U.PORTO

DOURORAMENTO

CIÊNCIAS BIOMÉDICAS

Chiral Stationary Phases for Liquid Chromatography: Development, Enantioseparation and Molecular Recognition Mechanism Studies

Ye Zaw Phyo

D

2019

U.PORTO

Ye Zaw Phyo. Chiral Stationary Phases for Liquid Chromatography: Development, Enantioseparation and Molecular Recognition Mechanism Studies

Chiral Stationary Phases for Liquid Chromatography: Development, Enantioseparation and Molecular Recognition Mechanism Studies

Ye Zaw Phyo

INSTITUTO DE CIÊNCIAS BIOMÉDICAS ABEL SALAZAR

D.ICBAS **2019**

YE ZAW PHYO

CHIRAL STATIONARY PHASES FOR LIQUID CHROMATOGRAPHY: DEVELOPMENT, ENANTIOSEPARATION AND MOLECULAR RECOGNITION MECHANISM STUDIES

Thesis submitted to Instituto de Ciências Biomédicas Abel Salazar, Universidade do Porto to obtain the degree of Doctor in Biomedical Sciences

Adviser - Dr. Carla Sofia Garcia Fernandes
Category - Assistant Professor
Affiliation - Faculdade de Farmácia da Universidade do Porto

Co-adviser - Dr. Anake Kijjoa
Category - Full Professor
Affiliation - Instituto de Ciências Biomédicas Abel Salazar da Universidade do Porto

IN ACCORDANCE WITH THE CURRENT LEGISLATION, ANY COPYING, PUBLICATION, OR USE OF THIS THESIS OR PARTS THEREOF SHALL NOT BE ALLOWED WITHOUT WRITTEN PERMISSION.

This work was developed in the Laboratório de Química Orgânica e Farmacêutica, Departamento de Ciências Químicas, Faculdade de Farmácia, Universidade do Porto and in the Departamento de Química, Instituto de Ciências Biomédicas Abel Salazar (ICBAS) da Universidade do Porto. The candidate performed this work with the PhD's scholarship provided by the "Lotus Plus Project under the ERASMUS MUNDUS ACTION 2-EU-Asia Mobility Project". This research was supported by the Strategic Funding UID/Multi/04423/2019 through national funds provided by FCT—Foundation for Science and Technology and European Regional Development Fund (ERDF), through the COMPETE – Programa Operacional Factores de Competitividade (POFC) program in the framework of the program PT2020; the project PTDC/MAR-BIO/4694/2014 (reference POCI-01-0145-FEDER-016790 and 3599-PPCDT) as well as by Project No. POCI-01-0145-FEDER-028736, co-financed by COMPETE 2020, under the PORTUGAL 2020 Partnership Agreement, through the European Regional Development Fund (ERDF), CHIRALBIOACTIVE-PI-3RL-IINFACTS-2019 and QOPNA research project (FCT UID/QUI/00062/2019) and Portuguese NMR network.

STATUS THESIS

It is hereby declared, as a communication of the candidate's role in the production of this thesis, that the author contributed to the design and execution of the experimental work which originated the results obtained, as well as their analysis, interpretation and drafting of the manuscripts that have been included in the thesis. The candidate also wrote the introductory material, the discussion and conclusions of the thesis, with the scientific suggestions, corrections and recommendations of the supervisors.

Scientific Publications

Articles in International Peer-Reviewed Journals

Review

Ye Zaw Phyo, João Ribeiro, Carla Fernandes, Anake Kijjoa and Madalena M.M. Pinto, "Marine Natural Peptides: Determination of absolute configuration using liquid chromatography methods and evaluation of bioactivities", *Molecules*, **2018**, 23(2), 306, doi:10.3390/molecules23020306.

Carla Fernandes, **Ye Zaw Phyo**, Ana Sofia Silva, Maria Elizabeth Tiritan, Anake Kijjoa and Madalena M.M. Pinto, "Chiral stationary phases based on small molecules: An update of the last 17 years", *Separation & Purification Reviews*, **2018**, 47: 89–123.

Original research

Ye Zaw Phyo, Sara Cravo, Andreia Palmeira, Maria Elizabeth Tiritan, Anake Kijjoa, Madalena M.M. Pinto and Carla Fernandes, "Enantiomeric resolution and docking studies of chiral xanthonic derivatives on chirobiotic columns", *Molecules*, **2018**, 23 (1),142.

Carla Fernandes, Maria Elizabeth Tiritan, Sara Cravo, **Ye Zaw Phyo**, Anake Kijjoa, Artur M.S. Silva, Quezia B. Cass and Madalena M.M. Pinto, "New chiral stationary phases based on xanthone derivatives for liquid chromatography", *Chirality*, **2017**, 29: 430–442.

Ye Zaw Phyo, Joana Teixeira, Maria Elizabeth Tiritan, Sara Cravo, Andreia Palmeira, Luís Gales, Artur M.S Silva, Anake Kijjoa, Madalena M.M Pinto, Carla Fernandes, "New chiral stationary phases for liquid chromatography based on small molecules: development, enantioresolution evaluation and chiral recognition mechanisms", *Chirality*, **2019** (Article submitted).

Ye Zaw Phyo, Joana Teixeira, Andreia Palmeira, Maria Elizabeth Tiritan, Anake Kijjoa, Madalena M.M Pinto, Carla Fernandes, "Enantioseparation of new xanthone and benzophenone derivatives by liquid chromatography on (*S*,*S*)-Whelk-O1 and cellulose based stationary phases, determination of enantiomeric purity and molecular docking studies", (Article in preparation for submission).

João P. do Carmo, **Ye Zaw Phyo**, Andreia Palmeira, Carla Fernandes, Maria Elizabeth Tiritan, Anake Kijjoa, Carlos Afonso, Madalena M. M. Pinto, "Enantioresolution, chiral recognition mechanisms and binding of xanthone derivatives on immobilized human serum albumin by liquid chromatography", *Bioanalysis*, **2019** (Article submitted).

Scientific Communications

Oral Communications

João P. do Carmo*, **Ye Zaw Phyo**, Andreia Palmeira, Carla Fernandes, Maria Elizabeth Tiritan, Anake Kijjoa, Carlos Afonso, Madalena M. M. Pinto, "Drug-protein binding of chiral derivatives of xanthones to immobilized human serum albumin by bioaffinity chromatography", 9th Meeting of Young Researches of University of Porto, 13-15 February, 2019.

Ye Zaw Phyo*, Carla Fernandes, Maria Elizabeth Tiritan, Sara Cravo, Artur M.S Silva, Anake Kijjoa, Madalena M.M. Pinto, "New chiral selectors for liquid chromatography based on xanthone derivatives", 11th International Symposium on Drug Analysis and the 29th International Symposium on Pharmaceutical and Biomedical Analysis, Leuven, Belgium, 09-12 September, 2018.**

João P. do Carmo*, **Ye Zaw Phyo**, Andreia Palmeira, Carla Fernandes, Maria Elizabeth Tiritan, Anake Kijjoa, Carlos Afonso, Madalena M. M. Pinto, "Enantioresolution, chiral recognition mechanisms and binding of xanthone derivatives on immobilized human serum albumin by liquid chromatography", XXIV ENCONTRO LUSO-GALEGO DE QUÍMICA, Porto, Portugal, 21-23 November, 2018.

A.S.Silva*, **Ye Zaw Phyo**, Madalena M.M. Pinto, Carla Fernandes, Anake Kijjoa, Artur M.S Silva, "Development and evaluation of a new chiral stationary phase for liquid chromatography", 6th Meeting of Young Researches of University of Porto, 17-19 February, 2016.

Poster Communications

Ye Zaw Phyo*, Joana Teixeira, Maria Elizabeth Tiritan, Sara Cravo, Artur M.S Silva, Anake Kijjoa, Madalena M.M Pinto, Carla Fernandes, "New chiral stationary phases for liquid chromatography based on small molecules: development, enantioresolution evaluation and chiral recognition mechanisms", 48th International Symposium on High-Performance Liquid Phase Separations and Related Techniques, Milan, Italy, 15-20 June, 2019.**

Joana Teixeira*, **Ye Zaw Phyo,** João Ribeiro, Bárbara Polónia, Carla Fernandes, Maria Elizabeth Tiritan, Artur M.S. Silva, Anake Kijjoa, Madalena M.M. Pinto, "Development of liquid chromatography chiral stationary phases for separation of enantiomeric drugs", Escola de Inverno de Farmácia, 4ª edição,18-27 March 2019.

Ye Zaw Phyo*, João Carmo, Andreia Palmeira, Maria Elizabeth Tiritan, Carla Fernandes, Carlos Afonso, Anake Kijjoa, Madalena M.M Pinto, "Enantioresolution and docking studies of xanthone derivatives on a human serum albumin stationary phase", 11th International Symposium on Drug Analysis and the 29th International Symposium on Pharmaceutical and Biomedical Analysis, Leuven, Belgium, 09-12 September, 2018.**

Ye Zaw Phyo*, Sara Cravo, Andreia Palmeira, Maria Elizabeth Tiritan, Artur M.S. Silva, Madalena M.M. Pinto, Anake Kijjoa, Carla Fernandes, "New chiral xanthonic stationary phases for liquid chromatography and studies of enantioresolution and chiral recognition mechanisms", First Meeting PhD in Biomedical Sciences, ICBAS, University of Porto, 07 May, 2018.

Ye Zaw Phyo*, Sara Cravo, Maria Elizabeth Tiritan, Anake Kijjoa, Madalena M.M. Pinto, Carla Fernandes, "Macrocyclic glycopeptide antibiotics: application as chiral selectors for enantioseparation of bioactive compounds", Escola de Inverno de Farmácia, 3ª edição, 07-15 March, 2018.

Catarina Leite*, Patrícia Barbosa, Krystyna Maslowska, Bárbara Polónia, João Ribeiro, **Ye Zaw Phyo**, Carla Fernandes, Maria Elizabeth Tiritan, Anake Kijjoa, Madalena M.M. Pinto, "Synthesis of xanthone derivatives: important chemical substrates to obtain bioactive compounds", Escola de Inverno de Farmácia, 3ª edição, 07-15 March, 2018.

Ye Zaw Phyo*, Andreia Palmeira, Sara Cravo, Maria Elizabeth Tiritan, Anake Kijjoa, Madalena M.M. Pinto, Carla Fernandes**,** "Enantiomeric separation and chiral recognition mechanisms of different macrocyclic glycopeptide-based chiral stationary phases", 10° Encontro National de Chromatografia, Bragança, Portugal, 04-06 December 2017.

Ye Zaw Phyo*, Carla Fernandes, Maria Elizabeth Tiritan, Sara Cravo, Artur M.S.Silva, Anake Kijjoa, Madalena M.M. Pinto, "Analytical application of xanthone derivatives as chiral selectors for liquid chromatography", Tramech IX: 9th Trans Mediterranean Colloquium on Heterocyclic Chemistry, Fez, Morocco, 22-25 November 2017.**

João Ribeiro*, **Ye Zaw Phyo**, Catarina Leite, Carla Fernandes, Maria Elizabeth Tiritan, Anake Kijjoa, Madalena M.M. Pinto, "Carboxyxanthone derivatives: synthesis and structure elucidation", Escola de Inverno de Farmácia, 2nd ed., 19-27 January 2017.

Ye Zaw Phyo*, A.S.Silva, Maria Elizabeth Tiritan, A.M.Silva, Madalena M.M. Pinto, Carla Fernandes, Anake Kijjoa, "Bioactive chiral derivatives of xanthones: Application as analytical tools", 5th Portuguese Young Chemists Meeting (5th PYChem) and 1st European Young Chemists Meeting (1st EYChem), Guimarães, 26-29 April 2016.**

Electronic Communications

Carla Fernandes*, **Ye Zaw Phyo**, João Ribeiro, Sara Cravo, Maria Elizabeth Tiritan, Artur M.S. Silva, Anake Kijjoa, Madalena M.M. Pinto, "Dual application of chiral derivatives of xanthones: in medicinal chemistry and liquid chromatography", 4th International Electronic Conference on Medicinal Chemistry, Sciforum Electronic Conference Series 4, 01-30 November, 2018.**

* Presenting author
** International conference

Awards

IUPAC Grant to participate in Transmediterranean Colloquium on Heterocyclic Chemistry (TRAMECH IX 2017) and present the poster: **Ye Zaw Phyo**, Carla Fernandes, Maria Elizabeth Tiritan, Sara Cravo, Artur M.S. Silva, Anake Kijjoa, Madalena M.M. Pinto, Analytical applications of xanthone derivatives as chiral selestors for liquid chromatography, Transmediterranean Colloquium on Heterocyclic Chemistry (TRAMECH IX 2017), Fez, Morocco, 22-25 November, 2017.

INDEX

ACKNOWLEDGMENTS…….. **xiv**
ABSTRACT…… **xviii**
RESUMO…… **xx**
ABBREVIATIONS……..... **xxii**
STRUCTURE AND ORGANIZATION OF THE THESIS …….. **xxiii**

CHAPTER I. INTRODUCTION…… 1
1. CHIRALITY…….. 2
2. STRATEGIES TO OBTAIN SINGLE ENANTIOMERS …… 4
3. CHIRAL STATIONARY PHASES FOR LIQUID CHROMATOGRAPHY… 7
4. CHIRAL RECOGNITION MECHANISMS …….. 11
5. CHIRAL DERIVATIVES OF XANTHONES ……..….. 13
6. SCOPE AND AIMS OF THE THESIS ……..…….. 16
REFERENCES…….. 19
CHAPTER II. MARINE NATURAL PEPTIDES: DETERMINATION OF ABSOLUTE CONFIGURATION USING LIQUID CHROMATOGRAPHY METHODS AND BIOACTIVITIES……. 44
CHAPTER III. CHIRAL STATIONARY PHASES BASED ON SMALL MOLECULES: AN UPDATE OF THE LAST SEVENTEEN YEAR……... 96
CHAPTER IV. NEW CHIRAL STATIONARY PHASES BASED ON XANTHONE DERIVATIVES FOR LIQUID CHROMATOGRAPHY…… 133
CHAPTER V. NEW CHIRAL STATIONARY PHASES FOR LIQUID CHROMATOGRAPHY BASED ON SMALL MOLECULES: DEVELOPMENT, ENANTIORESOLUTION EVALUATION AND CHIRAL RECOGNITION MECHANISMS ……. 147
ABSTRACT……. 150
1. INTRODUCTION…….. 150
2. MATERIALS AND METHODS…… 151

2.1 GENERAL METHODS…… 151
2.2 CHEMICALS AND REAGENTS…… 152
2.3 PREPARATION OF CSPs 1-12…… 152
2.4 X-RAY CRYSTALLOGRAPHY……... 165
2.5 CHROMATOGRAPHY…… 165
2.6 COMPUTATIONAL…….. 166
3. RESULTS AND DISCUSSION…… 166
4. CONCLUSION…… 180
REFERENCES AND NOTES…… 181

CHAPTER VI. ENANTIOSEPARATION OF NEW XANTHONE AND BENZOPHENONE DERIVATIVES BY LIQUID CHROMATOGRAPHY ON (*S,S*)-WHELK-O1 AND CELLULOSE BASED STATIONARY PHASES, DETERMINATION OF ENANTIOMERIC PURITY AND MOLECULAR DOCKING STUDIES…….. 188
ABSTRACT…….. 190
1. INTRODUCTION…… 190
2. MATERIALS AND METHODS…… 192
2.1 SYNTHESIS…… 192
2.2 CHROMATOGRAPHY……...195
2.3 COMPUTATIONAL……...196
3. RESULTS AND DISCUSSION……..…... 196
3.1 SYNTHESIS……... 196
3.2 CHROMATOGRAPHY……..…... 197
3.3 DOCKING STUDIES……... 202
4. CONCLUSIONS……..... 205
REFERENCES ……..……..... 206

CHAPTER VII. ENANTIOMERIC RESOLUTION AND DOCKING STUDIES OF CHIRAL XANTHONIC DERIVATIVES ON CHIROBIOTIC COLUMN…… 216

CHAPTER VIII. ENANTIOSEPARATION; CHIRAL RECOGNITION MECHANISMS AND BINDING OF XANTHONE DERIVATIVES ON IMMOBLIZED HUMAN SERUM ALBUMIN BY LIQUID CHROMATOGRAPHY …… 239
ABSTRACT…….. 242
1. INTRODUCTION…… 242
2. EXPERIMENTAL…… …… 245
2.1 CHEMICAL AND REAGENTS…….. 245
2.2 INSTRUMENTATION AND CHROMATOGRAPHIC CONDITIONS ……..…… 245
2.3 MOBILE PHASES…….. …… 246
2.4 SAMPLE SOLUTIONS……246
2.5 CHROMATOGRAPHIC AND BINDING PARAMETERS DETERMINATION……...246
2.6 COMPUTATIONAL…… 247
3. RESULTS AND DISCUSSION……... 247
3.1 SYSTEMATIC ENANTIOSEPARATION OF CDXs…… .. 248
3.2 COMPUTATIONAL DOCKING STUDIES…… 258
3.3 LIGAND-PROTEIN BIDING STUDIES……..…. 261
4. CONCLUSIONS……..... 266
FURTUER PERSPECTIVE……. 266
REFERENCES ……..……... 268

CHAPTER IX. CONCLUSIONS…… 286
APPENDIXES…….…… 290

FIGURES INDEX

FIGURE 1. LEFT AND RIGHT HUMAN HANDS TO ILLUSTRATE THE SPATIAL RELATIONSHIP BETWEEN A PAIR OF ENANTIOMERS……... 2

FIGURE 2. SCHEMATIC STEREOSELECTIVE BINDING OF A PAIR OF ENANTIOMERS…….. 3

FIGURE 3. ANNUAL DISTRIBUTION OF WORLDWIDE-APPROVED NEW MOLECULAR ENTITIES ACCORDING TO THE CHIRALITY, IN THE PERIOD OF 2002-2015…… 4

FIGURE 4. ROUTES TO OBTAIN ENANTIOMERICALLY PURE COMPOUNDS…… 5

FIGURE 5. DIFFERENT TYPES OF CSPs FOR LC…… 7

FIGURE 6. SUMMARY OF RECENT STRATEGIES FOR DEVELOPMENT OF NEW CSPs FOR LC……...…….. 9

FIGURE 7. STRUCTURE OF CELLULOSE *TRIS* (3-CHLORO-4-METHYLPHENYLCARBAMATE), THE CHIRAL SELECTOR OF THE COMMERCIAL COLUMN LUX® CELLULOSE-2. ……..……..… 10

FIGURE 8. 2D (**A**) AND 3D (**B**) STRUCTURE XANTHONE SCAFFOLD…… 14

FIGURE 9. COMMONLY USED METHODS FOR THE SYNTHESIS OF XANTHONE DERIVATIVES…… 15

FIGURE 10. EXAMPLE OF BIOLOGICAL ACTIVITIES OF SYNTHETIC CDXs…… 15

TABLE INDEX

TABLE 1. POSSIBLE CHIRAL RECOGNITION MECHANISM AND MAIN INTERACTIONS FOR DIFFERENT TYPES OF CSPs……..…… 12

ACKNOWLEDGEMENTS

It is with great pleasure I deliver my sincere appreciation to those who have contributed to this thesis and supported me in several ways during my doctoral study, without them, this work would not have been possible.

First and foremost, I would like to express my deepest gratitude to my supervisor Professor Dr. Carla Sofia Garcia Fernandes, the Laboratório de Química Orgânica e Farmacêutica (LQOF), Departamento de Ciências Químicas, Faculdade de Farmácia da Universidade do Porto (FFUP), for accepting and allowing me to pursue doctoral study under her effective supervision. There is no word to appreciate her enthusiasm, precious time, constructive criticism, inspiring ideas, unconditional support, numerous invaluable suggestions, kindness, guidance, teaching, encouraging and caring, being pivotal to the completion of this work. I am extremely fortunate to have been able to work with her and very proud to be her first Ph.D. candidate.

I am heartily thankful to my co-supervisor Professor Dr. Anake Kijjoa, Professor and Head of the Departamento de Química, Instituto de Ciências BiomédicasAbel Salazar (ICBAS), Universidade do Porto, for bringing and helping me to get a great opportunity in order to study my Ph.D. at the Universidade do Porto, Portugal. Without him, I could not imagine studying and graduating my Ph.D. I will forever be thankful to his unconditional support, enthusiasm, caring, and encouragement during my studies.

I would like to extend a most sincere thank to Professor Dr. Madalena Pinto, Professor and Head of the LQOF, Departamento de Ciências Químicas, FFUP, for allowing and supporting all the research facilities throughout my PhD study. Thank you very much for all suggestions, caring, supports and encouragement to successfully accomplish this study.

I am very grateful to Professor Dr. Maria Elizabeth Tiritan, from the Instituto Superior de Ciências da Saúde-Norte, for her valuable advice, suggestions, helps, inspiring discussions and knowledge as well as for providing chiral liquid chromatography columns during my study.

My grateful thanks to all Professors of LQOF, FFUP namely, Professor Dr. Carlos Afonso, Professor Dr. Honorina Cidade, Professor Dr. Emília Sousa and Professor Dr. Marta Correia Silva for their kindness, caring and helps throughout my study.

I am grateful to Professor Dr. Artur M. S. Silva, from the Departamento de Química, Universidade de Aveiro, for providing 1D and 2D NMR spectra throughout my research.

I would also like to thank Professor Dr. Eduardo Rocha, Head of the Departamento de Microscopia and Director of the PhD´s program in Biomedical Sciences, ICBAS, Universidade do Porto, for his support during my study.

A special thank goes to Professor Dr. Luis Gales, from Departamento de Biologia Molecular, ICBAS, Universidade do Porto, for his assistance in the X-Ray crystallography analysis.

I would like to acknowledge Dr Andreia Palmeira, from the LQOF, FFUP, Universidade do Porto, for her fruitful contribution and patience in helping and sharing valuable knowledge to allow me to understand and succeed in carrying out docking studies.

I would like to extend a most sincere thank you to Ms. Sara Cravo, LQOF, FFUP, for her valuable technical and practical assistance, support, discussions, teaching, sharing experiences as well as helping me in the use of HPLC and related issues.

I would like to thank the lab technicians Ms. Gisela Adriano and Mrs. Liliana Teixeira from LQOF, FFUP, for their help, support and friendship throughout my study.

I am very grateful to all the lab technicians of the Departamento de Química, ICBAS, Universidade do Porto, especially Mrs. Júlia Bessa, Ms. Sónia Santos and Mrs. Isabel Silva for their friendship, kindness, kind support, helps and encouragements during my study.

I would like to thank Professor Dr. José Augusto Caldeira and all professors from the Departamento de Química, ICBAS, for their friendship and encouragement.

I sincerely thank the Lotus Plus Project under the Erasmus Mundus Action 2-EU-Asia Mobility project for 34 months PhD's scholarship and Ms. Ulrica Ouline and all the staffs from International Office of Uppsala University, Sweden for their helps and support.

I am very grateful to Ms. Ana Castro Paiva, Ms. Ana Sofia Ferreira and all staff members from International Office of the Universidade do Porto for their help and support.

My special thanks go to Ms. Ana Paula Pereira and all staff members of the Secretariado de Pós-Graduação and Ms. Sara Pereira of the Mobility Office, ICBAS, Universidade do Porto, for their support and helps during my study.

Special thanks also go to Mrs. Joana Macedo and Mrs. Mónica Mendes from the technical office of the FFUP for providing and assisting in technical issues.

My special thanks to my respectful Professor Dr. Daw Hla Ngwe, Head of the Department of Chemistry (Retired), University of Yangon, Myanmar, for her constant support, kindness and helps to receive the PhD scholarship from the Erasmus Mundus to extend my horizon.

I wish to express my sincere thanks to my Professor Dr. Nwet Nwet Win, Post-doctoral researcher at Institute of Natural Medicine, University of Toyama, Japan (Former Associate Professor, Department of Chemistry, University of Yangon) for her kind suggestions, supports and motivation.

Thanks are also extended to the lecturers Dr. Khine Zar Wynn Lae and Dr. Nwe Ni Hlaing from Department of Chemistry, University of Yangon and Mawlamyine University for their kind suggestions and helps.

My thanks are also extended to the Ministry of Education, Myanmar, for giving the permission to study for four years at ICBAS, Universidade do Porto, Portugal.

My sincere thanks to Rector, Dr. Ba Han (Meiktila University), Professor Dr. Myatt Hla Wai (Department of Chemistry of Kyaukse University) and Professor Dr. Myo Myo Myat (Head of the Department of Chemistry of Dawei University) for their support, kind guidance and permission while I was doing the scholarship process at Dawei University.

I am thankful to Rector Dr. Aye Aye Myint, Pro-rectors and my second family members of Department of Chemistry of Yangon University of Education for their permission, assistance and taking responsibilities for my departmental workload and the duties during my stay at Universidade do Porto.

I wish to express my sincere thanks to Dr. Mu Mu Swe, Mr. Kyaw Min Htwe, Mr. Nay Ye Naing and all of my best friends who always give their hands in my difficult times, their friendship, encouragement and helps throughout my academic life.

My special thanks to my friends Dr. Suradet Buttachon, Dr. War War May Zin and my colleagues Solida Long (FFUP), Decha Kumla (ICABS) and all lab mates of Departamento de Química, ICBAS, for their true friendship, caring, many good memories, encouragement and constant readiness to help.

I also appreciate all of my lab colleagues, especially Maria Leticia Carraro, Ana Sofia Silva, Ana Catarina Lopes, Hélder Oliveira, João Pedro do Carmo, João Ribeiro, Joana Teixeira and Krystyna for sharing experiences, helps, friendship and for collaboration.

My thanks are also extended to Dr. Diana Resende (Post-doctoral fellow) and the PhD students Ana Rita Neves, Daniela Loureiro, Joana Moreira, and all others PhD students as well as integrated master's students, exchange students and master's students in medicinal chemistry whom I met during 2015-2019 academic years, for all of their helps, sharing the knowledge, friendship and a good times during my stay in LQOF, FFUP.

I wish to thank everyone who were directly or indirectly contributed their support towards the successful completion of this thesis.

Last but not least, the words cannot describe and express the gratitude and appreciation to my beloved mom for her unending concern, care, magnificent help, endless support and unlimited patience throughout my entire life. I am especially grateful to my brothers, sister and aunties for their supports and encouragement.

Finally, this thesis is dedicated to my beloved mom and all my respectful and admirable professors for their constant supports throughout my life.

SUCCESS IS THE SUM OF

SMALL EFFORTS,

REPEATED DAY IN AND DAY OUT.

"ROBERT COLLIER"

ABSTRACT

Liquid chromatography (LC) enantioresolution, using chiral stationary phases (CSPs), proved to be an essential separation tool with a wide range of applications, which plays more than ever a crucial role in academic research and industry. Actually, the development of CSPs for LC brought a new breath to enantioseparation processes, being their planning and development continuous and evolutionary issues.

This thesis reports the successful development of twelve new CSPs (**CSP1-CSP12**) by multi-step pathways starting from suitable functionalized small molecules, either derivatives of xanthones or benzophenones. Their planning was based on the most promising selectors based on chiral derivatives of xanthones (CDXs) recently reported, and aimed to obtain versatile and efficient CSPs as well as to explore the role of some structural characteristics that could be crucial for enantiorecognition. The chiral selectors, comprising one, two, three and four chiral moieties, were synthetized in enantiomerically pure form by coupling suitable functionalized carboxylated derivatives as chemical substrates with commercially available chiral building blocks (amino alcohols). The coupling reactions were carried out with the coupling reagent *O*-(benzotriazol-1-yl)-*N*-*N*-*N'*-*N'*-tetramethyluronium tetrafluoroborate (TBTU), in the presence of a catalytic amount of trimethylamine (TEA) in tetrahydrofuran (THF) as solvent, providing good yields. The enantiomeric purity of the new synthetized chiral selectors was evaluated by chiral LC and the enantiomeric ratio (e.r.) values were always higher than 99%. X-Ray analysis was used to establish a chiral selector 3D structure. The chemical substrates were also successfully synthetized using diverse synthetic approaches. The structure elucidation of all the synthesized chiral selectors and all intermediates was established on the basis of IR and NMR techniques. The synthesis of silylated derivatives of all chiral selectors, by reaction with 3-(triethoxysilyl)propylisocyanate, and further covalent linkage the to a chromatographic support, afforded **CSP1-CSP12**. Elemental analyses were performed to compare the extent of covalent binding of each chiral selector to silica. After packing into LC stainless-steel columns, the enantioselective capability of the new CSPs was evaluated using several commercial and “in house” chiral analytes. Specificity for enantioseparation of some CDXs, under normal-phase elution conditions, was

observed. Computational modeling studies by molecular docking were performed to gain an insight of structural features associated with chiral recognition mechanisms, which not only allowed the understanding of the chromatographic parameters at a molecular level but also gave a knowledge to improve the design of new selectors.

Enantioseparation and/or assessment of the chiral recognition mechanisms of several CDXs, prepared “in-house”, on different commercial chiral columns were also investigated to expand the investigation of the chromatographic behavior of this important class of small molecules. The selected CSPs encompassed four macrocyclic antibiotic CSPs (Chirobiotic® T, Chirobiotic® R, Chirobiotic® V and Chirobiotic® TAG), the Pirkle-type CSP (*S*,*S*)-Whelk-O1®, the polysaccharide-based CSP Lux® Celullose-2 and the protein-based CSP CHIRALPAK® HSA. Computational modeling studies were carried out by molecular docking approach using AutoDock Vina. The results obtained are important contributions to enlarge the knowledge of enantioseparation, to allow a closer look towards the mechanism of chiral molecular recognition as well as to have a better insight of structural requirements of the analytes to be enantioseparated.

The current work contributes to a better knowledge in the area of chiral LC in general and in the area of CDXs in particular, as well as to increase the number of developed CSPs based on small molecules and the understanding of the behavior of these important compounds (CDXs) toward different types of CSPs.

Keywords: Liquid chromatography; Chiral stationary phases; Chiral derivative of xanthones; Benzophenones; Enantioselectivity; Chiral recognition; Docking studies.

RESUMO

A resolução enantiomérica por cromatografia líquida com o uso de fases estacionárias quirais (FEQs) provou ser uma ferramenta de separação essencial com uma ampla gama de aplicações, que desempenha mais do que nunca um papel crucial na investigação a nível académico e na indústria. Efetivamente, o desenvolvimento de FEQs para cromatografia líquida trouxe um "novo fôlego" para os processos de separação de enantiómeros, sendo o seu planeamento e desenvolvimento, um processo contínuo e evolutivo.

Esta tese descreve a preparação de doze novas FEQs (**FEQ 1** - **FEQ 12**) através de vários passos reacionais utilizando pequenas moléculas adequadamente funcionalizadas, quer derivados de xantonas ou benzofenonas. O seu planeamento foi baseado nos seletores mais promissores baseados em derivados quirais de xantonas (DQXs) recentemente descritos, tendo como objetivos obter FEQs versáteis e eficientes, assim como explorar o papel de algumas características estruturais que podem ser cruciais para o reconhecimento molecular. Os seletores quirais, contendo uma, duas, três e quatro unidades quirais, foram sintetizados na forma enantiomericamente pura através do acoplamento de derivados carboxilados, usados como substratos químicos, a aminoálcoois quirais disponíveis comercialmente. As reações de acoplamento foram realizadas com o reagente de acoplamento tetrafluoroborato de *O*-(benzotriazol-1-il)-*N*-*N*-*N*′-*N*′-tetrametilurónio (TBTU), na presença de uma quantidade catalítica de trietilamina (TEA) e tetra-hidrofurano (THF) como solvente, com a obtenção de bons rendimentos. A pureza enantiomérica dos novos seletores quirais sintetizados foi avaliada por cromatografia líquida quiral e os valores obtidos de rácio enantiomérico (e.r.) foram superiores a 99%. Para estabelecer a estrutura tridimensional de um dos seletores quirais, foi efetuada análise de raios-X. Também foram sintetizados com sucesso os substratos químicos com a aplicação de diversas abordagens sintéticas. A elucidação estrutural de todos os seletores quirais sintetizados, assim como de todos os intermediários, foi estabelecida com base em técnicas de IV e RMN. A síntese de derivados sililados de todos os seletores quirais, através da reação com 3-(trietoxisilil)propilisocianato, e posterior ligação covalente a um suporte cromatográfico, permitou a obtenção das **FEQ 1**- **FEQ 12**. Foram realizadas análises elementares para comparar a extensão da ligação covalente de cada seletor quiral à sílica. Após o empacotamento em colunas de aço inoxidável para

cromatografia líquida, a capacidade enantiosseletiva das novas FEQs foi avaliada usando vários analitos quirais comerciais assim como analitos preparados pelo nosso grupo. Foi observada especificidade para a separação enantiomérica de alguns DQXs em condições de eluição de fase normal. Estudos computacionais de *docking* molecular foram realizados com o intuito de analisar as características estruturais associadas aos mecanismos de reconhecimento quiral, o que permitiu não só compreender melhor os parâmetros cromatográficos a nível molecular, mas também adquirir conhecimento para melhorar o *design* de novos seletores.

A separação enantiomérica e/ou avaliação dos mecanismos de reconhecimento quiral de vários DQXs preparados pelo nosso grupo, em diferentes colunas quirais comerciais, também foram investigadas, com a finalidade de ampliar a investigação relativa a esta importante classe de pequenas moléculas. As FEQs selecionadas englobaram quatro FEQs baseadas em antibióticos macrocíclicos (Chirobiotic® T, Chirobiotic® R, Chirobiotic® V e Chirobiotic® TAG), a FEQ do tipo Pirkle (*S*,*S*)-Whelk-O1®, a FEQ baseada em polissacarídeos Lux® Celullose-2 e a FEQ baseada em proteínas CHIRALPAK® HSA. Os estudos computacionais de *docking* molecular foram realizados com a utilização do programa AutoDock Vina. Os resultados obtidos constituem contribuições importantes para ampliar o conhecimento sobre separação enantiomérica, permitir um olhar mais próximo dos mecanismos de reconhecimento molecular quiral, assim como ter uma melhor compreensão das necessidades estruturais dos analitos a serem enantiosseparados.

O presente trabalho é uma importante contribuição para um melhor conhecimento na área de cromatografia líquida quiral em geral e na área dos DQXs em particular. Permitiu também aumentar o número de FEQs baseadas em pequenas moléculas e melhorar o entendimento do comportamento destas importantes moléculas (DQXs) em diferentes tipos de FEQs.

Palavras-chave: Cromatografia liquida; Fases estacionárias quirais; Derivados xantónicos quirais; Benzofenonas; Enantioseletividade; Reconhecimento quiral; Estudos de *docking*.

ABBREVIATIONS

AGP	α_1-Acid Glycoprotein
CBH I	Cellobiohydrolase I
CDX	Chiral derivative of xanthone
CE	Capillary electrophoresis
CSP	Chiral stationary phase
e.r.	Enantiomeric ratio
FFUP	Faculdade de Farmácia da Universidade do Porto
LC	Liquid chromatography
LQOF	Laboratório de Química Orgânica e Farmacêutica
HSA	Human serum albumin
HSA-CSP	Chiral stationary phase based on human serum albumin
ICBAS	Instituto de Ciências Biomédicas Abel Salazar
NMR	Nuclear magnetic resonance
OVM	Ovomucoid
SAR	Structure-activity relationship
SFC	Supercritical fluid chromatography
TBTU	*O*-(Benzotriazol-1-yl)-*N*-*N*-*N'*-*N'*-tetramethyluronium tetrafluoroborate
TEA	Triethylamine
THF	Tetrahydrofuran
UHPLC	Ultra-High-Performance Liquid Chromatographic

STRUCTURE AND ORGANIZATION OF THE THESIS

The present thesis is structured in nine chapters:

CHAPTER I - INTRODUCTION

In Chapter 1, a brief introduction of some key concepts about chirality is presented in section 1. The strategies to obtain single enantiomers are summarized in section 2. Examples of different types of CSPs, with especial emphasis on Pirkle-type, polysaccharide-based, macrocyclic antibiotics-based and protein-based CSPs are described in section 3. Section 4 deals with chiral recognition mechanisms and a brief description of CDXs and their importance in medicinal chemistry are highlighted in section 5. Finally, the scope and aims of this thesis are also included.

CHAPTER II - Marine Natural Peptides: Determination of Absolute Configuration Using Liquid Chromatography Methods and Evaluation of Bioactivities (review article)

In this chapter, a review covering the report on the determination of absolute configurations of amino acid residues of diverse marine peptides by chromatographic methodologies is presented. A brief summary of their biological activities was also included, emphasizing on the most promising marine peptides.

CHAPTER III - Chiral Stationary Phases Based on Small Molecules: An Update of the Last 17 Years (review article)

In this chapter, a review covering the report on Pirkle-type CSPs from January 2000 to March 2017 is presented. The chemical nature of the new chiral selectors, new insights in the development strategies and their applications in LC were emphasized.

CHAPTER IV - New chiral stationary phases based on xanthone derivatives for liquid chromatography (original research article)

This chapter includes an original article on the development of new CSPs based on xanthone derivatives for LC and evaluation of their enantioselective capability using several chemical classes of chiral compounds.

CHAPTER V - New chiral stationary phases for liquid chromatography based on small molecules: development, enantioresolution evaluation and chiral recognition mechanisms (submitted original research article)

This chapter reports the development and LC evaluation of new CSPs starting from suitable functionalized small molecules, including chiral derivatives of xanthones and benzophenones comprising one, two, three and four chiral moieties. The assessment of chiral recognition mechanisms by computational studies using molecular docking approach is also described.

CHAPTER VI - Enantioseparation of new xanthone and benzophenone derivatives by liquid chromatography on (*S*,*S*)-Whelk-O1 and cellulose based stationary phases, determination of enantiomeric purity and molecular docking studies (original research article in final preparation for submission)

This chapter contains the results of the original research describing the enantioseparation and determination of enantiomeric purity of new xanthone and benzophenone derivatives by liquid chromatography using (*S*,*S*)-Whelk-O1 and cellulose-based CSPs. The elucidation of chiral recognition mechanisms on (*S*,*S*)-Whelk-O1 CSP by computational studies using molecular docking approach is also described.

CHAPTER VII - Enantiomeric Resolution and Docking Studies of Chiral Xanthonic Derivatives on Chirobiotic Columns (original research article)

This chapter includes an original article describing a systematic study of enantioresolution of a library of xanthone derivatives, prepared “in-house”, using four commercially available macrocyclic glycopeptide-based columns. The effects of the mobile phase composition, the percentage of organic modifier, the pH of the mobile phase, the nature and concentration of different mobile phase additives on the chromatographic parameters are discussed. Considering the importance of understanding the chiral recognition mechanisms associated with the chromatographic enantioresolution, and the scarce data available for macrocyclic glycopeptide-based columns, computational studies by molecular docking are also reported.

CHAPTER VIII - Enantioresolution, chiral recognition mechanisms and binding of xanthone derivatives on immobilized human serum albumin by liquid chromatography (submitted original research article)

This chapter reports a systematic study of enantioseparation and further binding affinity of a library of enantiomeric mixtures of CDXs, prepared “in house”, by LC using a CSP based on human serum albumin (HSA-CSP). The chiral recognition mechanisms for CDXs on HSA-CSP are also described by molecular docking method using AutoDock Vina.

CHAPTER IX - Conclusions

This chapter gives the main conclusions of this thesis.

APPENDIXES

This chapter includes a table with the chemical structures of the developed CSPs based on small molecules as well as the numbering according to the thesis, chapters/research articles.

CHAPTER I

INTRODUCTION

1. Chirality

The word chirality, derived from the Greek word *cheir* meaning “hand”, is a spatial property describing the nature of a molecule, which makes it non-superimposable on its mirror image. These two non-superimposable object/mirror image forms of chiral molecules are called enantiomers, derived from the Greek word *enantios* meaning “opposite”.[1,2] The two hands are the most universally recognized example of enantiomers as shown in **Figure 1.**

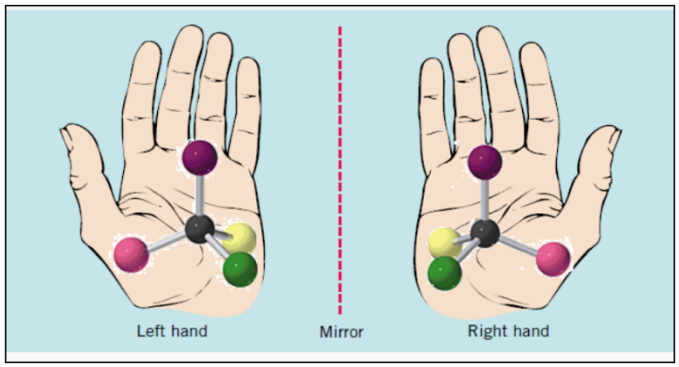


Fig. 1. Left and right human hands to illustrate the spatial relationship between a pair of enantiomers.

Chemically, two enantiomers of the same compound have equal chemical formula and identical physicochemical properties when they are in an achiral environment. However, it is possible to distinguish between them when they interact with chiral systems, such as biological systems, and by their optical activity.[3] Actually, the enantiomers rotate plane-polarized light in equal amounts but in opposite directions: one enantiomer rotates the light to clockwise (dextrorotatory) and the other to counterclockwise (levorotatory), referred by the symbols (+) and (-), respectively. For this reason, enantiomers are also called as optical isomers.[4]

Generally, the chiral molecules are characterized by the presence of an asymmetric center known as stereogenic center or stereocenter. In fact, most of the chiral molecules present central chirality, with one or more stereogenic centers, usually tetravalent carbon atoms bonded to four different substituents (atoms or groups of atoms).[5] Additionally, nitrogen, phosphorus, sulphur, selenium and boron can also produce stereogenic centers. The spatial arrangement of the substituents around the stereogenic centre is termed configuration. The nomenclature Cahn-Ingold-Prelog (CIP) is the most used system to differentiate the two enantiomers based on their

configuration. This system is based on the application of a set of priority rules, and subsequent assignment of the (*R*) (from the Latin word *rectus* which means right) or (*S*) (from the Latin word *sinister* which means left) configuration.[6]

Chirality is a property of the entire molecule, whereas a stereocenter is one of some causes of chirality. Actually, chirality can also be originated by a plane or an axis of chirality.[7] Recently, a new type of enantiomers were reported, the chiral akamptisomers.[8]

Chirality is a major concern in the pharmaceutical industry.[9] Biosystems comprising components with intrinsic chirality such as proteins, nucleic acids, and sugars, tend to be highly stereoselective environments.[10,11] Therefore, individual enantiomers of drugs may exhibit different pharmacokinetic and pharmacodynamic properties[12-14] as well as diverse toxicological effects[15-17] within the chiral environment of these biological systems. Considering biological activities, when one enantiomer is responsible for the activity of interest, the other enantiomer could be inactive, or possess lower activity, or be an antagonist of the active enantiomer or have a different activity that could be desirable or undesirable.[18-23] There are several examples of chiral drugs illustrating the referred situations.[24-26] Frequently, regarding a particular biological activity, one of the enantiomers has a high affinity for the receptor (eutomer) than the other (distomer) (**Figure 2**), being the ratio of the potencies termed eudismic ratio.[7]

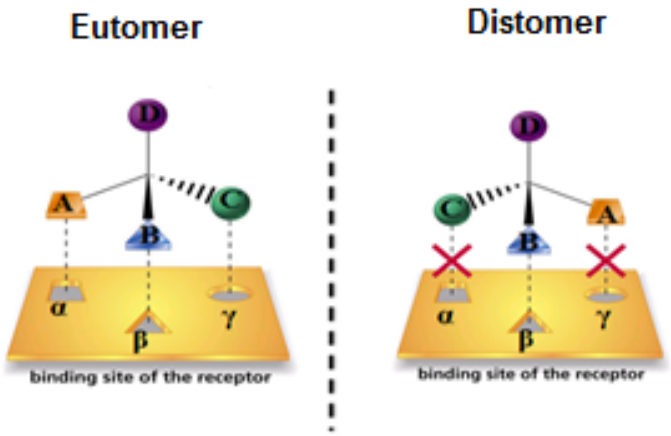


Fig. 2. Schematic stereoselective binding of a pair of enantiomers (adapted from [2]).

The pharmacological and biological differences exhibited by a pair of enantiomers as well as the potential benefits and safety of single enantiomeric drugs became crucial issues for the pharmaceutical industry and regulatory authorities.[27-29] Moreover, previously marketed racemic drugs are nowadays available as single enantiomers

("chiral switch") enhancing a new trend not only for public health consideration but also for economic purposes.[30-33]

The potential advantages of single enantiomeric drugs compared to racemates are numerous including, less side effects, reduction of the total administered dose, less complex pharmacokinetics and drug interactions, more selective pharmacological profile, better estimation of dose-response, reduced potential for complex drugs interactions and less complex relationship between plasma concentration and effect, among others.[13,34,35]

In addition to the several clinical advantages, the regulatory requirements and the "chiral switch", also the advances in synthetic methodologies, separation and analysis of the individual enantiomers contributed for the increasing number of single enantiomeric drugs rather than racemates (**Figure 3**).[28,36]

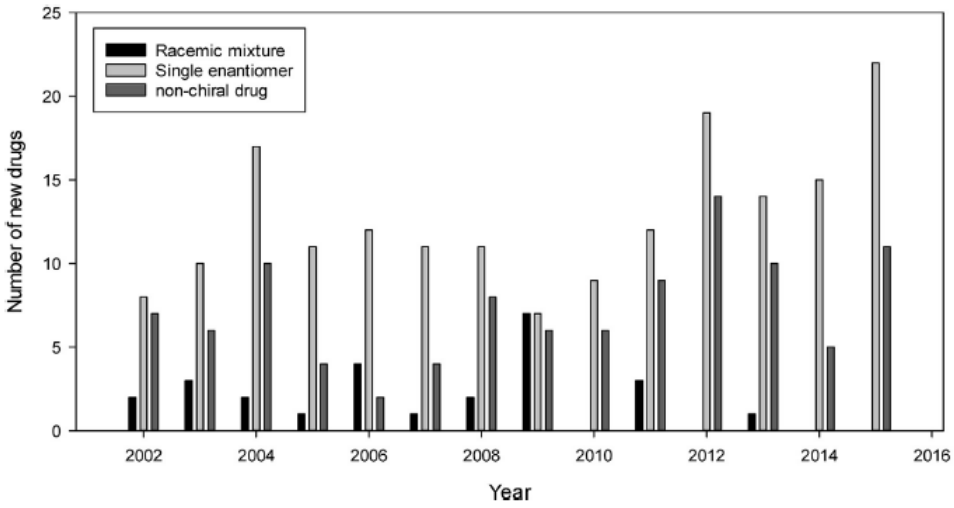


Fig. 3. Annual distribution of worldwide-approved new molecular entities according to chirality, in the period of 2002–2015.[36]

2. Strategies to obtain single enantiomers

The strategies to obtain and analyze both single enantiomers has become of pivotal importance in several research fields, including pharmaceutical and medicinal chemistry.[37,38] Three approaches can be used aiming to obtain enantiomerically pure compounds: chiral pool, stereoselective conversion of prochiral substrates (asymmetric synthesis), and chiral resolution[39,40] (**Figure 4**). Each of these strategies has advantages and drawbacks.

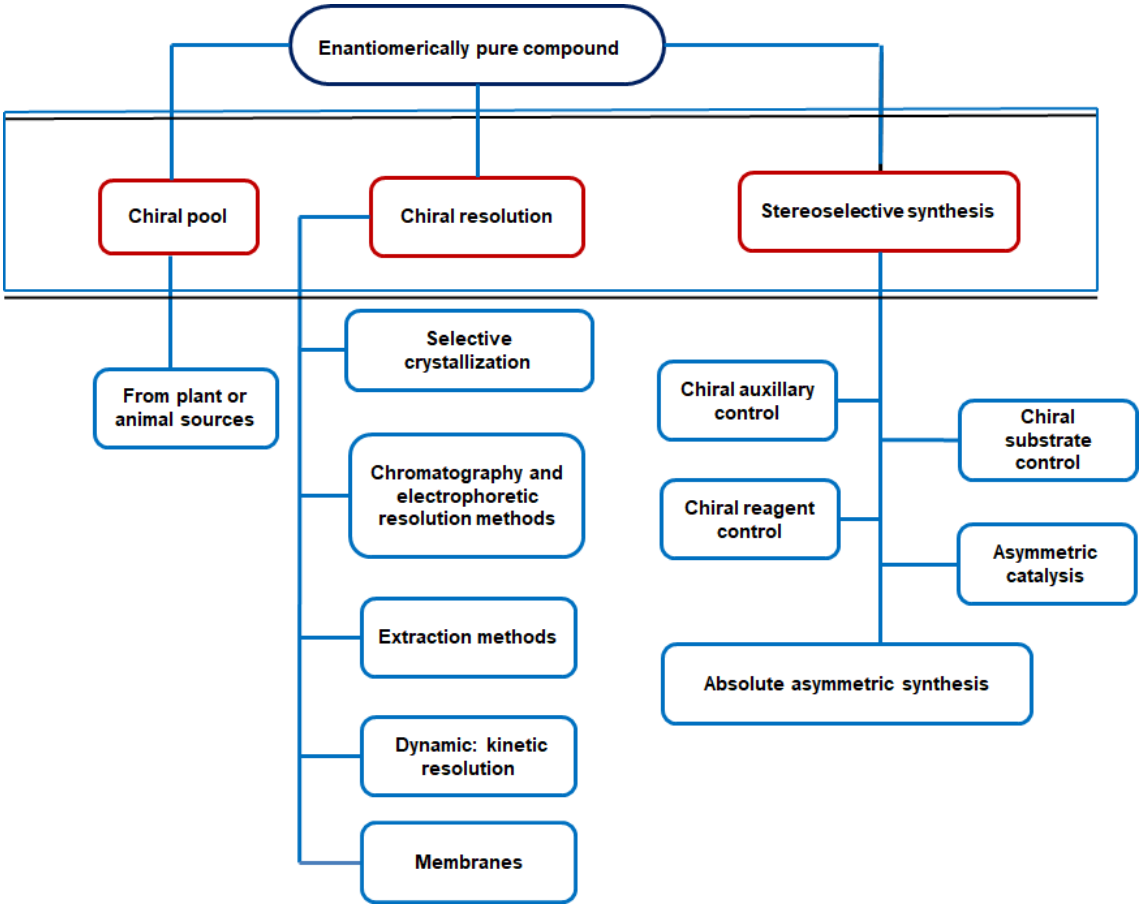


Fig. 4. Routes to obtain enantiomerically pure compounds (adapted from[39]).

The chiral pool and stereoselective synthesis involve the synthesis of the desired enantiomer being mainly useful when a large amount of only one enantiomer is required. If both enantiomers are needed it is necessary to develop two independent syntheses. The chiral pool uses an enantiomerically pure starting material and several achiral reagents followed by non-racemizing reaction to obtain the desired enantiomer, being economically advantageous but not suitable for all molecules. On the other hand, the stereoselective synthesis includes the production of new stereogenic center(s), starting from achiral precursors and using chiral synthons and auxiliaries, stereoselective catalysts or enzymes to obtain the enantiomeric molecule. Over the last few years, progresses in many new technologies, particularly in the catalytic asymmetric synthesis, have been achieved.[41-43]

The chiral resolution, also called “racemic approach”, involves the separation of a racemic mixture into the single enantiomers.[38] Regarding the early steps of drug development, resolution of a racemate is the preferential approach since it provides

both enantiomers with high enantiomeric purity for enantioselectivity studies.[40] Resolution of a racemate can be performed by several methodologies, including liquid chromatography (LC),[44,45] supercritical fluid chromatography (SFC),[46-48] capillary electrophoresis (CE),[49-51] diastereomeric crystallization,[52,53] membranes,[54,55] simulated moving bed,[56,57] dynamic and enzyme-mediated kinetic resolution,[58,59] among others. LC enantioresolution is considered as one of the most efficient tools for obtaining enantiomers with high enantiomeric purity.[44,60] The resolution of enantiomers can be carried out by two different approaches: direct or indirect methods.[61-63] Both separation methods provide different options to achieve separation of enantiomers.

The indirect method is based on the reaction of a racemate with an enantiomerically pure reagent providing a mixture of diastereomers. Due to the different physicochemical properties, they can be further separated by classical procedures such as crystallization, chromatography using a C_{18} or C_8 columns, extraction or distillation. After the resolution of the diastereoisomers, the enantiomers can be recovered by overturning the derivatization procedure. This method has a number of drawbacks: it is a laborious and time-consuming procedure that can fail in total separation of enantiomers by displaying different reaction rates; requires a 100% enantiomerically pure reagent to avoid the misleading formation of interfering diastereomeric pairs; is applicable only to enantiomers comprising a suitable functional group for derivatization; and further chemical treatment is necessary to recovered the starting enantiomers.[64,65]

The direct method is based on the formation of transient diastereomeric complexes between the enantiomers and a chiral selector present in the chromatographic system, being eluted first the enantiomer that forms the less stable complex. When compared to the indirect approach, this method has some advantages since it is more predictable for both preparative and analytical separations, no need prior manipulation (derivatization) of the compounds as well as no enantiomers regeneration after analysis. The direct method of separation is also often faster to obtain results without the need to set up laborious protocols. The chiral selector may be present as an additive in the mobile phase or, alternatively, as a component of the stationary phase.[66]

The direct method using chiral additives in mobile phase is rarely used due to their high cost and low efficiency.[67] Moreover, chiral additives modes of operation are complex and for preparative purposes, after elution, they need to be separated from the enantiomers and recovered.[64,65]

Nowadays, direct LC method using chiral stationary phases (CSPs) proved to be as one of the most significant separation approaches in academic research and industry[44,60] for both preparative[68-70] and analytical purposes.[71-73] The wide range of analytical applications include the determination of enantiomeric composition,[74,75] monitorization of asymmetric reactions,[76,77] pharmacokinetic,[78,79] forensic,[80,81] environmental,[82-84] and enantioselective studies,[85,86] analysis of the stereochemistry of natural compounds,[87-89] among others.

Regarding the application in evaluation of stereochemistry in natural products, a literature survey covering the report on the determination of absolute configurations of the amino acid residues of diverse marine peptides by LC is described in **Chapter II**. Both direct and indirect methods have proved to be suitable; however, in our opinion, the current trend is to use a chiral LC for stereochemical analysis due to many advantages of this method.

3. Chiral stationary phases for liquid chromatography

Over the last decades, several types of CSPs have been developed and, among them, more than a hundred were currently commercially available.[61,90] These comprise Pirkle-type, ligand-exchange-type, molecularly-imprinted, and based on macrocyclic antibiotics, proteins, polysaccharides, cyclodextrins, crown ethers, cyclofructans as well as synthetic polymers, among others (**Figure 5**).[91-98]

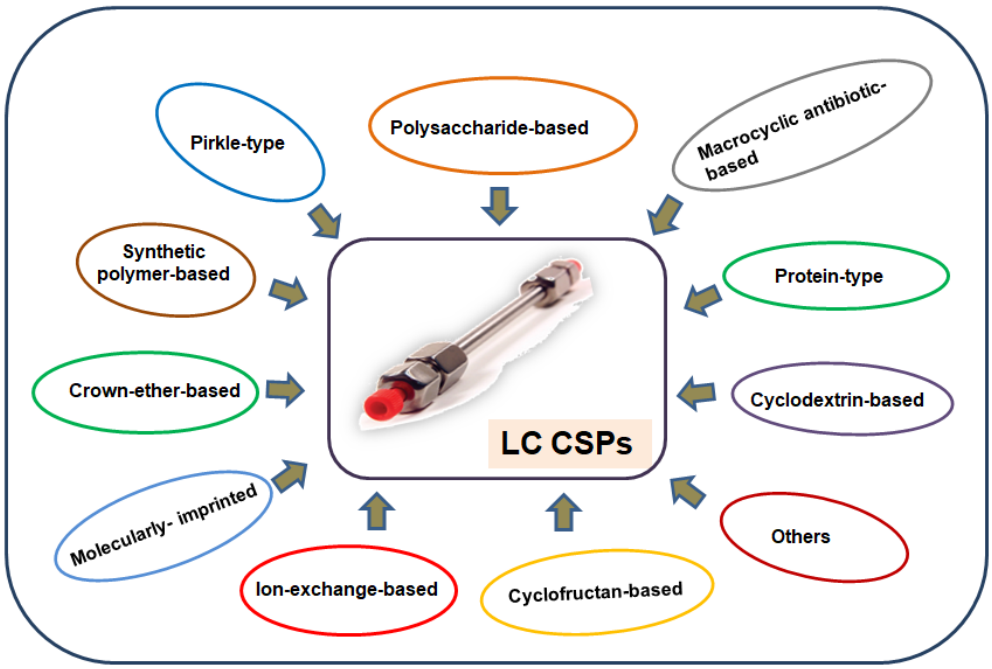


Fig. 5. Different types of CSPs for LC.

Since 1980s, a substantial effort has been made to find new CSPs of wide applicability or for specific target analytes, showing long durability and competitive cost. Additionally, the transition to ultra-high-performance liquid chromatographic (UHPLC) and the possibility of the new CSPs to be used in all elution modes or using mobile phases compatible with mass spectrometric detection were also taken into account.[99] The most recent development strategies comprise the introduction of new chiral selectors or new chromatographic supports, and the application of different immobilization or coating methodologies for preparation of the CSPs (**Figure 6**).[99] Recently, novel structures or analogues related to previously reported selectors were developed as well as the use of hybrid selectors.[100] The focus in chromatographic supports with lower particle size,[101,102] the innovation related to new materials such as monoliths[103-105] and core-shell particles,[106] as well as the use of hybrid supports,[107,108] were other approaches. Nevertheless, although many CSPs are described, the development of new CSPs continues to be a field of research with crucial importance. Nowadays, polysaccharide-based, macrocyclic antibiotic-based and Pirkle-type CSPs are pointed out as the most useful and broadly applied.[61] In this thesis, three of these types of CSPs were chosen for enantioseparation studies (**Chapters VI** and **VII**) and a brief description of these CSPs is presented below.

Pirkle-type or brush-type CSPs were introduced, in the late 1970s, by Pirkle *et col.*[109] This type of CSPs comprises small molecules as chiral selectors, typically with π-donor and/or π-acceptor moieties as attractive π-π interaction sites, being covalently bound to the chromatographic support *via* a spacer.[66,110] The advantages inherent to this type of CSPs are the excellent column durability, chemical and thermal inertness, good kinetic performance, high sample loading capacities, ability to invert elution order, good compatibility several mobile phases, among others.[111-113] (*S*,*S*)-Whelk-O1 CSP (**Figure 1** of **Chapter VI**), created by a rational approach,[114] is the most applied and versatile CSP in both academic and industrial fields. In fact, since the first reported CSP based on a chiral fluoro alcohol,[109] successive generations of CSPs have been developed, not only by Pirkle' group[66,110] but also by other research groups.[115]

A literature survey covering the report on Pirkle-type CSPs from January 2000 to March 2017 is described in **Chapter III**. The majority of the CSPs showed specificity for enantioseparation of some types of analytes, being an excellent choice to separate target analytes and analogues. It was found that appropriately chosen small molecules can be successfully used as chromatographic tools.

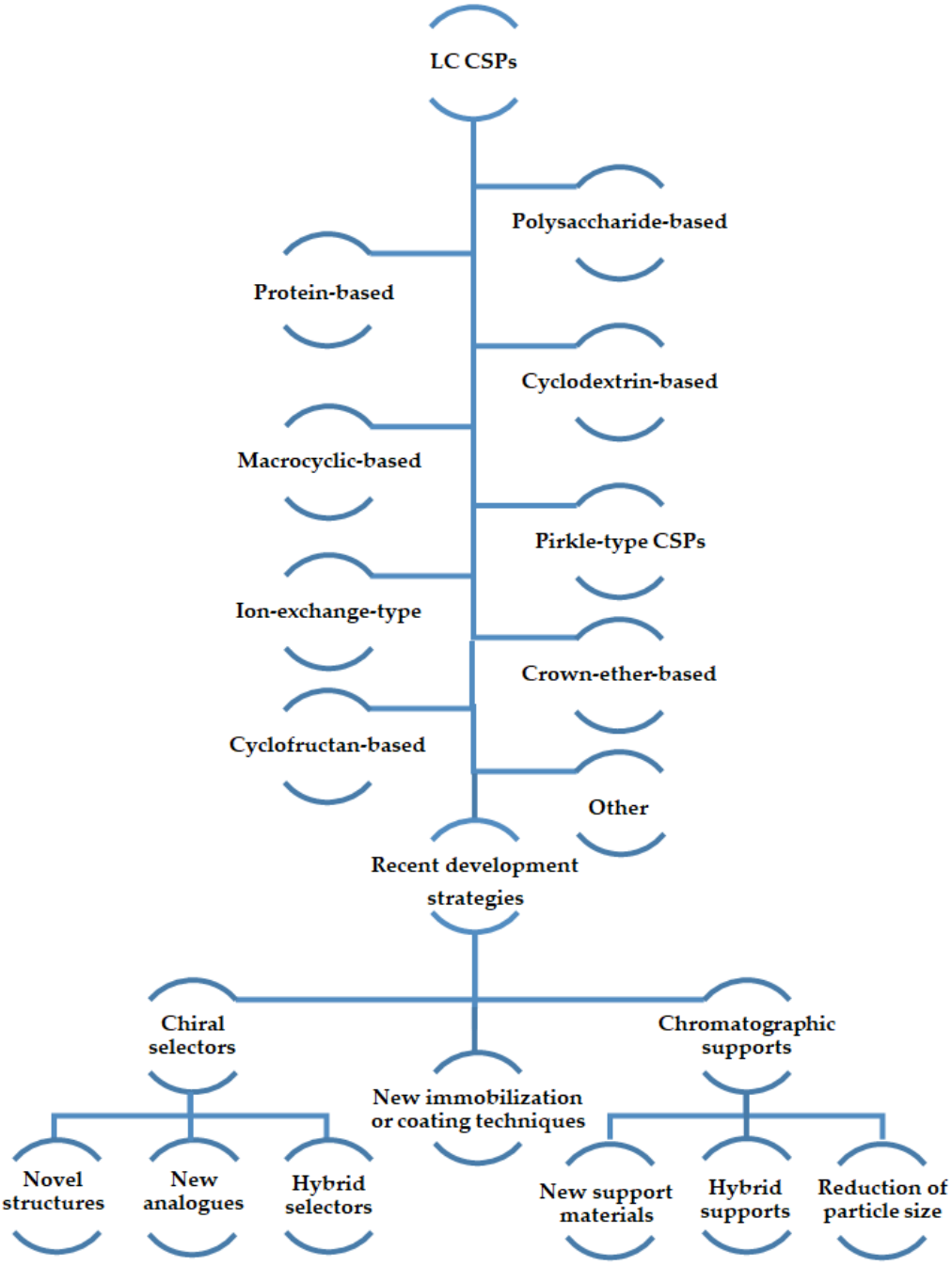


Fig. 6. Summary of recent strategies for development of new CSPs for LC.[99]

Polysaccharide-based CSPs are recognized as being the most successful and widely applied CSPs for both analytical[116-124] and preparative[125-131] enantioseparations, being responsible for about 99% of reported enantioseparations.[132] Amylose and cellulose are the main polysaccharides used to obtain CSPs, followed by chitosan and chitin.[133] Phenylcarbamates are the derivatives most studied due to their high chiral ability

recognition and the possibility to explore different aryl substituents, such as methyl, methoxy, among other groups, and/or chlorine,[134-140] affording different solubility and chiral recognition ability.[141] The position of the substituents in the aromatic ring also influence the enantioseparation performance of the chiral selector.[142] An example of a phenylcarbamate derivative of cellulose is illustrated in **Figure 7**. Among the developed polysaccharide-based CSPs, the 3,5-dimethylphenyl *tris*-phenylcarbamates of amylose and cellulose proved to have the best enantiorecognition performance.[143,144]

The phenylcarbamates of amylose and cellulose can be coated [143,145,146] or be immobilized[147-150] on a chromatographic support. Although the coated CSPs show high chiral recognition abilities for a wide variety of racemates, the range of mobile phases that can be used is very limited. Immobilized polysaccharides emerged as a reliable alternative allowing the use of a broader selection of solvents as mobile phases.[151,152] Nevertheless, despite the solvent versatility, in general, the potential of chiral recognition of immobilized polysaccharide-based CSPs is lower than the coated, which can be explained by the fact that stereospecific conformation can occur during the immobilization process.[148,151]

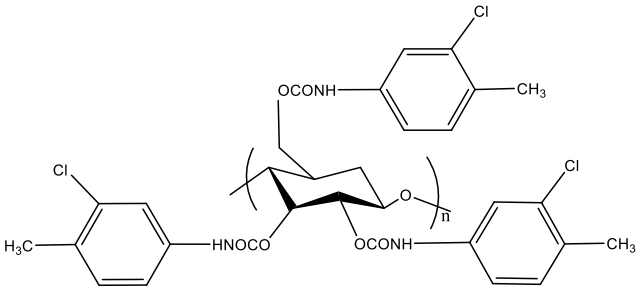


Fig. 7. Structure of cellulose *tris*(3-chloro-4-methylphenylcarbamate), the chiral selector of the commercial column Lux® Cellulose-2.

Macrocyclic antibiotic-based CSPs, introduced by Daniel W. Armstrong *et col.* in 1994,[153] are the second most versatile group of CSPs, being effective and versatile for the enantioseparation of a variety of chiral compounds.[154-175] This type of CSPs offers several advantages including high efficiency, short analysis time, low back pressure, high capacity, broad selectivity, among others.[176] Structurally, they comprise a variety of functional groups such as carboxyl, hydroxyl, amide, ester, and amino groups as well as multiple stereogenic centers and inclusion cavities.[177-180] These CSPs are able

to operate in all chromatographic elution modes.[181] Additionally, they provide a complementary enantioselective profile. [177] The macrocyclic antibiotics vancomycin, [153] teicoplanin,[159] ristocetin A[182] and the aglycone of teicoplanin[183] are the most used selectors, being commercially available as Chirobiotic® V, T, R and TAG, respectively (**Figure 1** of **Chapter VII**). Nevertheless, a diversity of other glycopeptides has been explored as chiral selectors, namely avoparcin,[184] norvancomycin,[185] eremomycin,[169] among others.

Protein-based CSPs are not considered as the most used type of CSPs due to their low capacity and efficiency. Moreover, their reduced chemical and biochemical stabilities as well as the possibility of denaturation of protein limit the ranges of pH, ionic strength, temperature and organic modifier composition of mobile phase.[181] Nevertheless, this type of CSPs demonstrate enantioselectivity for a broad range of chiral compounds.[186-189] Proteins are complex structures with a large surface comprising a variety of stereogenic centres and different binding sites, which allow multiple interactions with compounds.[190] One of the key applications of protein-based CSPs are on affinity and pharmacokinetic studies since they can mimic the *in vivo* systems, [191-195] being this feature very important in drug discovery. The most important used protein-based CSPs are human serum albumin (HSA),[196,197] α_1-acid glycoprotein (AGP),[198,199], and cellobiohydrolase I (CBH I) for chromatographic enantioseparations and for binding studies.[200-202] α_1-Acid glycoprotein (AGP) and ovomucoid (OVM) from chicken egg are mostly applied for resolution of a wide range of basic, acidic and neutral drugs.[203-205]

4. Chiral recognition mechanisms

Chiral recognition is a specific feature of a much broader area of the concept of molecular recognition.[206,207] Stereospecific recognition of chiral molecules plays a key role in nature as the basis of the interaction of chiral bioactive compounds with the biotarget molecules. In separation sciences such as chromatography technique, interactions between chiral analytes and chiral selectors are the basis for enantioseparations.[208] The formation of transient diastereomeric complexes in thermodynamic equilibria, which must differ in free energy, is a key condition for ultimate the separation of enantiomers. A variety of techniques, such as spectroscopic techniques, especially nuclear magnetic resonance (NMR) spectroscopy, X-Ray

crystallography as well as computational molecular modeling[61,209] can contribute to the understanding of the structure of the diastereomeric complexes, as well as to provide valuable information about intermolecular interactions. Computational modeling studies by using molecular docking approach proved to be an important tool to carry out this type of studies.[210,211]

Due to the large variety of chiral selectors, diverse structural characteristics contribute to the overall chiral recognition process and, consequently, different intermolecular interactions may be involved, namely ionic, ion-dipole or dipole–dipole, π-π, hydrogen bond interactions as well as steric (**Table 1**). It is important to highlight that the interactions can be either attractive or repulsive. Moreover, for same CSPs, such as based on macrocyclic antibiotic and proteins, the formation of inclusion complexes can occur.

Table 1. Possible chiral recognition mechanism and main interactions for different types of CSPs.[61,212-214]

CSP	Chiral recognition mechanism	Main interactions
Pirkle-type	Three-point interaction	Hydrogen bonding, π-π, dipole dipole and steric interactions
Polysaccharide derivatives	Helical structures	Hydrogen bonding, dipole dipole, π-π, steric interactions
Macrocyclic antibiotics	Multiple binding sites	Variable (e.g. Primary interactions: Ionic; Secondary interactions hydrogen bonding, dipole-dipole, π-π, hydrophobic interactions and steric repulsion)
Proteins	Multiple binding sites	Variable (e.g. Hydrophobic interactions, electrostatic interactions etc.)

Typically, to rationalize the observed stereoselective behavior of chiral selectors based on small molecules (Pirkle-type CSPs), the “3-point interaction” model explains the chiral recognition mechanisms.[215] This model stipulates that at least one of the enantiomers must undergo a minimum of three simultaneous interactions with the CSP, and that the overall interactions of the two enantiomers with the CSP must be energetically distinct. The predominant type of interactions that occur are dependent upon the functional groups present on both the analyte and CSP, and also the used

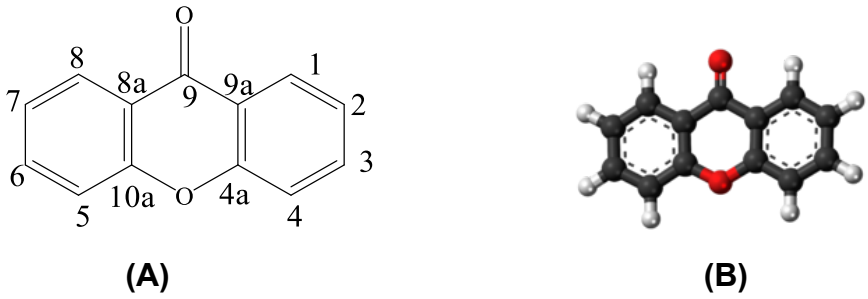
mobile phase.[93] This model was previously proposed by Easson and Stedman [216] to justify the differences in pharmacodynamic activity observed between enantiomers, considering their different interactions with a biomolecule (**Figure 3**). This model is very useful but it is a relatively simplistic representation of enantiomers-selector interactions since it assumes that the enantiomes must adopt a particular orientation in relation to the selector.[217] In addition, the molecular recognition between the enantiomers and the chiral selector may result in conformational changes in both the enantiomers and chiral selector. The difficulty in understanding the chiral recognition mechanisms increase when large molecules, such as macrocyclic antibiotics and proteins, or polymers are used as chiral selectors.

A closer look towards the chiral recognition mechanisms involved in an enantiomeric separation is fundamental to gain the insight of the kind of intermolecular interactions between each enantiomer and the chiral selector[208,218] as well as to understanding the chromatographic parameters at a molecular level.[211,219] Valuable information is also provided to predict which are the classes of racemates that may be enantioseparated, to establish the more suitable chromatographic conditions and to improve the design of new promising selectors.[220,221] In this thesis, insights of chiral recognitions mechanism are provided for CSPs based on small molecules, macrocyclic antibiotics and proteins, using computational modeling studies by molecular docking approach (**CHAPTERS VI**, **VII** and **VIII**).

5. Chiral derivatives of xanthones

One of the most important class of oxygenated heterocycles are xanthones or 9*H*-xanthen-9-ones comprising a dibenzo-*γ*-pyrone scaffold (**Figure 8**) being considered as a privileged structure.[222,223] Xanthone derivatives have an important role in Medicinal Chemistry, mainly considering their biological and pharmacological activities.[224,225] Naturally-occurring xanthones can be found as secondary metabolites in diverse terrestrial sources including higher plants, fungi, lichens[226,227] as well as isolated from marine invertebrates, such as sponges, tunicates, mollusks, bryozoans, in addition to algae and marine microorganisms (cyanobacteria and fungi).[228,229] The biosynthetic pathway of xanthones only allows the presence of specific groups in particular positions of the xanthone scaffold, which is a limiting factor for structural diversity. For this reason, in order to enlarge chemical space in this field, total synthesis needs to be considered[230,231] allowing the access to structures that otherwise could not

be reached only with natural product as a basis for molecular modification. Moreover, higher number of compounds can be obtained for structure-activity relationship (SAR) studies. For the last several years, the synthesis of new xanthone derivatives with potential biological properties has remained in the area of interest of our group.[232-243] They comprise a variety of different types of substituents in certain positions of the xanthone scaffold, leading to a vast diversity of biological/pharmacological activities[244] as well as different physicochemical and pharmacokinetic properties.[245,246] Additionally, other applications have been described for xanthone derivatives, such as preparation of fluorescence probes.[247,248]



(A) **(B)**

Fig.8. 2D (**A**) and 3D (**B**) structure xanthone scaffold.

In general, four methods can be applied for the synthesis of simple xanthones: Grover, Shah and Shah method, in one step reaction, synthesis *via* benzophenone and diaryl ether intermediates, which overcome the limitations of one-step methods, and synthesis via chromen-4-one derivatives[230,231] (**Figure 9**). Among the large number of xanthone derivatives, those containing a carboxylic group, carboxyxanthones, have shown great significance not only considering their interesting biological activities but also they proved to be suitable molecular scaffolds for synthesis of analogues and derivatives,[249] including chiral compounds.[250,251]

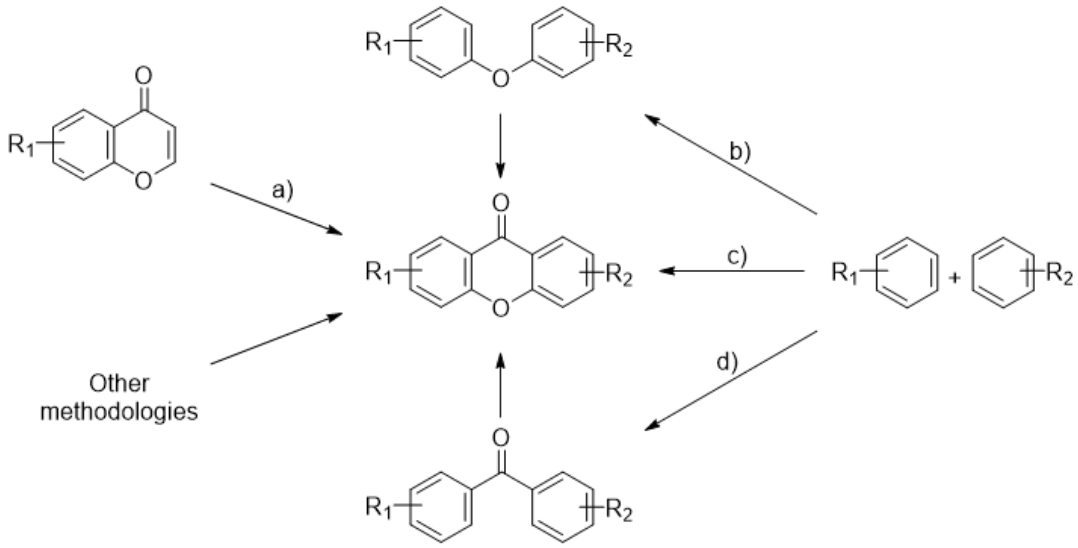


Fig. 9. Commonly used methods for the synthesis of xanthone derivatives.[249]

Synthetic chiral derivatives of xanthones (CDXs) are very interesting compounds leading to a large variety of biological activities (**Figure 10**).[252] These chiral derivatives can be obtained inspired in naturally occurring xanthones or by coupling chiral moieties to the xanthone scaffold.[252,253]

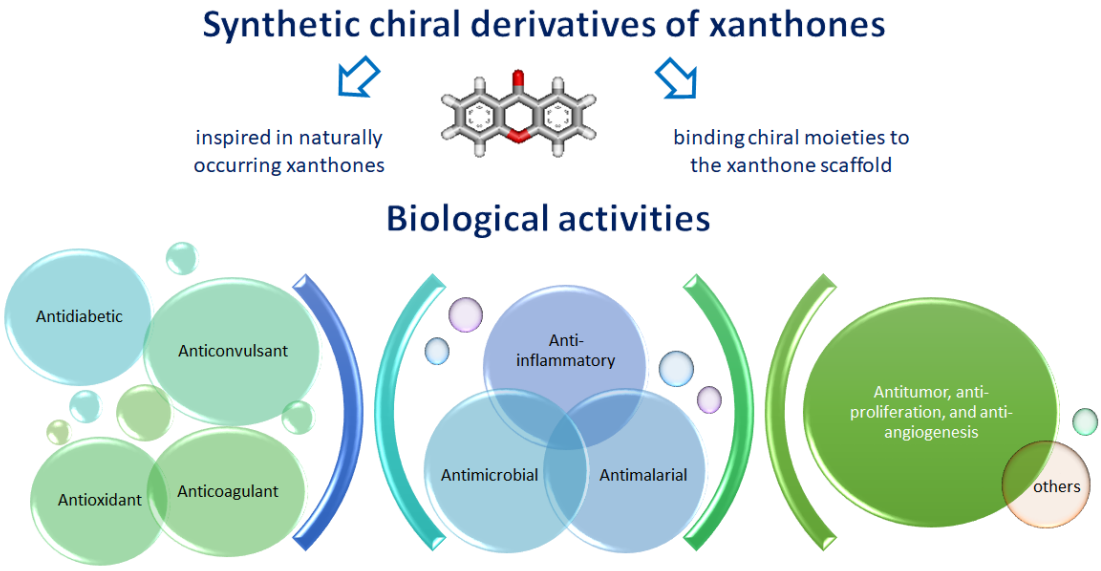


Fig. 10. Example of biological activities of synthetic CDXs.[252]

Recently, there has been an increase interest in new bioactive CDXs obtained by synthesis. Some reasons that can justify this trend were the interesting biological and pharmacological activities of some chiral members of this family, the clinical advantages of a single enantiomer than a racemate, the scarce examples of synthetic CDXs described, and the possibility to perform enantioselectivity studies. Actually, nature usually gives only one enantiomer and the synthetic procedures allow the preparation of both enantiomers to explore the enantioselectivity in biological screening assays.

Besides, another promising application has been described for CDXs, i.e. they can be used as chiral selectors for CSPs for LC, after covalently bounded to a chromatographic support through a spacer.[254] The CDXs comprise structural characteristics affording the establishment of different types of interactions as well as the three-dimensionality, factors that influence the enantioselectivity. In fact, the 3D *quasi*-planar structure and peculiar electronic properties of the xanthone scaffold,[255] associated with a diversity of functional groups and chiral moieties, are essential characteristics for enantioselective interactions with chiral analytes, through similar interactions of the same nature of Pirkle-type CSPs.[66,110]

The referred data support the choice of these compounds as an important part of this thesis.

6. Scope and aims of the thesis

The development of CSPs for LC revolutionized the enantioseparation approaches and, nowadays, several types of CSPs are available. Nevertheless, the development of new CSPs continues to be a field of research with great importance to follow the constant challenges on different areas as well as the advances in chromatographic instrumentation. Moreover, since there is no universal CSP, the choice of a CSP may become a difficult task and many chiral compounds remain to be resolved. These are reasons why the development of new CSPs continues to be a field of great interest. Of note are the Pirkle-type CSPs that have evolved over the years, showing more reported progress, mainly due to the possibility of using a wide variety of small molecules as chiral selectors. Recently, CDXs proved to be structurally promising chiral selectors for LC, in addition to their broad spectrum of bioactivities. Consequently, enantioseparation, enantiomeric purity evaluation and chiral recognition mechanism studies on different types of CSPs are crucial to expand the investigation on this

important class of small molecules as well as to guide for the development of more versatile and efficient chiral selectors.

Therefore, two main aims of this thesis were:

1. To develop new CSPs based on small molecules for LC,
2. To enantioseparate a series of CDXs, prepared “in-house”, on different commercial chiral columns and assess the chiral recognition mechanisms.

The specific objectives of this thesis are presented below.

- To synthesize suitable functionalized xanthone and benzophenone derivatives (carboxylated compounds) as chemical substrates by using different synthetic methodologies;
- To synthesize chiral xanthone and benzophenone derivatives in enantiomerically pure form as chiral selectors;
- To elucidate the structure of the chiral selectors, as well as the carboxylated chemical substrates and intermediates;
- To evaluate the enantiomeric purity of derivatives of chiral xanthones and benzophenones by LC;
- To synthesize silylated derivatives allowing the covalent linkage of the chiral selectors to a chromatographic support;
- To pack the CSPs into LC stainless-steel columns;
- To evaluate the enantioresolution performance of the chiral columns by LC using several commercial and “in house” chiral analytes;
- To separate enantiomeric mixtures of chiral derivatives of xanthones and/or benzophenones using commercial chiral columns to:
    - expand the systematic investigation on enantioseparation using different types of CSPs,
    - explore the influence of different mobile phases compositions on enantiomeric separation,
    - achieve the optimized chromatographic conditions for evaluation of enantiomeric purity;

- To perform computational modeling studies by molecular docking to gain the insight of structural features associated with chiral recognition mechanisms.

The major findings of the thesis were divided in eight chapters, corresponding to review and original articles, and are briefly described below.

Chapter II includes a review on analytical applications of chromatographic methodologies (direct and indirect methods) for the determination of absolute configurations of the amino acid residues of marine peptides.

Chapter III includes a review on Pirkle-type CSPs developed from January 2000 to March 2017, highlighting the chemical nature of the new chiral selectors, new insights in the development strategies and their applications in LC.

This thesis contains two articles, one has been already published and another was submitted to international Journals. These articles were originated from part of the results obtained in the experimental work, which are related to Aim 1 of this thesis, which are presented in the following chapters:

Chapter IV includes a research article describing, within the scope of this thesis, the synthesis of the xanthone derivative 6-methoxy-9-oxo-9*H*-xanthene-2-carboxylic acid, which was used as chemical substrate for coupling reaction with the enantiomerically pure amino alcohol (1*R*,2*R*)-(+)-2-amino-1,2-diphenylethanol, to afford a CDX. The development of a new CSP (**CSP1**) comprising this CDX as selector as well as the evaluation of its enantioselective capability by LC was also reported (see **Table 1** of compounds in **Appendixes** for correspondence).

Chapter V includes a research article describing, within the scope of this thesis, the development and LC evaluation of eleven new CSPs (**CSP2-CSP12**) based on chiral derivatives of xanthones and benzophenones (see **Table 1** of compounds in **Appendixes** for correspondence). The assessment of chiral recognition mechanisms of all described CSPs by computational studies using molecular docking approach is also emphasized.

Regarding the Aim 2 of this thesis, three other articles originated from part of the results obtained in the experimental work, were included. One of them was published, the second was submitted, and the third is in final preparation for submission to international Journal. They are presented in the following chapters:

Chapter VI includes a research article describing the enantioseparation and determination of enantiomeric purity of new xanthone and benzophenone derivatives by LC using (*S*,*S*)-Whelk-O1 and cellulose-based CSPs. The elucidation of chiral recognition mechanisms on (*S*,*S*)-Whelk-O1 CSP by computational studies using molecular docking approach is also emphasized.

Chapter VII presents a research article reporting a systematic study of enantioresolution of a library of CDXs, prepared “in-house”, using four commercially available macrocyclic glycopeptide-based columns. The effects of the mobile phase composition, the percentage of organic modifier, the pH of the mobile phase, the nature and concentration of different mobile phase additives on the chromatographic parameters are discussed as well as the assessment of chiral recognition mechanisms by molecular docking approach.

Chapter VIII presents a research article describing, within the scope of this thesis, the assessment of the chiral recognition mechanisms for CDXs on HSA-CSP by molecular docking method using AutoDock Vina. The student João Carmo performed the systematic study of enantioseparation and the binding affinity studies, within the scope of his master’s thesis.

REFERENCES

The search for the references used in the present thesis was made using the following browsers (last access in May of 2019).

http://www.scopus.com/scopus/home.url
http://atoz.ebsco.com/titles.asp?id=uniporto&sid=122887192&TabID=2
http://pubs.rsc.org/en/search/advancedsearch
http://onlinelibrary.wiley.com/advanced/search

http://www.google.pt/
http://www.sciencedirect.com/
http://pubs.acs.org/search/advanced

1. Davankov VA. Analytical chiral separation methods (IUPAC Recommendations 1997). *Pure Appl Chem* 1997;69(7):1469-1474.
2. Nguyen LA, He H, Pham-Huy C. Chiral drugs: an overview. *Int J Biomed Sci* 2006;2(2):85-100.
3. Leffingwell JC. Chirality & bioactivity I.: pharmacology. *Leffingwell Rep* 2003;3(1):1-27.
4. Wainer IW. Drug Stereochemistry: analytical methods and pharmacology. Dekker M, editor. New York, *J Appl Toxicol* 1993;18.
5. Francotte E, Lindner W, editors. Methods and Principles in Medicinal Chemistry - Chirality in Drug Research *Weinheim, Germany: WILEY-VCH*; 2006;33.
6. Gal J. Louis Pasteur, language, and molecular chirality. I. Background and Dissymmetry. *Chirality* 2011;23(1):1-16.
7. Tiritan ME, Ribeiro AR, Fernandes C, Pinto M. Chiral Pharmaceuticals. *Kirk-Othmer Encyclopedia of Chemicl Technology*: *John Wiley & Sons, Inc.*; 2016: 1-28.
8. Canfield PJ, Blake IM, Cai Z-L, Luck IJ, Krausz E, Kobayashi R, Reimers JR, Crossley MJ. A new fundamental type of conformational isomerism. *Nat Chem* 2018;10(6):615.
9. Blaser HU. Chirality and its implications for the pharmaceutical industry. *Rend Fis Acc Lincei* 2013;24(3):213-216.
10. Maier NM, Franco P, Lindner W. Separation of enantiomers: needs, challenges, perspectives. *J Chromatogr A* 2001;906(1-2):3-33.
11. Agranat I, Caner H, Caldwell J. Putting chirality to work: the strategy of chiral switches. *Nat Rev Drug Discov* 2002;1(10):753-768.
12. Mannschreck A, Kiesswetter R, von Angerer E. Unequal activities of enantiomers via biological receptors: Examples of chiral drug, pesticide, and fragrance molecules. *J Chem Educ.* 2007;84(12):2012-2017.
13. Triggle DJ. Stereoselectivity of drug action. *Drug Discov Today* 1997;2(4):138-147.

14. Cordato DJ, Mather LE, Herkes GK. Stereochemistry in clinical medicine: A neurological perspective. *J Clin Neurosci* 2003;10(6):649-654.
15. Smith SW. Chiral toxicology: It's the same thing only different. *Toxicol Sci* 2009;110(1):4-30.
16. Silva B, Fernandes C, Tiritan ME, Pinto MMM, Valente MJ, Carvalho M, de Pinho PG, Remião F. Chiral enantioresolution of cathinone derivatives present in “legal highs”, and enantioselectivity evaluation on cytotoxicity of 3,4-methylenedioxypyrovalerone (MDPV). *Forensic Toxicol* 2016;34(2):372-385.
17. Silva B, Fernandes C, de Pinho PG, Remião F. Chiral resolution and enantioselectivity of synthetic cathinones: A brief review. *J Anal Toxicol* 2018;42(1):17-24.
18. Eichelbaum MF, Testa B, Somogyi A. Stereochemical aspects of drug action and disposition: *SSBM* 2012;153.
19. Jamali F, Mehvar R, Pasutto F. Enantioselective aspects of drug action and disposition: therapeutic pitfalls. *J Pharm Sci* 1989;78(9):695-715.
20. McConathy J, Owens MJ. Stereochemistry in Drug Action. *Prim Care Companion J Clin Psychiatry* 2003;5(2):70-73.
21. Patočka J, Dvořák A. Biomedical aspects of chiral molecules. *J Appl Biomed* 2004;2:95-100.
22. Challener CA. Chiral drugs: *Routledge Revivals* 2017.
23. Ahuja S. The importance of chiral separations in pharmaceuticals. The Impact of Stereochemistry on Drug Development and Use. *New York: Wiley*,1997;142:287-315.
24. Ahuja S. A strategy for developing HPLC methods for chiral drugs. *LC GC N Am* 2007;25(11):1112.
25. Crossley RJ. Chirality and biological activity of drugs: *CRC Press* 1995;7.
26. Peepliwal A, Bagade S, Bonde C. A Review: Stereochemical consideration and eudismic ratio in chiral drug development. *J Biomed Sci and Res* 2010;2(1):29-45.
27. FDA'S policy statement for the development of new stereoisomeric drugs. *Chirality* 1992;4(5):338-340.
28. Caner H, Groner E, Levy L, Agranat I. Trends in the development of chiral drugs. *Drug discov today* 2004;9(3):105-110.

29. Cayen MN. Racemic mixtures and single stereoisomers: Industrial concerns and issues in drug development. *Chirality* 1991;3(2):94-98.
30. Somogyi A, Bochner F, Foster D. Inside the isomers: The tale of chiral switches. *Aust Prescr* 2004;27(2):47-49.
31. Sumithira G, Sujatha M. Drug chirality and its clinical significance evident, future for the development/separation of single enantiomer drug from racemates-The chiral switch. *Int J Pharm Gen Res* 2013;1(1):1-19.
32. Calcaterra A, D'Acquarica I. The market of chiral drugs: Chiral switches versus de novo enantiomerically pure compounds. *J Pharm Biomed Anal* 2018;147:323-340.
33. Agranat I, Wainschtein SR. The strategy of enantiomer patents of drugs. *Drug Discov Today* 2010;15(5-6):163-170.
34. Baumann P, Zullino DF, Eap CB. Enantiomers' potential in psychopharmacology - A critical analysis with special emphasis on the antidepressant escitalopram. *Eur Neuropsychopharmacol* 2002;12(5):433-444.
35. Baker GB, Prior TI, Coutts RT. Chirality and drugs used to treat psychiatric disorders. *J Psychiatry and Neurosci* 2002;27(6):401-403.
36. Sanganyado E, Lu Z, Fu Q, Schlenk D, Gan J. Chiral pharmaceuticals: A review on their environmental occurrence and fate processes. *Water Res* 2017;124:527-542.
37. Gübitz G, Schmid MG. Chiral Separations. *Kirk-Othmer Encyclopedia of Chemical Technology*: *John Wiley & Sons, Inc.* 2000.
38. Sekhon BS. Enantioseparation of chiral drugs—an overview. *Int J Pharm Technol Res* 2010;2:1584-1594.
39. Andrushko V, Andrushko N. Stereoselective Synthesis of Drugs and Natural Products. *New Jersey: Jonh Wiley & Sons;* 2013;1:1836.
40. Francotte ER. Enantioselective chromatography as a powerful alternative for the preparation of drug enantiomers. *J Chromatogr A* 2001;906(1-2):379-397.
41. Bhadra S, Yamamoto H. Substrate Directed Asymmetric Reactions. *Chemical Rev* 2018;118(7):3391-3446.
42. Xue YP, Cao CH, Zheng YG. Enzymatic asymmetric synthesis of chiral amino acids. *Chem Soc Rev* 2018;47(4):1516-1561.

43. Karimi B, Tavakolian M, Akbari M, Mansouri F. Ionic Liquids in Asymmetric Synthesis: An Overall View from Reaction Media to Supported Ionic Liquid Catalysis. *ChemCatChem* 2018;10(15):3173-3205.
44. Ward TJ, Ward KD. Chiral separations: A review of current topics and trends. *Anal Chem* 2012;84(2):626-635.
45. Ward TJ, Ward KD. Chiral Separations: Fundamental Review 2010. *Anal Chem* 2010;82(12):4712-4722.
46. Speybrouck D, Lipka E. Preparative supercritical fluid chromatography: A powerful tool for chiral separations. *J Chromatogr A* 2016;1467:33-55.
47. Bajpai L, Naidu H, Asokan K, Shaik KM, Kaspady M, Arunachalam P, Wu DR, Mathur A, Sarabu R. Integrating a post-column makeup pump into preparative supercritical fluid chromatography systems to address stability and recovery issues during purifications. *J Chromatogr A* 2017;1511:101-106.
48. Zehani Y, Lemaire L, Millet R, Lipka E. Small scale separation of isoxazole structurally related analogues by chiral supercritical fluid chromatography. *J Chromatogr A* 2017;1505:106-113.
49. Yu RB, Quirino JP. Chiral selectors in capillary electrophoresis: Trends during 2017–2018. *Molecules* 2019; 24(6):1135.
50. Voeten RLC, Ventouri IK, Haselberg R, Somsen GW. Capillary Electrophoresis: Trends and Recent Advances. *Anal Chem* 2018;90(3):1464-1481.
51. Stolz A, Jooß K, Höcker O, Römer J, Schlecht J, Neusüß C. Recent advances in capillary electrophoresis-mass spectrometry: Instrumentation, methodology and applications. *Electrophoresis* 2019;40(1):79-112.
52. Bishop R. Aspects of crystallization and chirality. In Chirality in Supramolecular Assemblies: Causes and Consequences. *Wiley Hoboken, NJ, USA* 2016(3):65-93.
53. Kovalenko VN, Kozyrkov YY. A simple method for resolution of endo-/exo-monoesters of trans-norborn-5-ene-2,3-dicarboxylic acids into their enantiomers. *Chirality* 2015;27(2):151-155.
54. Fernandes C, Tiritan ME, Pinto MMM. Chiral Separation in Preparative Scale: A Brief Overview of Membranes as Tools for Enantiomeric Separation. *Symmetry* 2017;9(206):1-19.

55. Afonso CAM, Crespo JG. Recent advances in chiral resolution through membrane-based approaches. *Angew Chem Int Ed Engl.* 2004;43(40):5293-5295.
56. Mun S, Wang NHL. Improvement of the performances of a tandem simulated moving bed chromatography by controlling the yield level of a key product of the first simulated moving bed unit. *J Chromatogr A* 2017;1488:104-112.
57. Song JY, Kim KM, Lee CH. High-performance strategy of a simulated moving bed chromatography by simultaneous control of product and feed streams under maximum allowable pressure drop. *J Chromatogr A* 2016;1471:102-117.
58. Kitamura M, Ohkuma T, Tokunaga M, Noyori R. Dynamic kinetic resolution in binap-ruthenium(ii) catalyzed hydrogenation of 2-substituted 3-oxo carboxylic esters. *Tetrahedron Asymmetry* 1990;1(1):1-4.
59. Schoemaker HE, Mink D, WubboLts MG. Dispelling the myths—Biocatalysis in industrial synthesis. *Science* 2003;299(5613):1694-1697.
60. Gumustas M, Ozkan SA, Chankvetadze B. Analytical and Preparative Scale Separation of Enantiomers of Chiral Drugs by Chromatography and Related Methods. *Curr Med Chem* 2018;25(33):4152-4188.
61. Lämmerhofer M. Chiral recognition by enantioselective liquid chromatography: Mechanisms and modern chiral stationary phases. *J Chromatogr A* 2010;1217(6):814-856.
62. Witte DT. High performance liquid chromatography for direct and indirect enantiomeric separations of chiral drugs. *Pharm World Sci* 1993;15(6):283-284.
63. Sellergren B. A Practical Approach to Chiral Separations by Liquid Chromatography; G. Subramanian (Editor). *Wiley-VCH Verlag GmbH* 1994:69-93.
64. Taylor DR, Maher K. Chiral separations by high-performance liquid chromatography. *J Chromatogr Sci* 1992;30(3):67-85.
65. Haginaka J. Pharmaceutical and biomedical applications of enantioseparations using liquid chromatographic techniques. *J Pharm Biomed Anal* 2002;27(3-4):357-372.

66. Fernandes C, Tiritan ME, Pinto M. Small molecules as chromatographic tools for HPLC enantiomeric resolution: Pirkle-type chiral stationary phases evolution. *Chromatographia* 2013;76(15-16):871-897.
67. Nagori BP, Deora MS, Saraswat P. Chiral drug analysis and their application. *Int J Pharm Sci Rev Res* 2011;6(2):106-113.
68. Sousa ME, Tiritan ME, Belaz KRA, Pedro M, Nascimento MSJ, Cass QB, Pinto MMM. Multimilligram enantioresolution of low-solubility xanthonolignoids on polysaccharide chiral stationary phases using a solid-phase injection system. *J Chromatogr A* 2006;1120(1-2):75-81.
69. Miller L, Potter M. Preparative chromatographic resolution of racemates using HPLC and SFC in a pharmaceutical discovery environment. *J Chromatogr B Anal Technol Biomed Life Sci* 2008;875(1):230-236.
70. Leek H, Andersson S. Preparative scale resolution of enantiomers enables accelerated drug discovery and development. *Molecules* 2017(22):1-9.
71. Fernandes C, Brandão P, Santos A, Tiritan ME, Afonso C, Cass QB, Pinto MM. Resolution and determination of enantiomeric purity of new chiral derivatives of xanthones using polysaccharide-based stationary phases. *J Chromatogr A* 2012;1269:143-153.
72. Fernandes C, Palmeira A, Santos A, Tiritan ME, Afonso C, Pinto MM. Enantioresolution of chiral derivatives of xanthones on (S,S)-Whelk-O1 and l -phenylglycine stationary phases and chiral recognition mechanism by docking approach for (S,S)-Whelk-O1. *Chirality* 2013;25(2):89-100.
73. Silva C, Ribeiro C, Maia AS, Gonçalves V, Tiritan ME, Afonso C. Enantiomeric separation of tramadol and its metabolites: Method validation and application to environmental samples. *Symmetry* 2017;9(9):170.
74. Kirkpatrick AD, Fain M, Yang J, Trehy M. Enantiomeric impurity analysis using circular dichroism spectroscopy with United States Pharmacopeia Liquid Chromatographic Methods. *J Pharm Biomed Anal* 2018;156:366-371.
75. Batista ANL, dos Santos FM, Batista JM, Cass QB. Enantiomeric mixtures in natural product chemistry: Separation and absolute configuration assignment. *Molecules* 2018;23:1-18.
76. Dawood AWH, de Souza ROMA, Bornscheuer UT. Asymmetric synthesis of chiral halogenated amines using amine transaminases. *ChemCatChem* 2018;10(5):951-955.

77. Chen J, Xu X, He Z, Qin H, Sun W, Fan B. Nickel/Zinc iodide co-catalytic asymmetric [2+2] cycloaddition reactions of azabenzonorbornadienes with terminal alkynes. *Adv Synth Catal* 2018;360(3):427-431.
78. Toki H, Ichikawa T, Mizuno-Yasuhira A, Yamaguchi J. A rapid and sensitive chiral LC-MS/MS method for the determination of ketamine and norketamine in mouse plasma, brain and cerebrospinal fluid applicable to the stereoselective pharmacokinetic study of ketamine. *J Pharm Biomed Anal* 2018;148:288-297.
79. Jiao H, Li Y, Sun L, Zhang H, Yu L, Yuan Z, Xie L, Chen J, Wang Y. A chiral LC-MS/MS method for the enantioselective determination of R-(+)- and S-(-)-pantoprazole in human plasma and its application to a pharmacokinetic study of S-(-).pantoprazole sodium injection. *Biomed Chromatogr* 2017;31(10):1-8.
80. Silva B, Pereira JA, Cravo S, Araújo AM, Fernandes C, Pinto MMM, Pinho PG, Pemião F. Multi-milligram resolution and determination of absolute configuration of pentedrone and methylone enantiomers. *J Chromatogr B Anal Technol Biomed Life Sci* 2018;1100:158-164.
81. Ribeiro C, Santos C, Gonçalves V, Ramos A, Afonso C, Tiritan ME. Chiral drug analysis in forensic chemistry: An overview. *Molecules* 2018;23(2):262.
82. Ribeiro AR, Maia AS, Cass QB, Tiritan ME. Enantioseparation of chiral pharmaceuticals in biomedical and environmental analyses by liquid chromatography: An overview. *J Chromatogr B Anal Technol Biomed Life Sci* 2014;968:8-21.
83. Ribeiro C, Ribeiro AR, Maia AS, Tiritan ME. Occurrence of chiral bioactive compounds in the aquatic environment: A review. *Symmetry* 2017;9(10):215.
84. Ribeiro AR, V.M.F. G, A.S. M, C. R, L. CPM, M.E. T. Dispersive liquid–liquid microextraction and HPLC to analyse fluoxetine and metoprolol enantiomers in wastewaters. *Environ Chem Lett* 2015;13(2):203-210.
85. Cosimelli B, Greco G, Laneri S, Novellino E, Sacchi A, Collina S, Rossi D, Cosconati S, Barresi E, Taliani S and others. Studies on enantioselectivity of chiral 4-acetylamino-6-alkyloxy-2-alkylthiopyrimidines acting as antagonists of the human adenosine receptor. *MedChemComm* 2018;9(1):81-86.
86. George R, Haywood A, Good P, Hennig S, Khan S, Norris R, Hardy J. Can saliva and plasma methadone concentrations be used for enantioselective

pharmacokinetic and pharmacodynamic studies in patients with advanced cancer? *Clin Ther* 2017;39(9):1840-1848.

87. Wu S, Harada S, Morikawa T, Nishidda A. Enantioselective total synthesis of a natural hydrocarbazolone alkaloid, identification of its stereochemistry, and revision of its spectroscopic data. *Tetrahedron Asymmetry* 2017(28):1083-1088.
88. Zin WWM, Buttachon S, Dethoup T, Fernandes C, Cravo S, Pinto MMM, Gales L, Pereira JA, Silva AMS, Sekeroglu N and others. New cyclotetrapeptides and a new diketopiperzine derivative from the marine sponge-associated fungus Neosartorya glabra KUFA 0702. *Mar Drugs* 2016;14(7):136.
89. Prompanya C, Fernandes C, Cravo S, Pinto MMM, Dethoup T, Silva AMS, Kijjoa A. A new cyclic hexapeptide and a new isocoumarin derivative from the marine sponge-associated fungus Aspergillus similanensis KUFA 0013. *Mar Drugs* 2015;13(3):1432-1450.
90. Felix G, A. B. Commercial chiral stationary phases for the separations of clinical racemic drugs. *Sep. Purif. Rev.* 2007;36(4):285-481.
91. Cavazzini A, Pasti L, Massi A, Marchetti N, Dondi F. Recent applications in chiral high performance liquid chromatography: A review. *Anal Chim Acta* 2011;706(2):205-222.
92. Tang M, Zhang J, Zhuang S, Liu W. Development of chiral stationary phases for high-performance liquid chromatographic separation. *TrAC, Trends Anal Chem.* 2012;39:180-194.
93. Okamoto Y, Ikai T. Chiral HPLC for efficient resolution of enantiomers. *Chem Soc Rev* 2008;37(12):2593-2608.
94. Beesley TE. Review of chiral stationary phase development and chiral applications. *LC GC Eur* 2011;24(5):270-276.
95. Mericko D, Lehotay J, Cizmarik J. HPLC separation of enantiomers using chiral stationary phases. *Ceska Slov farm* 2007;56(3):107-113.
96. Armstrong DW. Chiral stationary phases for high performance liquid chromatographic separation of enantiomers: A mini-review. *J Liq Chromatogr* 1984;7(sup2):353-376.
97. Armstrong DW, Zhang B. Chiral stationary phases for HPLC. *Anal Chem* 2001;73(19):557A-561A.

98. Kalíková K, Riesová M, Tesařová E. Recent chiral selectors for separation in HPLC and CE. *Cent Eur J Chem* 2012;10(3):450-471.
99. Teixeira J, Tiritan ME, Pinto MMM, Fernandes C. Chiral stationary phases for liquid chromatography: Recent developments. *Molecules* 2019;24(5):865.
100. Iuliano A, Attolino E, Salvadori P. (S)-leucine and [(S)-1-(1-naphthyl)ethyl]amine as chiral building blocks for a bifunctional system - Synthesis of a new chiral stationary phase and evaluation of its biselector properties in the HPLC resolution of racemic compounds. *Eur J Org Chem* 2001(18):3523-3529.
101. Cancelliere G, Ciogli A, D'Acquarica I, Gasparrini F, Kocergin J, Misiti D, Pierini M, Ritchie H, Simone P, Villani C. Transition from enantioselective high performance to ultra-high performance liquid chromatography: A case study of a brush-type chiral stationary phase based on sub-5-micron to sub-2-micron silica particles. *J Chromatogr A* 2010;1217(7):990-999.
102. Kotoni D, Ciogli A, Molinaro C, D'Acquarica I, Kocergin J, Szczerba T, Ritchie H, Villani C, Gasparrini F. Introducing enantioselective ultrahigh-pressure liquid chromatography (eUHPLC): Theoretical inspections and ultrafast separations on a new sub-2-μm Whelk-O1 stationary phase. *Anal Chem* 2012;84(15):6805-6813.
103. Wang Y, Ai F, Ng SC, Tan TTY. Sub-2μm porous silica materials for enhanced separation performance in liquid chromatography. *J Chromatogr A* 2012;1228:99-109.
104. Fekete S, Oláh E, Fekete J. Fast liquid chromatography: The domination of core-shell and very fine particles. *J Chromatogr A* 2012;1228:57-71.
105. Guillarme D, Ruta J, Rudaz S, Veuthey JL. New trends in fast and high-resolution liquid chromatography: A critical comparison of existing approaches. *Anal Bioanal Chem* 2010;397(3):1069-1082.
106. Wu X, You L, Di B, Hao W, Su M, Gu Y, Shen L. Novel chiral core-shell silica microspheres with trans-(1R,2R)-diaminocyclohexane bridged in the mesoporous shell: Synthesis, characterization and application in high performance liquid chromatography. *J Chromatogr A* 2013;1299:78-84.
107. Wang L, Dong S, Han F, Zhao Y, Zhang X, Zhang X, Qiu H, Zhao L. Spherical β-cyclodextrin-silica hybrid materials for multifunctional chiral stationary phases. *J Chromatogr A* 2015;1383:70-78.

108. Zhao B, Li L, Wang Y, Zhou Z. Preparation of polar group derivative β-cyclodextrin bonded hydride silica chiral stationary phases and their chromatography separation performances. *Chin Chem Lett* 2018;30(3):643-649.
109. Pirkle WH, House DW. Chiral high-performance liquid chromatographic stationary phases. 1. Separation of the enantiomers of sulfoxides , amines, amino acids, alcohols, hydroxy acids, lactones and mercaptans. *J Org Chem* 1979(44):1957-1960.
110. Welch CJ. Evolution of chiral stationary phase design in the Pirkle laboratories. *J Chromatogr A* 1994;666(1-2):3-26.
111. Pirkle WH, House DW, Finn JM. Broad spectrum resolution of optical isomers using chiral high-performance liquid chromatographic bonded phases. *J Chromatogr A* 1980;192(1):143-158.
112. Badaloni E, Cabri W, Ciogli A, Deias R, Gasparrini F, Giorgi F, Vigevani A, Villani C. Combination of HPLC “Inverted Chirality Columns Approach” and MS/MS Detection for Extreme Enantiomeric Excess Determination Even in Absence of Reference Samples. Application to Camptothecin Derivatives. *Anal Chem* 2007;79(15):6013-6019.
113. Blum AM, Lynam KG, Nicolas EC. Use of a new pirkle-type chiral stationary phase in analytical and preparative subcritical fluid chromatography of pharmaceutical compounds. *Chirality* 1994;6(4):302-313.
114. Pirkle WH, Welch CJ. An improved chiral stationary phase for the chromatographic separation of underivatized naproxen enantiomers. *J Liq Chromatogr* 1992;15(11):1947-1955.
115. Gasparrini F, Misiti D, Villani C. High-performance liquid chromatography chiral stationary phases based on low-molecular-mass selectors. *J Chromatogr A* 2001;906(1-2):35-50.
116. Khatiashvili T, Kakava R, Matarashvili I, Tabani H, Fanali C, Volonterio A, Farkas T, Chankvetadze B. Separation of enantiomers of selected chiral sulfoxides with cellulose *tris*(4-chloro-3-methylphenylcarbamate)-based chiral columns in high-performance liquid chromatography with very high separation factor. *J Chromatogr A* 2018;1545:59-66.

117. Cass QB, Bassi ALC, Calafatti SA, Matlin SA, Tiritan ME, de Campos LMM. Carbohydrate carbamate coated onto microporous silica: Application to chiral analysis of commercial pharmaceutical drugs. *Chirality* 1996;8(1):143-146.
118. Matlin SA, Tiritan ME, Cass QB, Boyd DR. Enantiomeric resolution of chiral sulfoxides on polysaccharide phases by HPLC. *Chirality* 1996;8(1):147-152.
119. Cass QB, Degani ALG, Tiritan ME, Matlin SA, Curran DP, Balog A. Enantiomeric resolution by HPLC of axial chiral amides using amylose *tris*[(*S*)-1-phenylethylcarbamate]. *Chirality* 1997;9(2):109-112.
120. Cass QB, Watanabe CS, Rabi JA, Bottari PQ, Costa MR, Nascimento RM, Cruz JE, Ronald RC. Polysaccharide-based chiral phase under polar organic mode of elution in the determination of the enantiomeric purity of emtricitabine an anti-HIV analogue nucleoside. *J Pharm Biomed Anal* 2003;33(4):581-587.
121. Lourenço TC, Armstrong DW, Cass QB. Enantiomeric Resolution of a Chiral Sulfoxide Series by LC on Synthetic Polymeric Columns with Multimodal Elution. *Chromatographia* 2010;71(5-6):361-372.
122. Jie Z, Qiuzheng D, Suzhen Z, Fang S, Xinyu L, Zhenzhong Z. Enantioseparation of Three Important Intermediates of Tanikolide with Immobilized Cellulose Chiral Stationary Phase. *J Chromatogr Sc.* 2015;53(6):959-962.
123. Zacharis CK, Vastardi E. A Validated LC Method for the Determination of Enantiomeric Purity of Clopidogrel Intermediate Using Amylose-Based Stationary Phase. *Chromatographia* 2015;78(11-12):819-824.
124. Ramisetti NR, Arnipalli MS, Nimmu NV, Bondigalla R. UHPLC Determination of Besifloxacin Enantiomers on Immobilized Amylose Tris(3,5-dichlorophenylcarbamate) Chiral Stationary Phase. *Chromatographia* 2017;80(10):1509-1515.
125. Tiritan ME, Cass QB, Del Alamo A, Matlin SA, Grieb SJ. Preparative enantioseparation on polysaccharide phase using microporous silica as a support. *Chirality* 1998;10(7):573-577.
126. Lourenco TC, Batista JM, Jr., Furlan M, He Y, Nafie LA, Santana CC, Cass QB. Albendazole sulfoxide enantiomers: preparative chiral separation and absolute stereochemistry. *J Chromatogr A* 2012;1230:61-65.
127. Belaz KR, Coimbra M, Barreiro JC, Montanari CA, Cass QB. Multimilligram enantioresolution of sulfoxide proton pump inhibitors by liquid chromatography

on polysaccharide-based chiral stationary phase. *J Pharm Biomed Anal* 2008;47(1):81-87.

128. Cass QB, Oliveira RV. Separation of Multi-Milligram Quantities of Gossypol Enantiomers on Polysaccharide-Based Stationary Phases. *J Liq Chromatogr Relat Technol* 2002;25(5):819-829.
129. Heydari R, Shamsipur M. Enantiomeric Separation and Quantitation of Tenofovir Disoproxil Fumarate Using Amylose-Based Chiral Stationary Phases by High-Performance Liquid Chromatography. *Acta Chromatogr* 2015;27(4):583-595.
130. Lal M, Bhushan R. Analytical and semi-preparative enantioresolution of (*RS*)-ketorolac from pharmaceutical formulation and in human plasma by HPLC. *Biomed Chromatogr* 2016;30(10):1526-1534.
131. Sadutto D, Ferretti R, Zanitti L, Casulli A, Cirilli R. Analytical and semipreparative high performance liquid chromatography enantioseparation of bicalutamide and its chiral impurities on an immobilized polysaccharide-based chiral stationary phase. *J Chromatogr A* 2016;1445:166-171.
132. Ali I, Saleem K, Hussain I, Gaitonde VD, Aboul-Enein HY. Polysaccharides chiral stationary phases in liquid chromatography. *Sep Purif Rev* 2009;38(2):97-147.
133. Ribeiro J, Tiritan ME, Pinto MMM, Fernandes C. Chiral stationary phases for liquid chromatography based on chitin and chitosan-derived marine polysaccharides. *Symmetry (Basel)* 2017;9(9):190.
134. Fanali C, Fanali S, Chankvetadze B. HPLC Separation of Enantiomers of Some Flavanone Derivatives Using Polysaccharide-Based Chiral Selectors Covalently Immobilized on Silica. *Chromatographia* 2016;79(3-4):119-124.
135. Belboukhari N, Lahmar N, Sekkoum K, Cheriti A, Aboul-Enein HY. Chiral Separation of Several Flavanones by Liquid Chromatography. *Curr Pharm Anal* 2015;11(3):201-209.
136. López-Ram-de-Víu P, Gálvez JA, Díaz-de-Villegas MD. High-performance liquid chromatographic enantioseparation of unusual amino acid derivatives with axial chirality on polysaccharide-based chiral stationary phases. *J Chromatogr A* 2015;1390:78-85.
137. Albals D, Heyden YV, Schmid MG, Chankvetadze B, Mangelings D. Chiral separations of cathinone and amphetamine-derivatives: Comparative study

between capillary electrochromatography, supercritical fluid chromatography and three liquid chromatographic modes. *J Pharm Biomed Anal* 2016;121:232-243.

138. Ghanem A, Hoenen H, Müller P, Aboul-Enein HY. Enantiomeric separation of cyclopropane derivatives on a polysaccharide-based chiral stationary phase. *Anal Chim Acta* 2005;538(1-2):15-24.
139. Lipka E, Yous S, Furman C, Carato P, Deghaye C, Bonte JP, Vaccher C. Analytical and preparative chiral separation of β-carboline derivatives, LDL oxidation inhibitors, using HPLC and CE methodologies: Determination of enantiomeric purity. *Chromatographia* 2012;75(7-8):337-345.
140. Gallinella B, Ferretti R, Zanitti L, Sestili I, Mosca A, Cirilli R. Comparison of reversed-phase enantioselective HPLC methods for determining the enantiomeric purity of (S)-omeprazole in the presence of its related substances. *J Pharm Biomed Anal* 2016;6(2):132-136.
141. Chankvetadze B. Recent developments on polysaccharide-based chiral stationary phases for liquid-phase separation of enantiomers. *J Chromatogr A* 2012;1269:26-51.
142. Chen X, Yamamoto C, Okamoto Y. Polysaccharide derivatives as useful chiral stationary phases in high-performance liquid chromatography. *Pure Appl Chem* 2007;79(9):1561-1573.
143. Witte DT, Bruggeman FJ, Franke JP, Copinga S, Jansen JM, De Zeeuw RA. Comparison between cellulose and amylose tris(3,5-dimethylphenylcarbamate) chiral stationary phases for enantiomeric separation of 17 amidotetralins. *Chirality* 1993;5(7):545-553.
144. Matlin SA, Tiritan ME, Crawford AJ, Cass QB, Boyd DR. HPLC with carbohydrate carbamate chiral phases: Influence of chiral phase structure on enantioselectivity. *Chirality* 1994;6(2):135-140.
145. Okamoto Y, Kawashima M, Hatada K. Useful chiral packing materials for high-performance liquid chromatographic resolution of enantiomers: Phenylcarbamates of polysaccharides coated on silica gel. *J Am Chem Soc* 1984;106(18):5357-5359.
146. Park JH, Whang YC, Jung YJ, Okamoto Y, Yamamoto C, Carr PW, McNeff CV. Separation of racemic compounds on amylose and cellulose

dimethylphenylcarbamate-coated zirconia in HPLC. *J Sep Sci* 2003;26(15-16):1331-1336.

147. Francotte E, Huynh D. Immobilized halogenophenylcarbamate derivatives of cellulose as novel stationary phases for enantioselective drug analysis. *J Pharm Biomed Anal* 2002;27(3-4):421-429.
148. Imran A, Hassan YA-E. Immobilized Polysaccharide CSPs: An Advancement in Enantiomeric Separations. *Curr Pharm Anal* 2007;3(1):71-82.
149. Ikai T, Okamoto Y. Structure control of polysaccharide derivatives for efficient separation of enantiomers by chromatography. *Chem Rev* 2009;109(11):6077-6101.
150. Al-Othman ZA, Ali I, Asim M, Khan TA. Recent trends in chiral separations on immobilized polysaccharides CSPs. *Comb Chem High Throughput Screen* 2012;15(4):339-346.
151. Ali I, Aboul-Enein HY. Impact of immobilized polysaccharide chiral stationary phase on enantiomeric separations*. J Sep Sci* 2006(29):762-769.
152. Ikai T, Okamoto Y. Structure control of polysaccharide derivatives for efficient separation of enantiomers by chromatography. *Chem Rev* 2009;109(11):6077-6101.
153. Armstrong DW, Tang Y, Chen S, Zhou Y, Bagwlll C, Chen JR. Macrocyclic Antibiotics as a New Class of Chiral Selectors for Liquid Chromatography. *Anal Chem* 1994;66(9):1473-1484.
154. Péter A, Árki A, Tourwé D, Forró E, Fülöp F, Armstrong DW. Comparison of the separation efficiencies of Chirobiotic T and TAG columns in the separation of unusual amino acids. *J Chromatogr A* 2004;1031(1-2):159-170.
155. Li J, Liu R, Wang L, Liu X, Gao H. Enantioseparation of chiral pharmaceuticals by vancomycin-bonded stationary phase and analysis of chiral recognition mechanism. *Chirality* 2019;31(3):236-247.
156. Svensson LA, Dönnecke J, Karlsson KE, Karlsson A, Vessman J. Polar organic phase liquid chromatography with packed capillary columns using a vancomycin chiral stationary phase. *Chirality* 2000;12(8):606-613.
157. Bosáková Z, Cuřínová E, Tesařová E. Comparison of vancomycin-based stationary phases with different chiral selector coverage for enantioselective separation of selected drugs in high-performance liquid chromatography. *J Chromatogr A* 2005;1088(1-2):94-103.

158. Aboul-Enein HY, Ali I. Macrocyclic antibiotics as effective chiral selectors for enantiomeric resolution by liquid chromatography and capillary electrophoresis. *Chromatographia* 2000;52(11-12):679-691.
159. Armstrong DW, Liu Y, Ekborgott KH. A covalently bonded teicoplanin chiral stationary phase for HPLC enantioseparations. *Chirality* 1995;7(6):474-497.
160. Zhang D, Xu X, Ma S. The study of enantioseparation of zolmitriptan on vancomycin-bonded chiral stationary phase. *J Sep Sci* 2005;28(18):2501-2504.
161. Rojkovičová T, Lehotay J, Čižmárik J. HPLC separation of racemic basic esters of alkoxyphenylcarbamic acid using two teicoplanin chiral stationary phases. *Ceska Slov Farma* 2005;54(4):173-177.
162. Péter A, Török G, Armstrong DW. High-performance liquid chromatographic separation of enantiomers of unusual amino acids on a teicoplanin chiral stationary phase. *J Chromatogr A* 1998;793(2):283-296.
163. Schlauch M, Frahm AW. Enantiomeric and diastereomeric high-performance liquid chromatographic separation of cyclic β-substituted α-amino acids on a teicoplanin chiral stationary phase. *J Chromatogr A* 2000;868(2):197-207.
164. Péter A, Török G, Armstrong DW, Tóth G, Tourwé D. High-performance liquid chromatographic separation of enantiomers of synthetic amino acids on a ristocetin A chiral stationary phase. *J Chromatogr A* 2000;904(1):1-15.
165. Hashem H, Tründelberg C, Attef O, Jira T. Effect of chromatographic conditions on liquid chromatographic chiral separation of terbutaline and salbutamol on Chirobiotic V column. *J Chromatogr A* 2011;1218(38):6727-6731.
166. Boesten JMM, Berkheij M, Schoemaker HE, Hiemstra H, Duchateau ALL. Enantioselective high-performance liquid chromatographic separation of N-methyloxycarbonyl unsaturated amino acids on macrocyclic glycopeptide stationary phases. *J Chromatogr A* 2006;1108(1):26-30.
167. Meng X, Shi L, Zhou H, Hou J. Preparation of vancomycin chiral stationary phase and study of racemate separation. *Chin J Chem* 2005;23(3):247-250.
168. Hrobonová K, Lehotay J, Cizmáriková R, Armstrong DW. Study of the mechanism of enantioseparation. I. Chiral analysis of alkylamino derivatives of aryloxypropanols by HPLC using macrocyclic antibiotics as chiral selectors. *J Liq Chromatogr Relat Technol* 2001;24(15):2225-2237.

169. Staroverov SM, Kuznetsov MA, Nesterenko PN, Vasiarov GG, Katrukha GS, Fedorova GB. New chiral stationary phase with macrocyclic glycopeptide antibiotic eremomycin chemically bonded to silica. *J Chromatogr A* 2006;1108(2):263-267.
170. Berthod A, Xiao TL, Liu Y, Jenks WS, Armstrong DW. Separation of chiral sulfoxides by liquid chromatography using macrocyclic glycopeptide chiral stationary phases. *J Chromatogr A* 2002;955(1):53-69.
171. Beesley TE, Lee JT. Method development strategy and applications update for CHIROBIOTIC chiral stationary phases. *J Liq Chromatogr Relat Technol* 2009;32(11-12):1733-1767.
172. Berthod A, Yu T, Kullman JP, Armstrong DW, Gasparrini F, D'Acquarica I, Misiti D, Carotti A. Evaluation of the macrocyclic glycopeptide A-40,926 as a high-performance liquid chromatographic chiral selector and comparison with teicoplanin chiral stationary phase. *J Chromatogr A* 2000;897(1-2):113-129.
173. Ding GS, Liu Y, Cong RZ, Wang JD. Chiral separation of enantiomers of amino acid derivatives by high-performance liquid chromatography on a norvancomycin-bonded chiral stationary phase. *Talanta* 2004;62(5):997-1003.
174. Aboul-Enein HY, Serignese V. Enantiomeric separation of several cyclic imides on a macrocyclic antibiotic (vancomycin) chiral stationary phase under normal and reversed phase conditions. *Chirality* 1998;10(4):358-361.
175. Péter A, Árki A, Vékes E, Tourwé D, Lázár L, Fülöp F, Armstrong DW. Direct and indirect high-performance liquid chromatographic enantioseparation of β-amino acids. *J Chromatogr A* 2004;1031(1-2):171-178.
176. Xiao TL, Armstrong DW. Enantiomeric separations by HPLC using macrocyclic glycopeptide-based chiral stationary phases: an overview. *Chiral Separation* 2004;243:113-171.
177. Cardoso PA, César IC. Chiral Method Development Strategies for HPLC using Macrocyclic Glycopeptide-Based Stationary Phases. *Chromatographia* 2018;81(6):841-850.
178. Ilisz I, Aranyi A, Pataj Z, Péter A. Enantioseparations by high-performance liquid chromatography using macrocyclic glycopeptide-based chiral stationary phases: An overview. *Chiral Separation* 2012:137-163.
179. Ďungelová J, Lehotay J, Rojkovičová T. HPLC chiral separations utilising macrocyclic antibiotics - A review. *Chem Anal Warsaw* 2004;49(1):1-17.

180. Ward TJ, Farris Iii AB. Chiral separations using the macrocyclic antibiotics: A review. *J Chromatogr A* 2001;906(1-2):73-89.
181. Tang M, Zhang J, Zhuang S, Liu W. Development of chiral stationary phases for high-performance liquid chromatographic separation. *TrAC-Trends Anal Chem* 2012;39:180-194.
182. Ekborg-Ott KH, Liu Y, Armstrong DW. Highly enantioselective HPLC separations using the covalently bonded macrocyclic antibiotic, ristocetin A, chiral stationary phase. *Chirality* 1998;10(5):434-483.
183. Berthod A, Chen X, Kullman JP, Armstrong DW, Gasparrini F, D'Acquarica I, Villani C, Carotti A. Role of the carbohydrate moieties in chiral recognition on teicoplanin- based LC stationary phases. *Anal Chem* 2000;72(8):1767-1780.
184. Ekborg-Ott KH, Kullman JP, Wang X, Gahm K, He L, Armstrong DW. Evaluation of the macrocyclic antibiotic avoparcin as a new chiral selector for HPLC. *Chirality* 1998;10(7):627-660.
185. Ding GS, Huang XJ, Liu Y, Wang JD. Chiral separation of racemates of drugs and amino acid derivatives by high-performance liquid chromatography on a norvancomycin-bonded chiral stationary phase. *Chromatographia* 2004;59(7-8):443-449.
186. Akapo S, McCrea C, Gupta J, Roach M, Skinner W. Chiral HPLC analysis of formoterol stereoisomers and thermodynamic study of their interconversion in aqueous pharmaceutical formulations. *J Pharm Biomed Anal* 2009;49(3):632-637.
187. Bhushan R, Kumar R. Analytical and preparative enantioseparation of dl-penicillamine and dl-cysteine by high-performance liquid chromatography on α-acid glycoprotein and β-cyclodextrin columns using ninhydrin as a reversible tagging reagent. *J Chromatogr A* 2009;1216(15):3413-3417.
188. Michishita T, Franco P, Zhang T. New approaches of LC-MS compatible method development on α1-acid glycoprotein-based stationary phase for resolution of enantiomers by HPLC. *J Sep Sci* 2010;33(23-24):3627-3637.
189. Millot MC, Taleb NL, Sebille B. Binding of human serum albumin to silica particles by means of polymers: a liquid chromatographic study of the selectivity of resulting chiral stationary phases. *J Chromatogr B Biomed Appl* 2002;768(1):157-166.

190. Moldoveanu SC, David V. Stationary phases and columns for chiral chromatography. Selection of the HPLC method in chemical analysis. *Elsevier* 2017:363-376.
191. Yang F, Zhang Y, Liang H. Interactive association of drugs binding to human serum albumin. *Int J Mol Sci* 2014;15(3):3580-3595.
192. Noctor TA, Diaz-Perez MJ, Wainer IW. Use of a human serum albumin-based stationary phase for high-performance liquid chromatography as a tool for the rapid determination of drug-plasma protein binding. *J Pharm Sci* 1993;82(6):675-676.
193. Wang H, Zou H, Zhang Y. Quantitative Study of Competitive Binding of Drugs to Protein by Microdialysis/High-Performance Liquid Chromatography. *Anal Chem* 1998;70(2):373-377.
194. Oravcova´ J, Bo¨hs B, Lindner W. Drug-protein binding studies new trends in analytical and experimental methodology. *J Chromatogr B Biomed Sci Appl* 1996;677(1):1-28.
195. Zsila F, Bikadi Z, Malik D, Hari P, Pechan I, Berces A, Hazai E. Evaluation of drug–human serum albumin binding interactions with support vector machine aided online automated docking. *Bioinformatics* 2011;27(13):1806-1813.
196. Domenici E, Bertucci C, Salvadori P, Félix G, Cahagne I, Motellier S, Wainer IW. Synthesis and chromatographic properties of an HPLC chiral stationary phase based upon human serum albumin. *Chromatographia* 1990;29(3-4):170-176.
197. Carlo B, Daniele T. Human Serum Albumin as Chiral Selector in Enantioselective High-Performance Liquid Chromatography. *Curr Med Chem* 2017;24(8):743-757.
198. Hermansson J. Direct liquid chromatographic resolution of racemic drugs using α1-acid glycoprotein as the chiral stationary phase. *J Chromatogr A* 1983;269:71-80.
199. Kirkland KM, Neilson KL, McCombs DA. Comparison of a new ovomucoid and a second-generation α1-acid glycoprotein-based chiral column for the direct high-performance liquid chromatography resolution of drug enantiomers. *J Chromatogr A* 1991;545(1):43-58.

200. Aboul-Enein HY, Serignese V. Direct enantiomeric separation of cathinone and one major metabolite on cellobiohydrolase (CBH-I) chiral stationary phase. *Biomed Chromatogr* 1997;11(1):47-49.
201. Wang QY, Xiong YJ, Lu BZ, Fan J, Zheng SR, Zhang WG. Effect of chromatographic conditions on enantioseparation of bovine serum albumin chiral stationary phase in HPLC and thermodynamic studies. *Chirality* 2013;25(9):487-492.
202. Bertucci C, Tedesco D. Human serum albumin as chiral selector in enantioselective high-performance liquid chromatography. *Curr Med Chem* 2017;24(8):743-757.
203. Barbato F, di Martino G, Grumetto L, La Rotonda MI. Retention of quinolones on human serum albumin and α1-acid glycoprotein HPLC columns: Relationships with different scales of lipophilicity. *Eur J Pharm Sci* 2007;30(3-4):211-219.
204. Bonato PS, De Abreu LRP, De Gaitani CM, Lanchote VL, Bertucci C. Enantioselective HPLC analysis of propafenone and of its main metabolites using polysaccharide and protein-based chiral stationary phases. *Biomed Chromatogr* 2000;14(4):227-233.
205. Mallik R, Xuan H, Hage DS. Development of an affinity silica monolith containing α1-acid glycoprotein for chiral separations. *J Chromatogr A* 2007;1149(2):294-304.
206. Davankov VA. The nature of chiral recognition: Is it a three-point interaction? *Chirality* 1997;9(2):99-102.
207. Peluso P, Dessì A, Dallocchio R, Mamane V, Cossu S. Recent studies of docking and molecular dynamics simulation for liquid-phase enantioseparations. *Electrophoresis* 2019:1-16.
208. Scriba GKE. Chiral recognition mechanisms in analytical separation sciences. *Chromatographia* 2012;75(15-16):815-838.
209. Scriba GKE. Recognition mechanisms of chiral selectors: An overview. *Chiral Separation Humana Press Inc* 2019;19851985:1-33.
210. Phyo YZ, Cravo S, Palmeira A, Tiritan ME, Kijjoa A, Pinto MMM, Fernandes C. Enantiomeric resolution and docking studies of chiral xanthonic derivatives on chirobiotic columns. *Molecules* 2018;23(1):142.

211. Fernandes C, Tiritan ME, Cass Q, Kairys V, Fernandes MX, Pinto M. Enantioseparation and chiral recognition mechanism of new chiral derivatives of xanthones on macrocyclic antibiotic stationary phases. *J Chromatogr A* 2012;1241:60-68.
212. Gübitz G, Schmid MG. Chiral separation by chromatographic and electromigration techniques. A Review. *Biopharm Drug Dispos* 2001;22(7-8):291-336.
213. Amini A. Recent developments in chiral capillary electrophoresis and applications of this technique to pharmaceutical and biomedical analysis. *Electrophoresis* 2001;22(15):3107-3130.
214. Berthod A. Chiral recognition mechanisms. *Anal Chem* 2006;78(7):2093-2099.
215. Pirkle WH, Pochapsky TC. Considerations of Chiral Recognition Relevant to the Liquid Chromatographic Separation of Enantiomers. *Chem Rev* 1989;89(2):347-362.
216. Easson LH, Stedman E. Studies on the relationship between chemical constitution and physiological action: Molecular dissymmetry and physiological activity. *Biochem J* 1933;27(4):1257-1266.
217. Booth TD, Wahnon D, Wainer IW. Is chiral recognition a three-point process? *Chirality* 1997;9(2):96-98.
218. Scriba GKE. Chiral recognition in separation science – an update. *J Chromatogr A* 2016;1467:56-78.
219. Carraro ML, Palmeira A, Tiritan ME, Fernandes C, Pinto MMM. Resolution, determination of enantiomeric purity and chiral recognition mechanism of new xanthone derivatives on (S,S)-Whelk-O1 stationary phase. *Chirality* 2017:1–10.
220. Blodgett J, Wang Y, Li T, Polavarapu PL, Drabowicz J, Pietrusiewicz KM, Zygo K. Resolution of tert-butyl-1-(2-methylnaphthyl)phosphine oxide using selectors identified from a chemical combinatorial library. *Anal Chem* 2002;74(20):5212-5216.
221. Brahmachary E, Ling FH, Svec F, Fréchet JMJ. Chiral recognition: Design and preparation of chiral stationary phases using selectors derived from Ugi multicomponent condensation reactions and a combinatorial approach. *J Comb Chem* 2003;5(4):441-450.

222. Muthukrishnan M, Basavanag UMV, Puranik VG. The first ionic liquid-promoted Kabbe condensation reaction for an expeditious synthesis of privileged bis-spirochromanone scaffolds. *Tetrahedron Lett* 2009;50(22):2643-2648.
223. Horton DA, Bourne GT, Smythe ML. The combinatorial synthesis of bicyclic privileged structures or privileged substructures. *Chem Rev* 2003;103(3):893-930.
224. Pinto MMM, Sousa ME, Nascimento MSJ. Xanthone derivatives: New insights in biological activities. *Curr Med Chem* 2005;12(21):2517-2538.
225. Ahmad I. Recent insight into the biological activities of synthetic xanthone derivatives. *Eur J Med Chem* 2016;116:267-280.
226. Masters KS, Brase S. Xanthones from fungi, lichens, and bacteria: the natural products and their synthesis. *Chem Rev* 2012;112(7):3717-3776.
227. Vieira LM, Kijjoa A. Naturally-occurring xanthones: recent developments. *Curr Med Chem* 2005;12(21):2413-46.
228. Pinto MMM, Castanheiro RAP, Kijjoa A. Xanthones from Marine-Derived Microorganisms: Isolation, Structure Elucidation, and Biological Activities. *Encyclopedia of Analytical Chemistry: Applications, Theory and Instrumentation* 2014;27:1-21.
229. Mayer AMS, Rodriguez AD, Taglialatela-Scafati O, Fusetani N. Marine Pharmacology in 2012-2013: Marine Compounds with Antibacterial, Antidiabetic, Antifungal, Anti-Inflammatory, Antiprotozoal, Antituberculosis, and Antiviral Activities; Affecting the Immune and Nervous Systems, and Other Miscellaneous Mechanisms of Action. *Mar Drugs* 2017;15(9):273.
230. Azevedo CMG, Afonso CMM, Pinto MMM. Routes to xanthones: An update on the synthetic approaches. *Curr Org Chem* 2012;16(23):2818-2867.
231. Sousa ME, Pinto MMM. Synthesis of xanthones: An overview. *Curr Med Chem* 2005;12(21):2447-2479.
232. Azevedo CMG, Afonso CMM, Sousa D, Lima RT, Helena Vasconcelos M, Pedro M, Barbosa J, Corrêa AG, Reis S, Pinto MMM. Multidimensional optimization of promising antitumor xanthone derivatives. *Bioorg Med Chem* 2013;21(11):2941-2959.
233. Castanheiro RAP, Pinto MMM, Cravo SMM, Pinto DCGA, Silva AMS, Kijjoa A. Improved methodologies for synthesis of prenylated xanthones by microwave

irradiation and combination of heterogeneous catalysis (K10 clay) with microwave irradiation. *Tetrahedron* 2009;65(19):3848-3857.

234. Castanheiro RAP, Pinto MMM, Silva AMS, Cravo SMM, Gales L, Damas AM, Nazareth N, Nascimento MSJ, Eaton G. Dihydroxyxanthones prenylated derivatives: Synthesis, structure elucidation, and growth inhibitory activity on human tumor cell lines with improvement of selectivity for MCF-7. *Bioorg Med Chem* 2007;15(18):6080-6088.
235. Correia-Da-Silva M, Sousa E, Duarte B, Marques F, Carvalho F, Cunha-Ribeiro LM, Pinto MMM. Polysulfated xanthones: Multipathway development of a new generation of dual anticoagulant/antiplatelet agents. *J Med Chem* 2011;54(15):5373-5384.
236. Cruz I, Puthongking P, Cravo S, Palmeira A, Cidade H, Pinto M, Sousa E. Xanthone and Flavone Derivatives as Dual Agents with Acetylcholinesterase Inhibition and Antioxidant Activity as Potential Anti-Alzheimer Agents. *J Chem* 2017;2017:1-16.
237. Sousa E, Paiva A, Nazareth N, Gales L, Damas AM, Nascimento MSJ, Pinto M. Bromoalkoxyxanthones as promising antitumor agents: Synthesis, crystal structure and effect on human tumor cell lines. *Eur J Med Chem* 2009;44(9):3830-3835.
238. Paiva AM, Sousa ME, Camões A, Nascimento MSJ, Pinto MMM. Prenylated xanthones: antiproliferative effects and enhancement of the growth inhibitory action of 4-hydroxytamoxifen in estrogen receptor-positive breast cancer cell line. *Med Chem Res* 2012;21(5):552-558.
239. Palmeira A. Design, synthesis and evaluation of xanthone derivatives for dual activity: antitumor and P-glycoprotein inhibition [thesis]. Porto: Universidade do Porto; 2011.
240. Palmeira A, Paiva A, Sousa E, Seca H, Almeida GM, Lima RT, Fernandes MX, Pinto M, Vasconcelos MH. Insights into the in vitro antitumor mechanism of action of a new pyranoxanthone. *Chem Biol Drug Des* 2010;76(1):43-58.
241. Pedro M, Cerqueira F, Sousa ME, Nascimento MSJ, Pinto M. Xanthones as inhibitors of growth of human cancer cell lines and their effects on the proliferation of human lymphocytes in vitro. *Bioorg Med Chem* 2002;10(12):3725-3730.

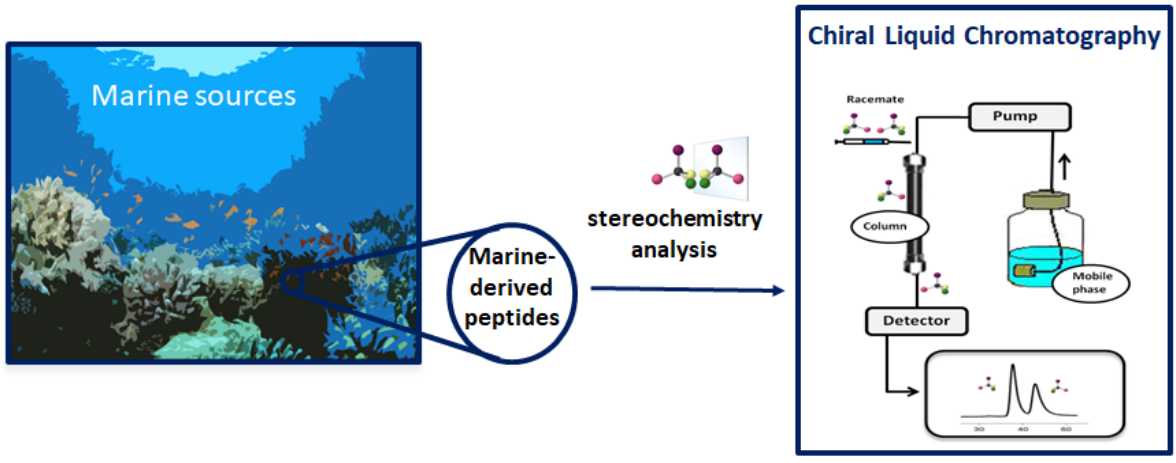
242. Alves A, Correia-da-Silva M, Nunes C, Campos J, Sousa E, Silva PMA, Bousbaa H, Rodrigues F, Ferreira D, Costa PC and others. Discovery of a new xanthone against glioma: Synthesis and Development of (Pro)liposome Formulations. *Molecules* 2019;24(3):409.
243. Cidade H, Rocha V, Palmeira A, Marques C, Tiritan ME, Ferreira H, Lobo JS, Almeida IF, Sousa ME, Pinto M. In silico and in vitro antioxidant and cytotoxicity evaluation of oxygenated xanthone derivatives. *Arab J Chem* 2017.
244. Pinto MM, Sousa ME, Nascimento MS. Xanthone derivatives: new insights in biological activities. *Curr Med Chem* 2005;12(21):2517-2538.
245. Gomes AS, Brandao P, Fernandes CSG, da Silva M, de Sousa M, Pinto MMM. Drug-like Properties and ADME of Xanthone Derivatives: The Antechamber of Clinical Trials. *Curr Med Chem* 2016;23(32):3654-3686.
246. Santos A, Soares JX, Cravo S, Tiritan ME, Reis S, Afonso C, Fernandes C, Pinto MMM. Lipophilicity assessement in drug discovery: Experimental and theoretical methods applied to xanthone derivatives. *J Chromatogr B Analyt Technol Biomed Life Sci* 2018;1072:182-192.
247. Sathyadevi P, Chen YJ, Wu SC, Chen YH, Wang YM. Reaction-based epoxide fluorescent probe for in vivo visualization of hydrogen sulfide. *Biosens Bioelectron* 2015;68:681-687.
248. Takashima I, Kawagoe R, Hamachi I, Ojida A. Development of an AND logic-gate-type fluorescent probe for ratiometric imaging of autolysosome in cell autophagy. *Chem Eur J* 2015;21(5):2038-2044.
249. Ribeiro J, Veloso C, Fernandes C, Tiritan ME, Pinto MMM. Carboxyxanthones: Bioactive agents and molecular scaffold for synthesis of analogues and derivatives. *Molecules* 2019;24(1):180.
250. Fernandes C, Masawang K, Tiritan ME, Sousa E, De Lima V, Afonso C, Bousbaa H, Sudprasert W, Pedro M, Pinto MM. New chiral derivatives of xanthones: Synthesis and investigation of enantioselectivity as inhibitors of growth of human tumor cell lines. *Bioorg Med Chem* 2014;22(3):1049-1062.
251. Fernandes C, Oliveira L, Tiritan ME, Leitao L, Pozzi A, Noronha-Matos JB, Correia-De-Sá P, Pinto MM. Synthesis of new chiral xanthone derivatives acting as nerve conduction blockers in the rat sciatic nerve. *Eur J Med Chem* 2012;55:1-11.

252. Fernandes C, Carraro ML, Ribeiro J, Araújo J, Tiritan ME, Pinto MMM. Synthetic chiral derivatives of xanthones: Biological activities and enantioselectivity studies. *Molecules* 2019;24(4):791.
253. Araújo J, Fernandes C, Pinto M, Elizabeth Tiritan M. Chiral derivatives of xanthones with antimicrobial activity. *Molecules* 2019;24(2).
254. Pinto M, Tiritan ME, Fernandes C, Cass Q. Fases Estacionárias Quirais baseadas em Derivados Xantónicos. In: Industrial BdP, editor. Porto; 2011.
255. Gales L, Damas AM. Xanthones - A structural perspective. *Curr Med Chem* 2005;12(21):2499-2515.

CHAPTER II

Marine Natural Peptides: Determination of Absolute Configuration using Liquid Chromatography Methods and Bioactivities

Reprinted from Molecules



molecules

MDPI

Review

Marine Natural Peptides: Determination of Absolute Configuration Using Liquid Chromatography Methods and Evaluation of Bioactivities

Ye' Zaw Phyo [1,2,†], João Ribeiro [3,†], Carla Fernandes [2,3,*], Anake Kijjoa [1,2,*] and Madalena M. M. Pinto [2,3]

1 ICBAS-Instituto de Ciências Biomédicas Abel Salazar, Universidade do Porto, Rua de Jorge Viterbo Ferreira, 228, 4050-313 Porto, Portugal; chemistkophyo.ckp@gmail.com
2 Interdisciplinary Centre of Marine and Environmental Research (CIIMAR), Edifício do Terminal de Cruzeiros do Porto de Leixões, Av. General Norton de Matos s/n, 4050-208 Matosinhos, Portugal; madalena@ff.up.pt
3 Laboratório de Química Orgânica e Farmacêutica, Departamento de Ciências Químicas, Faculdade de Farmácia da Universidade do Porto, Rua de Jorge Viterbo Ferreira, 228, 4050-313 Porto, Portugal; joaobigi@gmail.com
* Correspondence: cfernandes@ff.up.pt (C.F.); ankijjoa@icbas.up.pt (A.K.); Tel.: +351-22-042-8688 (C.F.); +351-220-428-331 (A.K.)
† These authors equally contributed to this work.

Received: 30 December 2017; Accepted: 27 January 2018; Published: 31 January 2018

Abstract: Over the last decades, many naturally occurring peptides have attracted the attention of medicinal chemists due to their promising applicability as pharmaceuticals or as models for drugs used in therapeutics. Marine peptides are chiral molecules comprising different amino acid residues. Therefore, it is essential to establish the configuration of the stereogenic carbon of their amino acid constituents for a total characterization and further synthesis to obtain higher amount of the bioactive marine peptides or as a basis for structural modifications for more potent derivatives. Moreover, it is also a crucial issue taking into account the mechanisms of molecular recognition and the influence of molecular three-dimensionality in this process. In this review, a literature survey covering the report on the determination of absolute configuration of the amino acid residues of diverse marine peptides by chromatographic methodologies is presented. A brief summary of their biological activities was also included emphasizing to the most promising marine peptides. A case study describing an experience of our group was also included.

Keywords: absolute configuration; bioactivity; chiral HPLC; Marfey's method; marine peptides; stereochemistry

1. Introduction

In recent years, it has become well known that the oceans represent a rich source of structurally unique bioactive compounds from the perspective of potential therapeutic agents [1,2]. Bioactive compounds can be isolated from a myriad of marine invertebrates such as mollusks, sponges, tunicates and bryozoans, in addition to algae and marine microorganisms, especially cyanobacteria, bacteria and fungi [3–5].

Over the last decades, novel bioactive compounds from marine organisms with important bioactivities, such as antifungal, antibacterial, cytotoxic and anti-inflammatory properties, have been widely explored, and many of them are considered as lead compounds for drug discovery as well as biologically useful agents in pharmaceutical research [6–10]. In fact, owing to their pharmacological

potential, either directly as drugs or as models for molecular modifications and/or total synthesis, marine natural products are certainly an interesting source, exploited by many researchers [11].

Ziconotide (Prialt®), a peptide first isolated from the venom of the cone snail (*Conus magus*), and trabectedin (Yondelis®), an alkaloid originally isolated from a marine tunicate *Ectenascidia turbinata* and now obtained by semisynthesis, are examples of marine natural products that have already been approved as human therapeutics [3,12–14]. Ziconotide is an analgesic used for treatment of patients suffering from chronic pain, and trabectedin for the treatment of soft tissue sarcomas and ovarian cancer.

In terms of the overall number of marine natural products, peptides are one of the most described due to their novel chemistry and diverse biological properties [15]. Actually, marine peptides are known to exhibit various biological activities such as antiviral, antiproliferative, antioxidant, anticancer, antidiabetic, anti-obesity, anticoagulant, antihypertensive, and calcium-binding activities [6,15–17].

Marine peptides are chiral molecules comprising different amino acid residue subunits. For their total characterization, and taking into account the mechanisms of molecular recognition and the influence of molecular three-dimensionality in this process, it is essential to define the configuration of the amino acids components of the peptide fractions, isolated from marine sources. Besides, it is also crucial to obtain the bioactive marine peptides by synthesis in order to achieve higher amount of compound for future assays or as a basis for structural modifications to obtain more potent derivatives.

Nowadays, there are different methodologies for the determination of the absolute configuration of amino acids, such as X-ray crystallography, NMR techniques, vibrational circular dichroism (VCD), enantioselective chromatography, optical rotatory dispersion (ORD), among others [18–26].

For the determination of the absolute configuration of amino acid residues of marine peptides, separation methodologies by using Marfey's method, chiral high performance liquid chromatography (HPLC) analysis or both have proved to be suitable and the most described, as will be shown in this review. Regardless of the method used, the evaluation of peptides stereochemistry is based on the determination of the amino acid composition in peptide hydrolysates. Two main steps are involved, specifically the total or partial hydrolysis of peptides to obtain amino acid residues followed by their analysis by comparison with appropriated standards [27] (Figure 1).

Marfey's method was first reported by Marfey in 1984 [28]. After the acid hydrolysis of peptides, the amino acid residues are derivatized with chiral Marfey's reagents such as 1-fluoro-2-4-dinitrophenyl-5-D,L-alanine amide (FDAA) or 1-fluoro-2-4-dinitrophenyl-5-D,L-leucine amide (FDLA). Subsequent analysis via reverse phase liquid chromatography (LC), using generally C_{18} columns, and by comparison the retention times of the derivatized amino acids with suitable standards, afforded the stereochemistry of the peptides [29–31]. This method is often used for determination of the absolute configuration of amino acids, mainly because it is a simple method, offering a better resolution when compared to chiral HPLC methodologies; furthermore, several derivatization agents, such as FDAA and FDLA, are commercially available. However, this methodology has some disadvantages, including low availability of some standards, and the possibility of occurring racemization of the analyte during the derivatization reaction, prior to the chromatographic analysis [30,31].

The chiral analysis by HPLC is based on a formation of transient diastereomeric complexes between the amino acids present in the hydrolysates and the chiral stationary phase (CSP) employed, being the less stable complex the first to elute [32]. There are several types of CSPs, such as polysaccharide-based, Pirkle-type, protein-based, macrocyclic antibiotic-based, crown ether-based, ligand exchange type, among others [33–35]; however, the last three types are the most used for the separation of primary amine-containing compounds and amino acids [36,37]. Chiral HPLC offers several advantages, when comparing to Marfey's method, including the direct analysis of the amino acid hydrolysates without further derivatization; moreover, the analysis often provides quicker results. However, poor chemical sensitivity, low sample capacity, and low availability and expensiveness of commercial chiral columns are some of the disadvantages of chiral HPLC method [38].

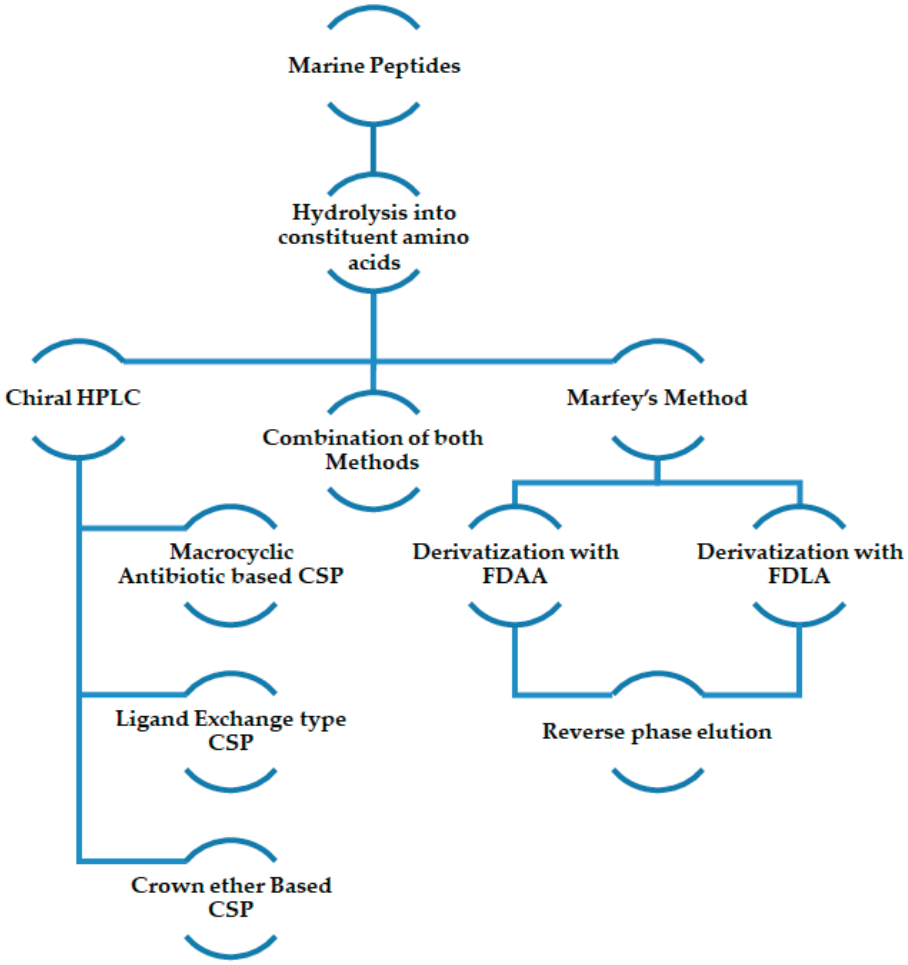


Figure 1. Schematic presentation of the methodologies generally used for determination of the configuration of amino acid residues of marine peptides. HPLC—High Performance Liquid Chromatography; CSP—Chiral Stationary Phase; FDAA—1-Fluoro-2-4-dinitrophenyl-5-D,L-alanine amide; FDLA—1-Fluoro-2-4-dinitrophenyl-5-D,L-leucine amide.

A number of reviews on marine peptides have appeared in recent years, focusing mainly on their biological activities, applications and biosynthesis as well as isolation procedures [16,39–57]. In this review, several works related to the methods used for determination of the absolute configuration of marine peptides by chromatographic methods are presented in different sections according to the source of the marine peptides. Diverse types of peptides such as cyclic peptides, cyclic depsipeptides and lipopeptides are reported. A literature survey covering all the reports on liquid chromatographic methods (Marfey's method and chiral HPLC) is presented (from 1996 to 2017). Furthermore, a case study describing an experience of our group is included.

2. Peptides from Marine Cyanobacteria and Other Bacteria

Cyanobacteria (blue-green algae), the most ancient known microorganisms on Earth, are a rich source of novel secondary metabolites possessing a broad spectrum of biological activities including antitumor, antibacterial, anticoagulant, antifungal, antiviral, antimalarial, antiprotozoal, and anti-inflammatory activities [58]. Currently, cyanobacteria are one of the most interesting sources of novel marine compounds [59]. Actually, the number of biologically active cyclic peptides, depsipeptides, lipopeptides, and other acyclic or small peptides, many of which containing unusual amino acid residues or modified amino acid units, is impressive. In addition to cyanobacteria, this type of compounds has also been isolated from other marine-derived bacteria.

2.1. Cyclic Peptides

Scattered publications concerning the stereochemistry determination of the amino acid residues of several cyclic peptides, isolated from marine cyanobacteria and other bacteria, were reported (Table 1). Marfey's method, using FDAA as derivatization reagent, allowed the successful determination of the absolute configuration of the amino acid residues of cyclic peptides **1**–**4** (Figure 2).

For the new cyclic tetrapeptide **1** isolated from the bacterium *Nocardiopsis* sp. [60], the absolute configuration of all the amino acid residues was found to be L. Similarly, the absolute configuration of the amino acid residues of three novel anabaenopeptins labeled NZ825 (**2**), NZ841 (**3**), and NZ857 (**4**) [61], were successfully determined by Marfey's method combined with HPLC.

However, as Marfey's method was not accurate enough to determine the absolute configuration of all the amino acid residues of some cyclic peptides **5**–**16** (Figure 2), it was necessary to associate this method with chiral HPLC.

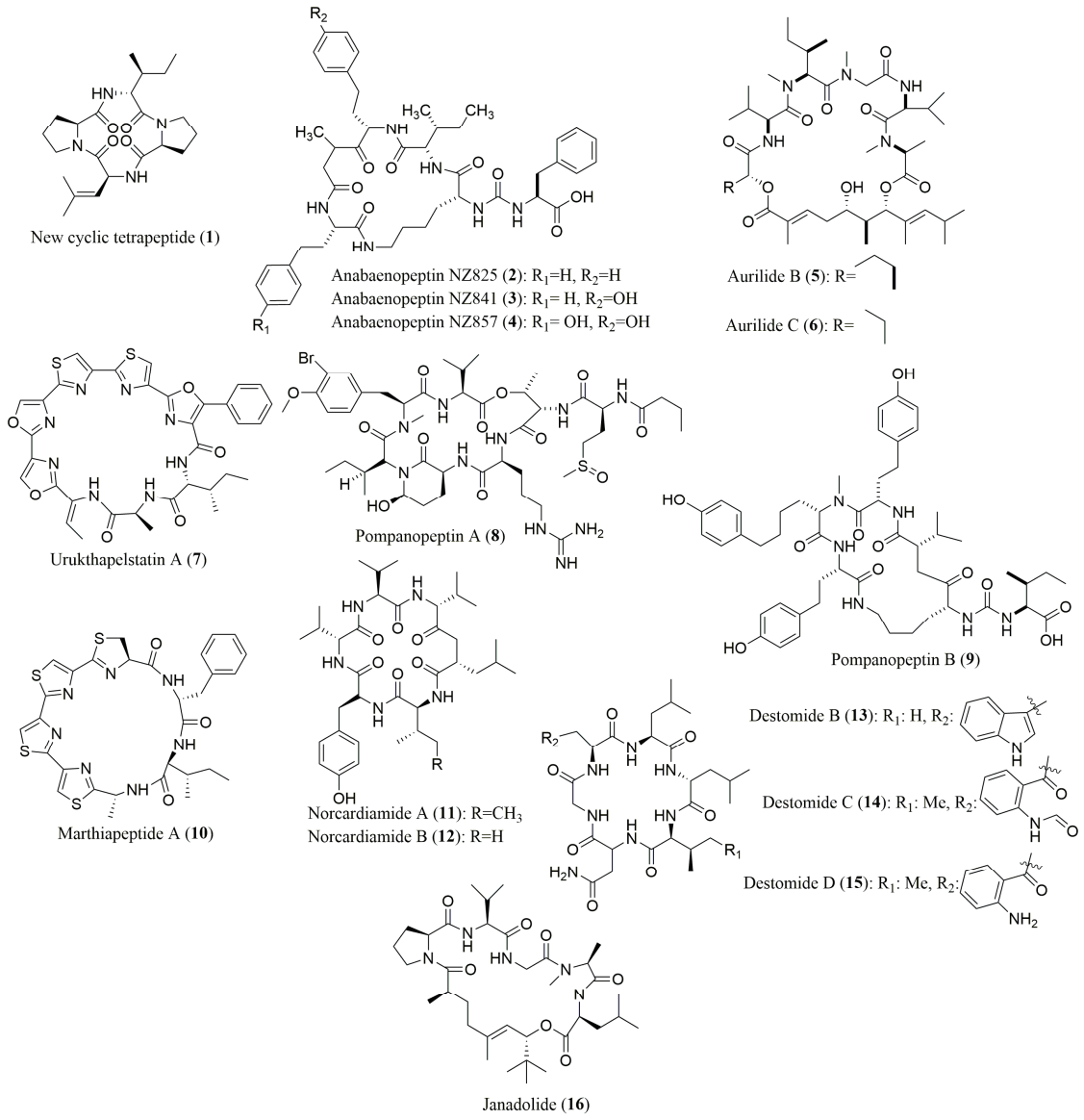


Figure 2. Structure of cyclic peptides **1**–**16**, isolated from marine cyanobacteria and other bacteria, whose stereochemistry determination of their amino acids was performed by Marfey's method (compounds **1**–**4**) and by a combination of both Marfey's method and chiral HPLC (compounds **5**–**16**).

This strategy, i.e., using a ligand exchange-type CSP in chiral HPLC associated with Marfey's method, was used for the determination of amino acids stereochemistry of several cyclic peptides, including aurilide B (**5**) and C (**6**), isolated from the cyanobacterium *Lyngbya majuscula* [62], urukthapelstatin A (**7**), isolated from a culture broth of thermoactinomycetaceae bacterium *Mechercharimyces asporophorigenens* YM11-542 [63], pompanoeptpins A (**8**) and B (**9**), isolated from the cyanobacterium *Lyngbya confervoides* [64], marthiapeptide A (**10**) isolated from the deep South China Sea-derived *Marinactinospora thermotolerance* SCSIO 00652 [65], norcardiamides A (**11**) and B (**12**), isolated from the marine-derived actinomycete *Nocardiopsis* sp. CNX037 [66], destomides B–D (**13**–**15**), isolated from the deep South China Sea-derived *Streptomyces scopuliridis* SCSIO ZJ46 [67], and jandolide (**16**) isolated from the marine cyanobacterium *Okeania* sp. [68].

The cyclic peptides aurilides B (**5**) and C (**6**) were reported to have the in vitro cytotoxicity toward NCl-H460, human lung tumor, and neuro-2a mouse neuroblastoma cell lines, with lethal concentration 50 (LC50) values between 0.01 and 0.13 μM [62]. Aurilide B (**5**) was evaluated in the NCl 60 cell line panel and was found to exhibit a high level of cytotoxicity, particularly against leukemia, renal, and prostate cancer cell lines [62]. The cyclic peptide pompanopeptpin A (**8**) was shown to exhibit trypsin inhibitory activity with an IC_{50} value of 2.4 ± 0.4 μg/mL [64]. A polythiazole cyclopeptide, marthiapeptide A (**10**) showed antibacterial activity against a panel of Gram-positive bacteria with minimum inhibitory concentration (MIC) values ranging from 2.0 to 8.0 μg/mL, and strong cytotoxicity against a panel of human cancer cell lines with IC_{50} values ranging from 0.38 to 0.52 μM [65]. The cyclohexapeptide destomide B (**13**) also showed antimicrobial activity against *Staphylococcus aureus* ATCC 29213, *Streptococcus pneumoniae* NCTC 7466 and MRSE shhs-E1 with MIC values of 16.0, 12.5, 32.0 μg/mL, respectively [67]. A cyclic polyketide-peptide hybrid, janadolide (**16**) exhibited potent antitrypanosomal activity with an IC_{50} value of 47 nM [68].

Recently, the configuration of the amino acids of a cytotoxic cyanobactin, wewakazole B (**17**), isolated from the cyanobacterium *Moorea producens* (Figure 3), was determined using only chiral HPLC [69]. Two different types of CSPs, under reverse phase mode, were used to perform the analysis. A macrocyclic antibiotic-based CSP afforded the assignment of the L-configuration for its Ala, Phe, and Pro residues, while a ligand exchange type CSP clearly identified the presence of L-Ile, which could not be distinguished by the first CSP [69].

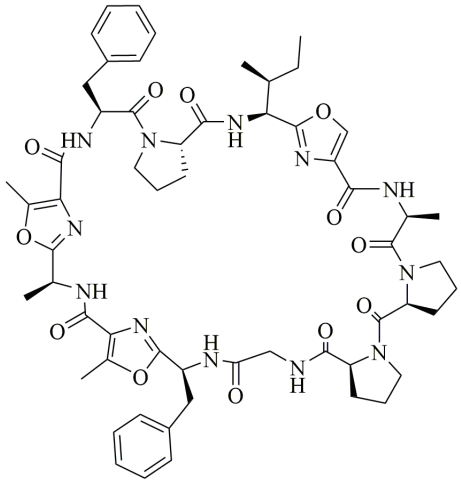


Figure 3. Structure of wewakazole B (**17**) isolated from a marine cyanobacteria.

Table 1. Cyclic peptides from marine cyanobacteria and other bacteria.

Peptide	Source	aa Composition	Chromatographic Conditions	Biological Activities	Refs.
Tetrapeptide (**1**)	Bacterium *Nocardiopsis* sp.	L-Ile, L-Leu, L-Pro	Marfey's method (FDAA) combined with HPLC C_{18} (YMC-ODS-A) (4.5 × 250 mm) Flow rate: 0.8 mL/min; UV detection at 340 nm MP: ACN(aq) (0–50% (*v*/*v*)) with 0.1% TFA	Cytotoxicity toward the leukemia cell-line K-562	[60]
Anabaenopeptins NZ825, NZ841, NZ857 (**2**–**4**)	Cyanobacterium *Anabaena* sp.	L-Ile, D-Lys, L-Phe; **2**: L-Hph; **3**: L-Hph, L-Hty; **4**: L-Hty	Marfey's method (FDAA) combined with HPLC Merck Chromolith performance RP-18e, (4.6 × 100 mm) MP: 50 mM TEAP buffer (pH 3)/ACN (9:1 to 1:1 *v*/*v*)	No inhibition of serine proteases	[61]
Aurilides B (**5**) and C (**6**)	Cyanobacterium *Lyngbya majuscula*	L-Val, *N*-Me-L-Ile, L-Ile	Ligand Exchange Type CSP; Phenomenex Chirex 3126 (D) (4.6 × 250 mm); Flow rate: 1.0 mL/min; UV detection at 254 nm; MP: 2 mM $CuSO_4$ in ACN/H_2O (5/95 *v*/*v*) or 2 mM $CuSO_4$ in ACN/H_2O (15/85 *v*/*v*)	Cytotoxicity against NCl-H460 and neuro-2a mouse neuroblastoma cell lines **5**: also active against leukemia, renal, and prostate cancer cell lines	[62]
		N-Me-L-Ala **6**: *N*-Me-L-*allo*-Ile, D-Hiva	Marfey's method (FDAA) combined with HPLC Microsob-MV C_{18} (4.6 × 250 mm) Flow rate: 1.0 mL/min; UV detection at 254 nm MP: 50 mM TEAP buffer pH 3/ACN (9:1 to 1:1 *v*/*v*)		
Urukthapelstatin A (**7**)	Marine Derived *Mechercharimyces asporophorigenens* YM11-542	L-Ala	Marfey's method (FDAA) combined with HPLC ODS-80Ts column (4.6 × 150 mm) Flow rate:1.0 mL/min; UV detection at 340 nm MP: MeOH, 0.1% TFA containing ACN or H_2O	Growth inhibition of human lung cancer A549 cells, cytotoxicity against a human cancer cell line panel	[63,70]
		D-*allo*-Ile	Ligand Exchange Type CSP Sumichiral OA-5000 column (4.6 × 150 mm) Flow rate: 1.0 mL/min; UV detection at 254 nm MP: 5% IPA containing 2 mM $CuSO_4$		
Pompanopeptins A (**8**) and B (**9**)	Cyanobacterium *Lyngbya confervoides*	**8**: L-Val, L-Thr, L-Met (O), *S*-Ahp, L-Ile, L-Arg **9**: L-Ile	Ligand Exchange Type CSP; Phenomenex Chirex 3126 *N*,*S*-dioctyl-(D)-penicillamine, 5 µm (4.6 × 250 mm) Flow rate: 1.0 mL/min; UV detection at 254 nm MP: 2 mM $CuSO_4$ or 2 mM $CuSO_4$/ACN (95:5 *v*/*v*)	**8**: Trypsin inhibitory activity	[64]
		8: *N*,*O*-diMe-Br-L-Tyr	Marfey's method (FDLA) combined with HPLC-MS Phenomenex Synergi 4u Hydro RP 80A (2 × 340 nm) Flow rate: 0.15 mL/min; UV detection at 254 nm MP: ACN/HCOOH (10–90:0.1 *v*/*v*) in gradient		
		9: D-Lys, L-Val, D-Glu	Marfey's method (FDLA) combined with HPLC-MS Alltech Altima HP C_{18} HL 54 (250 × 4.6 mm) Flow rate: 1.0 mL/min; PDA detection from 200–500 nm MP: ACN/aq TFA (30–70:0.1 *v*/*v*) in gradient		

Table 1. *Cont.*

Peptide	Source	aa Composition	Chromatographic Conditions	Biological Activities	Refs.
Marthiapeptide A (**10**)	Deep sea-derived *Marinactinospora thermotolerans* SCSIO 00652	L-Ile	Ligand Exchange Type CSP; MCIGELCR10W (4.6 × 150 mm); Flow rate: 0.5 mL/min; UV detection at 254 nm; MP: 2 mM $CuSO_6$ solution	Antibacterial and cytotoxic activities	[65]
		D-Phe, L-Ile	Marfey's method (FDAA) combined with HPLC Zorbax SB-C_8 column, 5 µm (2.1 × 30 mm)		
Nocardiamides A (**11**) and B (**12**)	Marine-derived Actinomycete *Nocardiopsis* sp. CNX037	L-Tyr, D-Leu, D- and L-Val	Marfey's method (FDAA or FDLA) combined with HPLC; Conditions not described	Antimicrobial activity and no cytotoxicity against HCT-116 cell line	[66]
		11: L-Ile	Ligand Exchange Type CSP; MCIGELCRS10W, (4.6 × 250 mm); Flow rate: 0.5 mL/min; UV detection at 254 nm; MP: 2 mM $CuSO_4/H_2O$		
Destomides B–D (**13**–**15**)	Deep sea-derived *Streptomyces scopuliridis* SCSIO ZJ46	L-Asn, D-Leu **13**: L-Trp, L-Val, L-Leu; **14**: L-Gly, L-Ile, **15**: L-Gly, L-Ile, L-Leu	Marfey's method (FDAA) combined with HPLC Phenomenex ODS column, 5 µm (4.6 × 150 mm) Flow rate: 1.0 mL/min; UV detection at 340 nm MP: ACN:H_2O:TFA (15:85:0.1 to 90:10:0.1)	**13**: Antimicrobial activity against *staphylococcus aureus* ATCC 29213, *Streptococcus pneumoniae* NCTC 7466 and MRSE shhs-E1 **13**–**15**: no cytotoxicity	[67]
		15: L-Kyn	Ligand Exchange Type CSP; MCIGELCRS10W column, 3 µm (4.6 × 50 mm); Flow rate: 0.5 mL/min; UV detection at 254 nm; MP: 2 mM $CuSO_4$ aqueous solution		
Janadolide (**16**)	Cyanobacterium *Okeania* sp.	*N*-Me-L-Leu, L-Pro, L-Val	Ligand Exchange Type CSP; Diacel CHIRALPAK (MA+) (4.6 × 50 mm); Flow rate: 1.0 mL/min; UV detection at 254 nm; MP: 2.0 mM $CuSO_4$	Antitrypanosomal activity	[68]
		N-Me-L-Ala	Marfey's method (FDAA) combined with HPLC Cosmosil Cholester (4.6 × 50 mm); Flow rate: 1.0 mL/min; UV detection at 340 nm MP: 0.02 M NaOAc(aq)/MeOH (45/55 *v*/*v*)		
Wewakazole B (**17**)	Cyanobacterium *Moorea producens*	L-Ala, L-Phe, L-Pro	Macrocyclic Antibiotic type CSP Chirobiotic TAG (2.1 × 250 mm); Flow rate: 0.3 mL/min; UV detection at 340 nm; MP: 0.1% aq. HCOOH and 1% (*v*/*v*) NH_4OAc in MeOH	Cytotoxicity against MCF7 and human 460 lung cancer cell lines	[69]
		L-Ile	Ligand Exchange type CSP; Sumichiral OA-5000 (4.6 × 150 mm); Flow rate: 1.0 mL/min; UV Detection at 254 nm; MP: MeOH/2.0 mM $CuSO_4$ in H_2O (5/95 *v*/*v*)		

aa—Amino acid; FDAA—1-Fluoro-2-4-dinitrophenyl-5-L-alanine amide; ESI—Electrospray Ionization; LC—Liquid Chromatography; MS—Mass spectrometry; HPLC—High Performance Liquid Chromatography; MP—Mobile Phase; TEAP—Triethylammonium phosphate; ACN—Acetonitrile; CPA—Carboxypeptidase A; TFA—Trifluoracetic acid; MeOH—Methanol; TEA—Triethylamine; IPA—Isopropyl alcohol; FDLA—1-fluoro-2-4-dinitrophenyl-5-D,L-leucine amide; NaOAc—Sodium acetate; NH_4OAc—Ammonium acetate.

2.2. Cyclic Depsipeptides

As mentioned above, there are many publications describing the isolation and characterization, including the determination of the stereochemistry of their amino acids, of new cyclic depsipeptides from marine cyanobacteria and other bacteria (Table 2). However, contrary to cyclic peptides, several works reported the use of chiral HPLC as the only method for determination of the configuration of amino acids. Figure 4 shows the structure of cyclic depsipeptides **18**–**46**, isolated from marine cyanobacteria and other bacteria, whose stereochemistry of the amino acids was determined only by this method.

The ligand exchange-type CSPs were the most widely used by different research groups. Cai et al. employed a penicillamine ligand exchange-type CSP to determine the absolute configuration of the amino acids constituent of malevamide B (**18**) and C (**19**) isolated from the cyanobacterium *Symploca laete-viridis* [71]. Three different mobile phases in reverse phase elution mode were used. Nevertheless, the stereochemistry of Amha and Amoa residues present in both compounds were not determined [71]. The same CSP was employed to establish that all the amino acids of the cytotoxic depsipeptide lyngbyapeptin B (**20**) [72], tasipeptins A (**21**) and B (**22**) [73], wewakamide A (**23**) [74], cocosamide A (**24**) and B (**25**) [75], and the antiparasitic depsipeptides dudawelamides A–D (**26**–**29**) [76], isolated from cyanobacteria *Lyngbya majuscula*, *Symploca* sp., *Lyngbya semiplena*, *Lyngbya majuscula*, and *Moorea producens*, respectively, has L-configuration. The only exception was for *allo*-Hiva amino acid of dudawelamide C (**29**), which has D-configuration [76]. The configuration of the amino acids of the cyclic depsipeptides pitipeptolides A (**30**) and B (**31**), isolated from cyanobacterium *Lyngbya majuscula*, was assigned to be L by a ligand exchange-type CSP comprising *N*,*N*-dioctyl-L-alanine as chiral selector (Chiralpack MA (+) from Daicel) and different proportion of $CuSO_4$:ACN as mobile phase [77]. By using the same CSP, the absolute configuration of three new cyclic depsipeptides, kohamamides A–C (**32**–**34**) were also successfully established [78].

Zhou et al. [79] described the determination of the absolute configuration of new anti-infective cycloheptadepsipeptides marformycins A–F (**35**–**40**), produced by the deep sea-derived *Streptomyces drozdowiczii* SCSIO 1014, using a ligand exchange type CSP containing the same chiral selector as the previous ones (*N*,*N*-dioctyl-L(or D)-alanine) but purchased from Mitsubishi Chemical Corporation (MCI GEL CRS10W). Another type of CSP, specifically the macrocyclic antibiotic-based Chirobiotic TAG, confirmed the presence of L-Pro and L-Val in an unusual cyclic depsipeptide, pitiprolamide (**41**), isolated from *Lyngbya majuscula* [80]. Interestingly, in some works, more than one CSP were employed to elucidate the configuration of all the amino acids contained in the hydrolysates of cyclic depsipeptides. For example, two different types of ligand exchange type CSPs were used to elucidate the stereochemistry of the amino acid residues of palau'amide (**42**), depsipeptide with strong cytotoxicity against KB cell line (IC_{50} value of 13 nM) [81].

In the case of pitipeptolides C–F (**43**–**46**), which were isolated from the cyanobacterium *Lyngbya majuscula*, the configuration of most of the amino acid residues was determined using the macrocyclic antibiotic-based Chirobiotic TAG under reverse phase elution conditions [82]. Then, the *N*,*N*-dioctyl-L-alanine ligand exchange CSP Chiralpack MA (+), under the same elution mode, was used for the assignment of *S* configuration for Hiva residue [82].

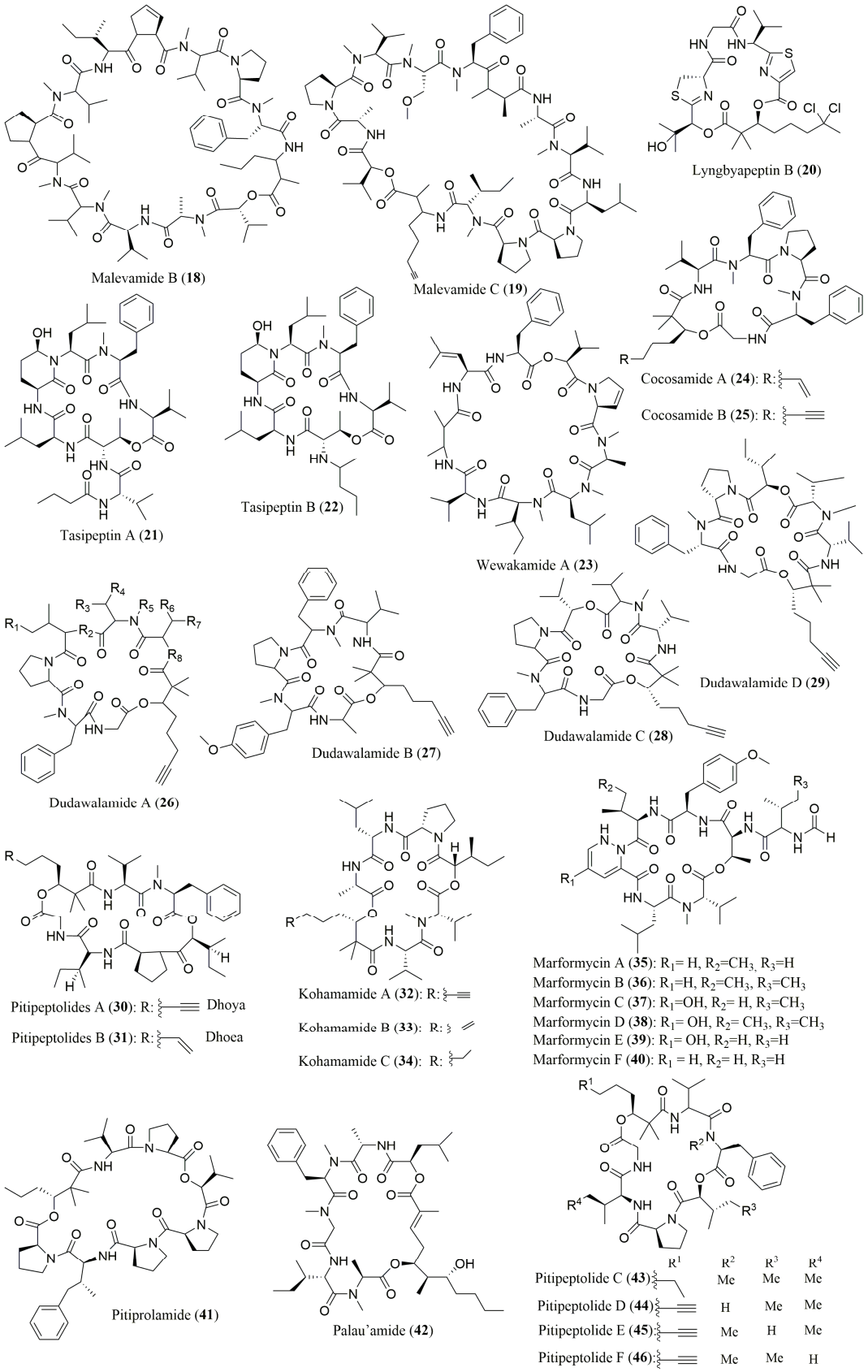


Figure 4. Structure of cyclic depsipeptides **18**–**46**, isolated from marine cyanobacteria and other bacteria, whose stereochemistry of their amino acids was determined only by chiral HPLC.

Table 2. Cyclic depsipeptides from marine cyanobacteria and other bacteria.

Peptide	Source	aa Composition	Chromatographic Conditions	Biological Activities	Refs.
Malevamides B (**18**) and C (**19**)	Cyanobacterium *Symploca laete-viridis*	L-Pro, *N*-Me-L-Val, *N*-Me-L-Phe **18**: L-Ile, *N*-Me-L-Ala, *N*-Me-D-Val, L-Val, (*R*)-Hiva; **19**: L-Ala, *N*-diMe-L-Ser, L-Leu, *N*-Me-D-Ala, *N*-Me-L-Ile, (*S*)-Hiva	Ligand Exchange Type CSP; Chirex (D) Penicillamine, Phenomenex 00G-3126E0 (4.6 × 250 mm) MP: 1.7 mM $CuSO_4$ in ACN/H_2O (14:86 *v*/*v*), 1.9 mM $CuSO_4$ in ACN/H_2O (5:95 *v*/*v*) or 2.0 mM $CuSO_4$ in H_2O Flow rate: 1.0 and 0.8 mL/min; UV detection at 245 nm	Inactive against P-388, A-549 and HT-29 cancer cells	[71]
Lyngbyapeptin B (**20**)	Cyanobacterium *Lyngbya majuscula*	*N*-Me-L-Ile, *N*-Me-L-Leu, *N*,*O*-diMe-L-Tyr	Ligand Exchange Type CSP; Chirex (D) Penicillamine, Phenomenex 00G-3126E0 (4.6 × 250 mm) MP: 2 mM $CuSO_4$ Flow: 0.8 mL/min; UV detection at 254 nm	Cytotoxicity against KB and LoVo cells	[72]
Tasipeptins A (**21**) and B (**22**)	Cyanobacterium *Symploca* sp.	L-Thr, L-Val, L-Leu, L-Glu, *N*-Me-L-Phe	Ligand Exchange Type CSP; Phenomenex Chirex Phase 3126 (D) (4.6 × 250 mm) MP: 2 mM $CuSO_4$; 2 mM $CuSO_4$/ACN (95:5 or 85:15 *v*/*v*) UV detection at 254 nm	Cytotoxicity toward KB cells	[73]
Wewakamide A (**23**)	Cyanobacteria *Lyngbya semiplena* and *Lyngbya majuscula*	L-M-Ala, L-Pro, L-Val, L-Me-Leu, L-Phe, L-Me-ILe, L-Hiv	Ligand Exchange Type CSP; Phenomenex Chirex 3126 (D) (4.6 × 250 mm); MP: 2 mM $CuSO_4$ in H_2O or 2 mM $CuSO_4$ in ACN/H_2O (15:85 or 5:95 *v*/*v*) Flow rate: 0.7, 0.8, 1.0 mL/min; UV detection at 254 nm	Brine shrimp toxicity	[74]
Cocosamide A (**24**) and B (**25**)	Cyanobacterium *Lyngbya majuscula*	L-Pro, L-Val, *N*-Me-L-Phe	Ligand Exchange Type CSP; Phenomenex Chirex (D), Penicillamine, 5 µm (4.6 × 250 mm) MP: 2.0 mM $CuSO_4$/ACN (85:15 or 90:10 *v*/*v*) Flow rate: 1.0 mL/min; UV detection at 254 nm	Cytotoxicity against MCF-7 (breast cancer) and HT-29 (colon cancer) cells	[75]
Dudawalamides A–D (**26**–**29**)	Cyanobacterium *Moorea producens*	L-Dhoya, L-Hiva, L-Val **29**: D-allo-Hiva	Ligand Exchange Type CSP; Chirex Phase 3126 (D) 5 µm (4.6 × 250 mm); MP: 2 mM $CuSO_4$-ACN (95:5 or 85:15 *v*/*v* or 87.5:12.5 *v*/*v*/*v*), ACN-H_2O-HCOOH (30:70:0.1 or 70:30:0.1 *v*/*v*/*v*) Flow rate: 0.8 mL/min; UV detection at 340 nm	Antiparasitic activity	[76]
Pitipeptolides A (**30**) and B (**31**)	Cyanobacterium *Lyngbya majuscula*	L-Gly, L-Pro, L-Val, L-Ile, *N*-Me-L-Phe, (2*S*,3*S*)-Hmp	Ligand Exchange Type CSP; Chiralpak MA (+) (4.6 × 50 mm); MP: 2 mM $CuSO_4$: ACN (90:10 or 85:15 *v*/*v*) Flow rate: 1.0 mL/min; UV detection at 254 nm	Cytotoxic, antimycobacterial and elastase inhibitory activities	[77]
Kohamamides A–C (**32**–**34**)	Cyanobacterium *Okeania* sp.	L-Pro, L-Ala, L-Val, *N*-Me-L-Val, L-Leu; **32**: L-Ile	Ligand Exchange Type CSP; Chiralpak MA (+) (4.6 × 250 mm); MP: 2 mM $CuSO_4$, ACN: 2 mM $CuSO_4$ (15:85 *v*/*v*); Flow rate: 1.0 mL/min; UV detection at 254 nm	No growth inhibition against HeLa and HL60 cells	[78]
Marformycins A–F (**35**–**40**)	Deep sea-derived *Streptomyces drozdowiczii*	**35**: D-allo-Ile, L-Val; **36**: D-allo-Ile, L-allo-Ile; **37**: D-Val, L-allo-Ile; **38**: D-allo-Ile, L-allo-Ile, L-Leu; **39** and **40**: L-Thr, L-Val, D-Val, L-Leu	Ligand Exchange Type CSP; MCIGELCRS10W (4.6 × 50 mm); MP: 2 mM $CuSO_4$ in H_2O Flow rate: 0.5 mL/min; UV detection at 254 nm	Anti-infective activity against *Micrococcus luteus*	[79]

Table 2. *Cont.*

Peptide	Source	aa Composition	Chromatographic Conditions	Biological Activities	Refs.
Pitiprolamide (**41**)	Cyanobacterium *Lyngbya majuscula*	L-Pro, L-Val	Macrocyclic Antibiotic Type CSP; Chirobiotic TAG (4.6 × 250 mm); MP: MeOH/10 mM NH_4OAc (40:60 *v*/*v*) (pH 5.6) Flow rate: 0.5 mL/min	Cytotoxicity against CT116 and MCF7 cancer cell lines and antibacterial activity	[80]
Palau'amide (**42**)	Cyanobacterium *Lyngbya* sp.	L-Ala, L-Ile, *N*-Me-L-Ala, *N*-Me-D-Phe and D-hydroxyisocaproic acid	Ligand Exchange Type CSP; Phenomenex Chirex Phase 3126 (D) (4.6 × 250 mm) MP: 1 mM $CuSO_4$; 2 mM $CuSO_4$/ACN (95:5 or 85:15 *v*/*v*) Flow rate: 0.8 mL/min; UV detection at 254 nm	Cytotoxicity against KB cell line	[81]
Pitipeptolides C–F (**43**–**46**)	Cyanobacterium *Lyngbya majuscula*	L-Pro, L-Val, L-Ile, L-Phe, *N*-Me-L-Phe	Macrocyclic Antibiotic Type CSP; Chirobiotic TAG (4.6 × 250 mm); MP: MeOH/10 mM NH_4OAc (40:60 *v*/*v*) (pH 5.6); Flow rate: 0.5 mL/min Detection by EIMS in positive ion mode (MRM scan)	**46**: Active against *Mycobacterium tuberculosis*	[82]
Ulongapeptin (**47**)	Cyanobacterium *Lyngbya* sp.	L-lactic acid, L-Val, *N*-Me-L-Val, *N*-Me-D-Val, *N*-Me-D-Phe	Ligand Exchange Type CSP; Phenomenex Chirex Phase 3126 (D), 4.6 × 250 mm MP: 2 mM $CuSO_4$; 2 mM $CuSO_4$/ACN (95:5 or 85:15 *v*/*v*) Flow rate: 1.00 mL/min; UV detection at 254 nm	Cytotoxicity against KB cells	[83]
		L-Val, *N*-Me-L-Val, *N*-Me-D-Val	Marfey's method (FDLA) combined with HPLC YMC-Pack AQ-ODS (10 × 250 mm); MP: 50% ACN in 0.01 N TFA Flow rate: 2.5 mL/min; UV detection at 254 nm		
		2-hydroxy-3-methylvaleric acid *N*-Me-L-Ala	Ligand Exchange Type CSP; CHIRALPAK MA (+) (4.6 × 50 mm); MP: 1 mM $CuSO_4$; 2 mM $CuSO_4$/ACN (95:5 or 85:15 *v*/*v*) Flow rate: 0.7 mL/min; UV detection at 254 nm		
Largamides A–H (**48**–**55**)	Cyanobacterium *Oscillatoria* sp.	**48**: L-Val, L-Thr, L-Ala, L-Leu, D-Gln, D-Tyr; **49**: L-Val, L-Thr, L-Ala, L-Ahppa, D-Gln, D-Tyr; **50**: L-Val, L-Thr, L-Ala, L-Ahpha, D-Gln, D-Tyr; **51**: L-Val, L-Thr, L-Ala, L-Leu, L-Ahp, *N*-MeBr-L-Tyr, L-Ahppa; **52**: L-Val, L-Thr, L-Ala, L-Leu, L-Ahp, *N*-MeCl-L-Tyr; **53**: L-Val, L-Thr, L-Ala, L-Tyr, L-Ahp, *N*-MeCl-L-Tyr; **54**: L-Val, L-Thr, L-Ala, L-hTyr, L-Ahp, *N*-MeCl-L-Tyr; **55**: L-Val, L-Thr, L-Ala, L-Amppa, L-Gln, *N*-Me-L-Asn	Marfey's method (FDLA) combined with HPLC Phenomenex Jupiter Proteo C_{12} column, 4 µm (4.6 × 150 mm); MP: ACN containing 0.01 M TFA Flow 0.5 mL/min; UV detection at 254 nm	**51**–**54**: Chymotrypsin inhibition	[84]
		D-Glyceric acid	Ligand Exchange Type CSP; Phenomenex Chirex 3126 (D) (4.6 × 150 mm); MP: 2 mM $CuSO_4$:ACN (90/10 *v*/*v*); Flow 0.5 mL/min; UV detection at 254 nm		

Table 2. *Cont.*

Peptide	Source	aa Composition	Chromatographic Conditions	Biological Activities	Refs.
Trungapeptins A–C (**56**–**58**)	Cyanobacterium *Lyngbya majuscula*	L-Val, L-*N*-MeVal, L-alloLeu, L-Pro	Marfey's method (FDLA) combined with HPLC. Alltech Econosil C_{18}; MP A:40% ACN with 0.04%TFA. MP B: 37.5% ACN with 0.05%TFA. Flow rate: 1.0 mL/min; UV detection at 254 nm	Brine shrimp toxicity and ichthyotoxicity	[85]
		Phenyllactic acid (*S*)	Ligand Exchange Type CSP; CHIRALPAK MA (+) (4.6 × 50 mm); MP: 2 mM $CuSO_4$/ACN (85:15) Flow rate: 0.5 mL/min; UV detection at 254 nm		
Carriebowmide (**59**)	Cyanbacterium *Lyngbya polychroa*	L-Ala, *N*-Me-L-Leu, *N*-Me-D-Phe, L-Phe, L-Met	Ligand Exchange Type CSP; Phenomenex, Chirex (D) Penicillamine, 5 µm (4.6 × 250 mm) MP: 2.0 mM $CuSO_4$-ACN (95:5, 90:10, or 85:15 *v*/*v*) Flow rate: 0.8 or 1.0 mL/min; UV detection at 254 nm	Lipophilic extract reduced feeding on agar food pellets	[86]
		R-Hmba	Ligand Exchange Type CSP; Chiralpak MA (+) (4.6 × 250 mm); MP: 2.0 mM $CuSO_4$-ACN (90:10 *v*/*v*) Flow rate: 1.0 mL/min; UV detection at 254 nm		
		L-Aba	Ligand Exchange Type CSP; Phenomenex, Chirex (D) Penicillamine, 5 µm (4.6 × 250 mm); MP: 2.0 mM $CuSO_4$ Flow rate:1.0 mL/min; UV detection at 254 nm		
		(2*R*,3*R*)-Amha	Marfey's method (FDAA) combined with HPLC Atlantis, C_{18}, (3.0 × 250 mm); MP: 50 mM NH_4COOCH_3(aq)-ACN (70:30 *v*/*v*) Flow rate: 1.0 mL/min; UV detection at 254 nm		
Symplocamide A (**60**)	Cyanobacterium *Symploca* sp.	L-Val, L-Thr, L-Ile, L-Cit, L-Gln, L-Btyr, L-But	Marfey's method (FDAA) combined with HPLC Phenomenex Jupiter C_{18} column (4.6 × 250 mm) MP: ACN:H_2O:HOAc (15:85:0.02 to 1:1:0.02 *v*/*v*/*v*) Flow rate: 0.5 mL/min; UV detection at 340 nm	Cytotoxicity and antimicrobial activities Chymotrypsin inhibitor	[87]
Kempopeptins A (**61**) and B (**62**)	Cyanobacterium *Lyngbya* sp.	**61**: *N*-*O*-diMe-Br-L-Tyr	Marfey's method (FDLA) combined with HPLC Conditions not described	**61**: Elastase and chymotrypsin inhibition **62**: Trypsin inhibition	[88]
		61: *N*-Me-L-Tyr, L-Val, L-Thr-2, L-Pro, L-Phe, L-Ahp, L-Leu **62**: L-Lys, L-Thr, L-Val, L-Ile	Ligand Exchange Type CSP; Phenomenex Chirex Phase 3126 *N*,*S*-dioctyl-(D)-penicillamine column, 5 µm (4.6 × 250 mm); MP: 2 mM CuSO4 in H_2O:ACN (95:5 *v*/*v*) or 2 mM $CuSO_4$ Flow rate: 1.0 mL/min; UV detection at 254 nm		

Table 2. *Cont.*

Peptide	Source	aa Composition	Chromatographic Conditions	Biological Activities	Refs.
Tiglicamides A–C (**63**–**65**)	Cyanobacterium *Lyngbya confervoides*	L-Ala, L-Thr, L-Val, D-Glu, D-Tyr; **63**: L-Htyr; **65**: L-Met (*O*)	Ligand Exchange Type CSP; Phenomenex, Chirex 3126, 5 μm (4.6 × 250 mm); Mobile Phase: 2 mM $CuSO_4$ Flow rate: 1.0 mL/min; UV detection at 254 nm	Porcine pancreatic elastase inhibition	[89]
		65: L-Phe	Marfey's method (FDLA) combined with HPLC Alltech Alltima HP C_{18}, 5μm (4.6 × 250 mm) MP: 50–100% MeOH in 0.1% (*v*/*v*) aqueous TFA Flow rate: 0.8 mL/min; PDA detection at 200–500 nm		
Hantupeptin B (**66**)	Cyanobacterium *Lyngbya majuscula*	L-Pro, L-Val, *N*-Me-L-Val, *N*-Me-L-Ile	Marfey's method (FDAA) combined with HPLC Phenomenex, Luna, 5 μm, (2.0 × 150 mm); MP: ACN in 0.1% (*v*/*v*) aqueous HCOOH; Flow rate: 0.2 mL/min	Cytotoxicity against MOLT-4 (leukemic) and MCF-7 (breast cancer) cell lines	[90]
		L-3-phenyllactic acid (*S*)	Ligand Exchange Type CSP; Chiralpak MA (+) (4.6 × 500 mm) MP: 2 mM $CuSO_4$/ACN (85:15 *v*/*v*) Flow rate: 0.7 mL/min; UV detection at 218 nm		
Palmyramide A (**67**)	Cyanobacterium (*Lyngbya majuscula*) and a red alga *Centroceras* sp. complex	L-Val, *N*-Me-L-Val, L-Pro	Marfey's method (FDAA) combined with HPLC/MS on a Merck LiChrospher 100 RP-18 (4.0 × 125 mm) MP: ACN:H_2O:HCOOH (30:70:0.1 to 70:30:0.1 *v*/*v*/*v*) or 2.0 mM $CuSO_4$ in H_2O Flow rate: 0.7 mL/min; UV detection at 254 nm	Sodium channel blocking activity in neuro-2a cells and cytotoxic activity in H-460 (human lung carcinoma) cells	[91]
		L-Lac, L-Pla	Ligand Exchange Type CSP; Phenomenex Chirex 3126 (4.6 × 250 mm); Conditions not described		
Veraguamides A–G (**68**–**74**)	Cyanobacterium *Symploca* cf. *hydnoides*	**68**–**71**, **73** and **74**: L-Val, *N*-Me-L-Val, L-Pro; **70**: (2*S*,3*R*) Br-Hmoya; **71**: *N*-Me-L-Ile; **72**: L-Ile, *N*-Me-L-Val, *N*-Me-L-Ile, L-Pro	Macrocyclic Antibiotic Type CSP; Chirobiotic TAG (4.6 × 250 mm); MP: MeOH/10 mM NH_4OAc (40:60 *v*/*v*) (pH 5.6); Flow rate: 0.5 mL/min	Cytotoxic activity against HT29 (colorectal adenocarcinoma) and HeLa (cervical carcinoma) cell lines	[92]
		74: 2*S*:3*R* dpv 2*R*:3*R* Dml	Marfey's method (FDAA) combined with HPLC-MS Phenomenex Synergi Hydro-RP (4.6 × 150 mm) MP: MeOH:H_2O:HCOOH (40–100% MeOH: 0.1% HCOOH); Flow rate: 0.5 mL/min		

Table 2. *Cont.*

Peptide	Source	aa Composition	Chromatographic Conditions	Biological Activities	Refs.
Porpoisamides A (**75**) and B (**76**)	Cyanobacterium *Lyngbya* sp.	**75** and **76**: L-Ala, L-Pro, *N*-Me-D-Phe, (2*S*,3*S*)-Hmpa	Ligand Exchange Type CSP; Phenomenex Chirex 3126 (4.6 × 250 mm); MP: 5% or 15% ACN in 2 mM $CuSO_4$ in H_2O; Flow rate: 1.0 mL/min	Cytotoxicity against HCT 116 (colorectal carcinoma) and U2OS (osteosarcoma) cells	[93]
		75: (2*S*,3*R*)-Amoa **76**: (2*R*,3*R*)-Amoa	Ligand Exchange Type CSP; Chiralpak MA (+) (4.6 × 50 mm); MP: 15% ACN in 2 mM $CuSO_4$ in H_2O Flow rate: 1.0 mL/min		
		(2*R*,3*R*) 3-NH_2-2-Me-octanoic acid	Marfey's method (FDAA) combined with HPLC YMC-Pack AQ-ODS (10 × 250 mm) MP: ACN:H_2O: *N*-TFA (57:43:0.1 *v*/*v*/*v*) Flow rate: 2.5 mL/min; UV detection at 340 nm		
		76: (2*S*)-Hiva	Ligand Exchange Type CSP; CHIRALPAK MA (+) (4.6 × 50 mm); MP: ACN/2 mM $CuSO_4$ (10:90 *v*/*v*) Flow: 1.0 mL/min; UV detection at 254 nm		
Companeramides A (**77**) and B (**78**)	Cyanobacterial assemblage collected from Coiba National Park, Panama	**77**: L-Ala, *N*-Me-L-Ala, L-Pro, L-Ile, *N*-Me-L-Leu, and *N*-Me-L-Val; **78**: L-Pro, *N*-Me-L-Val, L-Val, L-Ile, D- and *N*-Me-L-Ala	Marfey's method (FDAA) combined with HPLC C_{18} column (3.9 × 150 mm) MP: 40 mM NH_4OAc (pH 5.2):ACN (9:1 to 1:1 *v*/*v*) Flow rate: 1.0 mL/min; UV detection at 340 nm	Antiplasmodial activity against *Plasmodium falciparum*	[94]
		S-Hiva	Ligand Exchange Type CSP; Phenomenex Chirex 3126 (D) (4.6 × 250 mm); MP: $CuSO_4$/ACN Flow: 1.0 mL/min; UV detection at 254 nm		
Piperazimycins A–C (**79**–**81**)	Fermentation broth of a *Streptomyces* sp.	(*S*)-AMNA, (*S*,*S*)-OHPip1, (*R*,*R*)-γOHPip2, **79**: (*S*)-αMeSer	Marfey's method (FDAA) combined with HPLC C_{18}; MP: ACN in H_2O (10–100%) Flow rate: 1.0 mL/min; UV detection: 210, 254, 340 nm	**79**: Active against diverse cancer cell lines	[95]
Grassypeptolides D (**82**) and E (**83**)	Red sea cyanobacterium *Leptolyngbya* sp.	D-allo-Thr, *N*-Me-D-Leu, L-Thr, *N*-Me-L-Leu	Marfey's method (FDAA) combined with HPLC Gemini C_{18} 110 A, 5 µm (4.6 × 250 mm)	Cytotoxicity against HeLa and mouse neuro-2a blastoma cells	[96]
		L-PLa, *N*-Me-L-Val, L-Pro, *N*-Me-L-Phe, (2*S*)-MeCysA, D-Aba, L-Cya, (2*R*,3*R*)-Maba	Marfey's method (FDAA) combined with HPLC Kinetex XB-C_{18}, 110 A, 2.6 µm (4.6 × 100 mm) MP: ACN:H_2O:HCOOH (30:70:0.1 to 70:30:0.1 *v*/*v*/*v*) or ACN:H_2O:TFA (30:70:0.1 to 70:30:0.1 *v*/*v*/*v*); Flow rate: 0.2 mL/min; UV detection at 340 nm and ESIMS		

Table 2. *Cont.*

Peptide	Source	aa Composition	Chromatographic Conditions	Biological Activities	Refs.
Fijimycins A–C (**84**–**86**)	Fermentation broth of *Streptomyces* sp. strain CNS-575	**84**: D-PhSar, L-Ala, L-DiMe-Leu, Sar, D-Hyp, D-Leu, L-Thr; **85**: L-*N*-MeLeu, L-Ala, L-DiMeLeu, Sar, D-Hyp, D-Leu, L-Thr; **86**: L-PhSar, L-Ser, L-DiMeLeu, Sar, D-Hyp, D-Leu, L-Thr	Marfey's method (FDAA) combined with HPLC C_{18} column, Luna (4.6 × 100 mm) MP: ACN:H_2O:TFA (10:90:1 to 50:50:1 *v*/*v*/*v*) Flow rate: 0.7 mL/min; UV detection at 340 nm	Antibacterial activity against three MRSA strains of *Staphylococcus aureus*	[97]
Itralamides A (**87**) and B (**88**), and Carriebowmide sulfone (**89**)	Cyanobacterium *Lyngbya majuscula*	**87**: L-Ala, D-Ala, *N*-Me-L-Ala, *N*-Me-D-Phe, *N*-Me-L-Thr, *N*-Me-L-Val	Marfey's method (FDLA) combined with HPLC Eclipse XDB-18, Agilent (4.6 × 150 mm) MP: ACN:H_2O:HCOOH (20:80:0.1 to 80:20:0.1 *v*/*v*/*v*) Flow rate: 0.8 mL/min; Detection by ESI-MS	**88**: Cytotoxicity against HEK293 (human embryonic kidney) cell line	[98]
		88: *N*-Me-L-Ala, *N*-Me-D-Phe, *N*-Me-L-Thr, D-Val	Marfey's method (FDLA) combined with HPLC Luna C18, Phenomenex, 5 µm (4.6 × 250 mm) MP: ACN:H_2O:HCOOH (20:80:0.1 to 90:10:0.1 *v*/*v*/*v*) Flow rate: 0.8 mL/min		
		89: (2*S*,3*R*)-AMHA	Marfey's method (FDLA) combined with HPLC-PDA dC_{18}, 5 µm (3.0 × 250 mm); MP: ACN:H_2O:HCOOH (0:100:0.1 to 50:50:0.1 *v*/*v*/*v*); Flow rate: 0.3 mL/min		
Viequeamide A (**90**)	Marine button cyanobacterium *Rivularia* sp.	L-Val, L-Thr, *N*-Me-L-Val, L-Pro	Marfey's method (FDLA) combined with HPLC Conditions not described	Highly toxic to H460 (human lung cancer) cells	[99]
Ngercheumicin F–I (**91**–**94**)	Photobacterium related to *P. halotolerans*	L-Ser, L-*allo*-Thr, D-Ser, D-Thr, L-Leu, D-Leu	Marfey's method (FDLA) combined with HPLC Dionex RSLC Ultimate 300 with a diode array detector Kinetex C_{18} column, 2.6 µm at 60 °C (2.1 × 150 mm) ACN:H_2O:TFA (0:100:0.1 to 50:50:0.1 *v*/*v*/*v*) Flow rate: 0.8 mL/min	**91**–**93**: *rnaIII inhibiting* activities	[100]

aa—Amino acid; FDAA—1-Fluoro-2-4-dinitrophenyl-5-L-alanine amide; LC—Liquid Chromatography; MS—Mass Spectrometry; HPLC—High Performance Liquid Chromatography; MP—Mobile Phase; TEAP—Triethylammonium phosphate; ACN—Acetonitrile; TFA—Trifluoracetic acid; MeOH—Methanol; TEA—Triethylamine; IPA—Isopropyl alcohol; FDLA—1-Fluoro-2-4-dinitrophenyl-5-D,L-leucine amide; NaOAc—Sodium acetate; NH_4OAc—Ammonium acetate.

The concurrent applicability of chiral HPLC and Marfey's methods for determination of the absolute configuration of all the amino acid residues of cyclic depsipeptides **47**–**78** (Figure 5) was also described in several reports, among which ten described the use of ligand exchange-type CSPs to perform the analysis in association with Marfey's method [71,72,74–76,78,79,81]. Furthermore, the use of macrocyclic antibiotic-based CSPs was reported by Montaser et al. [82].

Considering the biological activities of cyclic depsipeptides, whose stereochemistry of the amino acids was determined by a combination of Marfey's method and chiral HPLC, it is worth mentioning the following compounds. Ulongapeptin (**47**), isolated from a Palauan marine cyanobacterium *Lyngbya* sp. displayed significant cytotoxic activity against KB cells with IC_{50} value of 0.63 μM [83]. Largamides A–H (**48**–**55**), isolated from the marine cyanobacterium *Oscillatoria* sp., inhibited chymotrypsin with IC_{50} values ranging from 4 to 25 μM [84]. Symplocamide A (**60**), isolated from the marine cyanobacterium *Symploca* sp., showed cytotoxicity against NCI-460, non-small cell lung cancer cells (IC_{50} = 40 nM), and neuro-2a mouse neuroblastoma cells (IC_{50} = 29 nM). It was also reported that **60** was active against three tropical parasites: malaria (*Plasmodium falciparum*, IC_{50} = 0.95 μM), chagas disease, (*Trypanasoma cruzi*, IC_{50} > 9.5 μM), and leishmaniasis (*Leishmania donovani*, IC_{50} > 9.5 μM) [87]. It was found that, kempopeptins A (**61**) and B (**62**), isolated from the marine cyanobacterium *Lyngbya* sp., exhibited inhibitory activity against elastase and chymotrypsin with IC_{50} values of 0.32 μM and 2.6 μM, respectively [88]. Palmyramide A (**67**), isolated from the marine cyanobacterium *Lyngbya majuscula*, showed sodium channel blocking activity in the neuro-2a cells as well as cytotoxic activity in H-460 human lung carcinoma cell line [91]. Companeramides A (**77**) and B (**78**), isolated from a marine cyanobacterial assemblage comprising a small filament *Leptolyngbya* species, showed high nanomolar in vitro antiplasmodial activity against *Plasmodium falciparum* strains D6, Dd2, and 7G8 [94].

Moreover, HPLC analysis after derivatization with a Marfey's reagent has been reported as the only method to determine the stereochemistry of the amino acid residues of cyclic depsipeptides **79**–**94** (Figure 6). FDAA was used as derivatization reagent for piperazimycins A–C (**79**–**81**), cyclic hexadepsipeptides isolated from the fermentation broth of a marine-derived bacterium *Streptomyces* sp. Strain, collected from a sediment [95], grassypeptolides D (**82**) and E (**83**), cyclic depsipeptides isolated from the marine cyanobacterium *Leptolyngbya* sp. [96], fijimycins A–C (**84**–**86**), cyclic depsipeptides isolated from a marine bacteria *Streptomyces* sp. [97]. The Marfey's reagent FDLA was employed for the assignment of the absolute configuration of the amino acid residues of several cyclic depsipeptides such as itralamide A (**87**) and B (**88**) and carriebowmide sulfone (**89**), isolated from the marine cyanobacterium *Lyngbya majuscula* [98], viequeamide A (**90**), isolated from the marine button cyanobacterium (*Rivularia* sp.) [99], ngercheumicins F–I (**91**–**94**) [100].

Many cyclic depsipeptides whose stereochemistry of their amino acids was determined only by Marfey's method, exhibited various interesting biological activities. Thus, piperazimycin A (**79**) was found to exhibit potent cytotoxicity against a panel of sixty cancer cell lines (mean values of growth inhibition (GI_{50}) = 100 nM, and LC_{50} = 2 μM) [95]. While, grassypeptolides D (**82**) and E (**83**) exhibited significant cytotoxicity to HeLa (IC_{50} = 335 and 192 nM, respectively) and mouse neuro-2a blastoma (IC_{50} = 559 and 407 nM, respectively) cell lines [96], itralamide B (**88**) was active against HEK293 cells (IC_{50} value of 6 ± 1 μM) [98]. Fijimycins A–C (**84**–**86**) exhibited strong growth inhibitory activity against three MRSA strains in a concentration range of 4–32 $\mu g/mL^{-1}$ [97].

2.3. Lipopeptides

To the best of our knowledge, there are only two reports describing simultaneously the isolation and characterization of lipopeptides from marine cyanobacteria (Figure 7) as well as the stereochemistry determination of the amino acids present in their hydrolysates (Table 3).

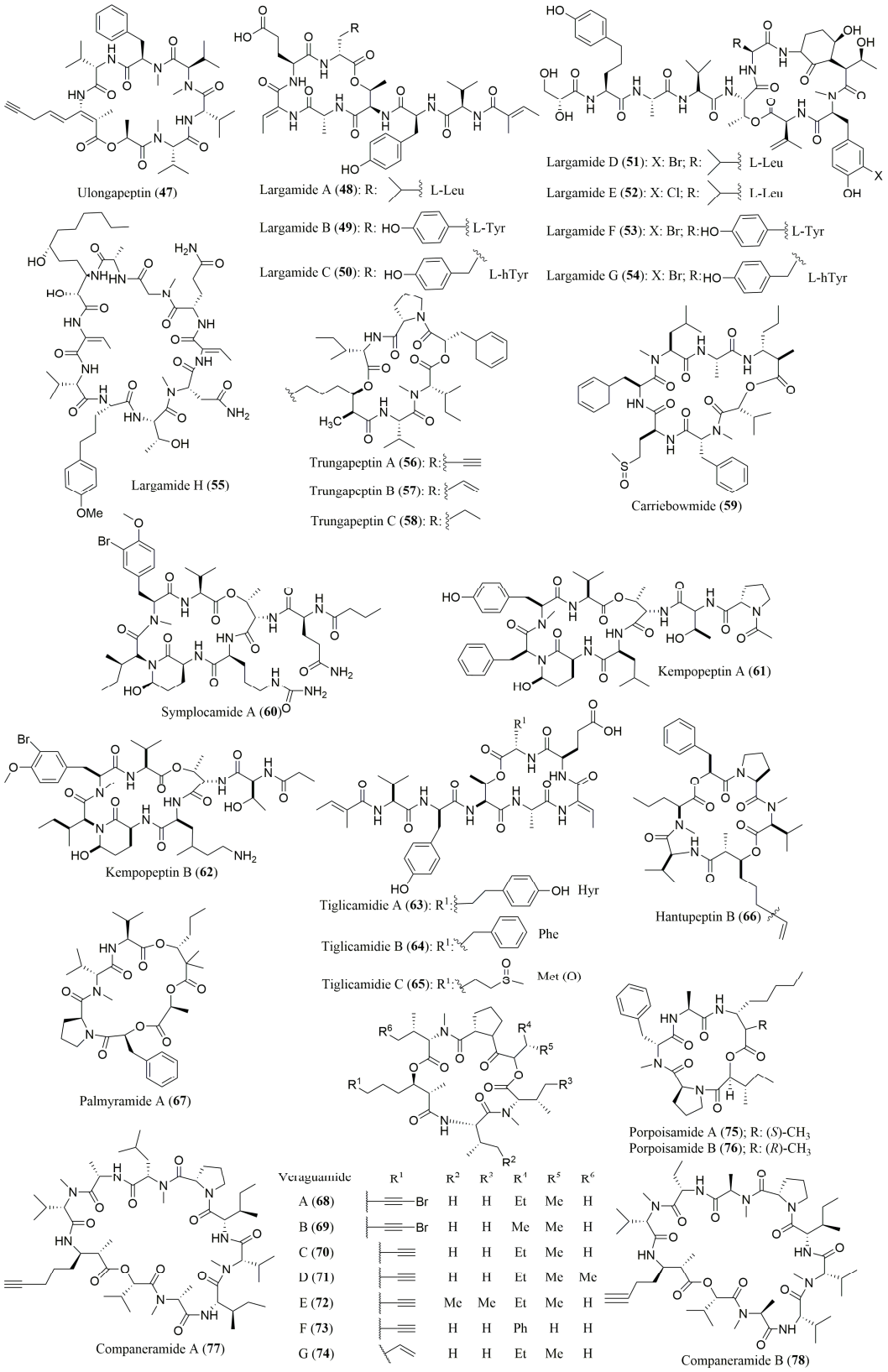


Figure 5. Structure of cyclic depsipeptides **47**–**78**, isolated from marine cyanobacteria and other bacteria, whose stereochemistry of their amino acids was determined by a combination of Marfey's method and chiral HPLC.

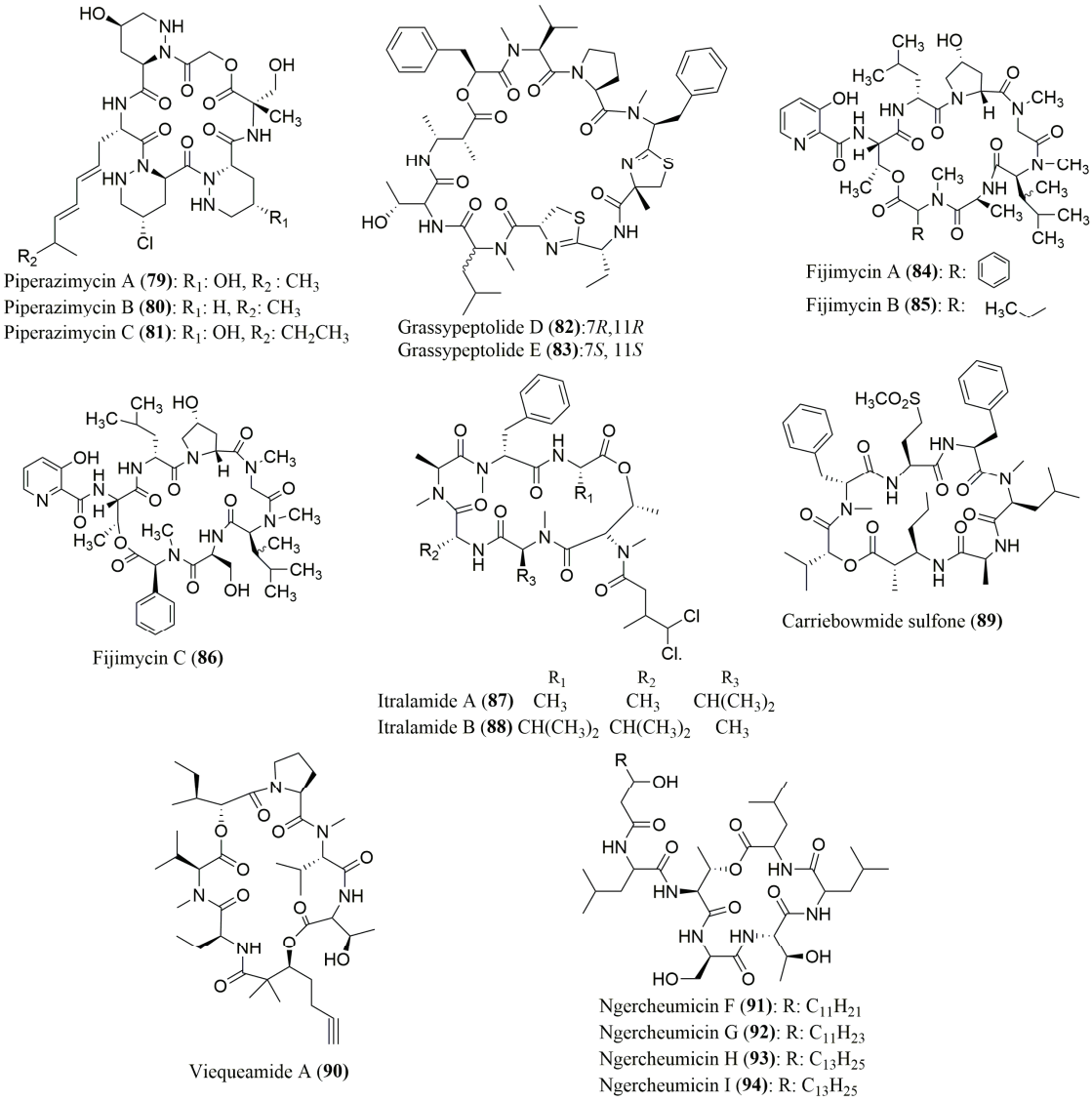


Figure 6. Structure of cyclic depsipeptides **79**–**94**, isolated from marine cyanobacteria and other bacteria, whose stereochemistry of their amino acids was determined by Marfey's method.

The configuration of *N*-Me-Hph of the lipopeptide antillatoxin B (**95**), isolated from the cyanobacterium *Lyngbya majuscula*, was assigned as L using FDAA as Marfey's derivatization reagent [101]. Compound **95** exhibited significant sodium channel activation (EC_{50} = 1.77 μM) and ichthyotoxicity (LC_{50} = 1 μM) [101]. The hydrolysates of lipopeptides lobocyclamides A–C (**96**–**98**), isolated from the cyanobacterium *Lyngbya confervoides*, were analyzed by either direct chiral HPLC, using the D-penicillamine ligand exchange type CSP or by prior derivatization by Marfey's method and reverse phase HPLC [102]. Both compounds displayed modest in vitro antifungal activity against a panel of *Candida* sp., including two fluconazole-resistant strains. Interestingly, synergistic antifungal activity was also observed [102].

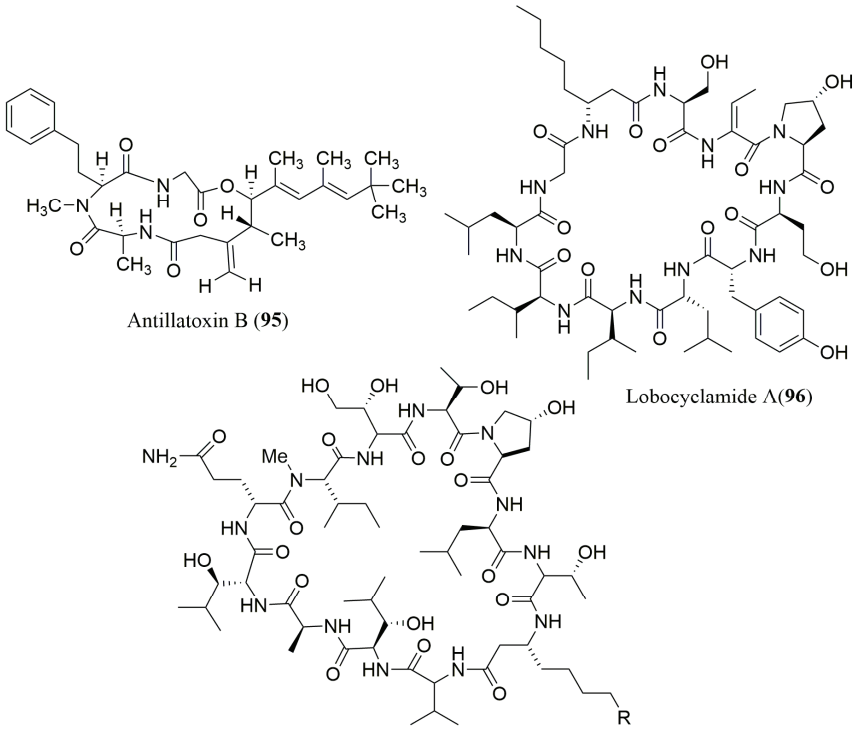


Figure 7. Structure of lipopeptides **95–98**, isolated from marine cyanobacteria.

Table 3. Lipopeptides from marine cyanobacteria.

Peptide	Source	aa Composition	Chromatographic Conditions	Biological Activities	Ref.
Antillatoxin B (**95**)	Cyanobacterium *Lyngbya majuscula*	*N*-Me-L-Hph	Marfey's method (FDAA) combined with HPLC Waters Nova-Pak C_{18} (3.9 × 150 mm), MP: 10 to 50% ACN in H_2O with 0.05% TFA, UV detection at 340 nm	Sodium channel-activating and ichthyotoxic activities	[101]
Lobocyclami-des A–C (**96–98**)	Cyanobacterium *Lyngbya confervoides*	**96**: *S*-Ile, *S-allo*-Ile, *S*-Leu, *R*-β-Aoa, *S*-Ser, *R*-Tyr, *S*-Hse, *R*-Hpr	Ligand Exchange Type CSP Chirex 3126 (D)-penicillamine column; MP: 2 mM aq $CuSO_4$/ACN (1:99, 95:5 or 86:14 *v*/*v*); Flow rate: 1.15–1.20 mL/min, UV detection at 254 nm	Antifungal activity against a panel of *Candida* sp.	[102]
		97: *S*-Ala, *S*-Thr, *N*-Me-*S*-Ile, *R*-Aoa, *R*-Ada, 2*R*,3*R*-4-OH-Hth, 2*R*,3*S*-3-OH-Leu, *trans*-3-OH-Pro	Marfey's method (FDAA) combined with HPLCC_{18} column (4.8 × 250 mm); MP: ACN: 0.1% aq. TFA buffer (pH 3) (1:9 to 1:1 *v*/*v*) Flow rate: 1.0 mL/min; UV detection at 340 nm		

aa—Amino acid; FDAA—1-Fluoro-2-4-dinitrophenyl-5-L-alanine amide; HPLC—High Performance Liquid Chromatography; MP—Mobile Phase; ACN—Acetonitrile; TFA—Trifluoracetic acid.

3. Peptides from Marine-Derived Fungi

Marine fungi have been isolated from various marine sources like algae, marine invertebrates, sediment or water, mangroves and sponges. Most of the fungal species isolated from marine sponges are related to the genera *Aspergillus* and *Penicillium* [103]. Marine fungi are a rich source of structurally unique and biologically active compounds with a wide range of biological activities, such as antimalarial, anticancer, antifungal, antibacterial, cytotoxicity and among others [104]. More than

1000 compounds have been already isolated from marine derived fungi and among them around 150–200 new compounds were bioactive [103,104].

3.1. Cyclic Peptides

A large number of cyclic peptides have been isolated from marine-derived fungi (Figure 8) and Table 4 shows the marine fungal cyclic peptides whose stereochemistry of their amino acid residues were determined. To the best of our knowledge, only three reports described the use of FDAA and FDLA as Marfey's derivatization reagents, specifically for analysis of the peptides **99**–**112**.

The cyclic peptide cyclo-(L-leucyl)-*trans*-4-hydroxyl-L-prolyl-D-leucyl-*trans*-4-hydroxy-L-proline) (**99**), isolated from the marine mangrove-derived fungi *Phomopsis* sp. K38, and *Alternaria* sp. E33, was found to exhibit antifungal activity, particularly the fungus *Helminthosporium sativum*. By using a combination of Marfey's method and a reverse phase HPLC, the presence of 4-OH-L-Pro and both L- and D-Leu residues in its structure was confirmed [105]. Scytalidamides A (**100**) and B (**101**), and clonostachysins A (**102**) and B (**103**), isolated from marine sponge derived fungus *Clonostachys rogersoniana* strain HJK9, were found to comprise L-configuration for all their amino acids [106,107]. Scytalidamides A (**100**) and B (**101**) showed cytotoxicity against human colon carcinoma tumor cell line (HCT-116) with IC_{50} values of 2.7 and 11.0 μM, respectively, and the NCI 60 cell-line, with 7.9 and 4.1 μM GI-50, respectively [106], while clonostachysins A (**102**) and B (**103**) exhibited inhibitory effect on the *Prorocentrum micans* alga at concentration higher than 30 μM [107].

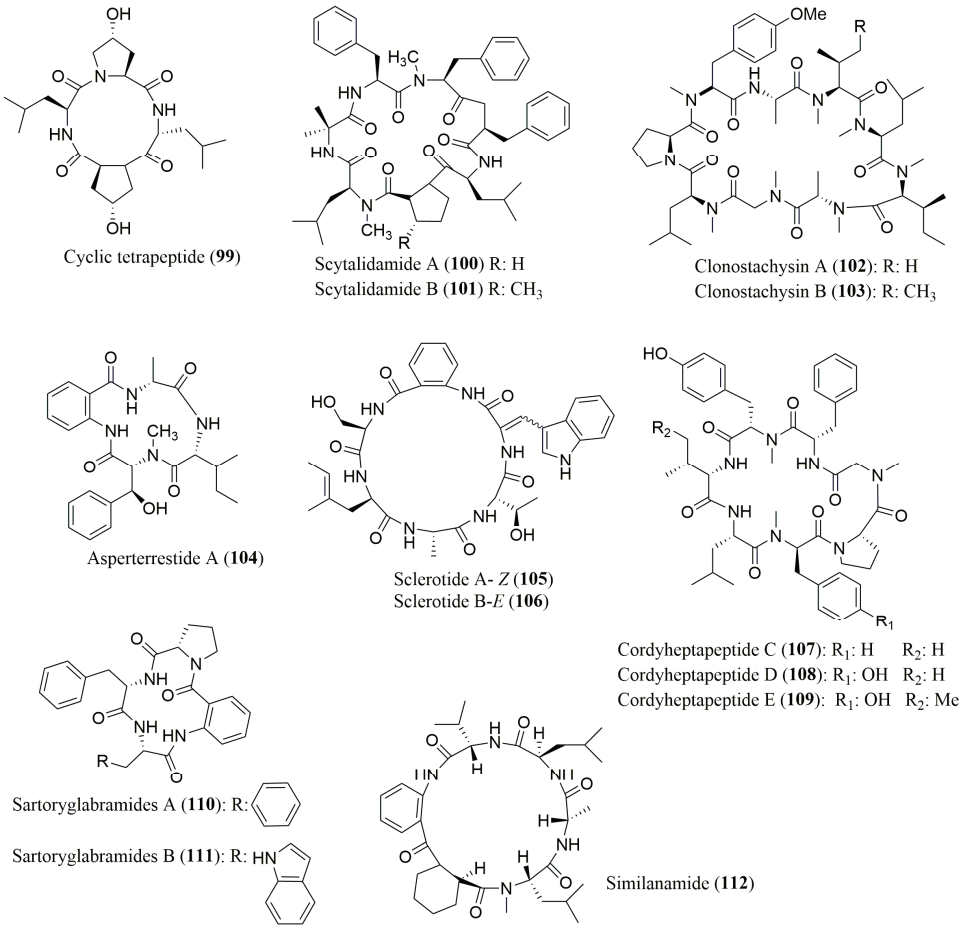


Figure 8. Structure of cyclic peptides **99**–**112**, isolated from marine-derived fungi.

Table 4. Cyclic peptides from marine-derived fungi.

Peptide	Source	aa Composition	Chromatographic Conditions	Biological Activities	Ref.
Cyclo-(L-leucyl-*trans*-4-hydroxyl-L-prolyl-D-leucyl-*trans*-4-hydroxy-L-proline) (**99**)	Marine mangrove-derived fungi *Phomopsis* sp. K38 and *Alternaria* sp. E33	4-OH-L-Pro, D-Leu, L-Leu	Marfey's method (FDAA) combined with LC/MS Alltima C_{18} column, 5 µm; (4.6 × 250 mm) MP: MeOH:H_2O:HCOOH (60:40:0.05 to 10:90:0.05 *v*/*v*/*v*); Flow rate: 0.6 mL/min	Inhibition against four crop-threatening fungi	[105]
Scytalidamides A (**100**) and B (**101**)	Marine Fungus of the genus *Scytalidium*	L-Phe, *N*-Me-L-Phe, L-Leu, *N*-Me-L-Leu, L-Pro, 3-Me-L-Pro	Marfey's method (FDLA) combined with HPLC Agilent Hypersil ODS column, 5 µm (4.6 × 100 mm); MP: ACN 25 to 65%; Flow rate: 0.7 mL/min	Cytotoxicity against HCT-116 and NCI 60 cell lines	[106]
Clonostachysins A (**102**) and B (**103**)	Marine sponge-derived fungus *Clonostachys rogersoniana* strain HJK9	*N*-Me-L-Ile, *N*-Me-L-Leu, L-Pro, L-Gly, *N*-Me-L-Tyr, *N*-Me-L-Ala **102**: *N*-Me-L-Val; **103**: *N*-Me-L-Ile	Marfey's method (FDLA) combined with LC-ESI MS/MS; Conditions not described	Inhibitory effect on dinoflagellate *Prorocentrum micans*	[107]
Asperterrestide A (**104**)	Marine-derived fungus *Aspergillus terreus* SCSGAF0162	D-Ala	Marfey's method (FDAA) combined with HPLC Alltima C_{18} column, 5 µm (4.6 × 250 mm); MP: ACN:H_2O:TFA (15:85:0.1 to 90:10:0.1 *v*/*v*/*v*); Flow rate: 0.5 mL/min; UV detection at 254 nm Ligand Exchange Type CSP; MCI GELCRS 10 W (4.6 × 50 mm); MP: 2 mM $CuSO_4$:H_2O solution Flow rate: 1.0 mL/min; UV detection at 254 nm	Cytotoxicity against U937 and MOLT4 human carcinoma cell lines and inhibitory effects on influenza virus	[108]
Sclerotides A (**105**) and B (**106**)	Marine-derived fungus, *Aspergillus sclerotiorum* PT06-1	L-Thr, L-Ala, D-Phe, D-Ser	Crown Ether CSP; Crownpak CR (+); MP: aq $HClO_4$ pH 2.0; Flow rate: 0.4 mL/min; UV detection at 200 nm	**105** and **106**: Antifungal activity **106**: Cytotoxicity and antibacterial activity	[109]
Cordyheptapeptides C–E (**107**–**109**)	Marine-derived fungus *Acremonium persicinum* SCSIO 115	*N*-Me-L-Tyr, L-Phe, L-Pro, L-Leu **107**–**109**: *N*-Me-D-Phe, L-Val **109**: *N*-Me-L-Gly, *N*-Me-D-Tyr, L-*allo*-Ile	Crown Ether Chiral CSP; Crownpak CR (+) MP: 2.0 mM $CuSO_4$:ACN (95:5 *v*/*v*) Flow rate: 1.0 mL/min; UV detection at 254 nm	**107** and **109**: Cytotoxicity against SF-268, MCF-7, and NCI-460 tumor cell lines	[110]
Similanamide (**110**)	Marine sponge-associated fungus *Aspergillus similanensis* KUFA 0013	L-Ala, D-Leu, L-Val, *N*-Me-L-Leu, D-pipecolic acid	Macrocyclic Antibiotic Type CSP; Chirobiotic T, 5 µm (4.6 × 150 mm); MP: MeOH:H_2O:CH_3COOH (70:30:0.02 *v*/*v*/*v*); Flow rate: 1.0 mL/min; UV detection at 210 nm	Cytotoxicity against MCF-7, NCI-H460 and A373 tumor cell lines	[111]
Sartoryglabramide A (**111**) and B (**112**)	Marine sponge-associated fungus *Neosartorya glabra* KUFA 0702	L-Phe, L-Pro **112**: L-Trp	Macrocyclic Antibiotic Type CSP; Chirobiotic T, 5 µm (4.6 × 150 mm); MP: MeOH:H_2O (80:20 *v*/*v*) Flow rate: 1.0 mL/min; UV detection at 210 nm	Neither antibacterial nor antifungal activity	[112]

aa—Amino acid; FDAA—1-Fluoro-2-4-dinitrophenyl-5-L-alanine amide; HPLC—High Performance Liquid Chromatography; MP—Mobile Phase; ACN—Acetonitrile; TFA—Trifluoracetic acid; MeOH—Methanol; FDLA—1-fluoro-2-4-dinitrophenyl-5-D,L-leucine amide.

Both Marfey's method and chiral HPLC analysis were also used for the analysis of the absolute configuration of the amino acids of asperterrestide A (**104**), a cyclic peptide isolated from the marine-derived fungus *Aspergillus terreus* SCSGAF0162 which revealed the presence of D-Ala in its structure [108]. Nevertheless, it was not possible to distinguish between D-Ile and D-*allo*-Ile. Compound **104** showed promising inhibitory effects to the influenza virus strains A/WSN/33, and A/Hong Kong/8/68 (IC_{50} values of 15 and 8.1 μM, respectively) as well as cytotoxicity against U937 and MOLT4 cell lines (IC_{50} values of 6.5 and 6.2 μM, respectively) [108].

There are some reports describing the application of different types of CSPs, including crown ethers and macrocyclic antibiotics, for a chiral HPLC as the only method for analysis of the absolute configuration of the amino acids of peptides. Thus, the determination of the stereochemistry of the amino acids in the cyclic peptides sclerotides A (**105**) and B (**106**), isolated from the marine-derived fungus *Aspergillus sclerotiorum* PT06-1 [109], and cordyheptapeptides C–E (**107**–**109**), isolated from the marine-derived fungus *Acremonium persicinum* SCSIO 115 [110], was achieved via chiral HPLC analysis of the hydrolysates using the crown ether-based CSP Crownpak CR (+). Sclerotides A (**105**) and B (**106**) were found to comprise L-Thr, L-Ala, D-Phe, and D-Ser [109]. Moreover, the presence of *N*-Me-D-Gly, and L-Val in cordyheptapeptides C (**107**) and D (**108**) and *N*-Me-L-Gly, *N*-Me-D-Tyr, and L-*allo*-Ile in cordyheptapeptide E (**109**) was confirmed, in addition to the present of other amino acids common to the three cyclic peptides [110]. Sclerotides A (**105**) and B (**106**) displayed antifungal activity against *Candida albicans*, with MIC values of 7.0 and 3.5 μM, respectively. Furthermore, sclerotide B (**106**) also exhibited cytotoxicity against HL-60 cell line as well as antibacterial activity against *Pseudomonas aeruginosa* [109] whereas cordyheptapeptides C (**107**) and E (**109**) exhibited cytotoxic activity against SF-268 (IC_{50} values of 3.7 and 3.2 μM, respectively), MCF-7 (IC_{50} values of 3.0 and 2.7 μM, respectively), and NCI-H460 (IC_{50} values of 11.6 and 4.5 μM, respectively) tumor cell lines [110]. Recently, the macrocyclic antibiotic-based CSP Chirobiotic T was employed in our group to determine the stereochemistry of amino acid residues of a new cyclic hexapeptide, similanamide (**110**), isolated from a marine sponge-associated fungus *Aspergillus similanensis* KUFA 0013 [111] which confirmed the presence of L-Ala, D-Leu, L-Val and D-pipecolic acid as its amino acids constituent. By using a similar approach, the absolute configuration of all the amino acids of two new cyclotetrapeptides, sartoryglabramides A (**111**) and B (**112**), isolated from the marine sponge-associated fungus *Neosartorya glabra* KUFA 0702, were assigned to be L-configuration in both cyclic peptides [112]. Further details are described in the case-study presented below.

3.2. Cyclic Depsipeptides

Most of the works describing the stereochemistry determination of amino acid residues of cyclic depsipeptides, isolated from marine fungus (Figure 9), employed Marfey's method coupled with HPLC, using FDAA or FDLA as derivatization reagents (Table 5).

The structures of exumolides A (**113**) and B (**114**), cyclic depsipeptides isolated from the marine fungus of the genus *Scytalidium*, were confirmed to have L-Pro, L-Phe and *N*-Me-L-Leu in their composition [113]. Moreover, guangomide A (**115**), isolated from an unidentified sponge-derived fungus, was found to comprise *N*-Me-D-Phe [114]. The absolute configuration of common amino acid residues in destruxin E chlorohydrin (**116**) and pseudodestruxin C (**117**), isolated from the marine-derived fungus *Beauveria felina*, indicated the presence of *N*-Me-L-Ala and L-Ile in **116**, L-Phe in **117**, and *N*-Me-L-Val in both cyclic depsipeptides [115]. Furthermore, the absolute configuration of amino acid residues in zygosporamide (**118**), isolated from the marine-derived fungus *Zygosporium masonii* [116], petriellin A (**119**), isolated from the coprophilous fungus *Petriella sordida* [117], alternaramdie (**120**), isolated from the marine derived fungus *Alternaria* sp. SF-5016 [118], petrosifungins A (**121**) and B (**122**), isolated from a *Penicillum brevicompac-tum* strain of the Mediterranean sponge *Petrosia ficiformis Poiret* [119], were also successfully determined by Marfey's method coupled with HPLC. Zygosporamide (**118**) displayed cytotoxic activity against RXF 393 and SF-268 cancer cell lines, with mean values of GI-50 of 6.0 and <5.6 nM, respectively [116]

whereas guangomide A (**115**) [114] and alternaramdie (**120**) [118] showed antibacterial activity against *Staphylococcus epidermidis* and *Staphylococcus aureus*, respectively.

In the last few years, ultra-high-pressure liquid chromatography (UHPLC) is becoming an essential technique for ultra-fast separations, since it offers many benefits, including high efficiency in short analysis time and low solvent consumption [120,121]. Thus, the absolute configuration of the amino acid residues of oryzamides A–E (**123**–**127**), isolated from the sponge-derived fungus *Nigrospora oryzae PF18*, was achieved by Marfey's analysis with FDLA, combined with UHPLC [122].

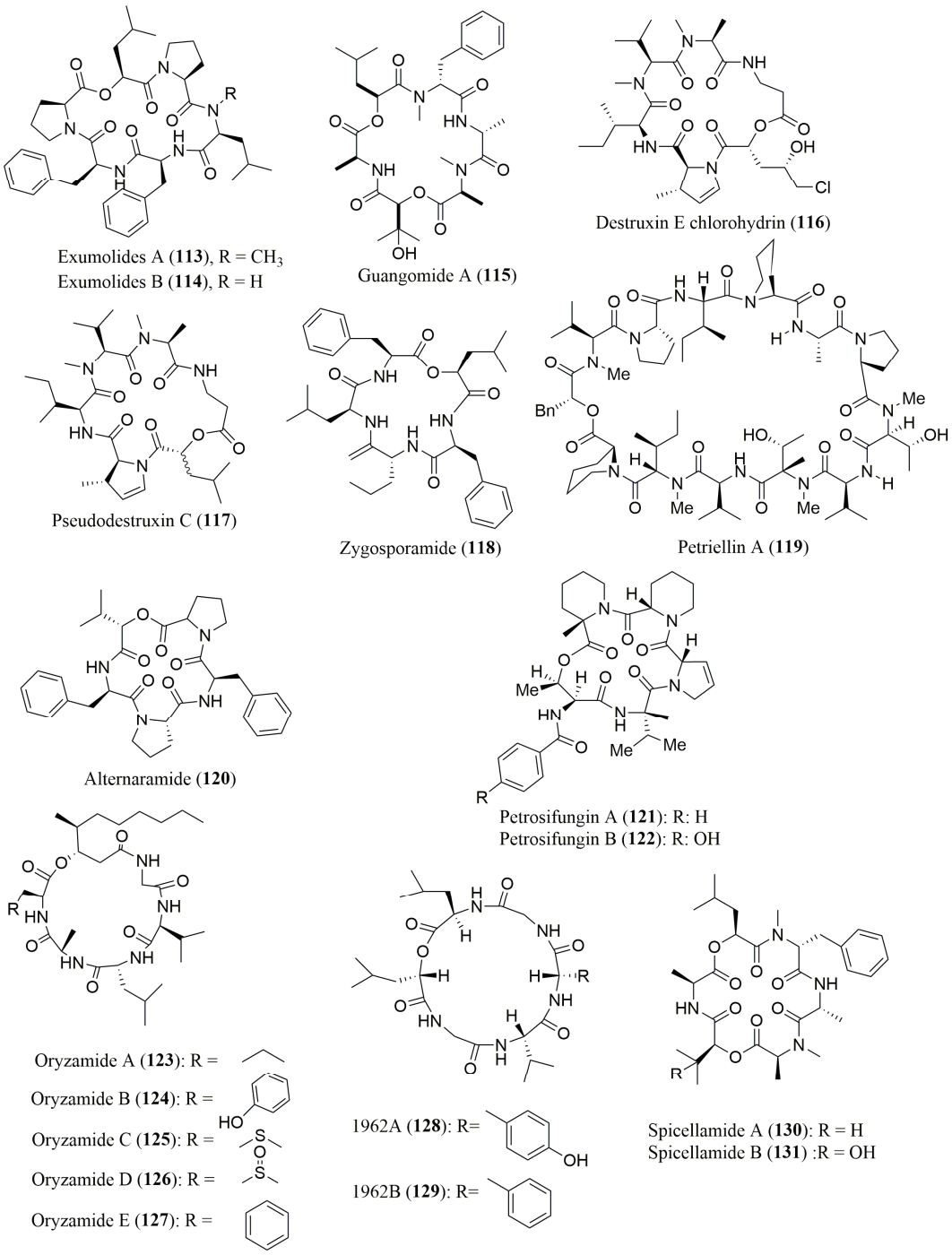


Figure 9. Structure of cyclic depsipeptides **113**–**131**, isolated from marine-derived fungi.

Table 5. Cyclic depsipeptides from marine-derived fungi.

Peptide	Source	aa Composition	Chromatographic Conditions	Biological Activities	Ref.
Exumolides A (**113**) and B (**114**)	Fungus of the genus *Scytalidium* sp.	L-Pro, L-Phe, *N*-Me-L-Leu	Marfey's method (FDAA) combined with HPLC Hewlett Packard 1090 Diode Array, 5 µm (10 × 250 mm); MP: 10–50% aq ACN (0.1% TFA) Flow rate: 1.0 mL/min; UV detection at 340 nm	Antimicroalgal activity against unicellular chlorophyte *Dunaliella* sp	[113]
Guangomide A (**115**)	Sponge-derived fungus	*N*-Me-D-Phe	Marfey's method (FDAA) combined with HPLC Alltech Altima C_{18} column, 5 µm (10 × 250 mm) MP: ACN:H_2O (4:1 to 1:1 *v*/*v*); Flow rate: 1.0 mL/min; UV detection at 340 nm	Antibacterial activity against *Staphylococcus epidermidis* and *Enterococcus durans*	[114]
Destruxin E chlorohydrin (**116**) and pseudodestruxin C (**117**)	Marine-derived fungus *Beauveria felina*	*N*-Me-L-Val **116**: *N*-Me-L-Ala, L-Ile **117**: L-Phe	Marfey's method (FDAA) combined with HPLC C_{18} column, 5 µm (4.6 × 250 mm); MP: 10–20% ACN in 0.1 M NH_4OAc (pH = 5) Flow rate: 1.0 mL/min; UV detection at 340 nm	Cytotoxicity in NCI's 60 cell line panel	[115]
Zygosporamide (**118**)	Marine-derived fungus *Zygosporium masonii*	L-Phe, L-Leu, D-Leu	Marfey's method (FDAA) combined with HPLC C_{18}, Agilent column, 5 µm (4.6 × 250 mm) MP: 10–50% ACN (0.1% TFA) Flow rate: 1.0 mL/min; UV detection at 340 nm	Cytotoxicity in RXF 393 and SF-268 cancer cell lines	[116]
Petriellin A (**119**)	Coprophilous fungus *Petriella sordida*	*N*-Me-L-Ile, *N*-Me-L-Thr D-Phenyllactate	Marfey's method (FDAA) combined with HPLC C_{18} column (4.6 × 250 mm); Conditions not described; UV detection at 260 nm	Antifungal activity	[117]
Alternaramide (**120**)	Marine derived fungus *Alternaria* sp. SF-5016	L-Pro, D-Phe	Marfey's method (FDAA) combined with HPLC Capcell Pak C_{18} column; MP: 30–60% ACN in H_2O (0.1% HCOOH); Flow rate: 1.0 mL/min	Antibacterial activity against *Bacillus subtilis* and *Staphylococcus aureus*	[118]
Petrosifungins A (**121**) and B (**122**)	*Penicillum brevicompac-tum*	L-Val, L-Pro, L-Thr, L-pipecolinic acids	Marfey's method (FDAA) combined with HPLC C_{18} column, Waters, 5 µm (2.1 × 150 mm); MP: H_2O or ACN (0.05% TFA); Flow rate: 1.0 mL/min	Not described	[119]
Oryzamides A–E (**123**–**127**)	Sponge-Derived fungus *Nigrospora oryzae* PF18	L-Ala, D-Leu, L-Val **123**: L-Leu; **124**: L-Tyr **125** and **126**: L-Met; **127**: L-Phe	Marfey's method (FDLA) combined with UHPLC Acquity UHPLC BEH column, 1.7 µm (2.1 × 250 mm); MP: 10–100% ACN in H_2O with 0.1% HCOOH; Flow rate: 0.5 mL/min; UV detection at 360 nm	No cytotoxicity, antibacterial, antiparasitic, and NF-*k*B activities	[122]
Spicellamide A (**128**) and B (**129**)	Marine-derived fungus *Spicellum roseum*	*N*-Me-D-Phe, *N*-Me-L-Ala, L-Ala	Marfey's method (FDAA) combined with HPLC C_{18} column; Macherey-Nagel Nucleodur 100, 5 µm (2.0 × 125 mm); MP: MeOH:H_2O (10:90 *v*/*v* to 100% MeOH) or 100% MeOH with NH_4Ac, 2 mmol	**129**: Cytotoxicity	[123]
		L-2-hydroxyisocaproic acid	Ligand Exchange Type CSP; Phenomenex Chirex 3126 *N*,*S*-dioctyl-(D)-penicillamine (4.6 × 50 mm) MP: 2 mM $CuSO_4$ in ACN:H_2O (15:85 *v*/*v*) Flow rate: 1.0 mL/min; UV detection at 254 nm		
Depsipeptides 1962A (**130**) and 1962B (**131**)	Endophytic fungus *Kandelia candel*	L-Tyr, L-Val, D-Leu, (*S*)-*O*-Leu	Crown Ether CSP; Crownpak CR (+) column (0.4 × 150 mm), MP: 2 mM $CuSO_4$ aq. solutions Flow rate: 0.5 mL/min; UV detection at 200 nm	**131**: Activity against MCF-7 tumor cell line	[124]

aa—Amino acid; FDAA—1-Fluoro-2-4-dinitrophenyl-5-L-alanine amide; HPLC—High Performance Liquid Chromatography; MP—Mobile Phase; ACN—Acetonitrile; TFA—Trifluoracetic acid; MeOH—Methanol; TEA—Triethylamine; FDLA—1-Fluoro-2-4-dinitrophenyl-5-D,L-leucine amide; NaOAc—Sodium acetate; NH_4OAc—Ammonium acetate.

Spicellamides A (**128**) and B (**129**), which were isolated from the marine-derived fungus *Spicellum roseum*, exhibited cytotoxicity against rat neuroblastoma B104 cell line, with an IC_{50} value of 6.2 μg/mL for spicellamide B (**129**) [123]. It is interesting to note that Marfey's method was not suitable for the determination of the configuration of all amino acid residues of these two peptides. Therefore, a chiral HPLC approach was also employed, using a ligand exchange type CSP [123]. Furthermore, the chiral HPLC, using the crown ether-based CSP Crownpak CR (+), was used as the only method for determination of the configuration of the amino acids residues to confirm the presence of L-Tyr, L-Val, D-Leu, and (*S*)-*O*-Leu in the cyclic depsipeptides 1962 A (**130**) and B (**131**), isolated from the endophytic fungus *Kandelia candel* [124]. The cyclic depsipeptide 1962 A (**130**) exhibited growth inhibitory activity against the human breast cancer cell line, MCF-7, with IC_{50} of 100 μg/mL [124].

4. Peptides from Marine Sponges

Marine sponges are an important source of new metabolites from the marine environment [125]. They are considered one of the most prolific sources of novel bioactive compounds, such as terpenoids, alkaloids, macrolides, nucleoside derivatives, polyethers, fatty acids, sterols, peroxides and other numerous organic compounds [17,126]. In addition, cyclic peptides and depsipeptides have also been isolated from marine sponges. Most bioactive compounds from sponges displayed myriad of biological activities including anti-inflammatory, antibiotic, antitumor, antimalarial, antiviral, antifouling, and immuno- or neurosuppressive [127]. However, a significant number of marine natural products isolated from sponges were tested for the anticancer activity, and many of them were successfully undergoing to preclinical and clinical trials [126,128]. More recently, among bioactive compounds discovered from marine sponges, bioactive peptides have aroused attention of many researchers [8,17].

4.1. Cyclic Peptides

Several works reported the determination of the stereochemistry of the amino acid residues of diverse peptides isolated from marine sponges (Figures 10 and 11), most of which described the application of Marfey's method, using FDAA as the derivatization reagent (Table 6). By using Marfey's method, Randazzo et al. [129] have showed that a 16-membered cyclic peptide, haliclamide (**132**), isolated from the Vanuatu marine sponge *Haliclona* sp., comprised the amino acid *N*-Me-L-Phe. The absolute configuration analysis of the amino acid residues of microsclerodermins J (**133**) and K (**134**), isolated from the sponge *Microscleroderma herdmani*, indicated, besides the amino acids common to both microsclerodermins, the presence of L-Phe, and L-Gly in **133**, and L-Val, and L-Ala in **134** [130]. Moreover, in the case of euryjanicins E–G (**135**–**137**), isolated from the Caribbean sponge *Prosuberites laughlini* [131], chujamide A (**138**), isolated from *Suberites waedoensis* [132], and kapakahines A–D (**139**–**142**), isolated from *Cribrochalina olemda* [133], all the amino acid residues were proved to have the L configuration. However, except for D-Phe, all the amino acid residues of koshikamide B (**143**), isolated from the marine sponge *Theonella* sp., were shown to possess L-configuration [134]. Furthermore, perthamides C–F (**144**–**147**), isolated from the sponge marine *Theonella swinhoei*, were found to comprise L-ThrOMe, and L-Phe; while perthamides C (**144**) and D (**145**) also comprise in their structures L-Asp, and (2*R*,3*S*)-βOHAsp [135,136]. Marfey's method was also successfully used for evaluation of the stereochemistry of the amino acids of the cyclic peptides stylisins 1 (**148**) and 2 (**149**), stylissatins B–D (**152**–**154**), and carteritins A (**150**) and B (**151**), isolated from marine sponge *Stylissa* sp. [137–139], as well as of callyaerin G (**155**), isolated from the marine sponge *Callyspongia aerizusa* [140].

The marine sponge cyclic peptides whose configuration of their amino acids constituent was determined by Marfey's method, were found to display interesting biological activities. For examples, haliclamide (**132**) exhibited cytotoxicity against NSCLC-N6 cell line, with an IC_{50} value of 4.0 μg/mL [129], while koshikamide B (**143**) showed growth inhibitory activity against P388 and HCT-116 cell lines, with IC_{50} values of 0.45 and 7.5 μg/mL, respectively [134]. Callyaerin G (**155**) also exhibited cytotoxicity against mouse lymphoma cell line (L5178Y), and HeLa cell line, with ED_{50} values of 0.53 and 5.4 μg/mL,

respectively [140]. Moreover, perthamides C (**144**), D (**145**) and F (**147**) showed anti-inflammatory activity, with perthamide F (**147**) having a promising antipsoriatic effect [135,136].

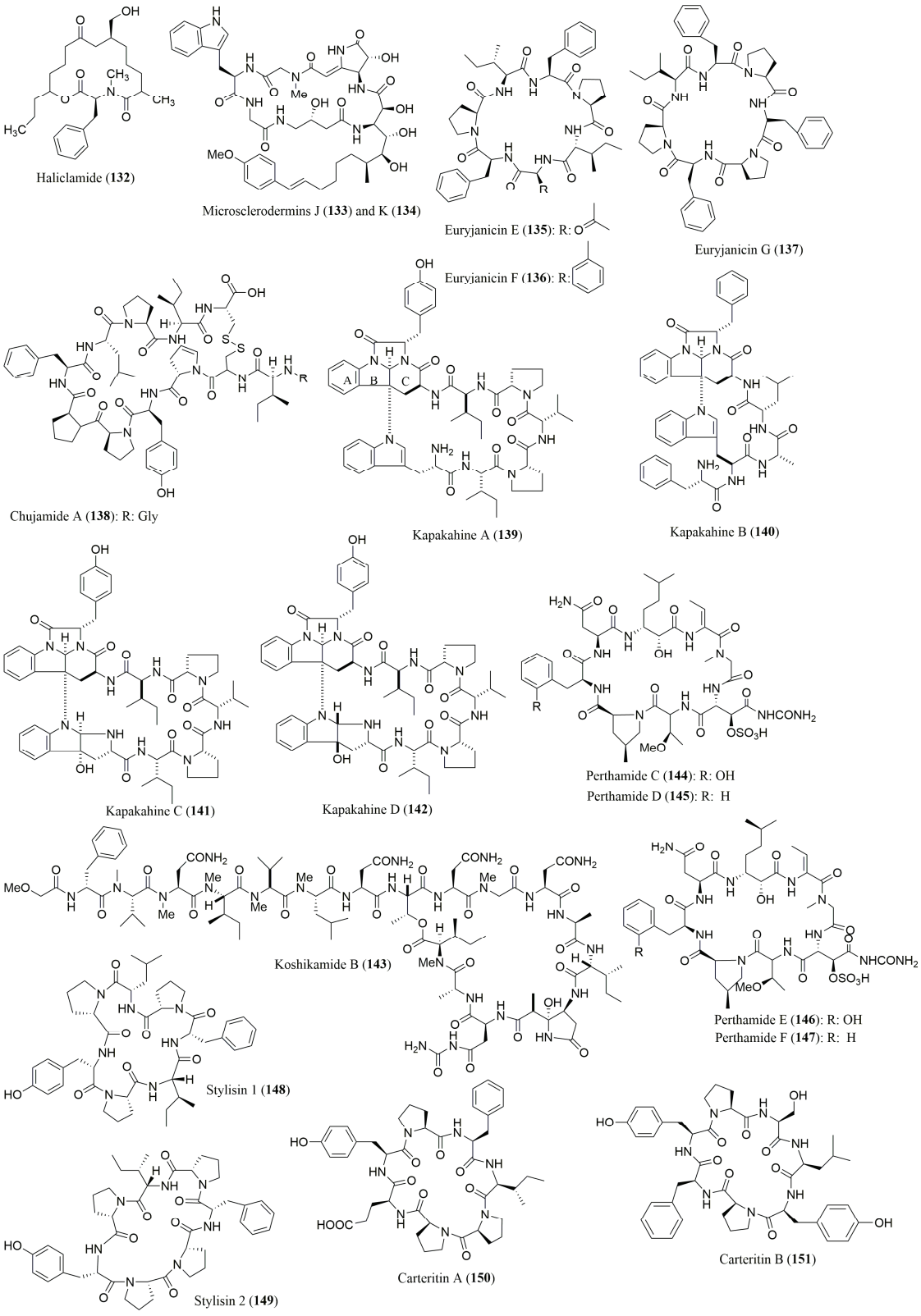


Figure 10. Structure of cyclic peptides **132**–**151**, isolated from marine sponges.

The simultaneous application of Marfey's method, using FDAA as derivatization reagent, and chiral HPLC, using a ligand exchange type CSP, afforded the total assignment of the configuration of all the amino acid residues of reniochalistatins A–E (**156–160**) [141]. Reniochalistatins A–E (**156–160**), the cyclic peptides isolated from the marine sponge *Reniochalina stalagmitis*, were found to have all the amino acid residues with L configuration, including L-Asn and L-Trp in reniochalistatins A (**156**) and E (**160**) respectively [141]. The octapeptide reniochalistatin E (**160**) exhibited cytotoxicity towards myeloma RPMI-8226, and gastric MGC-803 cell lines (IC_{50} values of 4.9 and 9.7 μM, respectively) [141].

Phakellistatins 15–18 (**161–164**) were analysed only by chiral HPLC, using the ligand exchange type Chirex 3126 D-penicillamine CSP, being able to identify that all the amino acids presented L-configuration. Furthermore, phakellistatins 15 (**161**) and 16 (**162**) exhibited cytotoxicity against P388 cancer cell line, with IC_{50} values of 8.5 and 5.4 μM, respectively, while phakellistatin 16 (**162**) was also active against BEL-7402 cancer cell line, with an IC_{50} value of 14.3 μM [142].

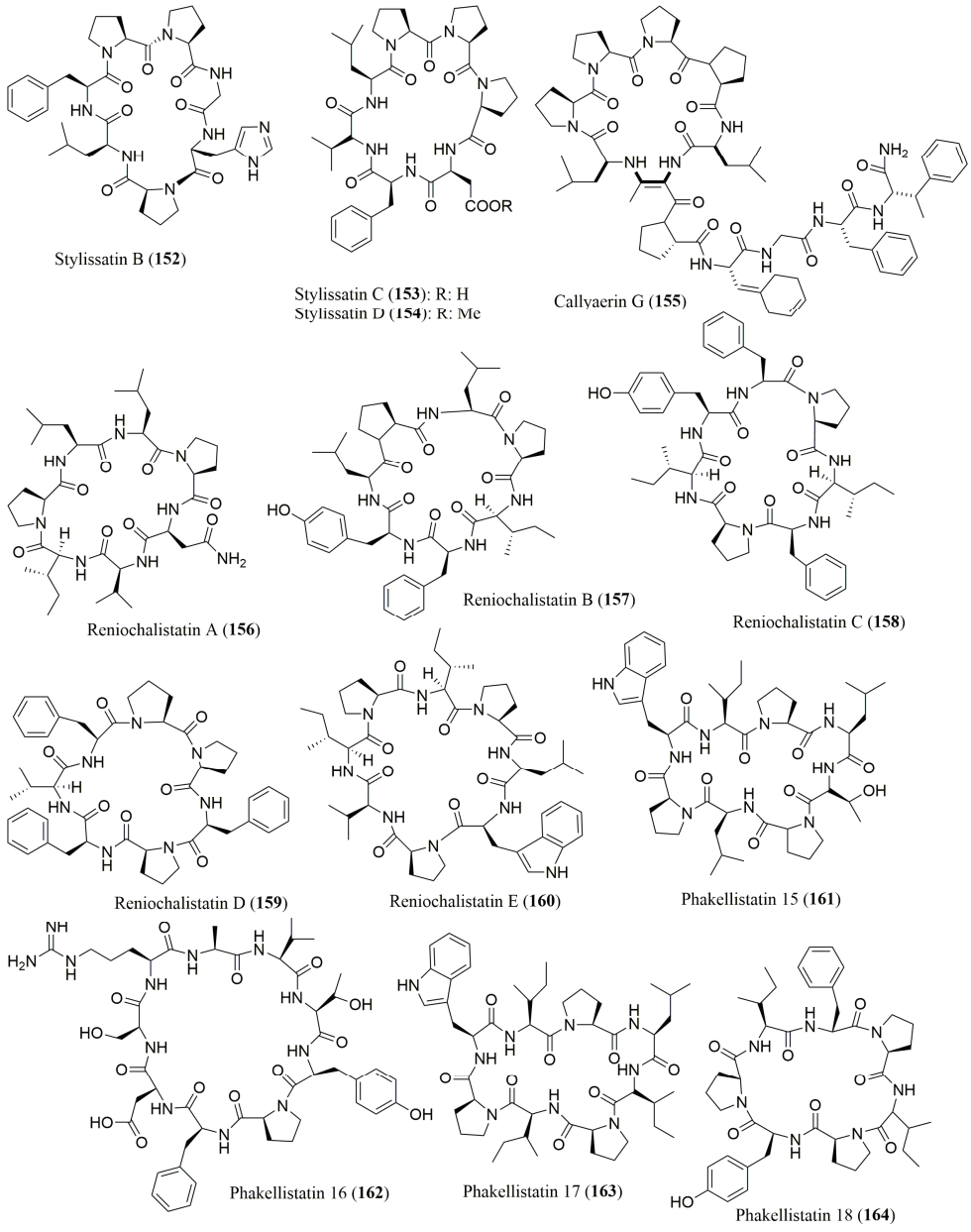


Figure 11. Structure of cyclic peptides **152–164**, isolated from marine sponges.

Table 6. Cyclic peptides from marine sponges.

Peptide	Source	aa Composition	Chromatographic Conditions	Biological Activities	Ref.
Haliclamide (**132**)	Vanuatu marine sponge *Haliclona* sp.	*N*-Me-L-Phe	Marfey's method (FDAA) combined with HPLC Vydac C18; MP: ACN in H_2O with 0.1% TFA (9:1 to 1:1 *v*/*v*); UV detection at 340 nm	Cytotoxicity against NSCLC-N6 carcinoma cell line	[129]
Microsclerodermins J (**133**) and K (**134**)	Deep water sponge *Microscleroderma herdmani*	L-Ile, L-Thr **133**: L-Phe, L-Gly **134**: L-Val, L-Ala	Marfey's method (FDAA) combined with HPLC C_{18} column, 5 µm (4.6 × 150 mm) Flow rate: 1.0 mL/min; UV detection at 340 nm	Activity against opportunistic pathogenenic fungi	[130]
Euryjanicins E–G (**135**–**137**)	The Caribbean Sponge *Prosuberites laughlini*	L-Pro, L-Ile, L-Phe **135**: L-Asp	Marfey's method (FDAA) combined with HPLC C_{18} column, 5 µm (4.6 × 150 mm) Flow rate: 1.0 mL/min; UV detection at 340 nm	No significant activity cytotoxicity against the National Cancer Institute 60 tumor cell line panel	[131]
Chujamide A (**138**)	Marine sponge *Suberites waedoensis*	L-Pro, L-Tyr, L-Cys, L-Leu, L-Phe L-Ile (*S*)	Marfey's method (FDAA) combined with HPLC ESI-LC/MS YMC ODS-A column, 5 µm (4.6 × 250 mm) MP: H_2O:ACN (80:20 to 30:70 *v*/*v*) Flow rate: 0.7 mL/min; UV detection at 360 nm	Weak cytotoxicity against A549 and K562 cell lines	[132]
Kapakahines A–D (**139**–**142**)	Marine Sponge *Cribrochalina olemda*	L-Val, L-Ile, L-Leu, L-Trp, L-Phe, L-Ala, L-Pro, L-Try	Marfey's method (FDAA) combined with HPLC Cosmosil C_{18}-MS column, 5 µm (4.6 × 250 mm) MP 37.5% ACN in 0.05% TFA or 20% or 38% ACN in 50 mM NH_4OAc	**139**–**141**: Cytotoxicity against P388 cell line **139**: Inhibition against protein phosphatase	[133]
Koshikamide B (**143**)	Marine sponge *Theonella* sp.	D-Phe, L-Thr, *N*-Me-L-Val, *N*-Me-L-Asn, *N*-Me-L-Leu	Marfey's method (FDAA) combined with HPLC ODS HPLC (10 × 250 mm); MP: ACN:H_2O:TFA (25:75:0.05 to 55:45:0.05 *v*/*v*/*v*); Flow rate: 1.0 mL/min; UV detection at 340 nm	Cytotoxicity against P388 and HCT-116 tumor cell lines	[134]
Perthamides C (**144**) and D (**145**)	Solomon Lithistid sponge *Theonella swinhoei*	L-Asp, L-ThrOMe, (2*R*,3*S*)-βOHAsp, L-Phe	Marfey's method (FDAA) combined with HPLC/MS Proteo C_{18} column (1.8 × 25 mm) MP: 10–50% aq ACN with 5% HCOOH and 0.05% TFA Flow rate: 0.15 mL/min	Anti-inflammatory activity	[135]
Perthamides E (**146**) and F (**147**)	Polar extracts of the sponge *Theonella swinhoei*	**146**: L-ThrOMe **147**: L-Phe	Marfey's method (FDAA) combined with HPLC Proteo C_{18} column, (1.8 × 25 mm); MP: 10–50% aq ACN with 5% HCOOH and 0.05% TFA Flow rate: 0.15 mL/min	**147**: IL-8 release inhibition	[136]
Stylisins 1 (**148**) and 2 (**149**)	Jamaican sponge *Stylissa caribica*	L-Pro, L-Tyr, L-Ile **148**: L-Leu, L-Phe	Marfey's method (FDAA) combined with HPLC HPLC water Nova Pack column (3.9 × 150 mm) MP: TEAP buffer (pH 3.0 ± 0.02):ACN (90 to 60% TEAP) UV detection at 340 nm	No antimicrobial, antimalarial, anticancer, anti-HIV-1, anti-Mtb and anti-inflammatory activities	[137]
Carteritins A (**150**) and B (**151**)	Marine sponge *Stylissa carteri*	**150**: L-Pro, L-Phe, L-Ile, L-Pro (*trans*), L-Pro (*cis*), L-Glu, L-Tyr; **151**: L-Pro (*trans*), L-Leu, L-Tyr, L-Pro(*cis*)	Marfey's method (FDAA) combined with HPLC Cosmosil C_{18} MS (4.6 × 250 mm); MP: H_2O:TFA (100:0.1) to ACN:H_2O:TFA (50:50:0.1 *v*/*v*/*v*); Flow rate: 1.0 mL/min; UV detection at 340 nm	**150**: Cytotoxicity against HeLa, HCT116, and RAW264 cells	[139]

Table 6. *Cont.*

Peptide	Source	aa Composition	Chromatographic Conditions	Biological Activities	Ref.
Stylissatins B–D (**152**–**154**)	Marine sponge *Stylissa massa*	L-Pro, L-Phe, L-Leu **152**: L-His **153**–**154**: L-Asp, L-Val	Marfey's method (FDAA) combined with HPLC Thermo BDS Hypersil C_{18} column, 5 µm (4.6 × 150 mm); MP: 30–70% MeOH:H_2O (H_3PO_4) Flow rate: 1.0 mL/min; UV detection at 340 nm	**152**: Inhibitory effects against a panel of human tumor cell lines including HCT-116, HepG2, BGC-823, NCI-H1650, A2780, and MCF7	[138]
Callyaerin G (**155**)	Indonesian sponge *Callyspongia aerizusa*	L-Pro, L-Leu, L-Phe, L-FGly	Marfey's method (FDAA) combined with HPLC/MS; Conditions not described	Cytotoxicity against L5178Y, Hela, and PC12	[140]
Reniochalistatins A–E (**156**–**160**)	Marine sponge *Reniochalina stalagmitis*	L-Pro, L-Phe, L-Val, L-Leu, L-Ile, L-Tyr	Ligand Exchange Type CSP; MCI GELCRS 10 W (4.6 × 50 mm); MP: 2 mM $CuSO_4$:H_2O solution Flow rate: 1.0 mL/min; UV detection at 254 nm	**160**: Cytotoxicity against RPMI-8226, MGC-803, HL-60, HepG2, and HeLa	[141]
		156: L-Asn **160**: L-Trp	Marfey's method (FDAA) combined with HPLC YMC-Park Pro C_{18}, 5 µm (4.6 × 250 mm) MP: 2 mM $CuSO_4$:H_2O solution Flow rate: 1.0 mL/min; UV detection at 254 nm		
Phakellistatins 15–18 (**161**–**164**)	South china sea sponge *Phakellia fusca*	L-Pro **161**: L-Trp, L-Ile, L-Leu, L-Thr; **162**: L-Phe, L-Asp, L-Ser, L-Arg, L-Ala, L-Val, L-Thr, L-Tyr; **163**: L-Trp, L-Val, L-Leu, L-Ile; **164**: L-Tyr, L-Ile, L-Phe	Ligand-exchange type CSP; Chirex 3126 (D)-penicillamine column (4.6 × 150 mm) MP: aq 2 mM $CuSO_4$:MeOH (85:15 to 70:30 *v*/*v*) or aq 1 mM/0.5 mM $CuSO_4$; Flow rate: 0.5 or 1.0 mL/min	**161**: Cytotoxicity against P388 cancer cell line **162**: Cytotoxicity against P388 and BEL-7402 cancer cell lines	[142]

aa—Amino acid; FDAA—1-Fluoro-2-4-dinitrophenyl-5-L-alanine amide; LC—Liquid Chromatography; MS—Mass spectrometry; HPLC—High Performance Liquid Chromatography; MP—Mobile Phase; TEAP—Triethylammonium phosphate; ACN—Acetonitrile; TFA—Trifluoracetic acid; MeOH—Methanol; TEA—Triethylamine; IPA—Isopropyl alcohol; NaOAc—Sodium acetate; NH_4OAc—Ammonium acetate.

4.2. Cyclic Depsipeptides

A number of cyclic depsipeptides (Figures 12 and 13), have been reported from marine sponges and Marfey's method using FDAA as the derivatization reagent was the most used for the determination of absolute configuration of the amino acid residues. Table 7 gives some examples of the cyclic depsipeptides, isolated from marine sponges, whose stereochemistry of their amino acid residues was determined by Marfey's method. By application of this method, callipeltins B (**165**) and C (**166**), isolated from the marine lithistida sponge *Callipelta* sp., were found to have in their structure L-Ala, *N*-Me-L-Ala, L-Leu, L-Thr and D-Arg [143]. For halipeptins A (**167**) and B (**168**), isolated from the marine sponge *Haliclona* sp., the referred method was only able to determine the configuration for L-Ala [144]. Marfey's method was successfully used to determine the absolute configuration of the amino acid constituents of several marine sponge cyclic peptides including phoriospongin A (**169**) and B (**170**), isolated from the marine sponges *Phoriospongia* sp. and *Callyspongia bilamellata* [145], mirabamides A–D (**171–174**), isolated from the marine sponge *Siliquarias-pongia mirabilis* [146], and neamphamides B–D (**175–177**), isolated from the marine sponge *Naemphius huxleyi* [147]. Furthermore, the stereochemistry determination of amino acid residues in pipecolidepsins A (**178**) and B (**179**), isolated from the marine sponge *Homophymia lamellose*, confirmed the presence of several L and D amino acid residues, besides the (3*S*,4*R*) diMe-L-Glu and (2*S*,3*S*)-EtO-Asp present in both peptides [148]. Stellatolide A (**180**), a cyclic depsipeptide isolated from *Ecionemia acervus*, was found to have *N*-Me-D-Ser and D-*allo*-Thr, among other L-configured amino acids [149]. The amino acid constituents of the cyclic depsipeptides cyclolithistide A (**181**) and nagahamide A (**182**), both isolated from the sponge *Theonella swinhoei*, were all found to have the *S* or L-configuration, and the 3-amino-5-hydroxybenzoic acid (AHBA) residue in nagahamide A (**182**) was established to have 3*S* configuration [150,151].

Almost all the cyclic peptides isolated from marine sponges displayed a variety of biological activities. Thus, callipeltin C (**166**) [143], cyclolithistide A (**181**) [150], and mirabamides A–D (**171–174**) [146] exhibited growth inhibitory activity against *Candida albicans*. Moreover, mirabamides A–D (**171–174**) also exhibited potent anti-HIV activities towards several HIV strains [146] whereas neamphamides B–D (**175–177**) displayed cytotoxic activity against several human cancer cell lines, including A549, HeLa, LNCaP, PC3, HEK, and NFF, with IC_{50} values ranging from 88 to 370 nM [147].

A simultaneous use of Marfey's method and chiral HPLC analysis for stereochemical analysis of the amino acids of this type of peptides have been reported (Table 7). For examples, the absolute configuration of the amino acids of theopapuamides B (**183**) and C (**184**) and celebesides A–C (**185–187**), isolated from an Indonesian sponge *Siliquariaspongia mirabilis*, was successful assigned by HPLC-MS analysis of FDAA derivatives as well as via chiral HPLC analysis using a ligand exchange type CSP [152]. In the case of theopapuamide (**188**), isolated from a papua new Guinea Lithistid Sponge *Theonella swinhoei*, Marfey's method was used to confirm the presence of D-*allo*-Thr, whereas chiral HPLC using a ligand exchange type CSP, revealed the presence of *N*-Me-L-Leu, D-Asp, L-Leu and *N*-Me-L-Glu in its structure [153]. The absolute configuration of the amino acid residues of a new sulfated cyclic depsipeptide, mutremdamide A (**189**) and six new highly *N*-methylated peptides, koshikamides C–H (**190–195**), isolated from different deep-water specimens of *Theonella swinhoei* and *Theonella cupola*, was also established by using both approaches. However, two different columns (C_{12} and C_{18}) were used in Marfey's method. By using chiral HPLC, it was possible to identify the amino acid residue *N*-Me-allo-L-Ile in koshikamide H (**195**) [154]. These cyclic peptides showed interesting biological activities. While theopapuamide (**188**) was cytotoxic against CEM-TART and HCT cell lines (IC_{50} values of 0.5 and 0.9 μM, respectively) [153], koshikamides F (**193**) and H (**195**) were active against a CCR5-using viral envelope, with IC_{50} values of 2.3 and 5.5 μM [154].

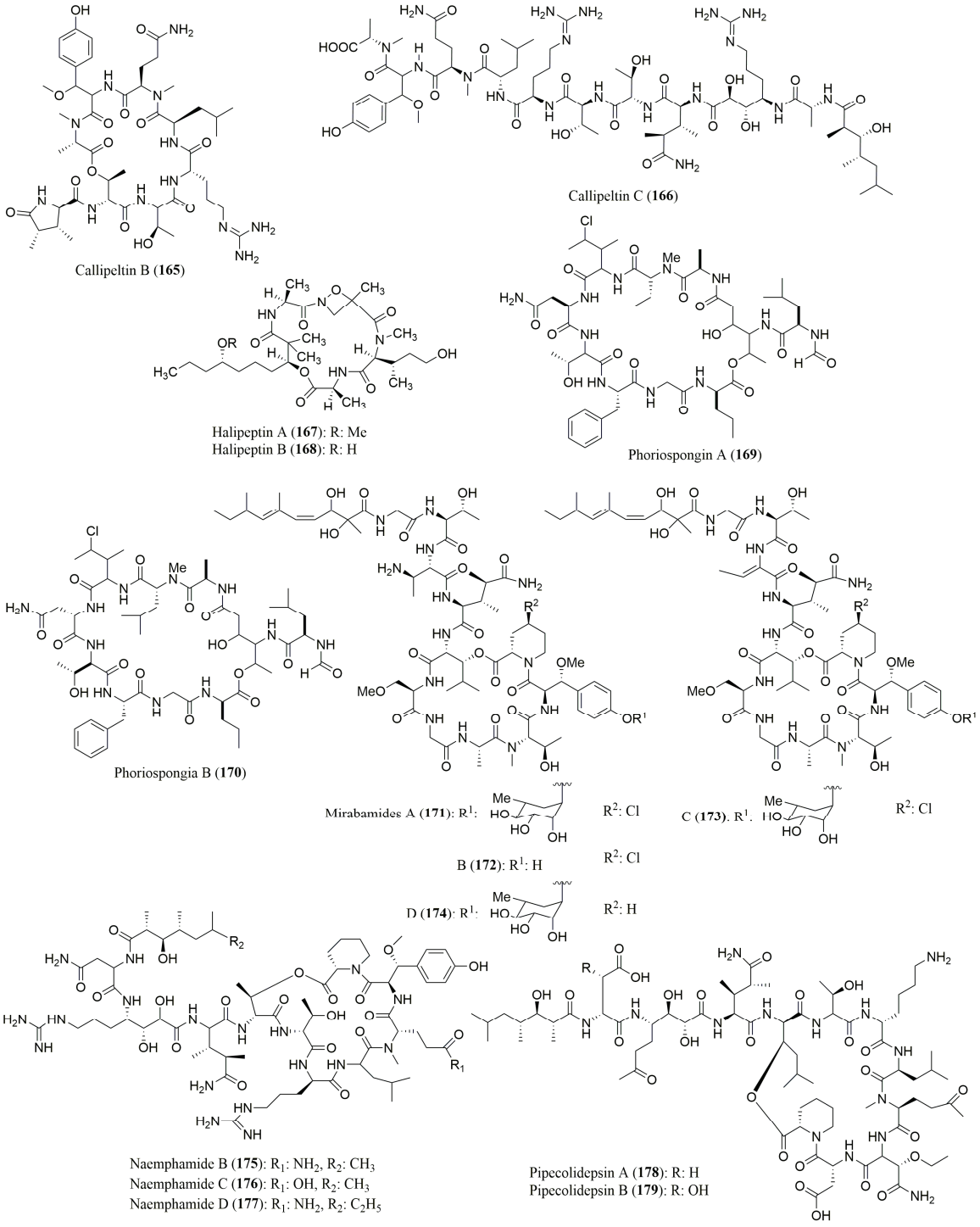


Figure 12. Structure of cyclic depsipeptides **165–179**, isolated from marine sponges.

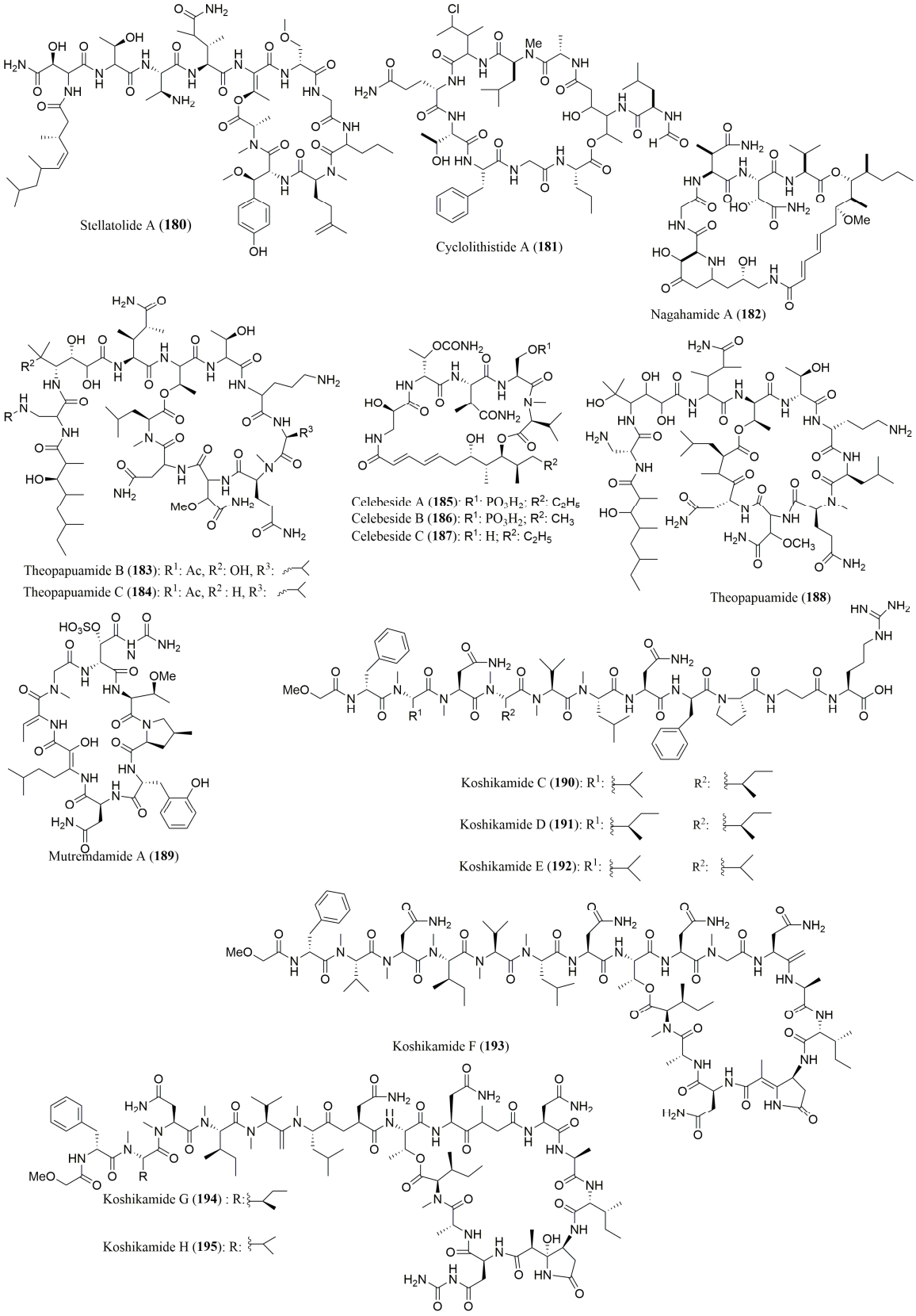


Figure 13. Structure of cyclic depsipeptides **180–195**, isolated from marine sponges.

Table 7. Cyclic depsipeptides from marine sponges.

Peptide	Source	aa Composition	Chromatographic conditions	Biological activities	Ref.
Callipeltins B (**165**) and C (**166**)	*Callipelta* sp.	L-Ala, D-Arg, L-Thr, *N*-Me-L-Ala, L-Leu	Marfey's method (FDAA) combined with HPLC; Column not described; MP: TEAP (50 nM, pH 3.0):ACN 90–50% TEAP Flow rate: 2.0 mL/min; UV detection at 340 nm	Cytotoxicity **166**: Growth inhibitory activity against *Candida albicans*	[143]
Halipeptiins A (**167**) and B (**168**)	*Haliclona* species	L-Ala	Marfey's method (FDAA) combined with HPLC Vydac C_{18} column; MP: H_2O (0.1% TFA):ACN (0:1 to 1:1 *v*/*v*) UV detection at 340 nm	**168**: Anti-inflammatory activity	[144]
Phoriospongin A (**169**) and B (**170**)	*Phoriospongia* sp. and *Callyspongia bilamellata*	D-Asp, D-*allo*-Thr, D-Ala, L-Phe, D-Leu, D-*nor*-Val, *N*-Me-D-*nor*-Val **170**: *N*-Me-L-Leu	Marfey's method (FDAA) combined with HPLC C_{18} column, 5 µm (4.6 × 250 mm) Flow rate: 1.0 mL/min; UV detection at 340 nm	Nematocidal activity against the parasite *Haemonchus contortus*	[145]
Mirabamides A–D (**171**–**174**)	*Siliquarias-pongia mirabilis*	*N*-Me-L-Thr, L-Thr, L-Ala, D-3-OMeAla, (2*R*,3*R*)-3-OH-Leu (3*S*,4*R*)-diMe-L-Glu, (2*S*,3*R*)-diaminobutanoic acid; **174**: L-HPr	Marfey's method (FDAA) combined with HPLC Phenomenex Jupiter Proteo C_{12} column, 4 µm (4.6 × 150 mm) MP: 25–70% ACN; Flow rate: 0.5 mL/min	**171**: Anti-HIV activity **173** and **174**: Antibacterial activity **171**–**173**: Antifungal activity	[146]
Neamphamides B (**175**), C (**176**) and D (**177**)	*Neamphius huxleyi*	D-Arg, L-Asn, L-Hpr, L-Leu, D-*allo*-Thr **175** and **177**: *N*-Me-L-Gln **176**: *N*-Me-L-Glu	Marfey's method (FDAA) combined with HPLC Phenomenex Luna Column C_{18}, 3 µm (2.0 × 150 mm) MP: H_2O:ACN:HCOOH (100:0:0.1 to 0:100:0.1 *v*/*v*/*v*) UV detection at 340 nm	Growth inhibition of human cell lines: A549, HeLa, LNCaP, PC3, and NFF	[147]
Pipecolidepsins A (**178**) and B (**179**)	*Homophymia lamellosa*	D-Asp, L-Leu, D-Lys, D-*allo*-Thr, (3*S*,4*R*) diMe-L-Glu, (2*S*,3*S*)-EtO-Asp, *N*-Me-L-Glu, L-Pip	Marfey's method (FDAA) combined with HPLC Symmetry C_{18}, 5 µm (4.6 × 150 mm); MP: 20–50% ACN (0.04% TFA) in H_2O (0.04% TFA); Flow rate: 0.8 mL/min	Cytotoxicity against three human tumor cell lines (A-549, HT-29, and MDA-MB-231)	[148]
Stellatolide A (**180**)	*Ecionemia acervus*	*N*-Me-L-Ala, L-Leu, *N*-Me-L-Gln, *N*-Me-D-Ser, D-*allo*-Thr	Marfey's method (FDAA) combined with HPLC Hewlett-Packard Hypersil BDS-C_{18}, 4 µm (4.0 × 100 mm); MP: H_2O (0.1% TFA):ACN (90:10 to 50:50 *v*/*v*); Flow rate: 1.0 mL/min	In in vitro antiproliferative activity	[149]
Cyclolithistide A (**181**)	*Theonella swinhoei*	nor-*S*-Val, *S*-Phe, S-Gln, *N*-Me-*S*-Leu, *S*-Ala, *S*-Allo-*S*-Thr	Marfey's method (FDAA) combined with HPLC ODS (4.6 × 250 mm); MP: 100% H_2O Flow rate: 2.0 mL/min; UV detection at 210 nm	Antifungal activity against *Candida albicans* (ATCC 24433)	[150]
Nagahamide A (**182**)	*Theonella swinhoei*	L-Val, L-Ser, 3*S*-AHBA	Marfey's method (FDAA) combined with HPLC ODS column (4.6 × 250 mm); Conditions not described	Antibacterial activity	[151]
Theopapuamides B (**183**) and C (**184**), Celebesides A–C (**185**–**187**)	*Siliquarias-pongia mirabilis*	**185**: L-βMeAsn	Marfey's method (FDAA) combined with HPLC/MS Phenomenex Jupiter Proteo C_{12} column, 4 µm (4.6 × 150 mm) MP: 25–70% ACN with 0.01 M TFA; Flow rate: 0.5 mL/min Ligand Exchange Type CSP Phenomenex column, Chirex Phase 3126 (D) (4.6 × 150 mm); MP: 1 mM $CuSO_4$:ACN (95:5 *v*/*v*) Flow rate: 0.5 mL/min; UV detection at 254 nm	**185**: Inhibits HIV-1 Entry **183**–**185**: Cytotoxic to human colon tumor cell line (HCT-116) **183** and **185**: Antifungal activity against *Candida albicans*	[152]

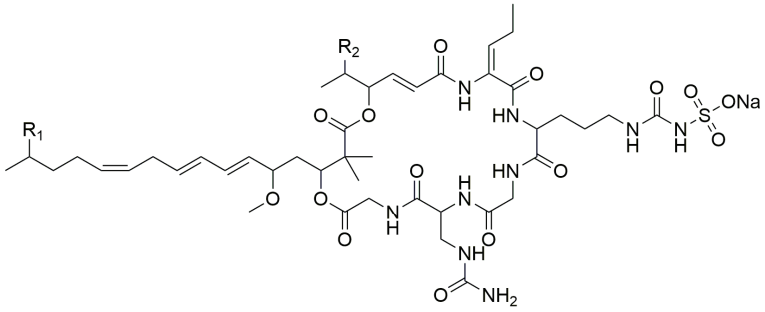
Table 7. *Cont.*

Peptide	Source	aa Composition	Chromatographic conditions	Biological activities	Ref.
Theopapuamide (**188**)	Lithistid sponge *Theonella swinhoei*	*N*-Me-L-Leu, D-Asp, L-Leu, *N*-Me-L-Glu	Ligand Exchange Type CSP Chirex Phase 3126 (D), 5 µm (4.6 × 250 mm); MP: IPA: 2 mM $CuSO_4$ (5:95 *v*/*v*) Flow rate: 1.0 mL/min; UV detection at 254 nm	Cytotoxicity against CEM-TART and HCT-cell lines	[153]
		D-allo-Thr	Marfey's method (FDAA) combined with HPLCPhenomenex C_{18}, 5 µm (4.6 × 250 mm); MP: 10–50% ACN in H_2O (0.05% TFA); Flow rate: 1.0 mL/min; UV detection at 340 nm		
Mutremdamide A (**189**) and Koshikamides C–H (**190**–**195**)	*Theonella swinhoei* and *Theonella cupola*	**189**: *N*-Me-L-Val; **190**: *N*-Me-L-Val, *N*-Me-L-Asn, L-Asn, *N*-Me-L-Leu, L-Pro, *N*-Me-allo-L-Ile, D-Phe	Marfey's method (FDAA) combined with HPLC LC-MS analysis using a C_{12} column, 4 µm (4.6 × 250 mm); MP: ACN with 0.01% TFA; Flow rate: 0.5 mL/min	**189**–**195**: Anti-HIV-1 activity	[154]
		191 and **192**: *N*-Me-*allo*-L-Ile, *N*-Me-L-Val; **192**–**194**: *N*-Me-*allo*-L-Ile, L-Ala 1, D-Ala2, L-Asn	Marfey's method (FDAA) combined with HPLC LC-MS, C_{18} column, 4 µm (4.6 × 250 mm); MP: 20 mM buffer (AF):ACN (3:1 to 3:7 *v*/*v*); Flow rate: 0.5 mL/min		
		195: *N*-Me-allo-L-Ile	Chiral HPLC (column not described); MP: 1 mM $CuSO_4$:ACN (95:5 *v*/*v*); Flow rate: 0.5 mL/min; UV detection at 254 nm		

aa—Amino acid; FDAA—1-Fluoro-2-4-dinitrophenyl-5-L-alanine amide; LC—Liquid Chromatography; MS—Mass spectrometry; HPLC—High Performance Liquid Chromatography; MP—Mobile Phase; TEAP—Triethylammonium phosphate; ACN—Acetonitrile; TFA—Trifluoracetic acid; MeOH—Methanol; TEA—Triethylamine; NaOAc—Sodium acetate; NH_4OAc—Ammonium acetate.

4.3. Lipopeptides

The absolute configuration of the amino acids of new *N*-sulfoureidylated lipopeptides sulfolipodiscamides A–C (**196–198**), isolated from the *n*-butanol fraction of the marine sponge *Discodermia kiiensis* (Figure 14), was determined by Marfey's method to be L-Uda and L-Gly (Table 8). Compound **196** was found to be cytotoxic against the murine leukemia cell line P388 with a IC_{50} value of 15 μM [155].



Sulfolipodiscamide A (**196**) R_1: CH_3; R_2: CH_3
Sulfolipodiscamide B (**197**) R_1: H; R_2: CH_3
Sulfolipodiscamide C (**198**) R_1: CH_3; R_2: CH_2CH_3

Figure 14. Structure of cyclic lipopeptides **196–198**, isolated from marine sponges.

Table 8. Lipopeptides from marine sponge.

Peptide	Source	aa Composition	Chromatographic Conditions	Biological Activity	Ref.
Sulfolipo-discamides A–C (**196–198**)	Sponge *Discoderma kiiensis*	L-Uda, L-Gly	Marfey's method (FDAA) combined with HPLC Cosmosil C_{18}-MSII column (4.6 × 250 mm); MP: 100 mM $NaClO_4$ in 60% ACN Flow rate: 0.8 mL/min	**196**: Cytotoxicity against P388 cell line	[155]

aa—Amino acid; FDAA—1-Fluoro-2-4-dinitrophenyl-5-L-alanine amide; HPLC—High Performance Liquid Chromatography; MP—Mobile Phase; ACN—Acetonitrile.

5. Peptides from Other Marine Invertebrates and Algae

A number of diverse bioactive peptides such as cyclic peptides, cyclic depsipeptides and linear peptides have been isolated from other marine invertebrates including ascidians, commonly called tunicates, mollusks, among others [17]. Moreover, the potential applications of many bioactive compounds from marine algae, mainly red and brown as well as some green algae, were reported [156].

5.1. Cyclic Peptides

To the best of our knowledge, only five works described the analysis of the stereochemistry of the cyclic peptides from marine invertebrates and algae (Figure 15). In all reported works, Marfey's method was employed (Table 9). Among these, the determination of the absolute configuration of the cyclic hexapeptides didmolamides A (**199**) and B (**200**) and mollamides B (**201**) and C (**202**), isolated from the marine ascidian *Didemnum molle* from Madagascar and Indonesia, respectively, was performed by Marfey's method using FDAA as derivatization reagent [157,158]. These compounds showed interesting biological activities, particularly, cytotoxicity against A549, HT29 MEL28 tumor cell lines, with IC_{50} values ranging from 10 to 20 μg/mL for didmolamides A (**199**) and B (**200**) [157] while **201** showed antimalarial activity against *Plasmodium falciprum*, clones D6 and W2, with IC_{50} values of 2.0 and 21 μg/mL, respectively [158].

Furthermore, the stereochemical determination of antatollamides A (**203**) and B (**204**), isolated from the marine ascidian *Didemnum molle*, sanguinamide A (**205**), isolated from the sea slug

Hexabranchus sanguineus, and gamakamide E (**206**), isolated from the oysters *Crassostrea giga*, was carried out by Marfey's method using FDLA as a derivatization reagent. The analysis demonstrated that most of their amino acids have the L-configuration, with the exception of D-Ala and D-Lys in antatollamides A (**203**) and B (**204**), and gamakamide E (**206**), respectively [159–161].

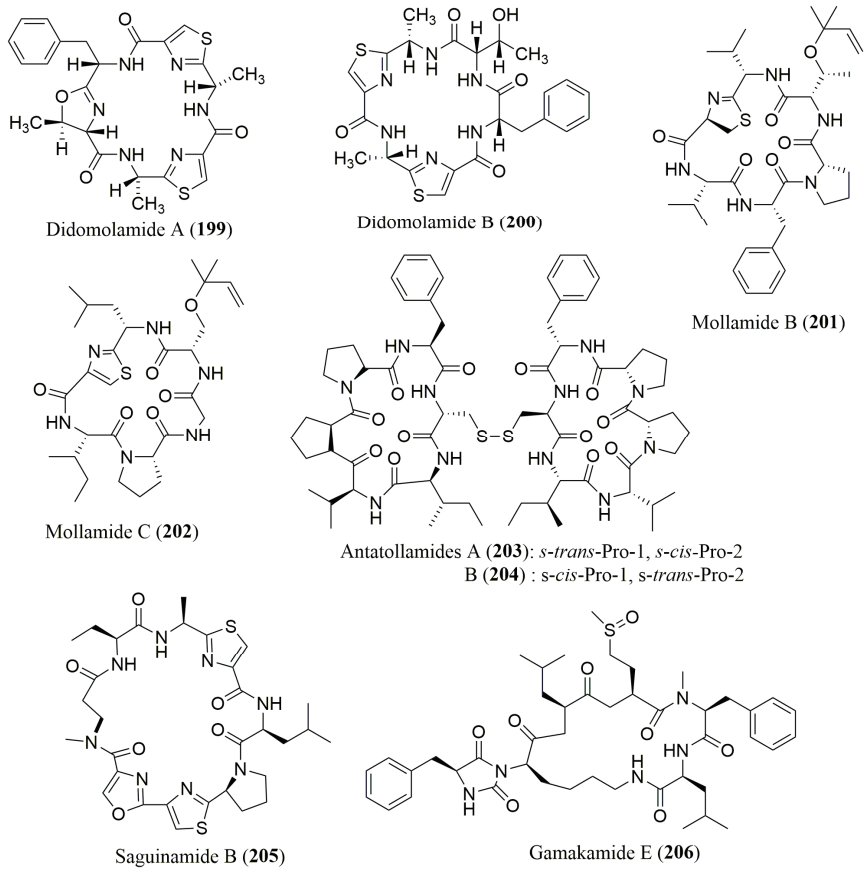


Figure 15. Structure of cyclic peptides **199**–**206**, isolated from marine invertebrates and marine algae.

Table 9. Cyclic peptides from marine invertebrates and algae.

Peptide	Source	aa Composition	Chromatographic Conditions	Biological Activities	Ref.
Didomolamides A (**199**) and B (**200**)	Ascidian *Didemnum molle*	L-Thr, L-Ala, L-Phe **200**: L-Tzl	Marfey's method (FDAA) combined with HPLC; MP: 50 mM (TEAP) buffer pH 3: ACN (9:1 to 1:1 *v*/*v*); Flow rate: 1.0 mL/min; UV detection at 340 nm	Cytotoxicity against A549, HT29 MEL28 tumor cell lines	[157]
Mollamides B (**201**) and C (**202**)	Tunicate *Didemnum molle*	L-Thr, L-Ile, L-Pro **201**: L-Val, L-Phe **202**: L-Ser, L-Leu	Marfey's method (FDAA) combined with HPLC; MP: 50 mM TEAP, pH 3.0: ACN (90:10 to 60:40 *v*/*v*) or 40 mM NH_4OAc, 70% ACN, and 30% MeOH (98:2 to 66:34 *v*/*v*) Flow rate: 1.0 or 0.8 mL/min; UV detection at 340 nm	**201**: Activity against HIV, *Plasmodium falciparum*, *Lieshmania donovan*, and cytotoxicity against H460, MCF7, SF-268 cell lines	[158]
Antatollamides A (**203**) and B (**204**)	Ascidian *Didemnum-molle*	L-Ile, L-Phe, L-Val, L-Pro, D-Ala	Marfey's method (FDLA) combined with HPLC/MSHypersil Gold C_{18} column, 1.9 µm (2.1 × 50 mm); MP: H_2O 0.1%; HCOOH:ACN (85:15 to 55:45 *v*/*v*) Flow rate: 0.5 mL/min	**203**: Weak cytotoxicity against a chronic lymphocytic leukemia cell line	[159]

Table 9. *Cont.*

Peptide	Source	aa Composition	Chromatographic Conditions	Biological Activities	Ref.
Sanguinamide A (**205**)	*Nudibranch Hexabranchs sanguineus*	L-Pro, L-Ile, L-Ala, L-Phe	Marfey's method (FDLA) combined with HPLC Agilent Zorbax SB-Aq C_{18} column, 5 µm (4.6 × 250 mm) MP: 80% (H_2O: 0.1% HCOOH), 20% (ACN)	Antifungal activity	[160]
Gamakamide E (**206**)	Oysters *Crassostrea giga*	L-Met(O), *N*-Me-L-Phe, L-Leu, D-Lys, L-Phe	Marfey's method (FDLA) combined with HPLC Conditions not described	No growth inhibition abilities	[161]

aa—Amino acid; FDAA—1-Fluoro-2-4-dinitrophenyl-5-L-alanine amide; HPLC—High Performance Liquid Chromatography; MP—Mobile Phase; ACN—Acetonitrile; TEAP—Triethylammonium phosphate; FDLA—1-Fluoro-2-4-dinitrophenyl-5-D,L-leucine amide; TFA—Trifluoracetic acid; MeOH—Methanol; TEA—Triethylamine; NH_4OAc—Ammonium acetate.

5.2. Cyclic Depsipeptides

To the best of our knowledge, only four works reported the determination of the stereochemistry of amino acid constituents of the cyclic depsipeptides from marine invertebrates and algae (Figure 16). Among these, three employed only Marfey's method, specifically for peptides **207**–**216**. However, for peptide **217**, Marfey's method was not efficient and, as a consequence, a ligand exchange type CSP was also used for complete determination of the configuration of its amino acids (Table 10).

The determination of the absolute configuration of the amino acids in kahalalides A–F (**207**–**212**), isolated from the marine mollusk *Elysia rufescens*, was performed by using FDLA as the derivatization reagent and the presence of diverse residues of L- and D-Val in these peptides was confirmed [162]. Using FDAA as the Marfey derivatization reagent, the absolute configuration of tamandarins A (**213**) and B (**214**), isolated from an unidentified Brazilian marine ascidian of the family Didemnidae [163], and kahalalides P (**215**) and Q (**216**), isolated from green algae *Bryopsis* species [164] were elucidated. In the case of kahalalide O (**217**), the absolute configuration of its amino acid constituents was determined by Marfey's method and chiral HPLC analysis, using a ligand exchange type CSP [165]. Tamandarin A (**213**) was found to display cytotoxicity against BX-PC3, DU-145, and UMSCC10b human cancer cell lines, with IC_{50} values of 1.79, 1.36, and 0.99 µg/mL, respectively [163].

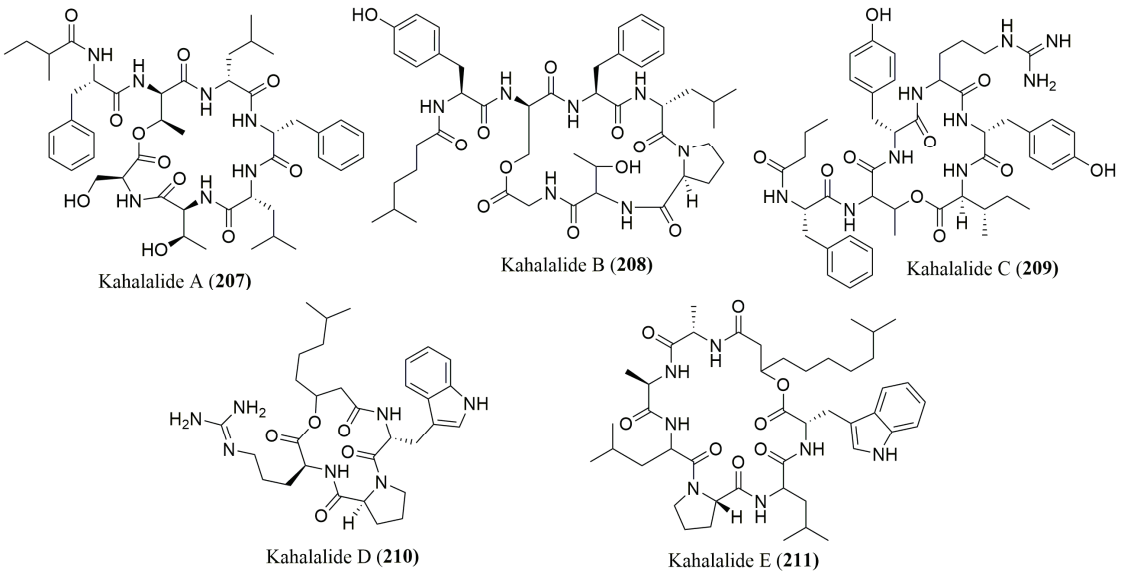


Figure 16. *Cont.*

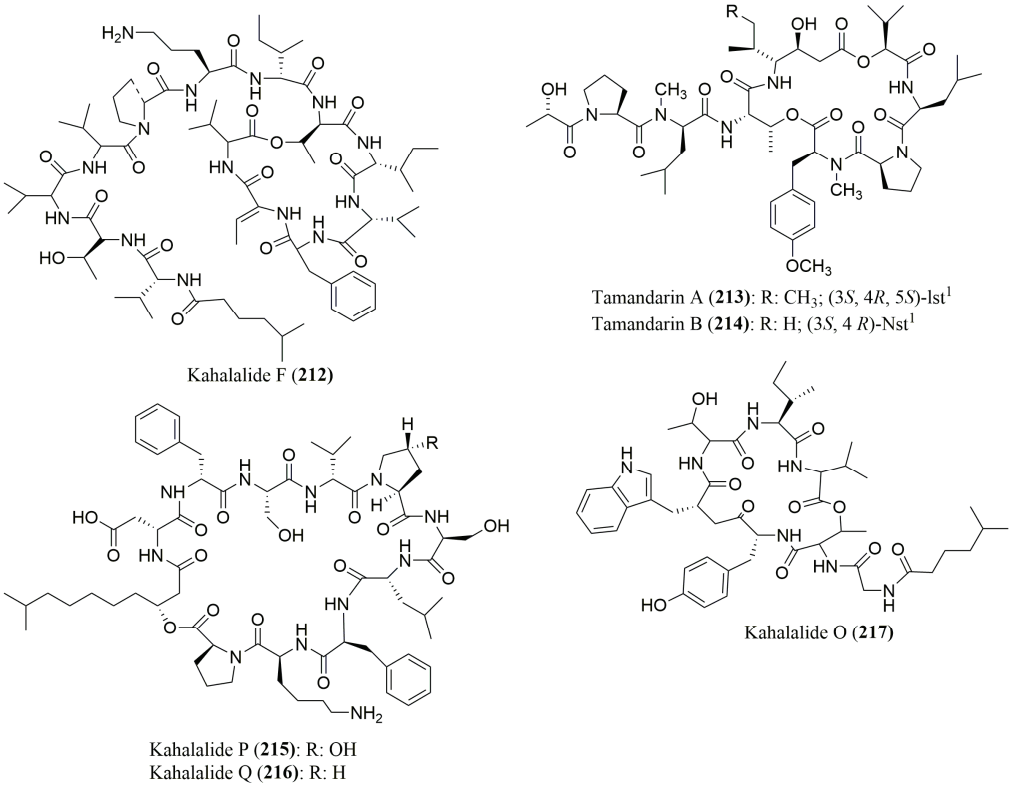


Figure 16. Structure of cyclic depsipeptides **207–217**, isolated from marine invertebrates and marine algae.

Table 10. Cyclic depsipeptides from marine invertebrates and algae.

Peptide	Source	aa Composition	Chromatographic Conditions	Biological Activities	Ref.
Kahalalides A–F (**207–212**)	Mollusk *Elysia rufescens*	**207**: D-Val-5; **208**: L-Val-1, D-Val-2, D-*allo*-Thr-1; **209**: L-Val-3, D-Val-4, L-Thr-2; **210**: D-Val-2, D-*allo*-Thr-1	Marfey's method (FDLA) combined with HPLC COSMOSIL 5C_{18}-AR MP: ACN:H_2O:TFA (42:48:0.05 *v*/*v*/*v*) or ACN:H_2O:50 mM NH_4OAc (20:80:0.01 *v*/*v*/*v*)	**207**: Antimalarial activity **211**: Activity against RSV II virus	[162]
Table 10. *Cont.* Tamandarins A (**213**) and B (**214**)	Ascidian of the family Didemni-dae	**213**: *S*-Lac, L-Pro, *N*-Me-D-Leu, L-Thr, (3*S*,4*R*,5*S*)-Ist **214**: *S*-Lac, L-Pro, *N*-Me-D-Leu, L-Thr 3*S*,4*R*)-Nst	Marfey's method (FDAA) combined with HPLC Hewlett-Packard ODS Hypersil 5 µm (4.6 × 200 mm); MP: 0.1% TFA in H_2O or MeOH; Flow rate: 1.0 mL/min; UV detection at 340 nm	**213**: Cytotoxicity against various human cancer cell lines	[163]
KahalalidesP (**215**) and Q (**216**)	Green alga *Bryopsis* sp.	L-Asp, L-Val, D-Leu, L-Ser, L-Hyp, L-Pro, L-Lys	Marfey's method (FDAA) combined with HPLC COSMOSIL 5C_{18}-AR-II (4.6 × 250 mm); MP: 0.1 M NH_4OAc pH 3 or 90% aq ACN	No antimicrobial and no hemolytic activities	[164]
Kahalalide O (**217**)	Mollusk *Elysia ornata* and green alga *Bryopsis* sp.	L-Ile, L-Thr, D-*allo*-Thr, D-Tyr, L-Val	Ligand Exchange Type CSP Chirex (D) Penicillamine Column (4.6 × 250 mm); MP: 1.9 mM $CuSO_4$ in ACN:H_2O (5:95) or 2.0 mM $CuSO_4$ in H_2O; UV detection at 254 nm	No growth inhibition of P-388, A549, HT29 and MEL28 cancer cell lines	[165]
		D-Trp	Marfey's method (FDAA) combined with HPLC COSMOSIL 5C_{18}-AR; MP: ACN:H_2O:TFA (37.5:62.5:0.05 *v*/*v*/*v*); Flow rate: 1.0 mL/min UV detection at 254 nm		

aa—Amino acid; FDAA—1-Fluoro-2-4-dinitrophenyl-5-L-alanine amide; HPLC—High Performance Liquid Chromatography; MP—Mobile Phase; ACN—Acetonitrile; FDLA—1-fluoro-2-4-dinitrophenyl-5-D,L-leucine amide; TFA—Trifluoracetic acid; MeOH—Methanol; TEA—Triethylamine; NH_4OAc—Ammonium acetate.

5.3. Lipopeptides

For lipopeptides isolated from other marine invertebrates and algae, there are only two works which reported the use of a chiral HPLC for the stereochemistry determination of the amino acid residues (Table 11) of the peptides **218**–**221** (Figure 17).

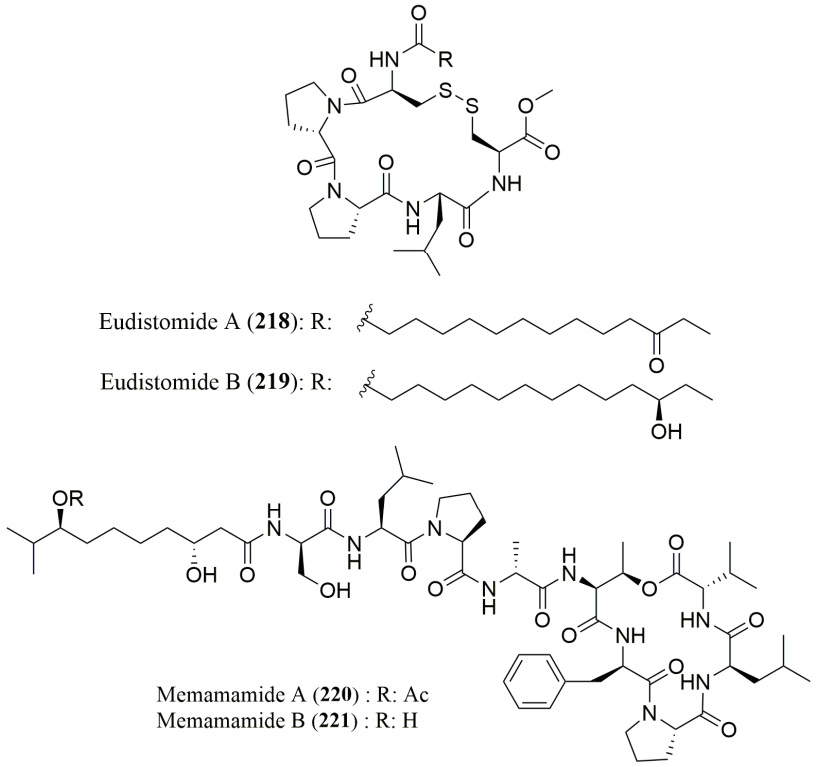


Figure 17. Structure of lipopeptides **218**–**221**, isolated from marine invertebrates and marine algae.

Table 11. Lipopeptides from marine invertebrates and algae.

Peptide	Source	aa Composition	Chromatographic Conditions	Biological Activities	Ref.
Eudistomides A (**218**) and B (**219**)	Ascidian *Eudistoma* sp.	L-Pro, L-Ala, L-Leu **219**: L-Cyp	Ligand Exchange Type CSP Phenomenex Chirex 3126 (D) (4.6 × 250 mm); MP: 2 mM $CuSO_4$, 2 mM $CuSO_4$:ACN (95:5 or 85:15 *v*/*v*); Flow rate: 1.0 mL/min UV detection at 254 nm	No activity reported	[166]
Mebamamides A (**220**) and B (**221**)	Green algae *Derbesia marina*	L-Leu, L-Pro, D-Ala, L-Thr, L-Val, D-Phe, D-Ser	Ligand Exchange Type CSP Diacel CHIRALPAK (MA+) (4.6 × 50 mm); MP: 2.0 mM $CuSO_4$, Flow rate: 1.0 mL/min; UV detection at 254 nm	No growth inhibitory activity against HeLa and HL60 cell lines	[167]

aa—Amino acid; MP—Mobile Phase; ACN—Acetonitrile.

Chiral HPLC analysis by using a ligand exchange type CSP (Phenomenex Chirex Phase 3126) was used to determine the configuration of the amino acid residues in eudistomides A (**218**) and B (**219**), isolated from an ascidian *Eudistoma* sp. It was possible to verify the presence of L-Pro, L-Ala and L-Leu in both compounds as well as the presence of L-Cyp in eudistomide A (**218**) [166]. Similarly, a chiral HPLC analysis using a ligand exchange type CSP (CHIRALPAK (MA+)) was able to confirm the presence of four L-amino acid residues and D-Ala, D-Phe, and D-Ser in mebamamides A (**220**) and B (**221**), isolated from the green alga *Derbesia marina* [167].

6. Case-Study: Chiral HPLC in the Analysis of the Stereochemistry of Cyclopeptides Isolated from Marine Sponge-Associated Fungi

Recently, the determination of the stereochemistry of the amino acid residues of three bioactive marine natural products, by chiral HPLC analysis of their acidic hydrolysates, using appropriate D- and L-amino acid standards was achieved in our group [111,112]. The marine sponge-associated fungus *Aspergillus similanensis* KUFA 0013 was the source of the cyclohexapeptide similanamide (**110**) (Figure 8), while cyclotetrapeptides sartoryglabramides A (**111**) and B (**112**) (Figure 8) were isolated from the marine sponge-associated fungus *Neosartorya glabra* KUFA 0702. The enantioseparations of the amino acids were successfully performed on Chirobiotic T column under reverse phase elution conditions. Actually, the teicoplanin selector of this column has several characteristic features that make it suitable for amino acid analysis [168,169]. Figure 18 shows selected chromatograms of the enantioseparation of standard amino acids.

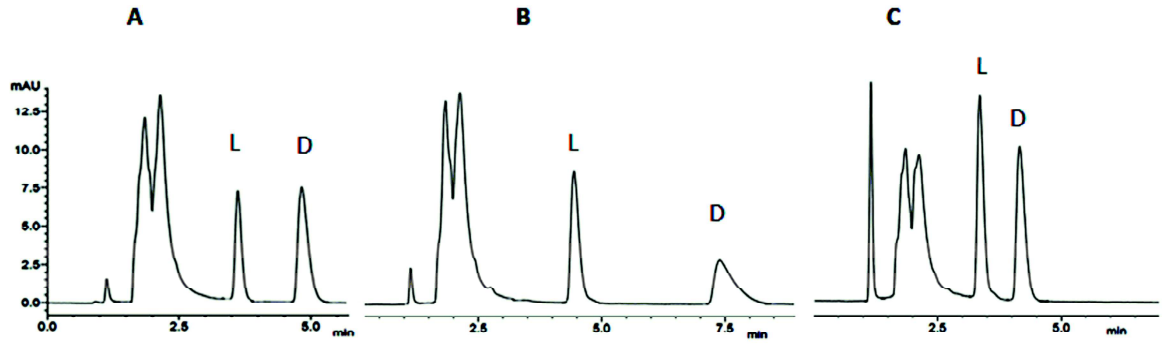


Figure 18. Chromatograms of enantiomeric mixture of DL-Ala (**A**), DL-pipecolic acid (**B**), and DL-Val (**C**). Column, Chirobiotic T; Mobile phase, MeOH:H_2O:acetic acid (70:30:0.02 *v*/*v*/*v*); Flow rate, 1.0 mL/min; UV detection, 210 nm.

The elution order of all the standard enantiomers of amino acids was confirmed by injecting solutions of the racemic or enantiomeric mixtures of amino acids and then each enantiomer separately. As an example, Figure 19 shows the chromatograms obtained during the method development for the determination of the elution order of Ala. As expected, the D-enantiomer was always more strongly retained than the corresponding L-enantiomer on Chirobiotic T column [168]. Mixed HPLC analyses of the acidic hydrolysates with appropriate standard amino acids (co-injection) (Table 12), confirmed the stereochemistry of the amino acids of the three cyclopeptides [111,112]. Chiral HPLC technique demonstrated to be decisive leading to the unambiguous elucidation of the amino acid constituents of the three marine natural products.

Additionally, the in vitro growth inhibitory activity against MCF-7, breast adenocarcinoma, NCI-H460, non-small cell lung cancer and A373, melanoma, cell lines, as well as antibacterial activity against reference strains and the environmental multidrug-resistant isolates (MRS and VRE) were evaluated for cyclopeptide **110**. Only weak activity against the three cancer cell lines was observed [111]. Moreover, cyclopeptides **111** and **112** were tested for their antifungal activity against filamentous (*Aspergillus fumigatus* ATCC 46645), dermatophyte (*Trichophyton rubrum* ATCC FF5) and yeast (*Candida albicans* ATCC 10231), as well as for their antibacterial activity against Gram-positive (*Escherichia coli* ATCC 25922) and Gram-negative (*Staphyllococus aureus* ATCC 25923) bacteria. None of them exhibited antibacterial or antifungal activities [112].

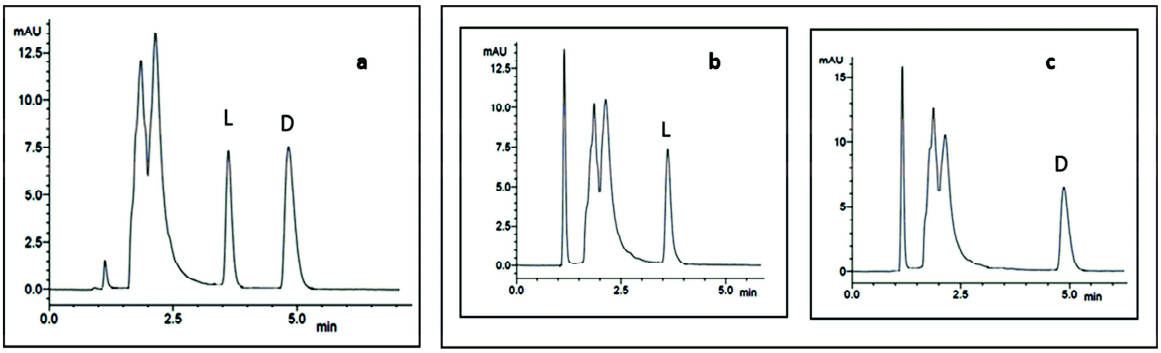


Figure 19. Chromatograms of enantiomeric mixture of DL-Ala (**a**), L-Ala (**b**), and D-Ala (**c**). Column, Chirobiotic T; Mobile phase, MeOH:H_2O:acetic acid (70:30:0.02 $v/v/v$); Flow rate, 1.0 mL/min; UV detection, 210 nm.

Table 12. Chiral HPLC analysis of the acidic hydrolysates of **110**, **111** and **112** by co-injection with amino acids standards.

	Retention Time (min)		Retention Time (min)
D-Trp (A)	5.20	D-pipecolic acid (B)	14.67
L-Trp (A)	4.51	Acidic hydrolysate of **110** (B)	6.59, 7.20, 8.09, 8.83, 9.67, 10.57, 14.69
L-Val (B)	6.60	Acidic hydrolysate of **110** + DL-Val (co-injection) (B)	6.61, 7.31, 8.30, 8.10, 8.84, 9.70, 10.50, 14.95
D-Val (B)	8.32	Acidic hydrolysate of **110** + DL-Ala (co-injection) (B)	6.59, 7.19, 8.04, 8.81, 9.37, 9.70, 10.50, 14.90
L-Ala (B)	7.16	Acidic hydrolysate of **110**+ DL-Leu (co-injection) (B)	6.60, 6.76, 7.26, 8.04, 8.83, 9.67, 10.54, 15.02
D-Ala (B)	9.36	Acidic hydrolysate of **110** + DL-pipecolic acid (co-injection) (B)	6.58, 7.20, 8.09, 8.64, 8.84, 9.77, 10.64, 14.64
L-Leu (B)	6.78	Acidic hydrolysate of **110** + *N*-Me-L-Leu (co-injection) (B)	6.59, 7.20, 8.09, 8.83, 9.67, 10.57, 14.69
D-Leu (B)	9.67	Acidic hydrolysate of **111** (A)	1.91, 2.55, 2.86, 3.49, 3.89, 6.79
N-Me-L-Leu (B)	8.09	Acidic hydrolysate of **111** + DL-Phe (co-injection) (A)	1.87, 2.50, 2.89, 3.68, 5.01, 6.82
L-Phe (A)	3.81	Acidic hydrolysate of **111** + DL-Pro (co-injection) (A)	1.96, 2.60, 2.96, 3.52, 3,92, 6.70, 21.09
D-Phe (A)	5.00	Acidic hydrolysate of **112** (A)	1.93, 3.07, 3.80, 4.29, 4.60, 6.62
L-Pro (A)	6.72	Acidic hydrolysate of **112** + DL-Phe (co-injection) (A)	1.90, 3.10, 3.78, 4.39, 5.04, 6.70
D-Pro (A)	20.10	Acidic hydrolysate of **112** + DL-Pro (co-injection) (A)	2.04, 3.02, 3.72, 4.30, 4.60, 6.66, 19.40
L-pipecolic acid (B)	8.68	Acidic hydrolysate of **112** + DL-Trp (co-injection) (A)	1.93, 2.99, 3.70, 4.29, 4.60, 5.07, 6.33

Column, Chirobiotic T; Mobile phase, MeOH:H_2O (80:20 v/v) (A) or MeOH:H_2O:acetic acid (70:30:0.02 $v/v/v$) (B); Flow rate, 1.0 mL/min (A) or 0.5 mL/min (B); UV detection, 210 nm.

7. Conclusions

In summary, concerning all the reported studies surveyed in this review, which are related to the determination of the absolute configuration of the marine peptides, their distribution according to the methods used, is shown in Figure 20. It is possible to conclude that Marfey's method is the most employed accounting for 52% of the reported studies, while only 21% of the studies described the use of chiral HPLC analysis. Moreover, 27% of the studies included the application of both methods. In fact, in some cases, the complementarity of both methods demonstrated to be crucial for the stereochemical analysis of all the amino acid residues.

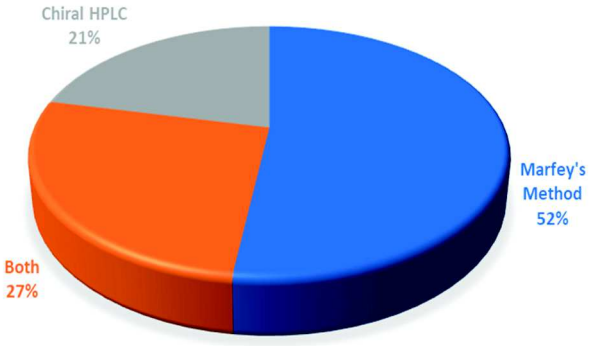


Figure 20. Distribution of the reported studies concerning the determination of the stereochemistry of marine peptides according to the methods used.

Figure 21 compares the reported studies before and after 2007. Interestingly, it is possible to observe that in the last ten years, Marfey's method is still the most used for determination of the absolute configuration of amino acid residues in marine peptides. However, it is important to point out a notable increase of the number of studies related to a chiral HPLC analysis, either as the only method or in a combination with Marfey's method.

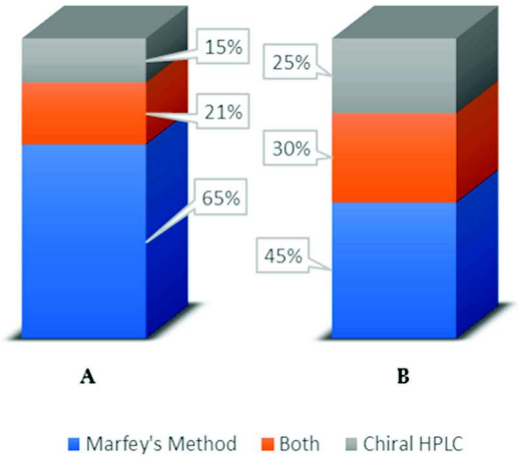


Figure 21. Distribution of the studies concerning the determination of the stereochemistry of marine peptides according to the method used before (**A**) and after 2007 (**B**).

In our opinion, the current trend is to use chiral HPLC for stereochemical analysis due to many advantages of this method. For examples, there is no need for prior derivatization, it requires much less sample manipulation and the results are more rapid to obtain. In contrast, Marfey's method involves time-consuming and labor-intensive procedure.

We believe that the reasons that can justify the actual low number of studies using chiral HPLC is due to the price of the commercially available CSPs and the fact that there is no universal CSP, i.e., one CSP can only separate a limited number of chiral compounds and, in many cases, the choice of CSP may become a very difficult task.

Acknowledgments: This research was partially supported by the Strategic Funding UID/Multi/04423/2013 through national funds provided by FCT—Foundation for Science and Technology and European Regional Development Fund (ERDF), in the framework of the programme PT2020, the project PTDC/MAR-BIO/4694/2014 (reference POCI-01-0145-FEDER-016790; Project 3599—Promover a Produção Científica e Desenvolvimento Tecnológico e a Constituição de Redes Temáticas (3599-PPCDT)) as well as by the project INNOVMAR—Innovation and Sustainability in the Management and Exploitation of Marine Resources (reference NORTE-01-0145-FEDER-000035, within Research Line NOVELMAR), supported by North Portugal Regional Operational Programme (NORTE 2020), under the PORTUGAL 2020 Partnership Agreement, through

the European Regional Development Fund (ERDF), and Chiral_Drugs_CESPU_2017. Phyo thanks the Erasmus Mundus Action 2 (Lotus Plus project) for a PhD's scholarship.

Author Contributions: Ye' Zaw Phyo collected the primary data, analyzed the references, and compiled the draft manuscript. João Ribeiro contributed in writing of the manuscript and data analysis. Carla Fernandes, Anake Kijjoa and Madalena M. M. Pinto supervised development of the manuscript, and assisted in data interpretation, manuscript evaluation, and editing.

Conflicts of Interest: The authors declare no conflict of interest.

References

1. Pinto, M.M.M.; Castanheiro, R.A.P.; Kijjoa, A. Xanthones from marine-derived microorganisms: Isolation, structure elucidation and biological activities. In *Encyclopedia of Analytical Chemistry*; John Wiley & Sons, Ltd.: Hoboken, NJ, USA, 2006.
2. Blunt, J.W.; Copp, B.R.; Keyzers, R.A.; Munro, M.H.G.; Prinsep, M.R. Marine natural products. *Nat. Prod. Rep.* **2017**, *34*, 235–294. [CrossRef] [PubMed]
3. Kijjoa, A.; Sawangwong, P. Drugs and cosmetics from the sea. *Mar. Drugs* **2004**, *2*, 73–82. [CrossRef]
4. Saleem, M.; Ali, M.S.; Hussain, S.; Jabbar, A.; Ashraf, M.; Lee, Y.S. Marine natural products of fungal origin. *Nat. Prod. Rep.* **2007**, *24*, 1142–1152. [CrossRef] [PubMed]
5. Xu, J. Biomolecules produced by mangrove-associated microbes. *Curr. Med. Chem.* **2011**, *18*, 5224–5266. [CrossRef] [PubMed]
6. Cheung, R.C.; Ng, T.B.; Wong, J.H. Marine peptides: Bioactivities and applications. *Mar. Drugs* **2015**, *13*, 4006–4043. [CrossRef] [PubMed]
7. Mayer, A.M.; Rodriguez, A.D.; Berlinck, R.G.; Fusetani, N. Marine pharmacology in 2007–8: Marine compounds with antibacterial, anticoagulant, antifungal, anti-inflammatory, antimalarial, antiprotozoal, antituberculosis, and antiviral activities; affecting the immune and nervous system, and other miscellaneous mechanisms of action. *Comp. Biochem. Physiol. C* **2011**, *153*, 191–222.
8. Aneiros, A.; Garateix, A. Bioactive peptides from marine sources: Pharmacological properties and isolation procedures. *J. Chromatogr. B Analyt. Technol. Biomed. Life Sci.* **2004**, *803*, 41–53. [CrossRef] [PubMed]
9. Donia, M.; Hamann, M.T. Marine natural products and their potential applications as anti-infective agents. *Lancet Infect. Dis.* **2003**, *3*, 338–348. [CrossRef]
10. Harada, K.-I.; Fujii, K.; Mayumi, T.; Hibino, Y.; Suzuki, M.; Ikai, Y.; Oka, H. A method usingL/CMS for determination of absolute configuration of constituent amino acids in peptide—Advanced Marfey's method. *Tetrahedron Lett.* **1995**, *36*, 1515–1518. [CrossRef]
11. Blunt, J.W.; Copp, B.R.; Hu, W.P.; Munro, M.H.; Northcote, P.T.; Prinsep, M.R. Marine natural products. *Nat. Prod. Rep.* **2009**, *26*, 170–244. [CrossRef] [PubMed]
12. Jimeno, J.; Faircloth, G.; Sousa-Faro, J.M.F.; Scheuer, P.; Rinehart, K. New marine derived anticancer therapeutics—A journey from the sea to clinical trials. *Mar. Drugs* **2004**, *2*, 14–29. [CrossRef]
13. Baker, D.D.; Chu, M.; Oza, U.; Rajgarhia, V. The value of natural products to future pharmaceutical discovery. *Nat. Prod. Rep.* **2007**, *24*, 1225–1244. [CrossRef] [PubMed]
14. Glaser, K.B.; Mayer, A.M. A renaissance in marine pharmacology: From preclinical curiosity to clinical reality. *Biochem. Pharmacol.* **2009**, *78*, 440–448. [CrossRef] [PubMed]
15. Gogineni, V.; Hamann, M.T. Marine natural product peptides with therapeutic potential: Chemistry, biosynthesis, and pharmacology. *Biochim. Biophys. Acta* **2018**, *1862*, 81–196. [CrossRef] [PubMed]
16. Anjum, K.; Abbas, S.Q.; Akhter, N.; Shagufta, B.I.; Shah, S.A.A.; Hassan, S.S.U. Emerging biopharmaceuticals from bioactive peptides derived from marine organisms. *Chem. Biol. Drug Des.* **2017**, *90*, 12–30. [CrossRef] [PubMed]
17. Jo, C.; Khan, F.F.; Khan, M.I.; Iqbal, J. Marine bioactive peptides: Types, structures, and physiological functions. *Food Rev. Int.* **2016**, *33*, 44–61. [CrossRef]
18. He, Y.; Wang, B.; Dukor, R.K.; Nafie, L.A. Determination of absolute configuration of chiral molecules using vibrational optical activity: A review. *Appl. Spectrosc.* **2011**, *65*, 699–723. [CrossRef] [PubMed]
19. Seco, J.M.; Quiñoá, E.; Riguera, R. The assignment of absolute configuration by NMR†. *Chem. Rev.* **2004**, *104*, 17–118. [CrossRef]

20. Hoye, T.R.; Jeffrey, C.S.; Shao, F. Mosher ester analysis for the determination of absolute configuration of stereogenic (chiral) carbinol carbons. *Nat. Protoc.* **2007**, *2*, 2451–2458. [CrossRef] [PubMed]
21. Li, X.; Hopmann, K.H.; Hudecova, J.; Isaksson, J.; Novotna, J.; Stensen, W.; Andrushchenko, V.; Urbanova, M.; Svendsen, J.S.; Bour, P.; et al. Determination of absolute configuration and conformation of a cyclic dipeptide by NMR and chiral spectroscopic methods. *J. Phys. Chem. A* **2013**, *117*, 1721–1736. [CrossRef] [PubMed]
22. Berova, N.; Di Bari, L.; Pescitelli, G. Application of electronic circular dichroism in configurational and conformational analysis of organic compounds. *Chem. Soc. Rev.* **2007**, *36*, 914–931. [CrossRef] [PubMed]
23. Toome, V.; De Bernardo, S.; Weigele, M. A simple method for determining the absolute configuration of α-amino acids. *Tetrahedron* **1975**, *31*, 2625–2627. [CrossRef]
24. Urriolabeitia, E.P.; Díaz-de-Villegas, M.D. A simple method for determining the absolute configuration of alpha-amino acids. *J. Chem. Ed.* **1999**, *76*, 77. [CrossRef]
25. Gomez, E.D.; Duddeck, H. A new method proposed for the determination of absolute configurations of alpha-amino acids. *Magn. Reson. Chem.* **2009**, *47*, 222–227. [CrossRef] [PubMed]
26. Calcaterra, A.; D'Acquarica, I. The market of chiral drugs: Chiral switches versus de novo enantiomerically pure compounds. *J. Pharm. Biomed. Anal.* **2018**, *147*, 323–340. [CrossRef] [PubMed]
27. Dolowy, M.; Pyka, A. Application of TLC, HPLC and GC methods to the study of amino acid and peptide enantiomers: A review. *Biomed. Chromatogr.* **2014**, *28*, 84–101. [CrossRef] [PubMed]
28. Marfey, P. Determination ofD-amino acids. II. Use of a bifunctional reagent, 1,5-difluoro-2,4-dinitrobenzene. *Carlsberg Res. Commun.* **1984**, *49*, 591–596. [CrossRef]
29. Vijayasarathy, S.; Prasad, P.; Fremlin, L.J.; Ratnayake, R.; Salim, A.A.; Khalil, Z.; Capon, R.J. C3 and 2D C3 Marfey's methods for amino acid analysis in natural products. *J. Nat. Prod.* **2016**, *79*, 421–427. [CrossRef] [PubMed]
30. Bhushan, R.; Bruckner, H. Use of Marfey's reagent and analogs for chiral amino acid analysis: Assessment and applications to natural products and biological systems. *J. Chromatogr. B Analyt. Technol. Biomed. Life Sci.* **2011**, *879*, 3148–3161. [CrossRef] [PubMed]
31. Bhushan, R.; Bruckner, H. Marfey's reagent for chiral amino acid analysis: A review. *Amino Acids* **2004**, *27*, 231–247. [CrossRef] [PubMed]
32. Tiritan, M.E.; Ribeiro, A.R.; Fernandes, C.; Pinto, M. Chiral pharmaceuticals. In *Kirk-Othmer Encyclopedia of Chemicl Technology*; John Wiley & Sons, Inc.: Hoboken, NJ, USA, 2016.
33. Okamoto, Y.; Ikai, T. Chiral HPLC for efficient resolution of enantiomers. *Chem. Soc. Rev.* **2008**, *37*, 2593–2608. [CrossRef] [PubMed]
34. Fernandes, C.; Phyo, Y.Z.; Silva, A.S.; Tiritan, M.E.; Kijjoa, A.; Pinto, M.M.M. Chiral stationary phases based on small molecules: An update of the last 17 years. *Sep. Purif. Methods* **2017**, *33*, 1–35. [CrossRef]
35. Ribeiro, J.; Tiritan, M.; Pinto, M.; Fernandes, C. Chiral stationary phases for liquid chromatography based on chitin- and chitosan-derived marine polysaccharides. *Symmetry* **2017**, *9*, 190. [CrossRef]
36. Fernandes, C.; Tiritan, M.E.; Pinto, M. Small molecules as chromatographic tools for hplc enantiomeric resolution: Pirkle-type chiral stationary phases evolution. *Chromatographia* **2013**, *76*, 871–897. [CrossRef]
37. Ribeiro, A.R.; Castro, P.M.L.; Tiritan, M.E. Chiral pharmaceuticals in the environment. *Environ. Chem. Lett.* **2012**, *10*, 239–253. [CrossRef]
38. Li, B.; T Haynie, D. Chiral Drug Separation. In *Encyclopedia of Chemical Processing*; Taylor & Francis: Boca Raton, FL, USA, 2006.
39. Auckloo, B.N.; Wu, B. Structure, biological properties and applications of marine-derived polysaccharides. *Curr. Org. Chem.* **2016**, *20*, 2002–2012. [CrossRef]
40. Bennur, T.; Ravi Kumar, A.; Zinjarde, S.S.; Javdekar, V. Nocardiopsis species: A potential source of bioactive compounds. *J. Appl. Microbiol.* **2016**, *120*, 1–16. [CrossRef] [PubMed]
41. Ciavatta, M.L.; Lefranc, F.; Carbone, M.; Mollo, E.; Gavagnin, M.; Betancourt, T.; Dasari, R.; Kornienko, A.; Kiss, R. Marine mollusk-derived agents with antiproliferative activity as promising anticancer agents to overcome chemotherapy resistance. *Med. Res. Rev.* **2017**, *37*, 702–801. [CrossRef] [PubMed]
42. Fang, W.Y.; Dahiya, R.; Qin, H.L.; Mourya, R.; Maharaj, S. Natural proline-rich cyclopolypeptides from marine organisms: Chemistry, synthetic methodologies and biological status. *Mar. Drugs* **2016**, *14*. [CrossRef] [PubMed]
43. Fernando, I.P.S.; Nah, J.W.; Jeon, Y.J. Potential anti-inflammatory natural products from marine algae. *Environ. Toxicol. Pharmacol.* **2016**, *48*, 22–30. [CrossRef] [PubMed]

44. França, P.H.B.; da Silva-Júnior, E.F.; Santos, B.V.O.; Alexandre-Moreira, M.S.; Quintans-Júnior, L.J.; de Aquino, T.M.; de Araújo-Júnior, J.X. Antileishmanial marine compounds: A review. *Rec. Nat. Prod.* **2017**, *11*, 92–113.
45. Hou, X.M.; Xu, R.F.; Gu, Y.C.; Wang, C.Y.; Shao, C.L. Biological and chemical diversity of coral-derived microorganisms. *Curr. Med. Chem.* **2015**, *22*, 3707–3762. [CrossRef] [PubMed]
46. Ji, N.-Y.; Wang, B.-G. Mycochemistry of marine algicolous fungi. *Fungal Divers.* **2016**, *80*, 301–342. [CrossRef]
47. Jin, Z. Muscarine, imidazole, oxazole and thiazole alkaloids. *Nat. Prod. Rep.* **2016**, *33*, 1268–1317. [CrossRef] [PubMed]
48. Lu, W.; Yu, W.; Sun, D. Advances in application of marine bioactive peptides in drug development. *Chin. J. Org. Chem.* **2017**, *37*, 1681. [CrossRef]
49. Maciel, E.; Costa Leal, M.; Lillebo, A.I.; Domingues, P.; Domingues, M.R.; Calado, R. Bioprospecting of marine macrophytes using MS-based lipidomics as a new approach. *Mar. Drugs* **2016**, *14*. [CrossRef] [PubMed]
50. Oh, G.-W.; Ko, S.-C.; Lee, D.H.; Heo, S.-J.; Jung, W.-K. Biological activities and biomedical potential of sea cucumber (Stichopus japonicus): A review. *Fish. Aquat. Sci.* **2017**, *20*. [CrossRef]
51. Pangestuti, R.; Kim, S.K. Bioactive peptide of marine origin for the prevention and treatment of non-communicable diseases. *Mar. Drugs* **2017**, *15*. [CrossRef] [PubMed]
52. Rangel, M.; Santana, C.; Pinheiro, A.; Anjos, L.; Barth, T.; Júnior, O.; Fontes, W.; Castro, M. Marine depsipeptides as promising pharmacotherapeutic agents. *Curr. Protein Pept. Sci.* **2016**, *18*, 72–91. [CrossRef]
53. Shannon, E.; Abu-Ghannam, N. Antibacterial derivatives of marine algae: An overview of pharmacological mechanisms and applications. *Mar. Drugs* **2016**, *14*. [CrossRef] [PubMed]
54. Shukla, S. Therapeutic importance of peptides from marine source: A mini review. *Indian J. Geo Mar. Sci.* **2016**, *45*, 1422–1431.
55. Sila, A.; Bougatef, A. Antioxidant peptides from marine by-products: Isolation, identification and application in food systems. A review. *J. Funct. Foods* **2016**, *21*, 10–26. [CrossRef]
56. Suleria, H.A.R.; Gobe, G.; Masci, P.; Osborne, S.A. Marine bioactive compounds and health promoting perspectives; innovation pathways for drug discovery. *Trends Food Sci. Technol.* **2016**, *50*, 44–55. [CrossRef]
57. Wang, L.; Dong, C.; Li, X.; Han, W.; Su, X. Anticancer potential of bioactive peptides from animal sources (Review). *Oncol. Rep.* **2017**, *38*, 637–651. [CrossRef] [PubMed]
58. Burja, A.M.; Banaigs, B.; Abou-Mansour, E.; Grant Burgess, J.; Wright, P.C. Marine cyanobacteria—A prolific source of natural products. *Tetrahedron* **2001**, *57*, 9347–9377. [CrossRef]
59. Blunt, J.W.; Copp, B.R.; Munro, M.H.G.; Northcote, P.T.; Prinsep, M.R. Marine natural products. *Nat. Prod. Rep.* **2006**, *23*, 26–78. [CrossRef] [PubMed]
60. Shin, J.; Seo, Y.; Lee, H.S.; Rho, J.R.; Mo, S.J. A new cyclic peptide from a marine-derived bacterium of the genus Nocardiopsis. *J. Nat. Prod.* **2003**, *66*, 883–884. [CrossRef] [PubMed]
61. Grach-Pogrebinsky, O.; Carmeli, S. Three novel anabaenopeptins from the cyanobacterium Anabaena sp. *Tetrahedron* **2008**, *64*, 10233–10238. [CrossRef]
62. Han, B.; Gross, H.; Goeger, D.E.; Mooberry, S.L.; Gerwick, W.H. Aurilides B and C, cancer cell toxins from a Papua New Guinea collection of the marine cyanobacterium Lyngbya majuscula. *J. Nat. Prod.* **2006**, *69*, 572–575. [CrossRef] [PubMed]
63. Matsuo, Y.; Kanoh, K.; Imagawa, H.; Adachi, K.; Nishizawa, M.; Shizuri, Y. Urukthapelstatin A, a novel cytotoxic substance from marine-derived Mechercharimyces asporophorigenens YM11–542. II. Physico-chemical properties and structural elucidation. *J. Antibiot.* **2007**, *60*, 256–260. [CrossRef] [PubMed]
64. Matthew, S.; Ross, C.; Paul, V.J.; Luesch, H. Pompanopeptins A and B, new cyclic peptides from the marine cyanobacterium Lyngbya confervoides. *Tetrahedron* **2008**, *64*, 4081–4089. [CrossRef]
65. Zhou, X.; Huang, H.; Chen, Y.; Tan, J.; Song, Y.; Zou, J.; Tian, X.; Hua, Y.; Ju, J. Marthiapeptide A, an anti-infective and cytotoxic polythiazole cyclopeptide from a 60 L scale fermentation of the deep sea-derived Marinactinospora thermotolerans SCSIO 00652. *J. Nat. Prod.* **2012**, *75*, 2251–2255. [CrossRef] [PubMed]
66. Wu, Z.C.; Li, S.; Nam, S.J.; Liu, Z.; Zhang, C. Nocardiamides A and B, two cyclohexapeptides from the marine-derived actinomycete Nocardiopsis sp. CNX037. *J. Nat. Prod.* **2013**, *76*, 694–701. [CrossRef] [PubMed]

67. Song, Y.; Li, Q.; Liu, X.; Chen, Y.; Zhang, Y.; Sun, A.; Zhang, W.; Zhang, J.; Ju, J. Cyclic Hexapeptides from the deep south china sea-derived streptomyces scopuliridis scsio zj46 active against pathogenic gram-positive bacteria. *J. Nat. Prod.* **2014**, *77*, 1937–1941. [CrossRef] [PubMed]
68. Ogawa, H.; Iwasaki, A.; Sumimoto, S.; Kanamori, Y.; Ohno, O.; Iwatsuki, M.; Ishiyama, A.; Hokari, R.; Otoguro, K.; Omura, S.; et al. Janadolide, a cyclic polyketide-peptide hybrid possessing a tert-butyl group from an okeania sp. marine cyanobacterium. *J. Nat. Prod.* **2016**, *79*, 1862–1866. [CrossRef] [PubMed]
69. Lopez, J.A.; Al-Lihaibi, S.S.; Alarif, W.M.; Abdel-Lateff, A.; Nogata, Y.; Washio, K.; Morikawa, M.; Okino, T. Wewakazole B, a cytotoxic cyanobactin from the cyanobacterium moorea producens collected in the red sea. *J. Nat. Prod.* **2016**, *79*, 1213–1218. [CrossRef] [PubMed]
70. Davyt, D.; Serra, G. Thiazole and oxazole alkaloids: Isolation and synthesis. *Mar. Drugs* **2010**, *8*, 2755–2780. [CrossRef] [PubMed]
71. Horgen, F.D.; Yoshida, W.Y.; Scheuer, P.J. Malevamides A–C, new depsipeptides from the marine cyanobacterium Symploca laete-viridis. *J. Nat. Prod.* **2000**, *63*, 461–467. [CrossRef] [PubMed]
72. Luesch, H.; Yoshida, W.Y.; Moore, R.E.; Paul, V.J. Isolation and structure of the cytotoxin lyngbyabellin b and absolute configuration of lyngbyapeptin a from the marine cyanobacteriumlyngbya majuscula. *J. Nat. Prod.* **2000**, *63*, 1437–1439. [CrossRef] [PubMed]
73. Williams, P.G.; Yoshida, W.Y.; Moore, R.E.; Paul, V.J. Tasipeptins A and B: New cytotoxic depsipeptides from the marine cyanobacterium Symploca sp. *J. Nat. Prod.* **2003**, *66*, 620–624. [CrossRef] [PubMed]
74. Han, B.; Gross, H.; McPhail, K.L.; Goeger, D.; Maier, C.S.; Gerwick, W.H. Wewakamide A and guineamide G, cyclic depsipeptides from the marine cyanobacteria Lyngbya semiplena and Lyngbya majuscula. *J. Microbiol. Biotechnol.* **2011**, *21*, 930–936. [CrossRef] [PubMed]
75. Gunasekera, S.P.; Owle, C.S.; Montaser, R.; Luesch, H.; Paul, V.J. Malyngamide 3 and cocosamides A and B from the marine cyanobacterium Lyngbya majuscula from Cocos Lagoon, Guam. *J. Nat. Prod.* **2011**, *74*, 871–876. [CrossRef] [PubMed]
76. Almaliti, J.; Malloy, K.L.; Glukhov, E.; Spadafora, C.; Gutierrez, M.; Gerwick, W.H. Dudawalamides A-D, antiparasitic cyclic depsipeptides from the marine cyanobacterium moorea producens. *J. Nat. Prod.* **2017**, *80*, 1827–1836. [CrossRef] [PubMed]
77. Luesch, H.; Pangilinan, R.; Yoshida, W.Y.; Moore, R.E.; Paul, V.J. Pitipeptolides A and B, new cyclodepsipeptides from the marine cyanobacterium Lyngbya majuscula. *J. Nat. Prod.* **2001**, *64*, 304–307. [CrossRef] [PubMed]
78. Iwasaki, A.; Shiota, I.; Sumimoto, S.; Matsubara, T.; Sato, T.; Suenaga, K. Kohamamides A, B, and C, cyclic depsipeptides from an okeania sp. marine cyanobacterium. *J. Nat. Prod.* **2017**, *80*, 1948–1952. [CrossRef] [PubMed]
79. Zhou, X.; Huang, H.; Li, J.; Song, Y.; Jiang, R.; Liu, J.; Zhang, S.; Hua, Y.; Ju, J. New anti-infective cycloheptadepsipeptide congeners and absolute stereochemistry from the deep sea-derived streptomyces drozdowiczii SCSIO 10141. *Tetrahedron* **2014**, *70*, 7795–7801. [CrossRef]
80. Montaser, R.; Abboud, K.A.; Paul, V.J.; Luesch, H. Pitiprolamide, a proline-rich dolastatin 16 analogue from the marine cyanobacterium Lyngbya majuscula from Guam. *J. Nat. Prod.* **2011**, *74*, 109–112. [CrossRef] [PubMed]
81. Williams, P.G.; Yoshida, W.Y.; Quon, M.K.; Moore, R.E.; Paul, V.J. The structure of Palau'amide, a potent cytotoxin from a species of the marine cyanobacterium Lyngbya. *J. Nat. Prod.* **2003**, *66*, 1545–1549. [CrossRef] [PubMed]
82. Montaser, R.; Paul, V.J.; Luesch, H. Pitipeptolides C-F, antimycobacterial cyclodepsipeptides from the marine cyanobacterium Lyngbya majuscula from Guam. *Phytochemistry* **2011**, *72*, 2068–2074. [CrossRef] [PubMed]
83. Williams, P.G.; Yoshida, W.Y.; Quon, M.K.; Moore, R.E.; Paul, V.J. Ulongapeptin, a cytotoxic cyclic depsipeptide from a Palauan marine cyanobacterium Lyngbya sp. *J. Nat. Prod.* **2003**, *66*, 651–654. [CrossRef] [PubMed]
84. Plaza, A.; Bewley, C.A. Largamides A–H, unusual cyclic peptides from the marine cyanobacterium Oscillatoria sp. *J. Org. Chem.* **2006**, *71*, 6898–6907. [CrossRef] [PubMed]
85. Bunyajetpong, S.; Yoshida, W.Y.; Sitachitta, N.; Kaya, K. Trungapeptins A–C, cyclodepsipeptides from the marine cyanobacterium Lyngbya majuscula. *J. Nat. Prod.* **2006**, *69*, 1539–1542. [CrossRef] [PubMed]
86. Gunasekera, S.P.; Ritson-Williams, R.; Paul, V.J. Carriebowmide, a new cyclodepsipeptide from the marine cyanobacterium Lyngbya polychroa. *J. Nat. Prod.* **2008**, *71*, 2060–2063. [CrossRef] [PubMed]

87. Linington, R.G.; Edwards, D.J.; Shuman, C.F.; McPhail, K.L.; Matainaho, T.; Gerwick, W.H. Symplocamide A, a potent cytotoxin and chymotrypsin inhibitor from the marine Cyanobacterium Symploca sp. *J. Nat. Prod.* **2008**, *71*, 22–27. [CrossRef] [PubMed]
88. Taori, K.; Paul, V.J.; Luesch, H. Kempopeptins A and B, serine protease inhibitors with different selectivity profiles from a marine cyanobacterium, Lyngbya sp. *J. Nat. Prod.* **2008**, *71*, 1625–1629. [CrossRef] [PubMed]
89. Matthew, S.; Paul, V.J.; Luesch, H. Tiglicamides A–C, cyclodepsipeptides from the marine cyanobacterium Lyngbya confervoides. *Phytochemistry* **2009**, *70*, 2058–2063. [CrossRef] [PubMed]
90. Tripathi, A.; Puddick, J.; Prinsep, M.R.; Lee, P.P.; Tan, L.T. Hantupeptins B and C, cytotoxic cyclodepsipeptides from the marine cyanobacterium Lyngbya majuscula. *Phytochemistry* **2010**, *71*, 307–311. [CrossRef] [PubMed]
91. Taniguchi, M.; Nunnery, J.K.; Engene, N.; Esquenazi, E.; Byrum, T.; Dorrestein, P.C.; Gerwick, W.H. Palmyramide A, a cyclic depsipeptide from a Palmyra Atoll collection of the marine cyanobacterium Lyngbya majuscula. *J. Nat. Prod.* **2010**, *73*, 393–398. [CrossRef] [PubMed]
92. Salvador, L.A.; Biggs, J.S.; Paul, V.J.; Luesch, H. Veraguamides A-G, cyclic hexadepsipeptides from a dolastatin 16-producing cyanobacterium Symploca cf. hydnoides from Guam. *J. Nat. Prod.* **2011**, *74*, 917–927. [CrossRef] [PubMed]
93. Meickle, T.; Gunasekera, S.P.; Liu, Y.; Luesch, H.; Paul, V.J. Porpoisamides A and B, two novel epimeric cyclic depsipeptides from a Florida Keys collection of Lyngbya sp. *Bioorg. Med. Chem.* **2011**, *19*, 6576–6580. [CrossRef] [PubMed]
94. Vining, O.B.; Medina, R.A.; Mitchell, E.A.; Videau, P.; Li, D.; Serrill, J.D.; Kelly, J.X.; Gerwick, W.H.; Proteau, P.J.; Ishmael, J.E.; et al. Depsipeptide companeramides from a Panamanian marine cyanobacterium associated with the coibamide producer. *J. Nat. Prod.* **2015**, *78*, 413–420. [CrossRef] [PubMed]
95. Miller, E.D.; Kauffman, C.A.; Jensen, P.R.; Fenical, W. Piperazimycins: Cytotoxic hexadepsipeptides from a marine-derived bacterium of the genus Streptomyces. *J. Org. Chem.* **2007**, *72*, 323–330. [CrossRef] [PubMed]
96. Thornburg, C.C.; Thimmaiah, M.; Shaala, L.A.; Hau, A.M.; Malmo, J.M.; Ishmael, J.E.; Youssef, D.T.; McPhail, K.L. Cyclic depsipeptides, grassypeptolides D and E and Ibu-epidemethoxylyngbyastatin 3, from a Red Sea Leptolyngbya cyanobacterium. *J. Nat. Prod.* **2011**, *74*, 1677–1685. [CrossRef] [PubMed]
97. Sun, P.; Maloney, K.N.; Nam, S.J.; Haste, N.M.; Raju, R.; Aalbersberg, W.; Jensen, P.R.; Nizet, V.; Hensler, M.E.; Fenical, W. Fijimycins A–C, three antibacterial etamycin-class depsipeptides from a marine-derived Streptomyces sp. *Bioorg. Med. Chem.* **2011**, *19*, 6557–6562. [CrossRef] [PubMed]
98. Jimenez, J.I.; Vansach, T.; Yoshida, W.Y.; Sakamoto, B.; Porzgen, P.; Horgen, F.D. Halogenated fatty acid amides and cyclic depsipeptides from an eastern Caribbean collection of the cyanobacterium Lyngbya majuscula. *J. Nat. Prod.* **2009**, *72*, 1573–1578. [CrossRef] [PubMed]
99. Boudreau, P.D.; Byrum, T.; Liu, W.T.; Dorrestein, P.C.; Gerwick, W.H. Viequeamide A, a cytotoxic member of the kulolide superfamily of cyclic depsipeptides from a marine button cyanobacterium. *J. Nat. Prod.* **2012**, *75*, 1560–1570. [CrossRef] [PubMed]
100. Kjaerulff, L.; Nielsen, A.; Mansson, M.; Gram, L.; Larsen, T.O.; Ingmer, H.; Gotfredsen, C.H. Identification of four new agr quorum sensing-interfering cyclodepsipeptides from a marine Photobacterium. *Mar. Drugs* **2013**, *11*, 5051–5062. [CrossRef] [PubMed]
101. Nogle, L.M.; Okino, T.; Gerwick, W.H. Antillatoxin B, a neurotoxic lipopeptide from the marine cyanobacterium Lyngbya majuscula. *J. Nat. Prod.* **2001**, *64*, 983–985. [CrossRef] [PubMed]
102. MacMillan, J.B.; Ernst-Russell, M.A.; de Ropp, J.S.; Molinski, T.F. Lobocyclamides A–C, lipopeptides from a cryptic cyanobacterial mat containing Lyngbya confervoides. *J. Org. Chem.* **2002**, *67*, 8210–8215. [CrossRef] [PubMed]
103. Rateb, M.E.; Ebel, R. Secondary metabolites of fungi from marine habitats. *Nat. Prod. Rep.* **2011**, *28*, 290–344. [CrossRef] [PubMed]
104. Blunt, J.W.; Copp, B.R.; Keyzers, R.A.; Munro, M.H.; Prinsep, M.R. Marine natural products. *Nat. Prod. Rep.* **2014**, *31*, 160–258. [CrossRef] [PubMed]
105. Li, C.; Wang, J.; Luo, C.; Ding, W.; Cox, D.G. A new cyclopeptide with antifungal activity from the co-culture broth of two marine mangrove fungi. *Nat. Prod. Res.* **2014**, *28*, 616–621. [CrossRef] [PubMed]
106. Tan, L.T.; Cheng, X.C.; Jensen, P.R.; Fenical, W. Scytalidamides A and B, new cytotoxic cyclic heptapeptides from a marine fungus of the genus Scytalidium. *J. Org. Chem.* **2003**, *68*, 8767–8773. [CrossRef] [PubMed]

107. Adachi, K.; Kanoh, K.; Wisespongp, P.; Nishijima, M.; Shizuri, Y. Clonostachysins A and B, new anti-dinoflagellate cyclic peptides from a marine-derived fungus. *J. Antibiot.* **2005**, *58*, 145–150. [CrossRef] [PubMed]
108. He, F.; Bao, J.; Zhang, X.Y.; Tu, Z.C.; Shi, Y.M.; Qi, S.H. Asperterrestide A, a cytotoxic cyclic tetrapeptide from the marine-derived fungus Aspergillus terreus SCSGAF0162. *J. Nat. Prod.* **2013**, *76*, 1182–1186. [CrossRef] [PubMed]
109. Zheng, J.; Zhu, H.; Hong, K.; Wang, Y.; Liu, P.; Wang, X.; Peng, X.; Zhu, W. Novel cyclic hexapeptides from marine-derived fungus, Aspergillus sclerotiorum PT06–1. *Org. Lett.* **2009**, *11*, 5262–5265. [CrossRef] [PubMed]
110. Chen, Z.; Song, Y.; Chen, Y.; Huang, H.; Zhang, W.; Ju, J. Cyclic heptapeptides, cordyheptapeptides C-E, from the marine-derived fungus Acremonium persicinum SCSIO 115 and their cytotoxic activities. *J. Nat. Prod.* **2012**, *75*, 1215–1219. [CrossRef] [PubMed]
111. Prompanya, C.; Fernandes, C.; Cravo, S.; Pinto, M.M.; Dethoup, T.; Silva, A.M.; Kijjoa, A. A new cyclic hexapeptide and a new isocoumarin derivative from the marine sponge-associated fungus Aspergillus similanensis KUFA 0013. *Mar. Drugs* **2015**, *13*, 1432–1450. [CrossRef] [PubMed]
112. May Zin, W.W.; Buttachon, S.; Dethoup, T.; Fernandes, C.; Cravo, S.; Pinto, M.M.; Gales, L.; Pereira, J.A.; Silva, A.M.; Sekeroglu, N.; et al. New cyclotetrapeptides and a new diketopiperzine derivative from the marine sponge-associated fungus neosartorya glabra KUFA 0702. *Mar. Drugs* **2016**, *14*. [CrossRef] [PubMed]
113. Jenkins, K.M.; Renner, M.K.; Jensen, P.R.; Fenical, W. Exumolides A and B: Antimicroalgal cyclic depsipeptides produced by a marine fungus of the genus Scytalidium. *Tetrahedron Lett.* **1998**, *39*, 2463–2466. [CrossRef]
114. Amagata, T.; Morinaka, B.I.; Amagata, A.; Tenney, K.; Valeriote, F.A.; Lobkovsky, E.; Clardy, J.; Crews, P. A chemical study of cyclic depsipeptides produced by a sponge-derived fungus. *J. Nat. Prod.* **2006**, *69*, 1560–1565. [CrossRef] [PubMed]
115. Lira, S.P.; Vita-Marques, A.M.; Seleghim, M.H.; Bugni, T.S.; LaBarbera, D.V.; Sette, L.D.; Sponchiado, S.R.; Ireland, C.M.; Berlinck, R.G. New destruxins from the marine-derived fungus Beauveria felina. *J. Antibiot.* **2006**, *59*, 553–563. [CrossRef] [PubMed]
116. Oh, D.-C.; Jensen, P.R.; Fenical, W. Zygosporamide, a cytotoxic cyclic depsipeptide from the marine-derived fungus Zygosporium masonii. *Tetrahedron Lett.* **2006**, *47*, 8625–8628. [CrossRef]
117. Aurelio, L.; Brownlee, R.T.C.; Dang, J.; Hughes, A.B.; Polya, G.M. Determination of the complete absolute configuration of petriellin A. *Aust. J. Chem.* **2006**, *59*, 407. [CrossRef]
118. Kim, M.Y.; Sohn, J.H.; Ahn, J.S.; Oh, H. Alternaramide, a cyclic depsipeptide from the marine-derived fungus Alternaria sp. SF-5016. *J. Nat. Prod.* **2009**, *72*, 2065–2068. [CrossRef] [PubMed]
119. Bringmann, G.; Lang, G.; Steffens, S.; Schaumann, K. Petrosifungins A and B, novel cyclodepsipeptides from a sponge-derived strain of Penicillium brevicompactum. *J. Nat. Prod.* **2004**, *67*, 311–315. [CrossRef] [PubMed]
120. Kotoni, D.; Ciogli, A.; D'Acquarica, I.; Kocergin, J.; Szczerba, T.; Ritchie, H.; Villani, C.; Gasparrini, F. Enantioselective ultra-high and high performance liquid chromatography: A comparative study of columns based on the Whelk-O1 selector. *J. Chromatogr. A* **2012**, *1269*, 226–241. [CrossRef] [PubMed]
121. Kotoni, D.; Ciogli, A.; Molinaro, C.; D'Acquarica, I.; Kocergin, J.; Szczerba, T.; Ritchie, H.; Villani, C.; Gasparrini, F. Introducing enantioselective ultrahigh-pressure liquid chromatography (eUHPLC): Theoretical inspections and ultrafast separations on a new sub-2-mum Whelk-O1 stationary phase. *Anal. Chem.* **2012**, *84*, 6805–6813. [CrossRef] [PubMed]
122. Ding, L.J.; Yuan, W.; Liao, X.J.; Han, B.N.; Wang, S.P.; Li, Z.Y.; Xu, S.H.; Zhang, W.; Lin, H.W. Oryzamides A-E, cyclodepsipeptides from the sponge-derived fungus nigrospora oryzae PF18. *J. Nat. Prod.* **2016**, *79*, 2045–2052. [CrossRef] [PubMed]
123. Kralj, A.; Kehraus, S.; Krick, A.; van Echten-Deckert, G.; Konig, G.M. Two new depsipeptides from the marine fungus Spicellum roseum. *Planta Med.* **2007**, *73*, 366–371. [CrossRef] [PubMed]
124. Huang, H.; She, Z.; Lin, Y.; Vrijmoed, L.L.; Lin, W. Cyclic peptides from an endophytic fungus obtained from a mangrove leaf (Kandelia candel). *J. Nat. Prod.* **2007**, *70*, 1696–1699. [CrossRef] [PubMed]
125. Kang, H.K.; Seo, C.H.; Park, Y. Marine peptides and their anti-infective activities. *Mar. Drugs* **2015**, *13*, 618–654. [CrossRef] [PubMed]

126. Kamalakkannan, P. Marine sponges a good source of bioactive compounds in anticancer agents. *Int. J. Pharm. Sci. Rev. Res.* **2015**, *31*, 132–135.
127. Muller, W.E.; Schroder, H.C.; Wiens, M.; Perovic-Ottstadt, S.; Batel, R.; Muller, I.M. Traditional and modern biomedical prospecting: Part II-the Benefits: Approaches for a sustainable exploitation of biodiversity (secondary metabolites and biomaterials from sponges). *Evid. Based Complement. Alternat. Med.* **2004**, *1*, 133–144. [CrossRef] [PubMed]
128. Mehbub, M.F.; Lei, J.; Franco, C.; Zhang, W. Marine sponge derived natural products between 2001 and 2010: Trends and opportunities for discovery of bioactives. *Mar. Drugs* **2014**, *12*, 4539–4577. [CrossRef] [PubMed]
129. Randazzo, A.; Debitus, C.; Gomez-Paloma, L. Haliclamide, a novel cyclic metabolite from the Vanuatu marine sponge Haliclona sp. *Tetrahedron* **2001**, *57*, 4443–4446. [CrossRef]
130. Zhang, X.; Jacob, M.R.; Rao, R.R.; Wang, Y.H.; Agarwal, A.K.; Newman, D.J.; Khan, I.A.; Clark, A.M.; Li, X.C. Antifungal cyclic peptides from the marine sponge Microscleroderma herdmani. *Res. Rep. Med. Chem.* **2012**, *2*, 7–14. [PubMed]
131. Aviles, E.; Rodriguez, A.D. Euryjanicins E-G, poly-phenylalanine and poly-proline cyclic heptapeptides from the Caribbean sponge Prosuberites laughlini. *Tetrahedron* **2013**, *69*, 10797–10804. [CrossRef] [PubMed]
132. Song, J.; Jeon, J.E.; Won, T.H.; Sim, C.J.; Oh, D.C.; Oh, K.B.; Shin, J. New cyclic cystine bridged peptides from the sponge Suberites waedoensis. *Mar. Drugs* **2014**, *12*, 2760–2770. [CrossRef] [PubMed]
133. Yeung, B.K.; Nakao, Y.; Kinnel, R.B.; Carney, J.R.; Yoshida, W.Y.; Scheuer, P.J.; Kelly-Borges, M. The kapakahines, cyclic peptides from the marine sponge cribrochalina olemda. *J. Org. Chem.* **1996**, *61*, 7168–7173. [CrossRef] [PubMed]
134. Araki, T.; Matsunaga, S.; Nakao, Y.; Furihata, K.; West, L.; Faulkner, D.J.; Fusetani, N. Koshikamide B, a cytotoxic peptide lactone from a marine sponge Theonella sp. *J. Org. Chem.* **2008**, *73*, 7889–7894. [CrossRef] [PubMed]
135. Festa, C.; De Marino, S.; Sepe, V.; Monti, M.C.; Luciano, P.; D'Auria, M.V.; Débitus, C.; Bucci, M.; Vellecco, V.; Zampella, A. Perthamides C and D, two new potent anti-inflammatory cyclopeptides from a Solomon Lithistid sponge Theonella swinhoei. *Tetrahedron* **2009**, *65*, 10424–10429. [CrossRef]
136. Festa, C.; De Marino, S.; Sepe, V.; D'Auria, M.V.; Bifulco, G.; Andrés, R.; Terencio, M.C.; Payá, M.; Debitus, C.; Zampella, A. Perthamides C–F, potent human antipsoriatic cyclopeptides. *Tetrahedron* **2011**, *67*, 7780–7786. [CrossRef]
137. Mohammed, R.; Peng, J.; Kelly, M.; Hamann, M.T. Cyclic heptapeptides from the Jamaican sponge Stylissa caribica. *J. Nat. Prod.* **2006**, *69*, 1739–1744. [CrossRef] [PubMed]
138. Sun, J.; Cheng, W.; de Voogd, N.J.; Proksch, P.; Lin, W. Stylissatins B–D, cycloheptapeptides from the marine sponge Stylissa massa. *Tetrahedron Lett.* **2016**, *57*, 4288–4292. [CrossRef]
139. Afifi, A.H.; El-Desoky, A.H.; Kato, H.; Mangindaan, R.E.P.; de Voogd, N.J.; Ammar, N.M.; Hifnawy, M.S.; Tsukamoto, S. Carteritins A and B, cyclic heptapeptides from the marine sponge Stylissa carteri. *Tetrahedron Lett.* **2016**, *57*, 1285–1288. [CrossRef]
140. Ibrahim, S.R.M.; Edrada-Ebel, R.; Mohamed, G.A.; Youssef, D.T.A.; Wray, V.; Proksch, P. Callyaerin G, a new cytotoxic cyclic peptide from the marine sponge Callyspongia aerizusa. *Arkivoc* **2008**, *2008*, 164. [CrossRef]
141. Zhan, K.X.; Jiao, W.H.; Yang, F.; Li, J.; Wang, S.P.; Li, Y.S.; Han, B.N.; Lin, H.W. Reniochalistatins A-E, cyclic peptides from the marine sponge Reniochalina stalagmitis. *J. Nat. Prod.* **2014**, *77*, 2678–2684. [CrossRef] [PubMed]
142. Zhang, H.J.; Yi, Y.H.; Yang, G.J.; Hu, M.Y.; Cao, G.D.; Yang, F.; Lin, H.W. Proline-containing cyclopeptides from the marine sponge Phakellia fusca. *J. Nat. Prod.* **2010**, *73*, 650–655. [CrossRef] [PubMed]
143. Valeria D'Auria, M.; Zampella, A.; Paloma, L.G.; Minale, L.; Debitus, C.; Roussakis, C.; Le Bert, V. Callipeltins B and C; bioactive peptides from a marine Lithistida sponge Callipelta sp. *Tetrahedron* **1996**, *52*, 9589–9596. [CrossRef]
144. Randazzo, A.; Bifulco, G.; Giannini, C.; Bucci, M.; Debitus, C.; Cirino, G.; Gomez-Paloma, L. Halipeptins A and B: Two novel potent anti-inflammatory cyclic depsipeptides from the Vanuatu marine sponge Haliclona species. *J. Am. Chem. Soc.* **2001**, *123*, 10870–10876. [CrossRef] [PubMed]
145. Capon, R.J.; Ford, J.; Lacey, E.; Gill, J.H.; Heiland, K.; Friedel, T. Phoriospongin A and B: Two new nematocidal depsipeptides from the Australian marine sponges Phoriospongia sp. and Callyspongia bilamellata. *J. Nat. Prod.* **2002**, *65*, 358–363. [CrossRef] [PubMed]

146. Plaza, A.; Gustchina, E.; Baker, H.L.; Kelly, M.; Bewley, C.A. Mirabamides A-D, depsipeptides from the sponge Siliquariaspongia mirabilis that inhibit HIV-1 fusion. *J. Nat. Prod.* **2007**, *70*, 1753–1760. [CrossRef] [PubMed]
147. Tran, T.D.; Pham, N.B.; Fechner, G.; Zencak, D.; Vu, H.T.; Hooper, J.N.; Quinn, R.J. Cytotoxic cyclic depsipeptides from the Australian marine sponge Neamphius huxleyi. *J. Nat. Prod.* **2012**, *75*, 2200–2208. [CrossRef] [PubMed]
148. Coello, L.; Reyes, F.; Martin, M.J.; Cuevas, C.; Fernandez, R. Isolation and structures of pipecolidepsins A and B, cytotoxic cyclic depsipeptides from the Madagascan sponge Homophymia lamellosa. *J. Nat. Prod.* **2014**, *77*, 298–303. [CrossRef] [PubMed]
149. Martin, M.J.; Rodriguez-Acebes, R.; Garcia-Ramos, Y.; Martinez, V.; Murcia, C.; Digon, I.; Marco, I.; Pelay-Gimeno, M.; Fernandez, R.; Reyes, F.; et al. Stellatolides, a new cyclodepsipeptide family from the sponge Ecionemia acervus: Isolation, solid-phase total synthesis, and full structural assignment of stellatolide A. *J. Am. Chem. Soc.* **2014**, *136*, 6754–6762. [CrossRef] [PubMed]
150. Clark, D.P.; Carroll, J.; Naylor, S.; Crews, P. An Antifungal Cyclodepsipeptide, Cyclolithistide A, from the SpongeTheonella swinhoei. *J. Org. Chem.* **1998**, *63*, 8757–8764. [CrossRef]
151. Okada, Y.; Matsunaga, S.; van Soest, R.W.; Fusetani, N. Nagahamide A, an antibacterial depsipeptide from the marine sponge Theonella swinhoei. *Org. Lett.* **2002**, *4*, 3039–3042. [CrossRef] [PubMed]
152. Plaza, A.; Bifulco, G.; Keffer, J.L.; Lloyd, J.R.; Baker, H.L.; Bewley, C.A. Celebesides A–C and theopapuamides B-D, depsipeptides from an Indonesian sponge that inhibit HIV-1 entry. *J. Org. Chem.* **2009**, *74*, 504–512. [CrossRef] [PubMed]
153. Ratnayake, A.S.; Bugni, T.S.; Feng, X.; Harper, M.K.; Skalicky, J.J.; Mohammed, K.A.; Andjelic, C.D.; Barrows, L.R.; Ireland, C.M. Theopapuamide, a cyclic depsipeptide from a Papua New Guinea lithistid sponge Theonella swinhoei. *J. Nat. Prod.* **2006**, *69*, 1582–1586. [CrossRef] [PubMed]
154. Plaza, A.; Bifulco, G.; Masullo, M.; Lloyd, J.R.; Keffer, J.L.; Colin, P.L.; Hooper, J.N.; Bell, L.J.; Bewley, C.A. Mutremdamide A and koshikamides C-H, peptide inhibitors of HIV-1 entry from different Theonella species. *J. Org. Chem.* **2010**, *75*, 4344–4355. [CrossRef] [PubMed]
155. Tan, K.C.; Wakimoto, T.; Abe, I. Sulfoureido lipopeptides from the marine sponge discodermia kiiensis. *J. Nat. Prod.* **2016**, *79*, 2418–2422. [CrossRef] [PubMed]
156. Cabrita, M.T.; Vale, C.; Rauter, A.P. Halogenated compounds from marine algae. *Mar. Drugs* **2010**, *8*, 2301–2317. [CrossRef] [PubMed]
157. Rudi, A.; Chill, L.; Aknin, M.; Kashman, Y. Didmolamide A and B, two new cyclic hexapeptides from the marine ascidian Didemnum molle. *J. Nat. Prod.* **2003**, *66*, 575–577. [CrossRef] [PubMed]
158. Donia, M.S.; Wang, B.; Dunbar, D.C.; Desai, P.V.; Patny, A.; Avery, M.; Hamann, M.T. Mollamides B and C, Cyclic hexapeptides from the indonesian tunicate Didemnum molle. *J. Nat. Prod.* **2008**, *71*, 941–945. [CrossRef] [PubMed]
159. Salib, M.N.; Molinski, T.F. Cyclic Hexapeptide Dimers, Antatollamides A and B, from the Ascidian Didemnum molle. A Tryptophan-Derived Auxiliary for l- and d-Amino Acid Assignments. *J. Org. Chem.* **2017**, *82*, 10181–10187. [CrossRef] [PubMed]
160. Dalisay, D.S.; Rogers, E.W.; Edison, A.S.; Molinski, T.F. Structure elucidation at the nanomole scale. 1. Trisoxazole macrolides and thiazole-containing cyclic peptides from the nudibranch Hexabranchus sanguineus. *J. Nat. Prod.* **2009**, *72*, 732–738. [CrossRef] [PubMed]
161. Lee, J.-S.; Satake, M.; Horigome, Y.; Oshima, Y.; Yasumoto, T. Gamakamide-E, a strongly bitter tasting cyclic peptide with a hydantoin structure from cultured oysters crassostrea gigas. *Fish. Aquatic. Sci.* **2012**, *15*, 15–19. [CrossRef]
162. Goetz, G.; Yoshida, W.Y.; Scheuer, P.J. The absolute stereochemistry of Kahalalide F. *Tetrahedron* **1999**, *55*, 7739–7746. [CrossRef]
163. Vervoort, H.; Fenical, W.; Epifanio, R.A. Tamandarins A and B: New cytotoxic depsipeptides from a Brazilian ascidian of the family Didemnidae. *J. Org. Chem.* **2000**, *65*, 782–792. [CrossRef] [PubMed]
164. Dmitrenok, A.; Iwashita, T.; Nakajima, T.; Sakamoto, B.; Namikoshi, M.; Nagai, H. New cyclic depsipeptides from the green alga Bryopsis species; application of a carboxypeptidase hydrolysis reaction to the structure determination. *Tetrahedron* **2006**, *62*, 1301–1308. [CrossRef]

165. Horgen, F.D.; delos Santos, D.B.; Goetz, G.; Sakamoto, B.; Kan, Y.; Nagai, H.; Scheuer, P.J. A new depsipeptide from the sacoglossan mollusk Elysia ornata and the green alga Bryopsis species. *J. Nat. Prod.* **2000**, *63*, 152–154. [CrossRef] [PubMed]
166. Whitson, E.L.; Ratnayake, A.S.; Bugni, T.S.; Harper, M.K.; Ireland, C.M. Isolation, structure elucidation, and synthesis of eudistomides A and B, lipopeptides from a Fijian ascidian Eudistoma sp. *J. Org. Chem.* **2009**, *74*, 1156–1162. [CrossRef] [PubMed]
167. Iwasaki, A.; Ohno, O.; Sumimoto, S.; Matsubara, T.; Shimada, S.; Sato, T.; Suenaga, K. Mebamamides A and B, Cyclic Lipopeptides Isolated from the Green Alga Derbesia marina. *J. Nat. Prod.* **2015**, *78*, 901–908. [CrossRef] [PubMed]
168. Berthod, A.; Liu, Y.; Bagwill, C.; Armstrong, D.W. Facile liquid chromatographic enantioresolution of native amino acids and peptides using a teicoplanin chiral stationary phase. *J. Chromatogr. A* **1996**, *731*, 123–137. [CrossRef]
169. Péter, A.; Török, G.; Armstrong, D. High-performance liquid chromatographic separation of enantiomers of unusual amino acids on a teicoplanin stationary phase. *J. Chromatogr. A* **1998**, *793*, 283–296. [CrossRef]



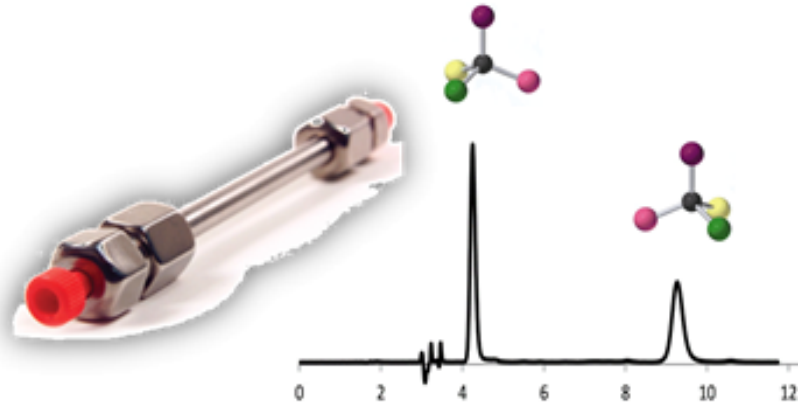
© 2018 by the authors. Licensee MDPI, Basel, Switzerland. This article is an open access article distributed under the terms and conditions of the Creative Commons Attribution (CC BY) license (http://creativecommons.org/licenses/by/4.0/).

CHAPTER III

Chiral stationary phases based on small molecules: an update of the last seventeen years

Reprinted from Separation & Purification Reviews

Copyright © (2019) with permission from Taylor & Francis



Taylor & Francis
Taylor & Francis Group



CHAPTER III

Separation & Purification Reviews

ISSN: 1542-2119 (Print) 1542-2127 (Online) Journal homepage: http://www.tandfonline.com/loi/lspr20

Chiral Stationary Phases Based on Small Molecules: An Update of the Last 17 Years

Carla Fernandes, Ye' Zaw Phyo, Ana Sofia Silva, Maria Elizabeth Tiritan, Anake Kijjoa & Madalena M.M. Pinto

To cite this article: Carla Fernandes, Ye' Zaw Phyo, Ana Sofia Silva, Maria Elizabeth Tiritan, Anake Kijjoa & Madalena M.M. Pinto (2018) Chiral Stationary Phases Based on Small Molecules: An Update of the Last 17 Years, Separation & Purification Reviews, 47:2, 89-123, DOI: 10.1080/15422119.2017.1326939

To link to this article: https://doi.org/10.1080/15422119.2017.1326939

Accepted author version posted online: 11 May 2017.
Published online: 11 Jul 2017.

Submit your article to this journal

Article views: 140

View related articles

View Crossmark data

Citing articles: 3 View citing articles

Full Terms & Conditions of access and use can be found at 97http://www.tandfonline.com/action/journalInformation?journalCode=lspr20

Separation & Purification Reviews, 47: 89–123, 2018
Copyright © Taylor & Francis Group, LLC
ISSN: 1542-2119 print / 1542-2127 online
DOI: https://doi.org/10.1080/15422119.2017.1326939

CHAPTER III

Taylor & Francis
Taylor & Francis Group

Check for updates

Chiral Stationary Phases Based on Small Molecules: An Update of the Last 17 Years

Carla Fernandes,[1,2] Ye' Zaw Phyo,[3] Ana Sofia Silva,[1] Maria Elizabeth Tiritan,[1,2,4] Anake Kijjoa,[2,3] and Madalena M.M. Pinto[1,2]

[1]*Laboratório de Química Orgânica e Farmacêutica, Departamento de Ciências Químicas, Faculdade de Farmácia, Universidade do Porto, Porto, Portugal*
[2]*Interdisciplinary Centre of Marine and Environmental Research (CIIMAR), Edifício do Terminal de Cruzeiros do Porto de Leixões, Matosinhos, Portugal*
[3]*ICBAS-Instituto de Ciências Biomédicas Abel Salazar, Universidade do Porto, Porto, Portugal*
[4]*CESPU, Instituto de Investigação e Formação Avançada em Ciências e Tecnologias da Saúde (IINFACTS), Gandra PRD, Portugal*

A literature survey covering the report on Pirkle-type chiral stationary phases (CSPs) from January 2000 to March 2017 is presented in this review. More than 200 CSPs comprising small molecules as chiral selectors covalently bound to the chromatographic support have been reported in this period. The chemical nature of these new chiral selectors, new insights into the development strategies and their applications in liquid chromatography were emphasized.

Keywords: Liquid chromatography, chiral stationary phases, Pirkle-type, enantioresolution, small molecule

INTRODUCTION

Chirality is vitally important in the development of pharmaceuticals, flavors, food, agrochemicals and related products from other industrial and research areas, due to the different biological/pharmacological or taste/odor effects that the two enantiomers can express (1, 2). Considering pharmaceuticals, this diversity ranges from no desired pharmacological/biological activity at all or less activity of the other enantiomer, to undesirable or different bioactivity, or worst, to severe side effects or even high toxicity (3, 4). Along with the development of efficient methodologies to obtain both enantiomers with high enantiomeric purity, major advances have been made in the field of chromatographic enantioresolution (5, 6). Over the years, liquid chromatography (LC) using chiral stationary phases (CSPs) has demonstrated to be the most useful, accurate and versatile technique for enantioresolution in diverse fields (7, 8). Pharmacokinetic and environmental studies (9, 10), analysis of the stereochemistry of natural compounds (11, 12), evaluation of enantiomeric purity in quality control, monitoring enantiomeric reactions (13–15) and preparative enantioresolution process (16, 17) often require LC with CSPs.

The success of an efficient enantioseparation is primarily determined by the chiral discriminative power of the employed CSP. Consequently, considerable attention has been devoted to finding new CSPs with wide applicability and/or for specific target analytes, long durability, robustness and competitive cost. Since the 1980s, considerable effort has been taken to develop new CSPs with these features as well as to understand and rationalize the structural basis for LC enantioseparations (18). Currently, different types of CSPs, according to the nature of chiral selectors, have been developed (19–21) and, among them, more than a hundred were commercialized and used for the separation of several chiral drugs (22, 23). These include Pirkle-type, polysaccharide-based, macrocyclic antibiotics-based, cyclodextrin-based, crown ether-based, ligand-exchange-type, protein-based, synthetic polymers, cyclofructans, among others (24, 25).

Received 9 October 2016, Accepted 30 April 2017.
Address correspondence to Carla Fernandes, Laboratório de Química Orgânica, Departamento de Ciências Químicas, Faculdade de Farmácia, Universidade do Porto, Rua de Jorge Viterbo Ferreira, 228, 4050-313 Porto, Portugal. E-mail: cfernandes@ff.up.pt

Polysaccharide-based CSPs are pointed out as one of the most useful and broadly applied for LC separations, including supercritical fluid chromatography (22–27). However, Pirkle-type or brush-type CSPs, in which the chiral selector is a small molecule covalently bound to the chromatographic support via a spacer, are the most widely investigated CSPs concerning the knowledge of chiral recognition mechanisms (19, 25). Such as mechanism, responsible for the enantiomer resolution, is easier to establish with small selectors compared to huge polymeric CSPs (18, 20, 25). In fact, elucidation of the chiral recognition mechanisms is essential to clarify the interactions between the CSP and the enantiomers, to estimate the enantioselectivity and elution order, to predict which other classes of analytes could be enantioseparated, as well as to improve the design of new selectors. The enantioresolution on Pirkle-type CSPs is generally based on several interactions between the selector's CSP and the enantiomers through a combination of hydrogen bonds, dipole–dipole, ionic intercations, van der Waals attractions and/or repulsions, and, especially, π–π interactions.

For the separation of enantiomers, Pirkle-type CSPs usually contain π-donor and/or π-acceptor moieties as attractive π–π interaction sites (28, 29). The key advantages of Pirkle-type CSPs are the facility of their preparation processes, applying a rational strategy planning (30) and, in some cases, the possibility of switching the configuration of the chemically synthesized chiral selector as well as using the inverted configuration column approach (19, 28). Furthermore, this type of CSPs has some important features such as universal solvent compatibility, stability at broader temperature and pressure ranges, and high loading capacity that can be scaled up to semi- and preparative chromatography.

PIRKLE-TYPE CSPS: RECENT DEVELOPMENTS

The evolution of several and successive generations of CSPs developed by Pirkle and co-workers (28, 29) was an inspiration to other research groups to dive into this fascinating field. The principle of reciprocity (31, 32) and the studies of chiral recognition phenomena, based on chromatographic (33, 34) and spectroscopic methods (35, 36), were the centerpieces of the evolution of their CSPs. Consequently, several new CSPs obtained by covalent linkage of low-molecular-mass selectors were developed until 2000, by different research groups (37). Gasparrini et al. extensively revised the achievement on this type of CSPs with an emphasis on those obtained by total synthesis (37). However, in the last 17 years, several scattered publications concerning the development and enantioresolution performance of new Pirkle-type CSPs were reported. Therefore, a literature survey on these new CSPs after the year 2000 is the objective for this review. The outline of this review is based on the chemical nature of the new chiral selectors. New insights into the strategies for the development of the CSPs and their applications in LC are emphasized.

CSPs Developed by Pirkle's Group

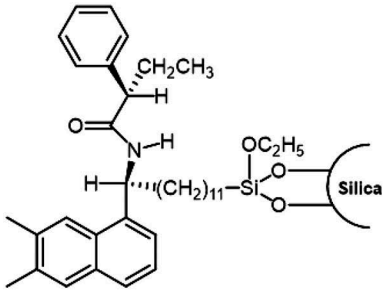
Pirkle's group has reported, after 2000, several studies related to enantioresolution, enantioselective reactions and chiral recognition (38–50); however, their work has not been so devoted to the development of new CSPs since Pirkle retired in 2006. To the best of our knowledge, only four new CSPs (CSP1–CSP4) were described (Table 1).

Similar to the previous CSPs that Pirkle and co-workers had planned to allow for both face-to-face and face-to-edge π–π interactions (28, 51–54), they prepared the diastereomeric CSP1 and CSP2 using (*S*)- or (*R*)-α-[1-(6,7-dimethyl) naphthyl]-10-dodecenylamine and (*S*)-2-phenylpropanoic acid, for the enantiomeric separation of several racemic thiazide diuretics and analogues (Table 1) (55). The rational basis for preparing CSP1 and CSP2 involved the development of a potential site for latter interactions with analytes by the introduction of an additional aromatic moiety (phenyl group) in the CSPs. Generally, the (*S,S*)-CSP (CSP1) gave better chromatographic results in separating the tested analytes (55). Therefore, it was found that the stereochemistry of the amine portion of the CSP plays a crucial role in the enantioselectivity. Presumably, the chiral pocket composed of two aromatic groups in CSP1 may be responsible for face-to-face and face-to-edge π–π interactions with the aryl moiety of the thiazides.

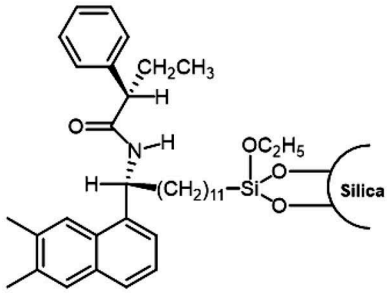
TABLE 1
CSPs developed by the Pirkle' group

CSPs	*Separated Analytes*	*Mobile Phase/Flow rate*	*Ref.*
CSP1-CSP2	Thiazide diuretics and analogues	Hex/2-PrOH (80:20); 2.0 mL/min	(55)
CSP3	β-Blockers and analogues	DCM/EtOH (95:5) containing 0.5 g/L of NH_4OAc; 2.0 mL/min	(56)
CSP4	Naphthylenecarboxamides, *N*-3,5-DNB derivatives of amino acids, esters and amides, NSAIDs, Benzodiazepines	Hex/2-PrOH (80:20); 2.0 mL/min	(57)

Hex: *n*-hexane; 2-PrOH: 2-propanol; DCM: dichloromethane; EtOH: ethanol; NSAIDs: non-steroidal anti-inflammatory drugs; DNB: dinitrobenzoyl; NH_4OAc: ammonium acetate.

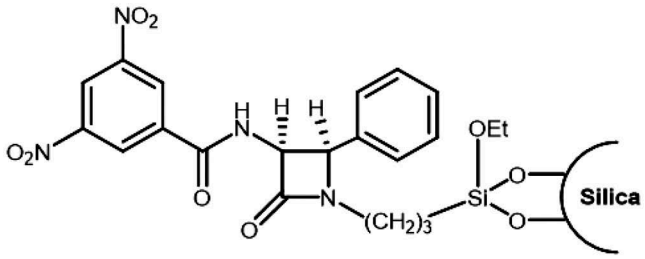


CSP1



CSP2

Recently, a CSP derived from α-amino β-lactam system was developed (CSP3) for a specific enantioresolution of several β-blockers and analogues with the use of various salt additives (Table 1) (56). The effect of the temperature on the chromatographic behavior was also investigated, affording considerable increase in enantioselectivity when the column temperature was reduced. For example, the separation factor of propranolol on CSP3 was 2.16 at 24°C and increased to 3.78 at –10°C.



CSP3

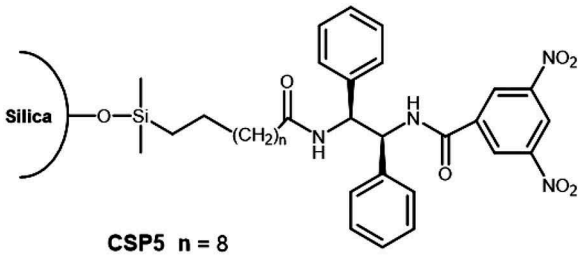
CSP4 was the newest stationary phase described by Pirkle and co-workers (57). CSP4, along with other previously described CSPs (29, 31), was used to resolve the enantiomers of their precursors in order to explore the chiral self-recognition phenomenon (57), in addition to other analytes such as some drugs (Table 1). The results revealed that a geometrically controlling π–π interaction has a strong influence on molecular recognition event.



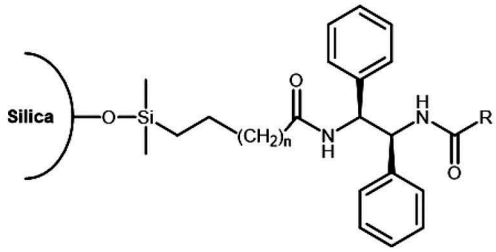
CSP4

Amine and Amino Alcohol-derived CSPs

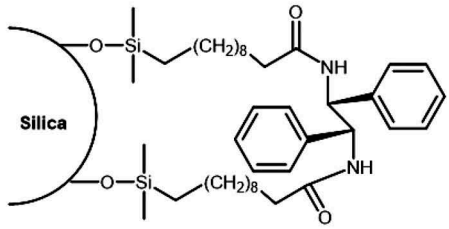
As previously mentioned, the largest number of Pirkle-type CSPs has been developed by other research groups in the last 17 years, and, among them, several amine and amino alcohol-derived CSPs were described and evaluated.



CSP5 n = 8
CSP6 n = 1



CSP7 R = 3,5-dinitrophenyl; n = 8
CSP8 R = 3,5-dinitrophenyl; n = 1
CSP9 R = phenyl; n = 8

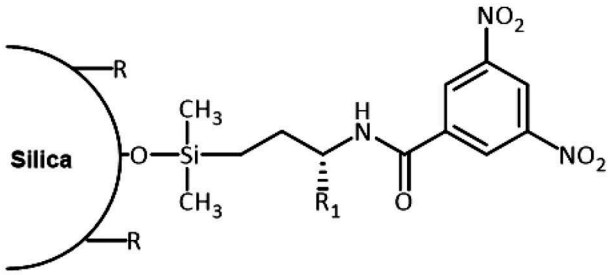


CSP10

A versatile, innovative and *in situ* procedure was followed to prepare new Pirkle-type CSPs based on undecanoyl- or butanoyl-bound (*R,R*)-1,2-diphenylethane-1,2-diamine (CSP5–CSP10) (58). The key step of this method was the preparation of *N*-hydroxysuccinimide activated silica, followed by the immobilization of the enantiomeric pure diamine with only one single amino group through a simple substitution reaction. Subsequently, the free second amino group was acylated with diverse acyl halogenides, providing a library of six new acylated Pirkle-type CSPs. A benzoylated analogue of the

commercially available ULMO CSP (CSP9) was demonstrated to be very useful in the separation of enantiomers of *N*-acyl amino acids (Table 2).

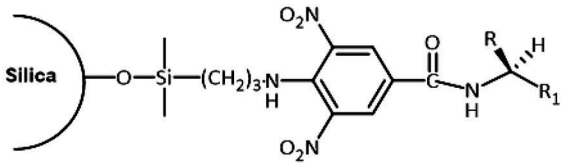
In a continuous interest in developing new Pirkle-type CSPs, CSP11–CSP14, which were based on chiral selectors containing pure aromatic amines and 3,5-dinitrobenzoic acid, were patented (59). The chiral selectors were then covalently bound to a chromatographic support through the allylic double bond (CSP11 and CSP13), and followed by end capping procedure (CSP12 and CSP14). Several analytes, including naproxen-type drugs and other similar nonsteroidal anti-inflammatory drugs (NSAIDs), were selected for the evaluation of the enantiodiscrimination power of these new CSPs, revealing good chromatographic results (Table 2). For example, CSP13 was found to resolve the enantiomers of fenoprofen with α and R_S values of 1.55 and 3.51, respectively.



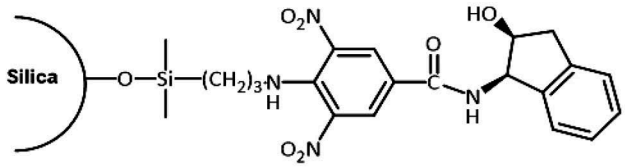
CSP11 R = OH; R_1 = phenyl
CSP12 R = $OSi(CH_3)_3$; R_1 = phenyl
CSP13 R = OH; R_1 = naphthyl
CSP14 R = $OSi(CH_3)_3$; R_1 = naphthyl

Chiral selectors comprising amides of 4-chloro-3,5-dinitrobenzoic acid and either enantiomerically pure α,β-aminoalcohols or α-substituted ethylamines were prepared (60). These chiral selectors were immobilized to aminopropyl silica gel, affording CSP15–CSP22. The π-acid properties of tetrasubstituted benzene rings and the amide of 3,5-dinitro-4-alkylaminobenzoic acid present in all CSPs were important for enantiorecognition, with the hydrophilic hydroxyl groups of CSP15–CSP18 and the lipophilic π-basic aromatic units of CSP20–CSP22 revealing a limited contribution. An important effect of the terminal π-donor aromatic ring was shown only for CSP22, which separated analytes containing nitrophenyl groups in suitable positions to match π-donor units (Table 2). Considering CSP15–CSP18, the phase derived from bicyclic (+)-2-amino-indanol (CSP18) showed the best efficacy for the majority of the racemates. In contrast, CSP15 derivative of L-alaninol showed the worst performance, suggesting that conformational rigidity of the CSP plays an essential role in chiral recognition.

In order to evaluate the influence of the free γ-aminopropyl groups on the silica surface in the vicinity of the chiral selector to enantiorecognition, another version of CSP22 was prepared from the same selector but devoid of the free aminopropyl groups. In general, best resolutions and higher retention factors were achieved on CSP22. As an example, high enantioselectivity (α = 1.24), resolution (R_S = 4.09) and retention factor (k_1 = 12.82) were obtained for warfarine on CSP22. However, by using the same elution conditions, these chromatographic parameters were found to be lower (α = 1.10, R_S = 0.74 and k_1 = 2.73) (60) in the other version of CSP22.

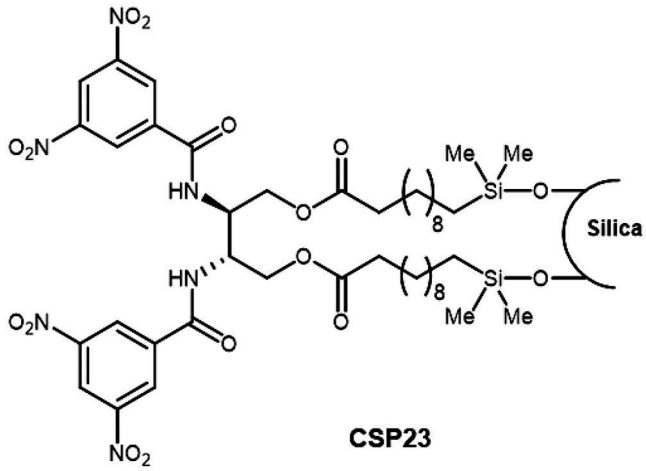


CSP15 R = CH_2OH; R_1 = CH_3
CSP16 R = CH_2OH; R_1 = phenyl
CSP17 R = CH(OH)Ph; R_1 = CH_3
CSP19 R = cyclohexyl; R_1 = CH_3
CSP20 R = phenyl; R_1 = CH_3
CSP21 R = 1-naphthyl; R_1 = CH_3
CSP22 R = 9-anthryl; R_1 = CH_3



CSP18

A new CSP (CSP23), having (2*S*,3*S*)-*O,O′*-bis-(10-undecenoyl)-*N,N′*-bis-(3,5-dinitrobenzoyl)-2,3-diamino-butane-1,4-diol as a selector, was developed using (2*R*,3*R*)-1,4-bis(benzyloxy)-butane-2,3-diol (61) as a starting material. The chiral recognition efficiency of the new CSP was good for the resolution of some π-basic chiral drugs including a diuretic bendroflumethiazide, and NSAIDs such as naproxen and alminoprofen (Table 2), with α values of 1.22, 1.25 and 1.16, respectively.



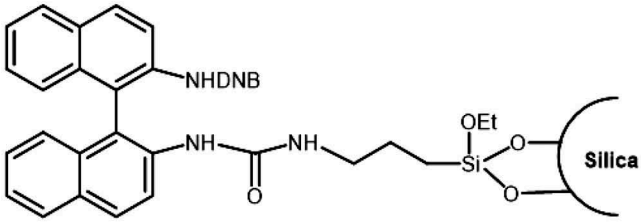
CSP23

TABLE 2
Amine and amino alcohol-derived CSPs

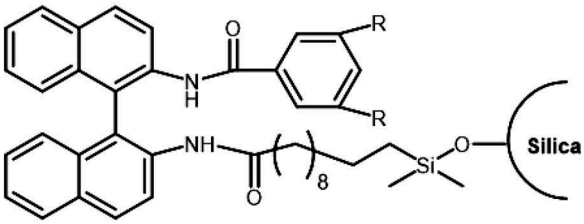
CSPs	*Separated Analytes*	*Mobile Phase/Flow rate*	*Ref.*
CSP5-CSP10	Aryl alcohols, Binaphthol, Naphthyl derivatives, Amides and Ureas, 3,5-DNB amino acids, Ketoprofene anilide	Hep/2-PrOH (70:30, 90:10, 98:2 or 99.5:0.5), Hep/2-PrOH/TFA (70:30:0.1 or 90:10:0.1), Hep/Dioxane (60:40 or 75:35); 1.0 mL/min	(58)
CSP11-CSP14	NSAIDs, Tröger base	Hex/2-PrOH (90:10, 80:20, 70:30); 1.0 mL/min	(59)
CSP15-CSP22	Isopropylesters of DNB-AAs, Tröger base, 1-(9-Anthryl)-2,2,2-trifluoro-1-ethanol, α-Arylethanols, Benzodiazepine derivatives, Arylamides, Dihydropyrimidine derivatives	Hex/2-PrOH (99:1, 80:20), Hex/DCM/2-PrOH (100:30:1); 1.0 mL/min	(60)
CSP23	Anilide derivatives of *N*-Acetyl-α-amino acids, 1,1'-bi-2-Naphthyl,3,3'-Diaryl-1,1'-bi-2 Naphthols, NSAIDs, Bendroflumethiazide, *N*-methyl-3,5-dimethylanilide derivative of naproxen	Hex/2-PrOH (98:2, 80:20); 1.0 and 2.0 mL/min	(61)
CSP24-CSP27	Naphthyl derivatives, Amides and Ureas, 3,5-DNB amino acids, 2,2,2-Trifluoro-1-(9-anthryl)-ethanol, *cis*-2,3-Dihydro-7α-methyl-3-phenylpyrollolo [2,1-b]-oxazol-5 (7a*H*)-one, 1,5-Dimethyl-4-phenyl-2-imidazolidinone, 5,5-Dimethyl-4-phenyl-2-oxazolidinone, α,α-Dimethyl-β-methyl-succinimide, *cis*-4,5-diphenyl-2-oxazolidinone, bis-α-Ethylbenzylsulfamide, 5-Chloro-1,3-dihydro-1,3,3-trimethylspiro-[2H-indole-2,3'-(3*H*)-naphth[2,1-b](1,4)oxazine], 1-Aminoindane, *N*-acyl-1-aryl-1-aminoalkanes	Hep/2-PrOH (97.5:2.5, 95:5, 90:10, 80:20); 1.0 or 1.2 mL/min	(62,63)
CSP28	*N*-(3,5-DNB)-α-amino acids, amides and esters	Hex/2-PrOH/TFA (95:5:0.1, 90:10:0.1, 80:20:0.1, 95:5:0.5, 90:10:0.5 or 80:20:0.5), Hex/EtOH/TFA (90:10:0.1); 0.5 mL/min	(64)
CSP29-CSP30	*N*-DNB derivatized amino acids,Benzodiazepines derivatives, α-Aryloxypropionic acids and α-Arylthiopropionic acids	Hex/$CHCl_3$ (90:10), MeCN/H_2O (60:40, 90:10), Hex/DCM/MeOH (75:20:5), MeCN/MeOH (85:15) + 10 mM NH_4HCO_2 buffer (pH= 7.45); 1.0 mL/min	(65)
CSP31-CSP34	Naphthol derivatives, 1-(9-Anthryl)-2,2,2-trifluoro-1-ethanol, *N*-(3,5-DNB)-amides, Oxazolidinones	Hex/2-PrOH (90:10), Hex/2-PrOH/TFA (90:10:0.1); 1.2 mL/min	(66)
CSP35-CSP36	*N*-acyl-1-naphthylaminoalkanes	Hex/2-PrOH (90:10); 1.5 mL/min	(67)
CSP37-CSP40	*N*-acyl-1-naphthylaminoalkanes	Hex/2-PrOH (80:20); 1.5 mL/min	(68)
CSP41-CSP42	*N*-(3,5-DNB)-α-amino acids	MeOH/H_2O/AcOH/TEA (80:20:0.1:0.1), MeCN/H_2O/AcOH/TEA (80:20:0.1:0.1), Hex/2-PrOH/AcOH/TEA (60:40:0.1:0.1), 20% DCM in Hex/2-PrOH/AcOH/TEA (60:40:0.1:0.1), 100% DCM/AcOH/TEA, DCM/AcOH/TEA (99.8:0.2:0.1); 0.8 and 1.2 mL/min	(69)
CSP43	*N*-(3,5-DNB)-α-amino acids, esters, and amides	Hex/EtOH/TFA (90:10:0.5), 2-PrOH/Hex/AcOH (60:40:0.5), different proportions of 2-PrOH/Hex/TFA; 0.5 mL/min	(70)

Hep: *n*-heptane; Hex: *n*-hexane; 2-PrOH: 2-propanol; EtOH: ethanol; MeOH: methanol; MeCN: acetonitrile; DCM: dichloromethane; AcOH: acetic acid; TEA: triethylamine; TFA: trifluoroacetic acid; DNB: dinitrobenzoyl; DNB-AAs: dinitrobenzoyl α-amino acids; NSAIDs: non-steroidal anti-inflammatory drugs.

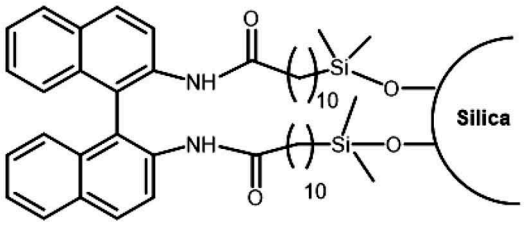
Another new CSP (CSP24), which was successfully used for the resolution of various *N*-(3,5-DNB)-α-amino amides and *N*-acyl-1-aryl-1-aminoalkanes (62) (Table 2), was prepared using (*R*)-(+)-1,1′-binaphthyl-2,2′-diamine as a starting material. Considering the performance of this new CSP, the chromatographic results for *N*-(3,5-DNB)-phenylglycine derivatives were better than those of other *N*-(3,5-DNB)-α-amino amides. Moreover, analytes with naphthyl and biphenyl substituents were better resolved than the corresponding those with a phenyl group. From these results, some conclusions concerning the chiral recognition mechanism were drawn. It was proposed that π–π and hydrogen bonding interactions were the major attractive interactions between the CSP and the two types of analytes. Another group reported the synthesis and chromatographic evaluation of the same CSP (CSP24) as well as three different 1,1′-binaphthyl-2,2′-diamine-derived CSPs (CSP25–CSP27). CSP24 and CSP25, which come under DNB group containing CSPs, showed much better separation results for the randomly selected commercially available chiral compounds (Table 2) (63).



CSP24



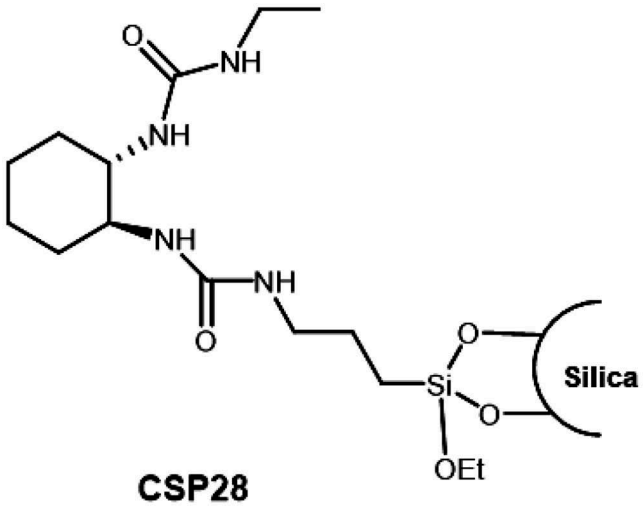
CSP25 R = NO_2
CSP26 R = H



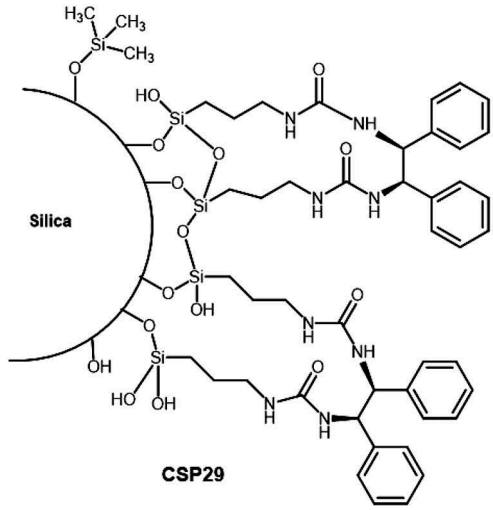
CSP27

Through continuous efforts to develop effective CSPs, the commercially available optically active *trans*-1,2-diaminocyclohexane (DACH) was explored as a chiral selector (64). The obtained CSP (CSP28), which has only two ureide functional groups, was successful in the resolution of various *N*-(3,5-DNB)-α-amino acids (Table 2), with α and R_S values within the range of 1.11–1.35 and 2.19–5.17, respectively. Considering these results, it was proposed that the complexation of the carboxylate anions of the analytes inside the double-ureide pocket of the CSP played an important role for the chiral recognition.

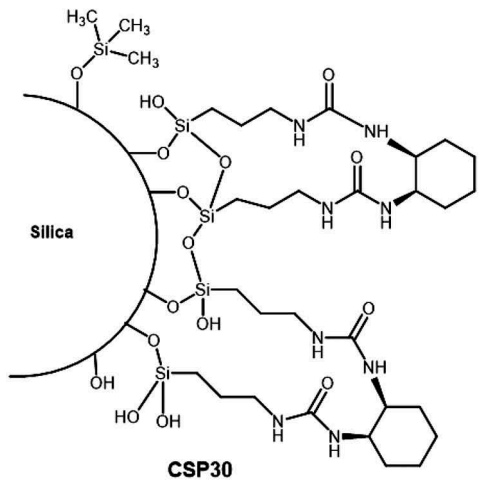
Two new totally synthetic "crab-like" Pirkle-type CSPs (CSP29 and CSP30) have been successfully prepared from 1,2-diaminocyclohexane and 1,2-diphenyl 1,2-ethylenediamine as chiral selectors (65). First, reactive ureido selectors were obtained by treating both enantiopure diamines with 3-(triethoxysilyl)propyl isocyanate that were, then, covalently bonded to unmodified silica gel through a bidentate tether. The enantioselectivity of the new CSPs was evaluated for a wide range of analytes, under multimodal elution conditions (Table 2). Particularly, CSP30 exhibited good enantioseparation for several racemates, including *N*-derivatized amino acids, benzodiazepines and free carboxylic acids, both in normal phase and polar organic modes.



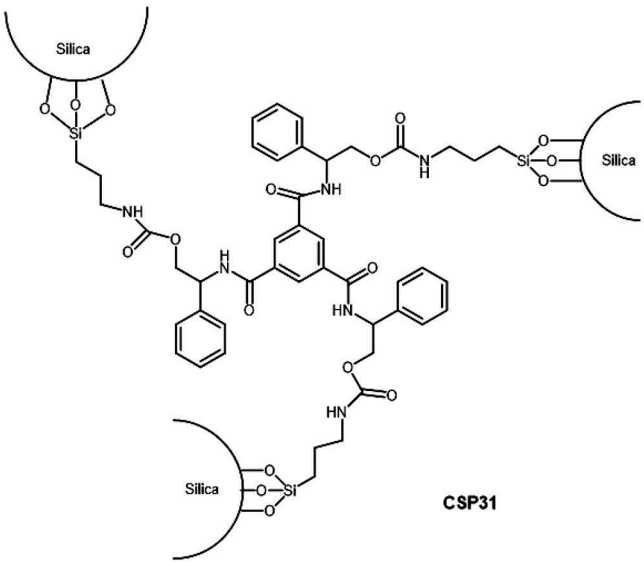
CSP28



CSP29



CSP30

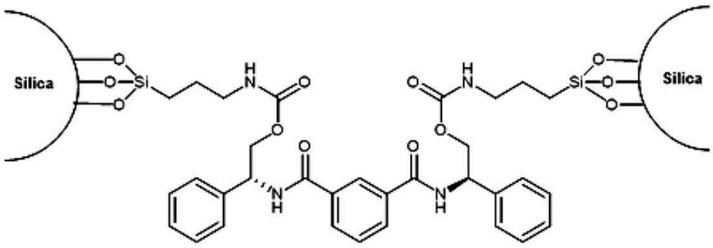


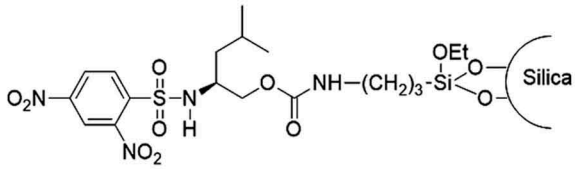
A new (*R*)-phenylglycinol *N*-1,3,5-benzenetricarboxylic acid-derived CSP (CSP31) with C3 symmetry was developed and evaluated for the enantioresolution of various π-basic, π-acidic compounds, and the oxazolidinone antibiotics (66) (Table 2).

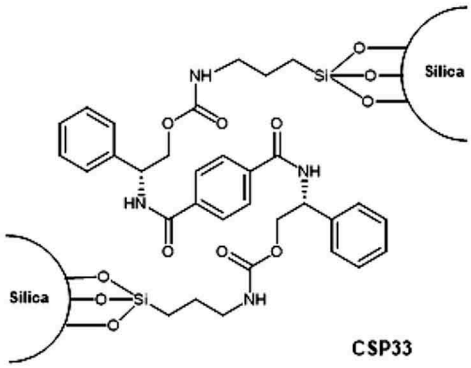
Additionally, three symmetric (*R*)-phenylglycinol CSPs (CSP32–CSP34) were prepared using *o-, m-* and *p*-phthaloyl dichlorides. Even though all CSPs have the same chiral moiety, the C3 symmetric CSP showed the best performance.

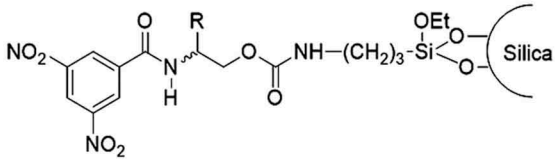
Other amino alcohol-derived CSPs (CSP35 and CSP36), prepared by connecting the 2,4-dinitrobenzenesulfonamide derivative or *N*-3,5-dinitrobenzamide derivative of (*S*)-leucinol to silica gel through a carbamate linkage (67), were described for the separation of the enantiomers of *N*-acyl-1-naphthylaminoalkanes (Table 2). Chromatographic results showed that CSP36 was useful to resolve the chosen analytes, which was in contrast to CSP35. It was assumed that CSP36 can interact more effectively with *N*-acyl-1-naphthylaminoalkanes by hydrogen bonding and π–π interactions considering that the amide group of this CSP has a conformational rigidity and is located co-planar with the π-acidic DNB group.

Other four π-acidic CSPs were also developed by the same group. These CSPs (CSP37–CSP40) were obtained by connecting the *N*-(3,5-dimethylbenzoyl) derivative of

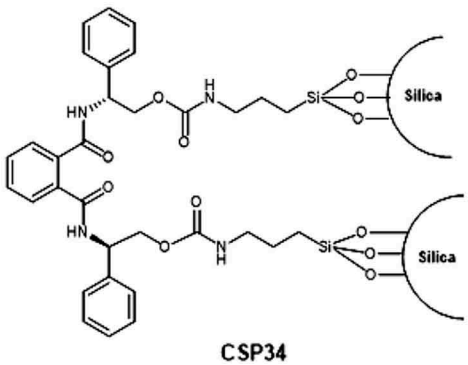


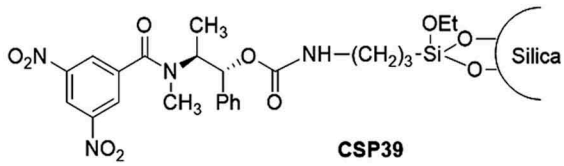


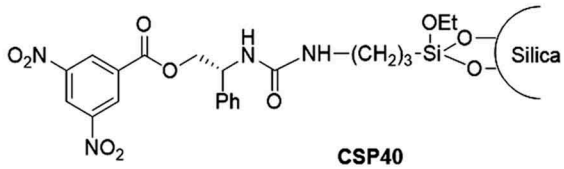




CSP36 (*S*) **R** = $CH_2CH(CH_3)_2$
CSP37 (*R*) **R** = CH_3
CSP38 (*S*) **R** = $C(CH_3)_3$

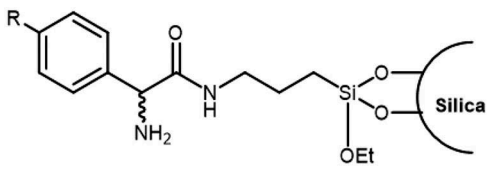




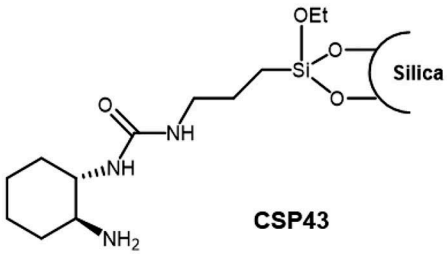


(*R*)-alaninol, (1*S*,2*R*)-ephedrine and (*S*)-*tert*-leucinol, and the *O*-3,5-DNB derivative of (*R*)-phenylglycinol to silica gel through a carbamate or urea linkage (68). These CSPs were applied to the separation of a broad range of *N*-acyl-1-naphthylaminoalkanes (Table 2).

CSP41 and CSP42 were prepared to demonstrate that ionic or electrostatic interactions are useful as attractive interactions for the resolution of ionic racemates such as *N*-3,5-DNB-α-amino acids on Pirkle-type CSPs (Table 2) (69). Accordingly, both CSPs contain a primary amino group, which becomes an ionic interaction site after being protonated. In addition, they contain a π-basic interaction site such as phenyl (CSP41) or *p*-methoxyphenyl group (CSP42), and an amide N–H hydrogen and amide carbonyl oxygen as hydrogen bonding donor and acceptor sites, respectively. Among different mobile phases used, dichloromethane containing 0.2% acetic acid and 0.1% triethylamine were the best. CSP42 was found to be the most effective chiral ion-pairing CSP in resolving *N*-3,5-DNB-α-amino acids, demonstrating that the π-basicity of



CSP41 (*S*) **R** = H
CSP42 (*R*) **R** = OCH_3



CSP43

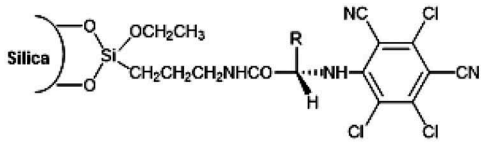
the aryl moiety of the CSP is crucial for enantiorecognition.

Following the same strategy, and aiming to resolve the same type of analytes, Hyun et al. prepared another ion-pairing CSP (CSP43) starting from (1*S*,2*S*)-1,2-diaminocyclohexane (70).

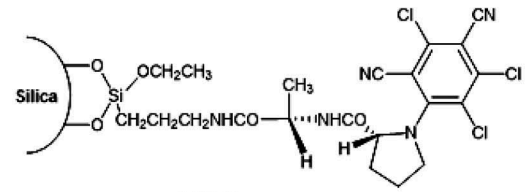
CSP43, comprising two simple functional groups such as a primary amino group and a ureide tethering linkage on a cyclohexane ring, was efficient for the resolution of different *N*-3,5-DNB-α-amino acids (Table 2), with separation and resolution factors ranging from 1.12 to 1.23 and 1.33 to 2.99, respectively. Accordingly, ionic or ion-pairing interaction between the CSP and analytes was found to play an important role in the chiral recognition.

Amino Acid-derived CSPs

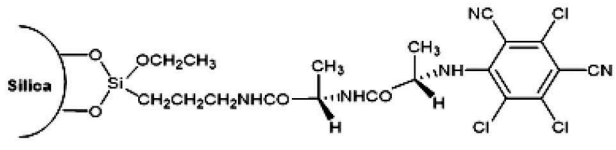
In the last 17 years, several amino acid-derived CSPs have been developed. Among them, six CSPs, based on *N*-4-(2,5,6-trichloro-1,3-dicyano)-phenyl derivatives of L-α-amino acids (CSP44–CSP49), were obtained by a Croatian team in Zagreb using aminopropyl or γ-L-alanylaminopropyl silica gel as chromatographic supports (71). The referred chiral selectors were prepared by nucleophilic substitution of the chlorine atom at C4 of 2,4,5,6-tetrachloro-1,3-dicyanobenzene (TCDCB) by a *N*-L-α amino acid residue. In order to improve hydrogen bonding interactions with the enantiomers of analytes, as well as to reduce the conformational mobility of the chiral selectors, CSP48 and CSP49 which contain dipeptide units, i.e., L-Ala-L-Pro and L-Ala-L-Ala, respectively, were prepared. The hydrogen bonding, via a sterically exposed amide group, and a π–π-type interaction, via a π-acid persubstituted benzene ring, in these CSPs were found to be essential for chiral recognition. The best resolution was obtained with CSP47 and CSP49. CSP47 was able to resolve the largest number of racemates (Table 3), acting probably as both hydrogen bonding donor and π-acceptor. CSP49 was found to



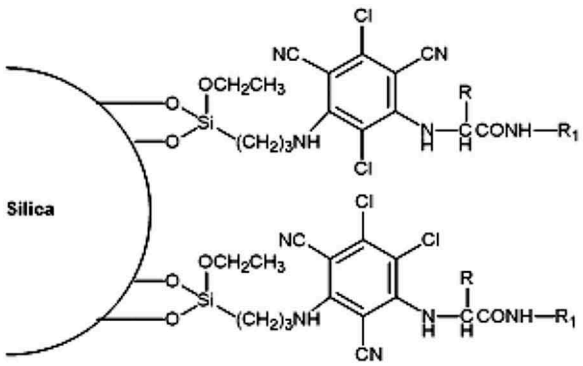
CSP44 R = $-H_2C-$
CSP45 R =
CSP46 R = $-CH_2CONH_2$
CSP47 R = $-CH_3$



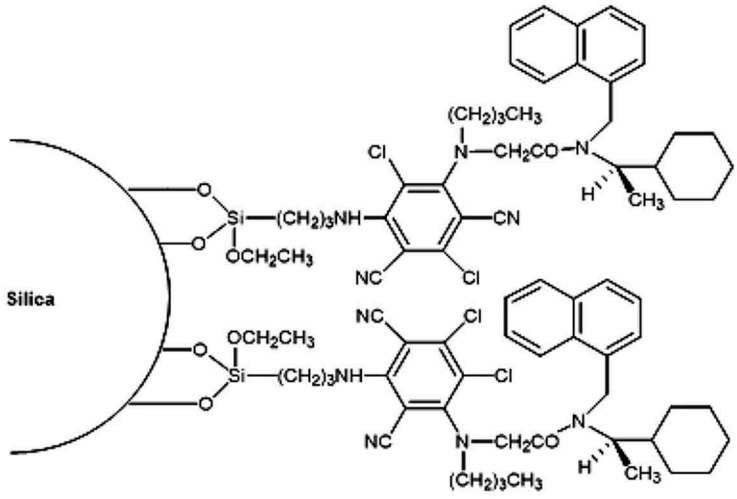
CSP48



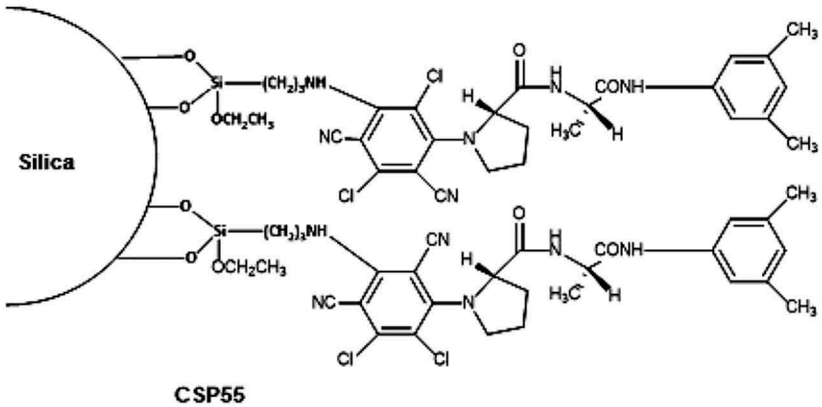
CSP49



CSP50 R = CH_3 R_1 = 3,5-dimethylanilide
CSP51 R = CH_2Ph R_1 = 3,5-dimethylanilide
CSP52 R = CH_3 R_1 = cyclohexyl
CSP53 R = CH_2Ph R_1 = 1-naphthyl



CSP54



CSP55

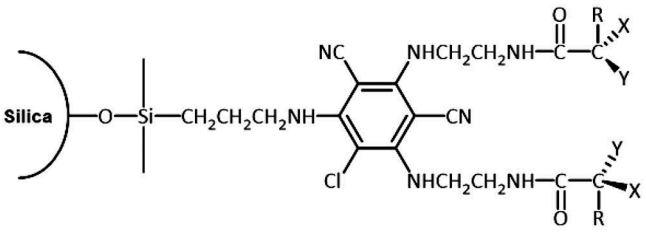
resolve all the isopropyl esters of *N*-3,5-dinitrobenzoyl derivatives of amino acids (DNB-AAs).

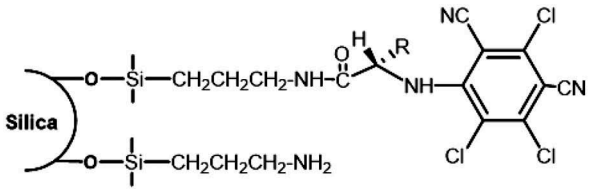
In order to improve the enantioresolution efficacy, a set of new CSPs (CSP50–CSP55), comprising the same structural unit (TCDCB), was described (72). In this case, after a nucleophilic substitution of the chlorine atom at C4 of TCDCB with L-α-amino acids, an amide-bond formation to lipophilic amines containing a strong π-donor group, followed by the introduction of the spacer 3-aminopropyltriethoxysilyl, was carried out. These new chiral selectors, in the form of a 1–2:1 mixture of 2,4 and 4,6-di(alkyl)amino regioisomers, were linked to silica gel

TABLE 3
Amino acid-derived CSPs

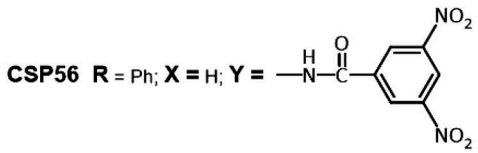
CSPs	*Separated Analytes*	*Mobile Phase/Flow rate*	*Ref.*
CSP44-CSP49	Isopropylesters of DNB-AAs, Arylamides, Benzodiazepine derivatives, Tröger base, 1,1′-bis-2-Naphthol, 1-(9-Anthryl)-2,2,2-trifluoro-1-Ethanol, *trans*-Stilbene oxide, Flavanone	Hex/2-PrOH (90:10), Hex/DCM/MeOH (100:30:1); 1.0 mL/min	(71)
CSP50-CSP55	Isopropylesters of DNB-AAs	Hex/2-PrOH (90:10), Hex/DCM/MeOH (100:30:1); 1.0 mL/min	(72)
CSP56-CSP57	Isopropylesters of DNB-AAs, Arylamides, Benzodiazepine derivatives, Tröger base, 1,1'-*bis*-2-Naphthol, 1-(9-Anthryl)-2,2,2-trifluoro-1-Ethanol, *trans*-Stilbene oxide, Flavanone	Hex/2-PrOH (90:10), Hex/DCM/MeOH (100:30:1); 0.5, 1.0, 2.0 and 2.5 mL/min	(73)
CSP58-CSP60	2-Aryloxypropionic acids	Hex/2-PrOH (80:20, 99.5:0.5); 1.0 mL/min	(74)
CSP61-CSP64	*N*-DNB α-amino acid, *N*-Benzoyl α-amino acid isopropylesters, BINAPO	Hex/2-PrOH (90:10), Hex/DCM/MeOH (100:30:1); 1.0 mL/min	(79,80)
CSP65-CSP71	BINAPO	Hex/2-PrOH (70:30), MTBE/MeOH (90:10); 1.0 mL/min	(80)
CSP72-CSP79	*N*-3,5-DNB derivatives of α-amino amides and esters, Benzodiazepine derivatives	Hex/2-PrOH (90:10); 2.0 mL/min	(82)
CSP80	Isopropyl esters of DNB-AAs, Tröger base, 1,1′-bis-2-Naphthol, 1-(9-Anthryl)-2,2,2-trifluoro-1-ethanol, Benzodiazepine derivatives, *N*-(1-phenylethyl)-amide derivatives	Hex/DCM/MeOH (100:30:1), Hex/2-PrOH (90:10); 1.0 mL/min	(83)
CSP81	*N*-Benzoyl amino acid methyl ester derivatives, Pyrethroid insecticides	Hex/2-PrOH (80:20), Hex/DCM/2-PrOH (79:20:1), Hex/EtOH (99.85:0.15, 99.5:0.5), Hex/DCM (94:6), Hex/DCM/EtOH (98.45:1.2:0.35, 93.95:6:0.05, 93.8:6:0.2); 1.0 mL/min	(84)
CSP82	Pyrethroid insecticides	Hex/2-PrOH (99.5:0.5), Hex/DCE:2-PrOH (97.45:2.5:0.05, 94.5:5:0.5, 96.8:3:0.2); 1.0 mL/min	(85)
CSP83-CSP85	Leucine derivatives, Pyrethroid insecticides	Hex/2-PrOH (80:20), Hex/DCM/2-PrOH (94.9:5:0.1); 1.0 mL/min	(86)
CSP86	β-Methylphenylethylamine	Phosphate buffer with different pH; 1.0 mL/min	(87)

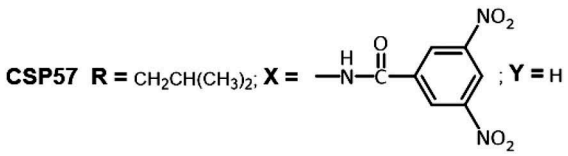
Hex: *n*-hexane; 2-PrOH: 2-propanol; EtOH: ethanol; MeOH: methanol; DCM: dichloromethane; DCE: dichloroethane; MTBE: *tert*-butyl methyl ether; DNB: dinitrobenzoyl; DNB-AAs: dinitrobenzoyl α-amino acids; NSAIDs: non-steroidal anti-inflammatory drugs.

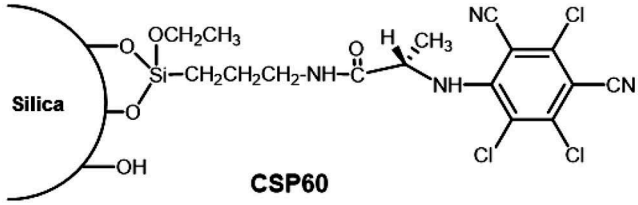




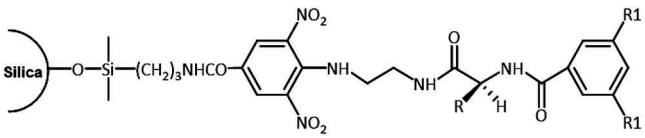
CSP58 R = $CH(CH_3)_2$
CSP59 R = $CH_2CH(CH_3)_2$



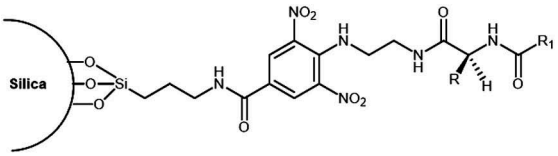




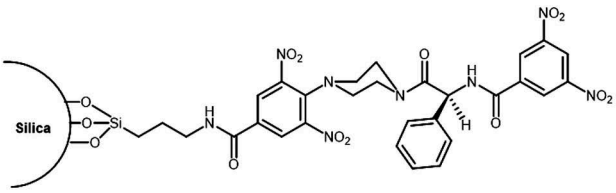
CSP60



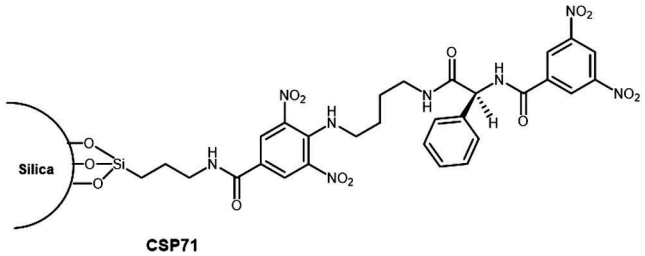
CSP61 R = CH_3 ; R_1 = NO_2
CSP62 R = $CH_2CH(CH_3)_2$; R_1 = NO_2
CSP63 R = Phenyl ; R_1 = NO_2
CSP64 R = Phenyl ; R_1 = H



CSP65 R = CH_2Phenyl ; R_1 = 3,5-Dinitrophenyl
CSP66 R = CH_3 ; R_1 = Phenyl
CSP67 R = $C(CH_3)_3$; R_1 = Phenyl
CSP68 R = Phenyl ; R_1 = Phenyl
CSP69 R = 1-Naphthyl



CSP70



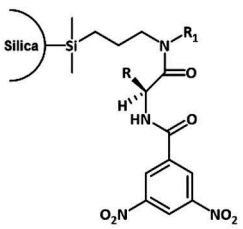
CSP71

as the chromatographic support. Good resolutions were recorded under normal-phase elution conditions, mainly for π-acid racemates (Table 3).

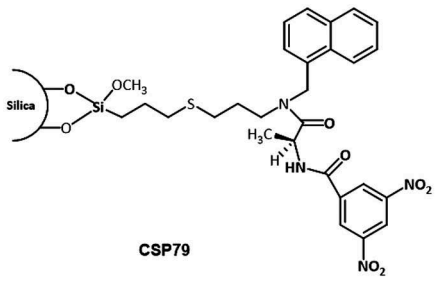
By a nonconventional synthetic approach, specifically by a solid-phase synthesis, the same Croatian group prepared two more new CSPs derived from the commercially available persubstituted benzene derivative TCDCB (CSP56 and CSP57) (73). These CSPs doubled the number of chiral units per binding site to the silica, resulting in an increased number of recognition sites. Accordingly, both CSPs comprise two chiral units, i.e., 3,5-dinitrobenzoyl (3,5-DNB) derivative of an amino acid, bound via 1,2-diaminoethane spacer, to the persubstituted benzene ring derived from TCDCB. The amino acid residues of CSP56 and CSP57 were D-PhGly and L-Leu, respectively. The presence of π-donor and π-acceptor aromatic rings in the chiral selectors was crucial for the separation of a broad spectrum of racemates, particularly DNB-AAs (Table 3). For example, resolution (R_S) values up to 5.2 were obtained for these amino acid derivatives with CSP57.

Another strategy adopted by the same group was developing new CSPs' analogues (CSP58–CSP60) for a specific resolution of racemic 2-aryloxypropionic acids (Table 3) (74). As previously mentioned, other groups also followed the same approach as Pirkle and co-workers which developed several CSPs for specific target analytes, such as β-blockers (75–77), NSAIDs (75, 78) and thiazide diuretics (55). One of these examples is the development of CSP58–CSP60. CSP58 and CSP59 comprise a *N*-3,5,6-trichloro-2,4-dicyanophenyl-L-α-amino acid unit bonded to γ-aminopropyl silica gel. CSP60, which contains the same chiral selector as the previously described CSP47 (71), was also prepared by binding *N*-3,5,6-trichloro-2,4-dicyanophenyl-L-alanyl-(3-triethoxysilyl) propylamide to an unmodified silica gel in order to verify the role of excess free aminopropyl groups (74). Comparing the performance of the two phases, CSP60 showed lower enantioseparation capability for racemic 2-aryloxypropionic acids than CSP47, presumably due to the lack of an achiral aminopropyl spacer.

Three new CSPs (CSP61–CSP63) containing a terminal *N*-DNB unit (a strong π-acid group) and CSP64, comprising the *N*-benzoyl unit (a π-neutral group), were synthesized (79). All CSPs include a linker unit which consists of 4-(alkyl)-amino-3,5-DNB amide moiety (a moderately π-acid group). To evaluate the enantiomeric performance of these



CSP72 R= CH_3 R_1= phenyl
CSP73 R= $CH_2CH(CH_3)_2$ R_1= 3,5-dimethylphenyl
CSP74 R= CH_3 R_1= 3,5-dimethylphenyl
CSP75 R= $CH_2CH(CH_3)_2$ R_1= 1-naphthyl
CSP76 R= $CH_2CH(CH_3)_2$ R_1= butyl
CSP77 R= CH_3 R_1= 1-naphthylmethyl
CSP78 R= $CH_2CH(CH_3)_2$ R_1= 1-anthryl

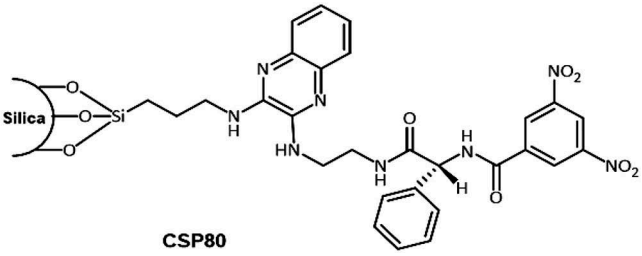


CSP79

new CSPs, a series of racemates that structurally match the chiral selector of these CSPs were selected (Table 3). The separations for racemic *N*-DNB amino acid isopropyl esters were more effective than separations for analogous

N-benzoyl derivatives. More interesting separations were observed with CSP62, prepared from (*S*)-leucine, followed by CSP63 and CSP61, derived from (*R*)-phenylglycine and (*S*)-alanine, respectively.

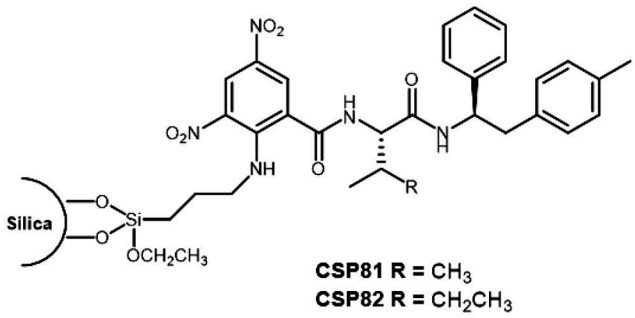
CSP61–CSP63 and a group of seven amino acid-derived CSPs (CSP65–CSP71), specifically designed and synthesized for the separation of 2,2′-bis(diphenylphosphino)-1,1′-binaphthyl oxide (BINAPO) atropisomers (Table 3), were tested in order to perform their chromatographic resolution (80). From the results obtained, it can be inferred that hydrogen bonding

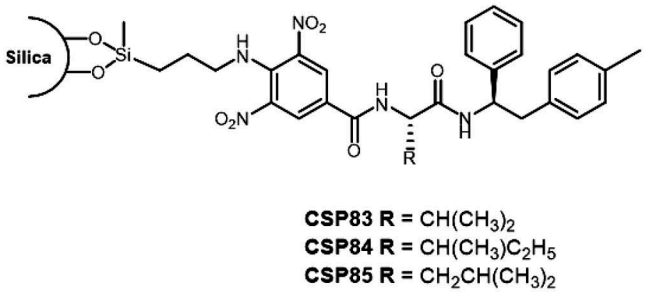


and electrostatic interactions are crucial for chiral recognition between the atropisomers of BINAPO and the CSPs.

It is well recognized that "superfluous" adsorption sites on a CSP can be responsible for increased retention and reduced enantioselectivity (81). With this in mind, new CSPs, based on the original Pirkle *N*-(3,5-DNB)-L-leucine stationary phase, were synthesized without the sites responsible for "competitive" interactions (CSP72–CSP79) (82). The strategy used to obtain these CSPs was the substitution of the hydrogen of the secondary amide tether of the leucine- or alanine-derived chiral selector with diverse π-basic aromatic or aliphatic groups, followed by immobilization on a silica gel. As expected, these new CSPs showed greater enantioselectivity and shorter retention times for the enantiomers of various racemates (Table 3). In most cases, the leucine-derived CSP73, containing a 3,5-dimethylphenyl substituent in the amide-attaching tether, showed the best performance. Accordingly, remarkable separations were achieved for *N*′,*N*′-dialkylamides of leucine and phenylglycine, with excellent α values (5.30 and 3.35, respectively).

Unexpected but interesting results were obtained with CSP76, the only stationary phase with an alkyl group in the tertiary amide. It should be noted that this CSP was developed in order to demonstrate the role of the π-donor aromatic unit as an electron-rich shield on the silica surface. Chromatographic data also revealed that the stationary phase with a 1-naphthylmethyl group, linked to the tertiary amide-attaching tether (CSP77), resolved inadequately the enantiomers of π-acidic racemates. Probably, the naphthyl group was pushed toward a chiral cavity due





to the effect of a silica surface, which hindered the approach of the analyte. However, evident differences in chiral discrimination ability were observed for CSP79, which contains the same chiral selector as CSP77; however, the synthetic procedure for its bonding to the silica gel surface was different. In fact, CSP77 was prepared by binding the chiral selector to the unmodified silica, while the chromatographic support of CSP79 was 3-mercaptopropyl silica. CSP79 was found to resolve enantiomers of several analytes substantially better than CSP77. The

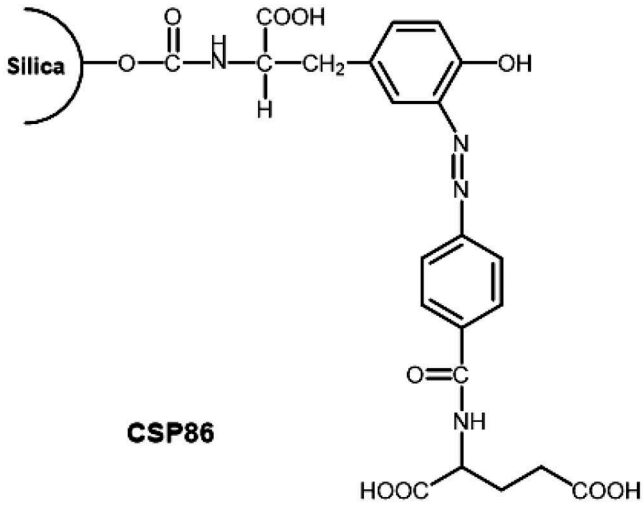


TABLE 4
Peptide CSPs

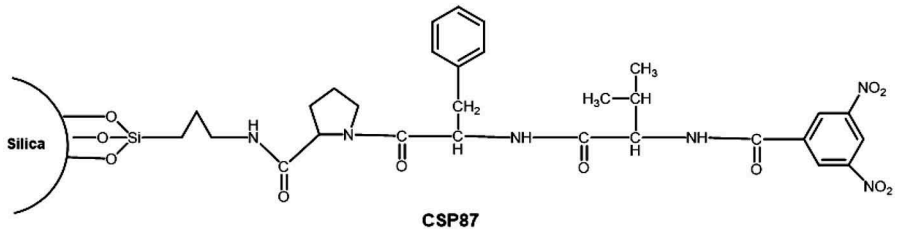
CSPs	*Separated Analytes*	*Mobile Phase/Flow rate*	*Ref.*
CSP87-88	2,2,2-Trifluoro-1-(9-anthryl)ethanol, Bupivacaine hydrochloride, Tiropramide, Proglumide, 1,1'-bi-2-Naphthol, Terbutaline, Norepinephrine	Hex/2-PrOH (95:5, 90:10, 60:40), Hex/2-PrOH/MeOH (50:25:25), Hex/2-PrOH/MeOH (50:25:25), Hex/2-PrOH/MeOH/TFA (50:25:25:0.1); 1.0 ml mL/min	(88)
CSP89-CSP93	*N*-Phenyl mandelic amide, 3-Phenyl-indol-2-one analogues, 1,1´-bi-2-Naphthol and derivatives	Hex/2-PrOH (70:30); 0.8 mL/min	(93)
CSP94-CSP100	1,1´-bi-2-Naphthol and derivatives	Hex/2-PrOH (60:40, 70:30, 80:20, 95:5, 90:10), Hex/2-PrOH/TFA (80:20:0.1), Hex/EtOH/TFA/TEA (70:30:0.2:0.1, 50:50:0.2:0.1); 0.8 mL/min	(94)
CSP101-CSP108	Binaphthol and analogues	Hex/2-PrOH (70:30, 95:5, 90:10), Hex/2-PrOH/TFA (90:10:0.1), Hex/2-PrOH/TFA/TEA (80:20:0.2:0.1, 50:50:0.2:0.1.); 0.8 mL/min	(95)
CSP109-CSP119	Binaphthol and analogues	Hex/2-PrOH (70:30); 0.8 mL/min	(97)
CSP120-CSP125	Binaphthol and analogues	Hex/$CHCl_3$ (50:50); 0.8 and 3 mL/min	(97)

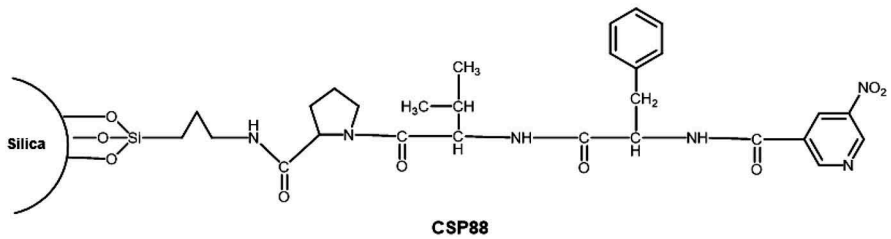
Hex: *n*-hexane; 2-PrOH: 2-propanol; EtOH: ethanol; MeOH: methanol; TEA:triethylamine; TFA: trifluoroacetic acid.

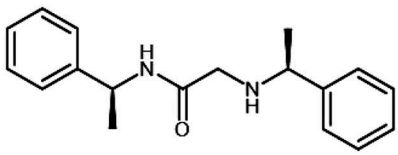
reason for this difference was probably the increase of the distance between the naphthyl moiety and the silica surface and, as a consequence, the naphthyl group could rotate freely and be positioned away from the chiral cavity.

A new CSP containing π-acidic *N*-(3,5-DNB)-D-α-phenylglycine chiral unit bound to the quinoxaline moiety of changed γ-aminopropyl silica gel by a 1,2-diaminoethane spacer was developed by solid-phase synthesis (CSP80) (83). Thus, this CSP possesses the *N,N*′-dialkyl-2,3-diaminoquinoxaline group as a connecting structure. It was expected that the introduction of this structurally different π-basic linking group could increase the enantiorecognition properties. In fact, CSP80 was proved to be able to resolving the enantiomers of a wide range of racemates (Table 3), namely isopropyl esters of DNB-AAs, with good enantioselectivity and resolutions values (α and R_S ranging from 1.14 to 1.45, and from 1.11 to 4.89, respectively).

A new CSP was prepared (CSP81) by connecting a (*R*)-1-phenyl-2-(4-methylphenyl) ethylamine amide derivative of (*S*)-valine to aminopropyl silica gel through a 2-amino-3,5-dinitro-1-carboxamido-benzene unit (84). CSP81 was used specifically for an efficient enantiomeric







$(Nspe)_2$

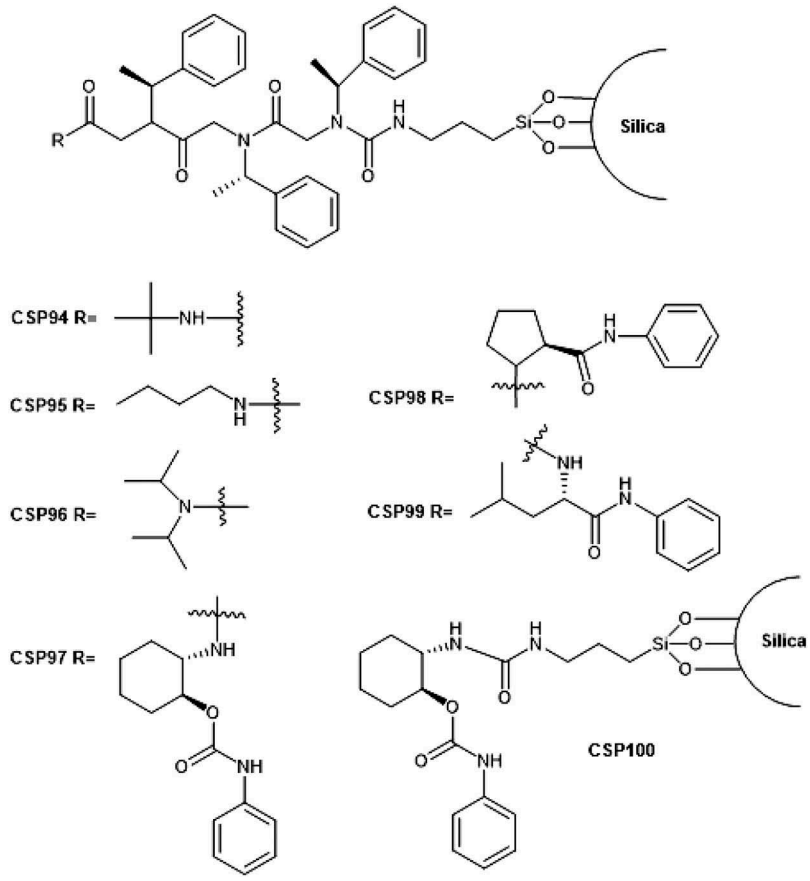
Selectors of:

CSP89 n= $(Nspe)_3$-$CONH(CH_2)_3$Silica
CSP90 n= $(Nspe)_4$-$CONH(CH_2)_3$Silica
CSP91 n= $(Nspe)_5$-$CONH(CH_2)_3$Silica
CSP92 n= $(Nspe)_6$-$CONH(CH_2)_3$Silica
CSP93 n= $(Nspe)_7$-$CONH(CH_2)_3$Silica

separation of amino acid derivatives and pyrethroid insecticides (Table 3). The use of dichloromethane as a modifier in the mobile phase proved to be decisive since the enantioseparation was improved to achieve baseline separations.

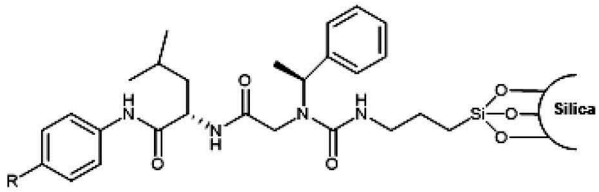
Based on the same strategy, another CSP (CSP82) was developed by the same group to separate pyrethroid insecticides, namely fenpropathrin, fenvalerate, brofluthrinate, cypermethrin and cyfluthrin (Table 3) (85). Compared with the previous CSP (CSP81), this CSP comprises (*S*)-isoleucine (instead of (*S*)-valine) as the linker between the two units [(*R*)-1-phenyl-2-(4-methylphenyl) ethylamine amide and 2-amino-3,5-dinitro-1-carboxamido-benzene]. Once again, it was found that this type of CSPs possessed enantioselectivity to pyrethroid insecticides (85).

Additionally, three new CSP analogues (CSP83–CSP85) were developed for the separation of the same type of analytes (Table 3) (86). These CSPs also have the (*R*)-1-phenyl-2-(4-methylphenyl)ethylamine unit connected to (*S*)-amino acid (valine, leucine or isoleucine); however, the π-acid unit is 4-amino-3,5-dinitro-1-carboxamido benzene. All the amino acid derivatives and pyrethroid insecticides were fairly resolved on these CSPs under the normal-phase condition, although the best

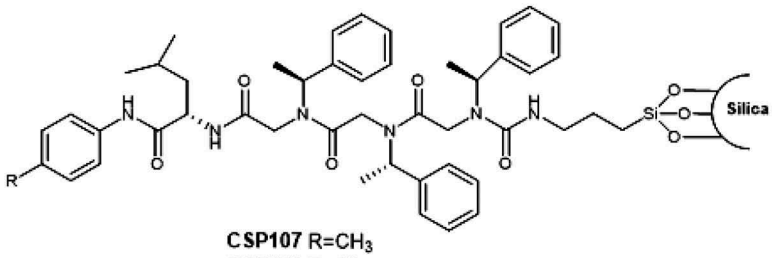




CSP101 R=H
CSP102 R=CH_3
CSP103 R=Cl



CSP104 R=H
CSP105 R=CH_3
CSP106 R=Cl



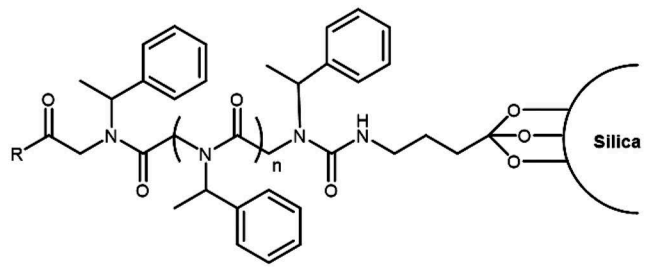
CSP107 R=CH_3
CSP108 R=Cl

chromatographic result was achieved with CSP85 (α = 1.70 for leucine derivative).

CSP86 was developed specifically for the enantioresolution of β-methylphenylethylamine (Table 3) (87). This specific target analyte is of interest since it belongs to the group of drugs related to amphetamines. The new CSP was prepared by using Sephorose 4B as a matrix, L-tyrosine as a spacer and an aromatic amino derivative of L-glutamic acid as a ligand. Several buffer solutions, at different pH values, were used as mobile phases in order to separate β-methylphenylethylamine into its enantiomers.

Peptide CSPs

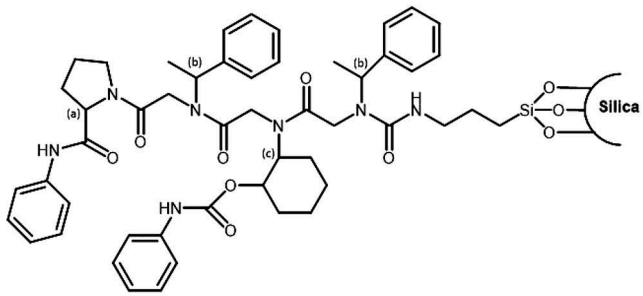
Recently, two new CSPs (CSP87 and CSP88), comprising peptides with three amino acids, have been prepared and



CSP109 R= *R-R-R*
CSP110 R= *S-R-R*
CSP111 R= *S-R-S*
CSP112 R= *S-S-R*
CSP113 R= *S-R-S-R-S*

CSP114 R= *S-R-R*
CSP115 R= *S-R-S*
CSP116 R= *S-S-R*

CSP117 R= *S-R-R*
CSP118 R= *S-R-S*
CSP119 R= *S-S-R*

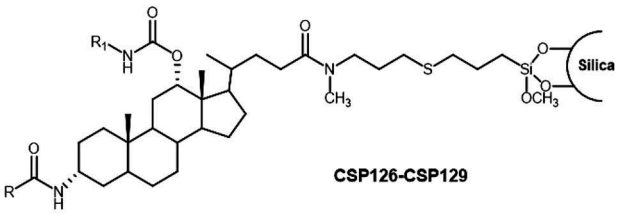


CSP120 (a) *R* **(b)** *S* **(c)** 1*R*,2*R*
CSP121 (a) *R* **(b)** *R* **(c)** 1*R*,2*R*
CSP122 (a) *R* **(b)** *S* **(c)** *rac*

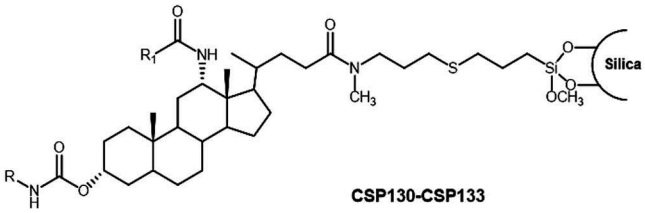
CSP123 (a) *R* **(b)** *S* **(c)** 1*S*,2*S*
CSP124 (a) *R* **(b)** *R* **(c)** 1*S*,2*S*
CSP125 (a) *S* **(b)** *R* **(c)** 1*R*,2*R*

evaluated. The effect of their amino acids sequence and 5-nitronicotinoyl terminal group on chiral separation was also investigated (88). Valine, phenylalanine and proline were chosen, and the obtained CSPs provided the effective recognition and enantioseparation of adrenoceptor agonists and analytes containing amide or naphthalene rings (Table 4).

Additionally, other CSPs comprising linear (89–91) and cyclopeptide-bonded stationary phases (92) were prepared and evaluated. Wu et al. described the development of several new CSPs that were based on poly-*N*-substituted glycines, and also called them peptoids. The first reported peptoid CSPs were based on peptoid oligomers with α-chiral aromatic side chains (CSP89–CSP93) (93). (*S*)-*N*-(1-Phenylethyl)glycine (Nspe) was used as the monomer for the peptoids and the chain length varied from three to seven chiral units. Binaphthol (BINOL) and its derivatives were chosen to investigate their performance as well as the influence of

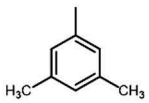


CSP126-CSP129

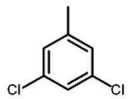


CSP130-CSP133

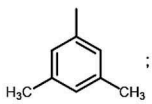
CSP126 and CSP130 R = R1 =



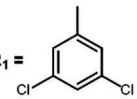
CSP127 and CSP131 R = R1 =



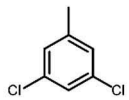
CSP128 and CSP132 R =



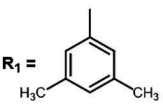
; R1 =



CSP129 and CSP133 R =



; R1 =

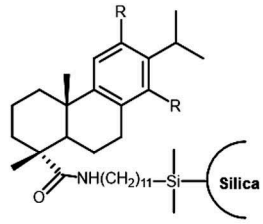


the peptidic chain length on enantiomeric ability (Table 4).

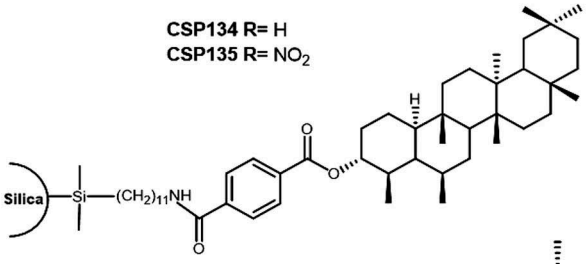
Subsequently, the terminal group of the peptoid selector was modified in order to improve the applicability of these CSPs (94). Therefore, six CSPs (CSP94–CSP99), comprising achiral alkyl groups, such as *n*-butyl, *t*-butyl and diisopropyl, or chiral groups, namely (1*R*, 2*R*)-2-aminocyclohexyl phenylcarbamate, *N*′-phenyl-L-proline amide and *N*′-phenyl-L-leucine amide, as terminal groups, were prepared. For comparison, CSP100 with (1*R*, 2*R*)-2-aminocyclohexyl phenylcarbamate directly bonded to silica was also synthesized. Based on chromatography, the results obtained for the BINOL atropisomers and their derivatives (Table 4) led to the conclusion that the introduction of these new chiral terminal groups was an effective way to broaden the applicability of the peptoid CSPs.

Other peptoid CSPs, terminated with *N*′-substituted phenyl-L-proline or L-leucine amide (CSP101–CSP108), were developed in order to investigate the influence of the introduction of *p*-methyl and *p*-chloro substituents to the terminal phenyl group (95). These CSPs were applied to the separation of a large number of analytes, under normal-phase elution conditions (Table 4). It was found that the influence of the substituent on selectivity varied along with the terminal amino acid and peptoid chain length.

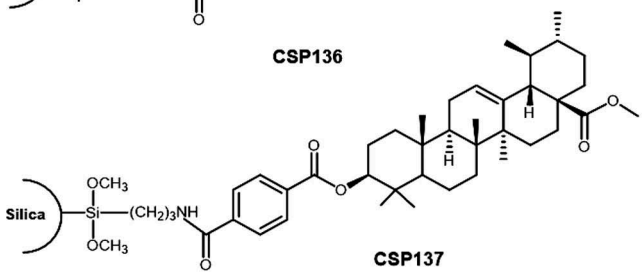
In order to further explore the role of the peptidic chain in enantiorecognition, a series of CSPs with selectors terminated with alkyl group, based on chiral *N*-(1-phenylethyl) glycine and varied in configurations was prepared (CSP109–CSP119) and investigated with axially chiral analytes (Table 4) (96). Selectors with heterogeneous configurations, such as *S-R-R, S-R-S, S-S-R*, generally performed better than homochiral selectors (*S-S-S* or *R-R-R*).



CSP134 R= H
CSP135 R= NO_2



CSP136



CSP137

TABLE 5
CSPs from natural source

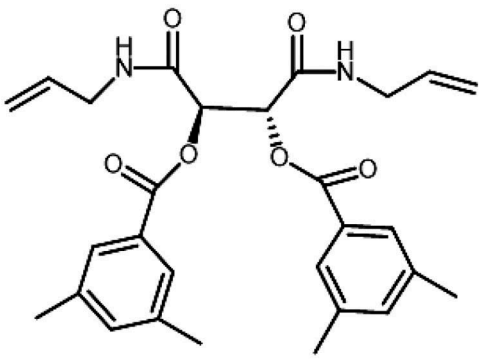
CSPs	*Separated Analytes*	*Mobile Phase/Flow rate*	*Ref.*
CSP126-CSP133	Benzodiazepines derivatives	Hex:DCM:2-PrOH (70:30:3);1.0 mL/min	(99)
CSP134-CSP136	*N*-Trifluoroacetyl and *N*-3,5-DNB methyl ester amino acids derivatives, *N*-Benzoyl tryptophan amino acid derivatives, Binaphthol, 9-Anthryl(trifluoromethyl) Carbinol, α-Methylbenzyl alcohol, 1,1′-*bis*-2-Naphthol, *cis*-β-Lactams	Hex:2PrOH (90:10, 80:20, 95.5, 99.1, 50:50), Hex:2-PrOH:TFA (99:1:0.09, 97:3:0.09), Hex:2-PrOH:MeOH (96:3.5:0.5), Hex:2-PrOH:EtOH (99:0.5:0.5, 95:2:3), Hex:DCM (80:20, 90:10, 95:5)	(101)
CSP138	Binaphthol, Trifluoromethyl-anthrylmethanol, Benzodiazepine derivatives	Hex:2-PrOH (95:5); 2.0 mL/min	(103)
CSP139-CSP147	*N*-protected Amino acid derivatives, DNB, DNP and DNZ derivatives of leucine derivatives, Profens	MeOH:0.1 M NH_4OAc (80:20); 0.75 mL/min	(107)
CSP148-CSP153	*N*-protected Amino acid derivatives, DNB, DNP and DNZ derivatives of leucine derivatives, Profens	MeOH:0.1 M NH_4OAc (80:20); 1.0 mL/min	(108)
CSP154	α-Aryloxycarboxylic acids, Profens	MeCN:AcOH:TEA (98:2:0.2), MeCN:NH_4OAc:AcOH (50:50:5); 0.75 mL/min	(109)
CSP155-CSP169	Acid type analytes	MeOH:AcOH:NH_4OAc (99:1:0.25); 1.0 mL/min	(110)
CSP170-CSP171 (not from natural source)	Amino alcohol type drugs	Different proportions of MeOH:MeCN with AB, DEA, DIEA, NH_4OAc and FA; 1.0 mL/min	(111,112)
CSP172-CSP176	*N*-Derivatized amino acids, 3,5-DNB amides, Cathinones, β-Methyl-1,2,3,4 tetrahydroisoquinoline-3-carboxylic acids, Cinchona alkaloids, Butoxamine, Celiprolol, Isoxsuprine, Mefloquine, Tocainide, Cyclic β-amino acids,1,2,3,4-Tetrahydroisoquinoline analogues, β-blockers, β-sympathomimetics, among others	Different proportions of MeOH:MeCN or H_2O containing NH_3, EA, DEA, TEA, PRA, TPA, TBA, BA, FA, AcOH or H_3PO_4; 0.4, 0.55, 0.6 and 1.0 mL/min	(113–115, 119,120, 122–132)
CSP177-CSP182	Amino acid derivatives, Modified mefloquine, Zwitterionic analytes	50 mM FA and 25 mM DEA in MeOH; 1.0 mL/min	(116,118,121)
CSP183-CSP190	Proteinogenic amino acids, Halogen atom-substituted amino acids, Hydroxy-substituted amino acids, Aminosulfonic acids, α and *N*-methylated amino acids, Aliphatic and aromatic amino acids	100% MeOH, MeCN:MeOH (50:50); 0.4 mL/min	(117)
CSP191-CSP192	Basic and acid derivatives of cinchona alkaloids	Hex:2-PrOH (70:30, 90:10, 95:5), Hex:2-PrOH:TFA:TEA (70:30:0.2:0.1, 80:20:0.2:0.1), Hex:2-PrOH:TFA (90:10:0.1, 80:20:0.1), MeOH:AcOH:TEA (97:3:0.45), MeOH:AcOH:NH_4OAc (98:2:1.5), MeOH:TFA (100:0.1); 0.8 mL/min	(133)

Hex: *n*-hexane; 2-PrOH: 2-propanol; EtOH: ethanol; DCM: dichloromethane; MeCN: acetonitrile; MeOH: methanol; AB: 2-amino-1-butanol; BA: butyl amine; DEA: diethylamine; DIEA: diisopropyl/ethyl amine; EA: ethylamine; TPA: tripropylamine; PRA: propylamine; TBA: tributylamine; TEA: triethylamine; TFA: trifluoroacetic acid; FA: formic acid; AcOH: acetic acid; NH_4OAc: ammonium acetate; DNB: dinitrobenzoyl; DNP: dinitrophenyl; DNZ: dinitrobenzyloxycarbonyl.

Additionally, a series of peptoid CSPs, incorporating several kinds of chiral blocks (CSP120–CSP125), were developed in order to further explore the influence of the absolute configurations of peptoid CSP on enantioselectivity (97). Considering the overall results, CSP120 and CSP121 provided better enantioresolution for the tested analytes, under normal-phase elution conditions (Table 4).

CSPs from Natural Source

Considering the enantiodiscrimination properties, exhibited by CSPs based on the natural product deoxycholic acid (98), two new families of CSP analogues comprising both arylamide and arylcarbamate moieties on the cholestane backbone were synthesized and covalently bonded to silica gel (CSP126–CSP133) (99). Benzodiazepine derivatives were selected as analytes to evaluate the performance of these eight CSPs (Table 5). Chromatographic data revealed that the enantioresolution capability depended either on the position of the arylamide on the cholestanic system or on electrostatic properties of the aryl substituent. Thereafter, these CSPs have been thoroughly evaluated using a larger library of racemates (Table 5), allowing to find similarities and differences in their enantiorecognition mechanisms, and suggesting that the arylcarbamoyl derivatives of bile acids



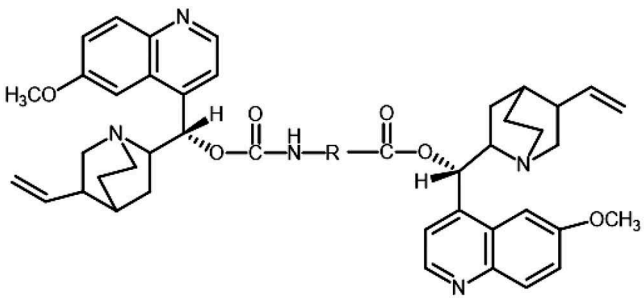
Selector of **CSP138**

can be successfully used as chiral selectors in enantioselective chromatography (100).

New Pirkle-type CSPs were obtained using natural compounds such as dehydroabietic acid and friedelin fixed onto a solid support of silica gel by a larger spacer 10-undecenylamine (CSP134–CSP136) (101). The chiral selector of CSP135 was synthesized by nitration of the selector of CSP134. These two selectors possess a rigid diterpenoid backbone covering an aromatic unit capable of enantioselective recognition of aromatic analytes by π–π interactions. However, they exhibit different electronic binding properties since the two electron-withdrawing nitro groups of the selector of CSP135 confer a π-acidic character while the selector of CSP134 has π-basic properties.

CSP136 possesses a long pre-organized triterpenoid backbone linked by an ester group to an aromatic moiety. All the three CSPs resolved racemates of *N*-trifluoracetyl and *N*-3,5-DNB ester of phenylalanine derivatives (Table 5). Additionally, CSP134 showed a good enantioseparation of β-lactams and *N*-benzoyl tryptophan amino acid derivatives, while CSP136 was suitable for separating free alcohols and their derivatives with fluorine substituents. CSP135 was the only phase to resolve efficiently 1,1′-binaphthol atropisomers. Molecular modeling studies were carried out in order to understand the structural features associated with chiral molecular recognition of these CSPs (101). The *in silico* results revealed that the stability of the transient diastereomeric complexes, formed between the chiral selectors of CSP134 and CSP135 and several amino acid derivatives, was achieved by van der Waals interactions, while the electrostatic binding interactions were mainly responsible for the enantioselectivity.

Recently, a new terpenoid chiral selector was covalently linked to 3-aminopropyl silica gel affording CSP137 (102). Four chiral analytes, namely methyl mandelate, aniline derivative of mandelic acid, benzoin and ibuprofen, were selected as the target analytes to evaluate enantiodiscriminating capability by static adsorption experiment (Table 5). The results showed that CSP137 has enantioselectivity for methyl mandelate and ibuprofen.



Selectors of:

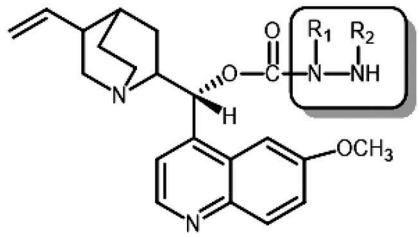
CSP139 R = -$(CH_2)_2$-
CSP140 R = -$(CH_2)_3$-
CSP141 R = -$(CH_2)_4$-
CSP142 R = -$(CH_2)_6$-

CSP143 R =

CSP144 R =

CSP145 R = (*R*,*R*)
CSP146 R = (*S*,*S*)

CSP147 R = (*R*,*R*)



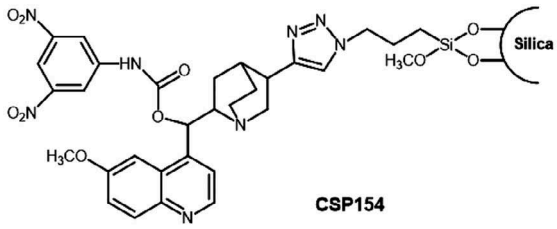
Selectors of:

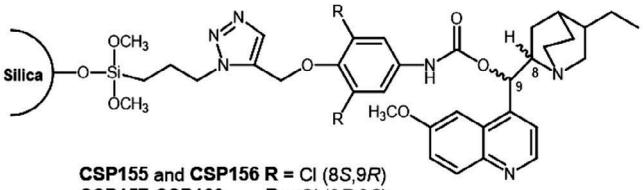
CSP148 R_1 = H, R_2 = H
CSP149 R_1 = CH_3, R_2 = H
CSP150 R_1 = H, R_2 = CO-*tert*-butyl
CSP151 R_1 = H, R_2 = CO-1-adamantyl
CSP152 R_1 = H, R_2 = CO-trityl
CSP153 R_1 = H, R_2 = 3,5-dinitrobenzoyl

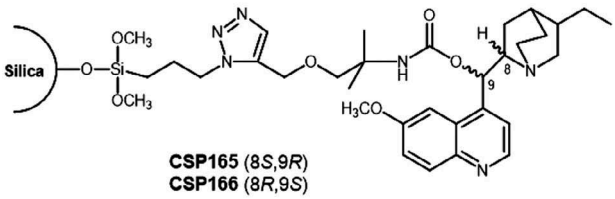
A Pirkle-type tartaric acid-based selector ((*R*,*R*)-*N*-allyl-*O*,*O*′-bis (dimethylbenzoyl) tartarimide) was synthesized, immobilized on mercaptopropyl silica and evaluated as CSP (CSP138) (103). The enantiodiscrimination of this new CSP was compared with the successful commercially available polymeric Kromasil CHI-DMB CSP, with a tartaric acid-based selector (*O*,*O*′-bis (dimethyl)benzoyl tartaric diamide). The principal aim of this study was to understand the influence of the effects from hydrogen bonding and rigidity on enantioselectivity. Accordingly, when compared with the Kromasil CHI-DMB CSP, the selector of CSP138 is more rigid and does not have the NH group. Considering the very low separation factors obtained (α between 1.00 and

1.06) with the new CSP, it was concluded that the introduction of rigidity and the absence of NH function resulted in lower resolving capacity toward the tested racemates (Table 5).

Several LC chiral anion-exchange CSPs, based on the cinchona alkaloid enantiomers quinine and quinidine, have been developed until 2000 by Lindner's group in Austria (104–106). These CSPs may be considered as a subset of Pirkle-type CSPs from which they differ in that they comprise ionizable chiral selectors. The ionic interaction between the oppositely charged selectors and

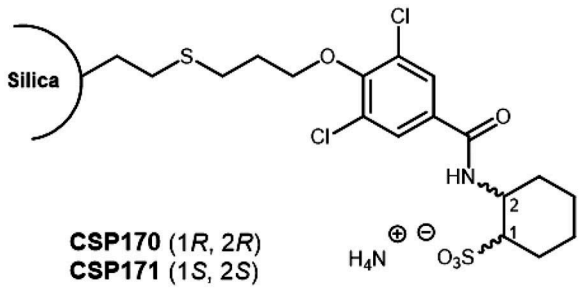






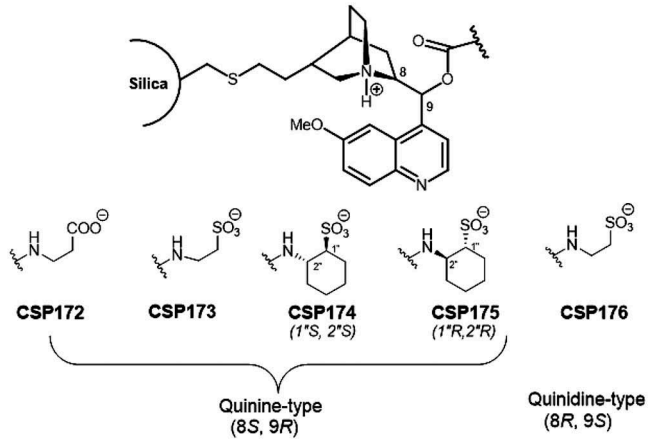
the analytes plays the key role for retention and enantioresolution (19). In the last 17 years, this trend was followed. In fact, these alkaloids continued to be used as starting materials for the preparation of new chiral ion-exchange CSPs and, more recently, zwitterionic CSPs.

Nine new dimeric CSPs (CSP139–CSP147), comprising two quinine units connected by different aliphatic and cyclic spacers, have been developed (107). A set of *N*-derivatized amino acids and other acidic drugs was chosen in order to clarify the role of the presence of a second quinine unit on the chiral selector, as well as the influence of the structure and length of the spacer, on the overall chiral recognition. An exceptional resolution was achieved with the CSPs possessing dimeric chiral selectors with a *trans*-1,2-diaminocyclohexylen-bridge (CSP145 and CSP146) for the separation of DNB derivatives of amino acids and certain acidic drugs such as profens (Table 5).



Another approach was exploited by the same group to develop chiral anion-exchange-type selectors by the introduction of a novel O_9-hydrazide functionality on the quinine template (108). Therefore, six new quinine O_9-hydrazide derivatives, with different substituents, have been synthesized and immobilized on silica gel affording CSP148–CSP153. A wide range of amino acid derivatives and acidic drugs of therapeutic interest, such as profens, were chosen to investigate the chiral resolving performance of these CSPs (Table 5). From the chromatographic results, generally the unsubstituted quinine-hydrazide derivative was the best chiral selector of the hydrazide series. Among the substituted hydrazide derivatives, the introduction of a tritylcarbonyl or a *tert*-butylcarbonyl group at the β position of the hydrazide moiety improved chiral recognition by the resulting CSPs.

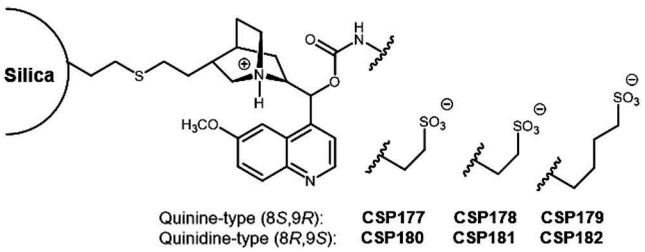
Click chemistry has been explored for the preparation of a new CSP using quinine derivative as starting material (CSP154) (109). This chiral selector comprises a π-basic quinoline group, a strong π-acid 3,5-dinitrophenyl moiety and an ionizable tertiary amino group. Thus, this CSP was able to establish π-donor–π-acceptor interactions in addition to ion-pairing/ion-exchange process toward specific analytes, such as herbicidal α-aryloxycarboxylic



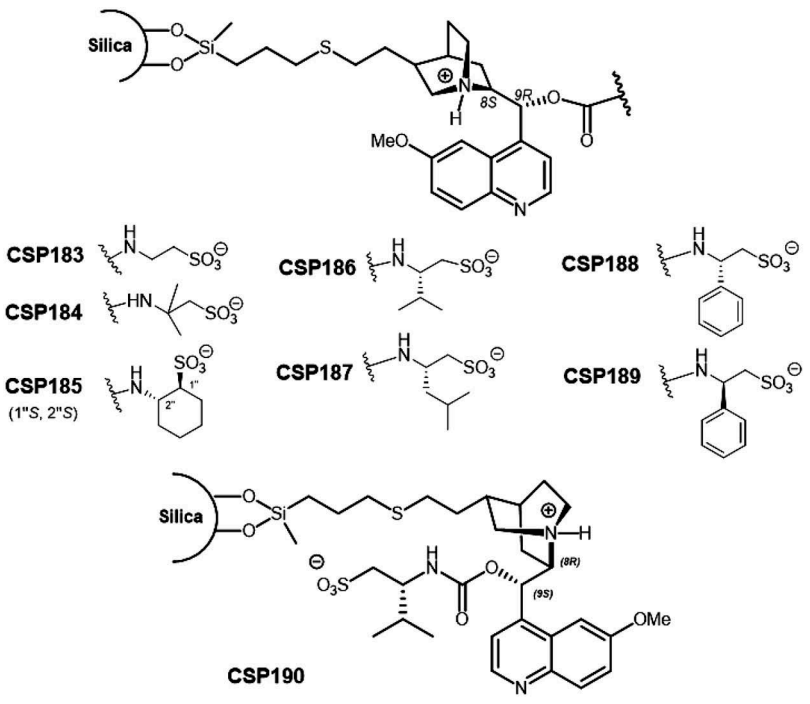
acids and nonsteroidal anti-inflammatory profens (Table 5).

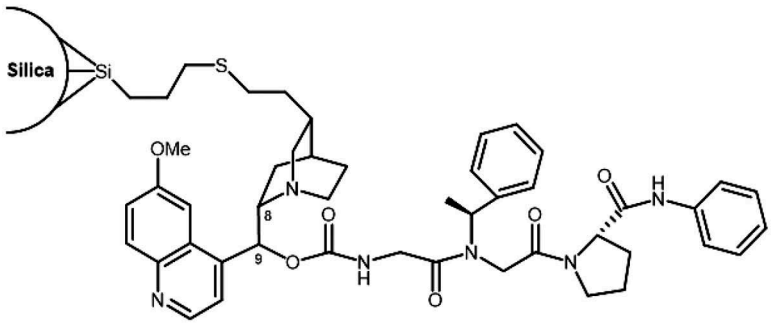
Using the same immobilization synthetic strategy, a series of new cinchona-derived CSPs was prepared (CSP155–CSP169) (110). To evaluate their chiral recognition performance, a set of representative chiral organic acids was used under polar organic elution conditions (Table 5). These authors also studied the effect of different selector loadings on selectivity and resolution by preparing four columns with the same selector but differing in the loading densities. Generally, the higher the selector loading, the longer the retention times and the worst the performance.

In a continuation of the work, two successful Pirkle-type strong cation-exchange CSPs (CSP170 and CSP171) for the chromatographic enantiomer separation of a variety of chiral amines by LC have been developed (Table 5) (111). The novel CSPs, containing a β-aminocyclohexanesulfonic acid moiety covalently attached to a chromatographic support, were prepared by nonenantioselective synthesis followed by preparative enantioseparation to afford CSPs of both configurations. The chromatographic evaluations were carried out under nonaqueous polar organic mobile phase conditions using a set of basic analytes, mostly common drugs (Table 5). All the analytes could be baseline separated. In a further work, CSP170 was successfully used for the resolution of a series of cinchona alkaloids and their synthetic derivatives to evaluate its effectiveness as alternative methodology for the separation of these alkaloids (112).



In an attempt to overcome the limited applicability scope of the described cinchona alkaloid-based weak anion exchangers CSPs as well as aminosulfonic acid-based strong cation exchangers CSPs, which are limited to oppositely charged analytes, Lindner and co-workers reported, in 2008, the merging of their individual chiral selectors in a combinatorial synthesis approach into single zwitterion exchanger-type CSPs (113). Indeed, the concept of zwitterionic CSPs is based on merging key cation- and anion-exchange moieties in one single chiral selector with the resulting CSPs allowing enantioresolution of a variety of chiral ionizable analytes. Hence, CSP172–CSP176 were successfully developed and demonstrated to be efficient for enantioseparations not only toward acids and amines but also for zwitterionic analytes like amino acids and dipeptides, using polar organic mobile-phase conditions (Table 5). Additionally, systematic investigations of the ion-exchange-type retention mechanisms, available with the zwitterionic CSP172–CSP175, in

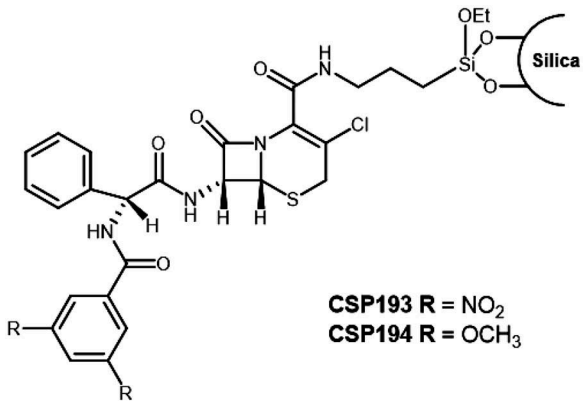




CSP191 (8*S*,9*R*)
CSP192 (8*R*,9*S*)

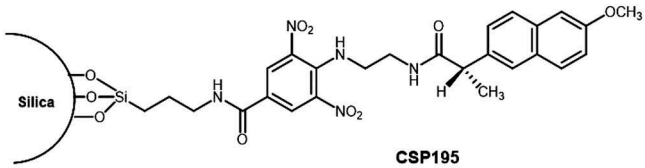
a nonaqueous polar organic mode (114), and the effects of mobile-phase composition on their chromatographic behavior (115) were carried out. Recently, CSP174 and CSP175 were commercialized as CHIRALPAK ZWIX(+) and ZWIX(–), respectively, from Chiral Technologies, Europe.

The same Austrian group also synthesized two pseudo-enantiomeric series of zwitterionic CSPs by fusion of quinine and quinidine with straight-chain aminoalkanesulfonic acids of different chain lengths (CSP177–CSP182) (116), aiming at a systematic evaluation of the influence of intramolecular distances between anion and cation exchanger sites on the enantioseparation as well as elucidation of the influence of a chiral element or a flexible alkyl chain close to the strong cation exchanger site. The six novel aminosulfonic acid/cinchona-based zwitterionic CSPs were successfully employed for enantiomer separations of chiral acids, bases and ampholytes in many cases (Table 5).

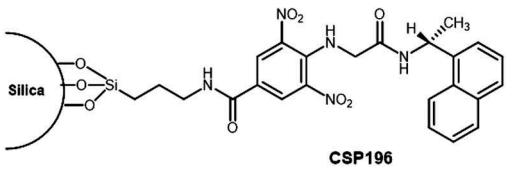


CSP193 R = NO_2
CSP194 R = OCH_3

Novel zwitterionic ion-exchange-type CSPs were developed by structural modifications at both the strong cation exchange site and weak anion-exchange moiety (CSP183–CSP190) (117). The influence of protic and aprotic solvent compositions of the nonaqueous mobile phase on their separation performance of various zwitterionic analytes was investigated (Table 5).



CSP195



CSP196

Several recent works developed by the Lindner group highlighted the versatility of cinchona-based chiral zwitterion-exchange stationary phases. Works described the enantiomer and diastereomer separation of underivatized oligopeptides (118, 119), the enantioseparation of free α-, β- and γ-aminophosphonic acids (120), the direct enantioseparation of underivatized aliphatic 3-hydroxyalkanoic acids (121), β-amino acids (122–126), secondary amino acids (127), bicyclo[2.2.2]octane-based 3-amino-2-carboxylic acids (128), monosubstituted tryptophan derivatives and metabolites (129), cationic 1,2,3,4-tetrahydroisoquinoline analogues (130), isoxazoline-fused-2-aminocyclopentane carboxylic acids (131), and cathinones (132).

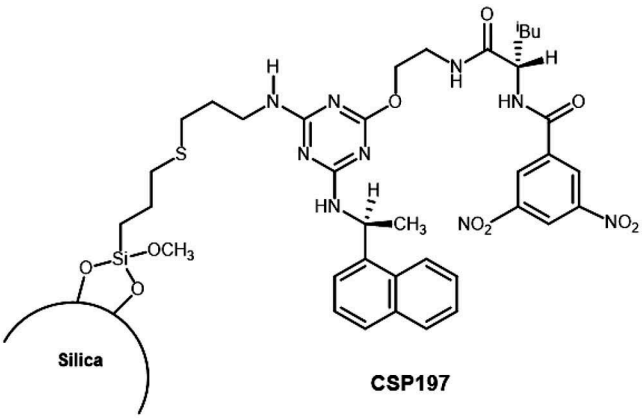
Additionally, the Liang group in Shanghai has also described the synthesis of novel CSPs, based on poly-*N*-

TABLE 6
CSPs from drugs

CSPs	*Separated Analytes*	*Mobile Phase/Flow rate*	*Ref.*
CSP193	*N*-(substituted benzoyl) Leucine ethyl esters, *N*-(substituted benzoyl) Leucine propyl amides, Anilide derivatives of *N*-acetyl-α-amino acids, Anilide derivatives of *O*-ethoxycarbonyl-2-hydroxycarboxylic acids, 3-substituted 1,4-Benzodiazepin-2-ones	Hex/2-PrOH (80:20); 1.0 mL/min	(134)
CSP194	*N*-(3,5-DNB)-α-amino acid, amide and ester derivatives, 3-substituted 1,4-Benzodiazepin-2-ones	Hex/EtOH (80:20), Hex/2-PrOH (80:20); 1.0 mL/min	(135)
CSP195-CSP196	BINAPO	Hex/2-PrOH (70:30), MTBE/MeOH (90:10); 1.0 mL/min	(80)

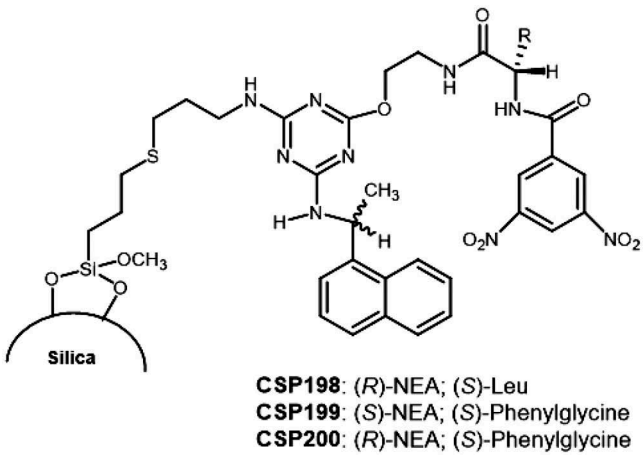
Hex: *n*-hexane; 2-PrOH: 2-propanol; EtOH: ethanol; MeOH: methanol; MTBE: *tert*-butyl methyl ether; DNB: dinitrobenzoyl.

substituted glycines (peptoids), which combines a quinidine moiety through a C9-position carbamate group (CSP191 and CSP192) (133). Neutral, acidic and basic chiral compounds were selected as analytes to investigate the chiral recognition performance of these two CSPs (Table 5). According to the chromatographic results, the strategy to obtain novel selectors by connecting a quinidine moiety to a peptoid chain was proved to be excellent.



CSPs from Drugs and Analogues

Two new Pirkle-type CSPs, based on the cephalosporin antibiotic cefaclor, were developed (134, 135). Cefaclor was chosen since it can be readily modified through the free amino and carboxylic acid groups, in addition to its commercial availability in an optically active form. CSP193 and CSP194 were prepared by bonding *N*-(3,5-DNB)-cefaclor (134) and *N*-(3,5-dimethoxybenzoyl)-cefaclor (135) to silica gel. CSP193 was the first to be prepared and was shown to be quite successful for the liquid chromatographic resolution of several π-basic analytes (Table 6). Moreover, the effective π–π interactions between the CSP and the analytes were proved to be of great importance for chiral recognition (134). Subsequently, and in order to separate π-acidic analytes, CSP194 comprising a π-basic moiety was prepared and proved to be effective on their chromatographic enantioresolution (135).



In addition to the previously described CSP61–CSP63, two CSPs based on the nonsteroid anti-inflammatory drug (*S*)-naproxen and its analogue (CSP195 and CSP196) were specifically designed and synthesized for the separation of BINAPO enantiomers (Table 6) (80). The best enantioresolution was achieved on CSP195, derived from (*S*)-naproxen, with an α value of 2.51 and R_S of 7.06, with this CSP being the option for scale-up separation of BINAPO enantiomers.

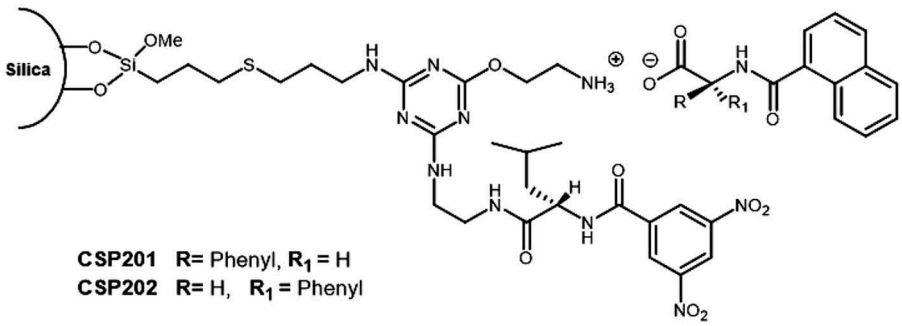


TABLE 7
CSPs with biselectors

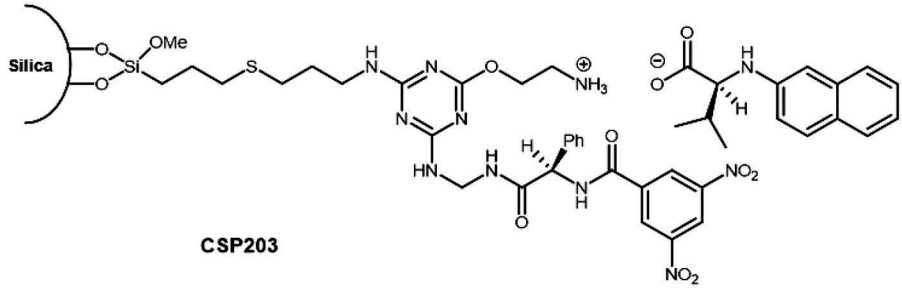
CSPs	*Separated Analytes*	*Mobile Phase/Flow rate*	*Ref.*
CSP197	3,5-Dinitrobenzamides of amine, 3,5-Dinitroanilides of ibuprofen, 4-Nitrobenzamides, Binaphthylic derivatives, 9-Anthryl(trifluoromethyl) carbinol, 3,5-DNP derivatives of amino acid alkyl esters	Hex/DCM/2-PrOH (70:30:1, 75:20:5, 90:10:1); 1.0 mL/min	(136)
CSP198-CSP200	3,5-DNP derivatives of 1-arylpropionic acids, Amino acid alkyl esters and methylamines, 3,5-Dinitroanilides of ibuprofen, 3,5-Dinitrobenzamides, 4-Nitrobenzamides, Binaphthylic derivatives, 1-(9-Anthryl)-2,2,2-trifluoro-ethanol	Hex/DCM/2-PrOH (70:30:1, 75:20:5, 90:10:1); 1.0 mL/min	(142)
CSP201-CSP202	Binaphthyl derivatives and alkylaryl carbinols, 4-Nitrobenzamide derivatives, 3,5-DNP derivatives of amino acid alkyl esters and amides	Hex/DCM/2-PrOH (70:30:1, 70:30:3, 70:30:5, 90:10:1, 95:5:0.5); 1.0 mL/min	(143)
CSP203	Binaphthols derivatives, Alkylaryl carbinols, π-basic Amides, 3,5-DNP derivatives of amino acid alkyl amides, 4-Nitrobenzamide derivatives, Methylamines	Hex/DCM/2-PrOH (70:30:1, 70:30:3, 70:30:5, 90:10:1, 95:5:0.5); 1.0 mL/min	(144)
CSP204	Binaphthol, Trifluoromethyl-anthrylmethanol, Benzodiazepine derivatives, DEABA	Hex/2-PrOH (95:5); 2.0 mL/min	(146)
CSP205-CSP207	Binaphthol, Aryl derivatives of amino acids, amino alcohols and amines, Arylamides and esters	Different proportions of Hex/2-PrOH, Hex/EtOH, Hex/BuOH, Hex/EtOH/MeOH, EtOH/MeOH, MeCN/MeOH, MeOH/H_2O, MeCN/H_2O, MeCN/MeOH/H_2O, MeOH/H_2O/TEA, MeOH or MeCN/Buffer (at different pH); 0.9 and 1.0 mL/min	(147)
CSP208-CSP211	Binaphthol and analogues, 2-Indolinone analogues, 2-Oxazolidone derivatives, 4-Phenyl-1,4-dihydropyridine derivatives, Amino acid derivatives	Mobile phase not specified; 0.8 mL/min	(148)

Hex: *n*-hexane; EtOH: ethanol; 2-PrOH: 2-propanol; BuOH: butanol; DCM: dichloromethane; MeCN: acetonitrile; MeOH: methanol; TEA: triethylamine; DNP: dinitrophenyl.

CSPs with Biselectors

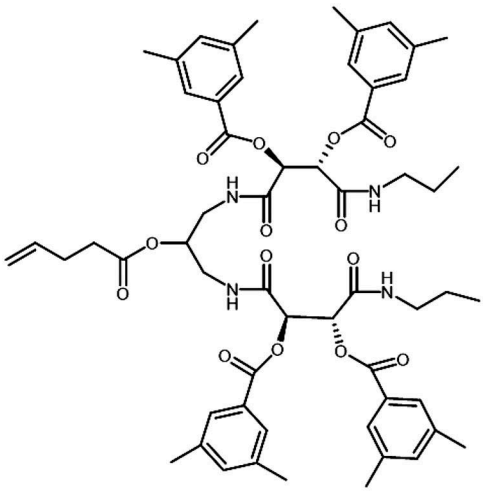
An interesting and efficient strategy, used to increase enantioselectivity, involved the development of CSPs comprising a biselector or combinatorial selectors.

A mixed CSP (CSP197) was developed by linking together two different effective selectors, and the resulting biselector was covalently attached to silica gel through a spacer (136). CSP197 comprises (*S*)-*N*-(3,5-DNB)-leucine and [(*S*)-1-(1-naphthyl) ethyl]amine [(*S*]-NEA) as selectors. It is interesting to note that (*S*)-*N*-(3,5-DNB)-leucine, when linked to silica gel, represents one of the most popular CSPs developed by Pirkle and co-workers (137–140). On the other hand, [(*S*)-1-(1-naphthyl) ethyl]amine [(*S*]-NEA), when bonded to s-triazine, gives the same selector as in one of Oi's s-triazine-based CSPs (141). s-Triazine was also chosen as the connecting moiety for the two chiral selectors of CSP197. As expected, the mixed CSP showed broader applicability than the two monoselector CSPs, and these features were due to the complementarity of the two selectors in the enantiodiscrimination of different analytes (Table 7).



CSP203

Once again, both NEA and (*S*)-*N*-(3,5-DNB)-leucine molecules, as well as (*S*)-*N*-(3,5-DNB)-phenylglycine, were used as chiral building blocks to prepare three new CSPs (CSP198–CSP200) increasing the number of biselector systems for enantioselective LC (142). Comparing the chromatographic data obtained using CSP198–CSP200 with the previously described biselector CSP (CSP197) (136) in the enantioresolution of tested analytes (Table 7), some insights about the enantiorecognition properties for this family of biselector



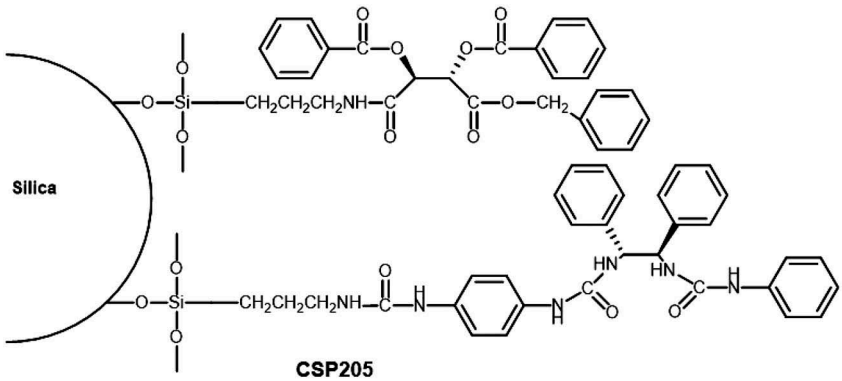
Selector of **CSP204**

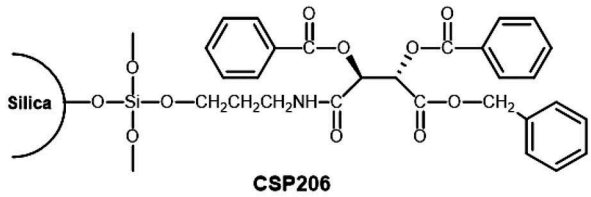
systems were obtained (142). Both stereochemistry and chemical structure of the derivatized amino acids have influenced the enantiodiscrimination properties of the 1-(1-naphthyl)ethylamino-s-triazine moiety of the CSPs. Considering efficiency and versatility toward π-acidic racemic compounds, the results for these new CSPs were found to be worse than those obtained for CSP197. In order to obtain a biselector system whose chiral moieties could act independently, i.e., their enantiodiscriminating capability does not depend on the nature and absolute configurations of the other chiral moiety (differently from the previous CSPs (136, 142), the same group has developed two new diastereoisomeric CSPs (CSP201 and CSP202) (143). In this circumstance, s-triazine was used only as a connection unit to which *N*-3,5-DNB-leucine and *N*-1-naphthoylphenylglycine were linked through a tether. According to the results obtained in the chromatographic resolution of both π-acidic and π-basic racemic analytes (Table 7), the desired goal was achieved. Indeed, both CSPs were able to resolve all classes of tested analytes, demonstrating a complete independence of the action of the two moieties of the biselector system.

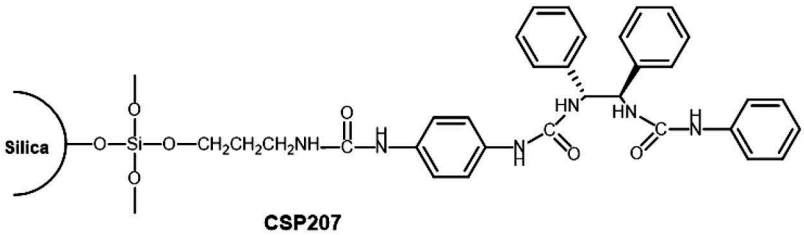
Once it was established that the use of s-triazine allowed to obtain a biselector system where the two components acted independently (143), the next step was to verify the applicability of this approach to the development of other biselector systems. Thus, CSP203, which was known to resolve different classes of racemic compounds (Table 7), was prepared (144), by embodying the selectors of two different original Pirkle's CSPs (137, 145). Taking into account the results obtained, in terms of elution order of the enantiomers tested and the trend of enantioresolution, it can be inferred that the enantiorecognition mechanism exhibited by each chiral moiety of the biselector CSP does not change significantly, when compared with the monoselector CSPs, thus proving the versatility of this approach.

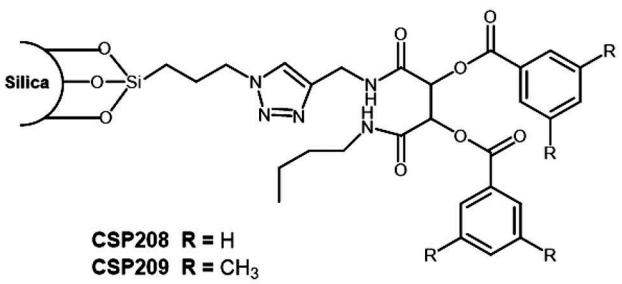
A twin version of the tartaric acid-based selector [*O,O*′-bis(dimethyl)benzoyl tartaric diamide] of the Kromasil CHI-DMB CSP was synthesized and immobilized on silica gel to obtain CSP204 (146). It was expected that this twin selector, which possesses an additional NH amide functionality, could work as a pair of molecular tweezers providing increased selectivity. Surprisingly, in general, the new Pirkle-type CSP revealed lower resolution capability when compared with polymeric Kromasil CHI-DMB CSP. However, two exceptions were observed, namely for the analytes lopirazepam and phenprocoumon, with α values of 1.30 and 1.06, respectively, vs α values of 1.00 or no separation for Kromasil CHI-DMB (Table 7).

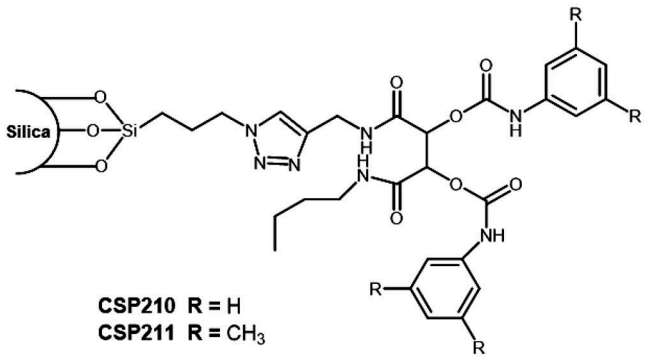
In an attempt to improve chiral recognition performances, another biselector CSP, derived from L-benzoylated tartaric acid and 1,2-diphenylethylenediamine, was obtained (147).











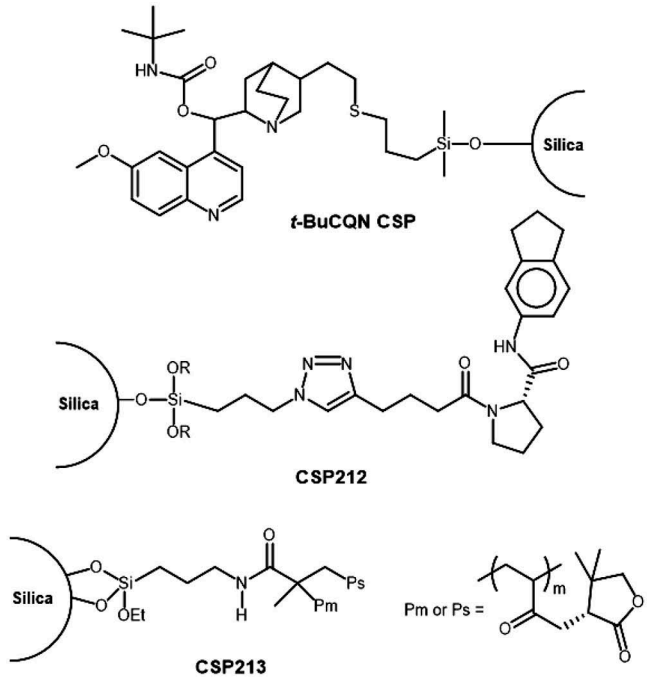
This mixed phase (CSP205) was prepared by simultaneous immobilization of both selectors of CSP206 and CSP207 on aminated silica gel. Analytes with a wide variety of structures were chosen to evaluate their performance, under both normal and reversed phase modes (Table 7). However, unfortunately, chromatographic data revealed that CSP205 did not demonstrate better enantioseparation ability for the tested racemates when compared with the single-selector CSPs (CSP205–CSP207).

Other selectors, based on *O,O′*-diaryl tartardiamide and *O,O′*-bis-(arylcarbamoyl) tartardiamine, were synthesized and immobilized on silica gel through click chemistry (148). The chiral recognition performance of the four obtained CSPs (CSP208–CSP211) was evaluated using a broad range of structurally different racemates (Table 7). CSPs with aryl carbamate moieties (CSP210 and CSP211) were more efficient for enantioresolution than those containing aryl ester moieties (CSP208 and CSP209). Moreover, additional hydrogen bond donors (NH) present in the carbamate groups were proved to be essential for enantioresolution (148).

TABLE 8
CSPs with new supports to improve column efficiency

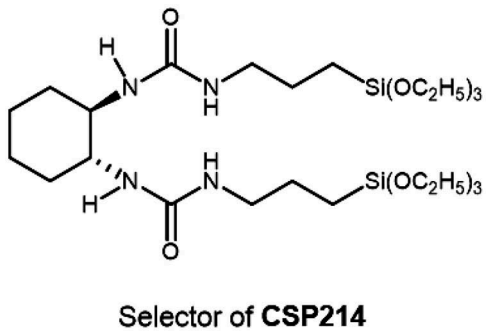
CSPs	*Separated Analytes*	*Mobile Phase/Flow rate*	*Ref.*
Monolithic *t*-BuCQN CSP	*N*-derivatized Amino acids, Suprofen	MeOH/AcOH (99:1, 99.05:0.05, 98:2), MeOH/0.1 M NH_4OAc (80:20); 1.0 mL/min	(153)
Monolithic CSP212	*N*-(3,5-DNB)-amino acid dialkyl amides	Hex/2-PrOH (90:10); 0.5 mL/min	(154)
Monolithic CSP213	1-Indanol, α-Phenyl glycinol, 1-(4-Bromophenyl) ethanol, 1-(2-Chlorophenyl) ethanol, 1-Phenylethylamine	Hex/2-PrOH (98:2); 0.4 mL/min	(155)
Core-shell CSP214	Binaphthyl derivatives, Biphenanthrol	Hex/DCM/EtOH (60:35:5, 60:30:10); 0.5 mL/min	(156)
Sub-2 µm DACH-DNB CSP	Sulfoxides, Phosphineoxide, Aromatic *bis*-Ketone, Naphthamide	Hex/1,4-dioxane/MeOH (70:30:3), Hex/DCM/1,4-dioxane/MeOH (30:30:40:5), DCM/2-PrOH (97:3)	(157)
Sub-2 µm (*R,R*)-Whelk-O1 CSP	NSAIDs, Sulfoxides, Phosphine oxides, Alcohols, Epoxides, Herbicides, Benzodiazepines	Hex/$CHCl_3$ (90:10), Hex/DCM/MeOH (80:20:3), MeCN/H_2O (60:40), Hex/2-PrOH (70:30), MeCN/AcOH/DEA (100:0.2:0.07)	(158,168)

Hex: *n*-hexane; 2-PrOH: 2-propanol; MeOH: methanol; DCM: Dichloromethane; MeCN: acetonitrile; DEA: diethylamine; AcOH: acetic acid; NH_4OAc: ammonium acetate; DNB: dinitrobenzoyl; MeCN: acetonitrile; NSAIDs: non-steroidal anti-inflammatory drugs.



CSPs with New Supports to Improve Column Efficiency

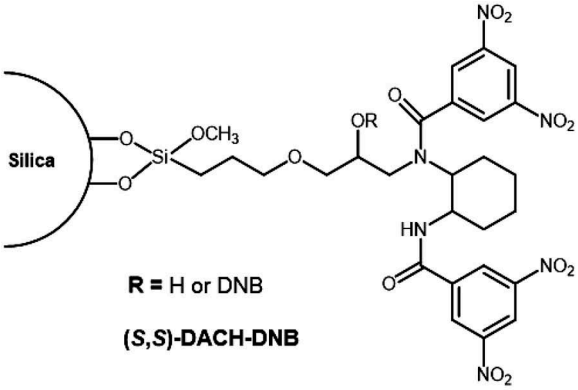
It is important to note that all the CSPs described until now were developed by binding small-molecule selectors to porous silica with 5 µm or bigger size. Nevertheless, the development of CSPs for enantioresolution can be regarded as a systematic and evolutionary process in chromatography. Therefore, a new approach to improve column efficiency was described by using new supports. Accordingly, silica support materials of different morphology, such as core–shell particles and sub-2-µm size, have been developed to improve separation performances in LC. The development of faster and high-throughput LC methods was also described by using monolithic columns (149–151).



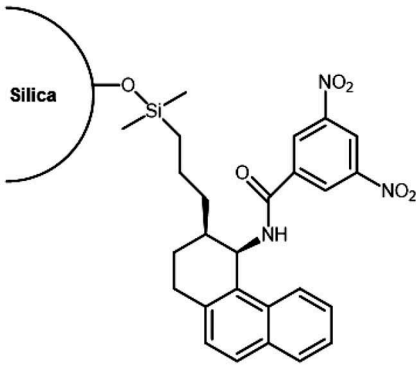
Lubda and Lindner have described the immobilization of *tert*-butyl-carbamoylquinine (*t*-BuCQN) anion-exchanger selector (152) on a silica monolith with unique properties of monolithic silica material (153). To the best of our knowledge, this was the first Pirkle-type monolithic silica column described until 2004. The chromatographic behavior of the monolithic *t*-BuCQN CSP was studied and compared with conventional silica particle-based CSPs. As expected, the silica-based monolith columns offered relatively low-column backpressure. Additionally, good selectivities were achieved for a spectrum of chiral analytes such as *N*-functionalized amino acids and suprofen (Table 8).

A new monolithic Pirkle-type CSP (CSP212) was obtained via an "*in-column* modification" process, which includes immobilization of the proline-derived chiral selector using

click chemistry (154). The same chiral selector was also attached to porous silica. Azide functionalities were first introduced on the pore surface of each type of chromatographic support by reaction with 3-(azidopropyl) trimethoxysilane, followed by immobilization of the selector containing an alkyne moiety. Interestingly, these CSPs possessed excellent enantioselectivity for all the analytes tested (Table 8), affording α values as high as 11.4.



(*S*,*S*)-DACH-DNB



(*R*,*R*)-Whelk-O1

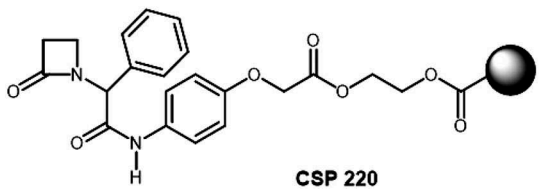
An "in-column" preparation of a new monolithic Pirkle-type CSP (CSP213) containing (*R*)-acryloyloxy-b-b-dimethyl-g-butyrolactone as a low-molecular-mass chiral selector was described (155). The modification of monolithic silica surface was easily performed with an anchor group containing an amide moiety, followed by copolymerization with lactone acrylate derivative to provide a chiral γ-lactone functionalized silica monolith. Several analytes were used to evaluate the performance of CSP213 (Table 8), revealing that a set of secondary alcohols was baseline separated.

New chiral core–shell silica microspheres with *trans*-(1*R*,2*R*)-diaminocyclohexane were synthesized using a layer-by-layer method, and studies on their application as CSP (CSP214) for chromatographic separation were carried out (156). The synthesized DACH silica particles exhibited well-formed spherical core–shell structure, narrow pore size distribution and homogenous distribution of DACH functional groups in the mesoporous shell. The functionalized mesoporous layers were formed by self-condensation of siliane precursors, which contain *N,N′-bis*-[(triethoxysilyl) propyl]-*trans*-(1*R*,2*R*)-*bis*-(ureido)-cyclohexane (DACH-BS) and tetraethoxysilane around the surfactants. CSP214 provided rapid and efficient enantioresolution of several chiral analytes with C2 symmetrical axes, including binaphthyl derivatives and biphenanthrol (Table 8).

The Gasparrini group has developed sub-2-μm Pirkle-type CSPs for fast enantioselective separation and reduced solvents consumption (157, 158). Three CSPs, differing in the particle size of the starting silica particles, specifically 4.3, 2.6 and 1.9 μm, have been prepared by covalent binding of the π-acidic *bis*-(3,5-dinitrobenzoyl)-derivative of *trans*-1,2-diaminocyclohexane (DACH-DNB) (157). DACH-DNB CSP has been designed in the 1990s (159, 160) and was proved to be very effective for separating many racemates (37, 161). Very high speed and high-resolution applications of several chiral analytes were achieved on the columns with reduced particle diameters (Table 9).

CSP215: DNB-D-Asn-L-Thr-L-Abu-NH$(CH_2)_3$silica
CSP216: DNB-D-Asn-L-Thr-L-Ahe-NH$(CH_2)_5$silica
CSP217: DNB-D-Asn-L-Thr-L-Aoc-NH$(CH_2)_7$silica
CSP218: DNB-D-Asn-L-Thr-L-Aun-NH$(CH_2)_{10}$silica
CSP219: DNB-L-Asn-L-Asn-L-Aun-NH$(CH_2)_{10}$silica

DNB: 3,5-dinitrobenzoyl; Asn: asparagine; Thr: threonine; Abu:4-aminobutyric acid; Ahe: 2-aminoheptanoic acid; Aoc:8-aminooctanoic acid; Aun:11-aminoundecanoic acid.



CSP 220

TABLE 9
CSPs obtained by design

CSPs	*Separated Analytes*	*Mobile Phase/Flow rate*	*Ref.*
CSP215-CSP219	*tert*-Butyl-1-(2-methylnaphthyl)-phosphine oxide	Hep/DCM (70:30); 1.2 mL/min	(177)
CSP220	3,5-DNB-amino acid derivatives	DCM/Hex (70:30); 1.0 mL/min	(178)

Hex: *n*-hexane; Hep: *n*-heptane; DCM: Dichloromethane; DNB: dinitrobenzoyl.

TABLE 10
CSPs with xanthone derivatives as small molecule selectors

CSPs	*Separated Analytes*	*Mobile Phase/Flow rate*	*Ref.*
CSP221-CSP226	Xanthone derivatives, bi-naphthol, 1-(9-anthryl)-2,2,2-trifluoroethanol, *N*-[1-(1-naphtyl)ethyl]-3,5-dinitrobenzamide	Hex/2-PrOH (90:10, 80:20, 70:30), Hex/EtOH (90:10, 85:15, 80:20), Hex/EtOH/TFA (90:10:0.01); 0.5 mL/min	(185, 186)

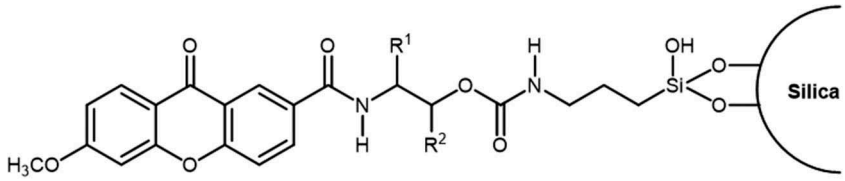
Hex: *n*-hexane; 2-PrOH: 2-propanol; EtOH: ethanol; TFA: trifluoroacetic acid.

By covalent attachment of the selector of (*R,R*)-Whelk-O1 CSP to spherical, high-surface area 1.7-µm porous silica particles, the Gasparrini group prepared another sub-2-µm Pirkle-type CSP (158). Among a large number of Pirkle-type CSPs described in the literature, the Whelk-O1 CSP is one of the most employed ones with the broadest application in industrial and academic laboratories (162–167). The Whelk-O1 CSP was designed in the 1990s (78), applying an immobilized guest strategy to undergo H-bonding, face-to-face, and edge-to-face π–π interactions with the enantiomers of naproxen. The new sub-2-µm (*R,R*)-Whelk-O1 CSP presented high stability and wide resolution applications for several tested analytes (Table 9) in considerably shorter times in both ultra-high and high-performance LC (158, 168).

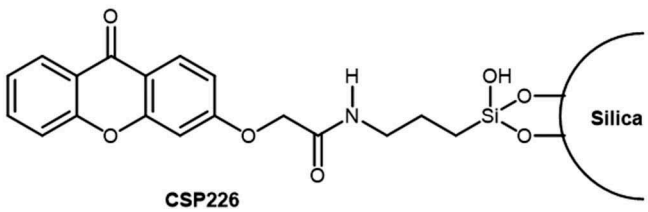
CSPs Obtained by Design

The chromatographic performance of Pirkle-type CSPs can be rationalized by chiral recognition models since they comprise small molecules as chiral selectors (28, 29). In recent years, computational studies of chromatographic separations have become essential for the elucidation of the chiral recognition mechanisms for diverse CSPs (19, 25), particularly Whelk-O1 CSP, which has been investigated in detail (15, 169–176).

Additionally, the development of chiral selectors from chemical combinatorial libraries together with high-throughput screening has been investigated to develop efficient enantioselective CSPs (177, 178).



CSP221 (*S*) R^1 = isopropyl R^2 = H
CSP222 (*R*) R^1 = phenyl R^2 = H
CSP223 (*S*) R^1 = phenyl R^2 = H
CSP224 (*R,S*) R^1 = phenyl R^2 = phenyl
CSP225 (*R,R*) R^1 = phenyl R^2 = phenyl



CSP226

Five new CSPs (CSP215–CSP219) were designed for a specific resolution of *tert*-butyl-1-(2-methylnaphthyl)-phosphine oxide (Table 9) from a small peptide library (177). The library consists of 81 peptide-based potential chiral selectors on polymeric synthesis resins, and the most promising selectors were then immobilized onto silica gel. It was found that the CSPs with longer linker (CSP218) provided a significantly higher enantioselectivity with an enantioresolution factor of 3.2.

In another study, libraries of potential chiral selectors have been prepared by the Ugi multicomponent condensation reactions, and screened for their enantioselectivity by the reciprocal approach using a CSP comprising *N*-(3,5-DNB)-α-L-leucine as the selector (178). The best candidate, containing a β-lactam unit, was then synthesized on a larger scale, resolved into single enantiomers by preparative enantioselective LC, and attached to porous poly(2-hydroxyethyl methacrylate-co-ethylene dimethacrylate) beads via an ester linkage to give CSP220. This new CSP afforded an enantioselectivity factor as high as 3.2 for the separation of a variety of 3,5-DNB-amino acid derivatives (Table 9).

CSPs with Xanthone Derivatives as Small-molecule Selectors

Xanthone derivatives comprise an important class of oxygenated heterocycles mainly concerning their broad spectrum of biological/pharmacological activities (179–182). Recently, some synthetic chiral derivatives of xanthones, in addition to the interesting biological activities (183, 184), were exploited as chiral selectors for LC (185, 186). Accordingly, six chiral derivatives of xanthones in enantiomerically pure form have been covalently linked to silica gel through a spacer yielding the corresponding CSP (CSP221–CSP226). The synthetic methodology involves only few steps and the reactions provided good yields. These new CSPs are based on a completely different type of small molecules from the Pirkle-type CSPs reported in the literature. The resolution capability of these CSPs was evaluated by LC using different chemical classes of chiral compounds (Table 10), under multimodal elution conditions. A library of chiral derivatives of xanthones was also evaluated in order to explore the principle of reciprocity as well as the chiral self-recognition phenomenon (the same strategy was described by Pirkle and co-workers to develop CSP4). In general, the CSPs provided high specificity for the enantiomeric mixtures of chiral derivatives of xanthones evaluated mainly under normal-phase elution conditions.

CONCLUSIONS

Although most of the CSPs described by Pirkle and co-workers are not commercial, the history of their planning and development is recognized as a great inspiration to other researchers to develop new CSPs. Consequently, several groups have developed Pirkle-type CSPs with chiral selectors based on small molecules. We have found 226 new Pirkle-type CSPs from the literature published during the last 17 years, and some of them were closely related to the previously described CSPs.

The research follows several different strategies, e.g., nonconventional synthetic approaches, such as solid-phase or click chemistry; development of CSPs comprising a biselector or combinatorial selectors; CSPs obtained by design, among others. Innovations with new chromatographic support materials, namely monolithic and core–shell particles, or sub-2-μm size particles were also reported. The majority of the new CSPs showed specificity for enantioseparation of some types of analytes, being an excellent choice to separate target analytes and analogues with the drawback that analyte derivation is often required.

Recently, several successful chiral ion-exchange or zwitterionic CSPs, based on the cinchona alkaloids, have been developed and some of them are commercialized. This subset of Pirkle-type CSPs demonstrated that ionic or electrostatic interactions are useful as attractive interactions for the resolution of ionic racemates in addition to hydrogen bonding, dipole–dipole and π–π interactions.

As a conclusion, it can be inferred that appropriately chosen small molecules can be successfully used as chromatographic tools. Moreover, the development of new CSPs continues to be a field of great importance. Even though several new CSPs for LC based on small molecules have been described in recent years, their applicability remains restricted and requires more research. Future development of new CSPs should be not only on the improvement of chiral selectors but also on column efficiency, like using sub-2-μm size particles.

FUNDING

This work was partially supported through national funds provided by FCT/MCTES—Foundation for Science and Technology from the Minister of Science, Technology and Higher Education (PIDDAC) and European Regional Development Fund (ERDF) through the COMPETE—Programa Operacional Factores de Competitividade (POFC) programme, under the Strategic Funding UID/Multi/04423/2013, the project PTDC/MAR-BIO/4694/2014 (reference POCI-01-0145-FEDER-016790; Project 3599—Promover a Produção Científica e Desenvolvimento Tecnológico e a Constituição de Redes Temáticas (3599-PPCDT)) in the framework of the programme PT2020 as well as by the project INNOVMAR—Innovation and Sustainability in the Management and Exploitation of Marine Resources (reference NORTE-01-0145-FEDER-000035, within Research Line NOVELMAR), supported

by North Portugal Regional Operational Programme (NORTE 2020), under the PORTUGAL 2020 Partnership Agreement, through the European Regional Development Fund (ERDF) and COXANT-CESPU-2016. Y.Z. Phyo thanks the Erasmus Mundus Action 2 (Lotus Plus project) for a PhD scholarship.

REFERENCES

1. Maier, N.M., Franco P. and Lindner W. (2001) Separation of enantiomers: needs, challenges, perspectives. *J. Chromatogr. A* 906: 3–33.
2. Mannschreck, A., Kiesswetter R. and von Angerer E. (2007) Unequal activities of enantiomers via biological receptors: Examples of chiral drug, pesticide, and fragrance molecules. *J. Chem. Educ*. 84: 2012–2017.
3. Triggle, D.J. (1997) Stereoselectivity of drug action. *Drug Discov. Today* 2: 138–147.
4. Caldwell, J. (1996) Importance of stereospecific bioanalytical monitoring in drug development. *J. Chromatogr. A* 719: 3–13.
5. Ward, T.J. and Ward K.D. (2010) Chiral Separations: Fundamental Review 2010. *Anal. Chem*. 82: 4712–4722.
6. Ward, T.J. and Ward K.D. (2012) Chiral separations: A review of current topics and trends. *Anal. Chem*. 84: 626–635.
7. Cavazzini, A., Pasti L., Massi A., Marchetti N. and Dondi F. (2011) Recent applications in chiral high performance liquid chromatography: A review. *Anal. Chim. Acta* 706: 205–222.
8. Bojarski, J., Aboul-Enein H.Y. and Ghanem A. (2005) What's New in Chromatographic Enantioseparations. *Cur. Anal. Chem*. 1: 59–77.
9. Ribeiro, A.R., Gonçalves V.M.F., Maia A.S., Ribeiro C., Castro P.M. L. and Tiritan M.E. (2015) Dispersive liquid–liquid microextraction and HPLC to analyse fluoxetine and metoprolol enantiomers in wastewaters. *Environ. Chem. Lett*. 13: 203–210.
10. Ribeiro, A.R., Maia A.S., Cass Q.B. and Tiritan M.E. (2014) Enantioseparation of chiral pharmaceuticals in biomedical and environmental analyses by liquid chromatography: An overview. *J. Chromatogr. B Anal. Technol. Biomed. Life Sci*. 968: 8–21.
11. Prompanya, C., Fernandes C., Cravo S., Pinto M.M.M., Dethoup T., Silva A.M.S. and Kijjoa A. (2015) A new cyclic hexapeptide and a new isocoumarin derivative from the marine sponge-associated fungus Aspergillus similanensis KUFA 0013. *Mar. Drugs* 13: 1432–1450.
12. Zin, W.W.M., Buttachon S., Dethoup T., Fernandes C., Cravo S., Pinto M.M.M., Gales L., Pereira J.A., Silva A.M.S., Sekeroglu N. and Kijjoa A. (2016) New cyclotetrapeptides and a new diketopiperzine derivative from the marine sponge-associated fungus Neosartorya glabra KUFA 0702. *Mar. Drugs* 14.
13. Fernandes, C., Brandão P., Santos A., Tiritan M.E., Afonso C., Cass Q.B. and Pinto M.M. (2012) Resolution and determination of enantiomeric purity of new chiral derivatives of xanthones using polysaccharide-based stationary phases. *J. Chromatogr. A* 1269: 143–153.
14. Fernandes, C., Tiritan M.E., Cass Q., Kairys V., Fernandes M.X. and Pinto M. (2012) Enantioseparation and chiral recognition mechanism of new chiral derivatives of xanthones on macrocyclic antibiotic stationary phases. *J. Chromatogr. A* 1241: 60–68.
15. Carraro, M.L., Palmeira A., Tiritan M.E., Fernandes C. and Pinto M. M.M. (2017) Resolution, determination of enantiomeric purity and chiral recognition mechanism of new xanthone derivatives on (S,S)-Whelk-O1 stationary phase. *Chirality* 1–10.
16. Sousa, M.E., Tiritan M.E., Belaz K.R.A., Pedro M., Nascimento M.S. J., Cass Q.B. and Pinto M.M.M. (2006) Multimilligram enantioresolution of low-solubility xanthonolignoids on polysaccharide chiral stationary phases using a solid-phase injection system. *J. Chromatogr. A* 1120: 75–81.
17. Silva, B., Fernandes C., Tiritan M.E., Pinto M.M.M., Valente M.J., Carvalho M., de Pinho P.G. and Remião F. (2016) Chiral enantioresolution of cathinone derivatives present in "legal highs", and enantioselectivity evaluation on cytotoxicity of 3,4-methylenedioxypyrovalerone (MDPV). *Forensic Toxicol*. : 1–14.
18. Scriba, G.K.E. (2016) Chiral recognition in separation science – an update. *J. Chromatogr. A* 1467: 56–78.
19. Lämmerhofer, M. (2010) Chiral recognition by enantioselective liquid chromatography: Mechanisms and modern chiral stationary phases. *J. Chromatogr. A* 1217: 814–856.
20. Scriba, G.K.E. (2012) Chiral recognition mechanisms in analytical separation sciences. *Chromatographia* 75: 815–838.
21. Kalíková, K., Riesová M. and Tesařová E. (2011) Recent chiral selectors for separation in HPLC and CE. *Cent. Eur. J. Chem*. : 1–22.
22. Felix, G. and Berthod A. (2007) Commercial chiral stationary phases for the separations of clinical racemic drugs. *Sep. Purif. Rev.* 36: 285–481.
23. Felix, G. and Berthod A. (2008) Part II: From dermatologicals to sensory organ and various drugs. *Sep. Purif. Rev.* 37: 1–227.
24. Francotte, E. and Lindner W., eds. (2006) *Methods and Principles in Medicinal Chemistry – Chirality in Drug Research*, Vols. 33. Wiley-VCH, Berlin, Germany..
25. Berthod, A., ed. (2010) *Chiral Recognition in Separation Methods: Mechanisms and Applications*. Springer-Verlag, Heidelberg, Germany..
26. Felix, G., Berthod A., Piras P. and Roussel C. (2008) Commercial chiral stationary phases for the separations of clinical racemic drugs: Part III: Supercritical fluid chromatographic separations. *Sep. Purif. Rev.* 37: 229–301.
27. Ali, I., Saleem K., Hussain I., Gaitonde V.D. and Aboul-Enein H.Y. (2009) Polysaccharides chiral stationary phases in liquid chromatography. *Sep. Purif. Rev.* 38: 97–147.
28. Fernandes, C., Tiritan M.E. and Pinto M. (2013) Small molecules as chromatographic tools for HPLC enantiomeric resolution: Pirkle-type chiral stationary phases evolution. *Chromatographia* 76: 871–897.
29. Welch, C.J. (1994) Evolution of chiral stationary phase design in the Pirkle laboratories. *J. Chromatogr. A* 666: 3–26.
30. Webster, G.K. and Szczerba T.J. (2013) Screening of Pirkle-type chiral stationary phases for HPLC enantioseparations. *Methods in molecular biology (Clifton, N.J.)* 970: 177–190.
31. Pirkle, W.H. and Däppen R. (1987) Reciprocity in Chiral Recognition. Comparison of several chiral stationary phases. *J. Chromatogr. A* 404: 107–115.
32. Schurig, V. (2016) The reciprocal principle of selectand-selector-systems in supramolecular chromatography. *Molecules* 21: 1535 doi:10.3390/molecules21111535.
33. Pirkle, W.H., Hyun M.H., Tsipouras A., Hamper B.C. and Banks B. (1984) A rational approach to the design of highly effective chiral stationary phases for the liquid chromatographic separation of enantiomers. *J. Pharm. Biomed. Anal*. 2: 173–181.
34. Pirkle, W.H. and Hyun M.H. (1985) Preparation and use of hydantion-based chiral stationary phases. *J. Chromatogr. A* 322: 309–320.
35. Pirkle, W.H., Murray P.G. and Wilson S.R. (1996) X-ray crystallographic evidence in support of a proposed chiral recognition mechanism. *J. Org. Chem*. 61: 4775–4777.
36. Pirkle, W.H. and Selness S.R. (1995) Chiral recognition studies: Intra- and intermolecular 1H{1H}-nuclear overhauser effects as effective tools in the study of bimolecular complexes. *J. Org. Chem*. 60: 3252–3256.
37. Gasparrini, F., Misiti D. and Villani C. (2001) High-performance liquid chromatography chiral stationary phases based on low-molecular-mass selectors. *J. Chromatogr. A* 906: 35–50.
38. Kosaka, M., Sugito T., Kasai Y., Kuwahara S., Watanabe M., Harada N., Job G.E., Shvet A. and Pirkle W.H. (2003) Enantioresolution and absolute configurations of chiral meta-substituted diphenylmethanols

as determined by x-ray crystallographic and 1H NMR anisotropy methods. *Chirality* 15: 324–328.
39. Naito, J., Kosaka M., Sugito T., Watanabe M., Harada N. and Pirkle W.H. (2004) Enantioresolution of Fluorinated Diphenylmethanols and Determination of Their Absolute Configurations by X-Ray Crystallographic and 1H NMR Anisotropy Methods. *Chirality* 16: 22–35.
40. Job, G.E., Shvets A., Pirkle W.H., Kuwahara S., Kosaka M., Kasai Y., Taji H., Fujita K., Watanabe M. and Harada N. (2004) The effects of aromatic substituents on the chromatographic enantioseparation of diarylmethyl esters with the Whelk-O1 chiral stationary phase. *J. Chromatogr. A* 1055: 41–53.
41. Koscho, M.E. and Pirkle W.H. (2005) Investigation of a broadly applicable chiral selector used in enantioselective chromatography (Whelk-O 1) as a chiral solvating agent for NMR determination of enantiomeric composition. *Tetrahedron Asymmetry* 16: 3345–3351.
42. Koscho, M.E., Spence P.L. and Pirkle W.H. (2005) Chiral recognition in the solid state: Crystallographically characterized diastereomeric co-crystals between a synthetic chiral selector (Whelk-O1) and a representative chiral analyte. *Tetrahedron Asymmetry* 16: 3147–3153.
43. Snyder, S.E., Carey J.R. and Pirkle W.H. (2005) Biphasic enantioselective partitioning studies using small-molecule chiral selectors. *Tetrahedron* 61: 7562–7567.
44. Snyder, S.E., Carey J.R., Shvets A.B. and Pirkle W.H. (2005) Formation of stable Meisenheimer adduct ion pairs in apolar solvents: Implications for stereoselective reactions. *J. Org. Chem*. 70: 4073–4081.
45. Snyder, S.E. and Pirkle W.H. (2002) Enantioselective hydrolysis of N-acylated Î±-amino esters at a biphasic interface: Tandem reaction kinetic resolution using a chiral complexing agent. *Org. Lett*. 4: 3283–3286.
46. Snyder, S.E., Shvets A.B. and Pirkle W.H. (2002) Enantioselective nucleophilic aromatic substitution with small-molecule chiral selectors. *Helv. Chim. Acta* 85: 3605–3615.
47. Snyder, S.E., Volkers P.I., Engebretson D.A., Lee W., Pirkle W.H. and Carey J.R. (2007) Strong enantioselective self-recognition of a small chiral molecule. *Org. Lett*. 9: 2341–2343.
48. Perrin, S.R., Hauck W., Ndzie E., Blehaut J., Ludemann-Hombouger O., Nicoud R.M. and Pirkle W.H. (2007) Purification of difluoromethylornithine by global process optimization: Coupling of chemistry and chromatography with enantioselective crystallization. *Org. Process Res. Dev*. 11: 817–824.
49. Pirkle, W.H. and Snyder S.E. (2001) Two-component chiral phase transfer catalysts: Enantioselective esterification of an N-acylated amino acid. *Org. Lett*. 3: 1821–1823.
50. Carey, J.R., Kim E., Hong J.H., Kang J.S., Pirkle W.H. and Lee W. (2011) Investigation of chiral self-recognition of π-acidic 3,5-dinitrobenzoylleucine derivatives. *Bull. Korean Chem. Soc*. 32: 4423–4426.
51. Pirkle, W.H. and Koscho M.E. (1999) Structural optimization of a chiral selector for use in preparative enantioselective chromatography. *J. Chromatogr. A* 840: 151–158.
52. Pirkle, W.H. and Liu Y. (1994) Design, synthesis, resolution, determination of absolute configuration, and evaluation of a chiral naproxen selector. *J. Org. Chem*. 59: 6911–6916.
53. Pirkle, W.H. and Liu Y. (1996) On the relevance of face-to-edge Ï€–Ï€ interactions to chiral recognition. *J. Chromatogr. A* 749: 19–24.
54. Pirkle, W.H. and Liu Y. (1996) Incremental development of chiral selectors for underivatized profens. *J. Chromatogr. A* 736: 31–38.
55. Hyun, M.H. and Pirkle W.H. (2000) Liquid chromatographic separation of the stereoisomers of thiazide diuretics. *J. Chromatogr. A* 876: 221–227.
56. Pirkle, W.H. and Lee W. (2010) Separation of the enantiomers of β-blockers using brush type chiral stationary phase derived from conformationally rigid α-amino β-lactam. *Bull. Korean Chem. Soc*. 31: 620–623.
57. Lee, W., Snyder S.E., Volkers P.I., Pirkle W.H., Engebretson D.A., Boulanger W.A., Lin H.S., Huang B.S. and Carey J.R. (2011) Assessing chiral self-recognition using chiral stationary phases. *Tetrahedron* 67: 7143–7147.
58. Kosjek, B. and Uray G. (2001) Immobilization of difunctional building blocks on hydroxysuccinimide activated silica: Versatile in situ preparation of chiral stationary phases. *Chirality* 13: 657–667.
59. Vinkovic, V., Kontrec D. and Landek G. (2012) Chiral stationary phases for chromatography based on aromatic allyl amines.Patent US, 8202417 B2.
60. Ranogajec, A., Kontrec D., Vinkovic V. and Sunjic V. (2003) Enantiomer separation and molecular recognition with new chiral stationary phases on 4-chloro-3,5-dinitrobenzoic acid amides of α,β-aminoalcohols and α-arylethylamines. *J. Liq. Chromatogr. Relat. Technol*. 26: 63–83.
61. Myung, H.H., Chang J.B., Hee J.C., Yun K.K., Bu S.K., Hyun J.H., Min K.C. and Tan G. (2006) Preparation of a new chiral stationary phase based on (2S,3S)-O,O′- bis-(10-undecenoyl)-N,N′-bis-(3,5-dinitrobenzoyl)-2,3-diamino-1, 4-butandiol and its application for the liquid chromatographic resolution of enantiomers. *Bull. Korean Chem. Soc*. 27: 1769–1774.
62. Zhang, D., Li F. and Myung H.H. (2007) Preparation and application of a novel Pirkle-type chiral stationary phase in liquid chromatography. *Pharmazie* 62: 258–261.
63. Jae, J.R. and Armstrong D.W. (2007) Preparation of binaphthyldiamine derived chiral stationary phases. *Bull. Korean Chem. Soc*. 28: 2103–2106.
64. Myung, H.H., Seung N.K., Hee J.C. and Sakthivel P. (2007) Liquid chromatographic resolution of N-(3,5-dinitrobenzoyl)-α-amino acids on a new chiral stationary phase: The first liquid chromatographic utilization of a double-ureide pocket for the recognition of chiral carboxylate anions. *Bull. Korean Chem. Soc*. 28: 1980–1984.
65. Kotoni, D., Villani C., Bell D.S., Capitani D., Campiglia P. and Gasparrini F. (2013) Bidentate urea-based chiral selectors for enantioselective high performance liquid chromatography: Synthesis and evaluation of "Crab-like" stationary phases. *J. Chromatogr. A* 1297: 157–167.
66. Yu, J., Ryoo D.H., Lee J.M. and Ryoo J.J. (2016) Synthesis and Application of C2 and C3 Symmetric (R)-Phenylglycinol-Derived Chiral Stationary Phases. *Chirality* 28: 186–191.
67. Ryoo, J.J., Heo K.S. and Song Y.A. (2003) Resolution of N-acyl-1-naphthylalkylamide on amide and sulfonamide-derived π-acidic chiral stationary phases. *Microchem. J*. 74: 215–221.
68. Ryoo, J.J., Kim T.H., Im S.H., Jeong Y.H., Park J.Y., Choi S.H., Lee K.P. and Park J.H. (2003) Enantioseparation of racemic N-acylarylalkylamines on various amino alcohol derived π-acidic chiral stationary phases. *J. Chromatogr. A* 987: 429–438.
69. Myung, H.H., Young K.C., Sang C.H. and Yoon J.C. (2002) Preparation and application of new ion-pairing chiral stationary phases for the liquid chromatographic separation of enantiomers. *J. Liq. Chromatogr. Relat. Technol*. 25: 573–588.
70. Hyun, M.H., Kim S.N., Choi H.J. and Sakthivel P. (2008) Preparation and application of a new ion-pairing chiral stationary phase for the liquid chromatographic resolution of N-(3,5-dinitrobenzoyl)-α- amino acids. *J. Liq. Chromatogr. Relat. Technol*. 31: 2363–2374.
71. Kontrec, D., Vinković V. and Šunjić V. (2000) Preparation and evaluation of the chiral stationary phases based on N- 4(2,5,6-trichloro-1,3-dicyano)-phenyl derivatives of L-α-amino acids. *J. Liq. Chromatogr. Relat. Technol*. 23: 1203–1215.
72. Kontrec, D., Vinković V. and Šunjić V. (2000) Preparation and evaluation of chiral stationary phases based on N,N-2,4- (or 4,6)-disubstituted 4,5-(or 2,5)-dichloro-1,3-dicyanobenzene. *Chirality* 12: 63–70.

73. Kontrec, D., Abatangelo A., Vinković V. and Šunjić V. (2001) Solid-phase synthesis of chiral stationary phases based on 2,4,5,6-tetrachloro-1,3-dicyanobenzene derivatives spaced from N-3,5-dinitrobenzoyl α-amino acids: Comparative study of their resolution efficacy. *Chirality* 13: 294–301.
74. Vinkovic, V., Kontrec D., Sunjic V., Navarini L., Zanetti F. and Azzolina O. (2001) Mechanism of chiral recognition in the enantioseparation of 2-aryloxypropionic acids on new brush-type chiral stationary phases. *Chirality* 13: 581–587.
75. Pirkle, W.H., Welch C.J., Burke J.A. and Lamm B. (1992) Target-directed design of chiral stationary phases. *Analytical Proceedings* 29: 225–227.
76. Pirkle, W.H. and Burke Iii J.A. (1991) Chiral stationary phase designed for β-blockers. *J. Chromatogr.* 557: 173–185.
77. Pirkle, W.H. and Burke J.A. (1989) Preparation of a chiral stationary phase from an α-amino phosphonate. *Chirality* 1: 57–62.
78. Pirkle, W.H. and Welch C.J. (1992) An improved chiral stationary phase for the chromatographic separation of underivatized naproxen enantiomers. *J. Liq. Chrom*. 15: 1947–1955.
79. Zafirova, B., Landek G., Kontrec D., Šunjić V. and Vinković V. (2004) Study of chromatographic enantioseparation of the esters of N-dinitrobenzoyl (N-DNB) and N-benzoyl (N-B) α-amino acids on novel chiral stationary phases containing structurally matching N-DNB and N-B-α-AA amides in the chiral selector. *Croat. Chem. Acta* 77: 573–579.
80. Vinković, V., Roje M., Kontrec D. and Šunjić V. (2008) Separation of BINAPO enantiomers on brush-type chiral stationary phases. *Arkivoc* 2008: 242–253.
81. Pirkle, W.H. and Welch C.J. (1992) Effect of superfluous remote polar functionality on chiral recognition. *J. Chromatogr. A* 589: 45–51.
82. Forjan, D.M., Kontrec D. and Vinković V. (2006) Performance of brush-type HPLC chiral stationary phases with tertiary amide in the connecting tether. *Chirality* 18: 857–869.
83. Forjan, D.M., Vinković V. and Kontrec D. (2006) Performance of a new HPLC chiral stationary phase derived from N-(3,5-dinitrobenzoyl)-D-α-phenylglycine with a quinoxaline branching unit. *Acta Chromatogr.* : 97–107.
84. Tan, X., Hou S., Jiang J. and Wang M. (2007) Preparation of a new chiral stationary phase for HPLC based on the (R)-1-phenyl-2-(-4-methylphenyl)ethylamine amide derivative of (S)-valine and 2-chloro-3,5-dinitrobenzoic acid: Enantioseparation of amino acid derivatives and pyrethroid insecticides. *J. Sep. Sci*. 30: 1888–1892.
85. Tan, X., Hou S. and Wang M. (2007) Enantioselective and diastereoselective separation of synthetic pyrethroid insecticides on a novel chiral stationary phase by high-performance liquid chromatography. *Chirality* 19: 574–580.
86. Tan, X.L., Hou S.C., Bian Q.H. and Wang M. (2007) Synthesis of novel chiral stationary phases for high-performance liquid chromatography. *Chin. Chem. Lett*. 18: 461–464.
87. Yilmaz, H., Topal G., Cakmak R. and Hosgoren H. (2010) Resolution of (±)-β-methylphenylethylamine by a novel chiral stationary phase for Pirkle-type column chromatography. *Chirality* 22: 252–257.
88. Li, Y., Jiang D., Huang D., Huang M. and Li L. (2015) Preparation and characterization of tripeptide chiral stationary phases with varying amino acid sequences and terminal groups. *Anal. Methods* 7: 3772–3778.
89. Lao, W. and Gan J. (2009) Evaluation of triproline and tri-α-methylproline chiral stationary phases. Retention and enantioseparation associated with hydrogen bonding. *J. Chromatogr. A* 1216: 5020–5029.
90. Huang, J., Chen H. and Li T. (2006) Improvement of proline chiral stationary phases by varying peptide length and linker. *J. Chromatogr. A* 1113: 109–115.
91. Huang, J., Chen H., Zhang P. and Li T. (2006) Improvement of proline enantioselective stationary phases by replacing the 9-fluorenylmethoxycarbonyl group. *J. Chromatogr. A* 1109: 307–311.
92. Li, J., Li Y., Chen T., Xu L., Liu X., Zhang X. and Zhang H. (2013) Preparation, chromatographic evaluation and comparison between linear peptide- and cyclopeptide-bonded stationary phases. *Talanta* 109: 152–159.
93. Wu, H., Liang T., Yin C., Jin Y., Ke Y. and Liang X. (2011) Enantiorecognition ability of peptoids with α-chiral, aromatic side chains. *Analyst* 136: 4409–4411.
94. Wu, H., Su X., Li K., Yu H., Ke Y. and Liang X. (2012) Improvement of peptoid chiral stationary phases by modifying the terminal group of selector. *J. Chromatogr. A* 1265: 181–185.
95. Wu, H., Song G., Liang X. and Ke Y. (2012) Investigation of peptoid chiral stationary phases terminated with N′-substituted phenyl-L-proline/leucine amide. *Chin. J. Chem*. 30: 2791–2797.
96. Wu, H., Li K., Yu H., Ke Y. and Liang X. (2013) Investigation of peptoid chiral stationary phases varied in absolute configuration. *J. Chromatogr. A* 1281: 155–159.
97. Wu, H., Song G., Wang D., Yu H., Ke Y. and Liang X. (2013) Study of stereomeric peptoid chiral stationary phases containing different chiral side chains. *J. Chromatogr. A* 1298: 152–156.
98. Iuliano, A., Salvadori P. and Félix G. (1999) Synthesis of a new family of four deoxycholic acid derived chiral stationary phases and their evaluation in the HPLC resolution of racemic compounds. *Tetrahedron Asymmetry* 10: 3353–3364.
99. Iuliano, A., Masini G., Félix G. and Salvadori P. (2001) Synthesis of deoxycholic-derived chiral stationary phases possessing both arylcarbamate and arylamide moieties: Evaluation of their chiral discrimination properties in the HPLC resolution of racemic compounds. *Tetrahedron Asymmetry* 12: 2811–2825.
100. Iuliano, A. and Félix G. (2004) Exhaustively substituted bile acids as chiral selectors for enantioselective chromatography: Aim, use and perspectives. *J. Chromatogr. A* 1031: 187–195.
101. Moiteiro, C., Fonseca N., Curto M.J.M., Tavares R., Lobo A.M., Ribeiro-Claro P., Félix V. and Drew M.G.B. (2006) Development of novel brush-type chiral stationary phases based on terpenoid selectors: HPLC evaluation and theoretical investigation of enantioselective binding interactions. *Tetrahedron Asymmetry* 17: 3248–3264.
102. Wang, D.C., Luo J., Yao S. and Song H. The synthesis and characterization of novel brush-type chiral stationary phase based on terpenoid selector for resolution of chiral drugs. *Proc.2nd International Conference on Chemical and Material Engineering, ICCME 2015*, 2016, 39: EDP Sciences.
103. Oxelbark, J. and Sellén I.B. (2003) Effects from Hydrogen Bonding and Rigidity on Selectivity in Tartaric Acid-Based Chiral Selectors for Enantioselective Liquid Chromatography. *Chirality* 15: 787–793.
104. Lämmerhofer, M. and Lindner W. (1996) Quinine and quinidine derivatives as chiral selectors. I. Brush type chiral stationary phases for high-performance liquid chromatography based on cinchonan carbamates and their application as chiral anion exchangers. *J. Chromatogr. A* 741: 33–48.
105. Piette, V., Lämmerhofer M., Bischoff K. and Lindner W. (1997) High-performance liquid chromatographic enantioseparation of N-protected α-amino acids using nonporous silica modified by a quinine carbamate as chiral stationary phase. *Chirality* 9: 157–161.
106. Maier, N.M., Nicoletti L., Lämmerhofer M. and Lindner W. (1999) Enantioselective anion exchangers based on cinchona alkaloid-derived carbamates: Influence of C8/C9 stereochemistry on chiral recognition. *Chirality* 11: 522–528.
107. Franco, P., Lämmerhofer M., Klaus P.M. and Lindner W. (2000) Novel cinchona alkaloid carbamate C9-dimers as chiral anion-exchange type selectors for high-performance liquid chromatography. *J. Chromatogr. A* 869: 111–127.
108. Franco, P., Lämmerhofer M., Klaus P.M. and Lindner W. (2000) Novel cinchona alkaloid O9-hydrazide derivatives as chiral anion-exchange-type selectors: Synthesis and chromatographic evaluation. *Chromatographia* 51: 139–146.

109. Kacprzak, K.M. and Lindner W. (2011) Novel Pirkle-type quinine 3,5-dinitrophenylcarbamate chiral stationary phase implementing click chemistry. *J. Sep. Sci*. 34: 2391–2396.
110. Hettegger, H., Kohout M., Mimini V. and Lindner W. (2014) Novel carbamoyl type quinine and quinidine based chiral anion exchangers implementing alkyne-azide cycloaddition immobilization chemistry. *J. Chromatogr. A* 1337: 85–94.
111. Hoffmann, C.V., Laemmerhofer M. and Lindner W. (2007) Novel strong cation-exchange type chiral stationary phase for the enantiomer separation of chiral amines by high-performance liquid chromatography. *J. Chromatogr. A* 1161: 242–251.
112. Hoffmann, C.V., Lämmerhofer M. and Lindner W. (2009) Separation of Cinchona alkaloids on a novel strong cation-exchange-type chiral stationary phase-comparison with commercially available strong cation exchanger and reversed-phase packing materials. *Anal. Bioanal. Chem*. 393: 1257–1265.
113. Hoffmann, C.V., Pell R., Lämmerhofer M. and Lindner W. (2008) Synergistic effects on enantioselectivity of zwitterionic chiral stationary phases for separations of chiral acids, bases, and amino acids by HPLC. *Anal. Chem*. 80: 8780–8789.
114. Hoffmann, C.V., Reischl R., Maier N.M., Lämmerhofer M. and Lindner W. (2009) Stationary phase-related investigations of quinine-based zwitterionic chiral stationary phases operated in anion-, cation-, and zwitterion-exchange modes. *J. Chromatogr. A* 1216: 1147–1156.
115. Hoffmann, C.V., Reischl R., Maier N.M., Lämmerhofer M. and Lindner W. (2009) Investigations of mobile phase contributions to enantioselective anion- and zwitterion-exchange modes on quinine-based zwitterionic chiral stationary phases. *J. Chromatogr. A* 1216: 1157–1166.
116. Wernisch, S., Pell R. and Lindner W. (2012) Increments to chiral recognition facilitating enantiomer separations of chiral acids, bases, and ampholytes using Cinchona-based zwitterion exchanger chiral stationary phases. *J. Sep. Sci*. 35: 1560–1572.
117. Pell, R., Sić S. and Lindner W. (2012) Mechanistic investigations of cinchona alkaloid-based zwitterionic chiral stationary phases. *J. Chromatogr. A* 1269: 287–296.
118. Wernisch, S. and Lindner W. (2012) Versatility of cinchona-based zwitterionic chiral stationary phases: Enantiomer and diastereomer separations of non-protected oligopeptides utilizing a multi-modal chiral recognition mechanism. *J. Chromatogr. A* 1269: 297–307.
119. Ianni, F., Sardella R., Carotti A., Natalini B., Lindner W. and Lämmerhofer M. (2016) Quinine-Based Zwitterionic Chiral Stationary Phase as a Complementary Tool for Peptide Analysis: Mobile Phase Effects on Enantio- and Stereoselectivity of Underivatized Oligopeptides. *Chirality* 28: 5–16.
120. Gargano, A.F.G., Kohout M., Macíková P., Lämmerhofer M. and Lindner W. (2013) Direct high-performance liquid chromatographic enantioseparation of free α-, β- And γ-aminophosphonic acids employing cinchona-based chiral zwitterionic ion exchangers Amino Acid Analysis. *Anal. Bioanal. Chem*. 405: 8027–8038.
121. Ianni, F., Pataj Z., Gross H., Sardella R., Natalini B., Lindner W. and Lämmerhofer M. (2014) Direct enantioseparation of underivatized aliphatic 3-hydroxyalkanoic acids with a quinine-based zwitterionic chiral stationary phase. *J. Chromatogr. A* 1363: 101–108.
122. Ilisz, I., Grecsó N., Aranyi A., Suchotin P., Tymecka D., Wilenska B., Misicka A., Fülöp F., Lindner W. and Péter A. (2014) Enantioseparation of β2-amino acids on cinchona alkaloid-based zwitterionic chiral stationary phases. Structural and temperature effects. *J. Chromatogr. A* 1334: 44–54.
123. Ilisz, I., Pataj Z., Gecse Z., Szakonyi Z., Fülöp F., Lindner W. and Péter A. (2014) Unusual temperature-induced retention behavior of constrained β-amino acid enantiomers on the zwitterionic chiral stationary phases ZWIX(+) and ZWIX(-). *Chirality* 26: 385–393.
124. Ilisz, I., Gecse Z., Lajkõ G., Forrõ E., Fülöp F., Lindner W. and Péter A. (2015) High-Performance Liquid Chromatographic Enantioseparation of Cyclic β-Amino Acids on Zwitterionic Chiral Stationary Phases Based on Cinchona Alkaloids. *Chirality* 27: 563–570.
125. Ilisz, I., Grecsó N., Papoušek R., Pataj Z., Barták P., Lázár L., Fülöp F., Lindner W. and Péter A. (2015) High-performance liquid chromatographic separation of unusual β3-amino acid enantiomers in different chromatographic modes on Cinchona alkaloid-based zwitterionic chiral stationary phases. *Amino Acids* 47: 2279–2291.
126. Ilisz, I., Grecsó N., Misicka A., Tymecka D., Lázár L., Lindner W. and Péter A. (2015) Comparison of the separation performances of cinchona alkaloid-based zwitterionic stationary phases in the enantioseparation of β2- And β3-amino acids. *Molecules* 20: 70–87.
127. Ilisz, I., Gecse Z., Pataj Z., Fülöp F., Tóth G., Lindner W. and Péter A. (2014) Direct high-performance liquid chromatographic enantioseparation of secondary amino acids on Cinchona alkaloid-based chiral zwitterionic stationary phases. Unusual temperature behavior. *J. Chromatogr. A* 1363: 169–177.
128. Ilisz, I., Grecsó N., Palkó M., Fülöp F., Lindner W. and Péter A. (2014) Structural and temperature effects on enantiomer separations of bicyclo[2.2.2]octane-based 3-amino-2-carboxylic acids on cinchona alkaloid-based zwitterionic chiral stationary phases. *J. Pharm. Biomed. Anal*. 98: 130–139.
129. Fukushima, T., Sugiura A., Furuta I., Iwasa S., Iizuka H., Ichiba H., Onozato M., Hikawa H. and Yokoyama Y. (2015) Enantiomeric separation of monosubstituted tryptophan derivatives and metabolites by HPLC with a cinchona alkaloid-based zwitterionic chiral stationary phase and its application to the evaluation of the optical purity of synthesized 6-chloro- L-Tryptophan. *Int. J. Trytophan Res*. 8: 1–5.
130. Ilisz, I., Grecsó N., Fülöp F., Lindner W. and Péter A. (2015) High-performance liquid chromatographic enantioseparation of cationic 1,2,3,4-tetrahydroisoquinoline analogs on Cinchona alkaloid-based zwitterionic chiral stationary phases ABCs 13th Anniversary. *Anal. Bioanal. Chem*. 407: 961–972.
131. Ilisz, I., Gecse Z., Lajkó G., Nonn M., Fülöp F., Lindner W. and Péter A. (2015) Investigation of the structure-selectivity relationships and van't Hoff analysis of chromatographic stereoisomer separations of unusual isoxazoline-fused 2-aminocyclopentanecarboxylic acids on Cinchona alkaloid-based chiral stationary phases. *J. Chromatogr. A* 1384: 67–75.
132. Wolrab, D., Frühauf P., Moulisová A., Kuchař M., Gerner C., Lindner W. and Kohout M. (2016) Chiral separation of new designer drugs (Cathinones) on chiral ion-exchange type stationary phases. *J. Pharm. Biomed. Anal*. 120: 306–315.
133. Wu, H., Wang D., Song G., Ke Y. and Liang X. (2014) Novel chiral stationary phases based on peptoid combining a quinine/quinidine moiety through a C9-position carbamate group. *J. Sep. Sci*. 37: 934–943.
134. Hwan, S.C., Hyun J.H., Hee J.C., Jong S.J. and Myung H.H. (2008) Preparation and application of a new liquid chromatographic chiral stationary phase based on cefaclor. *Bull. Korean Chem. Soc*. 29: 2135–2139.
135. Choi, H.J., Ha H.J., Shin M.S., Jin J.S. and Hyun M.H. (2009) Preparation of a new π-basic chiral stationary phase based on cefaclor and the liquid chromatographic resolution of-acidic analytes. *J. Liq. Chromatogr. Relat. Technol*. 32: 1879–1890.
136. Iuliano, A., Attolino E. and Salvadori P. (2001) (S)-leucine and [(S)-1-(1-naphthyl)ethyl]amine as chiral building blocks for a bifunctional system - Synthesis of a new chiral stationary phase and evaluation of its biselector properties in the HPLC resolution of racemic compounds. *Eur. J. Org. Chem*. 3523–3529.
137. Pirkle, W.H., House D.W. and Finn J.M. (1980) Broad spectrum resolution of optical isomers using chiral high-performance liquid chromatographic bonded phases. *J. Chromatogr*. 192: 143–158.

138. Pirkle, W.H. and Schreiner J.L. (1981) Chiral high-pressure liquid chromatographic stationary phases. 4. Separation of the enantiomers of bi-Î[2]-naphthols and analogues. *J. Org. Chem*. 46: 4988–4991.
139. Pirkle, W.H. and Welch C.J. (1984) Chromatographic separation of the enantiomers of acylated amines on chiral stationary phases. *J. Org. Chem*. 49: 138–140.
140. Pirkle, W.H., Welch C.J. and Hyun M.H. (1983) A chiral recognition model for the chromatographic resolution of N-acylated 1-aryl-1-aminoalkanes. *J. Org. Chem*. 48: 5022–5026.
141. Ôi, N., Nagase M. and Sawada Y. (1984) High-performance liquid chromatographic separation of enantiomers on s-triazine derivatives of a tripeptide ester and a chiral amine bonded to silica gel. *J. Chromatogr. A* 292: 427–431.
142. Iuliano, A., Attolino E. and Salvadori P. (2002) Biselector enantioselective stationary phases for HPLC: Dependence of the chiral discrimination properties on stereochemistry and chemical nature of each unit of the chiral auxiliary. *Tetrahedron Asymmetry* 13: 1805–1815.
143. Iuliano, A., Lecci C. and Salvadori P. (2003) The s-triazine moiety as a scaffold for connecting different chiral auxiliaries: Synthesis of new biselector CSPs for enantioselective chromatography. *Tetrahedron Asymmetry* 14: 1345–1353.
144. Lecci, C. and Iuliano A. (2005) Synthesis and evaluation of a new biselector s-triazine based chiral stationary phase for enantioselective HPLC: Potentiality of the approach and perspectives. *Biomed. Chromatogr*. 19: 439–446.
145. Pirkle, W.H. and Pochapsky T.C. (1986) A new, easily accessible reciprocal chiral stationary phase for the chromatographic separation of enantiomers. *J. Am. Chem. Soc*. 108: 352–354.
146. Oxelbark, J. and Gidlund P. (2005) Investigation of a tartaric acid-based linear polyamide and dimer as chiral selectors in liquid chromatography. *Chirality* 17: 79–84.
147. Wei, W.J., Deng H.W., Chen W., Bai Z.W. and Li S.R. (2010) Preparation and enantioseparation of a mixed selector chiral stationary phase derived from benzoylated tartaric acid and 1,2-diphenylethylenediamine. *Chirality* 22: 604–611.
148. Wu, H., Ji S., Yang B., Yu H., Jin Y., Ke Y. and Liang X. (2012) Investigation of brush-type chiral stationary phases based on O,O′-diaroyl tartardiamide and O,O′-bis-(arylcarbamoyl) tartardiamide. *J. Sep. Sci*. 35: 351–358.
149. Wang, Y., Ai F., Ng S.C. and Tan T.T.Y. (2012) Sub-2μm porous silica materials for enhanced separation performance in liquid chromatography. *J. Chromatogr. A* 1228: 99–109.
150. Fekete, S., Oláh E. and Fekete J. (2012) Fast liquid chromatography: The domination of core-shell and very fine particles. *J. Chromatogr. A* 1228: 57–71.
151. Guillarme, D., Ruta J., Rudaz S. and Veuthey J.L. (2010) New trends in fast and high-resolution liquid chromatography: A critical comparison of existing approaches. *Anal. Bioanal. Chem*. 397: 1069–1082.
152. Mandl, A., Nicoletti L., Lämmerhofer M. and Lindner W. (1999) Quinine-versus carbamoylated quinine-based chiral anion exchangers. A comparison regarding enantioselectivity for N-protected amino acids and other chiral acids. *J. Chromatogr. A* 858: 1–11.
153. Lubda, D. and Lindner W. (2004) Monolithic silica columns with chemically bonded tert-butylcarbamoylquinine chiral anion-exchanger selector as a stationary phase for enantiomer separations. *J. Chromatogr. A* 1036: 135–143.
154. Slater, M.D., Fréchet J.M.J. and Svec F. (2009) In-column preparation of a brush-type chiral stationary phase using click chemistry and a silica monolith. *J. Sep. Sci*. 32: 21–28.
155. Ghanem, A., Ikegami T. and Tanaka N. (2011) New silica monolith bonded chiral (R)-γ butyrolactone for enantioselective micro high-performance liquid chromatography. *Chirality* 23: 887–890.
156. Wu, X., You L., Di B., Hao W., Su M., Gu Y. and Shen L. (2013) Novel chiral core-shell silica microspheres with trans-(1R,2R)-diaminocyclohexane bridged in the mesoporous shell: Synthesis, characterization and application in high performance liquid chromatography. *J. Chromatogr. A* 1299: 78–84.
157. Cancelliere, G., Ciogli A., D'Acquarica I., Gasparrini F., Kocergin J., Misiti D., Pierini M., Ritchie H., Simone P. and Villani C. (2010) Transition from enantioselective high performance to ultra-high performance liquid chromatography: A case study of a brush-type chiral stationary phase based on sub-5-micron to sub-2-micron silica particles. *J. Chromatogr. A* 1217: 990–999.
158. Kotoni, D., Ciogli A., Molinaro C., D'Acquarica I., Kocergin J., Szczerba T., Ritchie H., Villani C. and Gasparrini F. (2012) Introducing enantioselective ultrahigh-pressure liquid chromatography (eUHPLC): Theoretical inspections and ultrafast separations on a new sub-2-μm Whelk-O1 stationary phase. *Anal. Chem*. 84: 6805–6813.
159. Gasparrini, F., Misiti D., Villani C. and La Torre F. (1991) Chromatographic resolution of 1,2-amino alcohols on a chiral stationary phase containing N,N′-(3,5-dinitrobenzoyl)-trans-1,2-diaminocyclohexane. Theoretical and practical aspects. *J. Chromatogr. A* 539: 25–36.
160. Galli, B., Gasparrini F., Misiti D., Pierini M., Villani C. and Bronzetti M. (1992) HPLC resolution of atropoisomeric compounds on a CSP derived from (1R;2R)- diaminocyclohexane: Thermodynamic data from variable temperature chromatography. *Chirality* 4: 384–388.
161. Cancelliere, G., D'Acquarica I., Gasparrini F., Maggini M., Misiti D. and Villani C. (2006) Twenty years of research on silica-based chiral stationary phases. *J. Sep. Sci*. 29: 770–781.
162. Pirkle, W.H., Koscho M.E. and Wu Z. (1996) High-performance liquid chromatographic separation of the enantiomers of N-aryloxazolinones, N-aryl thiazolinones and their sulfur derivatives on a synthetic chiral stationary phase. *J. Chromatogr. A* 726: 91–97.
163. Pirkle, W.H., Brice L.J., Caccamese S., Principato G. and Failla S. (1996) Facile separation of the enantiomers of diethyl N-(aryl)-1-amino-1-arylmethanephosphonates on a rationally designed chiral stationary phase. *J. Chromatogr. A* 721: 241–246.
164. Perera, R.W.H. and Lough W.J. (2011) Assessment of chiral stationary phases for suitability for combined enantiomeric impurity/related substances assays. *J. Chromatogr. A* 1218: 8655–8663.
165. Badaloni, E., Cabri W., Ciogli A., D'Acquarica I., Deias R., Gasparrini F., Giorgi F., Kotoni D. and Villani C. (2010) Extending the use of "Inverted Chirality Columns Approach" for enantiomeric excess determination in absence of reference samples: Application to a water-soluble camptothecin derivative. *J. Chromatogr. A* 1217: 1024–1032.
166. Pirkle, W.H. and Gan K.Z. (1997) Facile and predictable means of separating the enantiomers of 5- arylhydantoins. *J. Chromatogr. A* 790: 65–71.
167. Welch, C.J., Szczerba T. and Perrin S.R. (1997) Some recent high-performance liquid chromatography separations of the enantiomers of pharmaceuticals and other compounds using the Whelk-O 1 chiral stationary phase. *J. Chromatogr. A* 758: 93–98.
168. Kotoni, D., Ciogli A., D'Acquarica I., Kocergin J., Szczerba T., Ritchie H., Villani C. and Gasparrini F. (2012) Enantioselective ultra-high and high performance liquid chromatography: A comparative study of columns based on the Whelk-O1 selector. *J. Chromatogr. A* 1269: 226–241.
169. Fernandes, C., Palmeira A., Santos A., Tiritan M.E., Afonso C. and Pinto M.M. (2013) Enantioresolution of chiral derivatives of xanthones on (S,S)-Whelk-O1 and l -phenylglycine stationary phases and chiral recognition mechanism by docking approach for (S,S)-Whelk-O1. *Chirality* 25: 89–100.
170. Lipkowitz, K.B. (2001) Atomistic modeling of enantioselection in chromatography. *J. Chromatogr. A* 906: 417–442.
171. Del Rio, A., Hayes J.M., Stein M., Piras P. and Roussel C. (2004) Theoretical reassessment of Whelk-O1 as an enantioselective receptor for 1-(4-halogeno-phenyl)-1-ethylamine derivatives. *Chirality* 16:S1–S11.

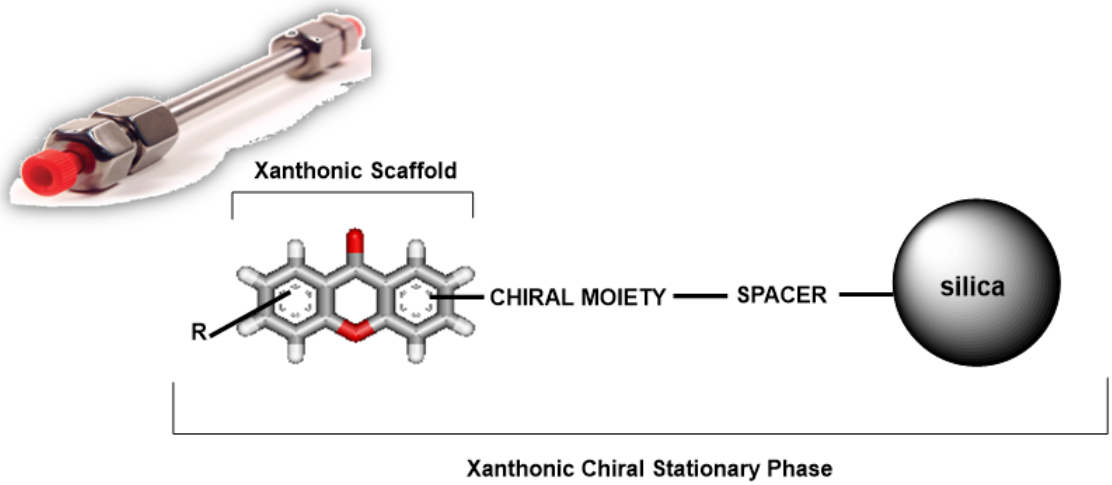
172. Del Rio, A., Piras P. and Roussel C. (2005) Data mining and enantiophore studies on chiral stationary phases used in HPLC separation. *Chirality* 17:S74–S83.
173. Del Rio, A., Piras P. and Roussel C. (2006) Enantiophore modeling in 3D-QSAR. A data mining application on Whelk-O1 chiral stationary phase. *Chirality* 18: 498–508.
174. Zhao, C. and Cann N.M. (2006) Solvation of the Whelk-O1 chiral stationary phase: A molecular dynamics study. *J. Chromatogr. A* 1131: 110–129.
175. Zhao, C. and Cann N.M. (2007) The docking of chiral epoxides on the Whelk-O1 stationary phase: A molecular dynamics study. *J. Chromatogr. A* 1149: 197–218.
176. Zhao, C.F., Diemert S. and Cann N.M. (2009) Rational optimization of the Whelk-O1 chiral stationary phase using molecular dynamics simulations. *J. Chromatogr. A* 1216: 5968–5978.
177. Blodgett, J., Wang Y., Li T., Polavarapu P.L., Drabowicz J., Pietrusiewicz K.M. and Zygo K. (2002) Resolution of tert-butyl-1-(2-methylnaphthyl)phosphine oxide using selectors identified from a chemical combinatorial library. *Anal. Chem*. 74: 5212–5216.
178. Brahmachary, E., Ling F.H., Svec F. and Fréchet J.M.J. (2003) Chiral recognition: Design and preparation of chiral stationary phases using selectors derived from Ugi multicomponent condensation reactions and a combinatorial approach. *J. Comb. Chem*. 5: 441–450.
179. Pinto, M.M.M., Sousa M.E. and Nascimento M.S.J. (2005) Xanthone derivatives: New insights in biological activities. *Curr. Med. Chem*. 12: 2517–2538.
180. Masters, K.S. and Bräse S. (2012) Xanthones from fungi, lichens, and bacteria: The natural products and their synthesis. *Chem. Rev.* 112: 3717–3776.
181. Wezeman, T., Bräse S. and Masters K.S. (2015) Xanthone dimers: A compound family which is both common and privileged. *Nat. Prod. Rep*. 32: 6–28.
182. Pinto, M.M.M., Castanheiro R.A.P. and Kijjoa A. (2014) Xanthones from marine-derived microorganisms: isolation, structure elucidation, and biological activities. In *Encyclopedia of Analytical Chemistry*, ed. L John Wiley & Sons, 27: 1–21. Number of 1–21 pp.
183. Fernandes, C., Masawang K., Tiritan M.E., Sousa E., De Lima V., Afonso C., Bousbaa H., Sudprasert W., Pedro M. and Pinto M.M. (2014) New chiral derivatives of xanthones: Synthesis and investigation of enantioselectivity as inhibitors of growth of human tumor cell lines. *Bioorg. Med. Chem*. 22: 1049–1062.
184. Fernandes, C., Oliveira L., Tiritan M.E., Leitao L., Pozzi A., Noronha-Matos J.B., Correia-De-Sá P. and Pinto M.M. (2012) Synthesis of new chiral xanthone derivatives acting as nerve conduction blockers in the rat sciatic nerve. *Eur. J. Med. Chem*. 55: 1–11.
185. Pinto, M., Tiritan M.E., Fernandes C. and Cass Q. (2011) *Fases Estacionárias Quirais baseadas em Derivados Xantónicos*. Portuguese Patent nº 104679.
186. Fernandes, C., Tiritan M.E., Cravo S., Phyo Y.Z., Kijjoa A., Silva A. M.S., Cass Q.B. and Pinto M.M.M. (2017) New chiral stationary phases based on xanthone derivatives for liquid chromatography. *Chirality* DOI: 10.1002/chir.22706.

CHAPTER IV

New chiral stationary phases based on xanthone derivatives for liquid chromatography

Reprinted from Chirality

Copyright © (2019) with permission from Wiley



Graphical abstract

Received: 6 January 2017 | Revised: 27 February 2017 | Accepted: 19 March 2017

DOI: 10.1002/chir.22706

REGULAR ARTICLE

WILEY

New chiral stationary phases based on xanthone derivatives for liquid chromatography

Carla Fernandes[1,2] | Maria Elizabeth Tiritan[1,2,3] | Sara Cravo[1,2] | Ye' Zaw Phyo[4] | Anake Kijjoa[2,4] | Artur M.S. Silva[5] | Quezia B. Cass[6] | Madalena M.M. Pinto[1,2]

[1] Laboratório de Química Orgânica e Farmacêutica, Departamento de Ciências Químicas, Faculdade de Farmácia, Porto, Portugal

[2] Interdisciplinary Centre of Marine and Environmental Research (CIIMAR), Matosinhos, Portugal

[3] CESPU, Instituto de Investigação e Formação Avançada em Ciências e Tecnologias da Saúde (IINFACTS), Gandra, PRD, Portugal

[4] ICBAS-Instituto de Ciências Biomédicas Abel Salazar, Universidade do Porto, Porto, Portugal

[5] Departamento de Química & QOPNA, Universidade de Aveiro, Aveiro, Portugal

[6] Departamento de Química, Universidade Federal de São Carlos, São Carlos, SP, Brasil

Correspondence
Prof. C. Fernandes, Laboratório de Química Orgânica e Farmacêutica, Departamento de Ciências Químicas, Faculdade de Farmácia, Rua de Jorge Viterbo Ferreira, 228, 4050-313 Porto, Portugal.
Email: cfernandes@ff.up.pt

Funding information
Coordenação de Aperfeiçoamento de Pessoal de Nível Superior (CAPES/FCT), Grant/Award Number: Project 214/08; Structured Program of R&D&I INNOVMAR - funded by the Programme NORTE2020 under the PORTUGAL 2020 Partnership Agreement, through ERDF and FCT, Grant/Award Number: NORTE-01-0145-FEDER-000035; Research Line NOVELMAR; Research project PTDC/MAR-BIO/4694 /2014 funded by FCT/MCTES, PIDDAC and ERDF through the COMPETE (POFC) programme in the framework of the programme PT2020 reference POCI-01-0145-FEDER-016790 3599-PPCDT; Cooperativa de Ensino

Abstract

Six chiral derivatives of xanthones (CDXs) were covalently bonded to silica, yielding the corresponding xanthonic chiral stationary phases (XCSPs). The new XCSPs were packed into stainless-steel columns with 150 x 4.6 mm i.d. Moreover, the greening of the chromatographic analysis by reducing the internal diameter (150 x 2.1 mm i.d.) of the liquid chromatography (LC) columns was also investigated. The enantioselective capability of these phases was evaluated by LC using different chemical classes of chiral compounds, including several types of drugs. A library of CDXs was evaluated in order to explore the principle of reciprocity as well as the chiral self-recognition phenomenon. The separation of enantiomeric mixtures of CDXs was investigated under multimodal elution conditions. The XCSPs provided high specificity for the enantiomeric mixtures of CDXs evaluated mainly under normal-phase elution conditions. Furthermore, two XCSPs were prepared with both enantiomers of the same xanthonic selector in order to confirm the inversion order elution.

KEYWORDS

chiral derivatives of xanthones, chiral stationary phase, enantioselectivity, liquid chromatography

Superior Politécnico e Universitário COXANT-CESPU-2016; Erasmus Mundus Action 2, Grant/Award Number: PhD's scholarship; QOPNA research project and Portuguese NMR network, Grant/Award Number: FCT UID/QUI/00062/2013

1 | INTRODUCTION

Analytical and preparative enantiomer separations by chromatography and related techniques play more than ever a crucial role in the chemical industry and academic research.[1] Over the years, liquid chromatography (LC) using chiral stationary phases (CSPs) has become a very helpful and highly applicable method for preparative resolution of racemates,[2] determination of the enantiomeric purity in quality control,[3] analysis of the stereochemistry of natural compounds,[4,5] monitoring enantiomeric reactions,[6,7] and for pharmacokinetic and environmental studies.[8,9] LC can be considered the method of choice in analytical laboratories due to its high speed, sensitivity, and reproducibility. Moreover, a number of CSPs based on polysaccharide derivatives, macrocyclic antibiotics, small chiral molecules, cyclodextrins, crown ethers, proteins, synthetic polymers, molecularly imprinted polymers, among others, have been developed for successful enantioseparations.[10-18] However, in spite of a large number of different types of CSPs described for enantiomeric separation by LC, there is no universal CSP, i.e., one CSP can only separate a limited number of chiral compounds and, in many cases, the choice of CSP may became a difficult task. Furthermore, even though there are many CSPs commercially available, many chiral compounds remain to be resolved. For this reason, the development of new CSPs continues to be a field of great importance.

Xanthone derivatives comprise an important class of oxygenated heterocycles, many of which possess a broad spectrum of biological/pharmacological activities.[19-23] In recent years, the synthesis of new bioactive xanthone derivatives using different synthetic methodologies, including chiral derivatives of xanthones (CDXs),[24,25] has been an area of great interest in our group.[26-29]

The CDXs, when anchored to a chromatographic support by covalent linkage through a spacer, possess all the necessary attributes to constitute chromatographic selectors.[30] The 3D *quasi*-planar structure and peculiar electronic properties of the xanthone scaffold,[31] associated with a diversity of functional groups and chiral moieties, constitute structural characteristics affording the establishment of different types of interactions, as well as contributing three-dimensionality factors that influence the enantioselectivity. In fact, the xanthone-based chiral selectors may contain aromatic, polar, and bulky nonpolar groups, forming interactions through hydrogen bonding, dipole–dipole, π–π interactions, and steric hindrance effects,[32] similar to what occurs with Pirkle-type CSPs.[33,34]

Herein we report the synthesis and evaluation of six new CSPs, based on xanthone derivatives (Figure 1). These xanthonic chiral stationary phases (XCSPs) are based on a completely different type of small molecule from those commercially available. The enantioresolution capability of the XCSPs was evaluated by LC using different chemical classes of chiral compounds, including drugs. A library of enantiomeric mixtures of CDXs was also evaluated in order to explore the principle of reciprocity,[34-36] as well as the chiral self-recognition phenomenon.[37,38] Two XCSPs possessing enantiomers of the same CDX were prepared to evaluate the resolving power of both enantiomers as selector and to confirm the inversion of the elution order. The greening choice of the chromatographic analysis, by reducing the internal diameter of the LC columns, was also investigated. To the best of our knowledge, this is the first report of the use of CDXs as LC chiral selectors.

2 | MATERIALS AND METHODS

2.1 | Chemicals

Enantiomerically pure reagents, (*S*)-(+)-valinol, (*R*)-(–)-α-phenylglycinol, (*S*)-(+)-α-phenylglycinol, (1*R*,2*S*)-(–)-2-amino-1,2-diphenylethanol, and (*R*,*R*)-(+)-2-amino-1,2-diphenylethanol, were obtained from Sigma-Aldrich (St. Louis, MO). *O*-(Benzotriazol-1-yl)-*N*-*N*-*N*'-*N*'-

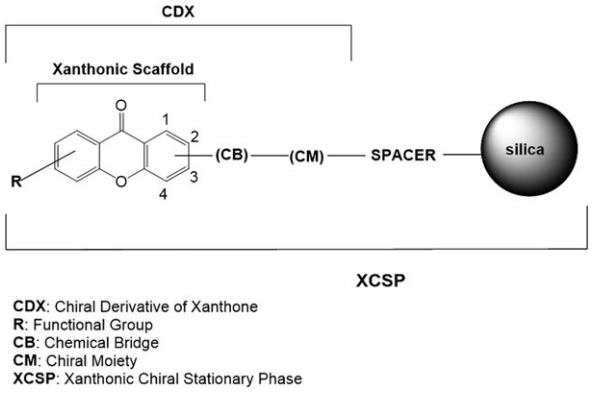


FIGURE 1 Schematic representation of a stationary phase based on chiral derivatives of xanthones

tetramethyluronium tetrafluoroborate (TBTU), 3-(triethoxysilyl)propylisocyanate, and other reagents and solvents were commercially available materials as *pro analysis*, from Sigma-Aldrich or Merck (Darmstadt, Germany), and were used without further purification. Porous spherical silica gel Nucleosil-100Å-5μm from Macherey-Nagel (Dören, Germany) was used as the support material of the six XCSPs. Ethanol (EtOH), 2-propanol (2-PrOH), *n*-hexane (Hex), methanol (MeOH), and acetonitrile (ACN) for high-performance liquid chromatography (HPLC) were purchased from Sigma-Aldrich. Triethylamine (TEA), diethylamine (DEA), and trifluoroacetic acid (TFA) (all p.a. grade) were also obtained from Sigma-Aldrich. Ultrapure water was produced by a Millipore Milli-Q system (Millipore, Bedford, MA). Commercial chiral test compounds used to evaluate the XCSPs were obtained from Sigma-Aldrich or from Merck. Kielcorins and CDXs were synthesized previously in our laboratory according to procedures described elsewhere.[24,25,39]

2.2 | Instrumentation and chromatography

Data melting points are uncorrected and were obtained with a Köfler microscope. Optical rotation measurements were carried out on a Polartronic Universal polarimeter. Infrared spectra were recorded in a KBr microplate (cm^{-1}) in an FTIR spectrometer Nicolet iS10 from Thermo Scientific (Waltham, MA) with Smart OMNI-Transmission accessory (Software OMNIC 8.3). ^{1}H and ^{13}C NMR spectra were taken in DMSO-d_6 at room temperature, on Bruker Avance 300 and 500 instruments (Billerica, MA; 300.13 and 500.13 MHz for ^{1}H and 75.47 and 125.77 MHz for ^{13}C). Chemical shifts are expressed in δ (ppm) values relative to tetramethylsilane (TMS) as an internal reference. Coupling constants are reported in Hz. ^{13}C nuclear magnetic resonance (NMR) assignments were made by 2D HSQC and HMBC experiments (long-range C, H coupling constants were optimized to 7 Hz). HRMS mass spectra were measured on a Bruker Daltonics micrOTOF Mass Spectrometer, recorded as ESI (electrospray) mode. Elemental analyses were conducted on an Elemental Carlo Erba 1108 apparatus. Flash chromatography was carried out using Grace Resolv, silica gel 5 g/25 mL cartridges. Thin-layer chromatography (TLC) was performed using Merck silica gel 60 (GF_{254}) plates, with appropriate mobile phases and detection at 254 and/or 365 nm. The column packing system was an SSI Lab Alliance – Pack in a Box, portable HPLC column packing system model CP constant pressure pump, nonflush, 0.1–24 mL/min, 10.000 psig, with transducer and RS-232 control, SS, 110/220V column packer assembly (50 mL reservoir, column adapter 5/16" 4.6 mm) with Quick-Set pump control software. A Shandon column packing pump was also used. The HPLC system used consisted of a JASCO (Tokyo, Japan) model 880-PU pump, equipped with a Rheodyne 7125 injector fitted with a 20 μL loop, a JASCO model 880-30 solvent mixer, a 875-UV Intelligent U*V*/Vis Detector, and a QR-2090 Plus Chiral Polarimeter Detector. Data acquisition was performed using Chromatography Station for Windows, v. 1.7 DLL. Two more HPLC systems were employed: a system consisted of one Shimadzu (Kyoto, Japan) LC-10ATVP pump, equipped with a Rheodyne 7725i injector fitted with a 100 μL loop, an SPD-10AV U*V*/Vis detector with an SCL-10Avp interface, controlled using Shimadzu CLASS-VP software; and a system consisted of two Shimadzu LC 10-ADvp pumps, an FCV-10AL solvent selector valve, an automatic injector SIL10-Advp, an SPD-10AV U*V*/Vis detector with an SCL-10Avp interface. A CD detector model JASCO CD 2095 Plus was also used. Data acquisition was performed using Shimadzu LC SOLUTIONS software. Analyses were performed at room temperature in an isocratic mode with a multimodal operation. The stock solutions of chiral test compounds were prepared by dissolution in EtOH at a concentration of 1 mg/mL and further diluted in the same solvent. Working solutions of mixtures of enantiomeric pure compounds were prepared mixing equal aliquots of each enantiomer. The mobile phase compositions were Hex and EtOH or 2-PrOH as a modifier, with or without TFA, TEA, or DEA, in normal-phase conditions. The evaluations in polar organic mode were carried out using MeOH, EtOH, ACN, or mixtures of these solvents. MeOH and water or ACN and water, with or without TFA or TEA, were used in reversed-phase conditions. The mobile phases were prepared in a volume/volume relation and degassed in an ultrasonic bath for 15 min before use. The flow rate used was 0.5 mL/min (columns with 150 x 4.6 mm i.d.) or 0.2 mL/min (columns with 150 x 2.1 mm i.d.) and the chromatograms were monitored by UV detection at a wavelength of 254 nm and/or polarimeter detection and/or CD detection. Sample injections (20 μL) were carried out in triplicate. The dead time (t_0) was considered to be equal to the peak of the solvent front and was taken from each particular run. The chromatographic parameters were established as follows: the retention factor (k) was determined as $[k = (t_R - t_0) / t_0]$ where t_R is the retention time for each enantiomer; the enantioselectivity factor (α) was calculated as $[\alpha = k_2 / k_1]$; the resolution (R_s) was determined as $[R_s = 1.18 \times (t_{R2} - t_{R1}) / (W_{1\ 0.5} + W_{2\ 0.5})]$ where t_{R1}, $W_{1\ 0.5}$ and t_{R2}, $W_{2\ 0.5}$ are the retention times and the peak width at half height of the first and second eluted enantiomer, respectively. The chiral selector loadings (μmol/m^2) were determined from the elemental analyses of carbon as follows: selector loading $= (10^6 \times \%C) / S\ [(100 \times n \times 12) - (\%C \times Mw)]$ where %C is the elemental analyses of carbon, *S* is the surface area, *n* is the number of carbon atoms in the modified chain, and *Mw* is the relative molecular mass.

2.3 | Development of XCSPs 1-6

XCSPs 1–6 were prepared following similar synthetic procedures according to Schemes 1 and 2.

2.4 | General procedure for the synthesis of CDXs 7–11 and 18

CDXs **7–11** and **18** were synthesized and characterized according to the described procedure.[24,25]

2.5 | General procedure for the synthesis of silylated derivative of CDXs 12–16 and 19

The appropriate CDX (2.12 mmol) was dissolved in anhydrous toluene (60 mL), and triethylamine (303 μL, 2.18 mmol) and 3-(triethoxysilyl)propylisocyanate (550 μL, 2.22 mmol) were added. The mixture was refluxed for 76 h. The solvent was evaporated under reduced pressure and the crude product was purified by flash chromatography (Grace Resolv, silica gel 5 g / 25 mL, *n*-hexane/ethyl acetate in gradient) and by crystallization from ethyl acetate / *n*-hexane affording the silylated derivative.

2.5.1 | (*S*)-2-(6-methoxyxanthone-2-carboxamido)-3-methylbutyl [3-(triethoxysilyl) propyl] carbamate (12)

Compound **12** was obtained as white crystals (yield: 91%); m.p.: 144–146°C (ethyl acetate / *n*-hexane); $[\alpha]_D^{20}$ = +15.8° (7.58 mg/mL, dichloromethane); ^{1}H NMR, ^{13}C NMR, IR, and HRMS data are shown in the Supplementary Material.

2.5.2 | (*R*)-2-(6-methoxyxanthone-2-carboxamido)-2-phenylethyl [3-(triethoxysilyl) propyl] carbamate (13)

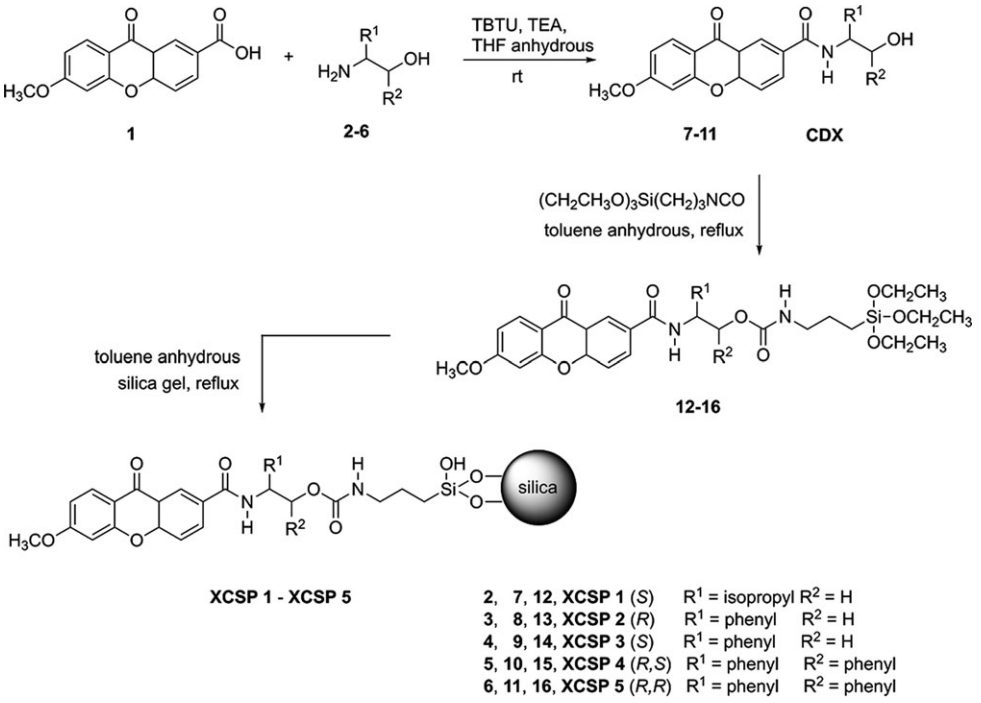
Compound **13** was obtained as white crystals (yield: 87%); m.p.: 96–98°C (ethyl acetate); $[\alpha]_D^{20}$ = +44.3° (7.5 mg/mL, ethyl acetate); ^{1}H NMR, ^{13}C NMR, IR, and HRMS data are shown in the Supplementary Material.

2.5.3 | (*S*)-2-(6-methoxy-9-oxo-9*H*-xanthene-2-carboxamido)-2-phenylethyl [3-(triethoxy-silyl) propyl] carbamate (14)

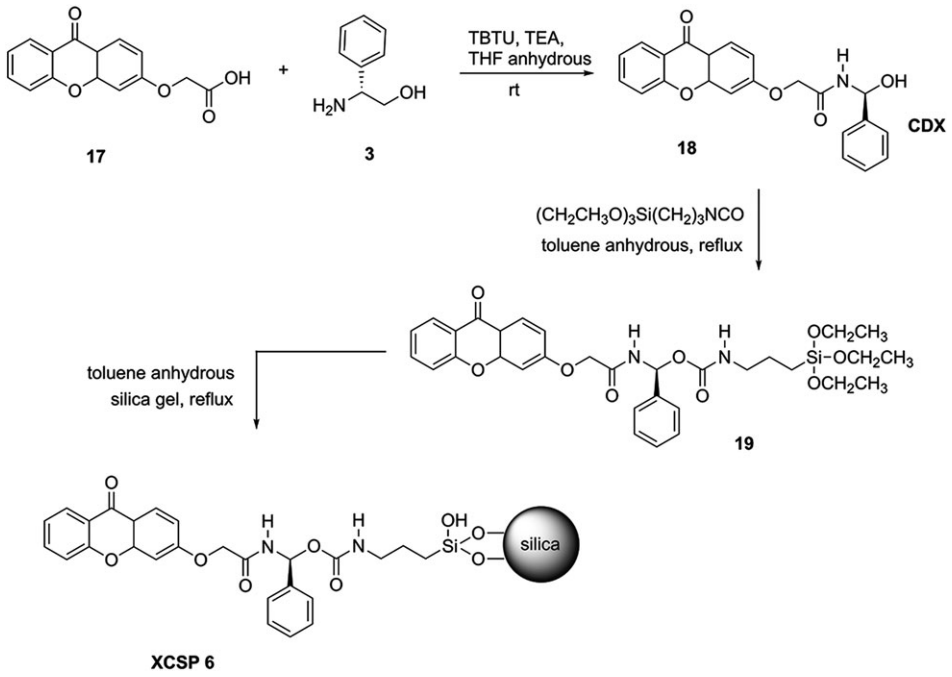
Compound **14** was obtained as white crystals (yield: 74%); m.p.: 96–98°C (ethyl acetate / *n*-hexane); $[\alpha]_D^{20}$ = –44.3° (7.5 mg/mL, ethyl acetate); ^{1}H NMR, ^{13}C NMR, IR, and HRMS data are shown in the Supplementary Material.

2.5.4 | (1*S*,2*R*)-2-(6-methoxy-9-oxo-9*H*-xanthene-2-carboxamido)-1,2-diphenylethyl [3-(triethoxysilyl)propyl] carbamate (15)

Compound **15** was obtained as white crystals (yield: 63%); m.p.: 219–220°C (ethyl acetate / *n*-hexane); $[\alpha]_D^{20}$ = –150.0° (0.20 mg/mL, dichloromethane); ^{1}H NMR, ^{13}C NMR, IR, and HRMS data are shown in the Supplementary Material.



SCHEME 1 Synthesis of XCSPs 1–5



SCHEME 2 Synthesis of XCSP 6

2.5.5 | (1*R*,2*R*)-2-(6-methoxy-9-oxo-9*H*-xanthene-2-carboxamido)-1,2-diphenylethyl [3-(triethoxysilyl)propyl] carbamate (16)

Compound **16** was obtained as white crystals (yield: 51%); m.p.: 155–158°C (ethyl acetate / *n*-hexane); $[\alpha]_D^{20}$ = +22.0° (0.5 mg/mL, chloroform); ^{1}H NMR, ^{13}C NMR, IR, and HRMS data are shown in the Supplementary Material.

2.5.6 | (*R*)-2-[2-(3-oxyxanthone)acetamide]-2-phenylethyl [3-(triethoxysilyl)propyl] carbamate (19)

Compound **19** was obtained as light pink crystals (yield: 76%); m.p.: 108–110°C (ethyl acetate / *n*-hexane); $[\alpha]_D^{20}$ = –19.2° (3.1 mg/mL, ethyl acetate); ^{1}H NMR, ^{13}C NMR, IR, and HRMS data are shown in the Supplementary Material.

2.6 | General procedure of covalent linkage of silylated derivative of CDXs onto the silica gel and HPLC column packing

Anhydrous toluene (30 mL) was added to silica gel Nucleosil (2890 mg, 100 Å-5µm, Macherey-Nagel), previously dried in a desiccator under vacuum and with phosphorus pentoxide for 24 h. Following this, the appropriate silylated derivative of CDX (1.42 mmol) dissolved in the same solvent (30 mL) was added. The mixture was gently stirred at reflux for 76 h. The solid was then filtered and washed successively with (100 mL) toluene, methanol, acetone, ethyl acetate, dichloromethane, and *n*-hexane. The bonded phase was dried in a desiccator under vacuum for 24 h, yielding the **XCSP**. Each new CSP (2.30 g) was mixed with Hex:2-PrOH (50:50 *v/v*) (50 mL), and then sonicated for 3 min. The suspension was poured into the chamber of a column packer and was packed into an empty HPLC column (150 x 4.6 mm i.d.) with Hex:2-PrOH (90:10 *v/v*) as packing solvent, under a pressure no more than 7500 psi.

3 | RESULTS AND DISCUSSION

Six new CSPs, based on xanthone derivatives (XCSP **1**–**6**), were developed according to Schemes 1 and 2. XCSPs **1**–**5** were prepared using the xanthone derivative 6-methoxy-9-oxo-9*H*-xanthene-2-carboxylic acid (**1**) (Scheme 1), synthesized via Ullmann reaction with the formation of diaryl ether intermediate according to the previously described procedure,[25] as a chemical substrate. For **XCSP 6**, the xanthone derivative 2-[(9-oxo-9*H*-xanthen-3-yl)oxy]acetic acid (**17**), synthesized via benzophenone intermediate,[24] was used as a substrate (Scheme 2). The CDXs were synthesized by coupling these two suitable functionalized xanthone derivatives with commercially available enantiomerically pure building blocks.[24,25] The activation of the carboxylic acid group of the xanthone scaffold was carried out with TBTU. Accordingly, xanthone **1** was coupled with the enantiomerically pure amino alcohols (*S*)-(+)-valinol (**2**), (*R*)-(–)-α-phenylglycinol (**3**), (*S*)-(+)-α-

phenylglycinol (**4**), (1*R*,2*S*)-(–)-2-amino-1,2-diphenylethanol (**5**), and (1*R*,2*R*)-(+)-2-amino-1,2-diphenylethanol (**6**), to afford CDXs (**7**–**11**), respectively. CDX **18** was synthesized by coupling xanthone **17** with the amino alcohol (*R*)-(–)-α-phenylglycinol (**3**). Our selection included enantiomerically pure building blocks with no tendency towards racemization or enantiomeric interconversion, having a primary amine as a reactive group for the coupling reaction with the carboxyxanthone derivative and a hydroxyl group to further linkage to the spacer.

The amino alcohols valinol and phenylglycinol were chosen to obtain XCSPs, similar to valine-derived[40] and phenylglycine-derived[41] CSPs developed by Pirkle et al. In fact, these amino acid-derived CSPs were shown to be useful to separate a broad spectrum of racemates on both analytical and preparative scales.[33,34] Recognizing the crucial role of π–π interactions between each enantiomer and this type of CSPs for chiral recognition, the amino alcohol 2-amino-1,2-diphenylethanol was also selected in order to increase these interaction types, as well as to obtain a more rigid structure (cleft type selector), similar to the most employed and successful Pirkle-type CSP, i.e., Whelk-O1 CSP.[42]

The strategy used for binding the CDXs (chiral selectors) to the chromatographic support was through the synthesis of derivatives that allowed the covalent linkage to the silica, specifically silylated derivatives.[43,44] Consequently, all CDXs reacted with 3-(triethoxysilyl) propylisocyanate giving the corresponding silylated derivatives. Then, the silylated derivatives of all the CDXs were anchored to silica gel (Nucleosil-100-5) giving the correspondent XCSPs **1**–**6** (Schemes 1 and 2). This synthetic methodology involves only a few steps and the reactions provided good yields.

The chiral selector loadings for all the XCSPs were calculated from the elemental analyses of carbon (Table 1).

Finally, all the XCSPs were packed in a column with 150 x 4.6 mm i.d. using Hex:2-PrOH (90:10 *v/v*). XCSP **2** and XCSP **5** were also packed in a column with 150 x 2.1 mm i.d.

The LC enantioselective resolution capabilities of **XCSPs 1-6** were evaluated with several enantiomeric mixtures of structurally different chiral compounds, including some types of drugs. Furthermore, a library of CDXs was also chosen that incorporates the enantiomeric precursors to XCSPs **1**–**3** and XCSP **5** and analogs.

The enantioseparation by XCSPs **1**–**6** was evaluated under normal, polar organic, and reversed-phase elution conditions. Table 2 shows the overall best results.

The results in Table 2 show that the best enantioselectivity was achieved mainly under normal-phase elution conditions using EtOH as a modifier.

It was found that **XCSP 1** showed enantioselective capabilities only for enantiomeric mixtures of CDXs. Concerning, for example, the enantiomeric mixtures of CDXs **23**, **24,** and **25**, good enantioselectivity (α = 1.14, 1.15, and 1.15) and resolution (R_S = 2.16, 2.24, and 2.18) were respectively obtained, with Hex:EtOH (90:10 *v/v*) as mobile phase.

XCSP 2 was found to have more versatility, showing enantioselectivity not only for the enantiomeric mixtures of CDXs (α ranging from 1.04 to 1.32) but also for the chiral compounds 1-(9-anthryl)-2,2,2-trifluoroethanol (**19**) (α = 1.07), *N*-[1-(1-naphthyl)ethyl]-3,5-dinitrobenzamide (**20**) (α = 1.31), and bi-naphthol (**22**) (α = 1.08). Unsurprisingly, in general, **XCSP 2** showed the best performance and versatility, when taking into account that: 1) **XCSP 2** is similar to the successfully commercially available Phenylglycine CSP[41]; 2) the selector of this CSP has another aromatic group in addition to the xanthone scaffold, both of which were essential for chiral recognition by this type of CSPs through π–π interactions between enantiomers and the CSP; and 3) an excellent enantioselectivity and resolution were achieved for the enantiomeric mixture of chiral selector of **XCSP 2** using macrocyclic antibiotics,[7] (*S*,*S*)-Whelk-O1,[32] and polysaccharide-based CSPs.[6]

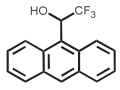
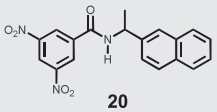
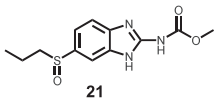
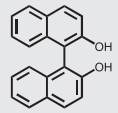
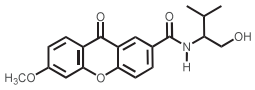
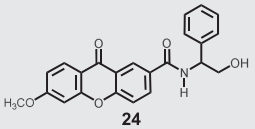
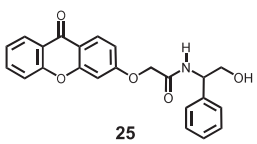
As expected, **XCSP 3** proved to have similar enantioselectivity capabilities to **XCSP 2**. Actually, these two XCSPs have the same chiral selector but with opposite configurations. However, the **XCSP 3** generally presented higher retention for the enantiomers, which can be explained by its slightly higher selector loading (1.31 μmol/m^2) when compared with **XCSP 2** (0.90 μmol/m^2).

Regarding **XCSP 4**, the additional aromatic groups of the chiral selector of this CSP did not contribute to its potential enantiorecognition. In fact, the steric hindrance of the bulky and rigid structural elements may be responsible for non-

TABLE 1 Elemental analysis and chiral selector loadings for XCSPs **1–6**

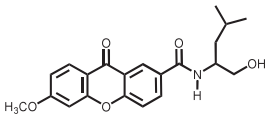
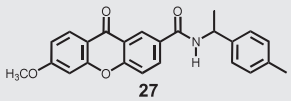
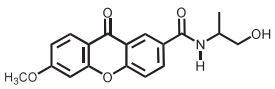
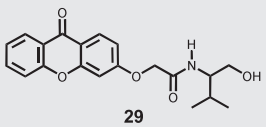
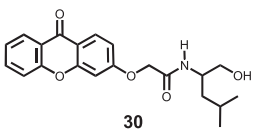
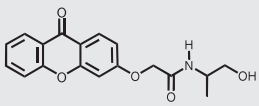
Elemental analysis	XCSP 1	XCSP 2	XCSP 3	XCSP 4	XCSP 5	XCSP 6
% C	7.09	8.66	11.87	8.36	10.11	9.87
% N	1.01	0.82	1.14	1.10	0.85	0.89
% H	2.60	1.84	1.65	1.59	0.97	1.76
Selector loading (based on C) μmol/m^2	0.80	0.90	1.31	0.70	0.85	1.04

TABLE 2 Chromatographic resolution of enantiomeric mixtures on XCSPs **1-6**

Enantiomeric mixture	XCSP	Mobile phase (*v/v*)	k_1	α	R_s
 **19** 1-(9-anthryl)-2,2,2-trifluoroethanol	XCSP 2	Hex/2-PrOH: 90/10	1.81	1.07	< 1.00
 **20** *N*-[1-(1-naphtyl)ethyl]-3,5-dinitrobenzamide	XCSP 2	Hex/EtOH: 80/20	2.90	1.17	1.95
		Hex/2-PrOH: 70/30	2.33	1.31	1.93
	XCSP 3	Hex/EtOH: 80/20	3.07	1.17	1.95
	XCSP 6	Hex/EtOH: 80/20	3.35	1.22	2.96
 **21** albendazole sulfoxide	XCSP 4	ACN/H_2O: 10/90	10.29	1.07	< 1.00
		MeOH/H_2O: 15/85	8.97	1.06	< 1.00
		EtOH/H_2O: 15/85	4.61	1.07	< 1.00
 **22** bi-naphthol	XCSP 2	Hex/EtOH: 90/10 with 0.01% TFA	3.96	1.08	< 1.00
 **23** *N*-(1-hydroxy-3-methylbutan-2-yl)-6-methoxy-9-oxo-9*H*-xanthene-2-carboxamide	XCSP 1	Hex/EtOH: 90/10	9.76	1.14	2.16
		Hex/EtOH: 80/20	5.27	1.13	1.49
		Hex/2-PrOH: 70/30	2.36	1.18	< 1.00
	XCSP 2	Hex/EtOH: 80/20	6.12	1.12	1.33
		Hex/EtOH: 85/15	9.59	1.13	1.57
		Hex/2-PrOH: 70/30	3.48	1.15	< 1.00
	XCSP 3	Hex/EtOH: 80/20	6.72	1.11	1.30
	XCSP 6	Hex/EtOH: 80/20	6.01	1.06	< 1.00
 **24** *N*-(2-hydroxy-1-phenylethyl)-6-methoxy-9-oxo-9*H*-xanthene-2-carboxamide	XCSP 1	Hex/EtOH: 90/10	18.79	1.15	2.24
		Hex/EtOH: 80/20	7.53	1.13	1.68
		Hex/2-PrOH: 70/30	4.35	1.16	< 1.00
	XCSP 2	Hex/EtOH: 80/20	10.99	1.15	1.98
		Hex/EtOH: 85/15	17.89	1.15	1.60
		Hex/2-PrOH: 70/30	6.82	1.32	< 1.00
		EtOH	0.96	1.10	< 1.00
		ACN/MeOH: 50/50	0.57	1.10	< 1.00
		ACN/MeOH: 5:95	0.96	1.08	< 1.00
	XCSP 3	Hex/EtOH: 80/20	10.67	1.12	1.95
	XCSP 6	Hex/EtOH: 80/20	12.35	1.05	< 1.00
	XCSP 5	Hex/EtOH: 80/20	4.45	1.10	< 1.00
 **25** *N*-(2-hydroxy-1-phenylethyl)-2-((9-oxo-9*H*-xanthen-3-yl)oxy) acetamide	XCSP 1	Hex/EtOH: 90/10	16.63	1.05	< 1.00
		Hex/EtOH: 80/20	6.94	1.04	< 1.00

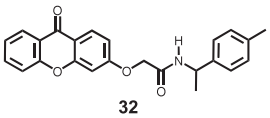
(*Continues*)

TABLE 2 (Continued)

Enantiomeric mixture	XCSP	Mobile phase (*v/v*)	k_1	α	R_s
 **26** *N*-(1-hydroxy-4-methylpentan-2-yl)-6-methoxy-9-oxo-9*H*-xanthene-2-carboxamide	XCSP 1	Hex/EtOH: 90/10	7.59	1.15	2.18
		Hex/EtOH: 80/20	3.55	1.13	1.38
		Hex/2-PrOH: 70/30	1.86	1.18	< 1.00
	XCSP 2	Hex/EtOH: 80/20	4.85	1.11	1.21
		Hex/EtOH: 85/15	6.69	1.11	1.40
		Hex/2-PrOH: 70/30	2.63	1.16	< 1.00
	XCSP 3	Hex/EtOH: 80/20	6.42	1.11	1.10
	XCSP 6	Hex/EtOH: 80/20	4.79	1.08	1.06
 **27** 6-methoxy-9-oxo-*N*-(1-(*p*-tolyl)ethyl)-9*H*-xanthene-2-carboxamide	XCSP 1	Hex/EtOH: 90/10	5.88	1.07	< 1.00
		Hex/EtOH: 80/20	3.66	1.06	< 1.00
		Hex/2-PrOH: 70/30	1.82	1.08	< 1.00
	XCSP 2	Hex/EtOH: 80/20	4.92	1.09	1.14
		Hex/EtOH: 85/15	7.07	1.10	1.38
		Hex/2-PrOH: 70/30	2.92	1.12	< 1.00
		EtOH	0.78	1.08	< 1.00
	XCSP 3	Hex/EtOH: 80/20	6.72	1.10	1.15
	XCSP 6	Hex/EtOH: 80/20	4.99	1.08	1.11
 **28** *N*-(1-hydroxypropan-2-yl)-6-methoxy-9-oxo-9*H*-xanthene-2-carboxamide	XCSP 1	Hex/EtOH: 90/10	18.08	1.06	< 1.00
		Hex/EtOH: 80/20	7.06	1.05	< 1.00
	XCSP 2	Hex/EtOH: 80/20	9.59	1.04	< 1.00
		Hex/EtOH: 85/15	13.52	1.04	< 1.00
	XCSP 3	Hex/EtOH: 80/20	12.54	1.03	< 1.00
 **29** *N*-(1-hydroxy-3-methylbutan-2-yl)-2-((9-oxo-9*H*-xanthen-3-yl)oxy)acetamide	XCSP 1	Hex/EtOH: 90/10	10.07	1.05	< 1.00
	XCSP 3	Hex/EtOH: 80/20	7.53	1.05	< 1.00
 **30** *N*-(1-hydroxy-4-methylpentan-2-yl)-2-((9-oxo-9*H*-xanthen-3-yl)oxy)acetamide	XCSP 1	Hex/EtOH: 90/10	8.40	1.08	< 1.00
		Hex/EtOH: 80/20	3.43	1.06	< 1.00
	XCSP 2	Hex/EtOH: 80/20	4.82	1.07	< 1.00
	XCSP 3	Hex/EtOH: 80/20	6.24	1.07	< 1.00
 **31** *N*-(1-hydroxypropan-2-yl)-2-((9-oxo-9*H*-xanthen-3-yl)oxy) acetamide	XCSP 1	Hex/EtOH: 90/10	18.44	1.04	< 1.00
	XCSP 3	Hex/EtOH: 80/20	12.35	1.02	< 1.00

(*Continues*)

TABLE 2 (Continued)

Enantiomeric mixture	XCSP	Mobile phase (*v/v*)	k_1	α	R_s
 **32** 2-((9-oxo-9*H*-xanthen-3-yl)oxy)-*N*-(1-(*p*-tolyl)ethyl)acetamide	XCSP 1	Hex/EtOH: 90/10	5.89	1.04	< 1.00
	XCSP 2	Hex/EtOH: 80/20	4.66	1.06	< 1.00
	XCSP 3	Hex/EtOH: 80/20	6.33	1.07	< 1.00
	XCSP 6	Hex/EtOH: 80/20	4.79	1.04	< 1.00

enantioselective interactions with the chiral compounds. Interestingly, it was found that **XCSP 4** presented some enantioselectivity (α ~1.07) only for the chiral compound albendazole sulfoxide (**21**) under reversed-phase mode. This result indicates that the chiral recognition mechanism of **XCSP 4** is different from other XCSPs.

Interestingly, although the chiral selector of **XCSP 5** differs only in the configuration of one stereogenic center compared with that of **XCSP 4**, the chromatographic behavior of **XCSP 5** was similar to that of **XCSPs 1–3**. However, **XCSP 5** revealed poor enantioresolution capabilities for the tested compounds.

On the other hand, the best chromatographic value was achieved with **XCSP 6**, with α = 1.22 and R_S = 2.96 for *N*-[1-(1-naphthyl)ethyl]-3,5-dinitrobenzamide (**7**) with Hex:EtOH (80:20 *v/v*) as a mobile phase. The selector of **XCSP 6** comprises the same chiral moiety as that of **XCSP 2,** but with different substituents on the xanthone scaffold. Nevertheless, in general, less discrimination ability was observed compared to **XCSP 1** and **XCSP 2** (Table 2).

It is important to highlight that the enantioselectivity for the enantiomeric mixtures of CDXs, tested on XCSPs, was mainly achieved using a low percentage of the modifier (5–30%). However, with those elution conditions high retention factors were observed (k_1 ranging from 1.82 to 18.79). To overcome this situation, the polarity of the mobile phase was increased to consequently decrease the retention time, but concomitantly the enantioselectivity also decreased. Considering evaluation on the polar organic and reversed-phase elution conditions, the chromatographic results were not satisfactory. In general, short retention times were observed with absence or very poor resolutions.

Characteristic chromatograms obtained during the evaluation of the enantioselective resolution capabilities of the XCSPs are shown in Figure 2.

Considering the overall chromatographic results, it was also found that all the XCSPs (except for **XCSP 4**) provided enantioselectivity for the enantiomeric mixtures of CDXs. Accordingly, for example, from the 12 enantiomeric mixtures of CDXs tested, 10 of them (83%) showed enantioselectivity on **XCSP 1** and 9 of them (75%) on **XCSP-2**. This specificity for the CDXs is very important, since previous studies, using commercial CSPs, namely, (*S*,*S*)-Whelk-O1 and *L*-Phenylglycine CSPs, demonstrated less versatility for this important class of chiral compounds.[32] In fact, the enantiomeric mixture of CDX **27** was the only pair resolved on *L*-Phenylglycine CSP, while (*S*,*S*)-Whelk-O1 CSP showed enantioselectivity only for CDXs possessing an aromatic moiety bonded to the stereogenic center.

The chromatographic results also suggested that XCSPs can be developed by applying the concept of reciprocity.[35,36] As an example, the best resolution achieved on **XCSP 1** was with the enantiomeric mixture of CDX **24**, with R_S = 2.24 using Hex:EtOH (90:10 *v/v*) as a mobile phase. Therefore, the immobilized enantiomers of CDX **24** (**XCSP 2** and **XCSP 3**), using similar interactions, were able to distinguish between the enantiomeric precursors of **XCSP 1**, i.e., CDX **23** (Table 2). For example, good enantioselectivity (α = 1.13) and resolution (R_S = 1.57) were obtained on **XCSP-2** with Hex:EtOH (85:15 *v/v*).

It was also found that the chiral self-recognition phenomenon occurs with the XCSPs. As, for example, **XCSP 1** and **XCSP 2** can effectively separate the enantiomeric mixtures of their precursors, namely, CDX **23** and CDX **24**, with R_S = 2.16 and 1.98, respectively. In both cases, the enantiomer that forms the homochiral diastereisomeric complex with the CSP was more retained. Similar results were described in the literature using Pirkle-type CSPs.[33,37,38]

In order to confirm the inversion of elution order of XCSPs, the two enantiomers of CDX **24** (compounds **8** and **9**) were also eluted separately on **XCSP 2**, and on the opposite enantiomeric XCSP (**XCSP 3**). The chromatograms are shown in Figure 3.

As shown in Figure 3, with these new CSPs, the elution order of the enantiomers of CDX **24** is inverted by using the same type of CSP. This is an important advantage for enantiomeric purity determinations or preparative separations, giving the possibility to elute before the trace enantiomer or the desired enantiomer, respectively.

Additionally, concerning ecological, practical and economic reasons, the greening of the chromatographic

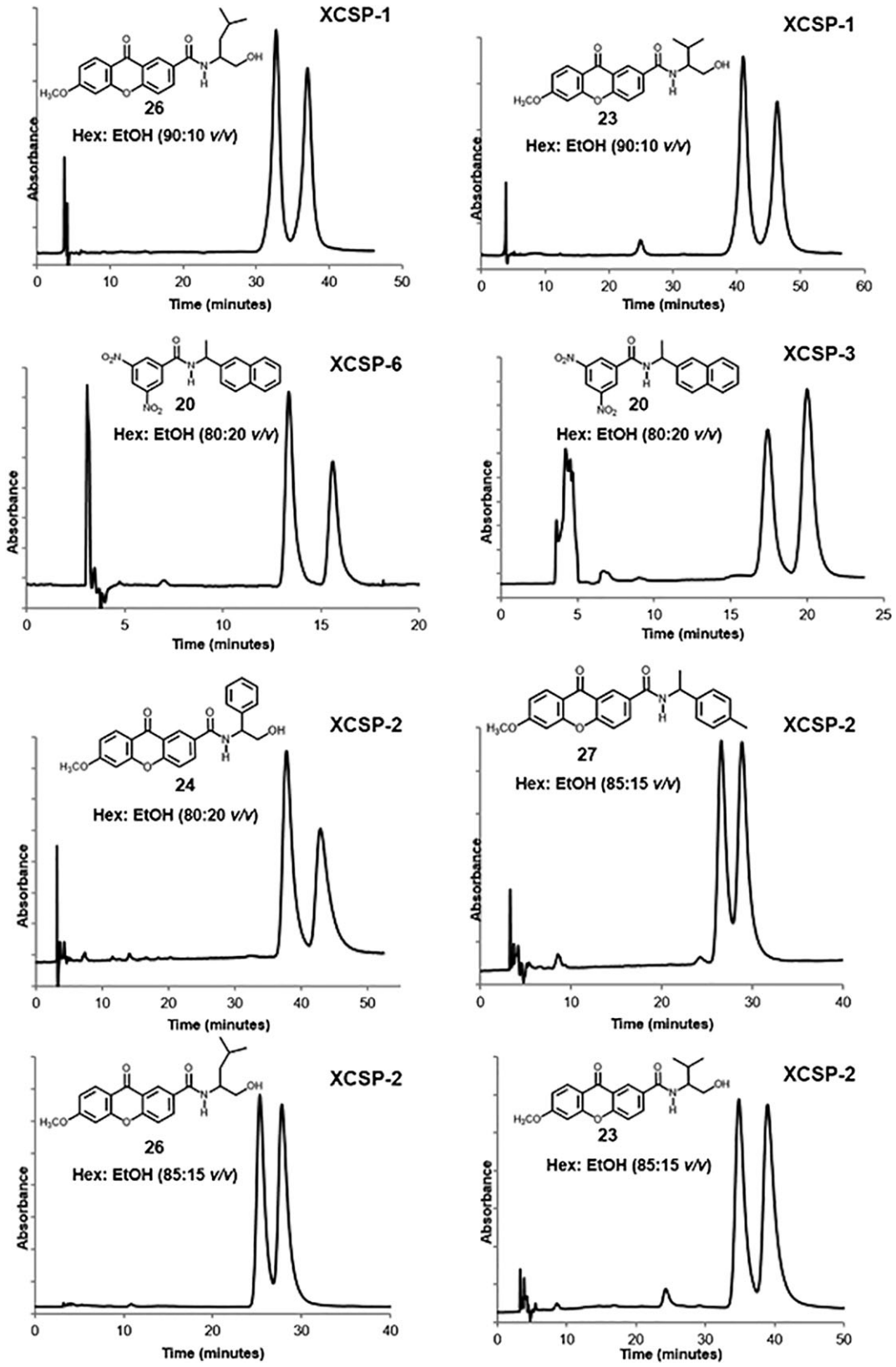


FIGURE 2 Chromatograms of enantiomeric mixtures of compounds 20, 23, 24, 26, and 27 on XCSPs. Flow rate, 0.5 mL/min; detection, 254 nm

analysis[45,46] was investigated by reducing the internal diameter of the LC columns from 4.6 to 2.1 mm i.d. Accordingly, the best obtained XCSPs, **XCSP 2,** and **XCSP 5** were packed in a column with 150 x 2.1 mm i.d. and their enantiomeric performance was evaluated using a flow rate of 0.2 mL/min. The major advantage

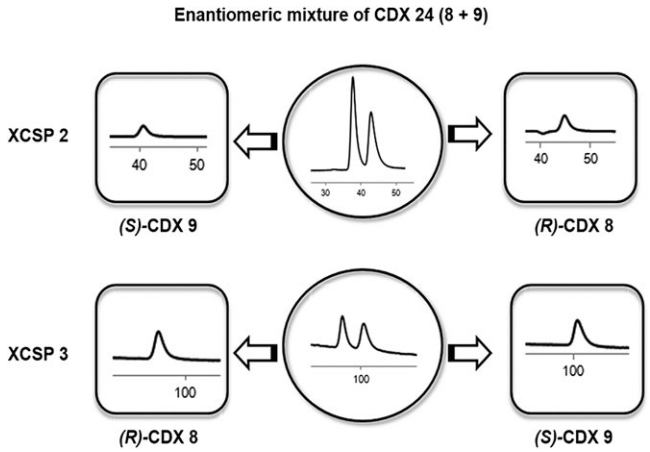


FIGURE 3 Schematic chromatograms of enantiomeric mixture of CDX 24, (S)-CDX 9, and (R)-CDX 8 on XCSP 2 and XCSP 3. Mobile phase, Hex:EtOH (80:20 *v*/*v*); flow rate, 0.5 mL/min; detection, 254 nm

was the decrease of the solvent consumption without compromising the enantioseparation.

4 | CONCLUSION

Six new xanthonic chiral stationary phases (XCSPs) were developed using a well-established synthetic methodology that involves only a few steps of reactions with good yields. The XCSPs were covalently bonded to fully porous silica, which guarantee long-lasting columns, and show high stability, versatility in the selection of the mobile phase composition, and reproducibility. It was found that, in general, they show enantioselectivity for CDXs and other chiral compounds, such as 1-(9-anthryl)-2,2,2-trifluoroethanol, *N*-[1-(1-naphthyl)ethyl]-3,5-dinitrobenzamide, binaphthol, and albendazole sulfoxide. Moreover, this type of chiral stationary phase gives the possibility to invert the elution order (by using the opposite enantiomer as chiral selector). Therefore, this work represents a breakthrough that is extremely interesting not only in the field of chiral LC but also as new chemical tools for further studies of chiral molecular recognition.

ACKNOWLEDGMENTS

This research was partially supported by the Structured Program of R&D&I INNOVMAR – Innovation and Sustainability in the Management and Exploitation of Marine Resources (reference NORTE-01-0145-FEDER-000035, Research Line NOVELMAR), funded by the Northern Regional Operational Programme (NORTE2020) through the European Regional Development Fund (ERDF) and by Foundation for Science and Technology (FCT), under the project PTDC/MAR-BIO/4694/2014 (reference POCI-01-0145-FEDER-016790) supported through national funds provided by FCT – Foundation for Science and Technology and European Regional Development Fund (ERDF) through the COMPETE – Programa Operacional Factores de Competitividade (POFC) programme and the Project 3599 – Promover a Produção Científica e Desenvolvimento Tecnológico e a Constituição de Redes Temáticas (3599-PPCDT), COXANT–CESPU-2016, QOPNA research project (FCT UID/QUI/00062/2013) and Portuguese NMR network. Y.Z. Phyo thanks the Erasmus Mundus Action 2 (Lotus Plus project) for a PhD's scholarship. We thank also Coordenação de Aperfeiçoamento Pessoal de Nível Superior (CAPES) and FCT for the joint international Project 214/08.

REFERENCES

1. Ward TJ, Ward KD. Chiral separations: A review of current topics and trends. *Anal Chem*. 2012;84(2):626-635.
2. Sousa ME, Tiritan ME, Belaz KRA, et al. Multimilligram enantioresolution of low-solubility xanthonolignoids on polysaccharide chiral stationary phases using a solid-phase injection system. *J Chromatogr A*. 2006;1120(1-2):75-81.
3. Silva B, Fernandes C, Tiritan ME, et al. Chiral enantioresolution of cathinone derivatives present in "legal highs", and enantioselectivity evaluation on cytotoxicity of 3,4-methylenedioxypyrovalerone (MDPV). *Forensic Toxicol*. 2016;1-14.
4. Prompanya C, Fernandes C, Cravo S, et al. A new cyclic hexapeptide and a new isocoumarin derivative from the marine sponge-associated fungus Aspergillus similanensis KUFA 0013. *Mar Drugs*. 2015;13(3):1432-1450.
5. Zin WWM, Buttachon S, Dethoup T, et al. New cyclotetrapeptides and a new diketopiperzine derivative from the marine sponge-associated fungus Neosartorya glabra KUFA 0702. *Mar Drugs*. 2016;14(7):
6. Fernandes C, Brandão P, Santos A, et al. Resolution and determination of enantiomeric purity of new chiral derivatives of xanthones using polysaccharide-based stationary phases. *J Chromatogr A*. 2012;1269:143-153.
7. Fernandes C, Tiritan ME, Cass Q, Kairys V, Fernandes MX, Pinto M. Enantioseparation and chiral recognition mechanism of new chiral derivatives of xanthones on macrocyclic antibiotic stationary phases. *J Chromatogr A*. 2012;1241:60-68.
8. Ribeiro AR, Gonçalves VMF, Maia AS, Ribeiro C, Castro PML, Tiritan ME. Dispersive liquid–liquid microextraction and HPLC to analyse fluoxetine and metoprolol enantiomers in wastewaters. *Environ Chem Lett*. 2015;13(2):203-210.
9. Ribeiro AR, Maia AS, Cass QB, Tiritan ME. Enantioseparation of chiral pharmaceuticals in biomedical and environmental analyses by liquid chromatography: An overview. *J Chromatogr B Analyt Technol Biomed Life Sci*. 2014;968:8-21.

10. Cavazzini A, Pasti L, Massi A, Marchetti N, Dondi F. Recent applications in chiral high performance liquid chromatography: A review. *Anal Chim Acta*. 2011;706(2):205-222.

11. Kalíková K, Riesová M, Tesařová E. Recent chiral selectors for separation in HPLC and CE. *Cent Eur J Chem*. 2011;1-22.

12. Lämmerhofer M. Chiral recognition by enantioselective liquid chromatography: Mechanisms and modern chiral stationary phases. *J Chromatogr A*. 2010;1217(6):814-856.

13. Chankvetadze B. Recent developments on polysaccharide-based chiral stationary phases for liquid-phase separation of enantiomers. *J Chromatogr A*. 2012;1269:26-51.

14. Tang M, Zhang J, Zhuang S, Liu W. Development of chiral stationary phases for high-performance liquid chromatographic separation. *Trends Anal Chem*. 2012;39:180-194.

15. Carreira EM, Yamamoto H. Comprehensive Chirality. In: *Volume 8: Separations and Analysis*. Amsterdam: Elsevier; 2012:96-310.

16. Bocian S, Skoczylas M, Buszewski B. Amino acids, peptides, and proteins as chemically bonded stationary phases — A review. *J Sep Sci*. 2016;39(1):83-92.

17. Zhou J, Tang J, Tang W. Recent development of cationic cyclodextrins for chiral separation. *Trends Anal Chem*. 2015;65:22-29.

18. Shen J, Okamoto Y. Efficient separation of enantiomers using stereoregular chiral polymers. *Chem Rev*. 2016;116(3):1094-1138.

19. Pinto MMM, Sousa ME, Nascimento MSJ. Xanthone derivatives: New insights in biological activities. *Curr Med Chem*. 2005;12(21):2517-2538.

20. Masters KS, Bräse S. Xanthones from fungi, lichens, and bacteria: The natural products and their synthesis. *Chem Rev*. 2012;112(7):3717-3776.

21. Wezeman T, Bräse S, Masters KS. Xanthone dimers: A compound family which is both common and privileged. *Nat Prod Rep*. 2015;32(1):6-28.

22. Pinto MMM, Castanheiro RAP, Kijjoa A. Xanthones from marine-derived microorganisms: isolation, structure elucidation, and biological activities. In: *Encyclopedia of Analytical Chemistry*. Vol.27 Hoboken, NJ: John Wiley & Sons L; 2014:1-21.

23. Shagufta AI. Recent insight into the biological activities of synthetic xanthone derivatives. *Eur J Med Chem*. 2016;116:267-280.

24. Fernandes C, Masawang K, Tiritan ME, et al. New chiral derivatives of xanthones: Synthesis and investigation of enantioselectivity as inhibitors of growth of human tumor cell lines. *Bioorg Med Chem*. 2014;22(3):1049-1062.

25. Fernandes C, Oliveira L, Tiritan ME, et al. Synthesis of new chiral xanthone derivatives acting as nerve conduction blockers in the rat sciatic nerve. *Eur J Med Chem*. 2012;55:1-11.

26. Azevedo CMG, Afonso CMM, Sousa D, et al. Multidimensional optimization of promising antitumor xanthone derivatives. *Bioorg Med Chem*. 2013;21(11):2941-2959.

27. Castanheiro RAP, Pinto MMM, Cravo SMM, Pinto DCGA, Silva AMS, Kijjoa A. Improved methodologies for synthesis of prenylated xanthones by microwave irradiation and combination of heterogeneous catalysis (K10 clay) with microwave irradiation. *Tetrahedron*. 2009;65(19):3848-3857.

28. Correia-Da-Silva M, Sousa E, Duarte B, et al. Polysulfated xanthones: Multipathway development of a new generation of dual anticoagulant/antiplatelet agents. *J Med Chem*. 2011;54(15):5373-5384.

29. Sousa E, Paiva A, Nazareth N, et al. Bromoalkoxyxanthones as promising antitumor agents: Synthesis, crystal structure and effect on human tumor cell lines. *Eur J Med Chem*. 2009;44(9):3830-3835.

30. Pinto M, Tiritan ME, Fernandes C, Cass Q. In: Industrial BdP, ed. *Fases Estacionárias Quirais baseadas em Derivados Xantónicos*. Porto, Portugal: In; 2011.

31. Gales L, Damas AM. Xanthones — A structural perspective. *Curr Med Chem*. 2005;12(21):2499-2515.

32. Fernandes C, Palmeira A, Santos A, Tiritan ME, Afonso C, Pinto MM. Enantioresolution of chiral derivatives of xanthones on (S,S)-Whelk-O1 and l -phenylglycine stationary phases and chiral recognition mechanism by docking approach for (S,S)-Whelk-O1. *Chirality*. 2013;25(2):89-100.

33. Welch CJ. Evolution of chiral stationary phase design in the Pirkle laboratories. *J Chromatogr A*. 1994;666(1–2):3-26.

34. Fernandes C, Tiritan ME, Pinto M. Small molecules as chromatographic tools for HPLC enantiomeric resolution: Pirkle-type chiral stationary phases evolution. *Chromatographia*. 2013;76(15-16):871-897.

35. Taylor DR, Maher K. Chiral separations by high-performance liquid chromatography. *J Chromatogr Sci*. 1992;30(3):67

36. Pirkle WH, Däppen R. Reciprocity in chiral recognition. Comparison of several chiral stationary phases. *J Chromatogr A*. 1987;404(C):107-115.

37. Pirkle WH, Pochapsky TC. Considerations of chiral recognition relevant to the liquid chromatographic separation of enantiomers. *Chem Rev*. 1989;89(2):347-362.

38. Lee W, Snyder SE, Volkers PI, et al. Assessing chiral self-recognition using chiral stationary phases. *Tetrahedron*. 2011;67(37):7143-7147.

39. Sousa EP, Silva AMS, Pinto MMM, Pedro MM, Cerqueira FAM, Nascimento MSJ. Isomeric kielcorins and dihydroxyxanthones: Synthesis, structure elucidation, and inhibitory activities of growth of human cancer cell lines and on the proliferation of human lymphocytes in vitro. *Helv Chim Acta*. 2002;85(9):2862-2876.

40. Pirkle WH, Finn JM. Chiral high-pressure liquid chromatographic stationary phases. 3. General resolution of arylalkylcarbinols. *J Org Chem*. 1981;46(14):2935-2938.

41. Pirkle WH, House DW, Finn JM. Broad spectrum resolution of optical isomers using chiral high-performance liquid chromatographic bonded phases. *J Chromatogr*. 1980;192(1):143-158.

42. Pirkle WH, Welch CJ. An improved chiral stationary phase for the chromatographic separation of underivatized naproxen enantiomers. *J Liq Chromatogr*. 1992;15(11):1947-1955.

43. Welch CJ, Perrin SR. Improved chiral stationary phase for ß-blocker enantioseparations. *J Chromatogr A*. 1995;690(2):218-225.

44. Ihara T, Sugimoto Y, Asada M, Nakagama T, Hobo T. Influence of the method of preparation of chiral stationary phases on enantiomer separations in high-performance liquid chromatography. *J Chromatogr A*. 1995;694(1):49-56.

45. Sandra P, Vanhoenacker G, David F, Sandra K. Pereira A. Green chromatography (Part 1): Introduction and liquid chromatography. *LC-GC Eur*. 2010;23(5)

46. Majors RE, Raynie D. The greening of the chromatography laboratory. *LC-GC N Am*. 2011;29(2):118-134.

SUPPORTING INFORMATION

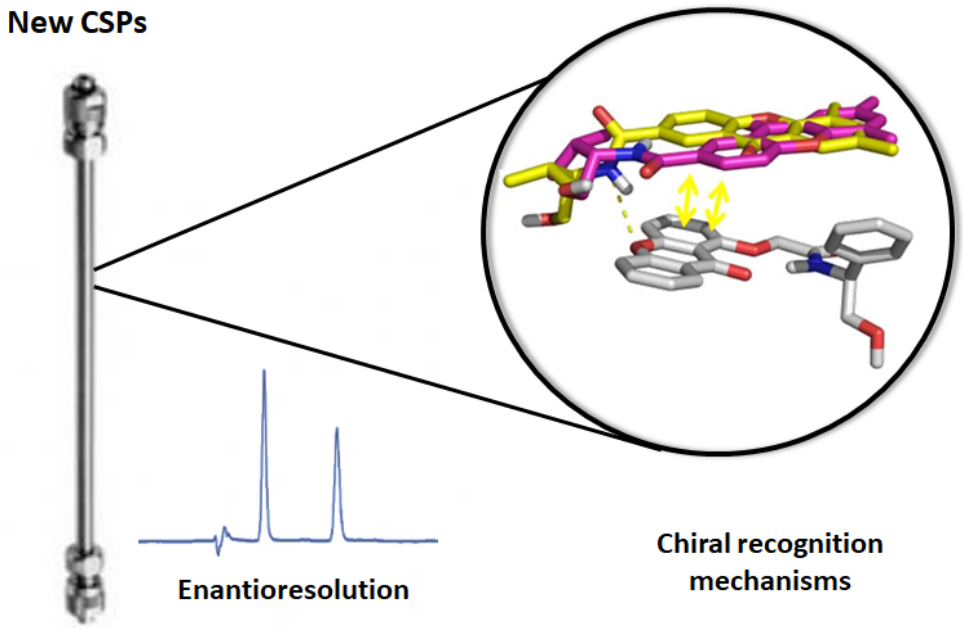
Additional Supporting Information may be found online in the supporting information tab for this article.

How to cite this article: Fernandes C, Tiritan ME, Cravo S, et al. New chiral stationary phases based on xanthone derivatives for liquid chromatography. *Chirality*. 2017;29:430-442. https://doi.org/10.1002/chir.22706

CHAPTER V

New chiral stationary phases for liquid chromatography based on small molecules: development, enantioresolution evaluation and chiral recognition mechanisms

Original research article submitted for publication in Chirality



Graphical abstract

Chirality

Home

Author

Review

Submission Confirmation

Print

Thank you for your submission

Submitted to
Chirality

Manuscript ID
CHIR-19-0080

Title
New chiral stationary phases for liquid chromatography based on small molecules: development, enantioresolution evaluation and chiral recognition mechanisms

Authors
Phyo, Ye' Zaw
Teixeira, Joana
Tiritan, Maria
Cravo, Sara
Palmeira, Andreia
Gales, Luís
Silva, Artur
Pinto, Madalena
Kijjoa, Anake
Fernandes, Carla

Date Submitted
10-May-2019

New chiral stationary phases for liquid chromatography based on small molecules: development, enantioresolution evaluation and chiral recognition mechanisms

Ye' Zaw Phyo[1,2], Joana Teixeira[3], Maria Elizabeth Tiritan[2,3,4], Sara Cravo[2,3], Andreia Palmeira[2,3], Luís Gales[1,5,6], Artur M.S. Silva[7], Madalena M.M. Pinto[2,3], Anake Kijjoa[1,2], Carla Fernandes[2,3*]

[1] *ICBAS*-Instituto de Ciências Biomédicas Abel Salazar, Universidade do Porto, Rua de Jorge Viterbo Ferreira, 228, 4050-313 Porto, Portugal

[2] Interdisciplinary Centre of Marine and Environmental Research (CIIMAR), Edifício do Terminal de Cruzeiros do Porto de Leixões, Av. General Norton de Matos s/n, 4050-208 Matosinhos, Portugal

[3] Laboratório de Química Orgânica e Farmacêutica, Departamento de Ciências Químicas, Faculdade de Farmácia, Rua de Jorge Viterbo Ferreira, 228, 4050-313 Porto, Portugal

[4] CESPU, Instituto de Investigação e Formação Avançada em Ciências e Tecnologias da Saúde (IINFACTS), Rua Central de Gandra, 1317, 4585-116 Gandra PRD, Portugal

[5] Instituto de Biologia Molecular e Celular (IBMC), Universidade do Porto, Rua de Jorge Viterbo Ferreira, 228, 4050-313 Porto, Portugal

[6] i3S – Instituto de Investigação e Inovação em Saúde, Rua Alfredo Allen, 208, Porto, Portugal.

[7] QOPNA & LAQV-REQUIMTE, Departamento de Química, Universidade de Aveiro, 3810-103 Aveiro, Portugal

Correspondence: cfernandes@ff.up.pt; Tel.: +35-122-042-8688

ABSTRACT

Recently, we reported the development of new chiral stationary phases (CSPs) for liquid chromatography (LC) based on chiral derivatives of xanthones (CDXs), a different type of small molecules from the commercially available CSPs. Based on the most promising CDX selectors twelve new CSPs were successfully prepared starting from suitable functionalized small molecules. The chiral selectors comprising one, two, three or four chiral moieties were covalently bonded to a chromatographic support, and further packed into LC stainless-steel columns (150 x 2.1 mm I.D.). Specificity for enantioseparation of some CDXs under normal-phase elution conditions was observed in the evaluation of the new CSPs. Besides, assessment of chiral recognition mechanisms was performed by computational studies using molecular docking approach, which are in accordance with the chromatographic parameters. X-Ray analysis was used to establish a chiral selector 3-D structure.

Keywords: Liquid chromatography; Chiral stationary phase; Chiral derivative of xanthone; Benzophenone; Enantioselectivity; Chiral recognition; Docking.

1. INTRODUCTION

Liquid chromatography (LC) enantioresolution using chiral stationary phases (CSPs) is one of the most significant separation approaches in academic research and industry,[1,2] for both analytical[3-5] and preparative purposes.[6-8] The development of CSPs for LC brought a new breath to enantioseparation processes and, nowadays, several types are available including Pirkle-type, ligand-exchange-type, molecularly-imprinted, and based on macrocyclic antibiotics, proteins, polysaccharides, cyclodextrins, crown ethers, cyclofructans as well as synthetic polymers.[9-12] Among them, more than a hundred are currently commercially available.[13] Nevertheless, although many different types are described, the development of new CSPs continues to be a field of research with great importance to follow the constant challenges on different areas as well as the advances in chromatographic instrumentation.[14] Of note are the Pirkle-type CSPs that have evolved over the years, showing more progress reported, mainly due to the possibility of using a wide variety of small molecules as chiral selectors.[15-17]

Recently, we described the development of new CSPs based on chiral derivatives of xanthones (CDXs),[18] a different type of small molecules from the commercially available CSPs. This class of small molecules is proved to be structurally promising chiral selectors for LC,[18] in addition to their broad spectrum of bioactivities.[19-21] The best enantioselectivity results were achieved for xanthone-(*R*)-(-)-α-phenylglycinol-derived CSPs.[18] In the last years, other amino

alcohol-derived CSPs can be found in literature and, among them, (*R*)-phenylglycinol-derived CSPs showed good results for the LC enantioseparation of many chiral analytes.[22-29]

In this study, twelve new CSPs were successfully prepared by multi-step pathways starting from suitable functionalized small molecules based on the most promising selectors (CDXs) previously reported.[18] Herein, the majority of the synthetized chiral selectors were (*R*)-phenylglycinol derivatives comprising one, two, three or four chiral moieties, and were covalently bonded through one or more sites to a chromatographic support.

Computational modeling studies by molecular docking were performed to gain the insight of structural features associated with chiral recognition mechanisms,[30,31] which not only allow the understanding the chromatographic parameters at a molecular level[32-34] but also to improve the design of new selectors.[35,36] These studies allowed a closer look towards the mechanisms involved in the enantiorecognition ability of this type of CSPs and the results are discussed in this work.

2. MATERIALS AND METHODS

2.1. GENERAL METHODS

^{1}H and ^{13}C NMR spectra were taken in DMSO-d_6 or acetone-d_6 at room temperature on a DRX-300 spectrometer. Chemical shifts are expressed in δ (ppm) values relative to TMS. ^{13}C NMR assignments were made by HSQC and HMBC experiments (long-range J_{C-H} were optimized to 7 Hz). Elemental analyses were conducted on an Elemental Carlo Erba 1108 apparatus in C.A.C.T.I.-University of Vigo, Spain. Melting points were obtained in a Kofler microscope and are uncorrected. The optical rotations were recorded on a Polartronic Universal polarimeter (ADP 410 polarimeter). IR spectra were recorded on a FTIR spectrometer Nicolet iS10 from Thermo Scientific with Smart OMNI-Transmission accessory (Software 188 OMNIC 8.3) in KBr. The column packing was performed in a SSI Lab Alliance® – Pack in a Box, portable HPLC column packing system model CP constant pressure pump, non-flush, 0.1-24 $mLmin^{-1}$, 10.000 psi, with transducer and RS-232 control, SS, 110/220V column packer assembly (50 mL reservoir, column adapter 5/16" 2.1 mm) Quick-Set pump control software. The empty stainless-steel columns were purchased from SSI Lab Alliance. The chiral selector loadings ($\mu molm^{-2}$) were determined from the elemental analyses of carbon as follows: selector loading = $(10^6 \times \%C) / S\,[(100 \times n \times 12) - (\%C \times Mw)]$ where %C is the elemental analyses of carbon, *S* is the surface area, *n* the number of carbon atoms in the modified chain and *Mw* is the relative molecular mass.

2.2. CHEMICALS AND REAGENTS

All reagents used in this study were purchased from Sigma-Aldrich Co (St. Louis, Missouri, USA) or Merck (Darmstadt, Germany). The organic solvents were obtained from Sigma-Aldrich Co (St. Louis, Missouri, USA) and were used without further purification. Silica gel 60 GF_{254} (Merck, Darmstadt, Germany) precoated plates were used for TLC. Silica gel 60 (0.04-0.063 mm, Macherey-Nagel, Düren, Germany) was used for flash column chromatography. Porous spherical silica gel Nucleosil® (100Å-5μm, Macherey-Nagel) was used as the support material of the CSPs.

2.3. Preparation of CSPs 1-12

CSPs 1-12 were prepared following similar synthetic procedures according to **Schemes 1-5**.

2.3.1. Synthesis of hydroxyxanthones 1-7

The following hydroxyxanthones were synthesized according to previously described procedures.[37-43]

*1-Hydroxy-9H-xanthen-9-one (**1**)*

Yield (51%). ^{1}H NMR (300.13 MHz, DMSO-d_6) δ: 12.50 (s,1-OH), 8.13 (dd, *J* = 8.1, 1.7 Hz,1H, H-8), 7.87 (ddd, *J* = 8.7, 7.1, 1.7 Hz, 1H, H-6), 7.69 (t, *J* = 8.3 Hz, 1H, H-3), 7.61 (dd, *J* = 8.7, 1.7 Hz, 1H, H-5), 7.46 (ddd, *J* = 8.1, 7.1, 1.7 Hz, 1H, H-7), 7.03 (dd, *J* = 8.3, 0.9 Hz, 1H, H-4), 6.78 ppm (dd, *J* = 8.3, 0.9 Hz, 1H, H-2); ^{13}C NMR (75.47 MHz, DMSO-d_6) δ: 181.8 (C-9), 160.9 (C-1), 155.8 (C-10a), 155.7 (C-4a), 137.6 (C-3), 136.5 (C-6), 129.6 (C-8), 125.4 (C-7), 121.9 (C-8a), 119.8 (C-5), 118.1 (C-2), 110.2 (C-9a), 108.3 ppm (C-4).

*1,3-Dihydroxy-9H-xanthen-9-one (**2**)*

Yield (51%). ^{1}H NMR (300.13 MHz, DMSO-d_6) δ: 12.81 (s, 1-OH), 11.13 (s, 3-OH), 8.10 (dd, *J* = 7.5, 1.7 Hz, 1H, H-8), 7.83 (td, *J* = 8.6, 7.5, 1.7 Hz, 1H, H-6), 7.56 (d, *J* = 8.6 Hz, 1H, H-5), 7.45 (t, *J* = 7.5 Hz, 1H, H-7), 6.38 (d, *J* = 2.1 Hz, 1H, H-4), 6.20 ppm (d, *J* = 2.1Hz, 1H, H-2); ^{13}C NMR (75.47 MHz, DMSO-d_6) δ: 179.8 (C-9), 166.0 (C-1), 162.9 (C-3), 157.4 (C-4a), 155.4 (C-10a), 135.7 (C-6), 125.3 (C-8), 124.4 (C-7), 119.8 (C-8a), 117.7 (C-5), 102.3 (C-9a), 98.2 (C-2), 94.1 ppm (C-4).

*1,3,6-Trihydroxy-9H-xanthen-9-one (**3**)*

Yield (69%). ^{1}H NMR (300.13 MHz, DMSO-d_6) δ: 13.09 (s, 1-OH), 10.97 (br, 2H), 7.91 (d, *J* = 8.7 Hz, 1H, H-8), 6.84 (dd, *J* = 8.7, 2.4 Hz, 1H, H-7), 6.76 (d, *J* = 2.4 Hz, 1H, H-5), 6.29 (d, *J* = 1.8 Hz, 1H, H-4), 6.12 ppm (d, *J* = 1.8 Hz, 1H, H-2); ^{13}C NMR (75.47 MHz, DMSO-d_6) δ: 179.1

(C-9), 165.2 (C-3), 164.3 (C-6), 162.9 (C-1), 157.5 (C-4a), 157.4 (C-10a), 127.2 (C-8), 114.1 (C-7), 112.3 (C-8a), 102.1 (C-9a), 101.6 (C-5), 97.9 (C-2), 93.9 ppm (C-4).

*1,3,8-Trihydroxy-9H-xanthen-9-one (**4**)*

Yield (26%). ^{1}H NMR (300.13 MHz, DMSO-d_6) δ: 11.89 (s, 1H, 1-OH), 11.81 (s, 1H, 8-OH), 6.79 (dd, *J* = 8.4, 0.9 Hz, 1H, H-7), 7.68 (t, *J* = 8.4 Hz, 1H, H-6), 7.00 (dd, *J* = 8.4, 0.9 Hz, 1H, H-5), 6.38 (d, *J* = 2.1 Hz, 1H, H-4), 6.21 ppm (d, *J* = 2.1 Hz, 1H, H-2); ^{13}C NMR (75.47 MHz, DMSO-d_6) δ: 183.3 (C-9), 167.1 (C-3), 162.2 (C-1), 160.3 (C-8), 157.5 (C-4a), 155.5 (C-10a), 137.2 (C-6), 110.6 (C-7), 107.1 (C-5), 106.9 (C-8a), 101.0 (C-9a), 98.7 (C-2), 94.5 ppm (C-4).

*1,3,6,8-Tetrahydroxy-9H-xanthen-9-one (**5**)*

Yield (24%). ^{1}H NMR (300.13 MHz, acetone-d_6) δ: 6.35 (d, *J* = 2.1 Hz, 2H, H-4 and H-5), 6.22 ppm (d, *J* = 2.1 Hz, 2H, H-2 and H-7); ^{13}C NMR (75.47 MHz, acetone-d_6) δ: 183.8 (C-9), 166.8 (C-3 and C-6), 163.6 (C-1 and C-8), 158.6 (C-4a and C-10a), 101.7 (C-8a and C-9a), 99.2 (C-2 and C-7), 95.0 ppm (C-4 and C-5).

*3,6-Dihydroxy-9H-xanthen-9-one (**6**)*

Yield (99%). ^{1}H NMR (300.13 MHz, DMSO-d_6) δ: 8.03 (d, *J* = 8.6 Hz, 2H, H-1 and H-8), 6.84 (dd, *J* = 8.6, 2.2 Hz, 2H, H-2 and H-7), 6.80 ppm (d, *J* = 2.2 Hz, 2H, H-4 and H-5); ^{13}C NMR (75.47 MHz, DMSO-d_6) δ: 174.5 (C-9), 163.1 (C-3 and C-6), 157.4 (C-4a and C-10a), 127.0 (C-1 and C-8), 113.9 (C-8a and C-9a), 113.0 (C-2 and C-7), 101.9 ppm (C-4 and C-5).

*3,4-Dihydroxy-9H-xanthen-9-one (**7**)*

Yield (70%). ^{1}H NMR (300.13 MHz, DMSO-d_6) δ: 9.72 (s, 2H, 3 and 4-OH), 8.16 (dd, *J* = 8.1, 1.8 Hz, 1H, H-8), 7.84 (ddd, *J* = 8.7, 7.1, 1.8 Hz, 1H, H-6), 7.65 (d, *J* = 8.7 Hz, 1H, H-1), 7.62 (d, *J* = 8.7 Hz, 1H, H-5), 7.44 (ddd, *J* = 8.1, 7.1, 1.8 Hz, 1H, H-7), 6.95 ppm (d, *J* = 8.8 Hz, 1H, H-2); ^{13}C NMR (75.47 MHz, DMSO-d_6) δ: 175.3 (C-9), 155.5 (C-10a), 151.6 (C-4a), 146.4 (C-1), 134.8 (C-2), 132.6 (C-6), 125.9 (C-8), 123.9 (C-3), 120.8 (C-7), 117.9 (C-8a), 116.6 (C-5), 114.7 (C-9a), 113.2 ppm (C-4).

2.3.2. Synthesis of acetate compounds 10-18

2.3.2.1. Starting from a mono-hydroxylated compound

The hydroxylated compound (**1**) (0.30 g, 1.40 mmol) was dissolved in anhydrous acetone (40 mL) and K_2CO_3 (0.58 g, 1.40 mmol) and $BrCH_2COOCH_3$ (0.2 mL, 1.70 mmol) were added. The mixture was kept under reflux and magnetic stirring for 24 h. Afterwards, the mixture was concentrated under reduced pressure and extracted with dichloromethane (2 × 100 mL) and

water (2 × 100 mL). The organic layer was evaporated under reduced pressure and the crude product was crystallized from methanol, to afford **10** as a white solid.

*Methyl 2-[(9-oxo-9H-xanthen-1-yl)oxy]acetate (**10**)*

Yield (95%, white solid). m.p.: 156-158 °C (MeOH); IR ν_{max} (cm^{-1}) (KBr): 1748, 1618, 1463, 1436, 1377, 1291, 1244, 821, 757; ^{1}H NMR (300.13 MHz, DMSO-d_6) δ: 8.10 (dd, *J* = 8.1, 1.7 Hz, 1H, H-8), 7.80 (ddd, *J* = 8.7, 7.1, 1.7 Hz, 1H, H-6), 7.70 (t, *J* = 8.3 Hz, 1H, H-3), 7.57 (dd, *J* = 8.1, 1.7 Hz, 1H, H-5), 7.43 (ddd, *J* = 8.1, 7.1, 1.7 Hz, 1H, H-7), 7.20 (dd, *J* = 8.3, 0.9 Hz, 1H, H-4), 6.88 (dd, *J* = 8.3, 0.9 Hz, 1H, H-2), 4.97 (s, 2H, OCH_2), 3.70 ppm (s, 3H, OCH_3); ^{13}C NMR (75.47 MHz, DMSO-d_6) δ: 175.0 (C-9), 168.9 (C=O, ester), 158.3 (C-1), 157.3 (C-10a), 154.4 (C-4a), 135.0 (C-3), 134.9 (C-6), 125.9 (C-8), 124.3 (C-7), 122.2 (C-8a), 117.5 (C-5), 111.9 (C-2), 110.7 (C-9a), 107.8 (C-4), 65.5 (OCH_2), 52.0 ppm (OCH_3).

2.3.2.2. Starting from a poly-hydroxylated compound

Compounds **11-18** were prepared from suitable hydroxylated compounds (**2-9**) using the same method as described for **10**, increasing the amount of K_2CO_3 and $BrCH_2COOCH_3$ according to the number of hydroxyl groups of the chemical substrate (**2-9**) and the stoichiometry of the reaction.

*Dimethyl 2,2'-[(9-oxo-9H-xanthene-1,3-diyl)bis(oxy)]diacetate (**11**)*

Yield (98%, white solid). m.p.: 157-159 °C (MeOH); IR ν_{max} (cm^{-1}) (KBr): 1750, 1620, 1466, 1458, 1377, 1292, 1243, 814, 757; ^{1}H NMR (300.13 MHz, DMSO-d_6) δ: 8.06 (dd, *J* = 7.5, 1.7 Hz, 1H, H-8), 7.75 (td, *J* = 8.7, 7.5, 1.7 Hz, 1H, H-6), 7.50 (d, *J* = 8.7 Hz, 1H, H-5), 7.39 (t, *J* = 7.5 Hz, 1H, H-7), 6.72 (d, *J* = 2.3 Hz, 1H, H-4), 6.45 (d, *J* = 2.3 Hz, 1H, H-2), 4.96 and 4.97 (2×s, 4H, 2×OCH_2), 3.69 and 3.70 ppm (2×s, 6H, 2×OCH_3); ^{13}C NMR (75.47 MHz, DMSO-d_6) δ: 179.8 (C-9), 168.6 and 168.7 (2×C=O, ester), 162.7 (C-1), 159.7 (C-3), 158.9 (C-4a), 154.4 (C-10a), 135.1 (C-6), 125.9 (C-8), 124.3 (C-7), 122.3 (C-8a), 117.7 (C-5), 107.1 (C-9a), 97.1 (C-2), 94.9 (C-4), 65.0 and 65.5 (2×OCH_2), 51.9 and 52.0 ppm (2×OCH_3).

*Trimethyl 2,2',2''-[(9-oxo-9H-xanthene-1,3,6-triyl)tris(oxy)]triacetate (**12**)*

Yield (91%, white solid). m.p.: 142-144 °C (MeOH); IR ν_{max} (cm^{-1}) (KBr): 1743, 1627, 1469, 1435, 1376, 1294, 1250, 828, 764; ^{1}H NMR (300.13 MHz, DMSO-d_6) δ: 7.98 (d, *J* = 8.7 Hz, 1H, H-8), 7.02 (dd, *J* = 8.7, 2.4 Hz, 1H, H-7), 7.00 (d, *J* = 2.4 Hz, 1H, H-5), 6.67 (d, *J* = 2.3 Hz, 1H, H-4), 6.45 (d, *J* = 2.3 Hz, 1H, H-2), 4.97 and 4.98 (2×s, 6H, 3×OCH_2), 3.70 and 3.71 ppm (2×s, 9H, 3×OCH_3); ^{13}C NMR (75.47 MHz, DMSO-d_6) δ: 173.1 (C-9), 168.7 (3×C=O, ester), 165.2 (C-3), 164.3 (C-6), 162.9 (C-1), 157.5 (C-4a), 157.4 (C-10a), 127.2 (C-8), 114.1 (C-7),

112.3 (C-8a), 102.1 (C-9a), 101.6 (C-5), 97.9 (C-2), 93.9 (C-4), 64.9-65.6 (3×OCH_2), 52.0 ppm (3×OCH_3).

*Trimethyl 2,2',2''-[(9-oxo-9H-xanthene-1,3,8-triyl)tris(oxy)]triacetate (**13**)*

Yield (93%, white solid). m.p.: 151-153 °C (MeOH); IR ν_{max} (cm^{-1}) (KBr): 1747, 1610, 1464, 1435, 1380, 1297, 1250, 816, 763; ^{1}H NMR (300.13 MHz, DMSO-d_6) δ: 7.00 (dd, *J* = 8.4, 0.7 Hz, 1H, H-7), 7.58 (t, *J* = 8.4 Hz, 1 H, H-6), 6.81 (dd, *J* = 8.4, 0.7 Hz, 1H, H-5), 6.65 (d, *J* = 2.3 Hz, 1H, H-4), 6.42 (d, *J* = 2.3 Hz, 1H, H-2), 4.91 and 4.95 (2×s, 6H, 3×OCH_2), 3.70 and 3.71 ppm (2×s, 9H, 3×OCH_3); ^{13}C NMR (75.47 MHz, DMSO-d_6) δ: 172.8 (C-9), 168.6 and 169.8 (3×C=O), 167.1 (C-3), 162.2 (C-1), 160.3 (C-8), 157.5 (C-4a), 155.5 (C-10a), 137.2 (C-6), 110.6 (C-7), 107.1 (C-5), 106.9 (C-8a), 101.0 (C-9a), 98.7 (C-2), 94.5 (C-4), 65.5 and 65.6 (3×OCH_2), 52.0 ppm (3×OCH_3).

*Tetramethy 2,2',2'',2'''-[(9-oxo-9H-xanthene-1,3,6,8 tetrayl)tetrakis(oxy)]tetraacetate (**14**)*

Yield (95%, white solid). m.p.: > 310 °C (MeOH); IR ν_{max} (cm^{-1}) (KBr): 1749, 1623, 1465, 1423, 1377, 1292, 1246, 814, 760; ^{1}H NMR (300.13 MHz, DMSO-d_6) δ: 6.56 (d, *J* = 2.1 Hz, 2H, H-4 and H-5), 6.39 (d, *J* = 2.1 Hz, 2H, H-2 and H-7), 4.94 and 4.96 (2×s, 8H, 4×OCH_2), 3.71 and 3.72 ppm (2×s, 12H, 4×OCH_3); ^{13}C NMR (75.47 MHz, DMSO-d_6) δ: 171.8 (C-9), 168.6 and 168.8 (4×C=O, ester), 161.7 (C-3 and C-6), 159.2 (C-1 and C-8), 157.5 (C-4a and C-10a), 103.9 (C-8a and C-9a), 97.3 (C-2 and C-7), 94.2 (C-4 and C-5), 65.0 and 65.6 (4×OCH_2), 52.0 ppm (4×OCH_3).

*2,2'-[(9-Oxo-9H-xanthene-3,6-diyl)bis(oxy)]diacetate (**15**)*

Yield (88%, white solid). m.p.: 228-230 °C (MeOH); IR ν_{max} (cm^{-1}) (KBr): 1750, 1613, 1453, 1435, 1382, 1286, 1250, 828, 768; ^{1}H NMR (300.13 MHz, DMSO-d_6) δ: 8.17 (d, *J* = 8.8 Hz, 2H, H-1 and H-8), 6.99 (dd, *J* = 8.8, 2.3 Hz, 2H, H-2 and H-7), 6.92 (d, *J* = 2.3 Hz, 2H, H-4 and H-5), 4.76 (s, 4H, 2×OCH_2), 3.79 ppm (s, 6H, 2×OCH_3); ^{13}C NMR (75.47 MHz, DMSO-d_6) δ: 174.4 (C-9), 169.2 (2×C=O, ester), 163.0 (C-3 and C-6), 157.2 (C-4a and C-10a), 127.5 (C-1 and C-8), 115.5 (C-8a and C-9a), 113.0 (C-2 and C-7), 100.9 (C-4 and C-5), 65.0 (2×OCH_2), 50.0 ppm (2×OCH_3).

*Dimethyl 2,2'-[(9-oxo-9H-xanthene-3,4-diyl)bis(oxy)]diacetate (**16**)*

Yield (95%, white solid). m.p.: > 310 °C (MeOH); IR ν_{max} (cm^{-1}) (KBr): 1767, 1605, 1470, 1431, 1380, 1300, 1267, 832, 763; ^{1}H NMR (300.13 MHz, DMSO-d_6) δ: 8.18 (dd, *J* = 8.1, 1.7 Hz, 1H, H-8), 7.92 (ddd, *J* = 9.0, 7.1, 1.7 Hz, 1H, H-6), 7.88 (d, *J* = 9.0, 1H, H-5), 7.65 (d, *J* = 8.5 Hz, 1H, H-1), 7.49 (ddd, *J* = 8.1, 7.1, 1.7 Hz, 1H, H-7), 7.22 (d, *J* = 8.5, 1H, H-2), 4.95 and 5.09 (2×s, 4H, 2×OCH_2), 3.71 and 3.72 ppm (2×s, 6H, 2×OCH_3); ^{13}C NMR (75.47 MHz, DMSO-d_6)

δ: 175.2 (C-9), 168.7 and 169.1 (2×C=O, ester), 155.6 (C-3), 154.9 (C-4), 149.5 (C-1), 135.4 (C-10a), 134.4 (C-4a), 125.9 (C-2), 124.5 (C-6), 121.4 (C-8), 120.8 (C-7), 118.2 (C-5), 116.4 (C-8a), 110.6 (C-9a), 65.4 and 69.1 (2×OCH_2), 51.8 and 52.1 ppm (2×OCH_3).

*Dimethyl 2,2'-[(carbonylbis(4,1-phenylene))bis(oxy)]diacetate (**17**)*

Yield (94%, white solid). m.p.: 175-177 °C (MeOH); IR v_{max} (cm^{-1}) (KBr): 1725, 1603, 1440, 1293, 1246, 829, 763; ^{1}H NMR (300.13 MHz, DMSO-d_6) δ: 7.65 (d, *J* = 8.9 Hz, 4H, H-2, H-2´, H-6, H-6´), 7.04 (d, *J* = 8.9 Hz, 4H, H-3, H-3´, H-5, H-5´), 4.89 (s, 4H, 2×OCH_2), 3.65 ppm (s, 6H, 2×OCH_3); ^{13}C NMR (75.47 MHz, DMSO-d_6) δ: 193.1 (C-9), 168.9 (2×C=O, ester), 160.8 (C-4 and C-4´), 131.3 (C-2, C-2´, C-6, C-6´), 130.6 (C-1 and C-1´), 114.3 (C-3, C-3´, C-5, C-5´), 64.7 (2×OCH_2), 55.2 ppm (2×OCH_3).

*Tetramethyl 2,2',2'',2'''-[(carbonylbis(benzene-4,1,3-triyl))tetrakis(oxy)]tetraacetate (**18**)*

Yield (93 %, white solid). m.p.: 128-130 °C (MeOH); IR v_{max} (cm^{-1}) (KBr): 1633, 1603, 1456, 1423, 1298, 1257, 834, 772; ^{1}H NMR (300.13 MHz, DMSO-d_6) δ: 7.38 (d, *J* = 8.6 Hz, 2H, H-6 and H-6´), 6.60 (dd, *J* = 8.6, 2.2 Hz, 2H, H-5 and H-5´), 6.50 (d, *J* = 2.2 Hz, 2H, H-3 and H-3´), 4.63 and 4.86 (2×s, 8H, 4×OCH_2), 3.60 and 3.71 ppm (2×s,12H, 4×OCH_3); ^{13}C NMR (75.47 MHz, DMSO-d_6) δ: 191.5 (C-9), 168.8 and168.9 (4×C=O, ester), 161.2 (C-4 and C-4´), 157.9 (C-2 and C-2´), 131.8 (C-6 and C-6´), 124.0 (C-1 and C-1´), 106.6 (C-5 and C-5´), 100.2 (C-3 and C-3´), 65.0 and 65.5 (4×OCH_2), 51.9 ppm (4×OCH_3).

2.3.3. Synthesis of carboxylated compounds 19-27

A suitable acetate compound (1.40 mmol) was dissolved in CH_2Cl_2/MeOH (1:1 *v/v*, 100 mL) and 8 M NaOH (15-30 mL) was added. The mixture was kept at room temperature and magnetic stirring for 24 h. Afterwards, the organic solvents were evaporated under reduced pressure and water (30 mL) was added. The aqueous phase was acidified with 5 M HCl solution resulting in the formation of a precipitate that was collected by filtration under reduced pressure, washed with water and crystallized from MeOH, to provide a carboxylated compound (**20-27**).

*2-[(9-Oxo-9H-xanthen-1-yl)oxy]acetic acid (**19**)*

Yield (93%, white solid). m.p.: 139-141 °C (MeOH); IR v_{max} (cm^{-1}) (KBr): 2860, 1713, 1606, 1470, 1431, 1374, 1231, 853, 753; ^{1}H NMR (300.13 MHz, DMSO-d_6) δ: 8.12 (dd, *J* = 8.1, 1.6 Hz,1H, H-8), 7.81 (ddd, *J* = 8.6, 7.2, 1.6 Hz, 1H, H-6), 7.72 (t, *J* = 8.4 Hz, 1H, H-3), 7.58 (dd, *J* = 8.1, 1.6 Hz, 1H, H-5), 7.44 (ddd, *J* = 8.1, 7.2, 1.6 Hz, 1H, H-7), 7.20 (dd, *J* = 8.4, 0.9 Hz, 1H, H-4), 6.87 (dd, *J* = 8.4, 0.9 Hz, 1H, H-2), 4.95 ppm (s, 2H, OCH_2); ^{13}C NMR (75.47 MHz, DMSO-d_6) δ: 175.0 (C-9), 169.8 (COOH), 158.6 (C-1), 157.4 (C-10a), 154.5 (C-4a), 135.5 (C-

3), 134.9 (C-6), 126.0 (C-8), 124.3 (C-7), 122.2 (C-8a), 117.6 (C-5), 111.9 (C-2), 110.4 (C-9a), 107.8 (C-4), 65.7 ppm (OCH_2).

*2,2'-[(9-Oxo-9H-xanthene-1,3-diyl)bis(oxy)]diacetic acid (**20**)*

Yield (94%, white solid). m.p.: 212-214 °C (MeOH); IR ν_{max} (cm^{-1}) (KBr): 2850, 1714, 1624, 1466, 1428, 1372, 1228, 855, 766; ^1H NMR (300.13 MHz, DMSO-d_6) δ: 8.08 (dd, *J* = 7.5, 1.7 Hz, 1H, H-8), 7.77 (td, *J* = 8.7, 7.5, 1.7 Hz, 1H, H-6), 7.53 (d, *J* = 8.7 Hz, 1H, H-5), 7.41 (t, *J* = 7,5 Hz, 1H, H-7), 6.68 (d, *J* = 2.3 Hz, 1H, H-4), 6.44 (d, *J* = 2.3 Hz, 1H, H-2), 4.85 and 4.86 ppm (2×s, 4H, 2×OCH_2); ^{13}C NMR (75.47 MHz, DMSO-d_6) δ: 173.7 (C-9), 169.5 and 169.6 (2×COOH), 163.1 (C-1), 159.9 (C-3), 158.9 (C-4a), 154.4 (C-10a), 134.6 (C-6), 125.9 (C-8), 124.3 (C-7), 122.3 (C-8a), 117.3 (C-5), 106.9 (C-9a), 97.1 (C-2), 94.4 (C-4), 65.1 and 65.7 ppm (2×OCH_2).

*2,2',2''-[(9-Oxo-9H-xanthene-1,3,6-triyl)tris(oxy)]triacetic acid (**21**)*

Yield (89%, white solid).m.p.: 225-226 °C (MeOH); IR ν_{max} (cm^{-1}) (KBr): 2852, 1718, 1612, 1450, 1435, 1376, 1236, 856, 764; ^1H NMR (300.13 MHz, DMSO-d_6) δ: 8.00 (d, *J* = 8.7 Hz, 1H, H-8), 7.03 (dd, *J* = 8.7, 2.4 Hz, 1H, H-7), 7.00 (d, *J* = 2.4 Hz, 1H, H-5), 6.66 (d, *J* = 2.2 Hz, 1H, H-4), 6.45 (d, *J* = 2.2 Hz, 1H, H-2), 4.85 and 4.87 ppm (2×s, 6H, 3×OCH_2); ^{13}C NMR (75.47 MHz, DMSO-d_6) δ: 173.1 (C-9), 169.6-169.7 (3×COOH), 162.7 (C-3), 162.5 (C-6), 159.8 (C-1), 158.9 (C-4a), 155.9 (C-10a), 127.6 (C-8), 116.4 (C-7), 113.3 (C-8a), 106.7 (C-9a), 100.8 (C-5), 97.5 (C-2), 94.5 (C-4), 65.0-65.6 ppm (3×OCH_2).

*2,2',2''-[(9-Oxo-9H-xanthene-1,3,8-triyl)tris(oxy)]triacetic acid (**22**)*

Yield (95%, white solid).m.p.: 219-221 °C (MeOH); IR ν_{max} (cm^{-1}) (KBr): 2863, 1732, 1605, 1458, 1434, 1380, 1236, 854, 755; ^1H NMR (300.13 MHz, DMSO-d_6) δ: 7.07 (dd, *J* = 8.4, 0.7 Hz, 1H, H-7), 7.61 (t, *J* = 8.4 Hz, 1 H, H-6), 6.81 (d, *J* = 8.4, 0.7 Hz, 1H, H-5), 6.58 (d, *J* = 2.3 Hz, 1H, H-4), 6.40 (d, *J* = 2.3 Hz, 1H, H-2), 4.79 and 4.80 ppm (2×s, 6H, 3×OCH_2); ^{13}C NMR (75.47 MHz, DMSO-d_6) δ: 173.4 (C-9), 169.6-169.7 (3×COOH), 162.5 (C-3), 159.4 (C-1), 158.1 (C-8), 157.7 (C-4a), 156.2 (C-10a), 137.2 (C-6), 110.6 (C-7), 107.1 (C-5), 106.9 (C-8a), 101.0 (C-9a), 97.4 (C-2), 93.7 (C-4), 65.5-65.9 ppm (3×OCH_2).

*2,2',2'',2'''-[(9-Oxo-9H-xanthene-1,3,6,8-tetrayl)tetrakis(oxy)]tetraacetic acid (**23**)*

Yield (88%, white solid). m.p.: > 310 °C (MeOH); IR ν_{max} (cm^{-1}) (KBr): 2860, 1714, 1624, 1466, 1428, 1372, 1230, 857, 763; ^1H NMR (300.13 MHz, DMSO-d_6) δ: 6.50 (d, *J* = 2.1 Hz, 2H, H-4 and H-5), 6.36 (d, *J* = 2.1 Hz, 2H, H-2 and H-7), 4.73 and 4.74 ppm (2×s, 8H, 4×OCH_2); ^{13}C NMR (75.47 MHz, DMSO-d_6) δ: 172.8 (C-9), 169.6 and 169.8 (4×C=O, COOH), 162.3 (C-3

and C-6), 159.4 (C-1 and C-8), 157.6 (C-4a and C-10a), 104.5 (C-8a and C-9a), 97.5 (C-2 and C-7), 93.4 (C-4 and C-5), 65.3 and 66.1 ppm (4×OCH_2).

*2,2'-[(9-Oxo-9H-xanthene-3,6-diyl)bis(oxy)]diacetic acid (**24**)*

Yield (88%, yellow solid). m.p.: 226-228 °C (MeOH); IR ν_{max} (cm^{-1}) (KBr): 2850, 1733, 1610, 1462, 1437, 1376, 1233, 851, 755; ^{1}H NMR (300.13 MHz, DMSO-d_6) δ: 8.19 (d, *J* = 8.9 Hz, 2H, H-1 and H-8), 7.03 (dd, *J* = 8.9, 2.4 Hz, 2H, H-2 and H-7), 6.97 (d, *J* = 2.4 Hz, 2H, H-4 and H-5), 4.79 ppm (s, 4H, 2×OCH_2); ^{13}C NMR (75.47 MHz, DMSO-d_6) δ: 174.3 (C-9), 169.2 (2×COOH), 163.0 (C-3 and C-6), 157.2 (C-4a and C-10a), 127.4 (C-1 and C-8), 115.4 (C-8a and C-9a), 113.0 (C-2 and C-7), 100.9 (C-4 and C-5), 64.7 ppm (2×OCH_2).

*2,2'-[(9-Oxo-9H-xanthene-3,4-diyl)bis(oxy)]diacetic acid (**25**)*

Yield (81%, white solid). m.p.: > 310 °C (MeOH); IR ν_{max} (cm^{-1}) (KBr): 2955, 1748, 1605, 1467.0, 1452, 1361, 1239, 902, 741; ^{1}H NMR (300.13 MHz, DMSO-d_6) δ: 13.09 (s, 2H, 2×COOH), 8.17 (dd, *J* = 7.6, 1.7 Hz, 1H, H-8), 7.91 (ddd, *J* = 8.1, 7.2, 1.7 Hz,1H, H-6), 7.86 (d, *J* = 8.1, 1H, H-5), 7.65 (d, *J* = 8.2 Hz, 1H, H-1), 7.48 (ddd, *J* = 7.6, 7.2, 1.7 Hz, 1H, H-7), 7.18 (d, *J* = 8.2 Hz, 1H, H-2), 4.84 and 4.97 ppm (2×s, 2H, 2×OCH_2); ^{13}C NMR (75.47 MHz, DMSO-d_6) δ: 175.2 (C-9), 169.6 and 170.1 (2×COOH), 155.5 (C-3), 155.1 (C-4), 149.6 (C-1), 135.2 (C-10a), 134.41 (C-4a), 125.9 (C-2), 124.4 (C-6), 121.1 (C-8), 120.8 (C-7), 118.2 (C-5), 116.2 (C-8a), 110.5 (C-9a), 65.2 and 68.9 ppm (2×OCH_2).

*2,2'-[(Carbonylbis(4,1-phenylene))bis(oxy)]diacetic acid (**26**)*

Yield (88%, white solid). m.p.: 234-236 °C (MeOH); IR ν_{max} (cm^{-1}) (KBr): 2850, 1725, 1603, 1459, 1420, 1360, 1236, 849; ^{1}H NMR (300.13 MHz, DMSO-d_6) δ: 13.13 (s, 2H, 2×COOH), 7.65 (d, *J* = 8.9 Hz, 4H, H-2, H-2´, H-6, H-6´), 7.04 (d, *J* = 8.9 Hz, 4H, H-3, H-3´, H-5, H-5´), 4.78 ppm (s, 4H, 2×OCH_2); ^{13}C NMR (75.47 MHz, DMSO-d_6) δ: 193.1 (C-9), 169.9 (2×COOH), 161.8 (C-4 and C-4´), 131.3 (C-2, C-2´, C-6, C-6´), 130.7 (C-1 and C-1´), 114.3 (C-3, C-3´, C-5, C-5´), 64.6 ppm (2×OCH_2).

*2,2',2'',2'''-[(Carbonylbis(benzene-4,1,3-triyl))tetrakis(oxy)]tetraacetic acid (**27**)*

Yield (80%, white solid). m.p.: 232-235 °C (MeOH); IR ν_{max} (cm^{-1}) (KBr): 1716, 1635, 1466, 1429, 1241, 1235, 857; ^{1}H NMR (300.13 MHz, DMSO-d_6) δ: 7.38 (d, *J* = 8.6 Hz, 2H, H-6 and H-6´), 6.55 (dd, *J* = 8.6, 2.2 Hz, 2H, H-5 and H-5´), 6.46 (d, *J* = 2.2 Hz, 2H, H-3 and H-3´), 4.52 and 4.71 ppm (2×s, 8H, 4×OCH_2); ^{13}C NMR (75.47 MHz, DMSO-d_6) δ: 192.0 (C-9), 170.2 (4×COOH), 161.7 (C-4 and C-4´), 158.5 (C-2 and C-2´), 132.3 (C-6 and C-6´), 124.1 (C-1 and C-1´), 106.4 (C-5 and C-5´), 100.8 (C-3 and C-3´), 65.5 and 65.9 ppm (4×OCH_2).

2.3.4. Synthesis of chiral selectors 28-39

2.3.4.1. Starting from a monocarboxylated compound

The carboxylated compound **19** (0.25 g, 0.93 mmol) was dissolved in THF (50 mL) and TEA (380 µL, 2.66 mmol) was added. Then, *O*-(benzotriazol-1-yl)-*N*,*N*,*N'*,*N'*-tetramethyluronium tetrafluoroborate (TBTU) (0.37 g, 1.11 mmol) and (*R*)-(-)-α-phenylglycinol (0.16 g 1.11 mmol) were added. The mixture was stirred at room temperature for 5 h. The solvent was evaporated under reduced pressure and the crude product was dissolved in chloroform (100 mL). This solution was washed with 1M HCl (2 × 50 mL), saturated solution of $NaHCO_3$ (2 × 50 mL) and water (3 × 50 mL). The organic layer was dried with anhydrous sodium sulphate, filtered and the solvent was evaporated under reduced pressure. The crude product was recrystallized from $CHCl_3$/MeOH to afford **28**.

*(R)-N-(2-Hydroxy-1-phenylethyl)-2-[(9-oxo-9H-xanthen-1-yl)oxy]acetamide (**28**)*

Yield (86%, white solid). m.p.: 168-170 °C ($CHCl_3$:MeOH); $[\alpha]_D^{25^\circ C}$ -219.0 (*c* = 0.32 × 10^{-3} gmL^{-1} in $CHCl_3$); IR ν_{max} (cm^{-1}) (KBr): 3433, 3299, 1660, 1619, 1547, 1464, 1435, 1260, 847; ^1H NMR (300.13 MHz, DMSO-d_6) δ: 9.17 (d, *J* = 8.9 Hz, 1H, NH), 8.10 (dd, *J* = 8.1, 1.6 Hz, 1H, H-8), 7.80 (ddd, *J* = 8.6, 7.2, 1.6 Hz, 1H, H-6), 7.70 (t, *J* = 8.4 Hz, 1H, H-3), 7.57 (dd, *J* = 8.6, 1.6 Hz, 1H, H-5), 7.43 (ddd, *J* = 8.1, 7.2, 1.6 Hz, 1H, H-7), 7.34 (d, *J* = 6.7 Hz, 2H, H-2´´ (Ar) and H-6´´ (Ar)), 7.27 (t, *J* = 6.7 Hz, 2H, H-3´´ (Ar) and H-5´´(Ar), 7.18 (d, *J* = 6.7 Hz, 1H, H-4´´ (Ar)), 7.01 (dd, *J* = 8.4, 0.9 Hz, 1H, H-4), 6.88 (dd, *J* = 8.4, 0.9 Hz, 1H, H-2), 5.03 (t, *J* = 5.7 Hz, OH), 4.85 (m, 1H, H-1´), 4.73 (s, 2H, OCH_2), 3.71 ppm (m, 2H, CH_2O); ^{13}C NMR (75.47 MHz, DMSO-d_6) δ: 175.9 (C-9), 167.1 (C=O, amide), 157.6 (C-1), 157.2 (C-10a), 154.7 (C-4a), 136.1 (C-3), 135.4 (C-6), 140.6 (C-1´´ (Ar)), 128.4 (C-3´´ (Ar) and C-5´´ (Ar)), 127.2 (C-2´´ (Ar) and C-6´´ (Ar)), 127.1 (C-4´´ (Ar)), 126.1 (C-8), 124.5 (C-7), 122.2 (C-8a), 117.7 (C-5), 111.7 (C-2), 110.8 (C-9a), 108.2 (C-4), 68.2 ppm (OCH_2), 65.0 (CH_2OH), 54.9 ppm (C-1´); e.r. > 99% (LC; Column: (*S,S*)-Whelk-O1® (25 cm × 4.6 mm I.D., 5 µm particle size), Mobile phase: MeOH/CH_3CN (50:50 v:v), 1.0 $mLmin^{-1}$, λ_{max} 254 nm). The structure of compound **28** was determined by X-Ray crystallography (please see subchapter 2.4).

2.3.4.2. Starting from polycarboxylated compounds

Compounds **29**-**39** were prepared from suitable carboxylated compounds (**20**-**27**) using the same method as described for **19**, increasing the amount of TEA, TBTU and appropriate chiral reagent according to the number of carboxylic groups of the chemical substrates (**20**-**27**) and the stoichiometry of the reaction.

*2,2'-{[9-Oxo-9H-xanthene-1,3-diyl)bis(oxy)]bis[N-((R)-2-hydroxy-1 phenylethyl]acetamide]} (**29**)*

Yield (85%, white solid). m.p.: 154-156 °C ($CHCl_3$:MeOH); $[\alpha]_D^{25^\circ C}$ -300.0 (*c* = 0.1 × 10^{-3} gmL^{-1} in $CHCl_3$); IR ν_{max} (cm^{-1}) (KBr): 3446, 3297, 1668, 1610, 1549, 1463, 1428, 1250, 848; ^{1}H NMR (300.13 MHz, DMSO-d_6) δ: 8.55 and 9.22 (2×d, *J* = 8.3-8.9 Hz, 2H, 2×NH), 8.18 (dd, *J* = 7.5, 1.7 Hz, 1H, H-8), 7.82 (td, *J* = 8.7, 7.5, 1.7 Hz, 1H, H-6), 7.53 (d, *J* = 8.7 Hz, 1H, H-5), 7.48 (t, *J* = 7.5 Hz, 1H, H-7), 7.21 (m, 10H, 2×H-Ar), 6.76 (d, *J* = 2.2 Hz, 1H, H-4), 6.67 (d, *J* = 2.2 Hz, 1H, H-2), 5.01 (t, *J* = 5.7 Hz, 2×OH), 4.92 (m, 2H, 2×H-1´), 4.68 and 4.80 (2×s, 4H, 2×OCH_2,), 3.63 and 3.72 ppm (2×m, 4H, 2×CH_2O); ^{13}C NMR (75.47 MHz, DMSO-d_6) δ: 174.7 (C-9), 166.5 and 166.8 (2×C=O, amide), 163.7 (C-1), 158.9 (C-3), 158.7 (C-4a), 154.6 (C-10a), 140.8 (2×C-1´´ (Ar)), 134.9 (C-6), 128.1 (2×C-3´´ (Ar) and C-5´´ (Ar)), 127.4 (C-8), 127.1 (2×C-2´´ (Ar) and C-6´´ (Ar)), 126.9 (2×C-4´´ (Ar)), 126.0 (C-8), 124.5 (C-7), 122.1 (C-8a), 117.5 (C-5), 106.5 (C-9a), 102.3 (C-2), 95.2 (C-4), 67.3 and 68.5 (2×OCH_2), 65.0 (2×CH_2OH), 55.0 ppm (2×C-1´); e.r. > 99% (LC; Column: (*S,S*)-Whelk-O1® (25 cm × 4.6 mm I.D., 5 µm particle size), Mobile phase: MeOH/CH_3CN (50:50 v:v), 1.0 $mLmin^{-1}$, λ_{max} 254 nm).

*2,2',2''-{[9-Oxo-9H-xanthene-1,3,6-triyl)tris(oxy)]tris[N-(R)-2-hydroxy-1-phenylethyl]acetamide} (**30**)*

Yield (88%, white solid). m.p.: 163-165 °C ($CHCl_3$:MeOH); $[\alpha]_D^{25^\circ C}$ -285.0 (*c* = 0.21 × 10^{-3} gmL^{-1} in $CHCl_3$); IR ν_{max} (cm^{-1}); 3360, 3328, 1669, 1610, 1540, 1460, 1430, 1261, 839; ^{1}H NMR (300.13 MHz, DMSO-d_6) δ: 8.56 and 9.22 (2×d, *J* = 8.6-8.9 Hz, 3H, 3×NH), 8.10 (d, *J* = 8.7 Hz, 1H, H-8), 7.27 (m, 15H, 3×H-Ar), 7.10 (dd, *J* = 8.7, 2.3 Hz, 1H, H-7), 7.02 (d, *J* = 2.3 Hz, 1H, H-5), 6.71 (d, *J* = 2.2 Hz, 1H, H-4), 6.65 (d, *J* = 2.2 Hz, 1H, H-2), 5.00 (t, *J* = 5.8 Hz, 3×OH), 4.90 (m, 3H, 3×H-1´), 4.66 and 4.78 (2×s, 6H, 3×OCH_2), 3.66 ppm (m, 6H, 3×CH_2O); ^{13}C NMR (75.47 MHz, DMSO-d_6) δ: 174.1 (C-9), 166.7-166.9 (3×C=O, amide), 163.3 (C-3), 162.9 (C-6), 158.7 (C-1), 157.4 (C-4a), 156.3 (C-10a), 140.6-140.7 (3×C-1´´ (Ar)), 128.3-128.8 (3×(C-3´´ (Ar) and C-5´´ (Ar))), 128.1 (C-8), 127.1-127.3 (3×C-2´´ (Ar) and C-6´´ (Ar)), 126.8-126.9 (3×C-4´´ (Ar)), 114.0 (C-7), 109.4 (C-8a), 106.4 (C-9a), 102.5 (C-5), 101.6 (C-2), 95.2 (C-4), 67.3-68.3 (3×OCH_2), 64.5-65.2 (3×CH_2OH), 54.8-54.9 ppm (3×C-1´); e.r. > 99% (LC; Column: (*S,S*)-Whelk-O1® (25 cm × 4.6 mm I.D., 5 µm particle size), Mobile phase: MeOH/CH_3CN (50:50 v:v), 1.0 $mLmin^{-1}$, λ_{max} 254 nm).

*2,2',2''-{[9-Oxo-9H-xanthene-1,3,8-triyl)tris(oxy)]tris[N-(R)-2-hydroxy-1-phenylethyl]acetamide} (**31**)*

Yield (90%, white solid). m.p.: 133-136 °C ($CHCl_3$:MeOH); $[\alpha]_D^{25^\circ C}$ -300.0 (*c* = 0.1 × 10^{-3} gmL^{-1} in $CHCl_3$); IR ν_{max} (cm^{-1}) (KBr): 3440, 3318, 1656, 1627, 1557, 1457, 1432, 1262, 851; ^{1}H NMR (300.13 MHz, DMSO-d_6) δ: 8.55 and 8.97 (2×d, *J* = 8.8-9.6 Hz, 3H, 3×NH), 7.35 (dd, *J* = 8.4,

0.7 Hz, 1H, H-7), 7.66 (t, *J* = 8.4 Hz, 1 H, H-6), 7.21 (m, 15H, 3×H-Ar), 6.93 (dd, *J* = 8.4, 0.7 Hz, 1H, H-5), 6.67 (d, *J* = 2.1 Hz, 1H, H-4), 6.60 (d, *J* = 2.1 Hz, 1H, H-2), 5.00 (t, *J* = 5.7 Hz, 3×OH), 4.93 (m, 3H, 3×H-1´), 4.69 and 4.72 (2×s, 6H, 3×OCH_2), 3.61 ppm (m, 6H, 3×CH_2O); ^{13}C NMR (75.47 MHz, DMSO-d_6) δ: 174.7 (C-9), 166.5-167.2 (3×C=O, amide), 163.1 (C-3), 161.5 (C-1), 159.3 (C-8), 158.1 (C-4a), 156.2 (C-10a), 140.6-140.7 (3×C-1´´(Ar)), 134.9 (C-6), 128.1 (3×C-3´´ (Ar) and C-5´´ (Ar)), 127.0 (3×C-2´´ (Ar) and C-6´´ (Ar)), 126.9 (3×C-4´´ (Ar)), 110.6 (C-7), 109.3 (C-5), 107.8 (C-8a), 104.7 (C-9a), 98.2 (C-2), 94.6 (C-4), 65.5-65.9 ppm (3×OCH_2), 68.3-68.5 (3×OCH_2), 64.4-65.0 (3×CH_2OH), 54.9 ppm (3×C-1´); e.r. > 99% (LC; Column: (*S,S*)-Whelk-O1® (25 cm × 4.6 mm I.D., 5 µm particle size), Mobile phase: MeOH/CH_3CN (50:50 v:v), 1.0 mLmin^{-1}, λ_{max} 254 nm).

*2,2',2'',2'''-{[(9-Oxo-9H-xanthene-1,3,6,8-tetrayl)tetrakis(oxy)]tetrakis[N-(R)-2-hydroxy-1-phenylethyl]acetamide} (**32**)*

Yield (78 %, white solid). m.p.: > 350 °C ($CHCl_3$:MeOH); $[\alpha]_D^{25^\circ C}$ -308.0 (*c* = 0.13 × 10^{-3} gmL^{-1} in $CHCl_3$); IR ν_{max} (cm^{-1}) (KBr): 3441, 3296, 1667, 1618, 1550, 1462, 1430, 1263, 849; ^1H NMR (300.13 MHz, DMSO-d_6) δ: 8.52 and 8.99 (2×d, *J* = 8.5-8.4 Hz, 4H, 4×NH), 7.25 (m, 20H, 4×H-Ar), 6.63 (d, *J* = 2.2 Hz, 2H, H-4 and H-5), 6.57 (d, *J* = 2.2 Hz, 2H, H-2 and H-7), 4.99 (t, *J* = 5.7 Hz, 4×OH), 4.92 (m, 4H, 4×H-1´), 4.71 and 4.72 (2×s, 8H, 4×OCH_2), 3.61 ppm (m, 8H, 4×CH_2O); ^{13}C NMR (75.47 MHz, DMSO-d_6) δ: 182.1 (C-9), 167.0-167.2 (4×C=O), 162.3 (C-3 and C-6), 159.4 (C-1 and C-8), 157.6 (C-4a and C-10a), 139.1-140.7 (4×C-1´´ (Ar)), 128.0-128.1 (4×C-3´´(Ar) and C-5´´(Ar)), 127.1 (4×C-2´´ (Ar) and C-6´´ (Ar)), 126.4-126.9 (4×C-4´´ (Ar)), 104.5 (C-8a and C-9a), 97.5 (C-2 and C-7), 94.5 (C-4 and C-5), 67.1-67.2 (4×OCH_2), 64.4-64.8 (4×CH_2OH), 55.0 ppm (4×C-1´); e.r. > 99% (LC; Column: (*S,S*)-Whelk-O1® (25 cm × 4.6 mm I.D., 5 µm particle size), Mobile phase: MeOH/CH_3CN (50:50 v:v), 1.0 mLmin^{-1}, λ_{max} 254 nm).

*2,2'-{[(9-Oxo-9H-xanthene-3,6-diyl)bis(oxy)]bis[N-(S)-2-hydroxy-1-phenylethyl]acetamide} (**33**)*

Yield (80 %, white solid). m.p.: 178-180 °C ($CHCl_3$:MeOH); $[\alpha]_D^{25^\circ C}$ +455.0 (*c* = 0.088 × 10^{-3} gmL^{-1} in $CHCl_3$); IR ν_{max} (cm^{-1}) (KBr): 3445, 3288, 1651, 1623, 1548, 1433, 1260, 837; ^1H NMR (300.13 MHz, DMSO-d_6) δ: 8.24 (d, *J* = 8.0 Hz, 2H, 2×NH), 8.17 (d, *J* = 8.9 Hz, 2H, H-1 and H-8), 7.28 (m, 10H, 2×(H-Ar), 7.08 (dd, *J* = 8.9, 2.3 Hz, 2H, H-2 and H-7), 7.00 (d, *J* = 2.3 Hz, 2H, H-4 and H-5), 5.06 (t, *J* = 5.7 Hz, 2×OH), 4.85 (m, 2H, 2×H-1´), 4.71 and 4.72 (2×s, 4H, 2×OCH_2), 3.75 ppm (m, 4H, 2×CH_2O); ^{13}C NMR (75.47 MHz, DMSO-d_6) δ: 174.3 (C-9), 166.7 (2×C=O, amide), 163.0 (C-3 and C-6), 157.3 (C-4a and C-10a), 140.8 (2×C-1´´ (Ar)), 128.1 (2×C-3´´ (Ar) and C-5´´ (Ar)), 127.4 (C-1 and C-8), 126.9 (2×C-2´´ (Ar) and C-6´´ (Ar)), 126.4 (2×C-4´´ (Ar)), 115.3 (C-8a and C-9a), 113.0 (C-2 and C-7), 101.6 (C-4 and C-5), 67.3

(2×OCH_2), 65.0 (2×CH_2OH), 55.0 ppm (2×C-1´); e.r. > 99% (LC; Column: (*S,S*)-Whelk-O1® (25 cm × 4.6 mm I.D., 5 µm particle size), Mobile phase: MeOH/CH_3CN (50:50 v:v), 1.0 $mLmin^{-1}$, λ_{max} 254 nm).

*2,2'-{[(9-Oxo-9H-xanthene-3,6-diyl)bis(oxy)]bis[N-(S)-1-hydroxy-4-methylpentan-2-yl]acetamide} (**34**)*

Yield (80%, white solid). m.p.: 228-230 °C ($CHCl_3$:MeOH); $[\alpha]_D^{25^\circ C}$ +400.0 (*c* = 0.12 × 10^{-3} gmL^{-1} in CH_3CN); IR v_{max} (cm^{-1}) (KBr): 3423, 3288, 1653, 1615, 1547, 1446, 1437, 1260, 761; ^1H NMR (300.13 MHz, DMSO-d_6) δ: 8.28 (d, *J* = 8.2 Hz, 2H, 2×NH), 8.17 (d, *J* = 8.9 Hz, 2H, H-1 and H-8), 7.05 (dd, *J* = 8.9, 2.4 Hz, 2H, H-2 and H-7), 7.00 (d, *J* = 2.3 Hz, 2H, H-4 and H-5), 4.63 and 4.64 (2×s, 4H, 2×OCH_2), 4.26 (t, *J* = 5.6 Hz, 3H, 3×OH), 4.14 (m, 2H, 2×H-1´), 3.61 (m, 4H, 2×CH_2O), 1.58 (m, 2H, 2×H-3´), 1.45 (m, 4H, 2×H-2´), 0.91 ppm (t, *J* = 6.0 Hz, 12H, H-4´); ^{13}C NMR (75.47 MHz, DMSO-d_6) δ: 174.3 (C-9), 166.4 (2×C=O, amide), 162.0 (C-3 and C-6), 157.2 (C-4a and C-10a), 128.0 (C-1 and C-8), 115.8 (C-8a and C-9a), 113.0 (C-2 and C-7), 101.5 (C-4 and C-5), 67.1 (2×OCH_2), 64.0 (2×CH_2OH), 50.0 (2×C-1´), 40.3 (2×C-2´), 24.2 (2×C-3´), 22.5 ppm (2×C-4´); e.r. > 99% (LC; Column: Lux® celullose-2 (15 cm × 4.6 mm I.D., 3 µm particle size), Mobile phase: 100 % EtOH, 0.5 $mLmin^{-1}$, λ_{max} 254 nm).

*2,2'-{[(9-Oxo-9H-xanthene-3,6-diyl)bis(oxy)]bis[N-(S)-1-hydroxy-3-methylbutan-2-yl]acetamide} (**35**)*

Yield (80%, white solid). m.p.: 236-238 °C ($CHCl_3$:MeOH); $[\alpha]_D^{25^\circ C}$ +417.0 (*c* = 0.12 × 10^{-3} gmL^{-1} in CH_3CN); IR v_{max} (cm^{-1}) (KBr): 3454, 2959, 2926, 1659, 1616, 1558, 1447; ^1H NMR (300.13 MHz, DMSO-d_6) δ: 8.23 (d, *J* = 8.9 Hz, 2H, 2×NH), 7.13 (d, *J* = 9.2 Hz, 2H, H-1 and H-8), 7.05 (dd, *J* = 8.9, 2.3 Hz, 2H, H-2 and H-7), 6.98 (d, *J* = 2.4 Hz, 2H, H-4 and H-5), 4.67 (s, 4H, 2×OCH_2), 4.27 (t, *J* = 5.3 Hz, 2H, 2×OH), 3.81 (m, 2H, 2×H-1´), 3.66 (m, 4H, 2×CH_2O), 1.95 (m, 2H, 2×H-2´), 0.96 ppm (t, *J* = 6.8 Hz, 6H, H-3a´), 0.91 ppm (t, *J* = 6.8 Hz, 6H, H-3b´); ^{13}C NMR (75.47 MHz, DMSO-d_6) δ: 175.0 (C-9), 166.5 (2×C=O, amide), 163.0 (C-3 and C-6), 157.2 (C-4a and C-10a), 127.0 (C-1 and C-8), 115.8 (C-8a and C-9a), 113.0 (C-2 and C-7), 101.3 (C-4 and C-5), 67.1 (2×OCH_2), 63.0 (2×CH_2OH), 55.8 (2×C-1´), 29.0 (2×C-2´), 19.0 (2×C-3´a), 18.5 ppm (2×C-3´b); e.r. > 99% (LC; Column: Lux® celullose-2 (15 cm × 4.6 mm I.D., 3 µm particle size), Mobile phase: 100 % EtOH, 0.5 $mLmin^{-1}$, λ_{max} 254 nm).

*2,2'-{[(9-Oxo-9H-xanthene-3,6-diyl)bis(oxy)]bis[N-(R)-2-hydroxy-1-phenylethyl]acetamide} (**36**)*

Yield (85%, white solid). m.p.: 177-179 °C ($CHCl_3$:MeOH); $[\alpha]_D^{25^\circ C}$ -455.0 (*c* = 0.088 × 10^{-3} gmL^{-1} in $CHCl_3$); IR v_{max} (cm^{-1}) (KBr): 3445, 3288, 1651, 1623, 1548, 1433, 1260, 837; ^1H NMR (300.13 MHz, DMSO-d_6) δ: 8.24 (d, *J* = 8.0 Hz, 2H, 2×NH), 8.17 (d, *J* = 8.9 Hz, 2H, H-1 and

H-8), 7.28 (m, 10H, 2×H-Ar), 7.08 (dd, *J* = 8.9, 2.3 Hz, 2H, H-2 and H-7), 7.00 (d, *J* = 2.3 Hz, 2H, H-4 and H-5), 5.06 (t, *J* = 5.7 Hz, 2H, 2×OH), 4.85 (m, 2H, 2×H-1´), 4.71 and 4.72 (2×s, 4H, 2×OCH_2), 3.75 ppm (m, 4H, 2×CH_2O); ^{13}C NMR (75.47 MHz, DMSO-d_6) δ: 174.3 (C-9), 166.7 (2×C=O, amide), 163.0 (C-3 and C-6), 157.3 (C-4a and C-10a), 140.8 (2×C-1´´ (Ar)), 128.1 (2×C-3´´ (Ar) and C-5´´ (Ar)), 127.4 (C-1 and C-8), 126.9 (2×C-2´´ (Ar) and C-6´´ (Ar)), 126.4 (2×C-4´´ (Ar)), 115.3 (C-8a and C-9a), 113.0 (C-2 and C-7), 101.6 (C-4 and C-5), 67.3 (2×OCH_2), 65.0 (2×CH_2OH), 55.0 ppm (2×C-1´); e.r. > 99% (LC; Column: (*S,S*)-Whelk-O1® (25 cm × 4.6 mm I.D., 5 µm particle size), Mobile phase: MeOH/CH_3CN (50:50 v:v), 1.0 mLmin^{-1}, λ_{max} 254 nm).

*2,2'-{[(9-Oxo-9H-xanthene-3,4-diyl)bis(oxy)]bis[N-(R)-2-hydroxy-1-phenylethyl]acetamide} (**37**)*

Yield (57%, white solid)**.** m.p.: 202-204 °C ($CHCl_3$:MeOH); $[\alpha]_D^{25^\circ C}$ -300.0 (*c* = 0.1 × 10^{-3} gmL^{-1} in $CHCl_3$); IR v_{max} (cm^{-1}) (KBr): 3388, 3272, 1668, 1616, 1529, 1463, 1448, 1255, 849; ^1H NMR (300.13 MHz, DMSO-d_6) δ: 8.51 and 8.65 (2×d, *J* = 8.3 Hz, 2H, 2×NH), 8.18 (dd, *J* = 8.1, 1.7 Hz, 1H, H-8), 7.84 (ddd, *J* = 8.7, 7.1, 1.7 Hz,1H, H-6), 7.90 (d, *J* = 8.7, 1H, H-5), 7.63 (d, *J* = 8.5 Hz, 1H, H-1), 7.48 (ddd, *J* = 8.1, 7.1, 1.7 Hz, 1H, H-7), 7.25 (m, 10H, 2×H-Ar), 7.15 (d, *J* = 8.5 Hz, 1H, H-2), 5.00 and 5.07 (2×t, *J* = 5.8 Hz, 2H, 2×OH), 4.95 and 4.98 (2×m, 2H, 2×H-1´), 4.81 and 4.83 (2×s, 4H, 2×OCH_2), 3.66 ppm (m, 4H, 2×CH_2O); ^{13}C NMR (75.47 MHz, DMSO-d_6) δ: 175.2 (C-9), 166.6 and 167.8 (2×C=O, amide), 155.5 (C-3), 155.4 (C-4), 140.7 and 140.8 (2×C-1´´ (Ar)), 135.25 (C-10a), 134.94 (C-4a), 128.1 (2×C-3´´(Ar) and C-5´´(Ar)), 126.9 (2×C-2´´(Ar) and C-6´´ (Ar)), 126.4 (2×C-4´´(Ar)), 125.9 (C-2), 124.5 (C-6), 121.6 (C-8), 120.8 (C-7), 118.3 (C-5), 116.3 (C-8a), 110.5 (C-9a), 67.4 (2×OCH_2), 64.3 and 64.4 (2×CH_2OH), 54.6 and 55.0 ppm (2×C1´); e.r. >99 % (LC; Column: (*S,S*)-Whelk-O1® (25 cm × 4.6 mm I.D., 5 µm particle size), Mobile phase: MeOH/CH_3CN (50:50 v:v), 1.0 mLmin^{-1}, λ_{max} 254 nm).

*2,2'-{[(Carbonylbis(4,1-phenylene)bis(oxy)]bis[N-(R)-2-hydroxy-1-phenylethyl]acetamide} (**38**)*

Yield (86%, white solid). m.p.: 173-175 °C ($CHCl_3$:MeOH); $[\alpha]_D^{25^\circ C}$ -238.0 (*c* = 0.21 × 10^{-3} gmL^{-1} in $CHCl_3$); IR v_{max} (cm^{-1}) (KBr)**:** 3413, 3273, 1604, 1540, 1456, 1449, 1254, 845; ^1H NMR (300.13 MHz, DMSO-d_6) δ: 8.46 (d, *J* = 8.3 Hz, 2H, 2×NH), 7.65 (d, *J* = 8.9 Hz, 4H, H-2, H-2´, H-6, H-6´), 7.21 (m, 10H, 2×H-Ar), 7.04 (d, *J* = 8.9 Hz, 4H, H-3, H-3´, H-5, H-5´), 4.90 (t, *J* = 5.7 Hz, 2H, 2×OH), 4.85 (m, 2H, 2×H-1´´), 4.64 and 4.65 (2×s, 4H, 2×OCH_2), 3.60 ppm (m, 4H, 2×CH_2O); ^{13}C NMR (75.47 MHz, DMSO-d_6) δ: 193.1 (C-9), 166.9 (2×C=O, amide), 161.8 (C-4 and C-4´), 140.8 (2×C-1´´´ (Ar)), 131.7 (C-2, C-2´, C-6, C-6´), 130.4 (C-1 and C-1´), 128.1 (2×C-3´´´ (Ar) and C-5´´´ (Ar)), 126.9 (2×C-2´´´ (Ar) and C-6´´´ (Ar)), 126.8 (2×C-4´´´ (Ar)), 114.3 (C-3, C-3´, C-5, C-5´), 66.5 (2×OCH_2), 64.9 (2×CH_2OH), 54.8 ppm (2×C-1´´); e.r. > 99%

(LC; Column: (*S,S*)-Whelk-O1® (25 cm × 4.6 mm I.D., 5 µm particle size), Mobile phase: MeOH/CH_3CN (50:50 v:v), 1.0 mLmin^{-1}, λ_{max} 254 nm).

*2,2',2'',2'''-{[(Carbonylbis(benzene-4,1,3-triyl)tetrakis(oxy)]tetrakis[N-(R)-2-hydroxy-1-phenylethyl]acetamide} (**39**)*

Yield (79 %, white solid). m.p.: > 350 °C ($CHCl_3$:MeOH); $[\alpha]_D^{25^\circ C}$ -333.0 (*c* = 0.12 × 10^{-3} gmL^{-1} in $CHCl_3$); IR v_{max} (cm^{-1}) (KBr): 3441, 3291, 1635, 1540, 1464, 1429, 1260; ^{1}H NMR (300.13 MHz, DMSO-d_6) δ: 8.29 and 8.62 (2×d, *J* = 8.2 Hz, 4H, 4×NH), 7.54 (d, *J* = 8.6 Hz, 2H, H-6 and H-6´), 7.42 (m, 20H, 4×H-Ar), 6.84 (dd, *J* = 8.6, 2.2 Hz, 2H, H-5 and H-5´), 6.80 (d, *J* = 2.2 Hz, 2H, H-3 and H-3´), 5.16 (t, *J* = 5.7 Hz, 4H, 4×OH), 5.01 (m, 4H, 4×H-1´´), 4.69 and 4.76 (2×s, 8H, 4×OCH_2), 3.68 ppm (m, 8H, 4×CH_2O); ^{13}C NMR δ: (75.47 MHz, DMSO-d_6): 199.2 (C-9), 167.0-167.2 (4×C=O, amide), 162.0 (C-4 and C-4´), 157.9 (C-2 and C-2´), 140.7 (4×C-1´´´ (Ar)), 133.0 (C-6 and C-6´), 128.3 (4×C-3´´´ (Ar) and C-5´´´ (Ar)), 127.1 (4×C-2´´´ (Ar) and C-6´´´ (Ar)), 126.8 (4×C-4´´´ (Ar)), 124.1 (C-1 and C-1´), 109.1 (C-5 and C-5´), 101.6 (C-3 and C-3´), 67.2 (4×OCH_2), 65.0 (4×CH_2OH), 55.0 ppm (4×C-1´´); e.r. > 99% (LC; Column: (*S,S*)-Whelk-O1® (25 cm × 4.6 mm I.D., 5 µm particle size), Mobile phase: MeOH/CH_3CN (50:50 v:v), 1.0 mLmin^{-1}, λ_{max} 254 nm).

2.3.5. Synthesis and covalent linkage of silylated selectors onto the silica gel

2.3.5.1. Starting from a selector with one chiral unit

The chiral compound **28** (0.51 mmol) was dissolved in anhydrous toluene (20 mL), and TEA (108 µL,1.51 mmol) and 3-(triethoxysilyl)propylisocyanate (200 µL, 1.51 mmol) were added. The mixture was refluxed for 72 h. The solvent was evaporated under reduced pressure and the crude product was dissolved in anhydrous toluene (30 mL). Silica gel Nucleosil® (800 mg, 100 A˚-5µm, Macherey-Nagel) previously dried, in a desiccator under vacuum with phosphorus pentoxide for 24 h, was suspended in the same solvent (30 mL). Following, the crude product solution was added. The reaction mixture was gently stirred at reflux for 72 h. The modified silica was filtered and washed successively with toluene, methanol, acetone, ethyl acetate, dichloromethane and *n*-hexane (100 mL). The bonded phase was dried in a desiccator under vacuum for 24 h, affording the CSP.

2.3.5.2. Starting from a selector with more than one chiral unit

The silylation reaction of selectors with more than one chiral unit (**29**-**39**) was performed using the same conditions as described for selector **28**, increasing the amount of TEA and 3-(triethoxysilyl)propylisocyanate, according to the number of chiral units of the selector (**29**-**39**) and the stoichiometry of the reaction. In some cases, anhydrous CH_3CN (**34**-**36**, **39**) or

anhydrous CH_3CN with few drops of DMSO (**29**, **33**) or anhydrous toluene with few drops of THF and DMSO (**30**) were used due to the low solubility of selectors. The covalent linkage of silylated selectors onto the silica gel and the determination of chiral selector loadings were performed using the same method as described for **28**.

2.3.6. LC column packing

Each packing material (*ca.*1.0 g) was sieved, slurried in Hex: 2-PrOH (50:50 v/v) (50 mL) and sonicated for 3 min. Then, the suspension was poured into the chamber of a column packer and packed into a stainless-steel column (150 × 2.1 mm I.D.) using Hex: 2-PrOH (90:10 v/v) as a packing solvent, under a pressure no more than 6000 psi.

2.4. X-RAY CRYSTALLOGRAPHY

A single crystal of (*R*)-*N*-(2-hydroxy-1-phenylethyl)-2-[(9-oxo-9*H*-xanthen-1-yl)oxy]acetamide (**28**) was mounted on a cryoloop using paratone. X-ray diffraction data were collected at 290 K with a Gemini PX Ultra equipped with CuK_α radiation (λ = 1.54184 Å). The structure was solved by direct methods using SHELXS-97 and refined with SHELXL-97.[44] Crystal was orthorhombic, space group $P2_12_12_1$, cell volume 3820.8(3) $Å^3$ and unit cell dimensions *a* = 8.3606(3) Å, *b* = 8.9346(3) Å and *c* = 51.149(3) Å (uncertainties in parentheses). There were two molecules in the asymmetric unit, one of them with an oxygen atom with alternate conformation. Non-hydrogen atoms were refined anisotropically. Hydrogen atoms were either placed at their idealized positions using appropriate HFIX instructions in SHELXL and included in subsequent refinement cycles or were directly found from difference Fourier maps and were refined freely with isotropic displacement parameters. The flack *x* parameter was refined with SHELXL-97 by means of TWIN and BASF to yield 0.097(3). The refinement converged to R (all data) = 8.44% and wR2 (all data) = 12.14%.

Full details of the data collection and refinement and tables of atomic coordinates, bond lengths and angles, and torsion angles have been deposited with the Cambridge Crystallographic Data Centre (CCDC 1908277).

2.5. CHROMATOGRAPHY

HPLC grade ethanol (EtOH), 2-propanol (2-PrOH) and *n*-hexane (Hex) were purchased from Sigma-Aldrich Co (St. Louis, Missouri, USA). Commercial chiral analytes (A1-A7, Figure S1, supplementary materials) used to evaluate the CSPs were obtained from Sigma-Aldrich (St. Louis, Missouri, USA) or Merck (Darmstadt, Germany) and “in-house” chiral analytes (A8-A38, Figure S1, supplementary materials) were synthesized previously by our group.[45,46] Working solutions of all chiral analytes were prepared using HPLC grade EtOH at a concentration of 10 μgmL^{-1}, and the injection volume was 10 µL. The HPLC system comprised a Jasco model 880-

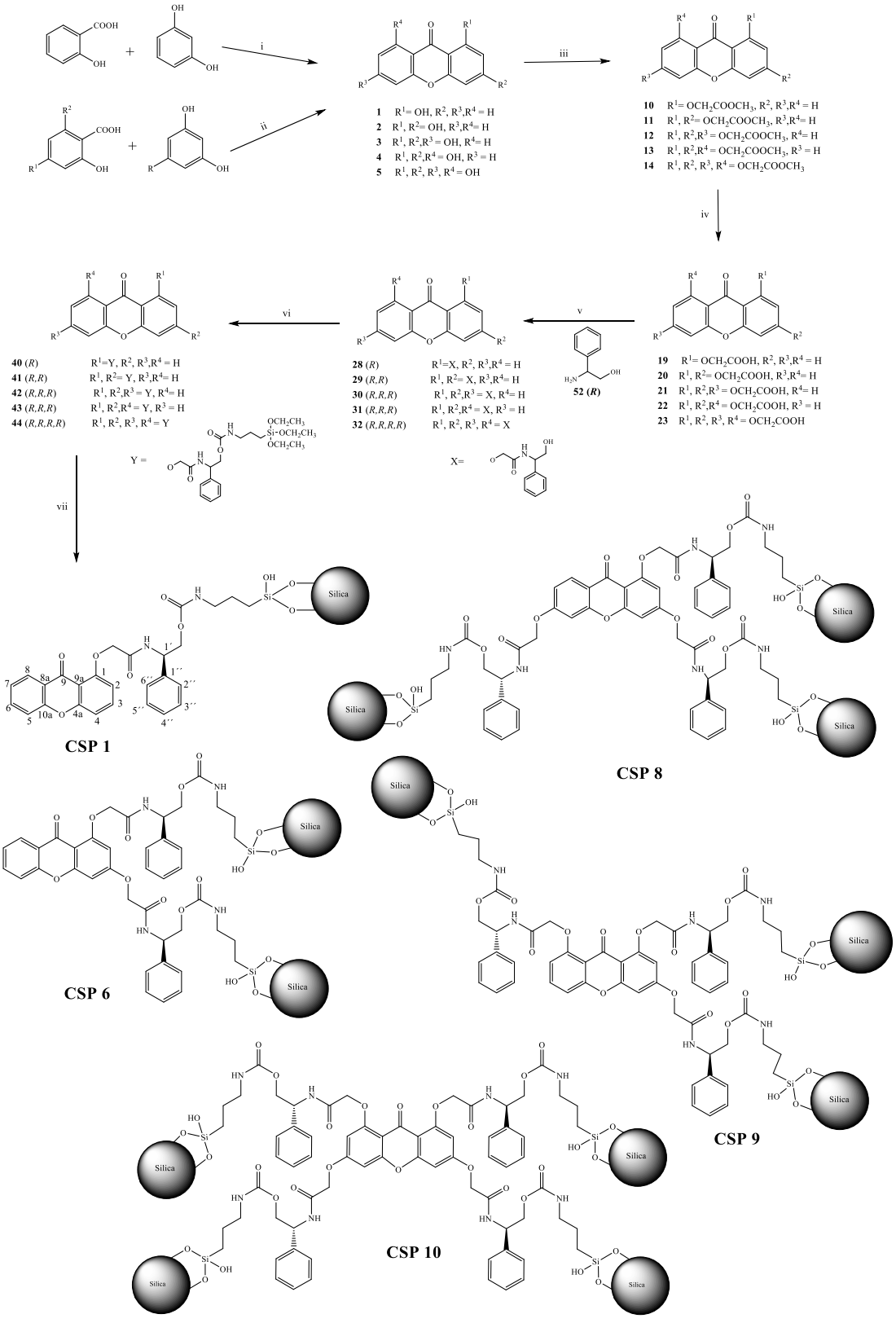
PU Intelligent HPLC pump (JASCO Corporation, Tokyo, Japan), equipped with a 7125 injector (Rheodyne LCC, Rohnert Park, CA, USA) fitted with a 20 µL loop, a JASCO model 880-30 solvent mixer involving an 875-UV intelligent UV/Vis detector. The data were handled on ChromNAC Chromatography Data System (version 1.19.1) from JASCO Corporation (Tokyo, Japan). The mobile phase consisted of mixtures of Hex and a modifier, EtOH or 2-PrOH, at a flow rate of 0.2 $mLmin^{-1}$. The mobile phases were prepared in a volume/volume ratio and degassed in an ultrasonic bath for 15 min before use. The chromatographic analyses were carried out in isocratic mode at 22 ± 2 °C, in triplicate. The UV detection was performed at a wavelength of 254 nm. The column void time was considered to be equal to the peak of the solvent front and was taken from each particular run.

2.6. COMPUTATIONAL

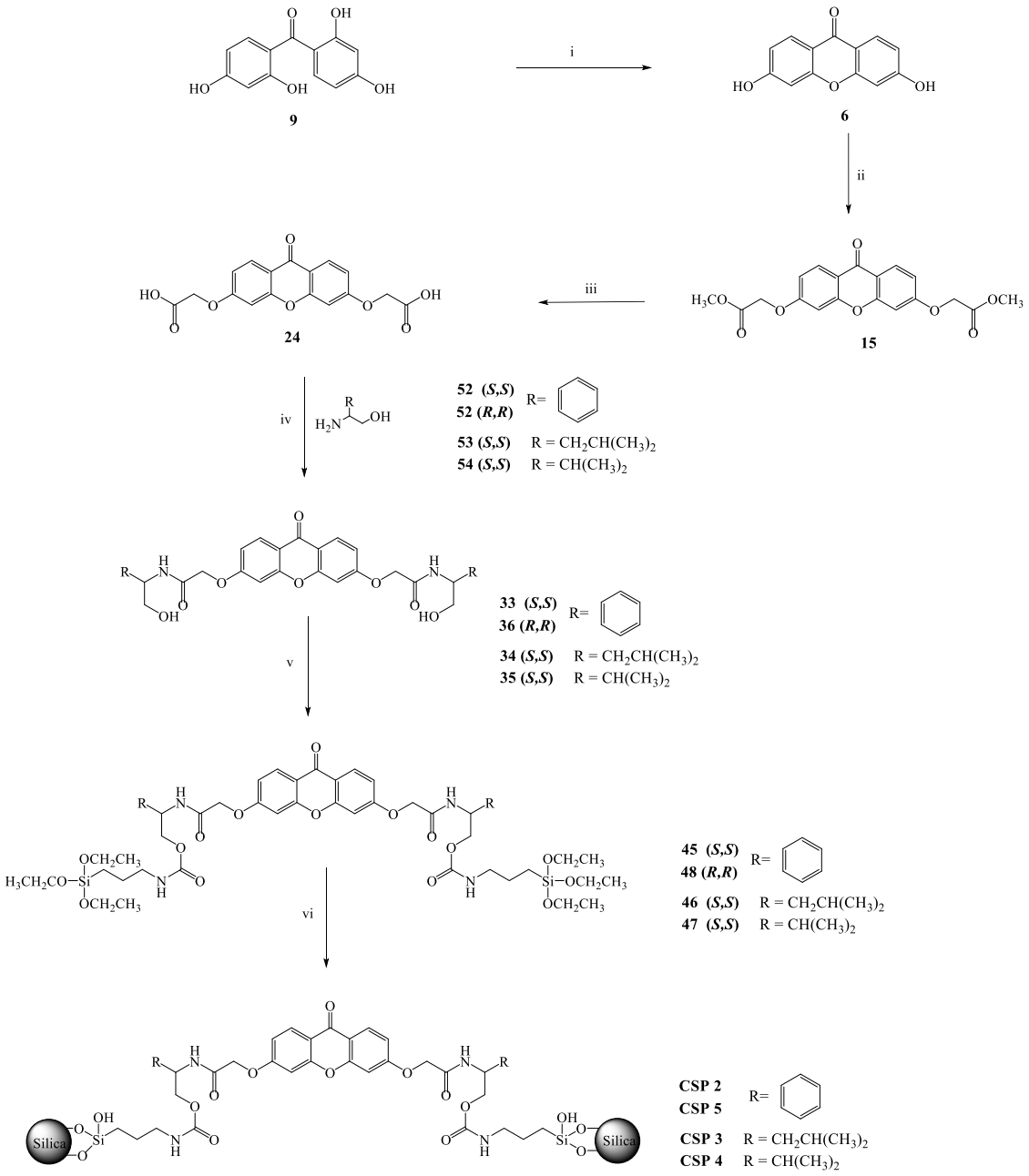
The structures of the synthesized selectors were drawn in Chemdraw and minimized in Chem3D 16.0, and both enantiomers of analytes were drawn and minimized using an Austin Model 1 (AM1) semi-empirical quantum mechanics force field.[47] The calculation was finished when the gradient between any two successive steps in the geometry search was less than 10^{-1} $kcalmol^{-1}Å^{-2}$ or the maximum steps were reached, whichever comes first. The line search used was the Broyden-Fletcher-Golfarb-Shanno search which uses an approximate Hessian matrix to guide the search.[48] Docking simulations between the synthesized chiral selectors and the analytes were undertaken in AutoDock Vina (Molecular Graphics Lab, La Jolla, CA, USA).[49] AutoDock Vina considered the target conformation as a rigid unit while the ligands were allowed to be flexible and adaptable to the target. Vina searched for the lowest binding affinity conformations and returned nine different conformations for each small molecule. The lowest binding energy docking poses of each compound were chosen. AutoDock Vina was run using an exhaustiveness of 8 and grid boxes with dimensions 16.0, 15.0, 13.0, engulfing the selectors were built. PyMol v1.3 (Schrödinger, New York, NY, USA)[50] was used to visualize the conformations and interactions as well as the graphical representations.

3. RESULTS AND DISCUSSION

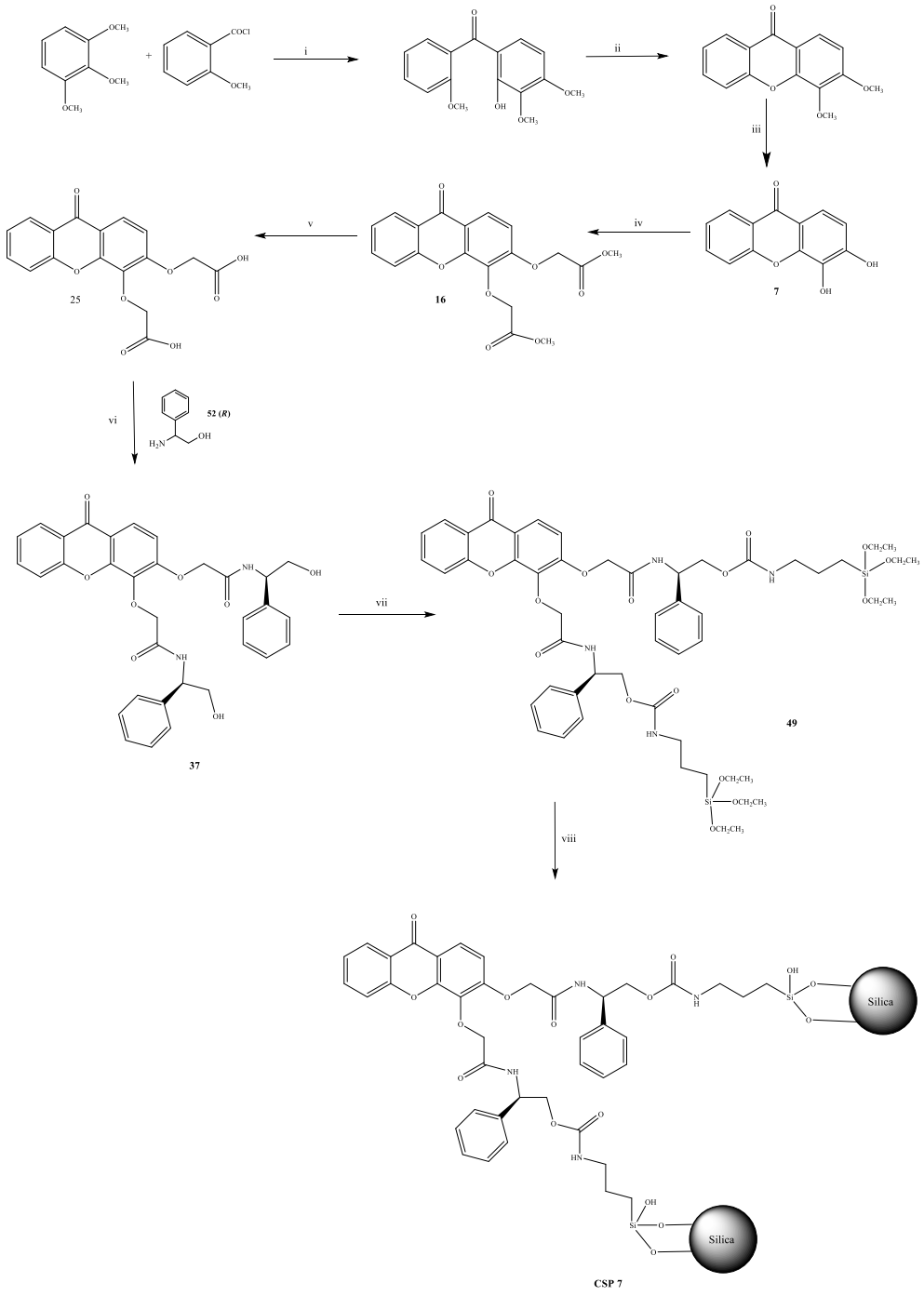
Our previous results of enantioselectivity obtained with recent CSPs based on CDXs,[18] the structural attributes of those small molecules for suitability as chiral selectors, and the high enantioselectivity observed for a series of CDXs in diverse CSPs[3,4,32-34] were crucial to pursue this approach and explore other strategies with CDXs as chiral selectors. Therefore, we report herein the preparation and evaluation of the LC enantioresolution behavior of twelve new CSPs (**CSP 1-12**). The synthetic routes for preparation of the new CSPs are shown in **Schemes 1-4**.



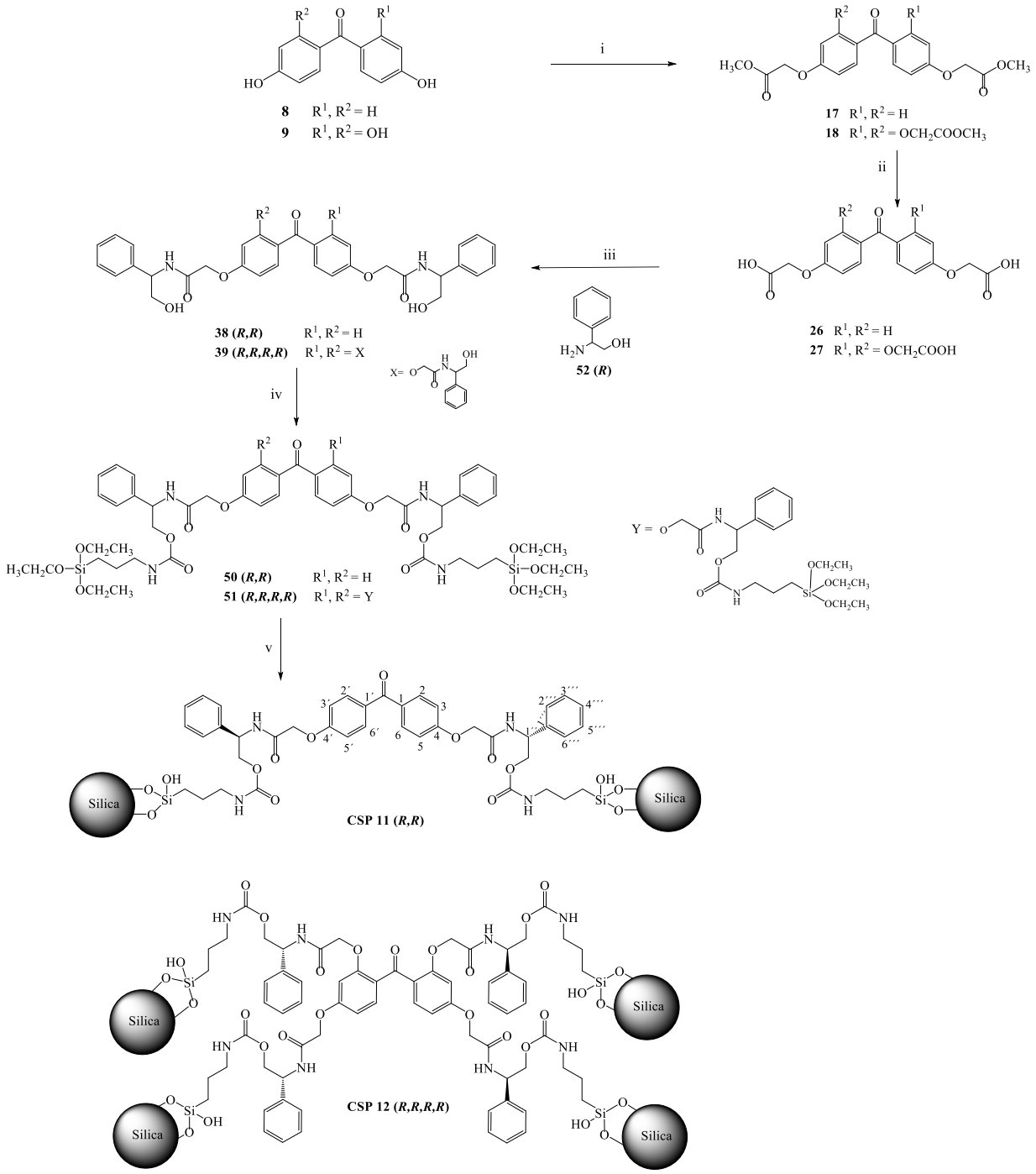
Scheme 1. Synthetic route for **CSP 1**, **CSP 6** and **CSPs 8**-**10**. Reagents and conditions: i. Anhydrous $ZnCl_2$, 160 °C, 6 h; ii. P_2O_5/CH_3SO_3H, 90 °C, 35 min; iii. Anhydrous acetone, $BrCH_2COOCH_3$, K_2CO_3, reflux, 24 h; iv. CH_2Cl_2:MeOH, 8M NaOH, r.t, 24 h; v. TBTU, TEA, THF, r.t, 8 h; vi. Anhydrous solvent, $(CH_3CH_2O)_3Si(CH_2)_3NCO$, TEA, reflux at 110 °C, 72 h; vii. Anhydrous toluene, silica gel, reflux, 72 h.



Scheme 2. Synthetic route for **CSPs 2-5**. Reagents and conditions: i. Furnace 200 °C, 8 h. ii. Anhydrous acetone, $BrCH_2COOCH_3$, K_2CO_3, reflux, 24 h; iii. CH_2Cl_2:MeOH, 8M NaOH, r.t, 24 h; iv. TBTU, TEA, THF, r.t, 8 h; v. Anhydrous solvent, $(CH_3CH_2O)_3Si(CH_2)_3NCO$, TEA, reflux, 72 h; vi. Anhydrous toluene, silica gel, reflux, 72 h.



Scheme 3. Synthetic route for **CSP 7**. Reagents and conditions: i. Anhydrous diethyl ether, $AlCl_3$, r.t, 22 h. ii. MeOH, H_2O, NaOH, reflux, 14 h. iii. Anhydrous toluene, $AlCl_3$, reflux, 40 min. iv. Anhydrous acetone, $BrCH_2COOCH_3$, K_2CO_3, reflux, 24 h; v. CH_2Cl_2:MeOH, 8M NaOH, r.t, 24 h; vi. TBTU, TEA, THF, r.t, 8 h; vii. Anhydrous toluene, $(CH_3CH_2O)_3Si(CH_2)_3NCO$, TEA, reflux, 72 h; viii. Anhydrous toluene, silica gel, reflux, 72 h.



Scheme 4. Synthetic route for **CSPs 11-12**. Reagents and conditions: i. Anhydrous acetone, $BrCH_2COOCH_3$, K_2CO_3, reflux, 24 h; ii. CH_2Cl_2:MeOH, 8M NaOH, r.t, 24 h; iii. TBTU, TEA, THF, r.t, 8 h; iv. Anhydrous solvent, $(CH_3CH_2O)_3Si(CH_2)_3NCO$, TEA, reflux, 72 h; v. Anhydrous toluene, silica gel, reflux, 72 h.

Nine different hydroxylated small molecules (**1-9**) were selected as a basis for molecular modifications. The hydroxy-9*H*-xanthen-9-ones **1-5** were obtained through the condensation of appropriate building blocks in the presence of Lewis acid $ZnCl_2$ (**1**)[41] or P_2O_5/$MeSO_3H$

(Eaton's reagent) (**2-5**)[37-39,42] (**Scheme 1**). A dehydrative cyclization of 2,2´,4,4´-tetrahydroxybenzophenone (**9**) in a furnace at 200 ^{o}C afforded the 3,6-dihydroxy-9*H*-xanthen-9-one (**6**)[40], in a very high yield (99%) (**Scheme 2**). The 3,4-dihydroxy-9*H*-xanthen-9-one (**7**) was synthetized by a classical intramolecular acylation of a benzophenone intermediate and further demethylation[41] (**Scheme 3**). The commercially available 2,2´,4,4´-tetrahydroxybenzophenone (**9**) and 4,4´-dihydroxybenzophenone (**10**) were also used as building blocks for preparation of new CSPs (**Scheme 4**). The hydroxylated small molecules (**1-9**) were further oxidized to afford acetate intermediates (**10-18**) and then carboxylated derivatives (**19-27**). The synthetic procedure to obtain the acetate intermediates (**10-18**) involved a Williamson ether synthesis using an alkyl halide containing an ester group ($BrCH_2COOCH_3$). Then, resorting to an alkaline hydrolysis of the respective esters, the carboxylated derivatives (**19-27**) were obtained. Compounds comprising a carboxylic acid, such as carboxyxanthones, have already proved to be suitable molecular scaffolds for synthesis of analogues and derivatives, including chiral compounds.[51] The chiral selectors (**28-39**) were synthetized by coupling the carboxylated derivatives (**19-27**) with commercially available enantiomerically pure amino alcohols at room temperature. The synthetic strategy was based on previous works using TBTU as a coupling reagent, in the presence of a catalytic amount of TEA in THF as solvent,[45,46] providing good yields. The structures of the chiral selectors **28-39** and all intermediates were established on the basis of IR and NMR techniques. For hydroxy-9*H*-xanthen-9-ones (**1-7**) all the data were in accordance with the literature.[38,40,52-55] The IR, ^{1}H NMR and ^{13}C NMR data of **10-39** are described for the first time (see Experimental section). The enantiomeric ratio (e.r.) of all chiral selectors was determined by LC[56] using two commercial chiral columns, (*S,S*)-Whelk-O1® and Lux® Celullose-2, and was higher than 99%. The next step was the synthesis of silylated derivatives, by reaction with 3-(triethoxysilyl)propylisocyanate,[57,58] to allow the further covalent linkage of the chiral selectors to a chromatographic support (silica gel, Nucleosil®-100-5), affording **CSPs 1-12** (**Schemes 1-4**). Therefore, after the synthesis of suitable chemical substrates, the carboxylated derivatives **19-27**, all CSPs were prepared through simple three steps: amidation, silylation and bonding to silica gel.

Elemental analyses were performed to compare the extent of covalent binding of each chiral selector to silica. The results are shown in **Table 1**. The majority of the new CSPs was covalently bonded to silica gel within appropriate levels (0.61-2.32 μmolm^{-2}) when compared to previous CSPs.[18] The silica gels in **CSP 9** and **CSP 12** contain about 0.30 μmolm^{-2}. It is assumed that the lower amount of loaded chiral selectors in those CSPs was caused by the low solubility of their silylated chiral selectors in toluene. Even though we conducted additional experiments by testing other solvents such as THF, CH_3CN and DMSO, the solubility remained low.

TABLE 1. Elemental analysis and chiral selector loadings for **CSPs 1–12**.

	Elemental analysis			
	%C	**%N**	**%H**	**% Selector loading (based on C) μmolm^{-2}**
CSP 1	18.21	2.91	1.99	2.32
CSP 2	13.49	2.21	1.99	1.03
CSP 3	13.66	2.26	2.13	1.22
CSP 4	7.58	0.98	1.29	0.61
CSP 5	18.84	4.21	2.91	1.67
CSP 6	21.63	4.37	2.44	2.09
CSP 7	13.11	2.55	2.02	1.00
CSP 8	23.66	5.95	3.91	1.87
CSP 9	6.15	0.91	1.21	0.30
CSP 10	14.06	2.19	3.06	0.67
CSP 11	14.81	2.19	2.19	1.18
CSP 12	9.13	1.15	1.33	0.38

All the CSPs were packed in LC columns with 150 x 2.1 mm I.D. This internal diameter was chosen because, previously, we demonstrated that columns containing the same chiral selector based on a CDX and only differing in the internal diameters, specifically 4.6 and 2.1 mm, showed similar enantiomeric behavior.[18] In fact, by reducing the internal diameter of the LC columns two main advantages can be pointed out such as a significant reduction of the material to be synthetized and packed, and a considerable decrease of the solvent consumption during the packing and chromatographic analysis. The ecological, practical and economic benefits are undeniable.[59,60]

Several commercial and "in house" chiral analytes (A1-A38) were selected (**Figure S1**, supplementary materials) to evaluate the LC enantioselective performance of **CSPs 1-12**. Additionally, enantiomeric mixtures of the chiral selectors (**28-39**) used for its preparation were included. The chromatographic analyses were performed under normal elution conditions, using different proportions of Hex and EtOH or 2-PrOH as mobile phases. **Table 2** shows the overall best results. For the enantioseparated analytes the elution order was determined by injecting each enantiomer separately.

Taking into account that in our previous work, the best enantioselectivity was achieved with two xanthone-(*R*)-(-)-α-phenylglycinol-derived CSPs,[18] we first developed the **CSP 1** comprising a chiral selector based on a xanthone derivative with a chiral moiety derived from (*R*)-(-)-α-phenylglycinol (**52**) in position 1 of the xanthone scaffold (**28**) (**Scheme 1**). The strategy was to use the same chiral moiety but changing its position in the xanthone scaffold. It was found that **CSP 1** showed baseline enantioseparation for analytes A24 and A30 (**Table**

2). For example, good enantioselectivity, α values of 2.02 and 2.04, and resolution, Rs values of 2.44 and 2.13, were obtained for A24 and A30 respectively, using Hex: EtOH (90:10 *v*/*v*) as mobile phase. For the other tested analytes short retention factors (analysis time generally lower than 3 min) and the absence or poor resolutions were found for all the combinations of mobile phases evaluated.

The next step was the introduction of an extra chiral moiety affording **CSP 2** (**Scheme 2**). The aim was to attempt to obtain more versatility and better enantioresolution by increasing the number of chiral moieties for enantiorecognition. Nevertheless, **CSP 2** comprising two chiral moieties in positions 3 and 6 of the xanthone scaffold (symmetrical structure) presented similar chromatographic performance to **CSP 1**, showing only a slightly increase of retention as well as enantioselectivity and resolution for A24 and A30 (**Table 2**). For comparison purposes, in addition to the (*R*)-(-)-α-phenylglycinol (**52**), the amino alcohols (*S*)-(+)-leucinol (**53**) and (*S*)-(+)-valinol (**54**) were chosen to obtain **CSP 3** and **CSP 4**, respectively (**Scheme 2**). Surprisingly, both CSPs showed similar enantioselectivity and resolution to those of **CSP 2** for the enantioseparated analytes (A24 and A30), as shown in **Table 2**.

Previously, we have confirmed the inversion of elution order for a selector based on a xanthone derivative comprising one chiral aromatic moiety.[18] To verify if with selectors comprising two chiral aromatic moieties the inversion of elution order would occur, **CSP 5** was prepared. The selector of this CSP is the enantiomeric pair of **CSP 2** selector. In this study, with more structurally complex xanthone selectors, it was found that the inversion of elution order did not occur.

Two more CSPs comprising two chiral moieties derived from (*R*)-(-)-α-phenylglycinol in different positions in the xanthone scaffold, specifically positions 1 and 3 (**CSP 6**) (**Scheme 1**) and positions 3 and 4 (**CSP 7**) (**Scheme 3**) were developed. It was found that, **CSP 7** enantioseparated the same two analytes with equivalent enantioselectivity and resolution, compared with **CSP 2**. As example, for analyte A30, using Hex:EtOH (80:20 *v*/*v*) as a mobile phase, the α and Rs values obtained on **CSP 2** were 2.13 and 3.81, while for **CSP 7** those values were 2.37 and 2.91, respectively. **CSP 6** showed some enantioselectivity only for analyte A24, however, with poor resolution (Rs <1.00 in all tested mobile phases).

The next step was to work with an increase of the number of chiral moieties to three (**CSP 8** and **CSP 9**) and four (**CSP 10**) (**Scheme 1**). It was found that both CSPs comprising three chiral moieties presented less discrimination ability. Nevertheless, **CSP 10** comprising chiral units in positions 1, 3, 6 and 8 of xanthone scaffold (symmetrical structure) showed good chromatographic results for both analytes A24 and A30, as shown in **Table 2**.

TABLE 2. Chromatographic enantioseparation of analytes A24 and A30 on CSPs 1-12.

		A24			A30		
	Mobile Phase (*v*/*v*)	**k_1**	**α**	**R_s**	**k_1**	**α**	**R_s**
CSP 1	Hex/EtOH: 90/10	1.50	2.02	2.44	1.84	2.04	2.13
	Hex/EtOH: 80/20	0.61	1.69	1.15	0.93	1.73	1.21
	Hex/2-PrOH: 80/20	0.64	2.26	1.66	0.79	2.21	1.52
CSP 2	Hex/EtOH: 80/20	2.40	1.92	3.50	2.39	2.13	3.81
	Hex/EtOH: 70/30	1.63	1.74	2.61	1.53	2.03	3.11
	Hex/2-PrOH: 80/20	3.22	2.51	3.38	3.00	3.02	3.71
	Hex/2-PrOH: 70/30	2.03	2.19	2.56	1.75	2.83	3.13
CSP 3	Hex/EtOH: 90/10	2.36	2.00	1.95	3.26	1.74	1.67
	Hex/EtOH: 80/20	1.58	1.86	1.88	1.83	1.63	1.36
	Hex/EtOH: 70/30	0.99	1.59	<1.00	0.99	1.62	1.06
	Hex/2-PrOH: 80/20	1.91	2.31	2.26	2.05	1.93	1.83
	Hex/2-PrOH: 70/30	1.36	1.49	1.15	1.21	1.87	1.29
CSP 4	Hex/EtOH: 90/10	2.24	2.16	3.20	2.59	2.22	3.73
	Hex/EtOH: 80/20	1.02	1.89	1.66	1.68	2.09	2.12
	Hex/EtOH: 70/30	0.86	1.46	1.17	0.71	1.93	2.08
	Hex/2-PrOH: 80/20	0.95	2.00	1.95	1.16	1.91	1.70
	Hex/2-PrOH: 70/30	0.61	1.80	1.46	0.91	1.52	1.00
CSP 5	Hex/EtOH: 80/20	2.09	2.29	1.33	1.75	3.33	1.74
	Hex/EtOH: 70/30	1.44	2.16	1.11	1.06	3.48	1.64
	Hex/2-PrOH: 80/20	1.82	2.29	1.09	3.28	2.24	1.76
	Hex/2-PrOH: 70/30	1.73	2.08	1.08	1.10	3.01	1.59
CSP 6	Hex/EtOH: 90/10	0.55	2.25	<1.00	0.99	1.00	ND
	Hex/EtOH: 80/20	0.34	1.27	<1.00	0.39	1.00	ND
	Hex/2-PrOH: 80/20	0.22	2.48	<1.00	0.26	1.00	ND
CSP 7	Hex/EtOH: 80/20	2.13	1.61	1.61	2.08	2.37	2.91
	Hex/2-PrOH: 80/20	2.01	1.81	1.48	1.65	2.98	2.54
CSP 8	Hex/EtOH: 90/10	2.63	2.43	<1.00	2.96	2.57	<1.00
	Hex/EtOH: 80/20	1.43	2.05	<1.00	1.46	1.00	<1.00
CSP 9	Hex/EtOH: 90/10	1.62	2.28	1.68	2.25	1.00	ND
	Hex/EtOH: 80/20	0.75	1.86	1.32	0.96	1.00	ND
	Hex/EtOH: 70/30	0.32	1.56	<1.00	0.38	1.00	ND
CSP 10	Hex/EtOH: 90/10	2.55	2.41	2.02	3.15	2.05	1.59
	Hex/EtOH: 80/20	1.43	2.02	1.36	1.29	2.12	1.22
	Hex/2-PrOH: 80/20	1.10	2.30	1.31	1.08	2.55	1.56

TABLE 2. Continuation

		A24			A30		
CSP 11	Hex/EtOH: 90/10	1.68	2.07	2.15	1.68	2.13	2.24
	Hex/EtOH: 80/20	1.14	1.84	1.56	0.99	2.17	1.88
	Hex/EtOH: 70/30	0.69	1.67	<1.00	0.59	1.98	1.24
	Hex/2-PrOH: 80/20	1.21	2.57	1.69	0.78	2.28	1.27
	Hex/2-PrOH: 70/30	0.75	1.77	1.11	0.55	1.25	1.38
CSP 12	Hex/EtOH: 90/10	3.00	2.20	3.56	3.70	1.96	3.04
	Hex/EtOH: 80/20	1.32	1.87	2.24	1.41	1.68	1.69
	Hex/EtOH: 70/30	0.70	1.71	1.30	0.70	1.56	1.15
	Hex/2-PrOH: 80/20	1.17	2.07	1.57	1.16	2.00	1.95
	Hex/2-PrOH: 70/30	1.02	2.13	1.75	0.89	2.09	1.72

ND: not determined. Detection at 254 nm; Flow rate, 0.2 $mLmin^{-1}$. Size of all columns: 150 mm length, 2.1 mm I.D.

In order to understand the role of the rigidity of the *quasi*-planar structure of the xanthone scaffold in the enantioresolution properties of these CSPs and also aiming to improve the enantioselectivity by increasing the flexibility of the central aromatic core, **CSPs 11** and **12** were prepared (**Scheme 4**). These CSPs are derived from benzophenone derivatives, one of the most common intermediates for the synthesis of xanthones.[61,62] It was found that **CSPs 11** and **12** afforded similar chromatographic results to their xanthone-based analogue CSPs, specifically **CSP 5** and **CSP 10** (**Table 2**).

Regarding the influence of the organic modifier in mobile phase, it was found that, despite a slight increase of enantioselectivity observed for Hex/2-PrOH combinations, shorter retention factors and higher resolution were obtained using mixtures of Hex and EtOH. For these reasons and considering the lower toxicity of this solvent compared to 2-PrOH, the use of EtOH was a better choice. Considering that, the majority of the analytes showed short retention times on the various CSPs, in normal phase elution mode, enantioseparation evaluation in polar organic and reversed-phase elution conditions were not considered. Regarding the elution order, for the enantioseparated analytes, the (*R*)-enantiomer was the more retained in all CSPs. In **Figures 1** and **2** a set of selected chromatograms for analytes A24 and A30 in different CSPs are presented.

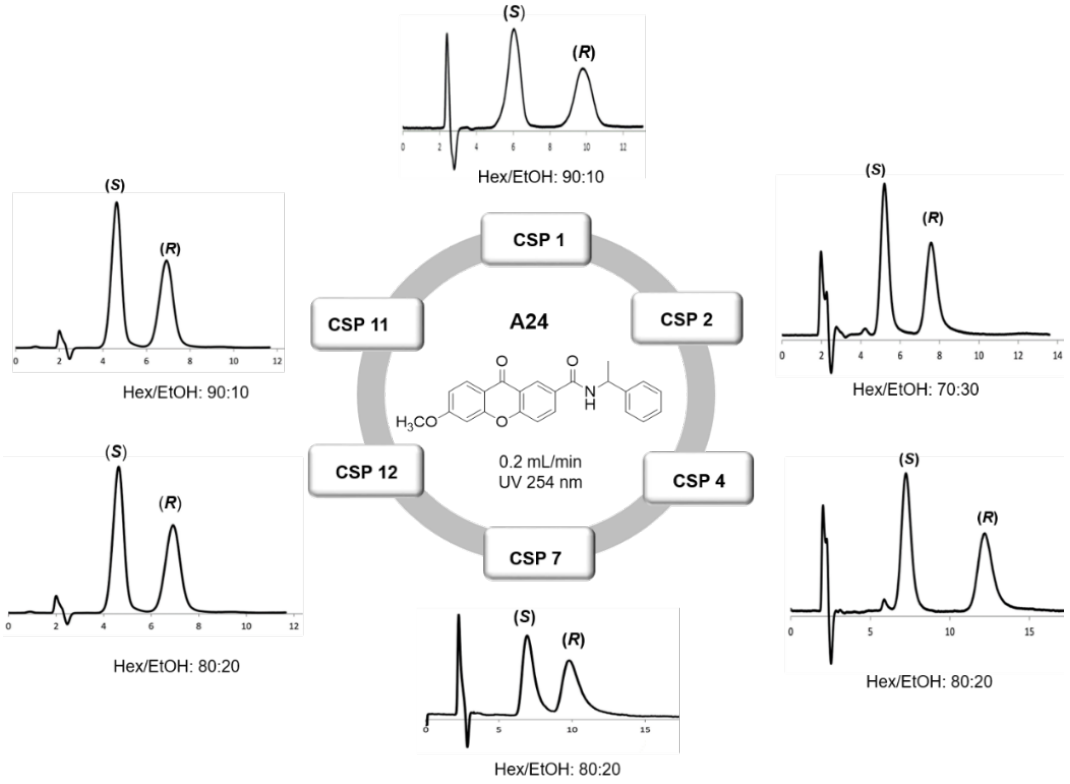


FIGURE 1. Chromatograms for the enantioseparation of analyte **A24** on different CSPs, at optimized chromatographic conditions.

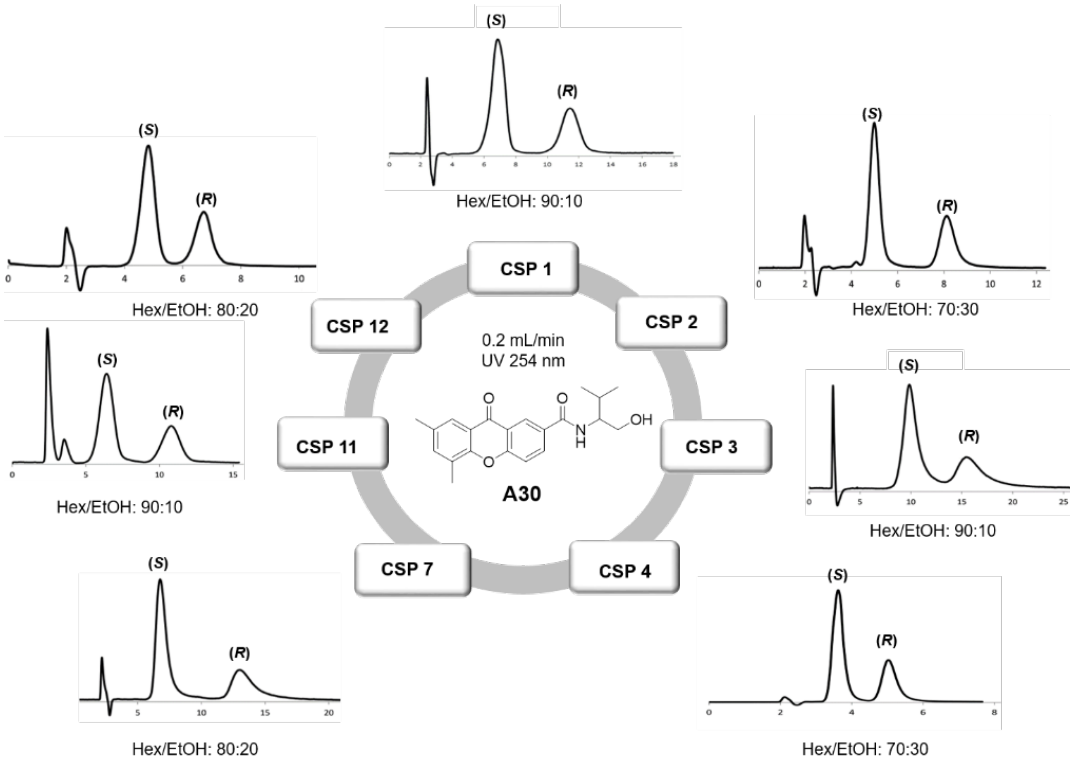


FIGURE 2. Chromatograms for the enantioseparation of analyte **A30** on different CSPs, in optimized chromatographic conditions.

In order to understand the binding mechanism behind the observed results of enantioresolution, docking studies were performed using the selectors of **CSPs 1**-**12**. The structure of the chiral selector of **CSP 1** (compound **28**) was determined by single crystal X-Ray diffraction and its ortep view is shown in **Figure 3**. The central pyranoid ring has a partial aromatic character and, as usual, the xanthone skeleton adopts a kind of flattened boat conformation.[63] The absolute configuration of the chiral center of the compound was confirmed to be (*R*).

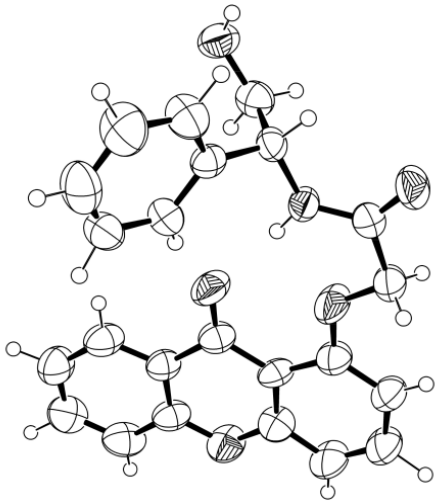


FIGURE 3. Ortep view of the crystal structure of chiral selector **28**.

Values of docking scores are presented on **Table 3**. The lower the docking score, the more stable the analyte-selector complex is. Docking scores between -3.4 and -6.5 kcalmol^{-1} and energy differences from -0.1 to -0.9 kcalmol^{-1} were obtained for A24; and docking scores between -4.0 and -6.1 kcalmol^{-1} and energy differences from 0 to -0.4 kcalmol^{-1} were obtained for A30.

The binding energies were different for the enantiomers of A24 in **CSPs 1-12** and A30 in **CSPs 1-5**, **7**, **8** and **10-12**, indicating that they have different affinities for these selectors, which is in accordance with the chromatographic data (separations were achieved, α = 1.25 to 3.02). In contrast, the binding energies were equal for both enantiomers of A30 in **CSP 6** (-5.2 kcalmol^{-1}) and **CSP 9** (-6.1 kcalmol^{-1}), indicating that they have identical affinity for these selectors, which is in agreement with the experimental results (no separation was achieved, α = 1.00). Docking analytes into selectors of **CSPs 1-12** revealed that, the (*R*)-enantiomers had higher affinity to the target (lower docking scores) than the corresponding (*S*)-enantiomers, although the average docking score difference was small in some cases. Consequently, there was 100% agreement between docking scores and experimental results for enantioselectivity and elution order of the enantiomers of the chiral analytes in all CSPs.

TABLE 3. Docking scores and elution order of both enantiomers of analytes A24 and A30 on **CSPs 1-12**.

	A24		A30	
	Docking Score (kcalmol^{-1})	**Energy difference (kcalmol^{-1})**	**Docking Score (kcalmol^{-1})**	**Energy difference (kcalmol^{-1})**
CSP 1 (X-ray structure)	(*S*): -4.5 (*R*): -4.8	-0.3	(*S*): -4.5 (*R*): -4.7	-0.2
CSP 2	(*S*): -5.4 (*R*): -5.5	-0.1	(*S*): -5.2 (*R*): -5.4	-0.2
CSP 3	(*S*): -5.0 (*R*): -5.1	-0.1	(*S*): -4.6 (*R*): -4.9	-0.3
CSP 4	(*S*): -5.5 (*R*): -5.7	-0.2	(*S*): -5.1 (*R*): -5.4	-0.3
CSP 5	(*S*): -5.1 (*R*): -5.6	-0.5	(*S*): -5.0 (*R*): -5.3	-0.2
CSP 6	(*S*): -5.5 (*R*): -5.7	-0.2	(*S*): -5.2 (*R*): -5.2	0.0
CSP 7	(*S*): -3.4 (*R*): -3.5	-0.1	(*S*): -4.0 (*R*): -4.4	-0.4
CSP 8	(*S*): -5.0 (*R*): -5.9	-0.9	(*S*): -4.1 (*R*): -4.2	-0.1
CSP 9	(*S*): -6.3 (*R*): -6.5	-0.2	(*S*): -6.1 (*R*): -6.1	0.0
CSP 10	(*S*): -6.0 (*R*): -6.1	-0.1	(*S*): -5.6 (*R*): -5.7	-0.1
CSP 11	(*S*): -5.3 (*R*): -5.4	-0.1	(*S*): -5.0 (*R*): -5.2	-0.2
CSP 12	(*S*): -6.0 (*R*): -6.1	-0.1	(*S*): -5.6 (*R*): -5.7	-0.1

In order to understand the binding mechanism and the chromatographic results, a visual inspection of the binding conformations and established interactions were performed.

Figure 4A illustrates a representative example of the most stable docked conformations for enantiomers of analyte A30 complexed with the chiral selector of **CSP 1**. The (*R*)-enantiomer of A30 was more retained in the CSP and, accordingly, presented lower docking score than (*S*)-enantiomer. In fact, only the (*R*)-enantiomer binds in a conformation that allows the establishment of a hydrogen interaction with the ether group of the xanthone tricyclic system of the selector. Furthermore, the tricyclic ring system of (*R*)-enantiomer establishes parallel π-stacking interactions with the xanthone scaffold of the selector, while its antipoda establishes parallel-displaced π-stacking interactions (**Figure 4A**). On the other hand, regarding for example analyte A17, which have the same chiral moiety as analyte A30 only differing in the

nature, number and positions of the substituents on the xanthone scaffold (**Figure 1**), both enantiomers docked on the identical docking pose with the tricyclic ring systems superimposed and an RMSD of only 1.5 Å (**Figure 4B**). It was found that A17 enantiomers, which were not separated on **CSP 1**, only established π-stacking interactions with selector of **CSP 1**.

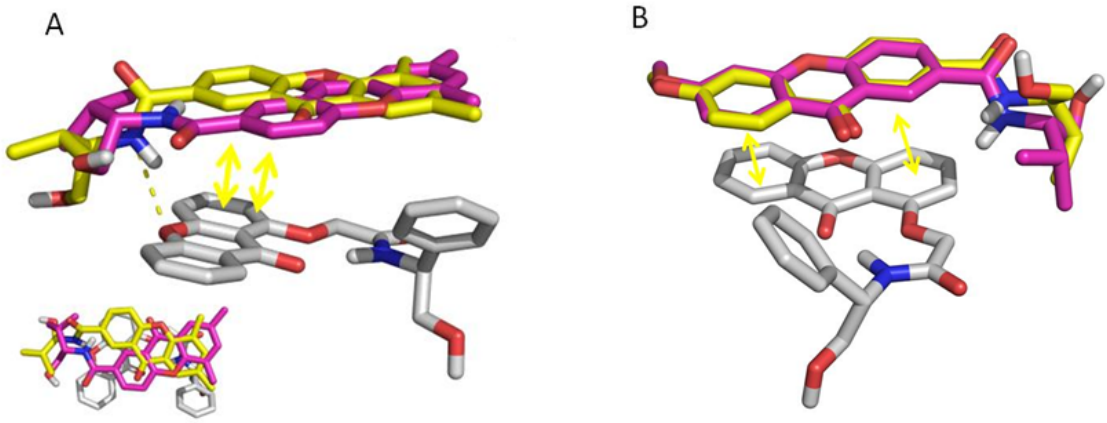


FIGURE 4. (**A**) Crystallographic **CSP 1** and docked A30 enantiomers (top-view of the docking poses is represented on the bottom-left corner of the image); (**B**) A17 docking pose of A17 enantiomers on crystallographic **CSP 1**. Selector of **CSP 1** is represented as grey sticks; (*R*) and (*S*) enantiomers are represented as yellow and pink sticks, respectively. Hydrogen interactions and π-stacking interactions are represented in yellow broken lines and yellow double arrow, respectively.

It is also important to highlight that, through docking studies, it was confirmed that the aromatic ring bonded to the stereogenic center of the side chain of the selector is not involved in interactions with analytes, as shown in **Figures 5A** and **5B**. The same occurs when the group is an alkyl chain. This justifies the reason why **CSP 2** and **CSP 5** (derived from phenylglycinol), **CSP 3** (derived from leucinol) and **CSP 4** (derived from valinol) have similar chromatographic behavior. It was found that with selectors of CSPs comprising three chiral units (**CSPs 8** and **9**) the interactions responsible for the enantioselectivity did not occur successfully due to steric hindrance of the three bulky chiral moieties preventing the establishment of parallel π-stacking interactions between the xanthone scaffolds of analytes and selectors. For selectors of CSPs comprising four bulky chiral moieties (**CSP 10** and **12**), they are in positions of the xanthone or benzophenone scaffold allowing to establish the interactions essential for enantiomeric discrimination (**Figure 5C** and **5D**). Regarding **CSP 10**, for example, enantiomers of A30 docks on the same side of the selector, but with the carbonyl group of the xanthone scaffold pointing in opposite directions. Therefore, (*R*)-enantiomer is able to form two hydrogen interactions through the xanthone carbonyl and side chain hydroxyl groups. The (*S*)-enantiomer establishes only one hydrogen interaction (**Figure 5C**). As far as **CSP 12** is concerned, enantiomers of A30 also dock on the same side of the selector. The (*S*)-enantiomer of A30 establishes three hydrogen interactions with the benzophenone carbonyl group, amide and

hydroxyl groups of the side chains of the selector. The (*R*)-enantiomer of A30 only establishes one hydrogen interaction by means of the side chain hydroxyl group, but it establishes additional π-stacking interactions (parallel and T-shaped) (**Figure 5D**).

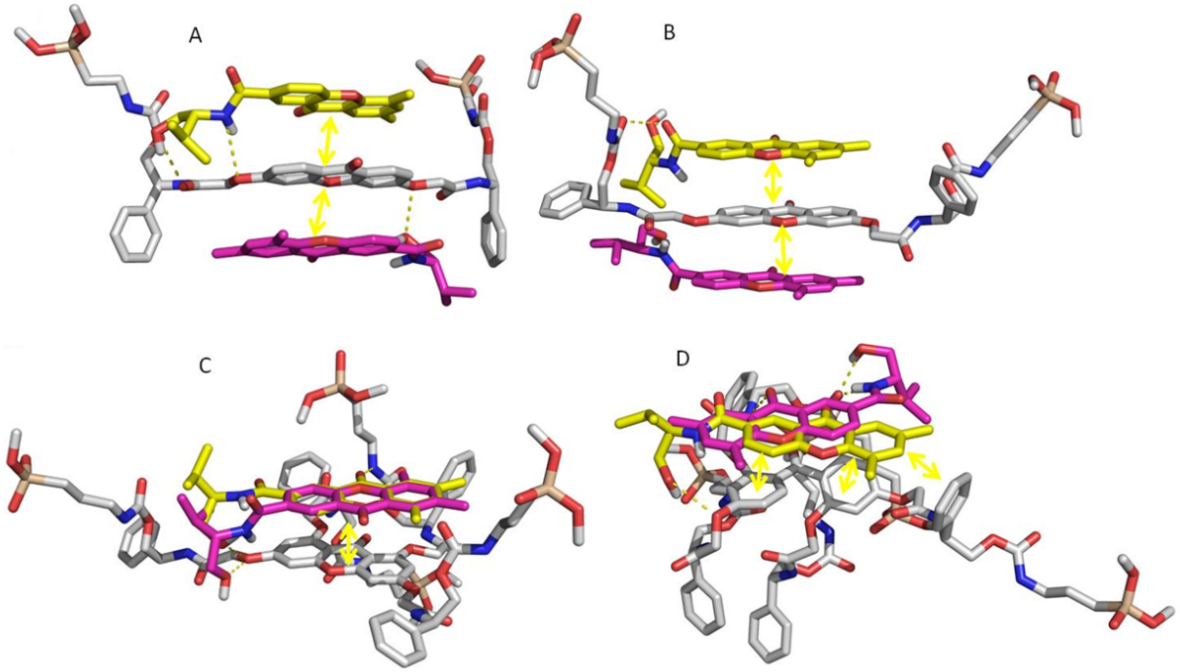


FIGURE 5. (**A**) **CSP 2** and docked A30 enantiomers; (**B**) **CSP 5** and docked A30 enantiomers; (**C**) **CSP 10** and docked A30 enantiomers; (**D**) **CSP 12** and docked A30 enantiomers. Selectors of **CSP 2**, **5**, **10** and **12** are represented as grey sticks; (*R*) and (*S*) enantiomers are represented as yellow and pink sticks, respectively. Hydrogen interactions and π-stacking interactions are represented in yellow broken lines and yellow double arrow, respectively.

Regardless the nature of the central aromatic core of the selector, xanthone for **CSP 10** or benzophenone for **CSP 12**, both CSPs were able to establish parallel π-stacking interactions with (*R*)-enantiomer of analyte A30 that, in addition to other interactions, are responsible for enantioselectivity which explains the similar enantioresolution properties of these CSPs.

4. CONCLUSION

Twelve new CSPs were successfully prepared aiming to obtain versatile and efficient CSPs as well as to explore the role of some structural characteristics that could be crucial for enantiorecognition. Although the chromatographic results obtained were not promising as expected, it was found that the number and position of the chiral units positioned in the xanthone scaffold of the chiral selectors can interfere with the chiral recognition mechanism by steric hindrance. Moreover, for the CSPs comprising equal number of chiral units in the same positions, the nature of the substituent next to the stereogenic center was shown not to be pivotal because either the CSPs having an aromatic ring or an alkyl chain showed similar

results. The central aromatic core of the selector, either xanthone or benzophenone scaffold, aligned with the xanthone tricyclic ring of the analytes to maximize π-stacking interactions, and the hydrogen bonding interactions between the donor and acceptor polar groups of analytes and selectors, demonstrated to be essential for enantioselective recognition. The docking studies were proved to be a meaningful tool for the structural requirements necessary for the effective elucidation of the intermolecular CSP-analyte interactions.

The development of new CSPs for LC is a continuous and challenging issue. This work is an important contribution to improve the design of new selectors and further preparation of more efficient CSPs based on xanthone and benzophenone derivatives possessing wider applicability.

Acknowledgements

This work was supported by the Strategic Funding UID/Multi/04423/2019 through national funds provided by FCT—Foundation for Science and Technology and European Regional Development Fund (ERDF), through the COMPETE – Programa Operacional Factores de Competitividade (POFC) program in the framework of the program PT2020; the project PTDC/MAR-BIO/4694/2014 (reference POCI-01-0145-FEDER-016790 and 3599-PPCDT), co-financed by COMPETE 2020, under the PORTUGAL 2020 Partnership Agreement, through the European Regional Development Fund (ERDF), CHIRALBIOACTIVE-PI-3RL-IINFACTS-2019 and QOPNA research project (FCT UID/QUI/00062/2019) and Portuguese NMR network. Y.Z. Phyo thanks the Erasmus Mundus Action 2 (Lotus Plus project) for a PhD's scholarship.

Supporting information

Additional supporting information may be found in the online version of this article at the publisher's website.

REFERENCES AND NOTES

1. Ward TJ, Ward KD. Chiral separations: A review of current topics and trends. *Anal Chem* 2012;84(2):626-635.
2. Gumustas M, Ozkan SA, Chankvetadze B. Analytical and Preparative Scale Separation of Enantiomers of Chiral Drugs by Chromatography and Related Methods. *Curr Med Chem* 2018;25(33):4152-4188.
3. Fernandes C, Brandão P, Santos A, Tiritan ME, Afonso C, Cass QB, Pinto MM. Resolution and determination of enantiomeric purity of new chiral derivatives of xanthones using polysaccharide-based stationary phases. *J Chromatogr A* 2012;1269:143-153.

4. Fernandes C, Palmeira A, Santos A, Tiritan ME, Afonso C, Pinto MM. Enantioresolution of chiral derivatives of xanthones on (S,S)-Whelk-O1 and l -phenylglycine stationary phases and chiral recognition mechanism by docking approach for (S,S)-Whelk-O1. *Chirality* 2013;25(2):89-100.
5. Silva C, Ribeiro C, Maia AS, Gonçalves V, Tiritan ME, Afonso C. Enantiomeric separation of tramadol and its metabolites: Method validation and application to environmental samples. *Symmetry* 2017;9(9).
6. Silva B, Fernandes C, Tiritan ME, Pinto MMM, Valente MJ, Carvalho M, de Pinho PG, Remião F. Chiral enantioresolution of cathinone derivatives present in “legal highs”, and enantioselectivity evaluation on cytotoxicity of 3,4-methylenedioxypyrovalerone (MDPV). *Forensic Toxicol* 2016:1-14.
7. Sousa ME, Tiritan ME, Belaz KRA, Pedro M, Nascimento MSJ, Cass QB, Pinto MMM. Multimilligram enantioresolution of low-solubility xanthonolignoids on polysaccharide chiral stationary phases using a solid-phase injection system. *J Chromatogr A* 2006;1120(1-2):75-81.
8. Silva B, Pereira JA, Cravo S, Araújo AM, Fernandes C, Pinto MMM, de Pinho PG, Remião F. Multi-milligram resolution and determination of absolute configuration of pentedrone and methylone enantiomers. *J Chromatogr B Analyt Technol Biomed Life Sci* 2018;1100-1101:158-164.
9. Lämmerhofer M. Chiral recognition by enantioselective liquid chromatography: Mechanisms and modern chiral stationary phases. *J Chromatogr A* 2010;1217(6):814-856.
10. Ribeiro J, Tiritan ME, Pinto MMM, Fernandes C. Chiral stationary phases for liquid chromatography based on chitin- and chitosan-derived marine polysaccharides. *Symmetry* 2017;9(190), 1-28.
11. Kalíková K, Riesová M, Tesařová E. Recent chiral selectors for separation in HPLC and CE. *Cent Eur J Chem* 2011:1-22.
12. Tang M, Zhang J, Zhuang S, Liu W. Development of chiral stationary phases for high-performance liquid chromatographic separation. *TrAC - Trends Anal Chem* 2012;39:180-194.
13. Felix G, Berthod A. Commercial chiral stationary phases for the separations of clinical racemic drugs. *Sep Purif Rev* 2007;36(4):285-481.
14. Teixeira J, Tiritan ME, Pinto MMM, Fernandes C. Chiral stationary phases for liquid chromatography: Recent developments. *Molecules* 2019, 24, 865; doi:10.3390/molecules24050865.

15. Fernandes C, Phyo YZ, Silva AS, Tiritan ME, Kijjoa A, Pinto MMM. Chiral Stationary Phases Based on Small Molecules: An Update of the Last 17 Years. *Sep. Pur Rev* 2018;47(2):89-123.
16. Fernandes C, Tiritan ME, Pinto M. Small molecules as chromatographic tools for HPLC enantiomeric resolution: Pirkle-type chiral stationary phases evolution. *Chromatographia* 2013;76(15-16):871-897.
17. Gasparrini F, Misiti D, Villani C. High-performance liquid chromatography chiral stationary phases based on low-molecular-mass selectors. *J Chromatogr A* 2001;906(1-2):35-50.
18. Fernandes C, Tiritan ME, Cravo S, Phyo YZ, Kijjoa A, Silva AMS, Cass QB, Pinto MMM. New chiral stationary phases based on xanthone derivatives for liquid chromatography. *Chirality* 2017;29(8):430-442.
19. Araújo J, Fernandes C, Pinto M, Elizabeth Tiritan M. Chiral derivatives of xanthones with antimicrobial activity. *Molecules* 2019;24(2), doi:10.3390/molecules24020314.
20. Fernandes C, Palmeira A, Ramos II, Carneiro C, Afonso C, Tiritan ME, Cidade H, Pinto PCAG, Saraiva MLMFS, Reis S and others. Chiral derivatives of xanthones: Investigation of the effect of enantioselectivity on inhibition of cyclooxygenases (COX-1 and COX-2) and binding interaction with human serum albumin. *Pharmaceuticals* 2017;10(2)50, doi:10.3390/ph10020050..
21. Fernandes C, Carraro ML, Ribeiro J, Araújo J, Tiritan ME, Pinto MMM. Synthetic chiral derivatives of xanthones: Biological activities and enantioselectivity studies. *Molecules* 2019, 24(4), 791, doi:10.3390/molecules24040791.
22. Yu J, Armstrong DW, Ryoo JJ. Synthesis of new C3 symmetric amino acid- and aminoalcohol-containing chiral stationary phases and application to HPLC enantioseparations. *Chirality* 2018;30(1):74-84.
23. Yu J, Lee JM, Ryoo JJ. Chiral separation on various modified amino alcohol-derived HPLC chiral stationary phases. *Chirality* 2016;28(4):276-281.
24. Yu J, Ryoo DH, Lee JM, Ryoo JJ. Synthesis and Application of C2 and C3 Symmetric (R)-Phenylglycinol-Derived Chiral Stationary Phases. *Chirality* 2016;28(3):186-191.
25. Ryoo JJ, Heo KS, Song YA. Resolution of N-acyl-1-naphthylalkylamide on amide and sulfonamide-derived π-acidic chiral stationary phases. *Microchem J* 2003;74(3):215-221.
26. Ryoo JJ, Im SH, Lee K-P, Park JH, Hyun MH. Resolution of Racemic N-Acyl-1-arylaminoalkanes on a (3,5-Dinitrobenzoyl)phenylglycinol-Derived High Performance Liquid Chromatography Chiral Stationary Phase. *Microchem J* 1999;63(1):128-133.

27. Ryoo JJ, Kim TH, Im SH, Jeong YH, Park JY, Choi S-H, Lee K-P, Park JH. Enantioseparation of racemic N-acylarylalkylamines on various amino alcohol derived π-acidic chiral stationary phases. *J Chromatogr A* 2003;987(1):429-438.
28. Hyun MH, Kim JI, Cho YJ, Ryoo JJ. Optical resolution of racemic α-hydroxycarboxylic acids on a dynamic chiral stationary phase derived from (S)-leucinol by ligand exchange chromatography. *B Korean Chem Soc* 2004;25(11):1707-1710.
29. Mayani VJ, Abdi SHR, Kureshy RI, Khan NH, Agrawal S, Jasra RV. Synthesis and characterization of (S)-amino alcohol modified M41S as effective material for the enantioseparation of racemic compounds. *J Chromatogr A* 2006;1135(2):186-193.
30. Scriba GKE. Chiral recognition mechanisms in analytical separation sciences. Chromatographia 2012;75(15-16):815-838.
31. Scriba GKE. Chiral recognition in separation science – an update. *J Chromatogr A* 2016;1467:56-78.
32. Phyo YZ, Cravo S, Palmeira A, Tiritan ME, Kijjoa A, Pinto MMM, Fernandes C. Enantiomeric resolution and docking studies of chiral xanthonic derivatives on chirobiotic columns. *Molecules* 2018;23(1), 142, doi:10.3390/molecules23010142.
33. Carraro ML, Palmeira A, Tiritan ME, Fernandes C, Pinto MMM. Resolution, determination of enantiomeric purity and chiral recognition mechanism of new xanthone derivatives on (S,S)-Whelk-O1 stationary phase. *Chirality* 2017:1–10.
34. Fernandes C, Tiritan ME, Cass Q, Kairys V, Fernandes MX, Pinto M. Enantioseparation and chiral recognition mechanism of new chiral derivatives of xanthones on macrocyclic antibiotic stationary phases. *J Chromatogr A* 2012;1241:60-68.
35. Blodgett J, Wang Y, Li T, Polavarapu PL, Drabowicz J, Pietrusiewicz KM, Zygo K. Resolution of tert-butyl-1-(2-methylnaphthyl)phosphine oxide using selectors identified from a chemical combinatorial library. *Anal Chem* 2002;74(20):5212-5216.
36. Brahmachary E, Ling FH, Svec F, Fréchet JMJ. Chiral recognition: Design and preparation of chiral stationary phases using selectors derived from Ugi multicomponent condensation reactions and a combinatorial approach. *J Comb Chem* 2003;5(4):441-450.
37. Chan KL, Lai-Yeng T, Yang ML, Syed AAS, Jean-Frederic FW. Synthesis of 1,3,6-Trioxygenated Prenylated Xanthone Derivatives as Potential Antitumor Agents. *Lett Org Chem* 2012;9(8):549-555.
38. Cruz I, Puthongking P, Cravo S, Palmeira A, Cidade H, Pinto M, Sousa E. Xanthone and Flavone Derivatives as Dual Agents with Acetylcholinesterase Inhibition and Antioxidant Activity as Potential Anti-Alzheimer Agents. *J Chem* 2017;2017.

39. Pillai RKM, Naiksatam P, Johnson F, Rajagopalan R, Watts PC, Cricchio R, Borras S. Thermorubin II. 1,3-Dihydroxy-9H-xanthones and 1,3-dihydroxy-9H-xanthenes. New methods of synthesis. *J Org Chem* 1986;51(5):717-723.
40. Pinto E, Afonso C, Duarte S, Vale-Silva L, Costa E, Sousa E, Pinto M. Antifungal Activity of Xanthones: Evaluation of their Effect on Ergosterol Biosynthesis by High-performance Liquid Chromatography. *Chem Biol Drug Des* 2011;77(3):212-222.
41. Sousa E, Paiva A, Nazareth N, Gales L, Damas AM, Nascimento MSJ, Pinto M. Bromoalkoxyxanthones as promising antitumor agents: Synthesis, crystal structure and effect on human tumor cell lines. *Eur J Med Chem* 2009;44(9):3830-3835.
42. Lin S, Koh JJ, Aung TT, Lim F, Li J, Zou H, Wang L, Lakshminarayanan R, Verma C, Wang Y and others. Symmetrically Substituted Xanthone Amphiphiles Combat Gram-Positive Bacterial Resistance with Enhanced Membrane Selectivity. *J Med Chem* 2017;60(4):1362-1378.
43. Grover P, Shah G, Shah R. Xanthones. Part IV. A new synthesis of hydroxyxanthones and hydroxybenzophenones. *J Chem Soc* (Resumed) 1955:3982-3985.
44. Sheldrick GM. A short history of SHELX. *Acta Crystallogr Section A: Foundations of Crystallograph*y 2008;64(1):112-122.
45. Fernandes C, Masawang K, Tiritan ME, Sousa E, De Lima V, Afonso C, Bousbaa H, Sudprasert W, Pedro M, Pinto MM. New chiral derivatives of xanthones: Synthesis and investigation of enantioselectivity as inhibitors of growth of human tumor cell lines. *Bioorg Med Chem* 2014;22(3):1049-1062.
46. Fernandes C, Oliveira L, Tiritan ME, Leitao L, Pozzi A, Noronha-Matos JB, Correia-De-Sá P, Pinto MM. Synthesis of new chiral xanthone derivatives acting as nerve conduction blockers in the rat sciatic nerve. *Eur J Med Chem* 2012;55:1-11.
47. Dewar MJS, Zoebisch EG, Healy EF, Stewart JJP. Development and use of quantum mechanical molecular models. 76. AM1: a new general purpose quantum mechanical molecular model. *J Am Chem Soc* 1985;107(13):3902-3909.
48. Mirzaei H, Zarbafian S, Villar E, Mottarella S, Beglov D, Vajda S, Paschalidis I, Vakili P, Kozakov D. Energy Minimization on Manifolds for Docking Flexible Molecules. *J Chem Theory Comput* 2015;11(3):1063-76.
49. Jaghoori MM, Bleijlevens B, Olabarriaga SD. 1001 Ways to run AutoDock Vina for virtual screening. *J Comput Aided Mol Des* 2016;30(3):237-249.
50. Seeliger D, de Groot BL. Ligand docking and binding site analysis with PyMOL and Autodock/Vina. *J Comput Aided Mol Des* 2010;24(5):417-422.
51. Ribeiro J, Veloso C, Fernandes C, Tiritan ME, Pinto MMM. Carboxyxanthones: Bioactive agents and molecular scaffold for synthesis of analogues and derivatives. *Molecules* 2019;24(1), 180, doi:10.3390/molecules24010180.

52. Carvalho MJ, Carvalho LM, Ferreira AM, Silva AMS. A new xanthone from Hedychium gardnerianum. *Nat Prod Res* 2003;17(6):445-449.
53. Lin C-N, Chung M-I, Liou S-J, Lee T-H, Wang J-P. Synthesis and Anti-inflammatory Effects of Xanthone Derivatives. *J Pharm Pharmacol* 1996;48(5):532-538.
54. Liu Y, Zou L, Ma L, Chen W-H, Wang B, Xu Z-L. Synthesis and pharmacological activities of xanthone derivatives as α-glucosidase inhibitors. *Bioorg Med Chem* 2006;14(16):5683-5690.
55. Zhang X-J, Ye S-F, Zhang Y, Meng H-Y, Zhang M-Q, Gao W-L, You Q-D. Microwave-Assisted Efficient and Green Synthesis of Hydroxyxanthone in Water. *Synth Commun* 2012;42(20):2952-2958.
56. Tiritan ME, Fernandes C, Maia AS, Pinto M, Cass QB. Enantiomeric ratios: Why so many notations? *J Chromatogr A* 2018;1569:1-7.
57. Welch CJ, Perrin SR. Improved chiral stationary phase for ß-blocker enantioseparations. *J Chromatogr A* 1995;690(2):218-225.
58. Ihara T, Sugimoto Y, Asada M, Nakagama T, Hobo T. Influence of the method of preparation of chiral stationary phases on enantiomer separations in high-performance liquid chromatography. *J Chromatogr A* 1995;694(1):49-56.
59. Sandra P, Vanhoenacker G, David F, Sandra K, Pereira A. Green chromatography (Part 1): Introduction and liquid chromatography. LC-GC Europe 2010;23(5).
60. Majors RE, Raynie D. The greening of the chromatography laboratory. *LC-GC N Am* 2011;29(2):118-134.
61. Azevedo CMG, Afonso CMM, Pinto MMM. Routes to xanthones: An update on the synthetic approaches. *Curr Org Chem* 2012;16(23):2818-2867.
62. Sousa ME, Pinto MMM. Synthesis of xanthones: An overview. *Curr Med Chem* 2005;12(21):2447-2479.
63. Gales L, Damas AM. Xanthones - A structural perspective. *Curr Med Chem* 2005;12(21):2499-2515.

Supplementary Material

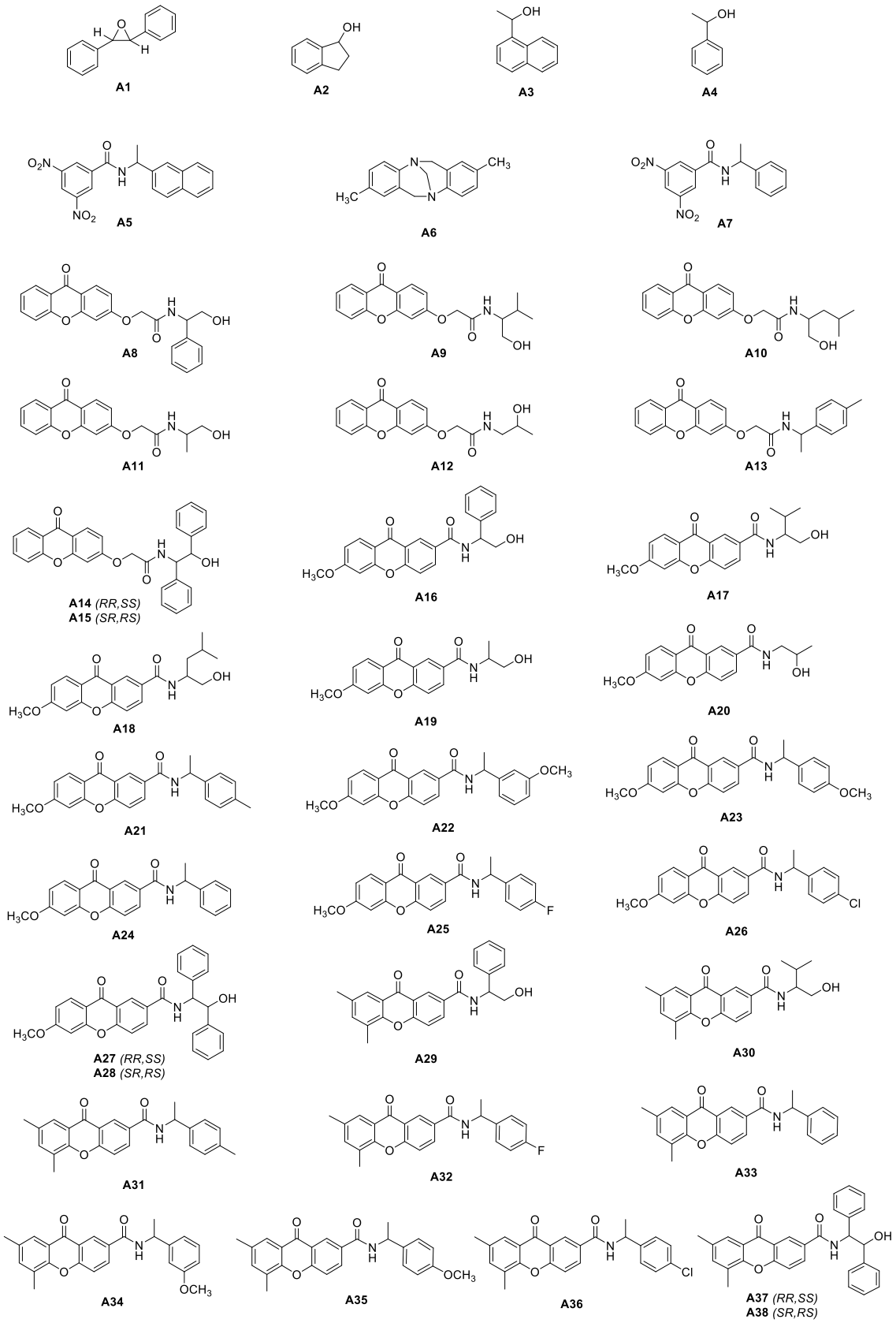
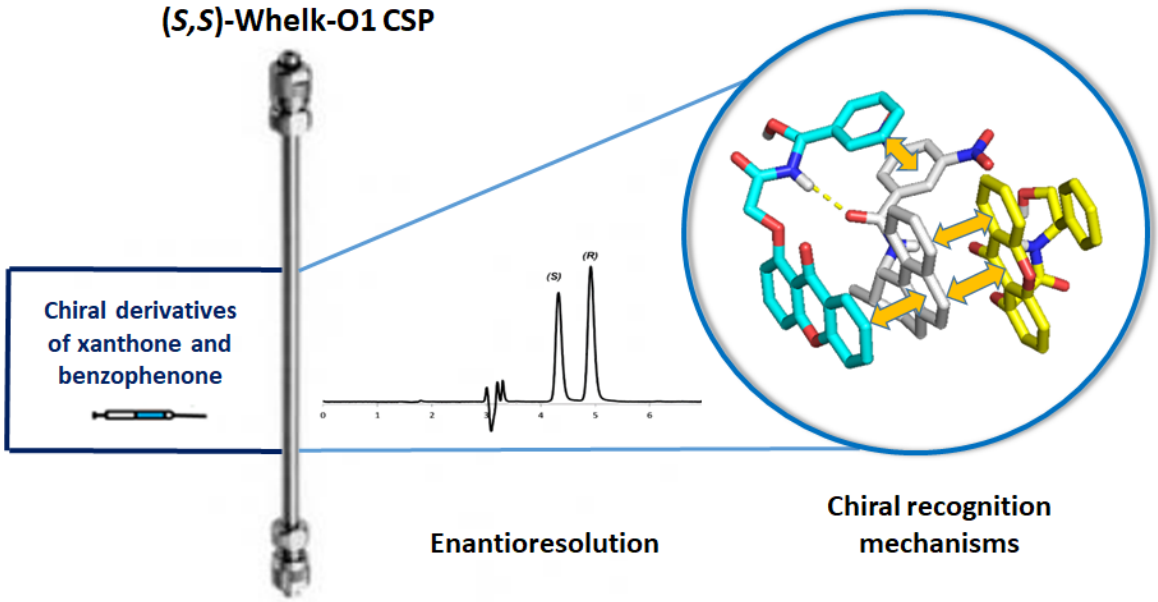


FIGURE S1. Chemical structures of analytes A1-A38.

CHAPTER VI

Enantioseparation of new xanthone and benzophenone derivatives by liquid chromatography on (*S*,*S*-Whelk-O1 and cellulose based stationary phases, determination of enantiomeric purity and molecular docking studies

Original research article in final preparation for submission



Graphical abstract

Enantioseparation of new xanthone and benzophenone derivatives by liquid chromatography on (*S*,*S*)-Whelk-O1 and cellulose based stationary phases, determination of enantiomeric purity and molecular docking studies

Ye‘ Zaw Phyo[1,2], Joana Teixeira[3], Andreia Palmeira[2,3], Maria Elizabeth Tiritan[2,3,4], Madalena M.M. Pinto[2,3], Carla Fernandes[2,3*], Anake Kijjoa[1,2]

[1] *ICBAS*-Instituto de Ciências Biomédicas Abel Salazar, Universidade do Porto, Rua de Jorge Viterbo Ferreira, 228, 4050-313 Porto, Portugal

[2] Interdisciplinary Centre of Marine and Environmental Research (CIIMAR), Edifício do Terminal de Cruzeiros do Porto de Leixões, Av. General Norton de Matos s/n, 4050-208 Matosinhos, Portugal

[3] Laboratório de Química Orgânica e Farmacêutica, Departamento de Ciências Químicas, Faculdade de Farmácia, Rua de Jorge Viterbo Ferreira, 228, 4050-313 Porto, Portugal

[4] CESPU, Instituto de Investigação e Formação Avançada em Ciências e Tecnologias da Saúde (IINFACTS), Rua Central de Gandra, 1317, 4585-116 Gandra PRD, Portugal

Correspondence: cfernandes@ff.up.pt; Tel.: +35-122-042-8688

ABSTRACT

Liquid chromatography enantioseparation and determination of enantiomeric purity of new xanthone and benzophenone derivatives comprising one or more chiral moieties are reported. High enantioselectivity and resolution were observed in (*S,S*)-Whelk-O1 chiral stationary phase (CSP) for the enantiomeric mixtures of compounds comprising an aromatic ring linked to the stereogenic center(s), with α values ranging from 1.35 to 4.15, and Rs values ranging from 2.22 to 13.87. Among all the tested enantiomeric mixtures, those comprising three chiral moieties positioned in the xanthone scaffold gave the best chromatographic results. Enantiomers comprising an alkyl chain linked to the stereogenic centers were enantioseparated on a Lux® Celullose-2 CSP. For both CSPs, the elution was performed in polar organic mode. The enantiomeric ratio (e.r.) values were always higher than 99%. Additionally, assessment of chiral recognition mechanisms on (*S*,*S*)-Whelk-O1 CSP was performed by molecular docking approach, which are in accordance with the chromatographic parameters. The nature and number of chiral moieties in the central aromatic scaffold of either xanthone or benzophenone derivatives are proved to be crucial for enantiorecognition.

Keywords: Liquid chromatography; Enantiomeric ratio; (*S*,*S*)-Whelk-O1; Chiral derivative of xanthone; Chiral derivative of benzophenone; Enantioselectivity; Chiral recognition; Docking studies.

1. INTRODUCTION

Separation of enantiomers has become a pivotal task in several research fields, including pharmaceutical and medicinal chemistry, since enantiomers of drugs and promising bioactive compounds may have different pharmacokinetic and pharmacodynamic properties[1-3] as well as diverse toxicological effects.[4-6] These are the reasons why the regulatory authorities advocate more on strict investigation and requirements for evaluating the safety and efficacy of new drugs containing stereogenic centers.[7-9] Accordingly, enantioseparation has acquired key relevance in all the stages of drug development with a wide range of applications, including monitorization of asymmetric reactions,[10,11] determination of enantiomeric purity,[12,13] preparative separation of enantiomers,[14,15] analysis of the stereochemistry of natural compounds,[16,17] pharmacokinetic,[18,19] and enantioselective studies,[20,21] among others. Over the last two decades, chiral liquid chromatography has become a powerful and widely employed analytical tool, and different types of chiral stationary phases (CSPs) were developed for these purposes.[22-25] Among the most successful CSPs described in the literature is the (*S*,*S*)-Whelk-O1 (**Figure 1**), a Pirkle-type CSP.[26,27] Although it was designed in the 1990s to isolate (*S*)-naproxen, a nonsteroidal anti-inflammatory drug,[28] this CSP is enantioselective

for a broad range of chiral analytes[29-31] and it can be used in diverse solvent systems.[32-34] Besides, the chiral recognition mechanism for (*S*,*S*)-Whelk-O1 CSP is the most widely investigated,[35,36] being essential to confirm the nature of interactions between analytes and the CSP, to better understand the chromatographic data and to predict enantioselectivity for other analytes.[27,37] Molecular docking is proved to be an important tool to carry out this type of studies.[38,39]

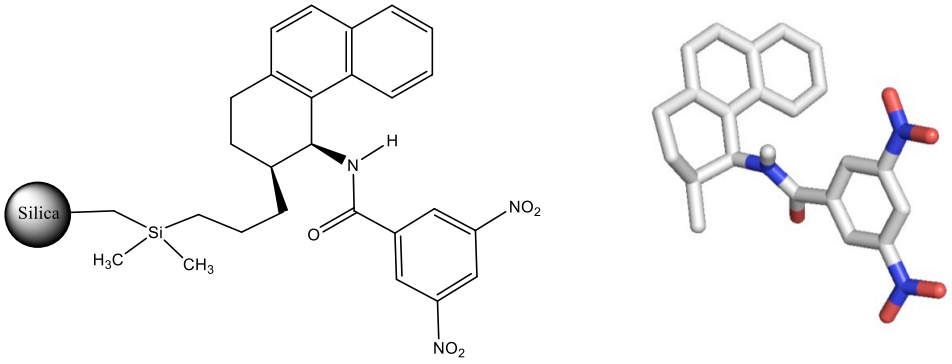


FIGURE 1. 2D (i) and 3D (ii) structures of (*S,S*)-Whelk-O1 selector. Chiral selector is represented in sticks with C, O and N colored in grey, red and blue, respectively.

Recently, (*S*,*S*)-Whelk-O1 CSP revealed good enantioselective performance for a series of derivatives of xanthones having a chiral moiety, mainly for those comprising an aromatic ring linked to the stereogenic center.[40,41] Chiral derivatives of xanthones, isolated from natural sources as well as obtained by synthesis, are very interesting compounds comprising a broad range of biological/pharmacological activities.[42,43] The synthesis of chiral derivatives of this class of compounds as single enantiomers for biological assays and to perform enantioselectivity studies is one of the main aims of our group.[44-46] In addition, this type of small molecules were also explored as selectors for CSPs.[47]

Herein, we report the liquid chromatography enantioseparation and determination of the enantiomeric purity of new xanthone derivatives comprising one, two, three and four chiral moieties in diverse positions of the central tricyclic scaffold. Two derivatives of benzophenone, one of the most common intermediates for the synthesis of xanthones,[48,49] having two and four chiral units were also included (**Figure 2**).

Additionally, molecular docking studies were performed to better understand the chromatographic data and shed light on the chiral recognition mechanism involved in enantioseparation. The analysis of the interactions between the enantiomerically pure compounds and the (*S*,*S*)-Whelk-O1 CSP and the role of the structural features of the compounds, specifically the nature, number and position of chiral moieties in the central aromatic scaffold, either xanthone or benzophenone, are discussed in this work.

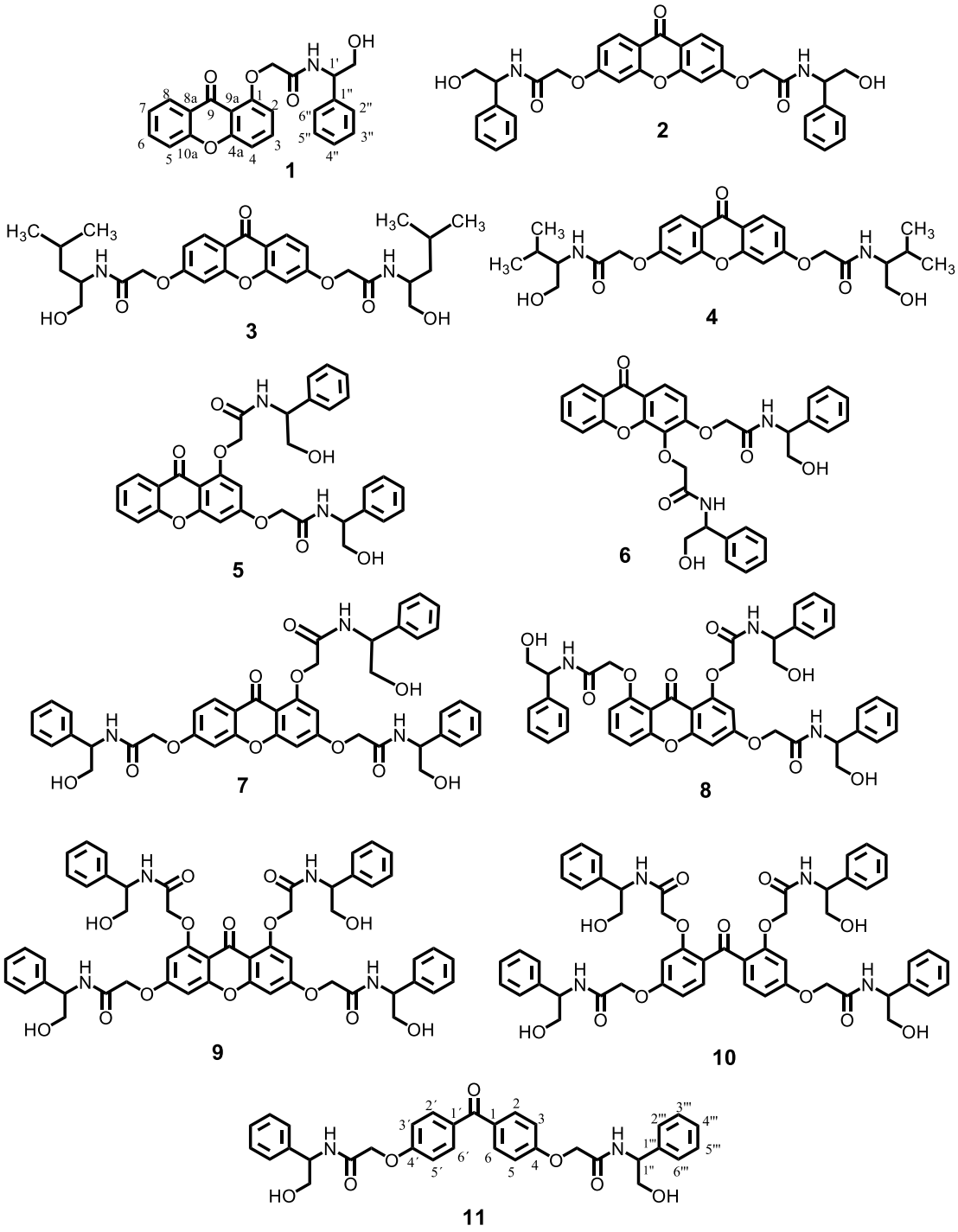


FIGURE 2. Chemical structures of derivatives of xanthones (**1-9**) and benzophenones (**10-11**).

2. MATERIALS AND METHODS

2.1. Synthesis

O-(1*H*-Benzotriazol-1-yl)-*N,N,N′,N′*-tetramethyluronium tetrafluoroborate (TBTU), (*S*)-(+)-α-phenylglycinol, (*R*)-(-)-leucinol, (*R*)-(-)-valinol, other reagents and solvents were commercially available materials at *pro analysis*, from Sigma-Aldrich Co (St. Louis, Missouri, USA) or Merck

(Darmstadt, Germany), and were used without further purification. ^{1}H and ^{13}C NMR were recorded on a Brucker DRX-300 spectrometer in DMSO-d_6 at room temperature. Chemical shifts are expressed in δ (ppm) values relative to TMS. Melting points were determined on a Kofler microscope and are uncorrected. The optical rotation measurements were performed on a Polartronic Universal polarimeter (ADP 410 polarimeter). IR spectra were obtained on a FTIR spectrometer Nicolet iS10 from Thermo Scientific (Waltham, MA, USA) with Smart OMNI-Transmission accessory (Software 188 OMNIC 8.3) in KBr.

2.1.1. General procedure for the synthesis of enantiomerically pure xanthone (1-9) and benzophenone (10-11) derivatives

Xanthone and benzophenone derivatives, in enantiomerically pure form, were prepared according to **Schemes 1** and **2**. The syntheses of (*R*)-enantiomers of **1** and **4**-**11**, both enantiomers of **2**, and (*S*)-enantiomers of **3** and **4** were recently reported by us (unpublished results[50]).

2.1.1.1. Synthesis of a compound with one chiral unit

The monocarboxylated compound **12** (0.25 g, 0.93 mmol) was dissolved in tetrahydrofuran (THF) (50 mL) and triethylamine (TEA) (380 µL, 2.66 mmol) was added. Then, TBTU (0.37 g, 1.11 mmol) and an appropriate enantiomerically pure reagent (1.11 mmol) were added. The mixture was stirred at room temperature for 5 h. The solvent was evaporated under reduced pressure and the crude product was dissolved in $CHCl_3$ (100 mL). This solution was washed with 1M HCl (2 × 50 mL), saturated solution of $NaHCO_3$ (2 × 50 mL) and water (3 × 50 mL). The organic layer was dried with anhydrous sodium sulphate, filtered and the solvent was evaporated under reduced pressure. The crude product was recrystallized from $CHCl_3$/MeOH to afford **1**.

***(S)-N-(2-Hydroxy-1-phenylethyl)-2-[(9-oxo-9H-xanthen-1-yl)oxy]acetamide* (1)**

(*S*)-Enantiomer of **1** was obtained as white crystals (yield: 86%); m.p. 168-170 °C ($CHCl_3$/MeOH); $[\alpha]_D^{25^{\circ}C}$ +219.0 (*c* = 0.32 mg/mL, $CHCl_3$); IR, ^{1}H NMR and ^{13}C NMR data are shown in the Supplementary Materials.

2.1.1.1. Synthesis of compounds with more than one chiral unit

Compounds **3**-**11** were prepared from suitable polycarboxylated compounds (**13**-**20**) using the same method as described for **1**, but increasing the amount of TEA, TBTU and the appropriate enantiomerically pure reagent according to the number of carboxylic groups of the chemical substrate and the stoichiometry of the reaction.

2,2'-{[(9-Oxo-9H-xanthene-3,6-diyl)bis(oxy)]bis[N-(R)-1-hydroxy-4-methylpentan-2-yl]acetamide} **(3)**

(*R*)-Enantiomer of **3** was obtained as white crystals (yield: 89%); m.p. 228-230 °C ($CHCl_3$/MeOH); $[\alpha]_D^{25^\circ C}$ -400.0 (*c* = 0.12 mg/mL, CH_3CN); IR, ^1H NMR and ^{13}C NMR data are shown in the Supplementary Materials.

2,2'-{[(9-Oxo-9H-xanthene-3,6-diyl)bis(oxy)]bis[N-(R)-1-hydroxy-3-methylbutan-2-yl]acetamide} **(4)**

(*R*)-Enantiomer of **4** was obtained as white crystals (yield: 87%); m.p. 236-238 °C ($CHCl_3$/MeOH); $[\alpha]_D^{25^\circ C}$ -417.0 (*c* = 0.12 mg/mL, CH_3CN); IR, ^1H NMR and ^{13}C NMR data are shown in the Supplementary Materials.

2,2'-{[9-Oxo-9H-xanthene-1,3-diyl)bis(oxy)]bis[N-((S)-2-hydroxy-1 phenylethyl]acetamide]} **(5)**

(*S*)-Enantiomer of **5** was obtained as white crystals (yield: 85%); m.p. 154-156 °C ($CHCl_3$/MeOH); $[\alpha]_D^{25^\circ C}$ +300.0 (*c* = 0.10 mg/mL, $CHCl_3$); IR, ^1H NMR and ^{13}C NMR data are shown in the Supplementary Materials.

2,2'-{[(9-Oxo-9H-xanthene-3,4-diyl)bis(oxy)]bis[N-(S)-2-hydroxy-1-phenylethyl]acetamide} **(6)**

(*S*)-Enantiomer of **6** was obtained as white crystals (yield: 85%); m.p. 202-204 °C ($CHCl_3$/MeOH); $[\alpha]_D^{25^\circ C}$ +300.0 (*c* = 0.10 mg/mL, $CHCl_3$); IR, ^1H NMR and ^{13}C NMR data are shown in the Supplementary Materials.

2,2',2''-{[9-Oxo-9H-xanthene-1,3,6-triyl)tris(oxy)]tris[N-(S)-2-hydroxy-1-phenylethyl]acetamide} **(7)**

(*S*)-Enantiomer of **7** was obtained as white crystals (yield: 86%); m.p. 163-165 °C ($CHCl_3$/MeOH); $[\alpha]_D^{25^\circ C}$ +285.0 (*c* = 0.21 mg/mL, $CHCl_3$); IR, ^1H NMR and ^{13}C NMR data are shown in the Supplementary Materials.

2,2',2''-{[9-Oxo-9H-xanthene-1,3,8-triyl)tris(oxy)]tris[N-(S)-2-hydroxy-1-phenylethyl]acetamide} **(8)**

(*S*)-Enantiomer of **8** was obtained as white crystals (yield: 88%); m.p. 133-136 °C ($CHCl_3$/MeOH); $[\alpha]_D^{25^\circ C}$ +300.0 (*c* = 0.10 mg/mL, $CHCl_3$); IR, ^1H NMR and ^{13}C NMR data are shown in the Supplementary Materials.

2,2',2",2"'-{[(9-Oxo-9H-xanthene-1,3,6,8-tetrayl)tetrakis(oxy)]tetrakis[N-(S)-2-hydroxy-1-phenylethyl]acetamide} **(9)**

(*S*)-Enantiomer of **9** was obtained as white crystals (yield: 77%); m.p. 173-175 °C ($CHCl_3$/MeOH); $[\alpha]_D^{25^\circ C}$ +238.0 (*c* = 0.21 mg/mL, $CHCl_3$); IR, ^1H NMR and ^{13}C NMR data are shown in the Supplementary Materials.

2,2',2",2"'-{[(Carbonylbis(benzene-4,1,3-triyl)tetrakis(oxy)]tetrakis[N-(S)-2-hydroxy-1-phenylethyl]acetamide} **(10)**

(*S*)-Enantiomer of **10** was obtained as white crystals (yield: 87%); m.p. > 350 °C ($CHCl_3$/MeOH); $[\alpha]_D^{25^\circ C}$ +308.0 (*c* = 0.13 mg/mL, $CHCl_3$); IR, ^1H NMR and ^{13}C NMR data are shown in the Supplementary Materials.

2,2'-{[(Carbonylbis(4,1-phenylene)bis(oxy)]bis[N-(S)-2-hydroxy-1-phenylethyl]acetamide} **(11)**

(*S*)-Enantiomer of **11** was obtained as white crystals (yield: 78%); m.p > 350 °C ($CHCl_3$/MeOH); $[\alpha]_D^{25^\circ C}$ +333.0 (*c* = 0.12 mg/mL, $CHCl_3$); IR, ^1H NMR and ^{13}C NMR data are shown in the Supplementary Materials.

2.2. Chromatography

The HPLC system used consisted of a Jasco model 880-PU Intelligent HPLC pump (JASCO Corporation, Tokyo, Japan) equipped with a 7125 injector (Rheodyne LCC, Rohnert Park, CA, USA) fitted with a 20 µL loop, a JASCO model 880-30 solvent mixer and a 875-UV intelligent UV/Vis detector. Data acquisition was performed on Chromatography Station for Windows, version 1.7 DLL. The chromatographic columns used were Whelk-O1® (*S,S*) (25 cm × 4.6 mm i.d., 5 µm particle size, 100-A° pore size) from Regis Technologies, Inc. (Morton Grove, IL, USA) and Lux® Celullose-2 (15 cm × 4.6 mm i.d., 3 µm particle size, 100A° pore size) from Phenomenex. HPLC grade EtOH, MeOH and CH_3CN were purchased from Sigma-Aldrich Co (St. Louis, Missouri, USA). The stock solution of (*R*) and (*S*) enantiomers of xanthone and benzophenone derivatives were prepared by dissolution in EtOH at concentration of 1 mg/mL. Working solutions of enantiomeric mixtures were further prepared by mixing aliquots of each enantiomer at a concentration of 10 µg/mL. The elution order and enantiomeric ratio (e.r.) determinations were performed with the stock solutions of each enantiomer diluted at the concentration of 10 µg/mL. The mobile phases were prepared in a volume/volume ratio and degassed in an ultrasonic bath for 15 min before use. Analyses were performed at room temperature in isocratic mode. The flow rate used was 0.5 or 1.0 mL/min, and the chromatograms were monitored by UV at a wavelength of 254 nm. The sample injections (10 µL) were carried out in triplicate. The column void time (t_o) was

considered to be equal to the peak of the solvent front and was taken from each particular run. The e.r. was determined by the relative percentages of the peak areas according to [e.r. (%) = 100 × ([*R*]/([*R*]+[*S*]) or 100 × ([*S*]/([*S*]+[*R*]), where [*S*] and [*R*] are the area of the peak of each enantiomer.[51]

2.3. Computational

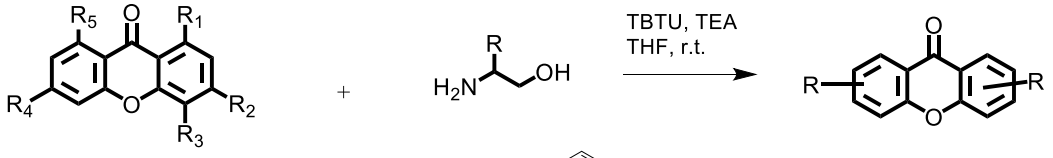
The structure of the selector of (*S,S*)-Whelk-O1 CSP was obtained from the Cambridge Crystallographic Data Centre (CCDC, UK) (deposition number 273851).[52,53] The enantiomerically pure xanthone and benzophenone derivatives were subjected to energy minimization by the Austin Model 1 (AM1) method with the Polak-Ribiere algorithm.[54] Docking simulations between the (*S,S*)-Whelk-O1 selector and the enantiomers were undertaken in AutoDock Vina (Molecular Graphics Lab, La Jolla, CA, USA).[55] AutoDock Vina considered the selector conformation as a rigid unit, while the ligands were allowed to be flexible and adaptable to the selector. Vina searched for the lowest binding affinity conformations and returned nine different conformations for each enantiomer. The lowest binding energy docking poses of each enantiomer were chosen. AutoDock Vina was run using exhaustiveness of 8 and a grid box with dimensions 21.0, 22.0, 24.0 engulfing the selector was built. PyMol v 1.3 (Schrodinger, New York, NY, USA)[56] was used for the visualization of the results and graphical representations.

3. RESULTS AND DISCUSSION

3.1. Synthesis

The synthetic strategy used to obtain the chiral derivatives of xanthones (**1-9**) and benzophenones (**10-11**), in enantiomerically pure form, is illustrated in **Schemes 1** and **2**. According to previous works,[44,45] the reaction of nine different carboxylated derivatives (**12-20**) with enantiomerically pure building blocks using TBTU as a coupling reagent offered an efficient method for preparing this type of compounds, in 77-89% yields. The synthetic routes for preparation of **12-20** were recently reported by us (unpublished results[50]). These compounds were selected because carboxyxanthones are not only suitable molecular scaffolds for synthesis of analogues and derivatives[57] but also give a possibility of preparing compounds comprising one, two, three and four chiral moieties in diverse positions of the xanthone scaffold. The employed chiral building blocks (**21-23**) were commercially available in enantiomerically pure form. In this study, we reported the synthesis of (*S*)-enantiomers of **1** and **4**-**11** as well as (*R*)-enantiomers of **3** and **4**. The IR, ^{1}H NMR and ^{13}C NMR data of these compounds are also described herein for the first time (see Supplementary Materials). The

syntheses of their enantiomeric pairs and both enantiomers of **2** were also developed (unpublished results[50]).



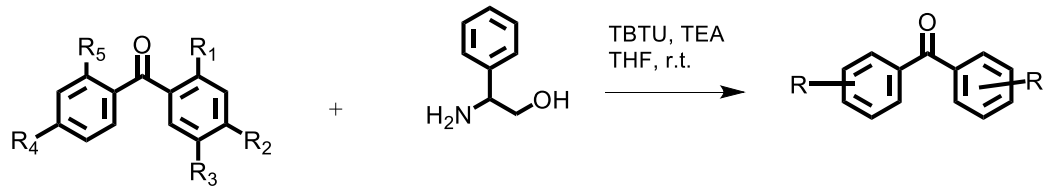
12 $R_1 = OCH_2COOH$, $R_2 = R_3 = R_4 = R_5 = H$
13 $R_1 = R_3 = R_5 = H$, $R_2 = R_4 = OCH_2COOH$
14 $R_1 = R_2 = OCH_2COOH$, $R_3 = R_4 = R_5 = H$
15 $R_1 = R_4 = R_5 = H$, $R_2 = R_3 = OCH_2COOH$
16 $R_1 = R_2 = R_4 = OCH_2COOH$, $R_3 = R_5 = H$
17 $R_1 = R_2 = R_5 = OCH_2COOH$, $R_3 = R_4 = H$
18 $R_1 = R_2 = R_4 = R_5 = OCH_2COOH$, $R_3 = H$

21 R= 

22 $R = CH_2CH(CH_3)_2$
23 $R = CH(CH_3)_2$

1-9

SCHEME 1. General synthetic route of chiral derivatives of xanthones **1-9**.



19 $R_1 = R_2 = R_4 = R_5 = OCH_2COOH$, $R_3 = H$
20 $R_1 = R_3 = R_5 = H$, $R_2 = R_4 = OCH_2COOH$

21

10-11

SCHEME 2. General synthetic route of chiral derivatives of benzophenones **10-11**.

3.2. Chromatography

One of the major aims of this study concerned the separation of the enantiomeric mixtures of the synthetized compounds by liquid chromatography for further determination of the enantiomeric purity. The high enantioselectivity and resolution observed in previous works,[40,41] for a series of chiral derivatives of xanthones on (*S*,*S*)-Whelk-O1 CSP using MeOH and CH_3CN (50:50 *v/v*) as mobile phase, led us to choose these chromatographic conditions. The chromatographic data obtained for all the enantiomeric mixtures is shown in **Table 1**. Nine out of eleven enantiomeric mixtures were successfully enantioseparated on (*S,S*)-Whelk-O1 CSP, with α values ranging from 1.35 to 4.15, and Rs values ranging from 2.22 to 13.87. Among all the tested enantiomeric mixtures, the one comprising three chiral moieties in positions C-1, C-3 and C-8 of the xanthone scaffold (**8**) (**Figure 2**) presented the best chromatographic parameters with α and Rs values of 4.15 and 13.87, respectively. It must be noted that, besides

the good α and Rs values obtained, all the enantioseparated compounds were eluted before 10 min.

Table 1. Separation performance of (*S,S*)-Whelk-O1 CSP for the enantiomeric mixtures of xanthone and benzophenone derivatives (**1-11**).

Enantiomeric mixture	k_1	k_2	α	R_s
1	0.63	0.85	1.35	2.68
2	0.72	1.77	2.46	9.38
3	0.56	0.61	1.09	<1.00
4	0.69	0.69	1.00	ND
5	0.61	1.33	2.18	7.33
6	0.53	1.21	2.28	7.28
7	0.61	1.90	3.11	11.03
8	0.60	2.49	4.15	13.87
9	0.42	0.62	1.48	2.22
10	0.39	0.62	1.57	2.40
11	0.43	0.77	1.79	5.79

Mobile phase: MeOH:CH_3CN (50:50 *v/v*), Flow rate 1.0 mL/min, UV Detection at 254 nm. ND: not determined.

Based on the separation profiles and chromatographic data achieved, the different enantiomeric mixtures were divided in four groups (**Figure 3**).

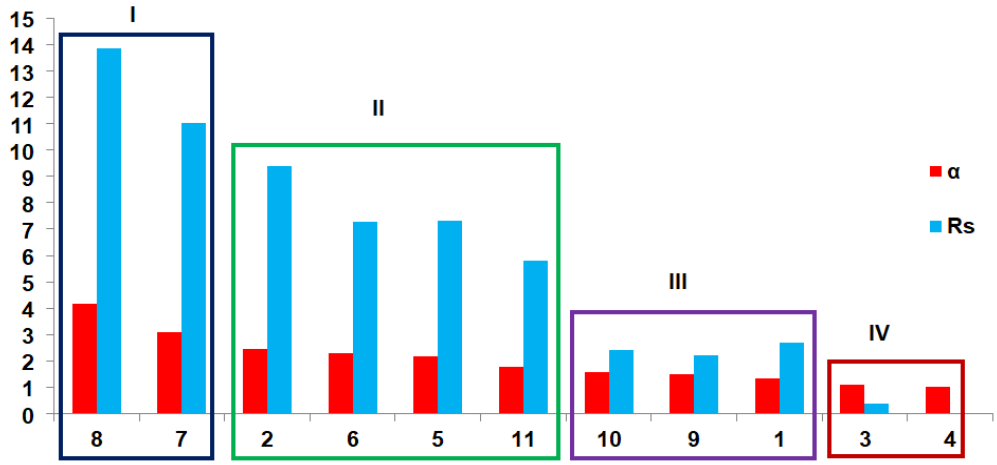


FIGURE 3 Schematic description of the overall performance of enantiomeric mixtures of xanthone and benzophenone derivatives.

In brief, group I contains the enantiomeric mixtures **7** and **8**, which showed the best chromatographic data (α > 3.11 and Rs > 11.03). Structurally, the enantiomers of both mixtures comprise three chiral moieties, with an aromatic ring linked to the stereogenic centers, in different positions of the xanthone scaffold (**Figure 2**). **Figure 4** displays the chromatograms obtained for both enantiomeric mixtures of this group.

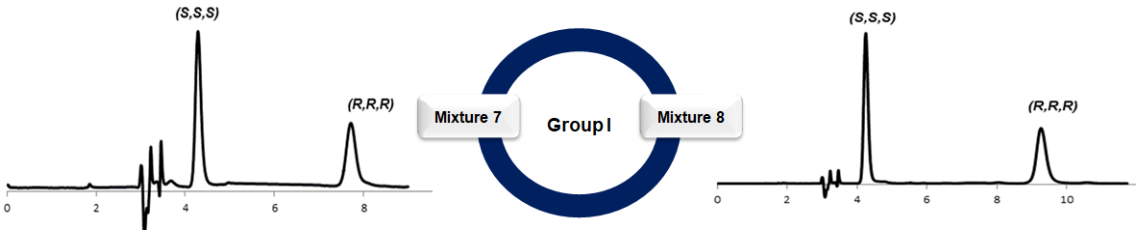


Figure 4 Chromatograms of enantiomeric mixtures of group I (**7** and **8**) on (*S,S*)-Whelk-O1®.

Group II consists of four enantiomeric mixtures (**2**, **5**, **6** and **11**), all of which having two chiral moieties, with an aromatic ring linked to the stereogenic centers, in different positions of the central scaffold (**Figure 2**). Although excellent chromatographic results, enantioselectivity and resolution were slightly lower when compared to the previous group (α and Rs values ranging from 1.79 to 2.46 and from 5.79 to 9.38, respectively). The chromatograms obtained for all the enantiomeric mixtures of this group are shown in **Figure 5**.

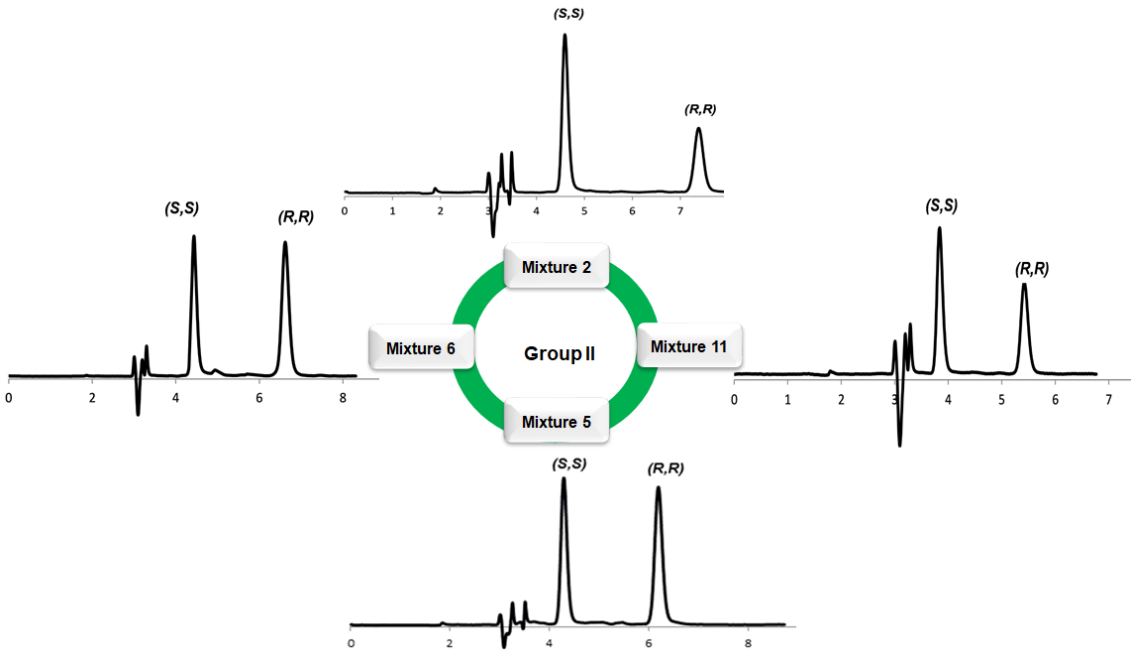


Figure 5 Chromatograms of enantiomeric mixtures of group II (**2**, **5**, **6** and **11**) on (*S,S*)-Whelk-O1®.

Group III includes the enantiomeric mixtures **1**, **9** and **10**, which exhibited similar enantioselectivity and resolution, with α and Rs values ranging from 1.35 to 1.57 and from 2.22 to 2.68, respectively. Curiously, the enantiomers of this group comprise either one or four chiral moieties, with an aromatic ring linked to the stereogenic centers, in different positions of the central scaffold (**Figure 2**). **Figure 6** shows the chromatograms obtained for the enantiomeric mixtures of this group.

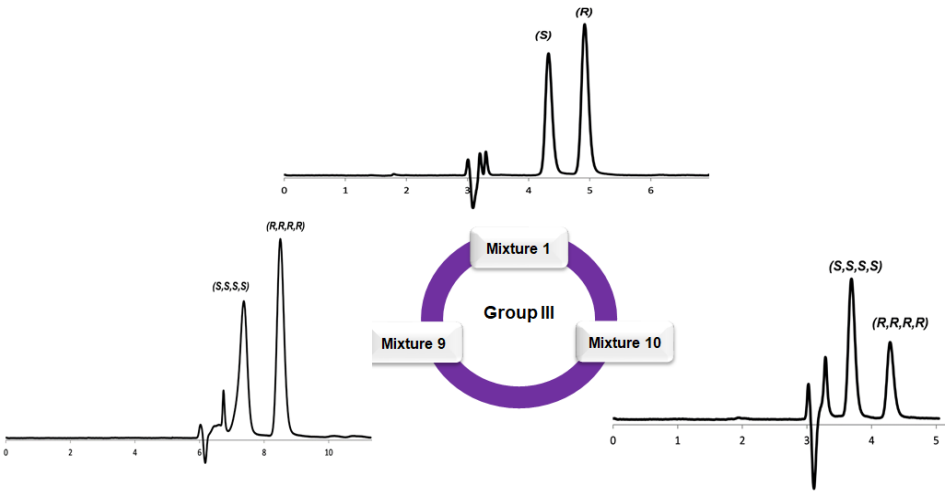


Figure 6 Chromatograms of enantiomeric mixtures of group III (**1**, **9** and **10**) on (*S,S*)-Whelk-O1®.

Finally, the two enantiomeric mixtures showing no or poor resolution (Rs <1.00), i.e. **3** and **4**, were included in group IV. Structurally, the enantiomers of this group comprise two chiral moieties in different positions of the central scaffold such as the compounds of group II, however, instead of an aromatic ring linked to the stereogenic centers, they have an alkyl chain (**Figure 2**). **Figure 7** shows the chromatograms obtained for both enantiomeric mixtures of this group.

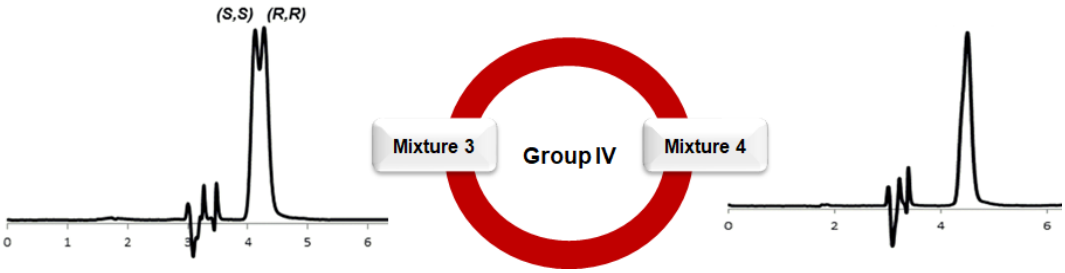


Figure 7 Chromatograms of enantiomeric mixtures of group IV (**3** and **4**) on (*S,S*)-Whelk-O1®.

The overall results confirmed that the nature of the substituents linked to the stereogenic center(s) and the number of chiral moieties in the central aromatic scaffold, either xanthone or benzophenone, played a key role for chiral recognition. As expected, all xanthone and benzophenone derivatives comprising an aromatic ring linked to the stereogenic center(s) (**1**-**2** and **5**-**11**, **Figure 2**) were successfully enantioseparated on (*S,S*)-Whelk-O1 CSP. Based on the literature[58] and on our own experience,[40] we have already anticipated that (*S,S*)-Whelk-O1 CSP could not efficiently separate the enantiomers of compounds comprising an alkyl chain linked to the stereogenic center(s) (**3** and **4**, **Figure 2**). Actually, the enantiomers that tend to be well resolved on this CSP typically exhibit an aromatic moiety in addition to a hydrogen bonding acceptor close to the stereogenic center.[31,58] As to the number of chiral moieties linked to the central aromatic scaffold, three was the optimal number affording the best resolution. Xanthone and benzophenone derivatives having two chiral moieties also presented good chromatographic results, followed by the compounds having either one or four chiral moieties, whose results were not so notable. Nevertheless, the position of the chiral moieties in the xanthone scaffold did not significantly interfere with the enantioselectivity. Additionally, it was found that the nature of the central aromatic core, xanthone or benzophenone, could also be an important structural characteristic for enantiorecognition mainly for the enantiomeric mixtures of compounds comprising two chiral moieties (**2** and **11**, **Figure 2**). For example, higher enantioselectivity (α = 2.46) and resolution (Rs = 9.38) were obtained for enantiomeric mixture **2**, having a xanthone scaffold, while for the benzophenone-analogue enantiomeric mixture (**11**) the α and Rs values were 1.79 and 5.79, respectively. In this case, the rigidity of the *quasi*-planar structure of the xanthone scaffold played an important role.

The same chromatographic conditions were used to evaluate the enantiomeric purity of the enantioseparated mixtures (**1**-**2** and **5**-**11**). For enantiomers comprising an alkyl chain linked to the stereogenic centers (**3** and **4**), the e.r. values were determined using the Lux® Celullose-2 CSP and 100% EtOH as mobile phase. This CSP was chosen due to the vast applicability and efficiency of polysaccharide-based CSPs for different classes of chiral compounds,[59-61] including xanthone derivatives.[62-64] Good enantioselectivity, α values of 2.16 and 1.86, and resolution, Rs values of 3.38 and 2.93, were obtained for enantiomeric mixtures **3** and **4**, respectively. The chromatograms are presented in **Figure S1** (Supplementary Materials). Regardless the CSP used, the e.r. values were higher than 99% for all the enantiomers. Moreover, in all the mixtures, the enantiomers comprising one or more stereogenic centers with (*R*)-configuration were more retained. The elution order was determined by injecting the enantiomers of each mixture separately.

3.3. Docking studies

Another key aim of this work was to shed light on the chiral recognition mechanism to better understand the chromatographic data, by performing molecular docking studies. Additionally, by analysis of the interactions between the tested enantiomers and the (*S*,*S*)-Whelk-O1 CSP, we expected to confirm the role of the structural characteristics of the compounds for enantiodiscrimination.

The values of binding affinity for the best scoring, i.e. the lowest binding affinity conformation, for all enantiomers, are shown in **Table 2**. The energy difference of the lowest binding affinity conformation of the (*S*)-enantiomer:CSP complex *versus* the (*R*)-enantiomer:CSP complex was used to determine the energy difference values. Docking scores ranging from -4.4 to -6.4 Kcal.mol^{-1} and energy differences from -0.1 to -1.8 Kcal.mol^{-1} were obtained.

Table 2. Calculated binding energy values of the top ranked conformations of each enantiomer of xanthone and benzophenone derivatives on (*S,S*)-Whelk-O1®.

Ligand (enantiomers)	Binding energy (kcal/mol)	Energy difference (kcal/mol)	Elution order
(*R*)-**1**	-5.4	-0.8	Second
(*S*)-**1**	-4.6		First
(*R,R*)-**2**	-6.4	-0.1	Second
(*S,S*)-**2**	-6.3		First
(*R,R*)-**3**	-5.0	-0.5	Second
(*S,S*)-**3**	-4.5		First
(*R,R*)-**4**	-4.9	0.0	-
(*S,S*)-**4**	-4.9		
(*R,R*)-**5**	-5.6	-0.2	Second
(*S,S*)-**5**	-5.4		First
(*R,R*)-**6**	-5.7	-1.1	Second
(*S,S*)-**6**	-4.6		First
(*R,R,R*)-**7**	-5.6	-0.2	Second
(*S,S,S*)-**7**	-5.4		First
(*R,R,R*)-**8**	-5.6	-1.8	Second
(*S,S,S*)-**8**	-3.8		First
(*R,R,R,R*)-**9**	-5.3	-0.4	Second
(*S,S,S,S*)-**9**	-4.9		First
(*R,R,R,R*)-**10**	-5.0	-0.6	Second
(*S,S,S,S*)-**10**	-4.4		First
(*R,R*)-**11**	-6.1	-0.3	Second
(*S,S*)-**11**	-5.8		First

As expected, the binding energies were different for the enantiomers of the same mixture, indicating that they have different affinities for the (*S*,*S*)-Whelk-O1 selector–which is in accordance with the chromatographic data (separations were achieved, α = 1.35 to 4.15). The only exception was for enantiomeric mixture **4** (-4.9 Kcal.mol^{-1} for both enantiomers) which is in agreement with the experimental results (no separation was achieved, α = 1.00). It is also important to highlight that the calculated binding affinity differences between the enantiomers of the same enantiomeric mixture are also related to the magnitude of the experimental separation factors. Accordingly, the enantiomeric mixture **8**, which presented the best chromatographic parameters also showed the higher binding affinity difference (-1.8 Kcal.mol^{-1}). Computational simulations using the PyRx/AutoDock Vina led to a successful reproduction of enantioselectivity and elution order for all the tested enantiomeric mixtures, with a 100% success rate between docking scores and experimental chromatographic data.

Figure 8 illustrates representative examples of enantiomers of the same enantiomeric mixture docked onto the (*S*,*S*)-Whelk-O1 selector, allowing the visualization of the docking pose differences. The selection included one enantiomeric mixture from each group (**Figure 3**).

Considering the enantiomeric mixture **7** of group I, the (*R*)-enantiomer binds more tightly with the chiral selector as there are more intermolecular interactions established when compared with the (*S*)-enantiomer. Accordingly, several face-to-face π-stacking interactions were established between the (*R*)-enantiomer and the selector, specifically between the xanthone scaffold and the 3,5-dinitrophenyl group of the selector as well as between the aromatic rings bonded to the stereogenic centers and the phenanthryl group of the selector (**Figure 8A**). In addition, two hydrogen interactions were also established. It was found that both nitro substituents of the 3,5-dinitrophenyl group of the selector are involved: one of them establishes a hydrogen interaction with the NH amide of one of the side chains of the (*R*)-enantiomer, whereas the other establishes the same type of interaction with the hydroxyl group of another side chain. The (*S*)-enantiomer has lower affinity for this selector because only π-stacking interactions were established (not shown).

As shown in **Figure 8B**, although the docking poses of the enantiomers of the mixture **11** (group II) are different, both enantiomer-CSP complexes display similar intermolecular interactions, namely two hydrogen interactions and two π-stacking interactions. The amide carbonyl group of the selector participates in all the hydrogen interactions. The polar groups of the enantiomers that are involved on such interactions are the hydroxyl group of one of the side chains and the NH amide of another. Additionally, the phenanthryl group of the selector establishes π-stacking interactions either with one of the aromatic rings of the benzophenone scaffold or with one the aromatic ring bonded to the stereogenic center of the (*R*)-enantiomer. The first π-stacking interaction is also observed for the (*S*)-enantiomer. Nevertheless, instead of the phenanthryl group of the selector, one the aromatic ring bonded to the stereogenic center

establishes the same type of interaction with the 3,5-dinitrophenyl group of the selector. This justifies the observed enantioselectivity.

Regarding the enantiomeric mixture **1** of group III, the enantiomers top docking poses are located on opposite sides of the selector cleft. The (*R*)-enantiomer presents higher binding affinity because, in addition to face-to-face π-stacking interactions, its NH amide establishes a hydrogen interaction with one nitro substituent of the 3,5-dinitrophenyl group of the selector (**Figure 8C**). The (*S*)-enantiomer only establishes π-stacking interactions, revealing lower affinity for this selector.

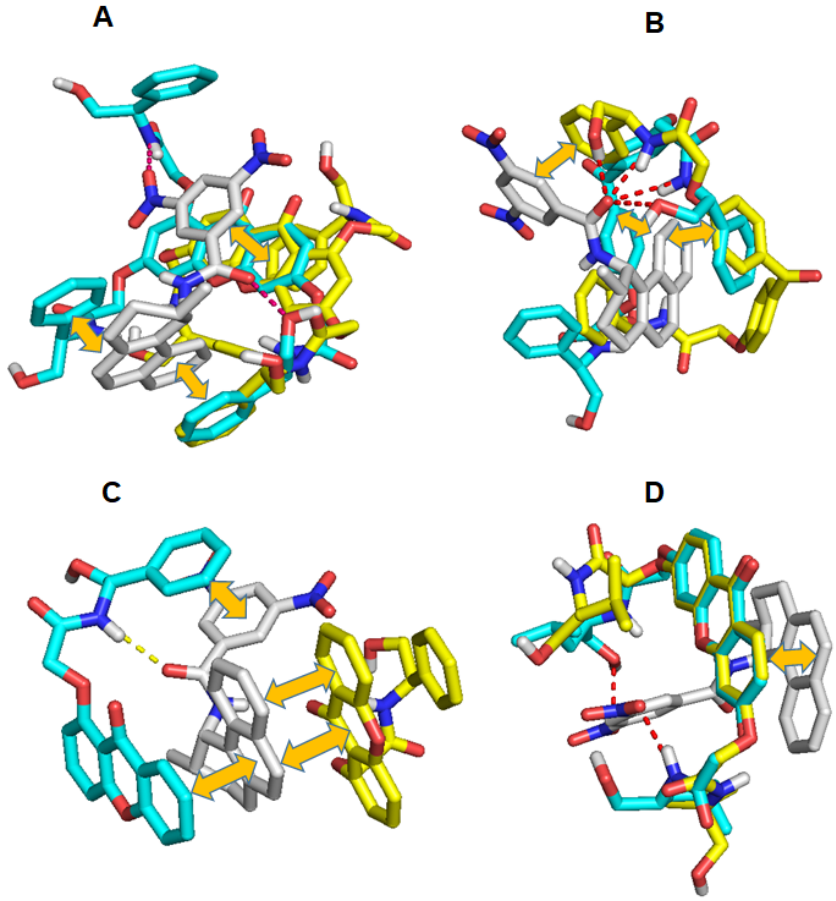


FIGURE 8. The most stable conformations of enantiomers **7** from group I (**A**), enantiomers **11** from group II (**B**), enantiomers **1** from group III (**C**), and enantiomers **3** from group IV (**D**), docked onto (*S,S*)-Whelk-O1® selector (gray). (*R*) and (*S*) enantiomers are represented as cyan and yellow sticks, respectively. Hydrogen interactions and π-stacking interactions are represented as a red broken line and a yellow double arrow, respectively.

Finally, both enantiomers of the enantiomeric mixture **3** (group IV) adopt similar conformations inside the cleft of the (*S*,*S*)-Whelk-O1 selector (**Figure 8D**). They establish similar intermolecular interactions, specifically hydrogen interactions and π-stacking interactions between the xanthone scaffold and the selector's phenanthryl group. This justifies the observed poor chromatographic resolution. Moreover, in addition to other intermolecular

interactions, the π-stacking interactions that may be established between the phenyl ring bonded to the stereogenic centers and the aromatic moiety of the selector are proved to be crucial for enantiorecognition, as observed for the more retained enantiomers representative of the other groups (**Figure 8A-C**).

4. Conclusions

The (*S,S*)-Whelk-O1® and Lux® Celullose-2 CSPs were used for enantioseparation and determination of enantiomeric purity of new synthetized xanthone and benzophenone derivatives comprising one or more chiral moieties. For both CSPs, polar organic elution mode were used and all the enantiomeric ratio (e.r.) values were higher than 99%. It was found that the nature and number of the chiral moieties positioned in the central aromatic scaffold play an important role in chiral recognition mechanism. Among all the tested enantiomeric mixtures, those comprising three chiral moieties with an aromatic ring bonded to the stereogenic centers presented the best chromatographic results on (*S,S*)-Whelk-O1® CSP, with α values ranging from 3.11 to 4.15 and Rs values ranging from 11.03 to 13.87. The simultaneous π-stacking interactions established by the aromatic ring at the stereogenic center and by the xanthone scaffold (with aromatic moieties of the selector) in addition to hydrogen interactions are shown to be essential for enantioselective recognition.

The results of the present study fulfilled the initial aims of this work, being an important contribution to enlarge the knowledge of the mechanism of chiral molecular recognition of (*S,S*)-Whelk-O1® CSP as well as to have a better insight of the structural requirements of the analytes to be enantioseparated.

Acknowledgements

This work was supported by the Strategic Funding UID/Multi/04423/2019 through national funds provided by FCT—Foundation for Science and Technology and European Regional Development Fund (ERDF), through the COMPETE – Programa Operacional Factores de Competitividade (POFC) program in the framework of the program PT2020; the project PTDC/MAR-BIO/4694/2014 (reference POCI-01-0145-FEDER-016790 and 3599-PPCDT), co-financed by COMPETE 2020, under the PORTUGAL 2020 Partnership Agreement, through the European Regional Development Fund (ERDF), and CHIRALBIOACTIVE-PI-3RL-IINFACTS-2019. Y.Z. Phyo thanks the Erasmus Mundus Action 2 (Lotus Plus project) for a PhD's scholarship.

REFERENCES

1. Mannschreck A, Kiesswetter R, von Angerer E. Unequal activities of enantiomers via biological receptors: Examples of chiral drug, pesticide, and fragrance molecules. *J Chem Ed* 2007;84(12):2012-2017.
2. Triggle DJ. Stereoselectivity of drug action. *Drug Discov Today* 1997;2(4):138-147.
3. Cordato DJ, Mather LE, Herkes GK. Stereochemistry in clinical medicine: A neurological perspective. Journal of Clinical Neuroscience 2003;10(6):649-654.
4. Smith SW. Chiral toxicology: It's the same thing only different. *Toxicol Sci* 2009;110(1):4-30.
5. Silva B, Fernandes C, Tiritan ME, Pinto MMM, Valente MJ, Carvalho M, de Pinho PG, Remião F. Chiral enantioresolution of cathinone derivatives present in “legal highs”, and enantioselectivity evaluation on cytotoxicity of 3,4-methylenedioxypyrovalerone (MDPV). *Forensic Toxicol* 2016:1-14.
6. Silva B, Fernandes C, de Pinho PG, Remião F. Chiral resolution and enantioselectivity of synthetic cathinones: A brief review. *J Anal Toxicol* 2018;42(1):17-24.
7. Investigation of chiral active substances. Directive 75/318/EEC 1993.
8. FDA. FDA's policy statement for the development of new stereoisomeric drugs. Fed. Reg. 1992;57:FR 22249.
9. Shimazawa R, Nagai N, Toyoshima S, Okuda H. Present state of new chiral drug development and review in Japan. *J Health Sci* 2008;54(1):23-29.
10. Dawood AWH, de Souza ROMA, Bornscheuer UT. Asymmetric synthesis of chiral halogenated amines using amine transaminases. *Chem Cat Chem* 2018(10):951-955.
11. Chen J, Xu X, He Z, Qin H, Sun W, Fan B. Nickel/Zinc iodide co-catalytic asymmetric [2+2] cycloaddition reactions of azabenzonorbornadienes with terminal alkynes. *Adv Synth Catal* 2018(360):427-431.
12. Kirkpatrick AD, Fain M, Yang J, Trehy M. Enantiomeric impurity analysis using circular dichroism spectroscopy with United States Pharmacopeia Liquid Chromatographic Methods. *J Pharm Biomed Anal* 2018(156):366-371.
13. Batista ANL, dos Santos FM, Batista JM, Cass QB. Enantiomeric mixtures in natural product chemistry: Separation and absolute configuration assignment. *Molecules* 2018(23):1-18.
14. Miller L, Potter M. Preparative chromatographic resolution of racemates using HPLC and SFC in a pharmaceutical discovery environment. *J Chromatogr B Anal Technol Biomed Life Sci* 2008(875):230-236.
15. Leek H, Andersson S. Preparative scale resolution of enantiomers enables accelerated drug discovery and development. *Molecules* 2017(22):1-9.

16. Wu S, Harada S, Morikawa T, Nishidda A. Enantioselective total synthesis of a natural hydrocarbazolone alkaloid, identification of its stereochemistry, and revision of its spectroscopic data. *Tetrahedrom Asymmetr* 2017(28):1083-1088.
17. Gholami H, Zhang J, Anyika M, Borhan B. Absolute stereochemical determination of asymmetric sulfoxides via central to axial induction of chirality. *Org Lett* 2017(19):1722-1725.
18. Toki H, Ichikawa T, Mizuno-Yasuhira A, Yamaguchi J. A rapid and sensitive chiral LC-MS/MS method for the determination of ketamine and norketamine in mouse plasma, brain and cerebrospinal fluid applicable to the stereoselective pharmacokinetic study of ketamine. *J Pharm Biomed Anal* 2018(148):288-297.
19. Jiao H, Li Y, Sun L, Zhang H, Yu L, Yuan Z, Xie L, Chen J, Wang Y. A chiral LC-MS/MS method for the enantioselective determination of *R*-(+)- and *S*-(-)-pantoprazole in human plasma and its application to a pharmacokinetic study of *S*-(-).pantoprazole sodium injection. *Biomed Chromatogr* 2017(31):1-8.
20. Cosimelli B, Greco G, Laneri S, Novellino E, Sacchi A, Collina S, Rossi D, Cosconati S, Barresi E, Taliani S and others. Studies on enantioselectivity of chiral 4-acetylamino-6-alkyloxy-2-alkylthiopyrimidines acting as antagonists of the human adenosine receptor. *Med Chem Comm* 2018(9):81-86.
21. George R, Haywood A, Good P, Hennig S, Khan S, Norris R, Hardy J. Can saliva and plasma methadone concentrations be used for enantioselective pharmacokinetic and pharmacodynamic studies in patients with advanced cancer? *Clin Ther* 2017(39):1840-1848.
22. Ribeiro J, Tiritan ME, Pinto MMM, Fernandes C. Chiral stationary phases for liquid chromatography based on chitin- and chitosan-derived marine polysaccharides. *Symmetry* 2017;9(190):1-28
23. Kalíková K, Riesová M, Tesařová E. Recent chiral selectors for separation in HPLC and CE. *Cent Eur J Chem* 2011:1-22.
24. Tang M, Zhang J, Zhuang S, Liu W. Development of chiral stationary phases for high-performance liquid chromatographic separation. *TrAC - Trends Anal Chem* 2012;39:180-194.
25. Teixeira J, Tiritan ME, Pinto MMM, Fernandes C. Chiral stationary phases for liquid chromatography: Recent developments. *Molecules* 2019; 24,865; doi:10.3390/molecules24050865.
26. Fernandes C, Phyo YZ, Silva AS, Tiritan ME, Kijjoa A, Pinto MMM. Chiral Stationary Phases Based on Small Molecules: An Update of the Last 17 Years. *Sep Purif Rev* 2018;47(2):89-123.

27. Lämmerhofer M. Chiral recognition by enantioselective liquid chromatography: Mechanisms and modern chiral stationary phases. *J Chromatogr A* 2010;1217(6):814-856.
28. Pirkle WH, Welch CJ. An improved chiral stationary phase for the chromatographic separation of underivatized naproxen enantiomers. *J Liq Chromatogr* 1992;15(11):1947-1955.
29. Perera RWH, Lough WJ. Assessment of chiral stationary phases for suitability for combined enantiomeric impurity/related substances assays. *J Chromatogr A* 2011;1218(48):8655-8663.
30. Badaloni E, Cabri W, Ciogli A, D'Acquarica I, Deias R, Gasparrini F, Giorgi F, Kotoni D, Villani C. Extending the use of "Inverted Chirality Columns Approach" for enantiomeric excess determination in absence of reference samples: Application to a water-soluble camptothecin derivative. *J Chromatogr A* 2010;1217(7):1024-1032.
31. Fernandes C, Tiritan ME, Pinto M. Small molecules as chromatographic tools for HPLC enantiomeric resolution: Pirkle-type chiral stationary phases evolution. *Chromatographia* 2013;76(15-16):871-897.
32. Dungelov J, Lehotay J, Cizmarik J, Armstrong D. Study of the Mechanism of Enantioseparation. IV. Study of Enantioseparation of Some Derivatives of Phenylcarbamic Acid Using π-Complex Stationary Phase in HPLC. *J Liq Chromatogr Relat Technol* 2003;26(14):2331-2350.
33. Asnin LD, Guiochon G. The adsorption of Naproxen enantiomers on the chiral stationary phase (R, R)-Whelk-O1 under reversed-phase conditions: The effect of mobile phase composition. *J Chromatogr A* 2010;1217(17):2871-2878.
34. Welch CJ, Szczerba T, Perrin SR. Some recent high-performance liquid chromatography separations of the enantiomers of pharmaceuticals and other compounds using the Whelk-O 1 chiral stationary phase. *J Chromatogr A* 1997;758(1):93-98.
35. Del Rio A, Hayes JM, Stein M, Piras P, Roussel C. Theoretical reassessment of Whelk-O1 as an enantioselective receptor for 1-(4-halogeno-phenyl)-1-ethylamine derivatives. *Chirality* 2004;16(S1):S1-S11.
36. Zhao C, Cann NM. The docking of chiral epoxides on the Whelk-O1 stationary phase: A molecular dynamics study. *J Chromatogr A* 2007;1149(2):197-218.
37. Scriba GKE. Chiral recognition in separation science – an update. *J Chromatogr A* 2016;1467:56-78.
38. Phyo YZ, Cravo S, Palmeira A, Tiritan ME, Kijjoa A, Pinto MMM, Fernandes C. Enantiomeric resolution and docking studies of chiral xanthonic derivatives on chirobiotic columns. *Molecules* 2018;23(1).

39. Fernandes C, Tiritan ME, Cass Q, Kairys V, Fernandes MX, Pinto M. Enantioseparation and chiral recognition mechanism of new chiral derivatives of xanthones on macrocyclic antibiotic stationary phases. *J Chromatogr A* 2012;1241:60-68.
40. Fernandes C, Palmeira A, Santos A, Tiritan ME, Afonso C, Pinto MM. Enantioresolution of chiral derivatives of xanthones on (S,S)-Whelk-O1 and l -phenylglycine stationary phases and chiral recognition mechanism by docking approach for (S,S)-Whelk-O1. *Chirality* 2013;25(2):89-100.
41. Carraro ML, Palmeira A, Tiritan ME, Fernandes C, Pinto MMM. Resolution, determination of enantiomeric purity and chiral recognition mechanism of new xanthone derivatives on (S,S)-Whelk-O1 stationary phase. *Chirality* 2017:1–10.
42. Araújo J, Fernandes C, Pinto M, Elizabeth Tiritan M. Chiral derivatives of xanthones with antimicrobial activity. *Molecule*s 2019;24(2).
43. Fernandes C, Carraro ML, Ribeiro J, Araújo J, Tiritan ME, Pinto MMM. Synthetic chiral derivatives of xanthones: Biological activities and enantioselectivity studies. *Molecules* 2019;24(4), 791, doi:10.3390/molecules24040791.
44. Fernandes C, Masawang K, Tiritan ME, Sousa E, De Lima V, Afonso C, Bousbaa H, Sudprasert W, Pedro M, Pinto MM. New chiral derivatives of xanthones: Synthesis and investigation of enantioselectivity as inhibitors of growth of human tumor cell lines. *Bioorg Med Chem* 2014;22(3):1049-1062.
45. Fernandes C, Oliveira L, Tiritan ME, Leitao L, Pozzi A, Noronha-Matos JB, Correia-De-Sá P, Pinto MM. Synthesis of new chiral xanthone derivatives acting as nerve conduction blockers in the rat sciatic nerve. *Eur J Med Chem* 2012;55:1-11.
46. Fernandes C, Palmeira A, Ramos II, Carneiro C, Afonso C, Tiritan ME, Cidade H, Pinto PCAG, Saraiva MLMFS, Reis S and others. Chiral derivatives of xanthones: Investigation of the effect of enantioselectivity on inhibition of cyclooxygenases (COX-1 and COX-2) and binding interaction with human serum albumin. *Pharmaceuticals* 2017;10(2) 50; doi:10.3390/ph10020050.
47. Fernandes C, Tiritan ME, Cravo S, Phyo YZ, Kijjoa A, Silva AMS, Cass QB, Pinto MMM. New chiral stationary phases based on xanthone derivatives for liquid chromatography. *Chirality* 2017;29(8):430-442.
48. Azevedo CMG, Afonso CMM, Pinto MMM. Routes to xanthones: An update on the synthetic approaches. *Curr Org Chem* 2012;16(23):2818-2867.
49. Sousa ME, Pinto MMM. Synthesis of xanthones: An overview. *Curr Med Chem* 2005;12(21):2447-2479.
50. Phyo YZ, Teixeira J, Tiritan ME, Cravo S, Palmeira A, Gales L, Silva AMS, Pinto MMM, Kijjoa A, Fernandes C. New chiral stationary phases for liquid chromatography based

on small molecules: development, enantioresolution evaluation and chiral recognition mechanisms. *Chirality* 2019 (submitted).

51. Tiritan ME, Fernandes C, Maia AS, Pinto M, Cass QB. Enantiomeric ratios: Why so many notations? *J Chromatogr A* 2018;1569:1-7.
52. Koscho ME, Pirkle WH. Investigation of a broadly applicable chiral selector used in enantioselective chromatography (Whelk-O 1) as a chiral solvating agent for NMR determination of enantiomeric composition. *Tetrahedron: Asymmetry* 2005;16(20):3345-3351.
53. Koscho ME, Spence PL, Pirkle WH. Chiral recognition in the solid state: crystallographically characterized diastereomeric co-crystals between a synthetic chiral selector (Whelk-O1) and a representative chiral analyte. *Tetrahedron: Asymmetry* 2005;16(19):3147-3153.
54. Li D-H, Zhang L, Zhou W. A descent modified Polak–Ribière–Polyak conjugate gradient method and its global convergence. *IMA J Numer Anal* 2006;26(4):629-640.
55. Trott O, Olson AJ. AutoDock Vina: improving the speed and accuracy of docking with a new scoring function, efficient optimization, and multithreading. *J comput chem* 2010;31(2):455-461.
56. Lill MA, Danielson ML. Computer-aided drug design platform using PyMOL. *J Comput Aided Mol Des* 2010;25(1):13-9.
57. Ribeiro J, Veloso C, Fernandes C, Tiritan ME, Pinto MMM. Carboxyxanthones: Bioactive agents and molecular scaffold for synthesis of analogues and derivatives. *Molecules* 2019;24(1), 180, doi:10.3390/molecules24010180.
58. Pirkle WH, Welch CJ. Use of simultaneous face to face and face to edge π-π interactions to facilitate chiral recognition. *Tetrahedron Asymmetry* 1994;5(5):777-780.
59. Silva B, Pereira JA, Cravo S, Araújo AM, Fernandes C, Pinto MMM, de Pinho PG, Remião F. Multi-milligram resolution and determination of absolute configuration of pentedrone and methylone enantiomers. *J Chromatogr B Anal Technol Biomed Life Sci* 2018;1100-1101:158-164.
60. Lopes A, Martins E, Silva R, Pinto MMM, Remião F, Sousa E, Fernandes C. Chiral Thioxanthones as Modulators of P-glycoprotein: Synthesis and Enantioselectivity Studies. *Molecules* 2018;23(3), 626, doi:10.3390/molecules23030626.
61. Okamoto Y, Ikai T. Chiral HPLC for efficient resolution of enantiomers. *Chem Soc Rev* 2008;37(12):2593-2608.
62. Sousa EP, Tiritan ME, Oliveira RV, Afonso CMM, Cass QB, Pinto MMM. Enantiomeric Resolution of Kielcorin Derivatives by HPLC on Polysaccharide Stationary Phases Using Multimodal Elution. *Chirality* 2004;16(5):279-285.

63. Fernandes C, Brandão P, Santos A, Tiritan ME, Afonso C, Cass QB, Pinto MM. Resolution and determination of enantiomeric purity of new chiral derivatives of xanthones using polysaccharide-based stationary phases. *J Chromatogr A* 2012;1269:143-153.

64. Sousa ME, Tiritan ME, Belaz KRA, Pedro M, Nascimento MSJ, Cass QB, Pinto MMM. Multimilligram enantioresolution of low-solubility xanthonolignoids on polysaccharide chiral stationary phases using a solid-phase injection system. *J Chromatogr A* 2006;1120(1-2):75-81.

Supplementary Materials

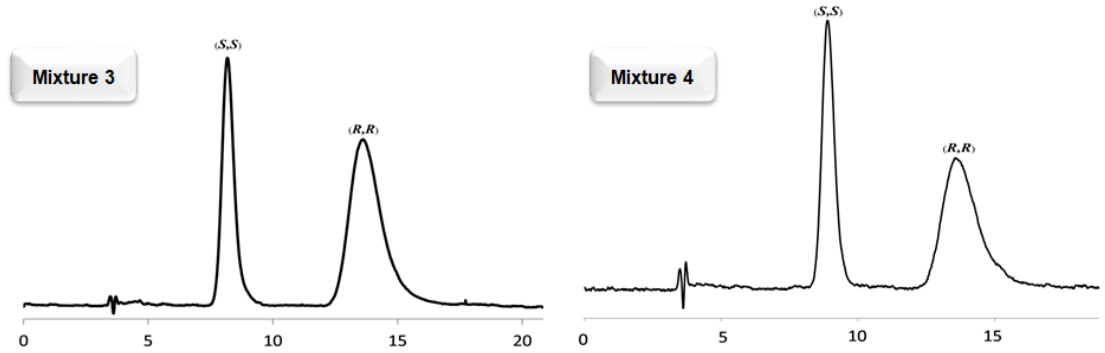


Figure S1. Chromatograms of enantiomeric mixtures **3** and **4** on Lux® Celullose-2 (15 cm × 4.6 mm i.d., 3 µm particle size, 100-A˚ pore size). Mobile phase, 100 % EtOH; Flow rate, 0.5 mL/min; UV Detection, 254 nm.

IR, ^{1}H NMR and ^{13}C NMR data:

***(S)-N-(2-Hydroxy-1-phenylethyl)-2-[(9-oxo-9H-xanthen-1-yl)oxy]acetamide* (1)**

IR ν_{max} (cm^{-1}) (KBr): 3433, 3299, 1660, 1619, 1547, 1464, 1435, 1260, 847; ^{1}H NMR (300.13 MHz, DMSO-d_6) δ: 9.17 (d, *J* = 8.9 Hz, 1H, NH), 8.10 (dd, *J* = 8.1, 1.6 Hz, 1H, H-8), 7.80 (ddd, *J* = 8.6, 7.2, 1.6 Hz, 1H, H-6), 7.70 (t, *J* = 8.4 Hz, 1H, H-3), 7.57 (dd, *J* = 8.6, 1.6 Hz, 1H, H-5), 7.43 (ddd, *J* = 8.1, 7.2, 1.6 Hz, 1H, H-7), 7.34 (d, *J* = 6.7 Hz, 2H, H-2´´ (Ar) and H-6´´ (Ar)), 7.27 (t, *J* = 6.7 Hz, 2H, H-3´´ (Ar) and H-5´´(Ar), 7.18 (d, *J* = 6.7 Hz, 1H, H-4´´ (Ar)), 7.01 (dd, *J* = 8.4, 0.9 Hz, 1H, H-4), 6.88 (dd, *J* = 8.4, 0.9 Hz, 1H, H-2), 5.03 (t, *J* = 5.7 Hz, OH), 4.85 (m, 1H, H-1´), 4.73 (s, 2H, OCH_2), 3.71 ppm (m, 2H, CH_2O); ^{13}C NMR (75.47 MHz, DMSO-d_6) δ: 175.9 (C-9), 167.1 (C=O, amide), 157.6 (C-1), 157.2 (C-10a), 154.7 (C-4a), 136.1 (C-3), 135.4 (C-6), 140.6 (C-1´´ (Ar)), 128.4 (C-3´´ (Ar) and C-5´´ (Ar)), 127.2 (C-2´´ (Ar) and C-6´´ (Ar)),

127.1 (C-4´´ (Ar)), 126.1 (C-8), 124.5 (C-7), 122.2 (C-8a), 117.7 (C-5), 111.7 (C-2), 110.8 (C-9a), 108.2 (C-4), 68.2 ppm (OCH_2), 65.0 (CH_2OH), 54.9 ppm (C-1´).

2,2'-{[(9-Oxo-9H-xanthene-3,6-diyl)bis(oxy)]bis[N-(R)-1-hydroxy-4-methylpentan-2-yl]acetamide} **(3)**

IR v_{max} (cm^{-1}) (KBr): 3423, 3288, 1653, 1615, 1547, 1446, 1437, 1260, 761; ^{1}H NMR (300.13 MHz, DMSO-d_6) δ: 8.28 (d, *J* = 8.2 Hz, 2H, 2×NH), 8.17 (d, *J* = 8.9 Hz, 2H, H-1 and H-8), 7.05 (dd, *J* = 8.9, 2.4 Hz, 2H, H-2 and H-7), 7.00 (d, *J* = 2.3 Hz, 2H, H-4 and H-5), 4.63 and 4.64 (2×s, 4H, 2×OCH_2), 4.26 (t, *J* = 5.6 Hz, 3H, 3×OH), 4.14 (m, 2H, 2×H-1´), 3.61 (m, 4H, 2×CH_2O), 1.58 (m, 2H, 2×H-3´), 1.45 (m, 4H, 2×H-2´), 0.91 ppm (t, *J* = 6.0 Hz, 12H, H-4´); ^{13}C NMR (75.47 MHz, DMSO-d_6) δ: 174.3 (C-9), 166.4 (2×C=O, amide), 162.0 (C-3 and C-6), 157.2 (C-4a and C-10a), 128.0 (C-1 and C-8), 115.8 (C-8a and C-9a), 113.0 (C-2 and C-7), 101.5 (C-4 and C-5), 67.1 (2×OCH_2), 64.0 (2×CH_2OH), 50.0 (2×C-1´), 40.3 (2×C-2´), 24.2 (2×C-3´), 22.5 ppm (2×C-4´).

2,2'-{[(9-Oxo-9H-xanthene-3,6-diyl)bis(oxy)]bis[N-(R)-1-hydroxy-3-methylbutan-2-yl]acetamide} **(4)**

IR v_{max} (cm^{-1}) (KBr): 3454, 2959, 2926, 1659, 1616, 1558, 1447; ^{1}H NMR (300.13 MHz, DMSO-d_6) δ: 8.23 (d, *J* = 8.9 Hz, 2H, 2×NH), 7.13 (d, *J* = 9.2 Hz, 2H, H-1 and H-8), 7.05 (dd, *J* = 8.9, 2.3 Hz, 2H, H-2 and H-7), 6.98 (d, *J* = 2.4 Hz, 2H, H-4 and H-5), 4.67 (s, 4H, 2×OCH_2), 4.27 (t, *J* = 5.3 Hz, 2H, 2×OH), 3.81 (m, 2H, 2×H-1´), 3.66 (m, 4H, 2×CH_2O), 1.95 (m, 2H, 2×H-2´), 0.96 ppm (t, *J* = 6.8 Hz, 6H, H-3a´), 0.91 ppm (t, *J* = 6.8 Hz, 6H, H-3b´); ^{13}C NMR (75.47 MHz, DMSO-d_6) δ: 175.0 (C-9), 166.5 (2×C=O, amide), 163.0 (C-3 and C-6), 157.2 (C-4a and C-10a), 127.0 (C-1 and C-8), 115.8 (C-8a and C-9a), 113.0 (C-2 and C-7), 101.3 (C-4 and C-5), 67.1 (2×OCH_2), 63.0 (2×CH_2OH), 55.8 (2×C-1´), 29.0 (2×C-2´), 19.0 (2×C-3´a), 18.5 ppm (2×C-3´b).

2,2'-{[9-Oxo-9H-xanthene-1,3-diyl)bis(oxy)]bis[N-((S)-2-hydroxy-1 phenylethyl]acetamide]} **(5)**

IR v_{max} (cm^{-1}) (KBr): 3446, 3297, 1668, 1610, 1549, 1463, 1428, 1250, 848; ^{1}H NMR (300.13 MHz, DMSO-d_6) δ: 8.55 and 9.22 (2×d, *J* = 8.3-8.9 Hz, 2H, 2×NH), 8.18 (dd, *J* = 7.5, 1.7 Hz, 1H, H-8), 7.82 (td, *J* = 8.7, 7.5, 1.7 Hz, 1H, H-6), 7.53 (d, *J* = 8.7 Hz, 1H, H-5), 7.48 (t, *J* = 7.5 Hz, 1H, H-7), 7.21 (m, 10H, 2×H-Ar), 6.76 (d, *J* = 2.2 Hz, 1H, H-4), 6.67 (d, *J* = 2.2 Hz, 1H, H-2), 5.01 (t, *J* = 5.7 Hz, 2×OH), 4.92 (m, 2H, 2×H-1´), 4.68 and 4.80 (2×s, 4H, 2×OCH_2,), 3.63 and 3.72 ppm (2×m, 4H, 2×CH_2O); ^{13}C NMR (75.47 MHz, DMSO-d_6) δ: 174.7 (C-9), 166.5 and 166.8 (2×C=O, amide), 163.7 (C-1), 158.9 (C-3), 158.7 (C-4a), 154.6 (C-10a), 140.8 (2×C-1´´ (Ar)), 134.9 (C-6), 128.1 (2×C-3´´ (Ar) and C-5´´ (Ar)), 127.4 (C-8), 127.1 (2×C-2´´ (Ar) and C-

6´´ (Ar)), 126.9 (2×C-4´´ (Ar)), 126.0 (C-8), 124.5 (C-7), 122.1 (C-8a), 117.5 (C-5), 106.5 (C-9a), 102.3 (C-2), 95.2 (C-4), 67.3 and 68.5 (2×OCH_2), 65.0 (2×CH_2OH), 55.0 ppm (2×C-1´).

2,2'-{[(9-Oxo-9H-xanthene-3,4-diyl)bis(oxy)]bis[N-(S)-2-hydroxy-1-phenylethyl]acetamide} **(6)**

IR v_{max} (cm^{-1}) (KBr): 3388, 3272, 1668, 1616, 1529, 1463, 1448, 1255, 849; ^{1}H NMR (300.13 MHz, DMSO-d_6) δ: 8.51 and 8.65 (2×d, *J* = 8.3 Hz, 2H, 2×NH), 8.18 (dd, *J* = 8.1, 1.7 Hz, 1H, H-8), 7.84 (ddd, *J* = 8.7, 7.1, 1.7 Hz,1H, H-6), 7.90 (d, *J* = 8.7, 1H, H-5), 7.63 (d, *J* = 8.5 Hz, 1H, H-1), 7.48 (ddd, *J* = 8.1, 7.1, 1.7 Hz, 1H, H-7), 7.25 (m, 10H, 2×H-Ar), 7.15 (d, *J* = 8.5 Hz, 1H, H-2), 5.00 and 5.07 (2×t, *J* = 5.8 Hz, 2H, 2×OH), 4.95 and 4.98 (2×m, 2H, 2×H-1´), 4.81 and 4.83 (2×s, 4H, 2×OCH_2), 3.66 ppm (m, 4H, 2×CH_2O); ^{13}C NMR (75.47 MHz, DMSO-d_6) δ: 175.2 (C-9), 166.6 and 167.8 (2×C=O, amide), 155.5 (C-3), 155.4 (C-4), 140.7 and 140.8 (2×C-1´´ (Ar)), 135.25 (C-10a), 134.94 (C-4a), 128.1 (2×C-3´´(Ar) and C-5´´(Ar)), 126.9 (2×C-2´´(Ar) and C-6´´ (Ar)), 126.4 (2×C-4´´(Ar)), 125.9 (C-2), 124.5 (C-6), 121.6 (C-8), 120.8 (C-7), 118.3 (C-5), 116.3 (C-8a), 110.5 (C-9a), 67.4 (2×OCH_2), 64.3 and 64.4 (2×CH_2OH), 54.6 and 55.0 ppm (2×C1´).

2,2',2''-{[9-Oxo-9H-xanthene-1,3,6-triyl)tris(oxy)]tris[N-(S)-2-hydroxy-1-phenylethyl]acetamide} **(7)**

IR v_{max} (cm^{-1}); 3360, 3328, 1669, 1610, 1540, 1460, 1430, 1261, 839; ^{1}H NMR (300.13 MHz, DMSO-d_6) δ: 8.56 and 9.22 (2×d, *J* = 8.6-8.9 Hz, 3H, 3×NH), 8.10 (d, *J* = 8.7 Hz, 1H, H-8), 7.27 (m, 15H, 3×H-Ar), 7.10 (dd, *J* = 8.7, 2.3 Hz, 1H, H-7), 7.02 (d, *J* = 2.3 Hz, 1H, H-5), 6.71 (d, *J* = 2.2 Hz, 1H, H-4), 6.65 (d, *J* = 2.2 Hz, 1H, H-2), 5.00 (t, *J* = 5.8 Hz, 3×OH), 4.90 (m, 3H, 3×H-1´), 4.66 and 4.78 (2×s, 6H, 3×OCH_2), 3.66 ppm (m, 6H, 3×CH_2O); ^{13}C NMR (75.47 MHz, DMSO-d_6) δ: 174.1 (C-9), 166.7-166.9 (3×C=O, amide), 163.3 (C-3), 162.9 (C-6), 158.7 (C-1), 157.4 (C-4a), 156.3 (C-10a), 140.6-140.7 (3×C-1´´ (Ar)), 128.3-128.8 (3×(C-3´´ (Ar) and C-5´´ (Ar))), 128.1 (C-8), 127.1-127.3 (3×C-2´´ (Ar) and C-6´´ (Ar)), 126.8-126.9 (3×C-4´´ (Ar)), 114.0 (C-7), 109.4 (C-8a), 106.4 (C-9a), 102.5 (C-5), 101.6 (C-2), 95.2 (C-4), 67.3-68.3 (3×OCH_2), 64.5-65.2 (3×CH_2OH), 54.8-54.9 ppm (3×C-1´).

2,2',2''-{[9-Oxo-9H-xanthene-1,3,8-triyl)tris(oxy)]tris[N-(S)-2-hydroxy-1-phenylethyl]acetamide} **(8)**

IR v_{max} (cm^{-1}) (KBr): 3440, 3318, 1656, 1627, 1557, 1457, 1432, 1262, 851; ^{1}H NMR (300.13 MHz, DMSO-d_6) δ: 8.55 and 8.97 (2×d, *J* = 8.8-9.6 Hz, 3H, 3×NH), 7.35 (dd, *J* = 8.4, 0.7 Hz, 1H, H-7), 7.66 (t, *J* = 8.4 Hz, 1 H, H-6), 7.21 (m, 15H, 3×H-Ar), 6.93 (dd, *J* = 8.4, 0.7 Hz, 1H, H-5), 6.67 (d, *J* = 2.1 Hz, 1H, H-4), 6.60 (d, *J* = 2.1 Hz, 1H, H-2), 5.00 (t, *J* = 5.7 Hz, 3×OH),

4.93 (m, 3H, 3×H-1´), 4.69 and 4.72 (2×s, 6H, 3×OCH_2), 3.61 ppm (m, 6H, 3×CH_2O); ^{13}C NMR (75.47 MHz, DMSO-d_6) δ: 174.7 (C-9), 166.5-167.2 (3×C=O, amide), 163.1 (C-3), 161.5 (C-1), 159.3 (C-8), 158.1 (C-4a), 156.2 (C-10a), 140.6-140.7 (3×C-1´´(Ar)), 134.9 (C-6), 128.1 (3×C-3´´ (Ar) and C-5´´ (Ar)), 127.0 (3×C-2´´ (Ar) and C-6´´ (Ar)), 126.9 (3×C-4´´ (Ar)), 110.6 (C-7), 109.3 (C-5), 107.8 (C-8a), 104.7 (C-9a), 98.2 (C-2), 94.6 (C-4), 65.5-65.9 ppm (3×OCH_2), 68.3-68.5 (3×OCH_2), 64.4-65.0 (3×CH_2OH), 54.9 ppm (3×C-1´).

2,2',2'',2'''-{[(9-Oxo-9H-xanthene-1,3,6,8-tetrayl)tetrakis(oxy)]tetrakis[N-(S)-2-hydroxy-1-phenylethyl]acetamide} **(9)**

IR v_{max} (cm^{-1}) (KBr): 3441, 3296, 1667, 1618, 1550, 1462, 1430, 1263, 849; ^{1}H NMR (300.13 MHz, DMSO-d_6) δ: 8.52 and 8.99 (2×d, *J* = 8.5-8.4 Hz, 4H, 4×NH), 7.25 (m, 20H, 4×H-Ar), 6.63 (d, *J* = 2.2 Hz, 2H, H-4 and H-5), 6.57 (d, *J* = 2.2 Hz, 2H, H-2 and H-7), 4.99 (t, *J* = 5.7 Hz, 4×OH), 4.92 (m, 4H, 4×H-1´), 4.71 and 4.72 (2×s, 8H, 4×OCH_2), 3.61 ppm (m, 8H, 4×CH_2O); ^{13}C NMR (75.47 MHz, DMSO-d_6) δ: 182.1 (C-9), 167.0-167.2 (4×C=O), 162.3 (C-3 and C-6), 159.4 (C-1 and C-8), 157.6 (C-4a and C-10a), 139.1-140.7 (4×C-1´´ (Ar)), 128.0-128.1 (4×C-3´´(Ar) and C-5´´(Ar)), 127.1 (4×C-2´´ (Ar) and C-6´´ (Ar)), 126.4-126.9 (4×C-4´´ (Ar)), 104.5 (C-8a and C-9a), 97.5 (C-2 and C-7), 94.5 (C-4 and C-5), 67.1-67.2 (4×OCH_2), 64.4-64.8 (4×CH_2OH), 55.0 ppm (4×C-1´).

2,2',2'',2'''-{[(Carbonylbis(benzene-4,1,3-triyl)tetrakis(oxy)]tetrakis[N-(S)-2-hydroxy-1-phenylethyl]acetamide} **(10)**

IR v_{max} (cm^{-1}) (KBr): 3441, 3291, 1635, 1540, 1464, 1429, 1260; ^{1}H NMR (300.13 MHz, DMSO-d_6) δ: 8.29 and 8.62 (2×d, *J* = 8.2 Hz, 4H, 4×NH), 7.54 (d, *J* = 8.6 Hz, 2H, H-6 and H-6´), 7.42 (m, 20H, 4×H-Ar), 6.84 (dd, *J* = 8.6, 2.2 Hz, 2H, H-5 and H-5´), 6.80 (d, *J* = 2.2 Hz, 2H, H-3 and H-3´), 5.16 (t, *J* = 5.7 Hz, 4H, 4×OH), 5.01 (m, 4H, 4×H-1´´), 4.69 and 4.76 (2×s, 8H, 4×OCH_2), 3.68 ppm (m, 8H, 4×CH_2O); ^{13}C NMR δ: (75.47 MHz, DMSO-d_6): 199.2 (C-9), 167.0-167.2 (4×C=O, amide), 162.0 (C-4 and C-4´), 157.9 (C-2 and C-2´), 140.7 (4×C-1´´´ (Ar)), 133.0 (C-6 and C-6´), 128.3 (4×C-3´´´ (Ar) and C-5´´´ (Ar)), 127.1 (4×C-2´´´ (Ar) and C-6´´´ (Ar)), 126.8 (4×C-4´´´ (Ar)), 124.1 (C-1 and C-1´), 109.1 (C-5 and C-5´), 101.6 (C-3 and C-3´), 67.2 (4×OCH_2), 65.0 (4×CH_2OH), 55.0 ppm (4×C-1´´).

2,2'-{[(Carbonylbis(4,1-phenylene)bis(oxy)]bis[N-(S)-2-hydroxy-1-phenylethyl]acetamide} **(11)**

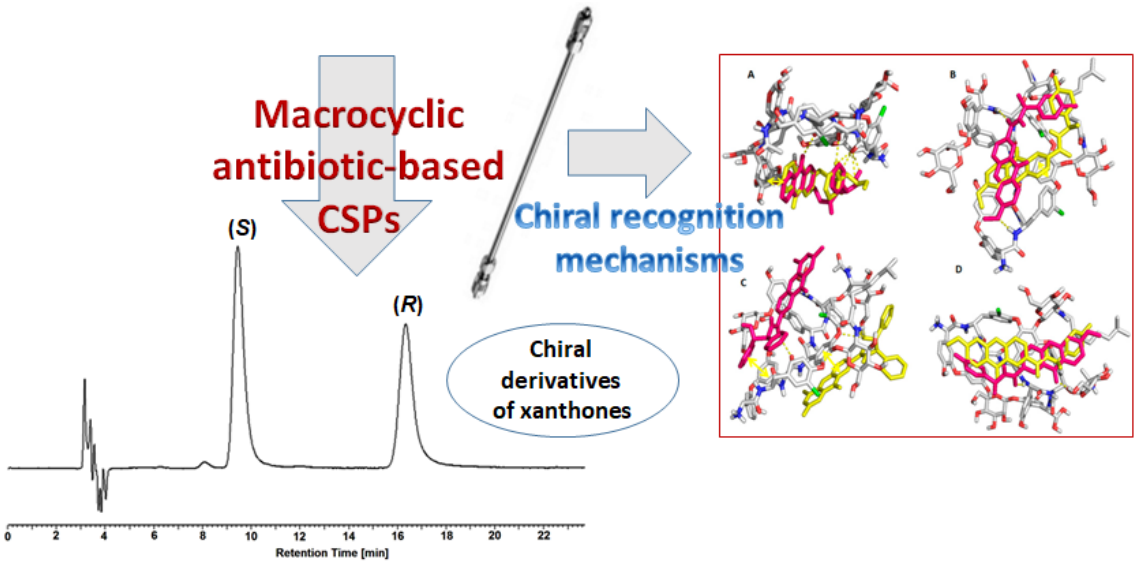
IR v_{max} (cm^{-1}) (KBr)**:** 3413, 3273, 1604, 1540, 1456, 1449, 1254, 845; ^{1}H NMR (300.13 MHz, DMSO-d_6) δ: 8.46 (d, *J* = 8.3 Hz, 2H, 2×NH), 7.65 (d, *J* = 8.9 Hz, 4H, H-2, H-2´, H-6, H-6´), 7.21 (m, 10H, 2×H-Ar), 7.04 (d, *J* = 8.9 Hz, 4H, H-3, H-3´, H-5, H-5´), 4.90 (t, *J* = 5.7 Hz, 2H,

2×OH), 4.85 (m, 2H, 2×H-1´´), 4.64 and 4.65 (2×s, 4H, 2×OCH_2), 3.60 ppm (m, 4H, 2×CH_2O); ^{13}C NMR (75.47 MHz, DMSO-d_6) δ: 193.1 (C-9), 166.9 (2×C=O, amide), 161.8 (C-4 and C-4´), 140.8 (2×C-1´´´ (Ar)), 131.7 (C-2, C-2´, C-6, C-6´), 130.4 (C-1 and C-1´), 128.1 (2×C-3´´´ (Ar) and C-5´´´ (Ar)), 126.9 (2×C-2´´´ (Ar) and C-6´´´ (Ar)), 126.8 (2×C-4´´´ (Ar)), 114.3 (C-3, C-3´, C-5, C-5´), 66.5 (2×OCH_2), 64.9 (2×CH_2OH), 54.8 ppm (2×C-1´´).

CHAPTER VII

Enantiomeric Resolution and Docking Studies of Chiral Xanthonic Derivatives on Chirobiotic Column

Reprinted from Molecules



Graphical abstract

molecules

MDPI

Article

Enantiomeric Resolution and Docking Studies of Chiral Xanthonic Derivatives on Chirobiotic Columns

Ye` Zaw Phyo [1,2], Sara Cravo [2,3], Andreia Palmeira [2,3], Maria Elizabeth Tiritan [2,3,4], Anake Kijjoa [1,2], Madalena M. M. Pinto [2,3,*] and Carla Fernandes [2,3,*]

1 ICBAS-Instituto de Ciências Biomédicas Abel Salazar, Universidade do Porto, Rua de Jorge Viterbo Ferreira, 228, 4050-313 Porto, Portugal; chemistkophyo.ckp@gmail.com (Y.Z.P.); ankijjoa@icbas.up.pt (A.K.)

2 Interdisciplinary Centre of Marine and Environmental Research (CIIMAR), Edifício do Terminal de Cruzeiros do Porto de Leixões, Av. General Norton de Matos s/n, 4050-208 Matosinhos, Portugal; scravo@ff.up.pt (S.C.); andreiapalmeira@gmail.com (A.P.); elizabeth.tiritan@iscsn.cespu.pt (M.E.T.)

3 Laboratório de Química Orgânica e Farmacêutica, Departamento de Ciências Químicas, Faculdade de Farmácia, Universidade do Porto, Rua de Jorge Viterbo Ferreira, 228, 4050-313 Porto, Portugal

4 CESPU, Instituto de Investigação e Formação Avançada em Ciências e Tecnologias da Saúde (IINFACTS), Rua Central de Gandra, 1317, 4585-116 Gandra PRD, Portugal

* Correspondence: madalena@ff.up.pt (M.M.M.P.); cfernandes@ff.up.pt (C.F.); Tel.: +35-122-042-8692 (M.M.M.P.); +35-122-042-8688 (C.F.)

Received: 29 November 2017; Accepted: 8 January 2018; Published: 11 January 2018

Abstract: A systematic study of enantioresolution of a library of xanthonic derivatives, prepared "in-house", was successfully carried out with four commercially available macrocyclic glycopeptide-based columns, namely Chirobiotic^{TM} T, Chirobiotic^{TM} R, Chirobiotic^{TM} V and Chirobiotic^{TM} TAG. Evaluation was conducted in multimodal elution conditions: normal-phase, polar organic, polar ionic and reversed-phase. The effects of the mobile phase composition, the percentage of organic modifier, the pH of the mobile phase, the nature and concentration of different mobile phase additives on the chromatographic parameters are discussed. Chirobiotic^{TM} T and Chirobiotic^{TM} V, under normal-phase and reversed-phase modes, respectively, presented the best chromatographic parameters. Considering the importance of understanding the chiral recognition mechanisms associated with the chromatographic enantioresolution, and the scarce data available for macrocyclic glycopeptide-based columns, computational studies by molecular docking were also carried out.

Keywords: Chirobiotic^{TM}; docking; enantioresolution; enantioselectivity; molecular recognition; xanthonic derivatives

1. Introduction

During the last few decades there has been widespread interest in oxygenated heterocyclic compounds such as molecules with a xanthone scaffold [1–3], mainly in consideration of their important roles as bioactive agents and because xanthone is an attractive core for molecular modifications [4–9] and the design of new molecular entities [10,11]. Xanthonic derivatives can be isolated from terrestrial [12,13] and marine [2] sources, or obtained by synthesis using different synthetic methodologies [14,15].

Recently, some synthetic enantiomerically pure xanthone derivatives prepared "in house" demonstrated highly interesting biological activities, namely inhibition of enzymes involved in inflammatory processes [16], growth inhibitory effects on different tumor cell lines [17], nerve sciatic conduction blockade [18], as well as the ability to behave as promising chiral selectors for liquid chromatography (LC) [19].

Since the enantiomeric purity of the final product is crucial regarding both biological activities and preparation of single enantiomer selectors for LC stationary phases, there is a great need for

suitable methods for enantioseparation and evaluation of the enantiomeric composition. One of the most frequently applied techniques is LC with chiral columns [20]. Consequently, systematic studies of enantioresolution using different types of LC chiral columns, i.e., macrocyclic glycopeptide-based [21], Pirkle-type [22,23] and polysaccharide-based [24], and further determination of the enantiomeric purity of the synthesized xanthonic compounds, were described. By comparison, of the overall chromatographic results for the same small library of xanthonic derivatives considering the different types of chiral columns, in general, macrocyclic glycopeptide-based showed enantioselectivity but low resolution [25]. These results were not expected considering that this type of chiral columns are one of the most versatile and broadly applied, allowing efficient enantioseparations of diverse classes of chiral compounds [26–33]. Moreover, their usefulness can be increased considering the complementary profile in enantioselectivity of the different macrocyclic glycopeptide-based selectors [34].

In order to further explore the effectiveness of this type of columns to separate the enantiomers of this important class of compounds, herein we describe a systematic study of enantioresolution using a larger library of chiral xanthonic derivatives and different mobile phases in normal-phase mode (NPM), polar organic mode (POM), polar ionic mode (PIM), and reversed-phase mode (RPM). The macrocyclic glycopeptide columns based on ristocetin, teicoplanin, teicoplanin aglycone, and vancomycin, Chirobiotic^{TM} R, T, TAG and V, respectively, were evaluated. The effects of the mobile phase composition, the percentage of organic modifier, the pH of the mobile phase, the nature and concentration of different mobile phase additives on the chromatographic parameters, for each Chirobiotic^{TM} column, are discussed. The elution order was also assessed in all cases. Finally, taking into account the importance in understanding the chiral recognition mechanisms associated with the chromatographic enantioresolution [35,36] and the scarce data for macrocyclic glycopeptide-based selectors [37–40], computational studies were also carried out.

2. Results and Discussion

In our previous work, LC columns containing macrocyclic glycopeptides as chiral selectors: Chirobiotic^{TM} R, T, TAG and V (Figure 1), were demonstrated to have enantioselectivity for six of the seven enantiomeric pairs of the xanthonic derivatives analyzed [21]. However, poor enantioresolution were obtained, which prompted us to pursue our investigation increasing the library of compounds and the variables of the mobile phase to better understand the behavior of these chiral columns towards the target analytes. In this work, a library of thirty-one chiral xanthonic analytes (Figure 2) was used for the systematic study of enantioresolution, including the previous seven enantiomeric pairs [21] and more twenty-four [22], applying the chiral columns based on these four macrocyclic glycopeptide selectors.

Chiral xanthonic analytes were obtained in enantiomeric pure form (enantiomeric excess between 98% and 99%) [21,22,24], by coupling carboxyxanthones with both enantiomers of commercially available chiral building blocks, using *O*-(benzotriazol-1-yl)-*N*,*N*,*N*′,*N*′-tetramethyluronium tetrafluoroborate (TBTU) as coupling reagent (Scheme 1), according to procedures described elsewhere [17,18].

The target library of this study, although comprising a common structural xanthone scaffold, is structurally diverse (Figure 2). The xanthone scaffold of analytes **1**–**8** has no substituents beyond an alkoxyamide chemical bridge for the link to the chiral moiety; analytes **9**–**21** have a methoxyl group at position 6 of the xanthone scaffold, and analytes **22**–**31** have methyl groups at positions 5 and 7. Additionally, the analytes **9**–**31** comprise an amide linkage with the chiral moiety at position 2. The majority of the analytes have only one stereogenic center with an alkyl or aromatic moiety, except **7**, **8**, **20**, **21**, **30** and **31** which have two stereogenic centers.

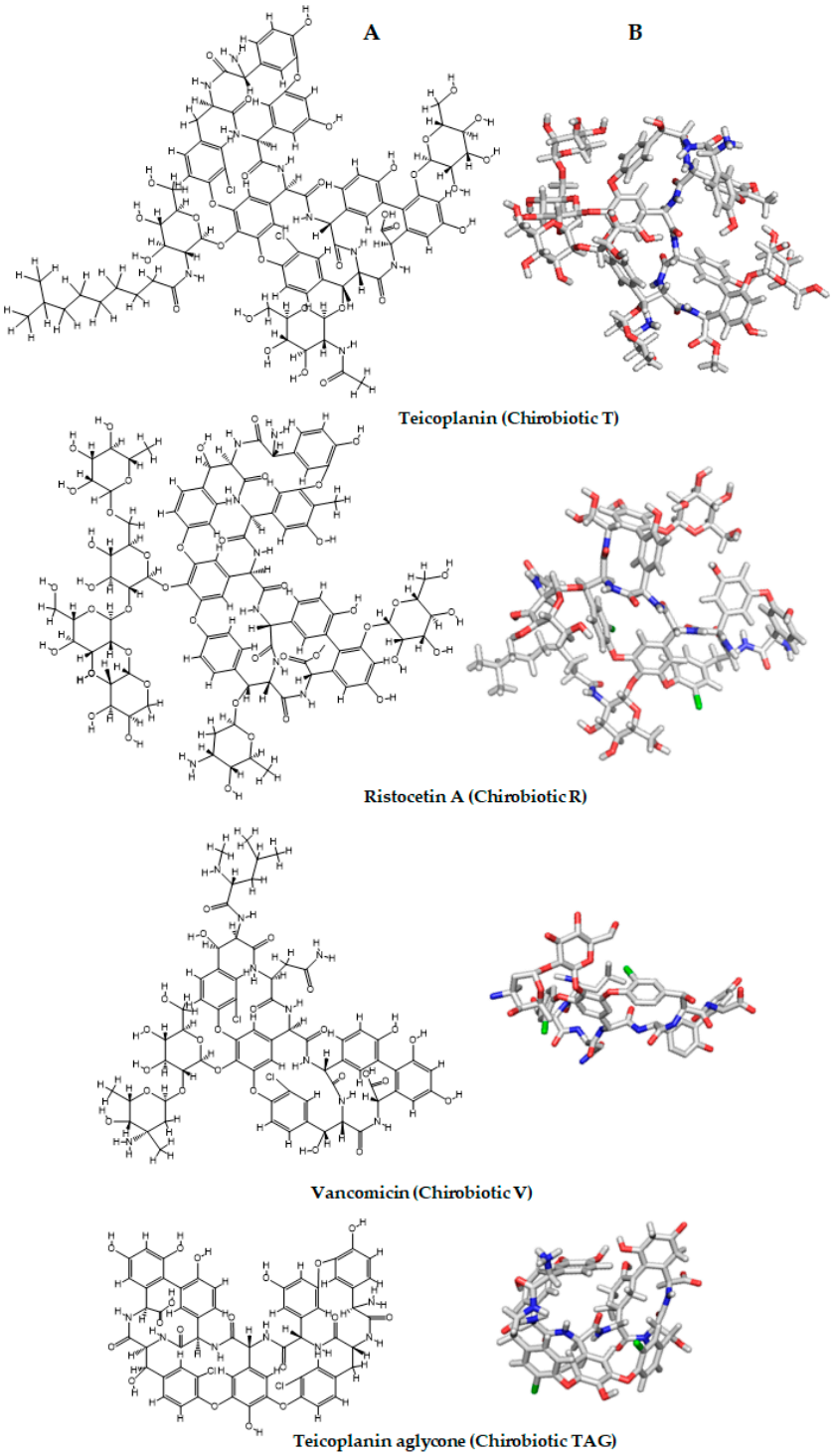


Figure 1. 2D (**A**) and 3D (**B**) structures of the four macrocyclic glycopeptide-based selectors. Chiral selectors are represented in sticks with C, O, N, and Cl atoms colored in grey, red, blue and green, respectively.

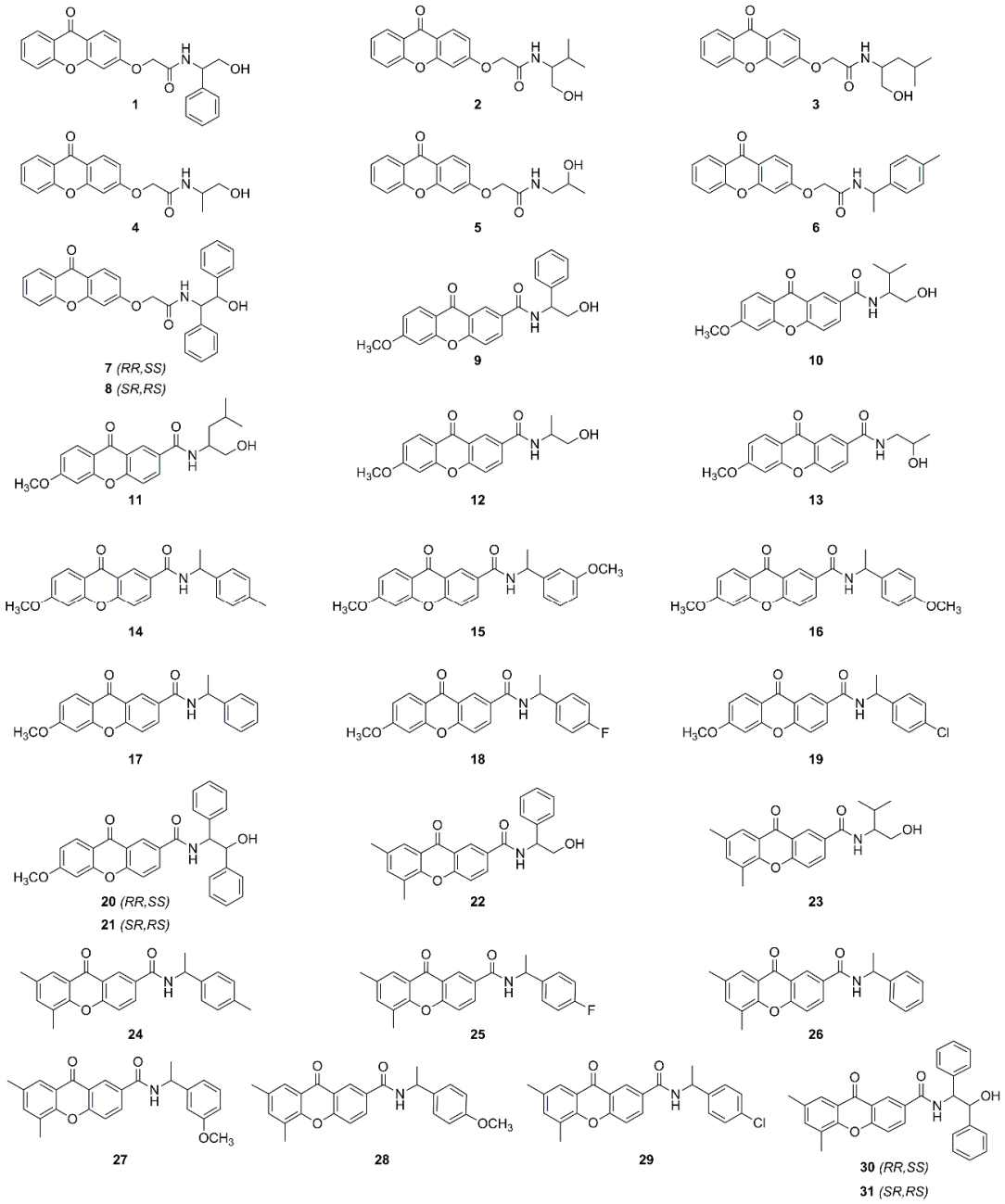
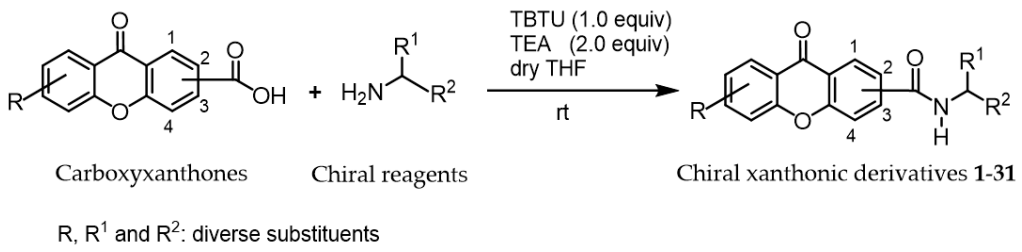


Figure 2. Chemical structures of chiral xanthonic analytes **1**–**31**.



Scheme 1. General scheme of synthesis of chiral xanthonic analytes **1**–**31**.

Considering that chromatographic separations are highly influenced by mobile phase components, all chiral analytes were evaluated under four chromatographic elution modes (NPM, POM, PIM and RPM). In NPM, *n*-hexane (Hex) and an organic modifier, ethanol (EtOH) or 2-propanol (2-PrOH), were

evaluated. Methanol (MeOH), EtOH, 2-PrOH or acetonitrile (ACN) in different proportions were used in POM. The mixture of MeOH with several percentages of triethylamine (TEA) and glacial acetic acid (AcOH) were employed in PIM. Regarding RPM, different proportions of MeOH or tetrahydrofuran (THF) and buffer (0.1 or 1% triethylammonium acetate (TEAA) or ammonium acetate (NH_4OAc)) with pH 4.0–6.0 were applied.

The experimental conditions, including the nature and proportion of the organic modifier, the pH of the mobile phase, the buffer type and concentration, were investigated in the course of the enantioseparation process.

2.1. Performance of Chirobiotic T Column for Enantioresolution of Chiral Xanthonic Analytes

Table 1 summarizes the best chromatographic results obtained with Chirobiotic™ T column, under multimodal elution conditions, with resolution factors ≥1.00. However, in some cases, results obtained with different mobile phases, but not leading to good enantioresolution, are also included for purposes of comparison.

Table 1. Chromatographic data, retention factor of first eluted enantiomer (k_1), separation factor (α), resolution (R_S), and elution order, for the chiral xanthonic analytes on Chirobiotic™ T column, under multimodal chromatographic conditions.

Analyte	Elution Mode	Mobile Phase	k_1	α	R_S	First Eluted Enantiomer
1	NPM	Hex:EtOH (80:20 *v*/*v*)	18.13	1.16	2.26	(*R*)
	NPM	Hex:2-PrOH (70:30 *v*/*v*)	33.19	1.47	1.93	(*R*)
	POM	100% EtOH	1.19	1.14	0.70	(*R*)
2	NPM	Hex:EtOH (40:60 *v*/*v*)	1.92	1.26	1.28	(*R*)
	NPM	Hex:2-PrOH (70:30 *v*/*v*)	15.98	1.62	1.49	(*R*)
	POM	100% EtOH	0.80	1.20	0.86	(*R*)
3	NPM	Hex:EtOH (80:20 *v*/*v*)	32.34	1.09	1.09	(*R*)
	NPM	Hex:2-PrOH (50:50 *v*/*v*)	2.93	1.32	1.00	(*R*)
4	NPM	Hex:EtOH (80:20 *v*/*v*)	19.56	1.42	2.95	(*R*)
	PIM	MeOH:AcOH:TEA (100:0.1:1 *v*/*v*/*v*)	1.13	1.09	0.80	(*R*)
	POM	100% EtOH	1.09	1.33	1.28	(*R*)
7	NPM	Hex:EtOH (90:10 *v*/*v*)	23.91	1.29	2.83	(*R*)
9	NPM	Hex:EtOH (70:30 *v*/*v*)	9.21	1.47	2.48	(*R*)
	NPM	Hex:2-PrOH (50:50 *v*/*v*)	7.11	1.46	1.07	(*R*)
	PIM	MeOH:AcOH:TEA (100:0.1:0.1 *v*/*v*/*v*)	1.34	1.08	0.60	(*R*)
	POM	100% EtOH	1.13	1.42	1.73	(*R*)
	POM	100% 2-PrOH	1.63	1.63	1.32	(*R*)
10	NPM	Hex:EtOH (70:30 *v*/*v*)	5.04	1.54	3.30	(*R*)
	NPM	Hex:2-PrOH (50:50 *v*/*v*)	4.05	1.61	1.56	(*R*)
	POM	100% EtOH	0.80	1.49	1.90	(*R*)
	POM	100% 2-PrOH	1.01	1.74	1.61	(*R*)
11	NPM	Hex:EtOH (80:20 *v*/*v*)	6.93	1.29	2.43	(*R*)
	NPM	Hex:2-PrOH (80:20 *v*/*v*)	8.35	1.33	0.84	(*R*)
	POM	100% EtOH	0.63	1.25	1.00	(*R*)
	POM	100% 2-PrOH	0.69	1.41	1.14	(*R*)
12	NPM	Hex:EtOH (80:20 *v*/*v*)	15.31	1.32	2.31	(*R*)
	NPM	Hex:2-PrOH (70:30 *v*/*v*)	22.72	1.38	0.50	(*R*)
	POM	100% EtOH	1.03	1.25	1.00	(*R*)
14	NPM	Hex:EtOH (90:10 *v*/*v*)	9.78	1.29	1.55	(*R*)
	NPM	Hex:2-PrOH (50:50 *v*/*v*)	1.53	1.15	0.78	(*R*)
	RPM	MeOH:TEAA pH 4.2 (40:60 *v*/*v*)	10.54	1.19	1.53	(*R*)
15	NPM	Hex:EtOH (90:10 *v*/*v*)	16.67	1.26	1.97	(*R*)
	NPM	Hex:2-PrOH (50:50 *v*/*v*)	2.33	1.23	0.89	(*R*)
	POM	100% EtOH	0.67	1.15	0.70	(*R*)
	RPM	MeOH:TEAA pH 4.2 (30:70 *v*/*v*)	20.59	1.33	2.46	(*R*)

Table 1. *Cont.*

Analyte	Elution Mode	Mobile Phase	k_1	α	R_S	First Eluted Enantiomer
16	NPM	Hex:EtOH (90:10 *v*/*v*)	17.86	1.18	1.51	(*R*)
	NPM	Hex:2-PrOH (50:50 *v*/*v*)	2.48	1.15	0.40	(*R*)
	POM	100% EtOH	0.70	1.08	0.50	(*R*)
	RPM	MeOH:TEAA pH 4.2 (30:70 *v*/*v*)	22.32	1.24	1.92	(*R*)
17 *	NPM	Hex:EtOH (80:20 *v*/*v*)	2.03	2.09	7.37	(*S*)
	NPM	Hex:2-PrOH (80:20 *v*/*v*)	3.33	2.71	3.31	(*S*)
	POM	100% EtOH	0.42	1.39	1.45	(*S*)
	POM	100% 2-PrOH	0.30	1.99	1.78	(*S*)
	RPM	MeOH:TEAA pH 4.2 (30:70 *v*/*v*)	21.13	1.49	3.20	(*R*)
18	NPM	Hex:EtOH (90:10 *v*/*v*)	12.05	1.16	1.43	(*R*)
	NPM	Hex:2-PrOH (50:50 *v*/*v*)	1.67	1.13	0.30	(*R*)
	RPM	MeOH:TEAA pH 4.2 (30:70 *v*/*v*)	18.89	1.18	1.37	(*R*)
19	NPM	Hex:EtOH (90:10 *v*/*v*)	10.68	1.13	1.28	(*R*)
	NPM	Hex:2-PrOH (50:50 *v*/*v*)	1.59	1.10	0.30	(*R*)
	RPM	MeOH:TEAA pH 4.2 (30:70 *v*/*v*)	29.61	1.17	1.30	(*R*)
20	NPM	Hex:EtOH (80:20 *v*/*v*)	11.20	1.31	2.24	(*R*)
	NPM	Hex:2-PrOH (50:50 *v*/*v*)	3.45	1.30	1.11	(*R*)
	PIM	MeOH:AcOH:TEA (100:0.1:1 *v*/*v*/*v*)	1.10	1.11	0.74	(*R*)
	POM	100% EtOH	0.85	1.30	1.32	(*R*)
	POM	100% 2-PrOH	1.09	1.46	0.99	(*R*)
	RPM	MeOH:TEAA pH 4.2 (30:70 *v*/*v*)	8.55	2.26	1.66	(*R*)
22	NPM	Hex:EtOH (80:20 *v*/*v*)	5.50	1.36	2.45	(*R*)
	NPM	Hex:2-PrOH (50:50 *v*/*v*)	2.62	1.39	1.18	(*R*)
	POM	100% EtOH	0.72	1.34	1.38	(*R*)
	POM	100% 2-PrOH	0.77	1.52	1.10	(*R*)
23 *	NPM	Hex:EtOH (50:50 *v*/*v*)	1.22	1.25	1.28	(*S*)
	NPM	Hex:2-PrOH (50:50 *v*/*v*)	1.57	1.19	0.87	(*S*)
	POM	100% EtOH	0.56	1.25	1.00	(*S*)
	POM	100% 2-PrOH	0.48	1.54	1.08	(*S*)
	RPM	MeOH:TEAA pH 4.2 (40:60 *v*/*v*)	4.68	2.83	6.79	(*R*)
24	NPM	Hex:EtOH (90:10 *v*/*v*)	3.57	1.11	0.79	(*R*)
	RPM	MeOH:TEAA pH 4.2 (30:70 *v*/*v*)	29.11	1.23	1.55	(*R*)
25	NPM	Hex:EtOH (90:10 *v*/*v*)	4.09	1.09	0.92	(*R*)
	RPM	MeOH:TEAA pH 4.2 (30:70 *v*/*v*)	22.38	1.16	1.08	(*R*)
26	NPM	Hex:EtOH (90:10 *v*/*v*)	4.53	1.12	1.16	(*R*)
	RPM	MeOH:TEAA pH 4.2 (30:70 *v*/*v*)	21.58	1.22	1.49	(*R*)
27	NPM	Hex:EtOH (90:10 *v*/*v*)	5.91	1.16	1.40	(*R*)
	RPM	MeOH:TEAA pH 4.2 (40:60 *v*/*v*)	10.87	1.26	1.97	(*R*)
28	NPM	Hex:EtOH (90:10 *v*/*v*)	6.41	1.11	1.13	(*R*)
	RPM	MeOH:TEAA pH 4.2 (30:70 *v*/*v*)	27.13	1.26	1.87	(*R*)
29	NPM	Hex:EtOH (90:10 *v*/*v*)	4.67	1.07	0.89	(*R*)
	RPM	MeOH:TEAA pH 4.2 (40:60 *v*/*v*)	13.04	1.16	1.18	(*R*)
30	NPM	Hex:EtOH (90:10 *v*/*v*)	15.16	1.24	1.93	(*R*)
	NPM	Hex:2-PrOH (80:20 *v*/*v*)	9.76	1.33	0.88	(*R*)
	POM	100% EtOH	0.56	1.17	0.70	(*R*)
	POM	100% 2-PrOH	0.49	1.43	1.05	(*R*)

Chromatographic conditions: flow rate: 0.5 mL/min, UV detection at 254 nm; * Elution order changed with the mobile phase.

Chirobiotic^{TM} T column presented good chromatographic parameters in our previous work [21], and in the present work the same pattern was achieved, with enantioseparation of twenty-five out of thirty-one enantiomeric mixtures of xanthonic analytes (81%) (Table 1).

In NPM, mixtures of Hex and EtOH or 2-PrOH as organic modifier, in different proportions, were evaluated in order to achieve optimized chromatographic conditions, i.e., high enantioselectivity and resolution in short analysis time. In general, the Hex:EtOH combinations afforded better chromatographic results. For example, excellent enantioselectivity (α = 2.09) and resolution (R_S = 7.37)

were obtained for analyte **17**, with a k_1 value of 2.03, when Hex:EtOH (80:20, v/v) was used as mobile phase. This was also the best chromatographic result achieved for Chirobiotic^{TM} T column. Moreover, under NPM very high enantioselectivity and resolution were achieved for twenty-two analytes with α and R_S values ranging from 1.11 to 2.09 and from 1.09 to 7.37, respectively. Additionally, it was found that, when using Hex:EtOH (90:10 v/v) as mobile phase, this column also showed enantioselectivity for analytes **24** and **29** but with slight resolution (R_S < 1.00). On the other hand, POM using EtOH or 2-PrOH as mobile phases proved to be an excellent alternative to NPM for ten xanthonic analytes (Table 1), since good enantioselectivity and resolution were obtained (α and R_S values ranging from 1.25 to 1.99 and from 1.00 to 1.90, respectively), with very short retention (values ranging from 0.30 to 1.63). As an example, high enantioselectivity (α = 1.49) and resolution (R_S = 1.90) were obtained for analyte **10**, when 100% EtOH was used as mobile phase, being the chromatographic run less than 10 min. The low toxicity of this solvent is also a significant advantage to be taken into account [41,42].

Following the systematic investigation, PIM were also evaluated for the Chirobiotic^{TM} T column. In spite of the shorted retention factors obtained, absence or poor enantioselectivity was observed with all the combination of mobile phases evaluated. Only for analytes **4**, **9** and **20** α values > 1.00 were achieved but with poor resolution (R_S < 1.00).

Similar to the achieved results in our previous work [21], high retention times were observed under RPM, however, for fourteen analytes good enantioselectivity and resolution were obtained, with α and R_S values ranging from 1.16 to 2.83 and from 1.08 to 6.79, respectively.

For example, the Chirobiotic^{TM} T column presented very high enantioseparation capabilities for analytes **15** and **23**, with α values of 1.33 and 2.83, respectively, and R_S values of 2.46 and 6.79, respectively, using MeOH:TEAA at pH 4.2 (30:70 v/v) as mobile phase. These chromatographic results were also the best achieved for both analytes in this column. Moreover, the proportion 30:70 v/v of MeOH:TEAA was the optimum for the majority of the obtained enantioseparations.

Considering the overall chromatographic data, it should be noted that analyte **17** could be baseline resolved under three different modes, namely NPM, POM and RPM. Figure 3 shows selected chromatograms of the enantioseparation of analyte **17** using different mobile phases.

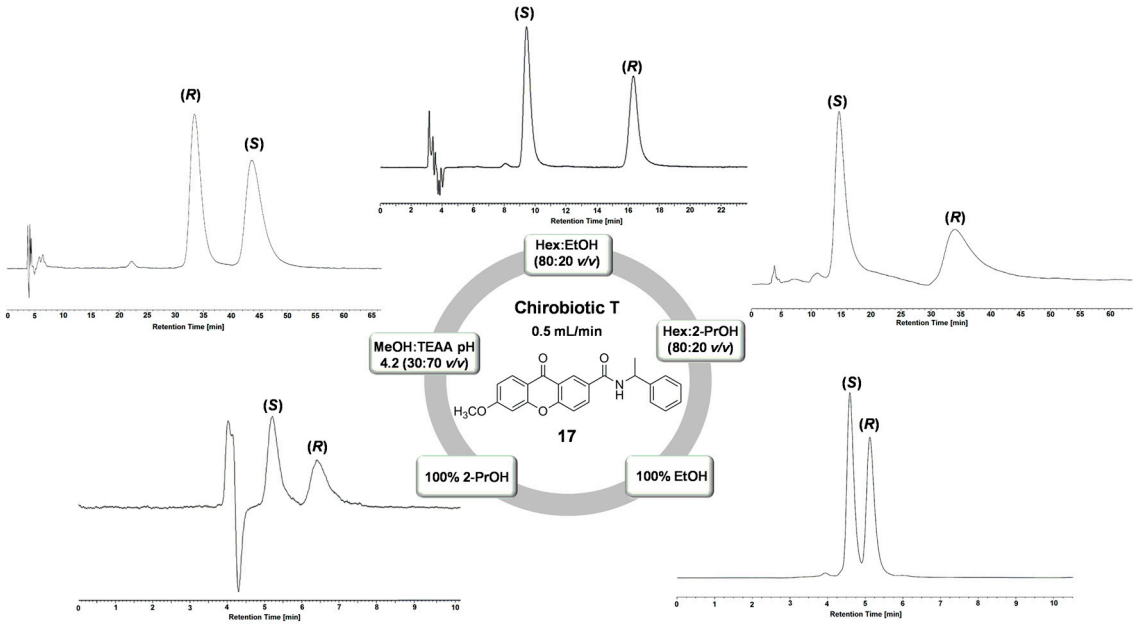


Figure 3. Chromatograms of the enantioseparation of analyte **17** on the Chirobiotic^{TM} T column using different mobile phases.

Regarding the elution order, for the enantioseparated xanthonic analytes, the (*R*)-enantiomer was the first to elute in this column. The exception was only observed for analytes **17** and **23**, which elution

order changed according to the elution mode: in NPM and POM the first eluted enantiomer was the (*S*), while (*R*) enantiomer eluted first in RPM.

2.2. Performance of Chirobiotic^{TM} R Column for Enantioresolution of Chiral Xanthonic Analytes

Considering the Chirobiotic^{TM} R column, a total of seventeen chiral xanthonic analytes (55%) was enantioseparated with resolution factors ≥1.00 (Table 2).

Table 2. Chromatographic data, retention factor of first eluted enantiomer (k_1), separation factor (α), resolution (R_S), and elution order, for the chiral xanthonic analytes on Chirobiotic^{TM} R column, under multimodal chromatographic conditions.

Analyte	Elution Mode	Mobile Phase	k_1	α	R_S	First Eluted Enantiomer
1	POM	100% MeOH	0.27	1.72	1.23	(*S*)
	PIM	MeOH:AcOH:TEA (100:0.1:1 *v*/*v*/*v*)	0.50	1.60	1.41	(*S*)
2	POM	100% MeOH	0.27	1.44	0.45	(*R*)
	PIM	MeOH:AcOH:TEA (100:0.01:0.01 *v*/*v*/*v*)	0.48	1.32	0.81	(*R*)
4	POM	100% MeOH	0.23	1.88	1.00	(*S*)
	PIM	MeOH:AcOH:TEA (100:0.1:1 *v*/*v*/*v*)	0.48	1.52	1.37	(*S*)
5	POM	100% MeOH	0.28	1.80	1.02	(*R*)
	PIM	MeOH:AcOH:TEA (100:0.1:1 *v*/*v*/*v*)	0.39	1.65	1.52	(*R*)
9	NPM	Hex:EtOH (80:20 *v*/*v*)	9.32	1.46	1.99	(*R*)
	NPM	Hex:2-PrOH (70:30 *v*/*v*)	7.59	1.88	1.49	(*R*)
	POM	100% 2-PrOH	1.44	1.85	1.32	(*R*)
	PIM	MeOH:AcOH:TEA (100:0.1:0.1 *v*/*v*/*v*)	0.22	1.72	0.87	(*R*)
10 *	NPM	Hex:EtOH (90:10 *v*/*v*)	15.78	1.24	1.77	(*R*)
	NPM	Hex:2-PrOH (80:20 *v*/*v*)	8.41	1.69	1.73	(*R*)
11	NPM	Hex:EtOH (90:10 *v*/*v*)	10.83	1.16	1.68	(*R*)
12	NPM	Hex:EtOH (90:10 *v*/*v*)	28.07	1.16	1.37	(*R*)
	PIM	MeOH:AcOH:TEA (100:0.1:1 *v*/*v*/*v*)	0.67	1.26	0.84	(*R*)
13 *	PIM	MeOH:AcOH:TEA (100:0.01:0.01 *v*/*v*/*v*)	0.44	1.47	1.15	(*S*)
17	NPM	Hex:EtOH (90:10 *v*/*v*)	2.32	2.91	3.95	(*S*)
	NPM	Hex:2-PrOH (70:30 *v*/*v*)	0.39	4.65	2.05	(*S*)
	POM	100% 2-PrOH	0.29	2.05	0.91	(*S*)
	RPM	MeOH:TEAA pH 4.2 (50:50 *v*/*v*)	1.09	1.35	0.70	(*S*)
19	RPM	MeOH:TEAA pH 4.2 (30:70 *v*/*v*)	1.90	1.21	1.00	(*R*)
20	NPM	Hex:EtOH (90:10 *v*/*v*)	20.33	1.11	1.18	(*R*)
	NPM	Hex:2-PrOH (50:50 *v*/*v*)	2.13	1.28	0.91	(*R*)
	PIM	MeOH:AcOH:TEA (100:0.1:1 *v*/*v*/*v*)	1.10	1.11	0.74	(*R*)
22	NPM	Hex:EtOH (90:10 *v*/*v*)	9.69	1.58	2.81	(*R*)
	NPM	Hex:2-PrOH (70:30 *v*/*v*)	2.06	2.21	1.83	(*R*)
	POM	100% 2-PrOH	0.61	1.97	1.00	(*R*)
23 *	NPM	Hex:2-PrOH (80:20 *v*/*v*)	2.42	1.52	1.12	(*R*)
	POM	100% 2-PrOH	0.41	1.36	0.50	(*R*)
	RPM	MeOH:TEAA pH 4.2 (40:60 *v*/*v*)	0.64	1.70	1.51	(*S*)
27	RPM	MeOH:TEAA pH 4.2 (30:70 *v*/*v*)	15.54	1.09	0.70	(*S*)
28	NPM	Hex:EtOH (90:10 *v*/*v*)	6.41	1.11	1.13	(*S*)
	RPM	MeOH:TEAA pH 4.2 (30:70 *v*/*v*)	15.45	1.25	1.12	(*S*)
29	RPM	MeOH:TEAA pH 4.2 (40:60 *v*/*v*)	13.04	1.16	1.18	(*S*)

Chromatographic conditions: flow rate: 0.2 mL/min, UV detection at 254 nm; * Elution order changed with the mobile phase.

Under NPM, this column showed very high enantioseparation capabilities for nine analytes, with α and R_S values ranging from 1.11 to 4.65 and from 1.12 to 3.95, respectively. The best chromatographic result was achieved for analyte **17**, with excellent enantioselectivity (α = 4.65), high resolution

(R_S = 2.05), and short retention time (k_1 = 0.39), when Hex:2-PrOH (70:30, v/v) was used as mobile phase. Nevertheless, in general, mixtures of Hex:EtOH afforded better chromatographic results.

It was found that none of the analytes which xanthone core has no substituents beyond an alkoxyamide chemical bridge for the link to the chiral moiety (**1**–**8**) were enantioseparated, under NPM. Actually, analytes **1**–**8** exhibited large k values and poor enantioresolution (data not shown). Consequently, under this elution mode, probably the nonspecific π-π interactions between the xanthonic and the aromatic moieties of the ristocetin selector resulted in high retention without chiral recognition. It is noteworthy that the nature of the substituents and their position on the xanthone core also have an important role in enantioselectivity.

Under POM, absence or poor resolution was observed for the majority of the xanthonic analytes. However, for the analytes comprising only one aromatic moiety and an hydroxyl group next to the stereogenic center (**1**, **9** and **22**) good enantioselectivity and resolution was obtained, with α and R_S values ranging from 1.72 to 1.85 and from 1.00 to 1.32, respectively, using 100% MeOH or 2-PrOH as mobile phases. Therefore, these structural molecular features of the analytes might be determining for enantiorecognition under this elution conditions. Moreover, the nature of the alcoholic modifier also exerted considerable effects in the retention factors. The polar nature of the mobile phase increased in the sequence 2-PrOH, EtOH and MeOH, while at a constant percentage of alcohol modifier. Increasing carbon number of the molecules of the organic solvent is disadvantageous for polar interactions between the mobile phase and analytes and, consequently, the retention factor may increase [43]. This behavior was more pronounced for 2-PrOH. In this case, the steric effect probably contributes to the decreased interactions between the mobile phase and the analytes. As an example, the retention time of analyte **1** decreased when changing the mobile phase from 2-PrOH, EtOH and MeOH, with k_1 values of 1.92, 0.56 and 0.27, respectively (data not shown).

Considering evaluation on the RPM the chromatographic results were only satisfactory for analytes **19**, **23**, **28** and **29**. The best enantioselectivity and resolution achieved were α = 1.70 and R_S = 1.51 for analyte **23** using MeOH:TEAA pH 4.2 (40:60 v/v) as mobile phase. When replacing water by pure MeOH, i.e., changing RPM to PIM, interesting results were obtained for four analytes (**1**, **4**, **5** and **13**). The presence of the protic but less polar MeOH may improve the ion-dipole interactions between those analytes and the ristocetin selector. Moreover, the acidic and basic additives added to the mobile phases are important to ensure the ionization of the selector.

In order to investigate the effect of ion content on chromatographic parameters, experiments were carried out with mobile phases containing MeOH:AcOH:TEA in the ratio of 100:1:0.1, 100:0.1:1, 100:1:1, 100:0.1:0.1 and 100:0.01:0.01 $v/v/v$) (Figure 4). Generally, when using MeOH:AcOH:TEA 100:0.1:1 $v/v/v$ high retention and resolution were obtained (k_1 ranging from 0.39 to 0.59 and R_S ranging from 1.03 to 1.52) with good enantioselectivity (α ranging from 1.35 to 1.65). Thus, using a slightly basic mobile phase, ion-dipole interactions between the amines of the selector and the amide or hydroxyl groups of the analytes, in addition to other selector-analyte interactions, may be responsible for chiral discrimination. Moreover, it was found that a higher ionic concentration resulted in lower retention. Probably, the ions existing in the mobile phase will compete for the interaction sites with the analytes.

In Chirobiotic^{TM} R column the elution order was also determined for all the enantioseparated xanthonic analytes. As shown in Table 2, for some analytes the first eluted enantiomer was the (*R*) while for others it was the (*S*). Accordingly, it was found that neither the xanthonic moiety of the analytes nor the chiral moiety determined the elution order. For example, comparing the results obtained with the analytes **19** and **29**, possessing the same chiral moiety but differing on the substituents linked to the xanthone scaffold, it can be seen that the first eluted enantiomer was the (*R*), while for the latter analyte was the (*S*)-enantiomer. Other situation can be observed when comparing the elution order of analytes **9** and **17**, possessing the same substituents linked to the xanthone scaffold but differing on the chiral moiety: for analyte **9** the first eluted enantiomer was the (*R*) while for analyte **17** was the (*S*)-enantiomer.

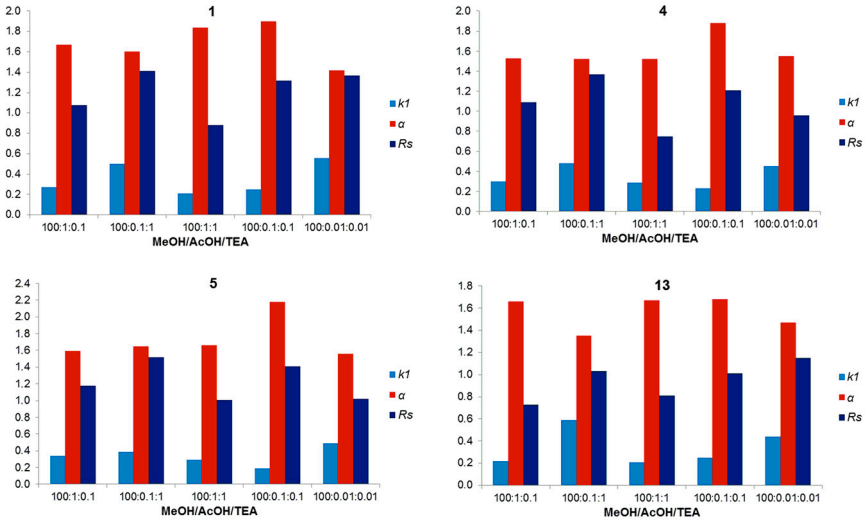


Figure 4. Effect of the different proportion of AcOH and TEA in MeOH on chromatographic parameters k_1, α and R_S for analytes **1**, **4**, **5** and **13**.

Moreover, in the case of analytes **10**, **13** and **23** the elution order changed according to the elution mode: in NPM and POM the first eluted enantiomer was the (*R*), differing for the opposite enantiomer in RPM (some data are not shown in Table 2 since it summarizes only the best chromatographic results obtained using Chirobiotic^{TM} R column for the tested xanthonic analytes).

2.3. Performance of Chirobiotic^{TM} V Column for Enantioresolution of Chiral Xanthonic Analytes

Considering the Chirobiotic^{TM} V column, NPM and RPM demonstrated to be the best elution modes for the enantioresolution of xanthonic analytes. A total of seven xanthonic analytes was successfully enantioseparated under NPM with α and R_S values ranging from 1.13 to 2.31 and from 1.16 to 7.71, respectively. Considering RPM, very high enantioselectivity and resolution were obtained for fourteen analytes with α and R_S values ranging from 1.21 to 3.32 and from 1.18 to 4.94, respectively. Relevant chromatographic results obtained using the Chirobiotic^{TM} V column for the target xanthonic analytes, under multimodal elution conditions are presented in Table 3.

Table 3. Chromatographic data, retention factor of first eluted enantiomer (k_1), separation factor (α), resolution (R_S), and elution order, for the chiral xanthonic analytes on the Chirobiotic^{TM} V column, under multimodal chromatographic conditions.

Analyte	Elution Mode	Mobile Phase	k_1	α	R_S	First Eluted Enantiomer
1	RPM	MeOH:NH_4OAc pH 6 (50:50 *v*/*v*)	2.32	1.12	0.92	(*R*)
2	NPM	Hex:EtOH (80:20 *v*/*v*)	8.72	1.09	0.88	(*R*)
4	NPM	Hex:EtOH (50:50 *v*/*v*)	3.37	1.08	0.66	(*R*)
6	NPM	Hex:EtOH (80:20 *v*/*v*)	4.69	1.09	0.89	(*R*)
	RPM	MeOH:NH_4OAc pH 6 (50:50 *v*/*v*)	3.21	1.39	2.29	(*R*)
	RPM	MeOH:NH_4OAc pH 4 (50:50 *v*/*v*)	2.68	1.39	2.67	(*R*)
9 *	NPM	Hex:EtOH (80:20 *v*/*v*)	15.72	1.19	1.16	(*S*)
	POM	100% EtOH	0.72	1.17	0.90	(*S*)
10	NPM	Hex:EtOH (80:20 *v*/*v*)	8.45	1.24	1.89	(*R*)
	POM	100% EtOH	0.39	1.23	0.60	(*R*)
	POM	100% 2-PrOH	1.24	1.29	0.60	(*R*)
11	NPM	Hex:EtOH (80:20 *v*/*v*)	6.14	1.15	1.39	(*R*)

Table 3. *Cont.*

Analyte	Elution Mode	Mobile Phase	k_1	α	R_S	First Eluted Enantiomer
12	NPM	Hex:EtOH (80:20 v/v)	13.56	1.13	1.35	(*R*)
	POM	100% 2-PrOH	1.79	1.11	0.60	(*R*)
14	RPM	MeOH:NH_4OAc pH 6 (50:50 v/v)	3.52	1.43	1.56	(*R*)
	RPM	MeOH:NH_4OAc pH 4 (50:50 v/v)	2.98	1.47	2.24	(*R*)
15	RPM	MeOH:NH_4OAc pH 6 (50:50 v/v)	3.41	1.42	2.32	(*R*)
	RPM	MeOH:NH_4OAc pH 4 (50:50 v/v)	2.87	1.44	2.49	(*R*)
16	RPM	MeOH:NH_4OAc pH 6 (50:50 v/v)	3.49	1.35	2.08	(*R*)
	RPM	MeOH:NH_4OAc pH 4 (50:50 v/v)	2.98	1.36	1.85	(*R*)
17 *	NPM	Hex:EtOH (80:20 v/v)	1.85	2.31	7.71	(*S*)
	POM	100% EtOH	0.13	2.20	1.29	(*S*)
	POM	100% 2-PrOH	0.20	2.00	1.71	(*S*)
	RPM	MeOH:NH_4OAc pH 6 (50:50 v/v)	3.11	1.21	1.18	(*R*)
	RPM	MeOH:NH_4OAc pH 4 (50:50 v/v)	2.61	1.21	1.05	(*R*)
18	RPM	MeOH:NH_4OAc pH 6 (50:50 v/v)	4.26	1.04	0.90	(*R*)
	RPM	MeOH:NH_4OAc pH 4 (50:50 v/v)	2.66	1.37	1.89	(*R*)
19	RPM	MeOH:NH_4OAc pH 6 (50:50 v/v)	4.09	1.53	2.79	(*R*)
	RPM	MeOH:NH_4OAc pH 4 (50:50 v/v)	3.03	1.55	2.47	(*R*)
20	NPM	Hex:EtOH (80:20 v/v)	3.39	1.21	1.32	(*R*)
	POM	100% EtOH	0.51	1.25	0.60	(*R*)
	POM	100% 2-PrOH	1.77	1.36	1.23	(*R*)
22	RPM	MeOH:NH_4OAc pH 6 (50:50 v/v)	2.38	1.13	0.75	(*R*)
	RPM	MeOH:NH_4OAc pH 4 (50:50 v/v)	2.51	1.15	0.78	(*R*)
23	NPM	Hex:EtOH (80:20 v/v)	3.45	1.31	2.68	(*R*)
	RPM	MeOH:NH_4OAc pH 6 (50:50 v/v)	1.34	2.34	4.94	(*R*)
	RPM	MeOH:NH_4OAc pH 4 (50:50 v/v)	1.35	3.32	4.65	(*R*)
24	RPM	MeOH:NH_4OAc pH 6 (50:50 v/v)	3.39	1.43	1.17	(*R*)
	RPM	MeOH:NH_4OAc pH 4 (50:50 v/v)	3.17	1.32	1.80	(*R*)
25	RPM	MeOH:NH_4OAc pH 6 (50:50 v/v)	3.00	1.10	1.45	(*R*)
	RPM	MeOH:NH_4OAc pH 4 (50:50 v/v)	2.55	1.35	1.66	(*R*)
26	RPM	MeOH:NH_4OAc pH 6 (50:50 v/v)	2.94	1.27	1.32	(*R*)
	RPM	MeOH:NH_4OAc pH 4 (50:50 v/v)	2.47	1.28	1.39	(*R*)
27	RPM	MeOH:NH_4OAc pH 6 (50:50 v/v)	3.14	1.38	1.91	(*R*)
	RPM	MeOH:NH_4OAc pH 4 (50:50 v/v)	2.29	1.41	1.79	(*R*)
28	RPM	MeOH:NH_4OAc pH 6 (50:50 v/v)	2.88	1.32	1.28	(*R*)
	RPM	MeOH:NH_4OAc pH 4 (50:50 v/v)	2.39	1.34	1.50	(*R*)
29	RPM	MeOH:NH_4OAc pH 6 (50:50 v/v)	3.31	1.49	1.97	(*R*)
	RPM	MeOH:NH_4OAc pH 4 (50:50 v/v)	2.99	1.54	2.08	(*R*)

Chromatographic conditions: flow rate: 0.5 mL/min, UV detection at 254 nm; * Elution order changed with the mobile phase.

Considering NPM, the combination of Hex and EtOH proved to be the most efficient. As an example, when Hex:EtOH (80:20 v/v) was used as mobile phase, excellent enantioselectivity (α = 2.31) and resolution (R_S = 7.71) were obtained for analyte **17**, in a good retention time (k_1 = 1.85). This is also the best chromatographic result achieved for all the chiral columns.

The Chirobiotic™ V column also afforded the best chromatographic results for other analytes (**6**, **14**, **15**, **16**, **18**, **19**, **24**, **25** and **29**) but under RPM. In this elution mode, the nature and proportion of the organic modifier, the pH of the mobile phase, the buffer type and concentration were investigated to study their influence on the enantioseparation process as well as to optimize the chromatographic parameters. It was found that the nature of the organic modifier exerted considerable effects on the separation, as example when MeOH was changed to THF the chromatographic parameters were not satisfactory (data not shown). Moreover, slight differences on enantioselectivity and resolution were observed at different pH (ranging from 4.0 to 6.0). This can be explained taking into account the

neutral character of the analytes that, consequently, do not undergo much influence to variations of pH. The best mobile phases were the following: MeOH:NH_4OAc pH 6 (50:50 v/v) and MeOH:NH_4OAc pH 4 (50:50 v/v).

It was found that all the analytes having methyl groups at positions 5 and 7 of the xanthone scaffold and only one stereogenic center (**22**–**29**) were successfully enantioseparated under RPM. Opposite situation occurred for the analytes which xanthone scaffold has no substituents beyond an alkoxyamide chemical bridge for the link to the chiral moiety (**1**–**8**) (with exception of analyte **6**). Consequently, under this elution mode, the nature and position of the substituents on the xanthone scaffold also have a relevant influence on the chiral recognition. In the case of analytes **1**–**8**, probably the nonspecific hydrophobic interactions between the xanthone scaffold and the vancomycin selector resulted in retention without chiral recognition.

Additionally, POM was found to be successful for the enantioseparation of two xanthonic analytes (**17** and **20**). The Chirobitic^{TM} V column provided excellent enantioselectivity (α = 2.00) and resolution (R_S = 1.71) and very short time of analysis (k_1 = 0.20) for analyte **17** with 100% 2-PrOH as mobile phase and, for analyte **20** the α and R_S values were 1.36 and 1.23, respectively. Considering evaluation on PIM the chromatographic parameters were not satisfactory (data not shown).

Regarding the elution order, likewise to the Chirobiotic^{TM} T column, the (*R*)-enantiomer of all the enantioseparated xanthonic analytes was the first to elute in Chirobiotic^{TM} V column, except for analytes **9** and **17**, which elution order changed according to the elution mode: in NPM and POM the first eluted enantiomer was (*S*), while in RPM was the (*R*)-enantiomer.

Selected chromatograms for the separation of chiral xanthonic analytes on the Chirobiotic^{TM} V column are shown in Figure 5.

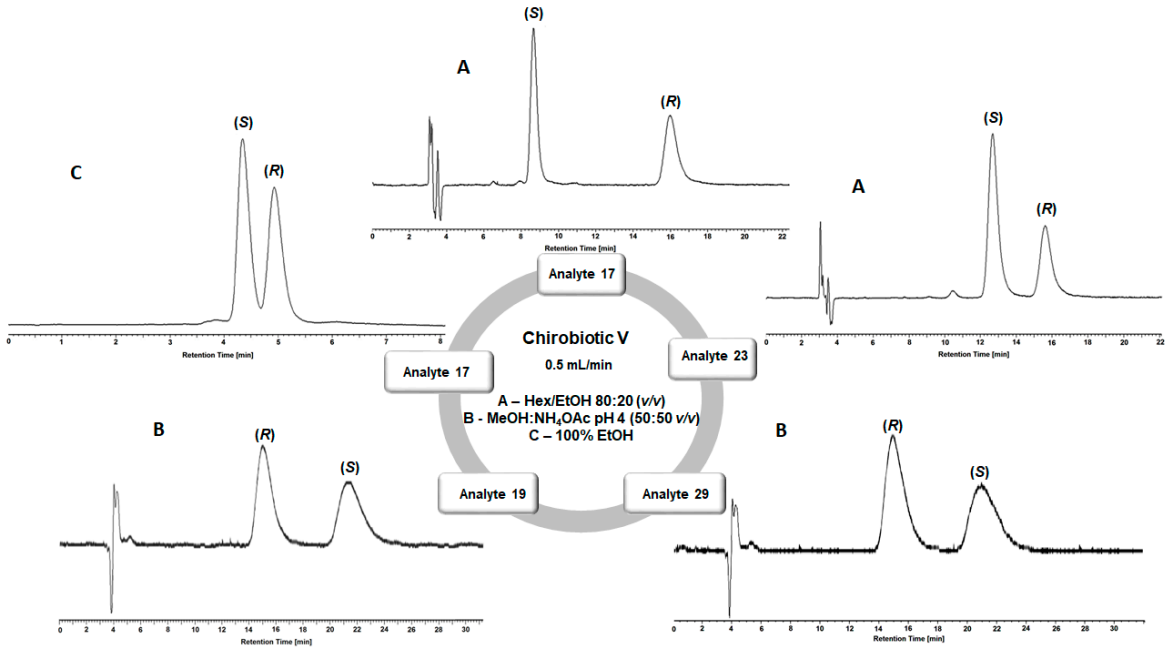


Figure 5. Chromatograms of xanthonic analytes **17**, **19**, **23** and **29** on the Chirobiotic^{TM} V column.

2.4. Performance of Chirobiotic^{TM} TAG Column for Enantioresolution of Chiral Xanthonic Analytes

The performance of Chirobiotic^{TM} TAG column to resolve the xanthonic analytes was also systematically evaluated under multimodal elution conditions. However, this column showed much lower discrimination capability compared to the others. Table 4 showed the relevant chromatographic results obtained for the tested xanthonic analytes, under multimodal elution conditions.

As shown in Table 4, good enantioseparation was observed under NPM for five xanthonic analytes using Hex:EtOH (70:30 v/v) as mobile phase with α and R_S values ranging from 1.37 to 1.45 and from

1.02 to 3.87, respectively. Partial enantioseparation was obtained for analytes **1** and **4**, under POM, using 100% EtOH as mobile phase.

Considering elution order of all the enantioseparated xanthonic analytes, the (*R*)-enantiomer was the first to elute on the Chirobiotic^{TM} TAG column. The only exception was also observed for analyte **17**.

Table 4. Chromatographic data, retention factor of first eluted enantiomer (k_1), separation factor (α), resolution (R_S), and elution order, for the chiral xanthonic analytes on the Chirobiotic^{TM} TAG column, under multimodal chromatographic conditions.

Analyte	Elution Mode	Mobile Phase	k_1	α	R_S	First Eluted Enantiomer
1	POM	100% EtOH	1.26	1.24	0.60	(*R*)
2	NPM	Hex:EtOH (70:30 *v*/*v*)	5.01	1.42	1.45	(*R*)
	POM	100% EtOH	0.73	1.39	0.80	(*R*)
4	NPM	Hex:EtOH (70:30 *v*/*v*)	10.66	1.38	1.76	(*R*)
	POM	100% EtOH	1.21	1.36	0.92	(*R*)
5	NPM	Hex:EtOH (70:30 *v*/*v*)	8.29	1.37	1.02	(*R*)
17	NPM	Hex:EtOH (70:30 *v*/*v*)	0.80	2.77	3.87	(*S*)
30	NPM	Hex:EtOH (70:30 *v*/*v*)	2.01	1.45	1.16	(*R*)
31	NPM	Hex:EtOH (70:30 *v*/*v*)	1.57	1.27	0.50	(*R*)

Chromatographic conditions: flow rate: 0.2 mL/min, UV detection at 254 nm.

2.5. Overall Effectiveness of Chirobiotic^{TM} Columns for Enantioresolution of Chiral Xanthonic Compounds under Multimodal Elution Conditions

After the systematic study of enantioseparation by LC under multimodal elution conditions, Chirobiotic^{TM} T demonstrated to be the most suitable for the xanthonic analytes evaluated. In fact, twenty-five out of thirty-one xanthonic analytes (81%) were enantioseparated with R_S values $\geq$ 1.00 (Figure 6).

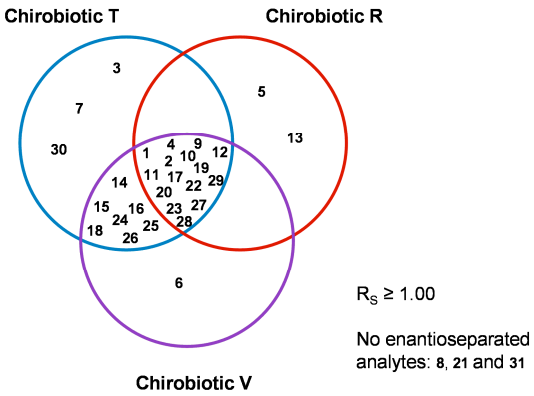


Figure 6. Diagram considering the xanthonic analytes enantioseparated by Chirobiotic^{TM} T, R and V columns, with resolution factors $\geq$1.00. Chirobiotic^{TM} TAG was not included considering its poor enantioselectivity for the evaluted analytes.

Moreover, this column was more efficient under NPM, allowing the efficient enantioseparation of twenty-two analytes (71%), as shown in Figure 7. This result is in agreement with our previous work [21]. Similar trend was observed by Armstrong *et col.* for dihydrofurocoumarins [44]. RPM and POM were also efficient elution modes for the efficient enantioseparation of fourteen (45%) and ten xanthonic analytes (32%), respectively, on a Chirobiotic^{TM} T column. Moreover, in some cases these elution modes proved to be good alternatives to NPM. Additionally, it should be highlight

that analytes **3**, **7** and **30** could only be enantioresolved with R_S value $\geq$ 1.00 on the Chirobiotic^{TM} T column.

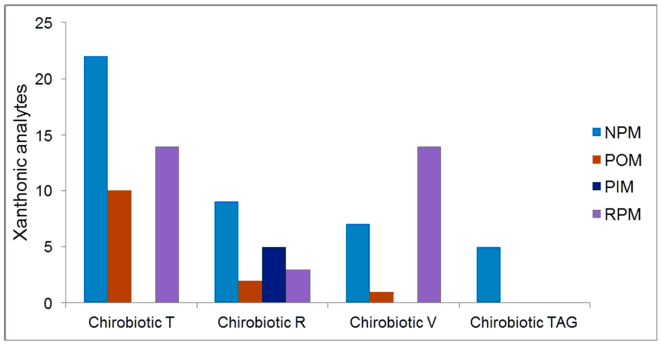


Figure 7. Comparative performance of Chirobiotic^{TM} T, R, V and TAG for baseline enantioseparation of xanthonic analytes under multimodal elution conditions.

Interestingly, Chirobiotic^{TM} V under RPM was very efficient for the tested xanthonic analytes (Figure 7) and, in some cases, exhibited the broadest enantioselectivity observed in all chiral columns. It was a surprising result considering that in our previous work, this chiral column was one of the less efficient. However, herein, for the new xanthonic analytes evaluated, particularly those having methyl groups at positions 5 and 7 on the xanthone scaffold, this column was very effective. In fact, a total of twenty-three analytes (74%) were baseline enantioseparated on the Chirobiotic^{TM} V column (Figure 6), and analyte **6** could only be baseline resolved in this column.

Chirobiotic^{TM} R and TAG columns showed the lowest discrimination ability, under multimodal elution conditions. However, under NPM nine (29%) and five (16%) analytes were baseline enantioseparated in Chirobiotic^{TM} R and TAG, respectively (Figure 7). Additionally, Chirobiotic^{TM} R column was the only one useful for the efficient enantioseparation of analytes **5** and **13** (Figure 6).

Finally, it should be emphasized that the xanthonic analytes comprising two stereogenic centers with the same configuration, i.e., analytes **8**, **21** and **31**, (Figure 2) were not enantioseparated in any of the four Chirobiotic^{TM} columns. Interestingly, their diastereoisomers were enantioseparated. These results suggest that the stereochemistry of both stereogenic centers on the xanthonic analytes play an important role in the enantioseparation of this class of chiral compounds on macrocyclic glycopeptide-based columns evaluated.

2.6. Computational Studies

In order to understand the binding mechanism behind the observed results of enantioresolution, docking studies were performed, using the chiral xanthonic analytes that were enantioseparated by LC with resolution factors $\geq$1.00. Values of docking scores are presented on Table 5. The lower the docking score, the more stable is the analyte:selector complex. Concerning Chirobiotic^{TM} T, R, V, and TAG columns, there was a 52%, 50%, 47%, and 80% agreement between docking scores and experimental results concerning the elution order of the enantiomers of the chiral analytes. The differences observed may be due to the complex structures of the macrocyclic glycopeptide-based selectors allowing different binding patterns with the molecules of the analytes. In fact, although all the structurally related glycopeptide antibiotics can establish the same type of interactions, including hydrogen, dipole-dipole, π-stacking, hydrophobic as well as steric repulsion [20], their morphological differences in the aglycon macrocyclic portions as well as other structural features, are responsible for their differences in enantioselectivity, retention times, and efficiency [45]. Moreover, computationally, AutodockVina has a hybrid scoring function (empirical and knowledge-based function) inspired in the X-Score function that consists of a weighted sum of steric interactions, hydrophobic interaction, and number of active rotatable bonds with different weights [46]. Therefore, similar selectors and/or ligands can originate very different docking scores, depending not only on the type of interactions

established, but also the number of interactions, maximizing favorable and minimizing unfavorable interactions, shape and property complementarities [47].

Table 5. Docking scores (Kcal.mol^{-1}) of both enantiomers of xanthonic analytes on Chirobiotic^{TM} T, R, V, TAG (**I**), and binding affinity difference between (*R*) and (*S*) enantiomers (**II**).

Analytes	R_S Value				I Docking Score				II Docking Score (*R*)–(*S*) (Delta) δ			
	T	R	V	TAG	T	R	V	TAG	T	R	V	TAG
(*R*)-**1** (*S*)-**1**	2.26	1.41	<1.00	<1.00	**−6.6** **−7.1**	**−7.1** **−6.9**	*	*	−0.5	−0.2	*	*
(*R*)-**2** (*S*)-**2**	1.49	<1.00	<1.00	1.45	−5.9 −5.4	*	*	**−4.9** **−5.1**	−0.5	*	*	−0.2
(*R*)-**3** (*S*)-**3**	1.09	<1.00	<1.00	<1.00	−5.8 −5.8	*	*	*	0.0	*	*	*
(*R*)-**4** (*S*)-**4**	2.95	1.37	<1.00	1.76	**−5.8** **−5.9**	**−6.2** **−6.0**	*	−4.9 −4.8	−0.1	−0.2	*	−0.1
(*R*)-**5** (*S*)-**5**	<1.00	1.52	<1.00	1.02	*	−6.3 −6.1	*	**−5.1** **−5.2**	*	−0.2	*	−0.1
(*R*)-**6** (*S*)-**6**	<1.00	<1.00	2.67	<1.00	*	*	−6.9 −6.6	*	*	*	−0.3	*
(*R*,*R*)-**7** (*S*,*S*)-**7**	2.83	<1.00	<1.00	<1.00	−7.0 −6.7	*	*	*	−0.3	*	*	*
(*S*,*R*)-**8** (*R*,*S*)-**8**	<1.00	<1.00	<1.00	<1.00	*	*	*	*	*	*	*	*
(*R*)-**9** (*S*)-**9**	2.48	1.99	1.16	<1.00	−6.2 −6.1	**−6.2** **−6.7**	**	*	−0.1	−0.5	**	*
(*R*)-**10** (*S*)-**10**	3.30	1.77	1.89	<1.00	−5.7 −5.7	**	−6.7 −6.6	*	0.0	**	−0.1	*
(*R*)-**11** (*S*)-**11**	2.43	1.68	1.39	<1.00	**−5.7** **−5.8**	−6.3 −6.1	**−6.1** **−6.3**	*	−0.1	−0.2	−0.2	*
(*R*)-**12** (*S*)-**12**	2.31	1.37	1.35	<1.00	−5.9 −5.8	**−6.2** **−6.5**	−6.7 −6.5	*	−0.1	−0.3	−0.2	*
(*R*)-**13** (*S*)-**13**	<1.00	1.15	<1.00	<1.00	*	**	*	*	*	**	*	*
(*R*)-**14** (*S*)-**14**	1.55	<1.00	2.24	<1.00	**−6.5** **−6.6**	*	**−6.5** **−6.6**	*	−0.1	*	−0.1	*
(*R*)-**15** (*S*)-**15**	2.46	<1.00	2.49	<1.00	−6.3 −6.3	*	−7.3 −7.1	*	0.0	*	−0.2	*
(*R*)-**16** (*S*)-**16**	1.92	<1.00	2.08	<1.00	−6.0 −5.9	*	**−7.1** **−7.4**	*	−0.2	*	−0.3	*
(*R*)-**17** (*S*)-**17**	7.37	3.95	7.71	3.87	**	−7.3 −7.3	**	**−4.9** **−4.6**	**	0.0	**	−0.3
(*R*)-**18** (*S*)-**18**	1.43	<1.00	1.89	<1.00	**−5.6** **−5.7**	*	**−7.7** **−7.9**	*	−0.1	*	−0.2	*
(*R*)-**19** (*S*)-**19**	1.30	1.00	2.79	<1.00	−6.5 −6.4	**−7.2** **−7.3**	−7.7 −7.5	*	−0.1	−0.1	−0.2	*
(*R*,*R*)-**20** (*S*,*S*)-**20**	2.24	1.18	1.32	<1.00	−6.5 −6.5	−7.4 −7.1	**−7.6** **−7.8**	*	0.0	−0.3	−0.2	*
(*S*,*R*)-**21** (*R*,*S*)-**21**	<1.00	<1.00	<1.00	<1.00	*	*	*	*	*	*	*	*
(*R*)-**22** (*S*)-**22**	2.45	2.81	<1.00	<1.00	−6.5 −6.2	−7.1 −7.0	*	*	−0.3	−0.1	*	*
(*R*)-**23** (*S*)-**23**	6.79	1.51	4.94	<1.00	**	**	−6.3 −6.7	*	**	**	−0.4	*
(*R*)-**24** (*S*)-**24**	1.55	<1.00	1.80	<1.00	**−6.7** **−7.2**	*	−8.0 −7.5	*	−0.5	*	−0.5	*
(*R*)-**25** (*S*)-**25**	1.08	<1.00	1.66	<1.00	**−6.1** **−6.7**	*	**−7.9** **−8.3**	*	−0.6	*	−0.4	*
(*R*)-**26** (*S*)-**26**	1.49	<1.00	1.39	<1.00	**−6.5** **−7.2**	*	**−7.6** **−7.8**	*	−0.5	*	−0.2	*

Table 5. *Cont.*

Analytes	R_S Value				I Docking Score				II Docking Score (*R*)–(*S*) (Delta) δ			
	T	R	V	TAG	T	R	V	TAG	T	R	V	TAG
(*R*)-**27** (*S*)-**27**	1.97	<1.00	1.91	<1.00	**−7.0** **−7.1**	*	**−7.5** **−7.6**	*	−0.1	*	−0.1	*
(*R*)-**28** (*S*)-**28**	1.87	1.13	1.50	<1.00	**−6.3** **−6.8**	**−7.5** **−7.2**	−7.8 −7.5	*	−0.5	−0.3	−0.3	*
(*R*)-**29** (*S*)-**29**	1.18	1.18	2.08	<1.00	**−6.6** **−7.1**	−7.6 −7.6	−7.7 −7.5	*	−0.5	0.0	−0.2	*
(*R*,*R*)-**30** (*S*,*S*)-**30**	1.93	<1.00	<1.00	1.16	**−6.6** **−6.8**	*	*	**−5.4** **−5.5**	−0.2	*	*	−0.1
(*S*,*R*)-**31** (*R*,*S*)-**31**	<1.00	<1.00	<1.00	<1.00	*	*	*	*	*	*	*	*

* not analyzed because R_S < 1.00; ** not analyzed because elution order was different according to the mobile phase used; **Bold numbers**: docking binding affinity in accordance with elution order.

In order to understand the binding mechanism, a visual inspection of the binding conformations and established interactions were performed for the molecules of the xanthonic analytes. Figures 8–10 illustrate representative examples of the most stable docked conformations for enantiomers complexes with the chiral selectors of the four chiral columns.

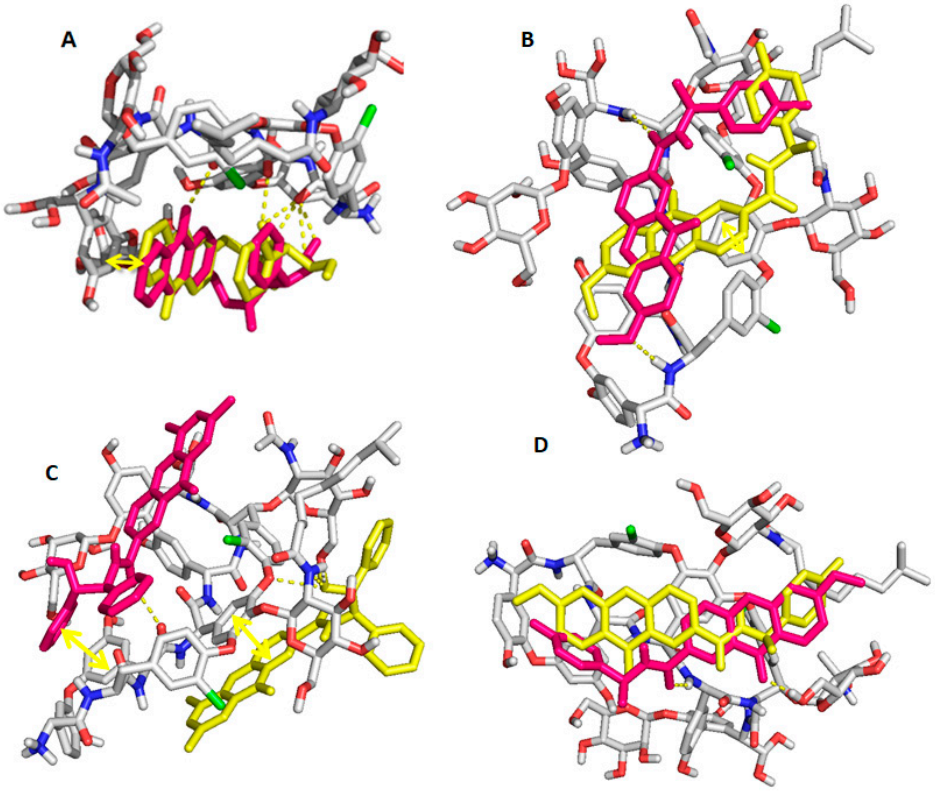


Figure 8. Analyte **1** (**A**), Analyte **14** (**B**), Analyte **30** (**C**), and Analyte **18** (**D**), docked on teicoplanin selector. Chiral selectors are represented in sticks with C, O, N, and Cl atoms colored in grey, red, blue, and green, respectively. (*S*) and (*R*) enantiomers are represented with magenta and yellow sticks, respectively. Hydrogen interactions and π-stacking interactions are represented with dashes and double arrow, respectively.

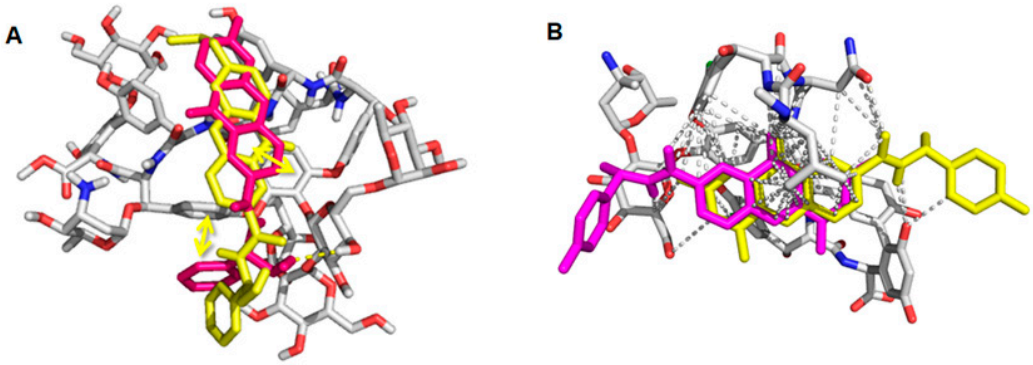


Figure 9. (**A**) Analyte **9** docked on ristocetin selector; (**B**) Analyte **25** docked on vancomycin selector. Chiral selectors are represented in sticks with C, O, N, and Cl atoms colored in grey, red, blue, and green, respectively. (*S*) and (*R*) enantiomers are represented with magenta and yellow sticks, respectively. In (**A**), hydrogen interactions and π-stacking interactions are represented with dashes and double arrow, respectively. In (**B**), all the interactions (apolar and polar) are represented as grey dashes.

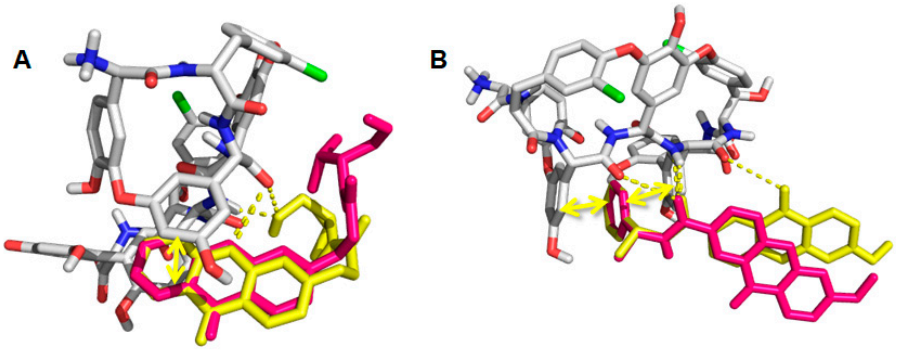


Figure 10. (**A**) Analyte **2** docked on teicoplanin aglycone selector; (**B**) Analyte **17** docked on teicoplanin aglycone selector. Chiral selectors are represented in sticks with C, O, N, and Cl atoms colored in grey, red, blue, and green, respectively. (*S*) and (*R*) enantiomers are represented with magenta and yellow sticks, respectively. Hydrogen interactions and π-stacking interactions are represented with dashes and double arrow, respectively.

Figure 8A show that both enantiomers of analyte **1** are folded in a "U" shape to maximize both the π stacking interactions between the xanthonic moiety and one of the teicoplanin aromatic rings; and the hydrogen interactions between –OH and –NH– groups of the xanthone molecule and the teicoplanin carbonyl groups. However, as the carbonyl group of the xanthone core of (*S*)-enantiomer is turned inside of the teicoplanin molecule, an additional hydrogen interaction with a teicoplanin carbonyl group was established. This last interaction can justify the stronger retention of (*S*)-enantiomer in the Chirobiotic™ T column.

However, this is not a general rule for the other enantioseparated analytes. As shown in Figure 8, for analytes **14** (Figure 8B), **30** (Figure 8C), and **18** (Figure 8D), the docking poses of both enantiomers of each xanthonic pair are very diverse. Consequently, different groups of both xanthonic and chiral moieties of the analytes are involved in the interactions.

Although both enantiomers of analyte **9** bind through π-stacking interactions between the xanthone scaffold and the aromatic rings of the ristocetin selector, only the aromatic ring of the chiral moiety of (*S*)-enantiomer is in such a way that allows an additional parallel π-stacking interaction (Figure 9A). Moreover, the terminal –OH group of (*S*)-enantiomer also establishes an additional hydrogen interaction with an –OH group of the chiral selector.

On the Chirobiotic™ V column, the majority of the chiral xanthonic analytes were enantioseparated under RPM. Concerning the enantiomers of analyte **25** docked onto the Chirobiotic™

V column, both enantiomers are bound to the selector through hydrophobic interactions between the xanthone scaffold and the aromatic rings and alkyl chain of vancomycin selector (Figure 9B). Additionally, hydrogen interactions (three) were also established. However, one of the hydrogen interactions on (*S*)-enantiomer is established with a fluorine atom [48], more electronegative than oxygen, thus resulting on a stronger interaction.

On the Chirobiotic™ TAG column, the (*S*)-enantiomers were always more retained, with exception of analyte **17**. Using analyte **2** as an example, both enantiomers are bound to the Chirobiotic™ TAG column by π stacking interactions established between the xanthone scaffold and aromatic rings of the selector. (*S*)-enantiomer binds more stably to the chiral selector creating additional hydrogen interactions with the amide groups of the chiral moiety (Figure 10A). Concerning analyte **17**, the aromatic ring and amide group of the chiral moiety on both enantiomers establish π-stacking and hydrogen interactions with the chiral selector, respectively. Nonetheless, only the (*R*)-enantiomer establishes an extra hydrogen interaction through the xanthone carbonyl group (Figure 10B). This different elution profile of analyte **17**, comparing to the other analytes, was due to its binding pose with the xanthone scaffold facing the outside medium, and the aromatic ring of the chiral moiety establishing double sided π-stacking interactions with two aromatic rings on the selector (Figure 10B); whereas for other analytes, such as **2**, the xanthone scaffold is the structural moiety that is holding the analyte to the selector through parallel π-stacking interactions (Figure 10A).

3. Materials and Methods

3.1. Chemicals and Reagents

Chiral xanthonic analytes (Figure 2) were obtained "in-house" according to procedures described elsewhere [17,18]. HPLC grade EtOH, MeOH, 2-PrOH, ACN, THF, and Hex were purchased from Sigma-Aldrich (St. Louis, MO, USA). TEA, AcOH, NH_4OAc, all p.a. grade, were also obtained from Sigma-Aldrich. Ultrapure water was purified by a Milli-Q system (Millipore, Bedford, MA, USA). TEAA buffers were prepared by titration of 0.1 or 1% (by volume) aqueous solutions of TEA with AcOH to adjust to a suitable pH.

3.2. Apparatus and Chromatography

Chromatographic measurements were carried out on two chromatographic systems. One LC system contained a model 880-PU Intelligent HPLC pump (JASCO Corporation, Tokyo, Japan), equipped with a 7125 injector (Rheodyne LCC, Rohnert Park, CA, USA) fitted with a 20 µL loop, a JASCO model 880-30 solvent mixer, a 875-UV intelligent UV/Vis detector A chromatography station for Microsoft Windows 95, version 1.7 DLL, was applied. The second LC was a Dionex Ultimate 3000 (Thermo Fisher Scientific Inc., Waltham, MA, USA) system equipped with a 3000 quaternary pump, a 3000 autosampler, and a 3000 Variable UV/Vis detector was also used. Chromeleon™ software version 7.2 Ultimate (Thermo Fisher Scientific Inc., Waltham, MA, USA) was employed to manage chromatographic data. Chromatographic separations were performed on four commercial macrocyclic glycopeptide-based columns: Chirobiotic™ T (150 × 4.6 mm id, 5 µm particle size), Chirobiotic™ TAG (150 × 2.1 mm id, 5 µm particle size), Chirobiotic™ V (250 × 4.6 mm id, 5 µm particle size) and Chirobiotic™ R (150 × 2.1 mm id, 5 µm particle size) (Figure 1), from ASTEC (Whippany, NJ, USA). Stock solutions of all chiral xanthonic analytes were prepared by dissolution in EtOH at a concentration of 1 mg/mL. Working solutions were further prepared by dilution of the stock solutions in the same solvent to a concentration of 10 µg/mL. The injection volume was 10 µL, and all the chromatographic analyses were performed in isocratic mode at 22 ± 2 °C, in triplicate. The dead times (t_0) were considered to be equal to the peak of the solvent front, and were taken from each particular run. The column flow rate was 0.5 mL/min (Chirobiotic™ T and V) or 0.2 mL/min (Chirobiotic™ R and TAG), and the chromatograms were recorded by UV detection at a wavelength of 254 nm. The mobile phases were prepared in a volume/volume relation, filtered using a Millipore

0.45 µm filter, and further degassed in an ultrasonic bath for 15 min before use. All the analytes mentioned in Figure 2 were evaluated with different mobile phases under NPM, POM, PIM and RPM. The elution order was determined for all the enantioseparated xanthonic analytes by injecting the solutions of the enantiomeric mixtures (prepared mixing equal aliquots of each enantiomer), and then each enantiomer separately.

3.3. Computational

The structures of the selectors were obtained from PubChem [49], and both enantiomers of all xanthonic compounds (Figure 2) were drawn and minimized using an Austin Model 1 (AM1) semi-empirical quantum mechanics force field [50]. The calculation was finished when the gradient between any two successive steps in the geometry search was less than 10^{-1} kcal/mol/Å or the maximum steps were reached, whichever comes first. The line search used was the Broyden-Fletcher-Golfarb-Shanno search which uses an approximate Hessian matrix to guide the search [51]. Docking simulations between the chiral selector and the xanthonic enantiomers were undertaken in AutoDock Vina (Molecular Graphics Lab, La Jolla, CA, USA) [46]. AutoDock Vina considered the target conformation as a rigid unit while the ligands were allowed to be flexible and adaptable to the target. Vina searched for the lowest binding affinity conformations and returned nine different conformations for each small molecule. The lowest binding energy docking poses of each compound were chosen. AutoDock Vina was run using an exhaustiveness of 9 and grid boxes engulfing the selectors were built. PyMol v1.3 (Schrödinger, New York, NY, USA) [52] was used for visual inspection of results and graphical representations.

4. Conclusions

The systematic study of enantioseparation for thirty-one chiral xanthonic analytes using four macrocyclic glycopeptide-based chiral columns confirmed the applicability of these columns in multimodal elution conditions for the enantioseparation of this class of compounds. It was found that their applicability increased considering the complementary profile in enantioselectivity of the different macrocyclic glycopeptide-based selectors. For some chiral xanthonic analytes, 100% EtOH as mobile phase presented excellent chromatographic parameters. EtOH is considered a green solvent due its low toxicity. As it was expected, the structural nature of the analytes and the chiral selectors as well as the mobile phase composition proved to be fundamental factors for the molecular interactions and consequently for chiral recognition.

The docking study showed that each macrocyclic glycopeptide-based selector allowed different binding patterns for both enantiomers of the analytes due to their complex structures. Due to the very diverse structural features of the thirty-one enantiomeric pairs of xanthonic analytes, with different alkyl and aryl substituents in different positions of the xanthone scaffold, and to the differences in spatial disposition (chirality) and tridimensional shape of the compounds, would not be suitable to establish a generalized chiral recognition mechanism or identify which chemical characteristics are more relevant for retention in the referred columns.

However, the results of the present study fulfilled the initial objectives since higher resolutions were obtained for the chiral xanthonic analytes evaluated compared to our previous work, and additional information about chiral recognition mechanisms was provided. In summary, we believe that this work contributes to a better knowledge in enantioseparation and chiral recognition in general and for chiral xanthonic derivatives in particular. Computational chemistry studies allowed an improvement to understand the behavior of these important class of compounds within macrocyclic glycopeptide-based chiral columns.

Acknowledgments: This research was partially supported by the Strategic Funding UID/Multi/04423/2013 through national funds provided by FCT—Foundation for Science and Technology and European Regional Development Fund (ERDF), in the framework of the programme PT2020, the project PTDC/MAR-BIO/4694/2014 (reference POCI-01-0145-FEDER-016790; Project 3599—Promover a Produção

Científica e Desenvolvimento Tecnológico e a Constituição de Redes Temáticas (3599-PPCDT)) as well as by the project INNOVMAR—Innovation and Sustainability in the Management and Exploitation of Marine Resources (reference NORTE-01-0145-FEDER-000035, within Research Line NOVELMAR), supported by North Portugal Regional Operational Programme (NORTE 2020), under the PORTUGAL 2020 Partnership Agreement, through the European Regional Development Fund (ERDF), and Chiral_Drugs_CESPU_2017. Phyo thanks the Erasmus Mundus Action 2 (Lotus Plus project) for a PhD's scholarship.

Author Contributions: Ye` Zaw Phyo performed both liquid chromatography enantioresolution and docking experiments, and contributed in writing the draft of the manuscript. Sara Cravo participated in liquid chromatography enantioresolution experiments. Andreia Palmeira participated in docking studies, and contributed in writing the manuscript. Maria Elizabeth Tiritan gave scientific advice for the development of liquid chromatography enantioresolution experiments, participated in discussion of the results and reviewed the final version of the manuscript. Anake Kijjoa contributed with discussion during the preparation of the manuscript and reviewed the final version of the manuscript. Madalena M. M. Pinto contributed with discussion during experiments, the preparation of the manuscript and reviewed the final version. Carla Fernandes coordinated and supervised both liquid chromatography enantioresolution and docking experiments, reviewed the data generated and wrote the paper.

Conflicts of Interest: The authors declare no conflict of interest.

References

1. Nguyen, H.T.; Lallemand, M.C.; Boutefnouchet, S.; Michel, S.; Tillequin, F. Antitumor psoropermum xanthones and sarcomelicope acridones: Privileged structures implied in DNA alkylation. *J. Nat. Prod.* **2009**, *72*, 527–539. [CrossRef] [PubMed]
2. Pinto, M.M.M.; Castanheiro, R.A.P.; Kijjoa, A. Xanthones from marine-derived microorganisms: Isolation, structure elucidation, and biological activities. In *Encyclopedia of Analytical Chemistry*; John Wiley & Sons: Hoboken, NJ, USA, 2014.
3. Lesch, B.; Bräse, S. A short, atom-economical entry to tetrahydroxanthenones. *Angew. Chem. Int. Ed.* **2004**, *43*, 115–118. [CrossRef] [PubMed]
4. Cruz, M.I.; Cidade, H.; Pinto, M. Dual/multitargeted xanthone derivatives for alzheimer's disease: Where do we stand? *Future Med. Chem.* **2017**, *9*, 1611–1630. [CrossRef] [PubMed]
5. Lima, R.T.; Sousa, D.; Paiva, A.M.; Palmeira, A.; Barbosa, J.; Pedro, M.; Pinto, M.M.; Sousa, E.; Vasconcelos, M.H. Modulation of autophagy by a thioxanthone decreases the viability of melanoma cells. *Molecules* **2016**, *21*, 1343. [CrossRef] [PubMed]
6. Barbosa, J.; Lima, R.T.; Sousa, D.; Gomes, A.S.; Palmeira, A.; Seca, H.; Choosang, K.; Pakkong, P.; Bousbaa, H.; Pinto, M.M.; et al. Screening a small library of xanthones for antitumor activity and identification of a hit compound which induces apoptosis. *Molecules* **2016**, *21*, 81. [CrossRef] [PubMed]
7. Silva, R.; Sousa, E.; Carmo, H.; Palmeira, A.; Barbosa, D.J.; Gameiro, M.; Pinto, M.; Bastos, M.D.; Remiao, F. Induction and activation of p-glycoprotein by dihydroxylated xanthones protect against the cytotoxicity of the p-glycoprotein substrate paraquat. *Arch. Toxicol.* **2014**, *88*, 937–951. [CrossRef] [PubMed]
8. Azevedo, C.M.G.; Afonso, C.M.M.; Soares, J.X.; Reis, S.; Sousa, D.; Lima, R.T.; Vasconcelos, M.H.; Pedro, M.; Barbosa, J.; Gales, L.; et al. Pyranoxanthones: Synthesis, growth inhibitory activity on human tumor cell lines and determination of their lipophilicity in two membrane models. *Eur. J. Med. Chem.* **2013**, *69*, 798–816. [CrossRef] [PubMed]
9. Genovese, S.; Fiorito, S.; Taddeo, V.A.; Epifano, F. Recent developments in the pharmacology of prenylated xanthones. *Drug Discov. Today* **2016**, *21*, 1814–1819. [CrossRef] [PubMed]
10. Pinto, M.M.; Sousa, M.E.; Nascimento, M.S. Xanthone derivatives: New insights in biological activities. *Curr. Med. Chem.* **2005**, *12*, 2517–2538. [CrossRef] [PubMed]
11. Shagufta; Ahmad, I. Recent insight into the biological activities of synthetic xanthone derivatives. *Eur. J. Med. Chem.* **2016**, *116*, 267–280.
12. Masters, K.S.; Bräse, S. Xanthones from fungi, lichens, and bacteria: The natural products and their synthesis. *Chem. Rev.* **2012**, *112*, 3717–3776. [CrossRef] [PubMed]
13. Vieira, L.M.M.; Kijjoa, A. Naturally-occurring xanthones: Recent developments. *Curr. Med. Chem.* **2005**, *12*, 2413–2446. [CrossRef] [PubMed]
14. Azevedo, C.M.G.; Afonso, C.M.M.; Pinto, M.M.M. Routes to xanthones: An update on the synthetic approaches. *Curr. Org. Chem.* **2012**, *16*, 2818–2867. [CrossRef]

15. Sousa, M.E.; Pinto, M.M.M. Synthesis of xanthones: An overview. *Curr. Med. Chem.* **2005**, *12*, 2447–2479. [CrossRef] [PubMed]
16. Fernandes, C.; Palmeira, A.; Ramos, I.I.; Carneiro, C.; Afonso, C.; Tiritan, M.E.; Cidade, H.; Pinto, P.C.A.G.; Saraiva, M.L.M.F.S.; Reis, S.; et al. Chiral derivatives of xanthones: Investigation of the effect of enantioselectivity on inhibition of cyclooxygenases (Cox-1 and Cox-2) and binding interaction with human serum albumin. *Pharmaceuticals* **2017**, *10*. [CrossRef] [PubMed]
17. Fernandes, C.; Masawang, K.; Tiritan, M.E.; Sousa, E.; de Lima, V.; Afonso, C.; Bousbaa, H.; Sudprasert, W.; Pedro, M.; Pinto, M.M. New chiral derivatives of xanthones: Synthesis and investigation of enantioselectivity as inhibitors of growth of human tumor cell lines. *Bioorg. Med. Chem.* **2014**, *22*, 1049–1062. [CrossRef] [PubMed]
18. Fernandes, C.; Oliveira, L.; Tiritan, M.E.; Leitao, L.; Pozzi, A.; Noronha-Matos, J.B.; Correia-de-Sa, P.; Pinto, M.M. Synthesis of new chiral xanthone derivatives acting as nerve conduction blockers in the rat sciatic nerve. *Eur. J. Med. Chem.* **2012**, *55*, 1–11. [CrossRef] [PubMed]
19. Fernandes, C.; Tiritan, M.E.; Cravo, S.; Phyo, Y.Z.; Kijjoa, A.; Silva, A.M.S.; Cass, Q.B.; Pinto, M.M.M. New chiral stationary phases based on xanthone derivatives for liquid chromatography. *Chirality* **2017**. [CrossRef] [PubMed]
20. Ward, T.J.; Ward, K.D. Chiral separations: A review of current topics and trends. *Anal. Chem.* **2012**, *84*, 626–635. [CrossRef] [PubMed]
21. Fernandes, C.; Tiritan, M.E.; Cass, Q.; Kairys, V.; Fernandes, M.X.; Pinto, M. Enantioseparation and chiral recognition mechanism of new chiral derivatives of xanthones on macrocyclic antibiotic stationary phases. *J. Chromatogr. A* **2012**, *1241*, 60–68. [CrossRef] [PubMed]
22. Carraro, M.L.; Palmeira, A.; Tiritan, M.E.; Fernandes, C.; Pinto, M.M.M. Resolution, determination of enantiomeric purity and chiral recognition mechanism of new xanthone derivatives on (*S*,*S*)-whelk-O1 stationary phase. *Chirality* **2017**, *29*, 247–256. [CrossRef] [PubMed]
23. Fernandes, C.; Palmeira, A.; Santos, A.; Tiritan, M.E.; Afonso, C.; Pinto, M.M. Enantioresolution of chiral derivatives of xanthones on (*S*,*S*)-Whelk-O1 and l-phenylglycine stationary phases and chiral recognition mechanism by docking approach for (*S*,*S*)-Whelk-O1. *Chirality* **2013**, *25*, 89–100. [CrossRef] [PubMed]
24. Fernandes, C.; Brandão, P.; Santos, A.; Tiritan, M.E.; Afonso, C.; Cass, Q.B.; Pinto, M.M. Resolution and determination of enantiomeric purity of new chiral derivatives of xanthones using polysaccharide-based stationary phases. *J. Chromatogr. A* **2012**, *1269*, 143–153. [CrossRef] [PubMed]
25. Fernandes, C.; Pinto, M.; Tiritan, M.E. Enantioresolution of chiral derivatives of xanthones on different types of liquid chromatography stationary phases: A comparative study. *Curr. Chromatogr.* **2014**, *1*, 139–150. [CrossRef]
26. Lämmerhofer, M. Chiral recognition by enantioselective liquid chromatography: Mechanisms and modern chiral stationary phases. *J. Chromatogr. A* **2010**, *1217*, 814–856. [CrossRef] [PubMed]
27. Ilisz, I.; Pataj, Z.; Aranyi, A.; Péter, A. Macrocyclic antibiotic selectors in direct hplc enantioseparations. *Sep. Purif. Rev.* **2012**, *41*, 207–249. [CrossRef]
28. Orosz, T.; Grecsó, N.; Lajkó, G.; Szakonyi, Z.; Fülöp, F.; Armstrong, D.W.; Ilisz, I.; Péter, A. Liquid chromatographic enantioseparation of carbocyclic β-amino acids possessing limonene skeleton on macrocyclic glycopeptide-based chiral stationary phases. *J. Pharm. Biomed. Anal.* **2017**, *145*, 119–126. [CrossRef] [PubMed]
29. Armstrong, D.W.; Tang, Y.; Chen, S.; Zhou, Y.; Bagwill, C.; Chen, J.R. Macrocyclic antibiotics as a new class of chiral selectors for liquid chromatography. *Anal. Chem.* **1994**, *66*, 1473–1484. [CrossRef]
30. Armstrong, D.W.; Liu, Y.; Ekborgott, K.H. A covalently bonded teicoplanin chiral stationary phase for hplc enantioseparations. *Chirality* **1995**, *7*, 474–497. [CrossRef]
31. Flieger, J.; Feder-Kubis, J.; Tatarczak-Michalewska, M.; Płazińska, A.; Madejska, A.; Swatko-Ossor, M. Natural terpene derivatives as new structural task-specific ionic liquids to enhance the enantiorecognition of acidic enantiomers on teicoplanin-based stationary phase by high-performance liquid chromatography. *J. Sep. Sci.* **2017**, *40*, 2374–2381. [CrossRef] [PubMed]
32. Flieger, J. Improvement of chiral discrimination of acidic enantiomers on teicoplanin stationary phase by the use of chaotropic effect. *J. Liq. Chromatogr. Relat. Technol.* **2009**, *32*, 948–963. [CrossRef]
33. Feder-Kubis, J.; Flieger, J.; Tatarczak-Michalewska, M.; Płazińska, A.; Madejska, A.; Swatko-Ossor, M. Renewable sources from plants as the starting material for designing new terpene chiral ionic liquids used for the chromatographic separation of acidic enantiomers. *RSC Adv.* **2017**, *7*, 32344–32356. [CrossRef]

34. Ward, T.J.; Farris Iii, A.B. Chiral separations using the macrocyclic antibiotics: A review. *J. Chromatogr. A* **2001**, *906*, 73–89. [CrossRef]
35. Scriba, G.K.E. Chiral recognition mechanisms in analytical separation sciences. *Chromatographia* **2012**, *75*, 815–838. [CrossRef]
36. Scriba, G.K.E. Chiral recognition in separation science—An update. *J. Chromatogr. A* **2016**, *1467*, 56–78. [CrossRef] [PubMed]
37. Bauvais, C.; Barbault, F.; Zhu, Y.; Petitjean, M.; Fan, B. Elucidation of chiral recognition processes of macrocyclic antibiotic vancomycin. *SAR QSAR Environ. Res.* **2006**, *17*, 253–264. [CrossRef] [PubMed]
38. Berthod, A.; Chen, X.; Kullman, J.P.; Armstrong, D.W.; Gasparrini, F.; D'Acquaric, I.; Villani, C.; Carotti, A. Role of the carbohydrate moieties in chiral recognition on teicoplanin-based LC stationary phases. *Anal. Chem.* **2000**, *72*, 1767–1780. [CrossRef] [PubMed]
39. Berthod, A.; Qiu, H.X.; Staroverov, S.M.; Kuznestov, M.A.; Armstrong, D.W. Chiral recognition with macrocyclic glycopeptides: Mechanisms and applications. In *Chiral Recognition in Separation Methods: Mechanisms and Applications*; Springer: Berlin/Heidelberg, Germany, 2010.
40. Berthod, A. Chiral recognition mechanisms with macrocyclic glycopeptide selectors. *Chirality* **2009**, *21*, 167–175. [CrossRef] [PubMed]
41. Sandra, P.; Vanhoenacker, G.; David, F.; Sandra, K.; Pereira, A. Green chromatography (part 1): Introduction and liquid chromatography. *LC-GC Eur.* **2010**, *23*, 242–259.
42. Majors, R.E.; Raynie, D. The greening of the chromatography laboratory. *LC-GC North. Am.* **2011**, *29*, 118–134.
43. Berkecz, R.; Ilisz, I.; Benedek, G.; Fülöp, F.; Armstrong, D.W.; Péter, A. High-performance liquid chromatographic enantioseparation of 2-aminomono- and dihydroxycyclopentanecarboxylic and 2-aminodihydroxycyclohexanecarboxylic acids on macrocyclic glycopeptide-based phases. *J. Chromatogr. A* **2009**, *1216*, 927–932. [CrossRef] [PubMed]
44. Xiao, T.L.; Rozhkov, R.V.; Larock, R.C.; Armstrong, D.W. Separation of the enantiomers of substituted dihydrofurocoumarins by hplc using macrocyclic glycopeptide chiral stationary phases. *Anal. Bioanal. Chem.* **2003**, *377*, 639–654. [CrossRef] [PubMed]
45. Gasper, M.P.; Berthod, A.; Nair, U.B.; Armstrong, D.W. Comparison and modeling study of vancomycin, ristocetin a, and teicoplanin for ce enantioseparations. *Anal. Chem.* **1996**, *68*, 2501–2514. [CrossRef] [PubMed]
46. Trott, O.; Olson, A.J. Software news and update autodock vina: Improving the speed and accuracy of docking with a new scoring function, efficient optimization, and multithreading. *J. Comput. Chem.* **2010**, *31*, 455–461. [PubMed]
47. Akhter, M. Challenges in docking: Mini review. *JSM Chem.* **2016**, *4*, 1–8.
48. Zhou, P.; Zou, J.; Tian, F.; Shang, Z. Fluorine bonding—How does it work in protein-ligand interactions? *J. Chem. Inf. Model.* **2009**, *49*, 2344–2355. [CrossRef] [PubMed]
49. Kim, S.; Thiessen, P.A.; Bolton, E.E.; Chen, J.; Fu, G.; Gindulyte, A.; Han, L.; He, J.; He, S.; Shoemaker, B.A.; et al. Pubchem substance and compound databases. *Nucleic Acids Res.* **2016**, *44*, D1202–D1213. [CrossRef] [PubMed]
50. Dewar, M.J.S.; Zoebisch, E.G.; Healy, E.F.; Stewart, J.J.P. Development and use of quantum mechanical molecular models. 76. Am1: A new general purpose quantum mechanical molecular model. *J. Am. Chem. Soc.* **1985**, *107*, 3902–3909. [CrossRef]
51. Mirzaei, H.; Zarbafian, S.; Villar, E.; Mottarella, S.; Beglov, D.; Vajda, S.; Paschalidis, I.; Vakili, P.; Kozakov, D. Energy minimization on manifolds for docking flexible molecules. *J. Chem. Theory Comput.* **2015**, *11*, 1063–1076. [CrossRef] [PubMed]
52. Lill, M.A.; Danielson, M.L. Computer-aided drug design platform using pymol. *J. Comput. Aided Mol. Des.* **2011**, *25*, 13–19. [CrossRef] [PubMed]

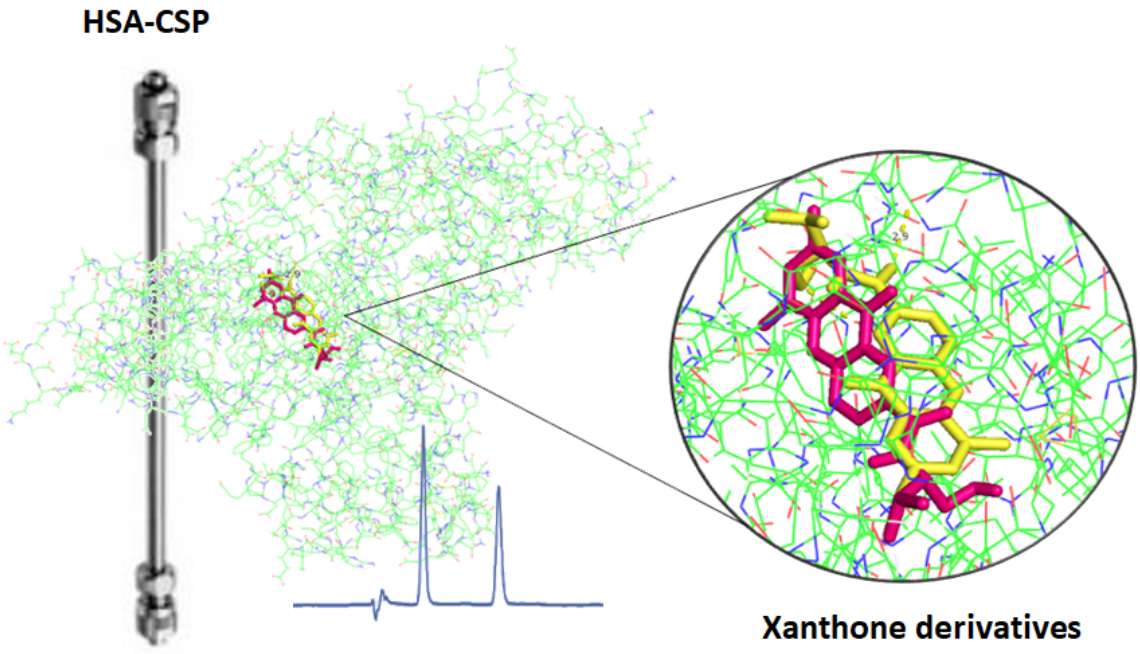
Sample Availability: Samples of the compounds **1–31** are available from the authors.

© 2018 by the authors. Licensee MDPI, Basel, Switzerland. This article is an open access article distributed under the terms and conditions of the Creative Commons Attribution (CC BY) license (http://creativecommons.org/licenses/by/4.0/).

CHAPTER VIII

Enantioseparation, chiral recognition mechanisms and binding of xanthone derivatives on immobilized human serum albumin by liquid chromatography

Original research article submitted for publication in Bioanalysis



Graphical abstract

Bioanalysis

Submission Confirmation

Print

Thank you for your submission

Submitted to
Bioanalysis

Manuscript ID
BIO-2019-0074

Title
Enantioseparation, recognition mechanisms and binding of xanthones on human serum albumin by liquid chromatography

Authors
Carmo, João
Phyo, Ye Zaw
Palmeira, Andreia
Tiritan, Maria
Afonso, Carlos M. M.
Kijjoa, Anake
Pinto, Madalena
Fernandes, Carla

Date Submitted
14-Mar-2019

Enantioseparation, chiral recognition mechanisms and binding of xanthone derivatives on immobilized human serum albumin by liquid chromatography

João P. do Carmo[1], Ye Zaw Phyo[2,3], Andreia Palmeira[1,2], Maria Elizabeth Tiritan[1,2,4], Carlos Afonso[1,2], Anake Kijjoa[2,3], Madalena M. M. Pinto[1,2], Carla Fernandes[1,2]

[1] Laboratório de Química Orgânica e Farmacêutica, Departamento de Ciências Químicas, Faculdade de Farmácia, Rua de Jorge Viterbo Ferreira, 228, 4050-313 Porto, Portugal

[2] Interdisciplinary Centre of Marine and Environmental Research (CIIMAR), Edifício do Terminal de Cruzeiros do Porto de Leixões, Av. General Norton de Matos s/n, 4050-208 Matosinhos, Portugal

[3] ICBAS-Instituto de Ciências Biomédicas Abel Salazar, Universidade do Porto, Rua de Jorge Viterbo Ferreira, 228, 4050-313 Porto, Portugal

[4] CESPU, Instituto de Investigação e Formação Avançada em Ciências e Tecnologias da Saúde (IINFACTS), Rua Central de Gandra, 1317, 4585-116 Gandra PRD, Portugal

Correspondence: cfernandes@ff.up.pt; Tel.: +35-122-042-8688

Abstract

A systematic study of enantioseparation of a library of thirty-one enantiomeric mixtures of chiral derivatives of xanthones (CDXs), prepared “in house”, was performed by liquid chromatography using a chiral stationary phase based on human serum albumin (HSA-CSP). The influence of the organic modifier, buffer type, pH and ionic strength of the mobile phase, and temperature were explored. Fourteen enantiomeric mixtures of CDXs were baseline enantioseparated with high enantioselectivity (α) and resolution (Rs). Under the optimized chromatographic conditions, α and Rs values were ranging from 1.40 to 9.16 and from 1.51 to 4.97, respectively. The binding affinity to HSA of each CDX has also been determined by bioaffinity chromatography, measuring the retention times of the CDXs on the HSA-CSP, and further calculation of bound percentage. In general, high affinity for HSA-CSP was observed, with bound percentages ranging from 79.02 to 99.99%. Moreover, chiral recognition mechanisms for CDXs on HSA-CSP were also investigated by molecular docking method using AutoDock Vina.

Keywords: Chiral Derivatives of Xanthones; Liquid Chromatography; Human Serum Albumin; Enantioseparation; Bioaffinity; Molecular Recognition.

1. Introduction

In the early stages of drug discovery, beyond the biological activity screening, each compound should also be evaluated and characterized by its lipophilicity, ionization, solubility, metabolic properties, and protein-binding affinity [1]. High-performance affinity liquid chromatography (HPALC) is a type of liquid chromatography (LC) that has become extremely useful and widely used to study intermolecular interactions between biomolecules and drugs [2]. This method is based on drug affinity to a biologically-related stationary phase. Fast and convenient determination of drug-protein interactions by using small amount of immobilized protein is one of the main advantages of this method [3], being automatic and reproducible, having the possibility of working under near-physiological conditions (buffer pH, ionic strength and temperature). Additionally, by using a chiral stationary phase (CSP), it is possible to analyze the behavior of both enantiomers of racemic or enantiomeric mixtures in the same run [4]. Another advantage is the possibility to perform other type of analyses in addition to bioaffinity binding studies, including: displacement studies with the presence of a competitive agent [5], thermodynamic and variability studies of chromatographic conditions [6], quantitative structure-retention relationship studies [7], and enantioseparation of racemic or enantiomeric mixtures [8]. Nevertheless, the immobilization process of the protein to a chromatographic support can bring some variations comparatively to the protein in soluble form, namely conformational changes, denaturation, steric hindrance at the binding sites, nonspecific binding by the

support, and anchor matrix [9, 10]. There are various approaches, which can counterbalance this disadvantage, namely covalent immobilization, biospecific adsorption, and entrapment [11]. As a consequence, a high concordance of this method compared to other techniques, such as ultrafiltration, is found [12].

Although there are other proteins in human blood plasma to which drugs are able to binding, human serum albumin (HSA) is the most abundant and, subsequently, the most used to predict how drugs behave in the human body [13], as well as plays an important role in the transport of drugs, metabolites, and endogenous ligands [14]. Binding to HSA controls the free and active concentration of a drug, provides a reservoir for a long duration of action, and affects drug absorption, metabolism, distribution, excretion and toxicological profile (ADMET), determining the overall pharmacological activity of a drug [15].

Several studies reported that HSA-CSPs were efficiently used for enantioseparation of chiral analytes, and the chromatographic results reflected their binding to HSA *in vivo* [15-17]. HSA exhibit a broad affinity and chiral recognition for a variety of classes of analytes due to its flexible structure comprising multiple binding sites [18]. The interactions of chiral analytes with HSA are often stereoselective, and information on these interactions by computational methods may be valuable to provide insights about chiral recognition mechanisms and to design and optimize further chiral separations [19, 20], particularly for HSA [21-23].

During the last few decades, there has been a widespread interest in oxygenated heterocyclic compounds, such as molecules with a xanthone scaffold, mainly due to their variety of biological and pharmacological activities [24-26]. Our group have also dived into this fascinating class of compounds to found new promising xanthones showing not only interesting biological activities [27-32] and suitable physicochemical properties [33, 34] but also other applications such as chiral selectors in LC [35, 36]. Among them, some chiral derivatives of xanthones (CDXs) proved to act as blockers of sciatic nerve transmission [37], as inhibitors of growth of human tumor cell lines [38] and cyclooxygenase enzymes [39]; in some cases, being the activity dependent on the stereochemistry. Additionally, enantioseparation studies and enantiomeric purity evaluation of the CDXs have been conducted using different types of CSPs, namely Pirkle-type [40, 41], macrocyclic glycopeptide-based [41, 42], and polysaccharide-based [43] CSPs.

In a continuation of our work, herein, we report a systematic study of enantioseparation of a library of thirty-one enantiomeric mixtures of CDXs (**Fig.1**) prepared “in house”, on a commercially available HSA-CSP, to expand the chiral recognition studies of this class of compounds on different types of CSPs. Computational studies by molecular docking approach were also performed to corroborate the experimental results and to better understand the chromatographic behavior at a molecular level, as well as the structural features associated with the chiral recognition mechanism.

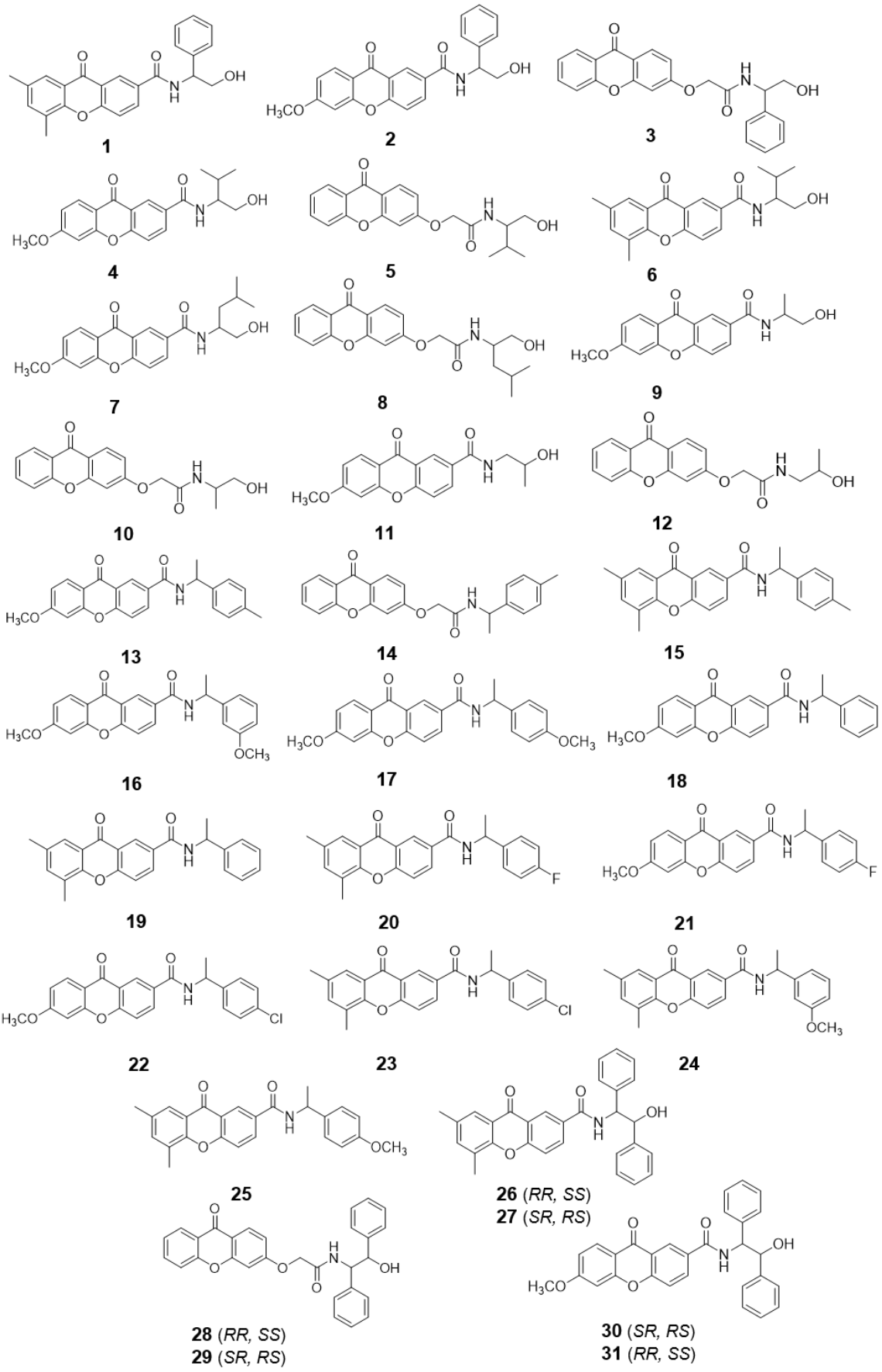


Fig. 1. Chemical structures of enantiomeric mixtures of CDXs **1-31**.

Recently, we reported the measurement of HSA binding affinity of three enantiomeric mixtures of CDXs by using *in vitro* spectrofluorimetric assays [39]. All CDXs demonstrated to bind with high affinity to HSA, and enantioselectivity was observed for one pair. To extend the binding affinity studies and to develop and optimize a fast and reliable method for screening CDX-HSA affinity, determinations for each enantiomer of CDXs were performed by HPALC, using a HSA-CSP.

To the best of our knowledge, LC systematic study and binding affinity of CDXs on HSA-CSP are presented here for the first time, highlighting the contribution of this work to expand the applications of this type of CSPs for a new class of chiral compounds.

2. Experimental

2.1. Chemical and reagents

CDXs were previously synthesized in enantiomerically pure form, by coupling different carboxyxanthones with both enantiomers of commercially available chiral reagents, according to described procedure [37, 38]. Chlorpromazine, indomethacin and metronidazole (all in p.a. grade) were purchased from Merck (Darmstadt, Germany). Methanol (MeOH), ethanol (EtOH), 2-propanol (2-PrOH), acetonitrile (ACN) for HPLC were purchased from Merck (Darmstadt, Germany). Ammonium acetate, sodium acetate, sodium phosphate dibasic, sodium phosphate monobasic, potassium phosphate monobasic, di-potassium hydrogen phosphate 3-hydrate (all in p.a. grade) were purchased from Carlo Erba (Barcelona, Spain) or from Merck (Darmstadt, Germany). Ultrapure water was generated by a Milli-Q system (Millipore, Bedford, MA). All other reagents and solvents were of analytical grade or ultrapure.

2.2. Instrumentation and chromatographic conditions

Analytical LC analyses were performed on a Thermo® Scientific HPLC equipped with an Thermo® Scientific Spectra System P4000 pump, detection was carried out using an Thermo® Scientific Spectra System UV8000 diode array detector (DAD) and the samples were injected by an autosampler Thermo® Scientific Spectra System AS3000. Data acquisition was performed using ChromQuest 5.0™. The chromatography analyses were achieved in reversed-phase mode on a CHIRALPAK® HSA column (150 mm × 40 mm, I.D., 5 µm) purchased at ChromTech, Lda (Congelton, Cheshire, UK). The flow rate used was 0.9 mL/min and the chromatograms were monitored by a DAD detector with the wavelength of 254 nm. The sample injections (20 µL) were carried out in duplicate or triplicate and the mean of the values were considered. The HPLC temperature and mobile phases were controlled by AS3000 autosampler oven. The analysis temperature was 22 ± 2°C or 37 ± 2°C.

2.3. Mobile phases

Aqueous buffers of sodium phosphate, potassium phosphate, ammonium acetate and sodium acetate were prepared at 10 mM; potassium phosphate buffer was also prepared at 67 mM. Buffers at 10 mM were prepared at pH 5.0 and 7.0, and the 67 mM buffers were prepared at pH 7.0 and 7.4. All aqueous buffers pH was controlled by a Gondo® PL-700PV pH monitor. The mobile phases were prepared in a volume/volume relation (*v*/*v*), degassed in an ultrasonic bath (Sonorex Digitec, Bandelin) for at least 15 min before use and were filtered through polyamide membrane filters of 0.2 µm pore size from Whatman® GmbH (Dassel, Germany). In the systematic study and optimization of the method, several mobile phases were tested. The organic modifiers used were ACN, MeOH, EtOH and 2-PrOH. For binding studies, the mobile phase composition used was a mixture of 67 mM potassium phosphate buffer at pH 7.4 with ACN as organic modifier, in nine different percentages ranging from 2-25%.

2.4. Sample solutions

Stock solutions of enantiomerically pure CDXs were prepared in EtOH at the concentration of 1 mg/mL and further diluted to working solutions of 100 µg/mL. Working solutions of enantiomeric mixtures were prepared mixing equal aliquots of each enantiomer. The working solutions for ligand-protein binding determinations were prepared by dilution of each enantiomer stock solution at the concentration of 50 µg/mL. The same strategy was used to prepare the working solutions of the drugs, to obtain a final concentration of 50 µg/mL.

2.5. Chromatographic and binding parameters determination

The retention factor (k) was calculated using the equation (1):

$$k = \frac{t_R - t_0}{t_0} \quad (1)$$

The dead time (t_0) was considered to be equal to the peak of the solvent front and was taken from each particular run. The separation factor (α) was calculated using the equation (2):

$$= \frac{k_2}{k_1} \quad (2)$$

The resolution factor (R_s) was calculated using the equation (3):

$$R_S = 1.18 \frac{t_{R2} - t_{R1}}{W_{1\,0.5} + W_{2\,0.5}} \quad (3)$$

where t_{R1} and t_{R2} are the retention times of the first and second enantiomers, respectively, and $W_{1\,0.5}$ and $W_{2\,0.5}$ are the corresponding peak width measured on half height.

The bound drug percentage (%*b*) was calculated from the k values, obtained by zonal elution chromatography, according to equation (4) [44]:

$$b = \frac{k}{1+k} \quad (4)$$

The bound drug parameter calculation in only aqueous phase was extrapolated by linearly plotting the log k values (averages of triplicate measurements) against the percentage (*v/v*) of ACN in the mobile phase.

2.6. Computational

The X-ray crystal structure of HSA (PDB code: 2bxg) was downloaded from the Protein Data Bank of Brookhaven [45], and both enantiomers of all CDXs were drawn and minimized using an Austin Model 1 (AM1) semi-empirical quantum mechanics force field [46]. The calculation was finished when the gradient between any two successive steps in the geometry search was less than 10^{-1} kcal/mol/Å or the maximum steps were reached, whichever comes first. The line search used was the Broyden-Fletcher-Golfarb-Shanno search which uses an approximate Hessian matrix to guide the search [47]. Docking simulations between the chiral selector and the CDXs were performed in AutoDock Vina (Molecular Graphics Lab, La Jolla, CA, USA) [48]. AutoDock Vina considered the target conformation as a rigid unit while the ligands were allowed to be flexible and adaptable to the target. Vina searched for the lowest binding affinity conformations and returned nine different conformations for each small molecule. The lowest binding energy docking poses of each compound were chosen. AutoDock Vina was run using an exhaustiveness of 8 and a grid boxes with the dimension of X: 2.8, Y: 0.669, Z: 0.128 for HSA. PyMol v1.3 (Schrödinger, New York, NY, USA) [49] was used for visual inspection of results and graphical representations.

3. Results and discussion

A CHIRALPAK® HSA column was employed for a systematic study of enantioseparation of a library of thirty-one enantiomeric mixtures of CDXs (**Fig. 1.**), where several chromatographic conditions were explored. Affinity binding studies, under chromatographic conditions that mimic the physiological environment, and computational studies were also conducted. Both enantiomers of all enantiomeric mixtures of CDXs **1-31** were previously synthesized, in enantiomerically pure form, by coupling carboxyxanthones (CXs) with both enantiomers of commercially available chiral reagents using *O*-(benzotriazol-1-yl)-*N*,*N*,*N'*,*N'*-tetramethyluronium tetrafluoroborate (TBTU) as coupling reagent [37, 38].

3.1. Systematic enantioseparation of CDXs

Optimization of the chromatographic conditions were performed to achieve the best conditions to obtain a higher number of separations of enantiomeric mixtures of CDXs **1-31** (**Fig. 1.**), with good enantioselectivity and resolution as well as short analysis time. Firstly, the organic modifier type and content, the buffer type and pH were explored. Then, modifications to approach to the physiological environment, by changing the buffer ionic strength to 67 mM, and its pH to 7.4 as well as the temperature of analysis to 37^{o}C were also carried out.

3.1.1. Organic modifier selection

The first step was to choose the most suitable organic modifier for the resolution of enantiomeric mixtures of CDXs **1-31**. Columns with immobilized HSA, such as a CHIRALPAK® HSA, are very susceptible to the presence and variation of organic modifiers [50]. They may differentially affect the reversible spatial conformation of the protein leading to changes in the number of available selective and non-selective binding sites, and may further accelerate protein denaturation leading to a significant shortening of CSP lifetime [51]. The purpose of choosing the best organic modifier took into consideration three factors: (i) using the minor proportion as possible of organic modifier; (ii) shorten CDXs retention and, consequently, analysis time; (iii) maintaining the enantioselective capacity of the CSP. Based on the technical data sheet provided by the column manufacturer [52], and considering that the tested CDXs are neutral, a mobile phase comprising 10 mM ammonium acetate buffer at pH 7.0 was chosen to start the systematic study of enantioseparation. The solvent ratio chosen took in consideration the high HSA affinity showed by this class of compounds in a previous work [39]. Four organic modifiers were used, namely ACN, EtOH, 2-PrOH and MeOH. Initially, all enantiomeric mixtures were tested using four different mobile phases comprising mixtures of ammonium acetate buffer (pH 7.0; 10 mM) with each one of the organic modifiers, in a proportion of 85:15 *v/v*. The analyses were carried out at 22 ± 2°C. Under these conditions, the majority of the enantiomeric mixtures of CDXs were not baseline enantioseparated. Nevertheless, for some of them enantioselectivity was observed; however, very high retention and poor resolution were obtained. As example, **Fig. 2.** shows the chromatograms obtained for enantiomeric mixture of CDX **30** using different organic modifiers in the mobile phase.

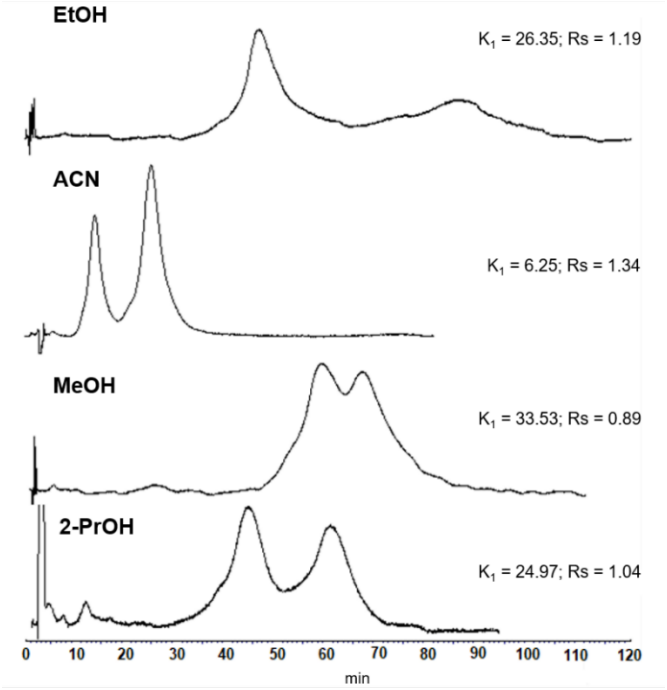


Fig. 2. Chromatograms for enantiomeric mixture of CDX **30** on a CHIRALPAK® HSA using different organic modifiers in the mobile phase: EtOH, ACN, MeOH and 2-PrOH. Mobile phase, ammonium acetate buffer (pH 7.0; 10 mM)/organic modifier (85:15 *v/v*); Flow rate, 0.9 mL/min.; Temperature, 22 ± 2°C; Detection, 254 nm.

According to **Fig. 2.**, the mobiles phases comprising MeOH, EtOH and 2-PrOH as organic modifier afforded the highest retention factors, with k_1 = 33.53, 26.35 and 24.97, respectively. The organic modifier ACN showed a significantly lower retention factor, with k_1 = 6.25 as well as better resolution, when compared to the other mobile phases. Similar behavior was observed for the other enantiomeric mixtures of CDXs. Accordingly, ACN was the organic modifier selected for further method optimization since it allowed the shortest analysis time for the enantioseparated mixtures of CDXs.

3.1.2. Buffer and pH selection

Different buffers were tested as aqueous phase, namely ammonium acetate, sodium acetate, potassium phosphate and sodium phosphate [52]. The choice of phosphate buffers is intrinsically related to the stability of the HSA as chiral selector [9]. In addition, several studies described the use of this type of buffers mimicking the physiological conditions of human plasma and, consequently, being used in protein binding studies [50, 53, 54]. Acetate buffers were also widely used in several enantioseparation studies, demonstrating good applicability [55, 56]. A great advantage of acetate buffers compared to phosphate buffers is the possibility to be used as component of the mobile phase for LC-MS analysis [57]. The effect of pH variation is also a determining factor for this type of study. interfering g in Coulomb interactions,

leading to conformational alterations of the albumin molecule which possesses negative or positive charges when the buffer pH is higher or lower than its isoelectric point [58]. HSA will be more negatively charged with increasing pH, for example. In addition, the control of pH is essential for analysis of ionized analytes [59]. In this work, since all tested CDXs are neutral, no significant changes in their ionization are expected to occur varying the pH of the mobile phase.

For CHIRALPAK® HSA column, a variation of mobile phase pH from 5.0 to 7.0 is possible to be used without shortening the life of the CSP [52]. Therefore, both values of pH were selected for the various buffers using different proportions of ACN as organic modifier (ranging from 25 to 0%). The overall best chromatographic results are shown on **Table 1**. Under all the chromatographic conditions evaluated among the thirty-one injected over the CHIRALPAK® HSA column, fourteen enantiomeric mixtures of CDXs, were baseline enantioseparated. It was found that six out of the fourteen enantiomeric mixtures of CDXs were separated in all evaluated chromatographic conditions.

Table 1

Chromatographic data obtained for enantiomeric mixtures of CDXs on CHIRALPAK® HSA, using different buffer types, at pH 5.0 and 7.0, on mobile phases.

Enantiomeric mixture		**Ammonium acetate** (10mM)		**Sodium acetate** (10mM)		**Potassium phosphate** (10mM)		**Sodium phosphate** (10mM)	
		pH 5.0	**pH 7.0**	**pH 5.0**	**pH 7.0**	**pH 5.0**	**pH 7.0**	**pH 5.0**	**pH 7.0**
CDX **1**	ACN %	18	20	16	20	20	18	20	20
	k_1	3.36	2.69	4.70	5.87	2.64	4.77	2.53	2.78
	k_2	9.67	8.03	14.05	19.44	9.88	19.64	9.68	12.45
	α	2.87	2.98	2.99	3.31	3.75	4.12	3.83	4.47
	Rs	3.27	3.55	2.70	3.30	4.04	2.04	3.12	6.41
CDX **6**	ACN %	-	-	-	-	-	20	-	-
	k_1	-	-	-	-	-	0.82	-	-
	k_2	-	-	-	-	-	10.28	-	-
	α	-	-	-	-	-	12.53	-	-
	Rs	-	-	-	-	-	4.81	-	-
CDX **14**	ACN %	-	-	-	-	-	16	-	15
	k_1	-	-	-	-	-	6.52	-	10.51
	k_2	-	-	-	-	-	9.03	-	14.87
	α	-	-	-	-	-	1.39	-	1.42
	Rs	-	-	-	-	-	1.02	-	1.27

Table 1 Continuation

Enantiomeric mixture		**Ammonium acetate** (10mM)		**Sodium acetate** (10mM)		**Potassium phosphate** (10mM)		**Sodium phosphate** (10mM)	
		pH 5.0	**pH 7.0**	**pH 5.0**	**pH 7.0**	**pH 5.0**	**pH 7.0**	**pH 5.0**	**pH 7.0**
CDX **15**	ACN %	22	22	21	21	24	21	22	23
	k_1	2.82	4.84	4.05	3.85	2.43	4.06	3.55	3.40
	k_2	8.88	18.71	12.84	12.58	10.55	19.63	16.29	14.52
	α	3.15	3.87	3.17	3.27	4.34	4.84	4.59	4.27
	Rs	2.79	4.73	2.49	1.78	4.36	6.11	4.91	4.77
CDX **16**	ACN %	10	-	11	-	12	-	-	-
	k_1	13.01	-	15.28	-	14.94	-	-	-
	k_2	19.58	-	23.33	-	21.98	-	-	-
	α	1.51	-	1.53	-	1.47	-	-	-
	Rs	1.61	-	2.08	-	1.02	-	-	-
CDX **18**	ACN %	-	-	-	-	24	21	-	-
	k_1	-	-	-	-	1.17	1.79	-	-
	k_2	-	-	-	-	9.57	17.41	-	-
	α	-	-	-	-	8.19	9.70	-	-
	Rs	-	-	-	-	5.29	3.93	-	-
CDX **19**	ACN %	22	22	21	21	24	21	22	22
	k_1	2.03	3.06	2.93	2.56	1.72	2.66	2.47	3.43
	k_2	9.98	20.30	10.66	10.53	8.89	15.69	20.19	20.89
	α	4.91	6.63	3.64	4.11	5.17	5.90	8.16	6.10
	Rs	3.87	5.24	2.57	2.03	4.88	5.72	4.32	5.17
CDX **20**	ACN %	22	22	22	21	22	20	22	23
	k_1	2.03	3.12	2.26	2.70	3.52	3.99	2.49	2.20
	k_2	7.55	15.14	11.02	10.36	20.37	20.44	14.25	16.77
	α	3.72	4.85	4.88	3.84	5.78	5.12	5.73	7.62
	Rs	3.08	4.38	3.10	2.37	3.94	3.41	4.17	4.40
CDX **22**	ACN %	-	-	-	20	-	18	-	20
	k_1	-	-	-	4.94	-	15.75	-	6.71
	k_2	-	-	-	11.27	-	19.95	-	19.13
	α	-	-	-	2.28	-	1.27	-	1.36
	Rs	-	-	-	2.52	-	0.90	-	1.07
CDX **23**	ACN %	-	-	20	-	22	22	-	-
	k_1	-	-	3.59	-	8.14	6.75	-	-
	k_2	-	-	7.79	-	34.53	26.79	-	-
	α	-	-	2.17	-	4.25	3.97	-	-
	Rs	-	-	1.38	-	1.97	2.31	-	-
CDX **24**	ACN %	18	22	18	18	20	19	20	20
	k_1	5.90	2.76	5.04	6.04	4.12	4.09	4.09	5.50
	k_2	16.39	7.05	13.21	16.75	13.53	12.06	12.59	18.95
	α	2.78	2.55	2.62	2.77	3.28	2.95	3.08	3.44
	Rs	3.07	2.87	2.70	2.52	3.28	4.20	2.86	4.93

Table 1 Continuation

Enantiomeric mixture		**Ammonium acetate** (10mM)		**Sodium acetate** (10mM)		**Potassium phosphate** (10mM)		**Sodium phosphate** (10mM)	
		pH 5.0	**pH 7.0**	**pH 5.0**	**pH 7.0**	**pH 5.0**	**pH 7.0**	**pH 5.0**	**pH 7.0**
CDX **25**	ACN %	18	20	16	20	18	19	18	20
	k_1	6.73	6.24	9.37	4.49	5.85	7.29	8.12	5.73
	k_2	15.22	14.81	21.31	9.72	17.66	21.67	23.15	16.86
	α	2.26	2.37	2.27	2.16	3.02	2.97	2.85	2.94
	Rs	2.40	2.30	2.45	2.27	4.27	4.90	3.49	5.23
CDX **27**	ACN %	22	22	21	21	22	21	22	22
	k_1	2.39	3.84	3.47	3.22	4.05	3.15	2.93	4.06
	k_2	7.23	15.86	10.32	10.78	19.79	17.07	13.31	22.31
	α	3.02	4.13	2.98	3.35	4.89	5.42	4.55	5.50
	Rs	2.64	3.97	2.38	2.35	4.53	4.45	3.46	3.97
CDX **30**	ACN %	-	13	11	10	-	15	13	15
	k_1	-	12.95	19.69	23.46	-	9.04	12.00	8.98
	k_2	-	24.06	36.24	44.21	-	23.49	26.82	20.56
	α	-	1.86	1.84	1.88	-	2.60	2.23	2.29
	Rs	-	2.20	3.04	2.12	-	3.73	2.36	2.90

Conditions: Flow rate: 0.9 mL/min; Temperature, 22 ± 2°C; Detection, 254nm.

Regarding the influence of ammonium acetate buffer at pH 5.0 on mobile phase, eight enantiomeric mixtures of CDXs were baseline enantioseparated, with α values ranging from 1.51 to 4.91 and Rs from 1.61 to 3.87. The same number of enantiomeric mixtures were baseline enantioseparated when changing the buffer pH to 7.0; moreover, best chromatographic data were achieved (α values ranging from 1.86 to 6.63 and R_S from 2.20 to 5.24).

Ten enantiomeric mixtures of CDXs were baseline enantioseparated using 10 mM sodium acetate buffer at pH 5.0 and ACN as mobile phase. Good enantioselectivity and resolution were achieved, with α values ranging from 1.53 to 4.88 and Rs from 1.38 to 3.10. When the pH of buffer changed to 7.0, only nine enantiomeric mixtures of CDXs were baseline enantioseparated, with α and Rs values being slightly higher, ranging from 1.88 to 4.11 and from 1.78 to 3.30, respectively.

Considering the effect of sodium phosphate buffer on mobile phase at both tested pH, eight enantiomeric mixtures of CDXs were baseline enantioseparated at pH 5.0, with α and Rs values ranging from 2.23 to 8.16 and 2.36 to 4.91; while at pH 7.0, the number increased to nine, with α and Rs values ranging from 1.42 to 7.62 and from 1.27 to 6.41.

Nine enantiomeric mixtures of CDXs were baseline enantioseparated with good enantioselectivity and resolution, using potassium phosphate buffer at pH 5.0 on mobile phase,

with α values ranging from 3.02 to 8.19 and Rs from 1.97 to 5.29. Nevertheless, the mobile phases comprising the same buffer at pH 7.0 afforded the highest number of baseline enantioseparations, namely eleven. Good enantioselectivity and resolution were also obtained, with α and Rs values ranging from 2.60 to 12.53 and from 2.04 to 6.11, respectively. Besides, enantiomeric mixtures of CDXs **14** and **22** were partially enantioseparated, using this mobile phase.

Taking into account the influence of pH on retention factors, in general, higher k_1 and k_2 values were found at buffer pH 7.0 compared to pH 5.0. As shown in **Fig. 3** for enantiomeric mixture of CDX **25** this behavior was consistent not depending on the various proportions of ACN on mobile phase. Moreover, it is important to highlight that slight variations of organic modifier content in mobile phase caused a significant change on retention factors, as exemplified in **Fig. 3**. By reducing the proportion of organic modifier, at both pH values, a substantial increase of retention factors was observed. Regarding resolution, the behavior was not linear depending on the pH of the mobile phase. For enantiomeric mixture of CDX **25**, for example, at pH 5.0 the resolution increased as the percentage of organic modifier reduced, while at pH 7.0 the opposite situation was observed. The chromatographic parameter that was most influenced by changing the percentage of organic modifier in the mobile phase was the retention factor of the second eluted enantiomer (k_2 values) (**Fig. 3**).

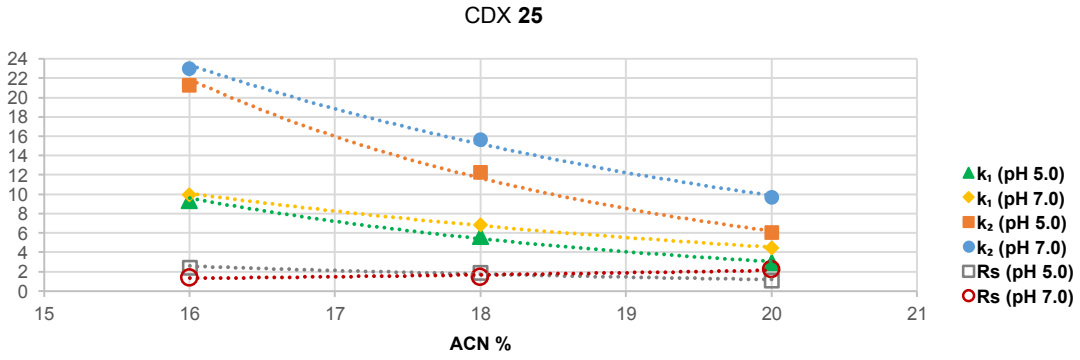


Fig. 3. Effect of the ACN percentage on mobile phase on retention factors and resolution of enantiomeric mixture of CDX **25**, on both pH buffers. Conditions: Mobile phase, sodium acetate buffer (pH 5.0 or 7.0; 10 mM):ACN, in different proportions; Flow rate: 0.9 mL/min; Temperature, 22 ± 2°C; Detection, 254nm.

The substantial variation of retention in the column with an increase of organic modifier in the mobile phase may be justified by the chemical structure of the tested CDXs (**Fig. 1**), comprising various hydrogen bonding acceptors or donors sites as well as aromatic moieties, which may be involved in hydrogen and hydrophobic interactions, respectively [60]. Actually, the molecules of organic modifier can act as hydrogen bonding acceptors or donors and establish strong hydrogen interactions with immobilized HSA and CDXs. Consequently, solvent

molecules occupy binding sites of HSA through formation of hydrogen bond interactions, and the interactions between these sites and analytes will be reduced, resulting in a trend for retention decrease. On the other hand, hydrophobic interactions between analytes and the CSP will become weaker with increasing the hydrophobicity of the mobile phase, which also causes a reduction of retention of analytes in the column [51].

Considering that the highest number of baseline enantioseparations was obtained using mixtures of potassium phosphate buffer at pH 7.0 and ACN as mobile phase, this buffer was chosen to pursue the best chromatographic conditions.

3.1.3. Optimizations to approach the physiological conditions

Modifications of the chromatographic conditions were carried out to mimic in *vivo* environment, by changing the ionic strength of the buffer to 67 mM, its pH to 7.4 and the temperature of analysis to 37 ^{o}C. From this step forward, only the thirteen enantiomeric mixtures of CDXs enantioseparated by using mixtures of potassium phosphate buffer and ACN as mobile phase were evaluated.

3.1.3.1. Buffer ionic strength

Buffer ionic strength is an important chromatographic condition for optimization [61], having influence on chiral recognition of a CSP [62, 63]. Nevertheless, its influence on retention time is not linear being always dependent on the characteristics of the compounds to be analyzed [15]. Moreover, an increase in buffer concentration has been shown to be an important ionization suppressor, increasing the quality of the separations [64]. Several drug-protein binding studies use the buffer concentration of 67 mM to mimic the physiological conditions [65, 66]. In addition, that concentration is also used for immobilization procedures of HSA to a chromatographic support, for packing the CSP into columns as well as for in their storage [9]. Accordingly, the next step was to increase the buffer ionic strength 67 mM.

A total of ten among the thirteen enantioseparated mixtures of CDXs were baseline enantioseparated, using mixtures of potassium phosphate (pH 7.0; 67 mM) and ACN as mobile phases. Good enantioselectivity and resolution were obtained, with α values ranging from 2.37 to 10.35 and Rs from 2.01 to 4.12. The overall best results are shown on **Table S1** (Supplementary Materials). As expected, the results obtained by increasing buffer ionic concentration on the mobile phase afforded a slight increase in the retention times of the enantiomeric mixtures of CDXs; however, for some analytes, such as enantiomeric mixture of CDX **1**, a significant variation on Rs values was observed (**Fig. 4**).

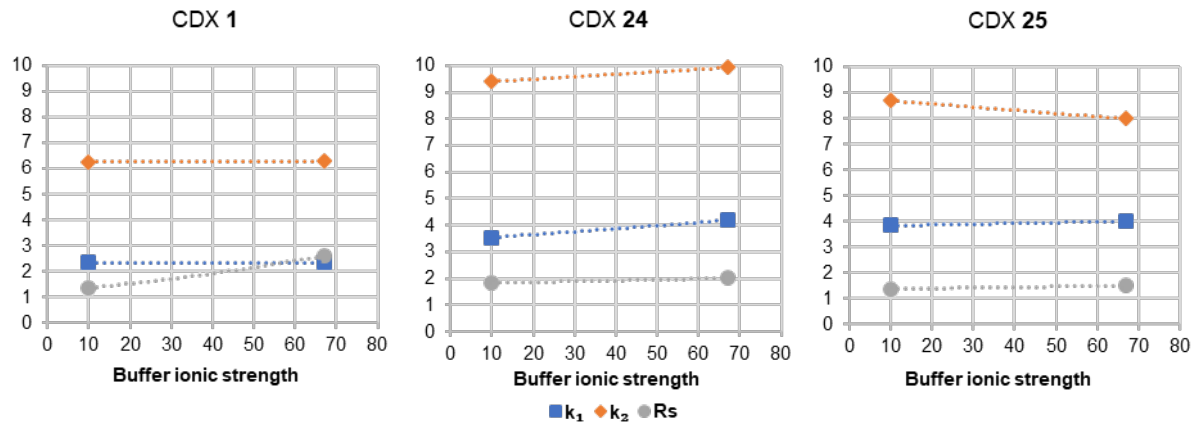


Fig. 4. Effect of buffer ionic strength on retention factors and resolution of enantiomeric mixtures of CDXs **1**, **24** and **25.** Conditions: Mobile phase, potassium phosphate buffer (pH 7.0; 10 or 67 mM):ACN (80:20 *v/v*); Flow rate: 0.9 mL/min; Temperature, 22 ± 2°C; Detection, 254nm.

3.1.3.2. Buffer pH 7.4

The physiological pH of human plasma is considered as 7.4 and it is assumed that HSA has a higher stability in this condition. To mimic the physiological conditions and aiming to optimize the enantioresolution method, the buffer pH was increased to 7.4. Among the thirteen enantiomeric mixtures of CDXs, eleven were baseline enantioseparated, with α values ranging from 1.40 to 11.76 and R_S from 1.51 to 5.41, using mixtures of potassium phosphate (pH 7.4; 67 mM) and ACN as mobile phases. The overall best results are shown on **Table S2** (Supplementary Materials).

Fig. 5 shows examples of how the chromatographic parameters k_1, k_2 and Rs of some enantiomeric mixtures of CDXs changed according to the increment of buffer pH to 7.4. In general, a decreasing in both retention factors were observed, being more slightly for k_1 and more significant for k_2, as exemplified in **Fig. 6**. Regarding resolution, it was found to be similar in both mobile phase pH value. The only exception was observed for enantiomeric mixture of CDX **24**, although the enantioselectivity and resolution improved, the retention time was longer.

3.1.3.3. Increase the system temperature

As a major protein in human blood, the normal function of HSA is carried out at the physiological temperature of 37°C. Consequently, in this systematic study, retention factors, enantioselectivity and resolution values of thirteen enantiomeric mixtures of CDXs were determined at 37°C ± 2°C, using mobile phases comprising potassium phosphate buffer (pH 7.4; 67 mM) and ACN. Ten of them were baseline enantioseparated, with α values ranging from 1.79 to 9.16 and Rs from 2.20 to 4.97. The overall best results are shown on **Table S3**.

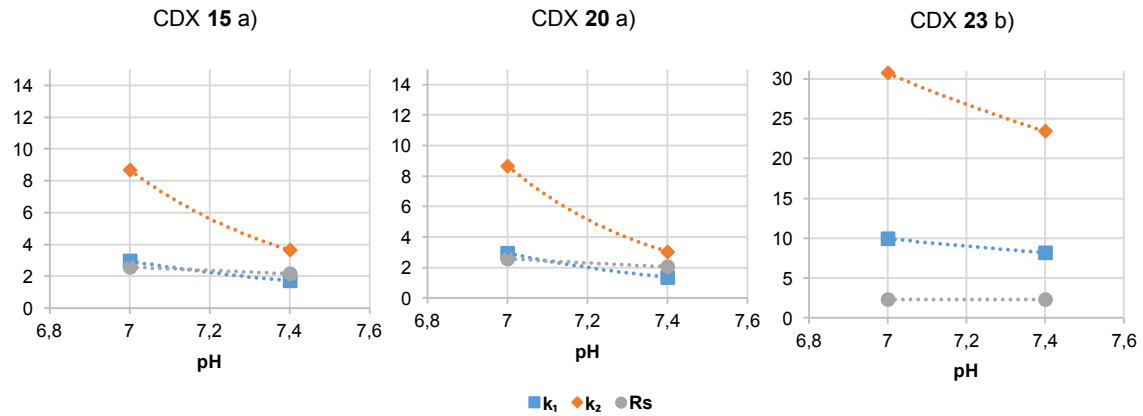


Fig. 5 Effect of buffer pH on retention factors and resolution of enantiomeric mixtures of CDXs **15**, **20** and **23**. Conditions: Mobile phase a), potassium phosphate (pH 7.0 or 7.4; 67 mM): ACN (76:24 *v/v*); Mobile phase b), potassium phosphate (pH 7.0 or 7.4; 67 mM): ACN (79:21 *v/v*); Flow rate: 0.9 mL/min; Temperature, 22 ± 2°C; Detection, 254nm.

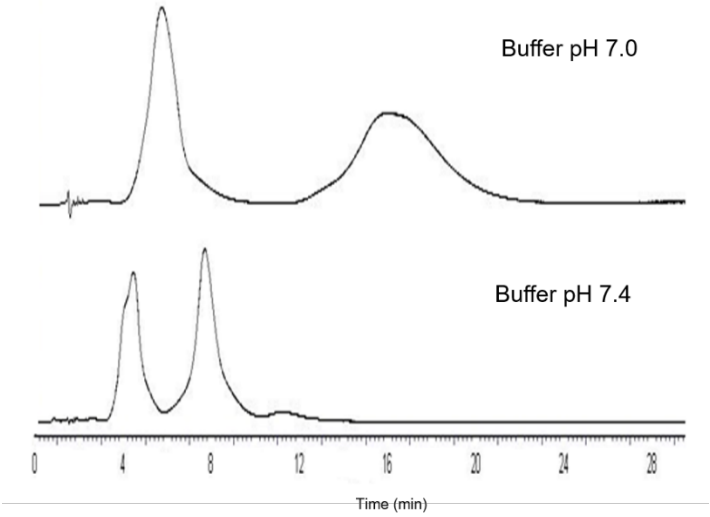


Fig. 6 Chromatograms of the enantioseparation of enantiomeric mixture of CDX **20** on CHIRALPAK® HSA column; Conditions: mobile phase, potassium phosphate (pH 7.0 or 7.4; 67 mM):ACN (76:24 *v/v*); Flow rate: 0.9 mL/min; Detection, 254 nm; Temperature, 22 ± 2°C.

Regarding the effect of the change of temperature of analysis, **Fig. 7** shows, as example, the variations of chromatographic parameters of three enantiomeric mixtures of CDXs. As expected, a strong decrease in the retention times of all the enantiomeric mixtures of CDXs, particularly for k_2 values, was observed at the mimic physiological temperature. The proportion of organic modifier had to be decreased to maintain similar enantioselectivity. The increase of temperature may lead to the decrease of hydrophobicity of the CDXs, as well as the viscosity of the mobile phase and the pressure of the LC system.

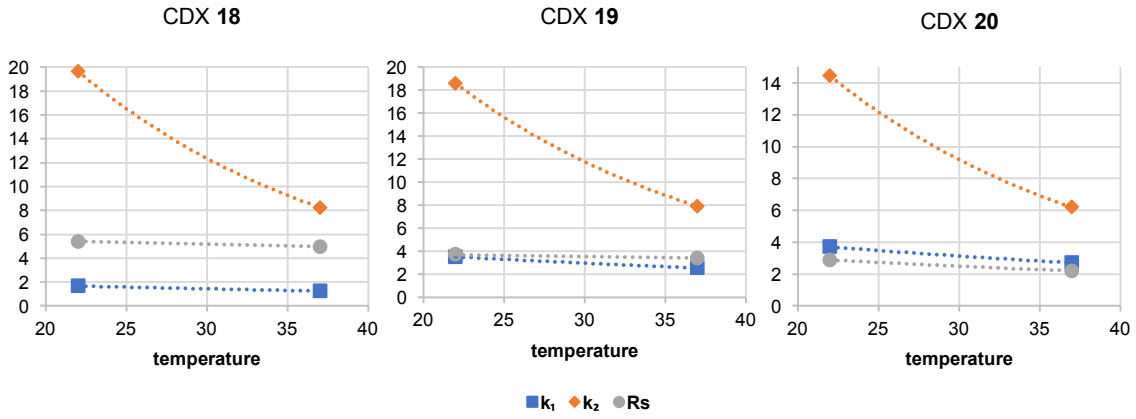


Fig. 7. Effect of the temperature on retention factors and resolution of enantiomeric mixtures of CDXs **18**, **19** and **20**; Conditions: Mobile phase, potassium phosphate (pH 7.4); 67 mM:ACN (78:22 *v/v*); Flow rate: 0.9 mL/min; Temperature: 22 or 37 ± 2°C.

3.1.4. Best performance of CHIRALPAK® HSA column for enantioseparation of CDXs

Table 2 summarizes the best chromatographic results obtained for the enantioseparated mixtures of CDXs on CHIRALPAK® HSA column, under reversed-phase mode.

According to the results, the majority of the best enantioselectivities and resolutions for the enantiomeric mixtures of CDXs, obtained in a shorter analysis time, were achieved using mixtures of potassium phosphate buffer (pH 7.4; 67 mM) and ACN as mobile phase. Exceptions were enantiomeric mixtures of CDX **16**, **22** and **30**, which obtained better results using ammonium acetate buffer (pH 5.0; 10mM), sodium acetate buffer (pH 7.0; 10mM) and sodium phosphate buffer (pH 7.0; 10mM), respectively. Moreover, 57% for the best chromatographic results were obtained at 37 ± 2°C, while 43% at 22 ± 2°C. The elution order of the enantioseparated CDXs was determined by injecting the solutions of the enantiomeric mixtures, and then each enantiomer separately, at the best chromatographic conditions.

A set of chromatograms, at optimized chromatographic conditions for enantiomeric mixtures of CDXs, are depicted in **Fig. 8**.

Table 2

The best chromatographic data obtained on CHIRALPAK® HSA column, under reversed-phase elutions conditions, for the enantiomeric mixtures of CDXs.

Enantiomeric mixture	Chromatographic conditions	k_1	k_2	α	R_s
CDX **1**	PP (pH 7.4; 67 mM):ACN (78:22 *v/v*); Temp.: 22 ± 2°C	1.82	4.62	2.54	2.35
CDX **6**	PP (pH 7.4; 67 mM):ACN (78:22 *v/v*); Temp.: 37 ± 2°C	0.48	4.38	9.16	4.31
CDX **14**	PP (pH 7.4; 67 mM):ACN (86:14 *v/v*); Temp.: 22 ± 2°C	14.51	20.37	1.40	1.51
CDX **15**	PP (pH 7.0; 67 mM):ACN (76:24 *v/v*); Temp.: 22 ± 2°C	2.96	8.68	2.93	2.59
CDX **16**	AA (pH 5.0; 10 mM):ACN (90:10 *v/v*); Temp.: 22 ± 2°C	13.01	19.58	1.51	1.61
CDX **18**	PP (pH 7.4; 67 mM):ACN (78:22 *v/v*); Temp.: 37 ± 2°C	1.02	7.28	7.14	4.97
CDX **19**	PP (pH 7.4; 67 mM):ACN (78:22 *v/v*); Temp.: 37 ± 2°C	2.17	6.96	3.20	3.39
CDX **20**	PP (pH 7.4; 67 mM):ACN (78:22 *v/v*); Temp.: 37 ± 2°C	2.32	5.44	2.34	2.20
CDX **22**	SA (pH 7.0; 10 mM):ACN (80:20 *v/v*); Temp.: 22 ± 2°C	4.94	11.27	2.28	2.52
CDX **23**	PP (pH 7.4; 67 mM):ACN (78:22 *v/v*); Temp.: 37 ± 2°C	4.75	9.67	2.04	2.45
CDX **24**	PP (pH 7.4; 67 mM):ACN (82:18 *v/v*); Temp.: 37 ± 2°C	5.23	11.16	2.13	2.66
CDX **25**	PP (pH 7.4; 67 mM):ACN (84:16 *v/v*); Temp.: 37 ± 2°C	8.18	14.65	1.79	2.32
CDX **27**	PP (pH 7.4; 67 mM):ACN (77:23 *v/v*); Temp.: 37 ± 2°C	0.48	4.38	9.16	4.31
CDX **30**	SP (pH 7.0; 10 mM):ACN (85:15 *v/v*); Temp.: 22 ± 2°C	8.98	20.56	2.29	2.90

Other conditions: Flow rate, 0.9 mL/min; Detection, UV at 254 nm. PP: potassium phosphate buffer; SA: sodium acetate buffer; AA: ammonium acetate buffer; SP: sodium phosphate buffer

3.2. Computational docking studies

In order to understand the chiral recognition mechanism behind the experimental chromatographic results, docking studies were performed using the fourteen enantiomeric mixtures of CDXs that were baseline enantioseparated on CHIRALPAK® HSA column. Values of docking scores are presented in **Table 3**. The lower the docking score, the more stable is the analyte-selector complex. The differences in energy of the docking score of (*S*)-enantiomer-CSP complex versus (*R*)-enantiomer-CSP complex were used to calculate the energy difference values. In the case of CDXs comprising two stereogenic centers, the energy differences were calculated by the difference between (*S,R*)-enantiomer-CSP complex and (*R,S*)-enantiomer-CSP complex. A previous study indicates that CDXs fit within the hydrophobic pocket of subdomain IIIA, presenting low negative docking scores [39]. In this study this pocket was selected for the docking studies as it was described as being the binding

pocket for (*S*)-ibuprofen and most ligands [67]. Actually, it was found that CDXs bind in a similar position in the binding groove, with the central xanthone ring aligned with ibuprofen ring [67].

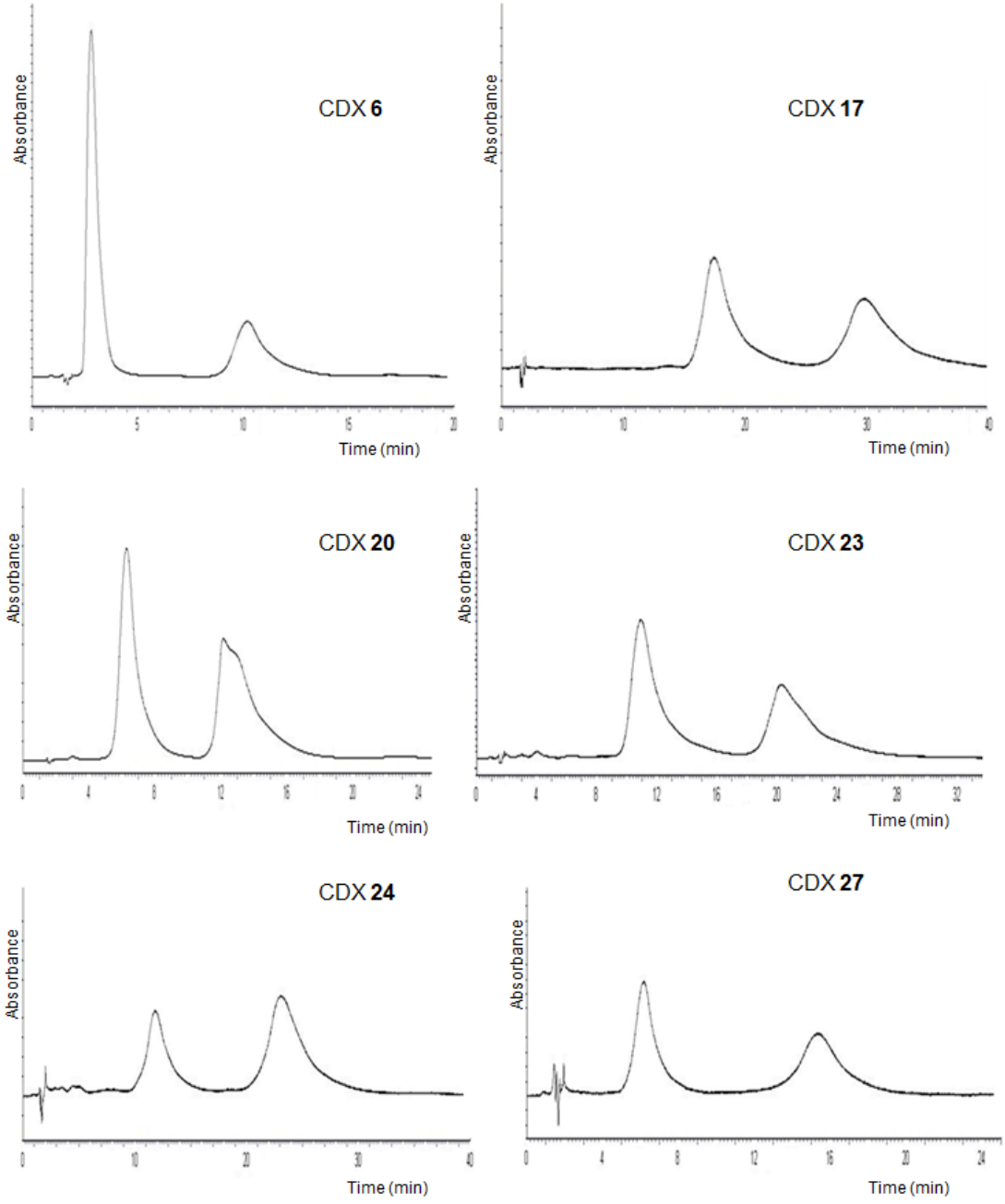


Fig. 8. Chromatograms of enantiomeric mixtures on CHIRALPAK® HSA column under optimized chromatographic conditions. Flow rate: 0.9 mL/min; Detection, UV at 254 nm.

Table 3

Chromatographic data, docking scores of both enantiomers of CDXs on a CHIRALPAK® HSA column and the energy difference between (*S*) and (*R*) or (*S,R*) and (*R,S*) enantiomers.

Enantiomeric mixture	α	Rs	First eluted enantiomer	Docking score (kcal.mol^{-1})	Energy difference (kcal.mol^{-1})
CDX **1**	2.54	2.35	(*S*)	(*S*): -8.9 (*R*): -9.5	0.6
CDX **6**	9.16	4.31	(*S*)	(*S*): -8.4 (*R*): -8.8	0.4
CDX **14**	1.40	1.51	(*R*)	(*S*): -9.8 (*R*): -8.6	-1.2
CDX **15**	2.93	2.59	(*R*)	(*S*): -10.6 (*R*): -9.8	-0.8
CDX **16***	1.51	1.61	(*R*)	(*S*): -9.0 (*R*): -9.3	0.3
CDX **18**	7.14	4.97	(*R*)	(*S*): -9.5 (*R*): -9.1	-0.4
CDX **19**	3.20	3.39	(*R*)	(*S*): -10.3 (*R*): -9.8	-0.5
CDX **20***	2.34	2.20	(*R*)	(*S*): -9.8 (*R*): -10.1	0.3
CDX **22**	2.28	2.52	(*R*)	(*S*): -9.0 (*R*): -8.9	-0.1
CDX **23**	2.04	2.45	(*R*)	(*S*): -11.2 (*R*): -9.9	-1.3
CDX **24**	2.13	2.66	(*R*)	(*S*): -10.1 (*R*): -9.4	-0.7
CDX **25**	1.79	2.32	(*R*)	(*S*): -10.1 (*R*): -9.4	-0.7
CDX **27***	9.16	4.31	(*R,S*)	(*S,R*): -9.9 (*R,S*): -10.0	0.1
CDX **30***	2.29	2.90	(*R,S*)	(*S,R*): -9.0 (*R,S*): -9.6	0.6

* docking scores not in accordance to experimental elution order

The overall results indicate that CDXs fit within the hydrophobic pocket of subdomain IIIA, presenting low negative docking scores. It was found that, a 71% agreement between docking scores and experimental chromatographic results were achieved concerning enantiomers elution order. The differences observed may be due to the complex structure of the HSA selector allowing different binding patterns with the molecules of CDXs. Moreover, it is not sure that all CDXs molecules bind only to one pocket of the protein structure, or if there may be a competition between both enantiomers for the same binding site when they are injected into the column as enantiomeric mixture. Moreover, computationally, AutodockVina has a hybrid scoring function (empirical and knowledge-based function) inspired in the X-Score function that consists of a weighted sum of steric interactions, hydrophobic interaction, and

number of active rotatable bonds with different weights [48]. Therefore, similar ligands can originate very different docking scores, depending not only on the type of interactions established, but also the number of interactions, maximizing favorable and minimizing unfavorable interactions, shape and property complementarities [68].

In order to understand the binding energy scores, a visual inspection of the binding conformations was performed for the CDXs molecules on HSA-CSP. **Fig. 9** illustrates representative examples of the most stable docked conformations for enantiomers complexes with the HSA-CSP. As shown in **Fig. 9A**, the docking poses of the enantiomers were diverse, leading to different binding interactions. The superimposition of (*R*) and (*S*) enantiomers of the same enantiomeric mixture shows that their positions are not in fact similar. Both (*R*)-enantiomers of CDXs **6** and **1** have higher affinity to HSA selector that the (*S*)-enantiomer. In fact, although the predicted docking positions of both enantiomers are similar, (*R*) enantiomers establish more polar interactions that (*S*)-enantiomers. Thus, (*R*)-CDX **6** establishes two hydrogen interactions with Tyr-452 and Asn-429 (**Fig. 9B**), and (*R*)-CDX **1** establishes two hydrogen interactions with Asp-187 and Lys-432 (**Fig. 9C**).

The (*S*)-enantiomers of CDXs **19**, **23** and **14** have higher affinity to HSA selector that the (*R*)-enantiomer. (*S*)-CDX **19** (**Fig. 9D**) and (*S*)-CDX **23** (**Fig. 9E**) establish one hydrogen interaction with Tyr-451 and Tyr-452, respectively. (*S*)-CDX **14** establishes hydrogen interactions with residues Arg-218, Trp-214, and Lys-436, and parallel π-stacking interaction with Trp-214 (**Fig. 9F**).

3.3. Ligand-Protein binding studies

Each enantiomer of the thirty-one enantiomeric mixtures of CDXs (**Fig. 1**) were analyzed at a fixed concentration (50 µg/mL). The ligand-protein binding affinity was measured based on the retention times using a zonal chromatography approach [8]. The chromatographic conditions were selected to mimic the physiological environment and to overcome the low solubility of CDXs in aqueous solution. Mixtures of potassium phosphate buffer (pH 7.4; 67 mM) and different percentages ACN ranging from 25 to 2% were chosen as mobile phases. The analyses were performed at 37 ± 2°C. Chlorpromazine, binding to HSA in subdomain IIIA [69], indomethacin, having affinity mainly for subdomain IIA [69] and metronidazole, having affinity for both subdomain IIA and IIIA [70] were selected as positive controls. The bound drug percentage (*%b*) was calculated from the k values obtained according to equation (4); the *%b* calculation in only aqueous phase was extrapolated by linearly plotting the log *k* values (average of triplicate measurements) against the percentage (*v/v*) of ACN in the mobile phase (**Table 4**). The k and R^2 values are detailed in **Table S4** (Supplementary Materials).

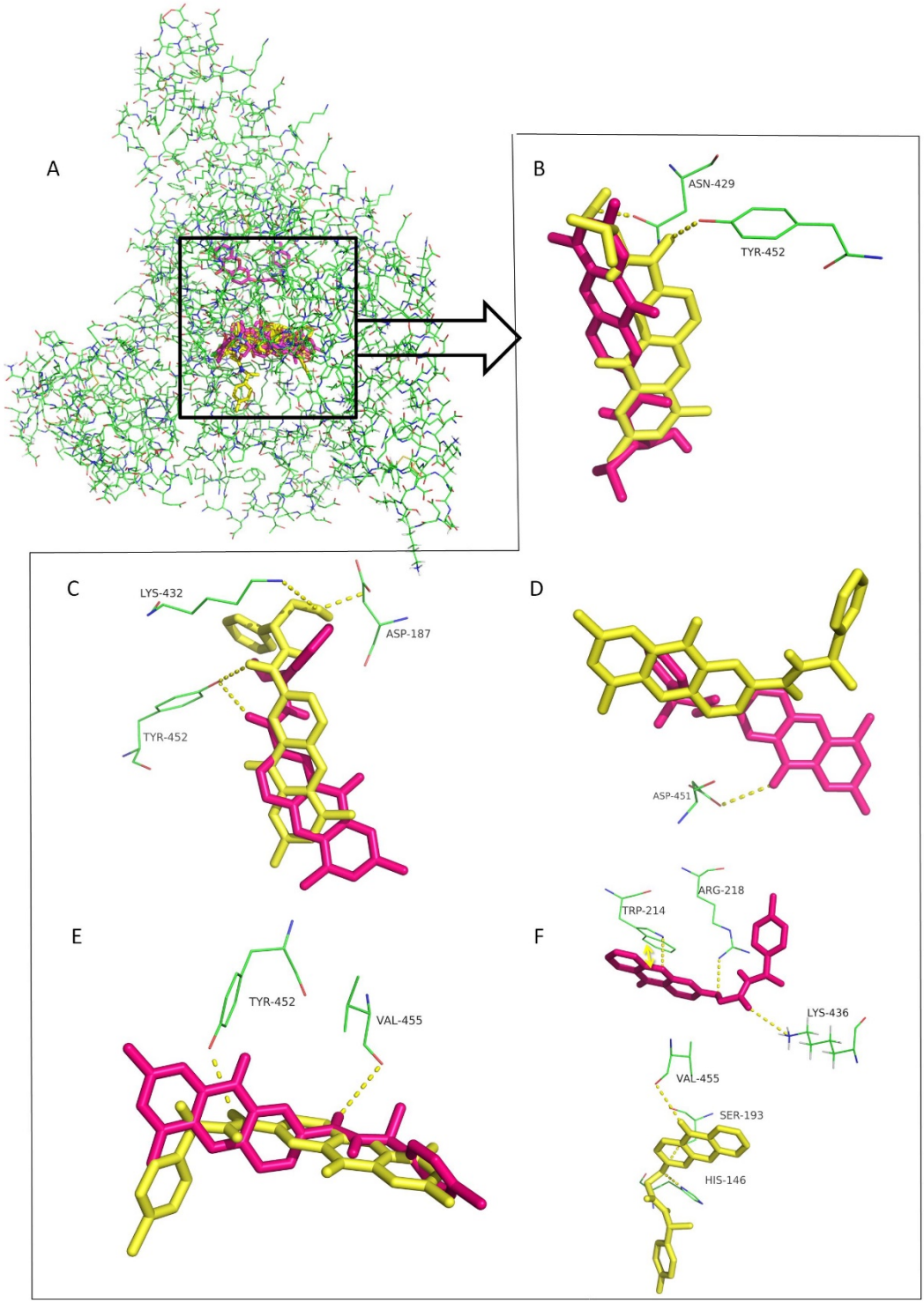


Fig. 9. Enantiomeric pairs docked onto HSA selector (**A**): CDX **6** (**B**), CDX **1** (**C**), CDX **19** (**D**), CDX **23** (**E**), and CDX **14** (**F**) enantiomers. Carbons, nitrogens and oxygens in the chiral selector are represented as green, blue and red lines, respectively. (*S*) and (*R*) enantiomers are represented as magenta and yellow sticks, respectively. Hydrongen interactions are represented as a yellow broken line. π-stacking interactions are represented as a yellow doble arrow. Residues evolved in those interactions are labeled.

Table 4

Bound percentage values (*%b*) of CDXs, injected as single enantiomers on CHIRALPAK® HSA column, using different ACN proportions in mobile phase, and by extrapolation to 100% aqueous buffer.

Compound	Bound percentage, *%b*									
	25[a]	**22**[a]	**20**[a]	**17**[a]	**15**[a]	**12**[a]	**10**[a]	**7**[a]	**2**[a]	**0**[a]
Chlorpromazine	-	-	87.79	89.26	92.75	94.31	94.75	-	-	98.12
Indomethacin	-	-	86.30	90.78	92.02	91.93	-	-	-	96.89
Metronidazole	-	-	-	-	5.16	7.27	8.22	-	16.78	19.78
(*S*)-CDX **1**	-	-	66.54	85.22	90.96	95.77	96.48	-	-	99.79
(*R*)-CDX **1**	64.74	77.34	88.01	92.42	95.99	-	-	-	-	99.90
(*S*)-CDX **2**	-	-	48.02	74.77	83.11	90.96	92.39	-	-	99.50
(*R*)-CDX **2**	-	-	48.07	74.60	83.08	90.87	92.26	-	-	99.48
(*S*)-CDX **3**	-	-	36.48	67.70	76.86	86.48	88.36	-	-	99.19
(*R*)-CDX **3**	-	-	38.42	68.90	78.29	88.06	89.87	-	-	99.36
(*S*)-CDX **4**	-	-	23.97	58.51	67.74	78.28	80.28	-	-	98.46
(*R*)-CDX **4**	-	-	-	57.56	66.82	77.17	79.02	85.85	-	94.48
(*S*)-CDX **5**	-	-	-	56.12	65.63	76.84	79.57	82.81	-	93.33
(*R*)-CDX **5**	-	-	21.33	59.86	69.14	80.78	83.07	-	-	99.09
(*S*)-CDX **6**	-	-	44.59	72.80	81.06	89.29	90.79	-	-	99.33
(*R*)-CDX **6**	74.88	86.21	92.76	95.67	97.70	-	-	-	-	99.95
(*S*)-CDX **7**	-	-	-	67.19	76.89	86.63	88.49	93.01	-	98.05
(*R*)-CDX **7**	-	-	-	66.49	76.36	85.97	87.67	91.92	-	97.59
(*S*)-CDX **8**	-	-	-	62.69	72.88	84.16	86.21	91.50	-	97.60
(*R*)-CDX **8**	-	-	-	65.97	75.59	86.38	88.34	92.55	-	97.99
(*S*)-CDX **9**	-	-	-	50.53	58.99	69.35	71.00	73.63	-	86.52
(*R*)-CDX **9**	-	-	-	50.79	60.10	69.99	71.94	74.45	-	87.25
(*S*)-CDX **10**	-	-	-	47.41	55.20	65.11	67.28	67.91	-	81.94
(*R*)-CDX **10**	-	-	-	51.19	56.31	62.90	67.55	67.10	-	79.02
(*S*)-CDX **11**	-	-	-	52.20	59.76	70.41	73.22	74.70	-	87.52
(*R*)-CDX **11**	-	-	-	52.54	59.48	69.98	72.47	73.83	-	86.51
(*S*)-CDX **12**	-	-	-	47.63	54.20	64.60	67.11	66.72	-	80.91
(*R*)-CDX **12**	-	-	-	48.07	54.45	64.78	67.22	66.82	-	80.82
(*S*)-CDX **13**	-	74.37	84.05	90.06	94.04	97.51	-	-	-	99.86
(*R*)-CDX **13**	-	75.11	84.42	90.44	94.39	97.77	-	-	-	99.89
(*S*)-CDX **14**	-	66.52	78.10	85.76	91.27	96.38	-	-	-	99.79
(*R*)-CDX **14**	-	64.31	75.19	83.14	89.19	95.15	-	-	-	99.65
(*S*)-CDX **15**	78.69	89.73	95.74	98.08	-	-	-	-	-	99.99
(*R*)-CDX **15**	71.26	83.55	90.43	94.57	96.85	-	-	-	-	99.92
(*S*)-CDX **16**	-	-	61.30	84.94	90.44	95.79	96.68	-	-	99.85

Table 4 Continuation

Compound	Bound percentage, *%b*									
	25[a]	**22**[a]	**20**[a]	**17**[a]	**15**[a]	**12**[a]	**10**[a]	**7**[a]	**2**[a]	**0**[a]
(*R*)-CDX **16**	-	-	58.43	82.51	88.72	94.86	95.98	-	-	99.80
(*S*)-CDX **17**	-	-	60.73	84.74	90.33	95.74	96.63	-	-	99.85
(*R*)-CDX **17**	-	-	63.47	87.15	92.16	96.77	97.64	-	-	99.92
(*S*)-CDX **18**	77.95	89.04	95.69	98.16	-	-	-	-	-	99.99
(*R*)-CDX **18**	-	-	61.90	84.02	89.47	94.98	95.96	-	-	99.76
(*S*)-CDX **19**	77.46	88.70	95.63	97.89	-	-	-	-	-	99.99
(*R*)-CDX **19**	-	-	76.78	91.44	94.88	97.77	-	-	-	99.95
(*S*)-CDX **20**	-	-	56.88	79.56	92.24	97.06	-	-	-	99.98
(*R*)-CDX **20**	-	-	78.13	90.28	95.25	97.97	-	-	-	99.96
(*S*)-CDX **21**	-	-	66.07	87.07	91.75	95.90	97.89	-	-	99.90
(*R*)-CDX **21**	-	-	63.81	85.13	90.47	95.22	97.67	-	-	99.88
(*S*)-CDX **22**	-	80.05	87.96	92.65	95.62	96.47		-	-	99.70
(*R*)-CDX **22**	-	78.96	87.46	92.29	95.31	-	-	-	-	99.85
(*S*)-CDX **23**	83.11	92.15	95.02	97.07	-	-	-	-	-	99.95
(*R*)-CDX **23**	77.30	87.64	93.02	96.07	98.13	-	-	-	-	99.96
(*S*)-CDX **24**	69.11	82.71	91.40	95.52	97.96	-	-	-	-	99.98
(*R*)-CDX **24**	-	76.08	85.10	90.90	95.21	-	-	-	-	99.87
(*S*)-CDX **25**	67.50	81.42	90.55	94.99	97.61	-	-	-	-	99.97
(*R*)-CDX **25**	-	77.14	86.15	91.80	95.77	-	-	-	-	99.91
(*S,S*)-CDX **26**	74.45	86.00	92.13	95.58	98.00	-	-	-	-	99.96
(*R,R*)-CDX **26**	74.75	86.30	92.78	96.28	-	-	-	-	-	99.97
(*S,R*)-CDX **27**	82.18	91.99	95.00	97.63	-	-	-	-	-	99.98
(*R,S*)-CDX **27**	69.66	82.19	90.93	93.70	95.51	-	-	-	-	99.85
(*S,S*)-CDX **28**	-	70.70	81.38	87.83	93.58	-	-	-	-	99.81
(*R,R*)-CDX **28**	-	67.92	77.69	84.59	91.12	-	-	-	-	99.68
(*S,R*)-CDX **29**	-	64.26	-	82.43	89.27	94.02	96.07	-	-	99.54
(*R,S*)-CDX **29**	-	65.07	78.86	84.54	90.63	94.90	96.54	-	-	99.61
(*S,R*)-CDX **30**	-	72.13	82.66	90.19	94.10	97.12		-	-	99.86
(*R,S*)-CDX **30**	-	-	78.86	86.43	91.39	95.22	96.70	-	-	99.59
(*S,S*)-CDX **31**	-	75.02	83.95	90.56	94.29	97.02	-	-	-	99.82
(*R,R*)-CDX **31**	-	74.33	83.34	90.23	94.12	97.04	-	-	-	99.83

[a] Acetonitrile %

As expected, all sixty-two enantiomers of CDXs showed a high affinity for HSA protein. All values presented a good correlation with the decrease of organic modifier, increasing its affinity with the protein, praising the importance of the hydrophobic interactions between this type of ligands and the protein. Extrapolation by linearly plotting the log k values against the

percentage of ACN in the mobile phase indicates that, in 100% aqueous buffer, the *%b* of the CDXs enantiomers to the HSA protein ranges from 79.02 to 99.99, with a R^2 generally higher than 0.98 (see **Fig. S1** in Supplementary Materials). Regarding the number of CDX enantiomers per each range of *%b* summarized in **Fig. 10**, it was found that 87% of the compounds have a high HSA affinity (> 90%).

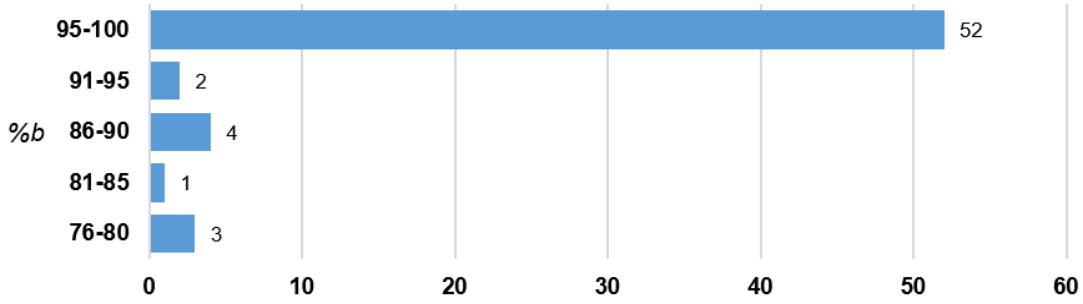


Fig. 10. Number of CDX enantiomers for each range of HSA bound percent (%*b*), values extrapolated to 100% aqueous buffer solution.

Regarding the structures of CDXs (**Fig. 1.**) it was found that affinity resulted significantly affected by the nature of the chiral side chain. Actually, CDXs bearing a methyl group in the chiral moiety (CDXs **9-12**), showed a lower affinity (*%b* ranging from 79.02 to 87.52) compared to all the other CDXs that comprise bulky alkyl or aryl groups (*%b* ranging from 936.33 to 99.99). These results suggest that the hydrophobicity of the ligand is fundamental in the HSA binding process [53].

A good agreement between the experimental and the reported *%b* values was achieved for the positive controls, specifically, 98.12% for chlorpromazine (reported value: > 90% [71]), 96.89% for indomethacin (reported value: 97.8% [67]) and 19.78% for metronidazole (reported value: 20% [72]).

It is known that the presence of an organic solvent may affect the drug–protein binding process, either by generating a change in the secondary or tertiary structure of the protein, and/or modifying the microenvironment at the binding site and, as a consequence, low energy interactions such as hydrophobic, dipole–dipole or hydrogen-bond may be absent [73]. The analysis of the log *k* values variation of each enantiomer of CDXs when changing the ACN percentage in the mobile phase showed a nearly linear relationship between log *k* and the organic solvent concentration, as for (*R*)-CDX **15** and (*R*)-CDX **17** (**Figure 11**). Moreover, due to the different structure of the enantiomers, they had a different behavior for the same proportions of organic modifier; however, when extrapolated to 100% aqueous buffer, both had a similar *%b* of 99.92.

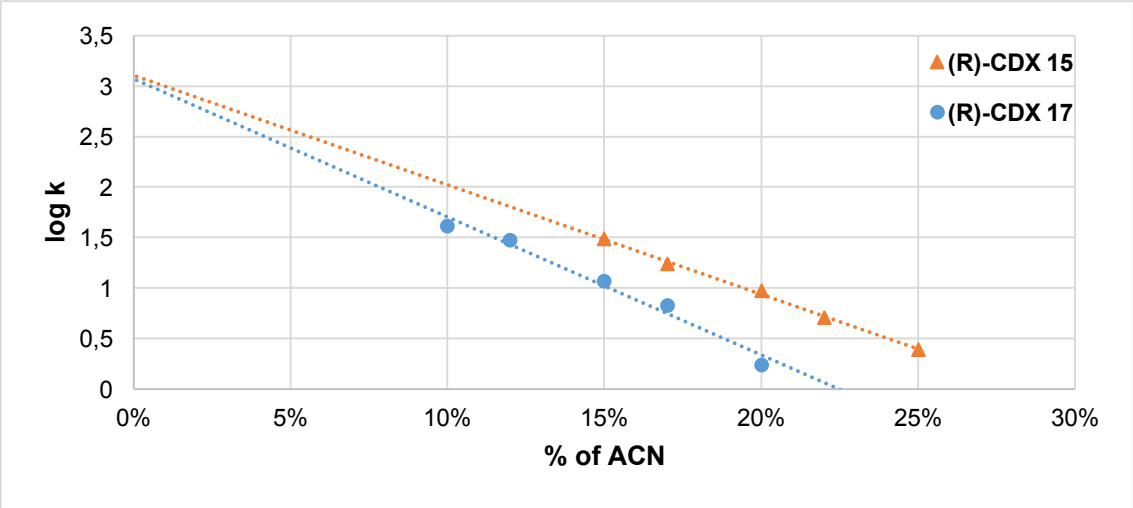


Fig. 11. Linear plotting of log k values of (*R*)-CDX **15** and (*R*)-CDX **17**, on CHIRALPAK® HSA column, using different percentages of ACN in the mobile phase. Conditions: Mobile phase potassium phosphate (pH 7.4; 67 mM):ACN; Flow rate, 0.9 mL/min; Detection, 254 nm; Temperature, 37 ± 2°C.

4. Conclusions

During the development of the systematic study of enantioseparation of CDXs on CHIRALPAK® HSA column, several experimental conditions were investigated, including the nature and proportion of the organic modifier, the type, concentration and pH of the buffer, as well as the temperature of analysis. Under the optimized chromatographic conditions, fourteen out of thirty-one enantiomeric mixtures of CDXs were successfully enantioseparated. For the majority of the enantiomeric mixtures, the analysis performed at 37 ± 2°C and using mixtures of potassium phosphate buffer (pH of 7.4; 67 mM) and ACN as mobile phases, afforded the best chromatographic data. Good agreement between docking studies and experimental results was achieved. Additionally, binding affinity studies of sixty-two enantiomers of CDXs on HSA-based CSP were performed. In general, high affinity for HSA-CSP was obtained, with bound percentage ranging from 79.02 to 99.99% in 100% aqueous buffer. The higher affinity values were achieved for the CDXs bearing bulky alkyl or aryl groups in the chiral side chain, suggesting that the hydrophobicity of the CDXs was important for HSA binding process. The results of the present study fulfilled the objectives of this work and confirmed the applicability of HSA-based column to this class of chiral compounds.

Future perspective

In the last few years, an exponential interest in synthetic bioactive CDXs has been witnessed. Nevertheless, although to pursue the development of these derivatives into drug candidates it is crucial to study their pharmacokinetics and toxicity properties. According to current point of views in the drug discovery pipeline, the binding of new bioactive compounds to plasma

proteins, especially HSA, at an early stage is of crucial importance, insofar as it affects not only distribution and elimination but also duration and intensity of the pharmacological action. This fast and reliable LC method could be of help and widely used to extend the HSA binding affinity studies and screening of other new xanthone derivatives.

Summary points

Background

- LC using a HSA-CSP has become widely used for enantioseparation of chiral analytes and to study protein-binding affinity.
- CDXs present a variety of biological and pharmacological activities being, in some cases, dependent on the stereochemistry.
- In the early stages of drug discovery, beyond the biological activity screening, each compound should also be evaluated and characterized by protein-binding affinity, among other properties.

Materials & methods

- LC analyses were performed on HSA-CSP under reversed-phase elution conditions.
- The influence of the organic modifier, buffer type, pH and ionic strength of the mobile phase, and temperature were explored.
- The binding affinity was determined by measuring the retention times of CDXs on HSA-CSP and further calculation of bound percentage (*%b)*.
- The *%b* calculation in only aqueous phase was extrapolated by linearly plotting the log *k* values against the percentage (*v/v*) of ACN in the mobile phase.
- Chiral recognition mechanisms were investigated by molecular docking using AutoDock Vina.

Results

- Fourteen enantiomeric mixtures of CDXs were baseline enantioseparated with high enantioselectivity and resolution.
- Under the optimized chromatographic conditions, α and Rs values were ranging from 1.40 to 9.16 and from 1.51 to 4.97, respectively.
- In general, high affinity for HSA-CSP was observed, with bound percentages ranging from 79.02 to 99.99%, being strongly affected by the presence of even low concentration of organic solvent in the mobile phase.
- The higher affinity values were achieved for the CDXs bearing bulky alkyl or aryl groups in the chiral side chain, suggesting that the hydrophobicity of the CDXs was important for HSA binding process.

- A good agreement (71%) between docking studies and experimental results was achieved, indicating that CDXs fit within the hydrophobic pocket of subdomain IIIA.

Acknowledgements

This research was developed under the projects PTDC/ MAR-BIO/4694/2014 and PTDC/AAG-TEC/0739/2014 supported through national funds provided by Fundação da Ciência e Tecnologia (FCT/MCTES, PIDDAC) and European Regional Development Fund (ERDF) through the COMPETE – Programa Operacional Factores de Competitividade (POFC) programme (POCI-01-0145-FEDER-016790 and POCI-01-0145-FEDER-016793) and– Reforçar a Investigação, o Desenvolvimento Tecnológico e a Inovação (RIDTI, Project 3599 and 9471) in the framework of the programme PT2020, as well as Project No. POCI-01-0145-FEDER-028736, co-financed by COMPETE 2020, Portugal 2020 and the European Union through the ERDF, and by FCT through national funds, and CHIRALXANT-CESPU-2018. Ye Zaw Phyo thanks the Erasmus Mundus Action 2 (Lotus Plus project) for a PhD's scholarship.

References

1. Gomes, A.S., et al., *Drug-like properties and ADME of xanthone derivatives: The antechamber of clinical trials.* Current Medicinal Chemistry, 2016. **23**(32): p. 3654-3686.
2. Hage, D.S., et al., *Characterization of drug–protein interactions in blood using high-performance affinity chromatography.* J. Sep. Sci., 2009. **32**(5-6): p. 835-853.
3. Kim, H.S. and I.W. Wainer, *Rapid analysis of the interactions between drugs and human serum albumin (HSA) using high-performance affinity chromatography (HPAC).* J. Chromatogr. B Analyt. Technol. Biomed. Life Sci., 2008. **870**(1): p. 22-26.
4. Patel, S., I. Wainer, and W. Lough, *Affinity-based chiral stationary phases.* Handbook of Affinity Chromatography, 2006. **2**: p. 571-592.
5. Aubry, A.F., N. Markoglou, and A. McGann, *Comparison of drug binding interactions on human, rat and rabbit serum albumin using high-performance displacement chromatography.* Comp. Biochem. Physiol. Part C: Comparative, 1995. **112**(3): p. 257-266.
6. Esmaeilzadeh, S., H. Valizadeh, and P. Zakeri-Milani, *The effects of pH, temperature and protein concentration on the in vitro binding of flutamide to human serum albumin.* Pharm. Dev. Technol., 2017. **22**(8): p. 982-991.
7. Ashton, D.S., et al., *Quantitative structure-retention relationships of acyclovir esters using immobilised albumin high-performance liquid chromatography and reversed-phase high-performance liquid chromatography.* J. Chromatogr. A, 1995. **707**(2): p. 367-372.

8. Li, Z. and D.S. Hage, *Analysis of stereoselective drug interactions with serum proteins by high-performance affinity chromatography: A historical perspective.* J. Pharm. Biomed. Anal., 2017. **144**: p. 12-24.
9. Kim, H.S., Y.S. Kye, and D.S. Hage, *Development and evaluation of N-hydroxysuccinimide-activated silica for immobilizing human serum albumin in liquid chromatography columns.* J. Chromatogr. A, 2004. **1049**(1-2): p. 51-61.
10. Millot, M.C., et al., *Structural changes of human serum albumin immobilized on chromatographic supports: A high-performance liquid chromatography and Fourier-transform infrared spectroscopy study.* J. Chromatogr. B Biomed. Sci. Appl., 2001. **753**(1): p. 101-113.
11. Hage, D.S., et al., *Pharmaceutical and biomedical applications of affinity chromatography: Recent trends and developments.* J. Pharmac. Biomed. Anal., 2012. **69**: p. 93-105.
12. Singh, S.S. and J. Mehta, *Measurement of drug–protein binding by immobilized human serum albumin-HPLC and comparison with ultrafiltration.* J. Chromatogr. B, 2006. **834**(1): p. 108-116.
13. Trainor, G.L., *The importance of plasma protein binding in drug discovery.* Expert Opin. Drug Discov., 2007. **2**(1): p. 51-64.
14. Ascoli, G.A., E. Domenici, and C. Bertucci, *Drug binding to human serum albumin: Abridged review of results obtained with high-performance liquid chromatography and circular dichroism.* Chirality, 2006. **18**(9): p. 667-679.
15. Kamble, S., et al., *Structural properties governing drug-plasma protein binding determined by high-performance liquid chromatography method.* J. Pharm. Biomed. Anal., 2018. **149**: p. 16-21.
16. Li, Z., et al., *High-Performance Affinity Chromatography: Applications in Drug-Protein Binding Studies and Personalized Medicine*, in *Advances in Protein Chemistry and Structural Biology*. 2016. p. 1-39.
17. Valkó, K.L., *Lipophilicity and biomimetic properties measured by HPLC to support drug discovery.* J. Pharm. Biomed. Anal., 2016. **130**: p. 35-54.
18. Carter, D.C. and J.X. Ho, *Structure of Serum Albumin*, in *Advances in Protein Chemistry*, C.B. Anfinsen, et al., Editors. 1994, Acad. Press. p. 153-203.
19. Scriba, G.K.E., *Chiral recognition in separation science – an update.* J. Chromatogr. A, 2016. **1467**: p. 56-78.
20. Lämmerhofer, M., *Chiral recognition by enantioselective liquid chromatography: Mechanisms and modern chiral stationary phases.* J. Chromatog. A, 2010. **1217**(6): p. 814-856.

21. Zhao, P., et al., *Drug-protein binding mechanism of juglone for early pharmacokinetic profiling: Insights from ultrafiltration, multi-spectroscopic and molecular docking methods.* J. Pharm. Biomed. Anal., 2017. **141**: p. 262-269.
22. Poureshghi, F., et al., *Interaction of an antiepileptic drug, lamotrigine with human serum albumin (HSA): Application of spectroscopic techniques and molecular modeling methods.* J. Photochem. Photobiol. B, 2017. **166**: p. 187-192.
23. Pragna Lakshmi, T., et al., *Molecular interaction of 2,4-diacetylphloroglucinol (DAPG) with human serum albumin (HSA): The spectroscopic, calorimetric and computational investigation.* Spectrochim. Acta A Mol. Biomol. Spectrosc., 2017. **183**: p. 90-102.
24. Shagufta and I. Ahmad, *Recent insight into the biological activities of synthetic xanthone derivatives.* Eur. J. Med. Chem., 2016. **116**: p. 267-280.
25. Pinto, M.M.M., M.E. Sousa, and M.S.J. Nascimento, *Xanthone derivatives: New insights in biological activities.* Curr. Med. Chem., 2005. **12**(21): p. 2517-2538.
26. Masters, K.-S. and S. Bräse, *Xanthones from fungi, lichens, and bacteria: the natural products and their synthesis.* Chem. Rev., 2012. **112**(7): p. 3717-3776.
27. Sousa, E., et al., *Bromoalkoxyxanthones as promising antitumor agents: Synthesis, crystal structure and effect on human tumor cell lines.* Eur. J. Med. Chem., 2009. **44**(9): p. 3830-3835.
28. Lopes, A., et al., *Chiral Thioxanthones as Modulators of P-glycoprotein: Synthesis and Enantioselectivity Studies.* Molecules, 2018. **23**(3).
29. Cruz, I., et al., *Xanthone and Flavone Derivatives as Dual Agents with Acetylcholinesterase Inhibition and Antioxidant Activity as Potential Anti-Alzheimer Agents.* J. Chem., 2017. **2017**.
30. Cidade, H., et al., *In silico and in vitro antioxidant and cytotoxicity evaluation of oxygenated xanthone derivatives.* Arab. J. Chem., 2016.
31. Barbosa, J., et al., *Screening a small library of xanthones for antitumor activity and identification of a hit compound which induces apoptosis.* Molecules, 2016. **21**(1).
32. Sousa, E., et al., *Bioactive xanthones with effect on P-glycoprotein and prediction of intestinal absorption.* Med. Chem. Res., 2013. **22**(5): p. 2115-2123.
33. Santos, Á., et al., *Lipophilicity assessement in drug discovery: Experimental and theoretical methods applied to xanthone derivatives.* J. Chromatogr. B Analyt. Technol. Biomed. Life Sci., 2018. **1072**: p. 182-192.
34. Azevedo, C.M.G., et al., *Pyranoxanthones: Synthesis, growth inhibitory activity on human tumor cell lines and determination of their lipophilicity in two membrane models.* Eur. J. Med. Chem., 2013. **69**: p. 798-816.
35. Fernandes, C., et al., *New chiral stationary phases based on xanthone derivatives for liquid chromatography.* Chirality, 2017. **29**(8): p. 430-442.

36. Fernandes, C., et al., *Chiral Stationary Phases Based on Small Molecules: An Update of the Last 17 Years.* Sep.Purif. Rev., 2018. **47**(2): p. 89-123.
37. Fernandes, C., et al., *Synthesis of new chiral xanthone derivatives acting as nerve conduction blockers in the rat sciatic nerve.* Eur. J. Med. Chem., 2012. **55**: p. 1-11.
38. Fernandes, C., et al., *New chiral derivatives of xanthones: Synthesis and investigation of enantioselectivity as inhibitors of growth of human tumor cell lines.* Bioorg. Med. Chem., 2014. **22**(3): p. 1049-1062.
39. Fernandes, C., et al., *Chiral derivatives of xanthones: Investigation of the effect of enantioselectivity on inhibition of cyclooxygenases (COX-1 and COX-2) and binding interaction with human serum albumin.* Pharmaceuticals, 2017. **10**(2).
40. Fernandes, C., et al., *Enantioresolution of chiral derivatives of xanthones on (S,S)-Whelk-O1 and l -phenylglycine stationary phases and chiral recognition mechanism by docking approach for (S,S)-Whelk-O1.* Chirality, 2013. **25**(2): p. 89-100.
41. Phyo, Y.Z., et al., *Enantiomeric resolution and docking studies of chiral xanthonic derivatives on chirobiotic columns.* Molecules, 2018. **23**(1).
42. Fernandes, C., et al., *Enantioseparation and chiral recognition mechanism of new chiral derivatives of xanthones on macrocyclic antibiotic stationary phases.* J. Chromatogr. A, 2012. **1241**: p. 60-68.
43. Fernandes, C., et al., *Resolution and determination of enantiomeric purity of new chiral derivatives of xanthones using polysaccharide-based stationary phases.* J. Chromatogr. A, 2012. **1269**: p. 143-153.
44. Noctor, T.A., M.J. Diaz-Perez, and I.W. Wainer, *Use of a human serum albumin-based stationary phase for high-performance liquid chromatography as a tool for the rapid determination of drug-plasma protein binding.* J. Pharm. Sci., 1993. **82**(6): p. 675-676.
45. Rose, P.W., et al., *The RCSB Protein Data Bank: views of structural biology for basic and applied research and education.* Nucleic Acids Res., 2015. **43**(Database issue): p. D345-D356.
46. Dewar, M.J.S., et al., *Development and use of quantum mechanical molecular models. 76. AM1: a new general purpose quantum mechanical molecular model.* J. Am. Chem. Soc., 1985. **107**(13): p. 3902-3909.
47. Mirzaei, H., et al., *Energy minimization on manifolds for docking flexible molecules.* J. Chem. Theory Comput., 2015. **11**(3): p. 1063-1076.
48. Trott, O. and A.J. Olson, *AutoDock Vina: improving the speed and accuracy of docking with a new scoring function, efficient optimization and multithreading.* J. Comput. Chem., 2010. **31**(2): p. 455-461.
49. Lill, M.A. and M.L. Danielson, *Computer-aided drug design platform using PyMOL.* J. Comput. Aided Mol. Des., 2011. **25**(1): p. 13-19.

50. Haginaka, J., *Recent progresses in protein-based chiral stationary phases for enantioseparations in liquid chromatography.* J. Chromatogr. B Analyt. Technol. Biomed. Life Sci., 2008. **875**(1): p. 12-19.
51. Noctor, T.A.G. and I.W. Wainer, *The Use of Displacement Chromatography to Alter Retention and Enantioselectivity on a Human Serum Albumin-Based HPLC Chiral Stationary Phase: A Mini-Review.* J. Liq. Chromatogr., 1993. **16**(4): p. 783-800.
52. Daicel-Corporation. *INSTRUCTION MANUAL FOR CHIRALPAK® HSA*. 2018 [cited 2018 13/12/2018]; Available from: http://chiraltech.com/wp-content/uploads/2018/09/CHIRALPAK-HSA-2018.pdf.
53. Bertucci, C., et al., *Binding studies of taxanes to human serum albumin by bioaffinity chromatography and circular dichroism.* J. Pharm. Biomed. Anal., 2006. **42**(1): p. 81-87.
54. Bertucci, C. and D. Tedesco, *Human serum albumin as chiral selector in enantioselective high-performance liquid chromatography.* Curr. Med. Chem., 2017. **24**(8): p. 743-757.
55. Cheng, Y., et al., *Measurements of drug–protein binding by using immobilized human serum albumin liquid chromatography–mass spectrometry.* J. Chromatogr. B, 2004. **809**(1): p. 67-73.
56. Valko, K., et al., *Fast gradient HPLC method to determine compounds binding to human serum albumin. Relationships with octanol/water and immobilized artificial membrane lipophilicity.* J. Pharm. Sci., 2003. **92**(11): p. 2236-2248.
57. Eberherr, W., et al., *Investigations on the Coupling of High-Performance Liquid Chromatography to Direct Analysis in Real Time Mass Spectrometry.* Anal. Chem., 2010. **82**(13): p. 5792-5796.
58. Gianazza, E., et al., *The behavior of serum albumin upon isoelectric focusing on immobilized pH gradients.* Electrophoresis, 1984. **5**(5): p. 310-312.
59. Peyrin, E., Y.C. Guillaume, and C. Guinchard, *Interactions between dansyl amino acids and human serum albumin using high-performance liquid chromatography: mobile-phase pH and temperature considerations.* Anal. Chem., 1997. **69**(24): p. 4979-4984.
60. Wang, Q.Y., et al., *Effect of chromatographic conditions on enantioseparation of bovine serum albumin chiral stationary phase in HPLC and thermodynamic studies.* Chirality, 2013. **25**(9): p. 487-492.
61. Bertucci, C. and E. Domenici, *Reversible and covalent binding of drugs to human serum albumin: Methodological approaches and physiological relevance.* Curr. Med. Chem., 2002. **9**(15): p. 1463-1481.
62. Berthod, A., *Chiral recognition mechanisms.* Anal. Chem. (Washington), 2006.

63. Shen, G., et al., *Thermodynamic study of chiral recognition between serum albumin and tryptophan enantiomers by surface plasmon resonance.* Chem. J. Chinese U., 2015. **36**(5): p. 881-885.

64. Gritti, F. and G. Guiochon, *Effect of the pH, the concentration and the nature of the buffer on the adsorption mechanism of an ionic compound in reversed-phase liquid chromatography II. Analytical and overload band profiles on Symmetry-C-18 and Xterra-C-18.* J. Chromatogr. A, 2004. **1041**: p. 63-75.

65. Mallik, R., T. Jiang, and D.S. Hage, *High-performance affinity monolith chromatography: Development and evaluation of human serum albumin columns.* Anal. Chem., 2005. **76**(23): p. 7013-7022.

66. Maddi, S., G. Scriba, and M.R. Yamsani, *Stereoselective binding of chiral anti-diabetic drug nateglinide to plasma proteins.* Drug Metabol Drug Interact, 2011. **26**(2): p. 81-6.

67. Ghuman, J., et al., *Structural Basis of the Drug-binding Specificity of Human Serum Albumin.* J. Mol. Biol., 2005. **353**(1): p. 38-52.

68. Sousa, S.F., P.A. Fernandes, and M.J. Ramos, *Protein–ligand docking: current status and future challenges.* Proteins: Struct., Funct., Bioinf., 2006. **65**(1): p. 15-26.

69. Varshney, A., et al., *Ligand binding strategies of human serum albumin: how can the cargo be utilized?* Chirality, 2010. **22**(1): p. 77-87.

70. Równicka-Zubik, J., et al., *Effect of ageing of human serum albumin in vitro on surface hydrophobicity and binding sites of metronidazole.* J. Mol. Struct., 2011. **993**(1): p. 477-484.

71. Lázaro, E., et al., *New Approach To Measure Protein Binding Based on a Parallel Artificial Membrane Assay and Human Serum Albumin.* J. Med. Chem., 2008. **51**(7): p. 2009-2017.

72. Chen, H., Z. Gong, and Z. Zhang, *Coupling microdialysis with flow-injection chemiluminescence detection for a protein–drug interaction study.* J. Pharm. Biomed. Anal., 2006. **41**(4): p. 1412-1417.

73. Domenici, E., et al., *Synthesis and chromatographic properties of an HPLC chiral stationary phase based upon human serum albumin.* Chromatographia, 1990. **29**(3-4): p. 170-176.

Supplementary Materials

Table S1

The best chromatographic data obtained for enantiomeric mixtures of CDXs, on CHIRALPAK® HSA, using 67 mM potassium phosphate at pH 7.0 as buffer.

Enantiomeric mixture	k_1	k_2	α	R_s	ACN %
CDX **1**	2.36	6.30	2.67	2.62	20
CDX **6**	1.09	8.12	7.49	3.92	20
CDX **15**	2.96	8.68	2.93	2.59	24
CDX **18**	0.98	10.18	10.35	3.81	24
CDX **19**	2.00	9.98	4.98	3.43	24
CDX **20**	2.02	7.38	3.65	2.26	24
CDX **23**	9.95	30.70	3.08	2.30	21
CDX **24**	4.19	9.92	2.37	2.01	20
CDX **25**	9.92	29.96	3.02	4.12	21
CDX **27**	5.95	26.51	4.45	3.48	20

CHIRALPAK® HSA column; Mobile phase, potassium phosphate buffer (pH 7.0; 67 mM):ACN (variable proportion); Flow rate 0.9 mL/min; Temperature 22 ± 2°C; Detection UV 254nm.

Table S2

The best chromatographic data obtained for enantiomeric mixtures of CDXs, on CHIRALPAK® HSA, using 67 mM potassium phosphate at pH 7.4 as buffer.

Enantiomeric mixture	k_1	k_2	α	Rs	ACN %
CDX **1**	1.82	4.62	2.54	2.35	22
CDX **6**	0.69	7.63	11.01	5.29	22
CDX **14**	14.51	20.37	1.40	1.51	14
CDX **15**	3.10	8.44	2.72	2.27	23
CDX **18**	1.67	19.66	11.76	5.41	22
CDX **19**	3.52	18.58	5.28	3.71	22
CDX **20**	3.71	14.44	3.89	2.89	22
CDX **23**	8.18	23.36	2.86	2.27	22
CDX **24**	3.01	6.71	2.23	1.83	22
CDX **25**	6.00	12.07	2.01	1.81	20
CDX **27**	2.97	9.64	3.24	2.83	23
CDX **30**	8.53	13.72	1.61	1.21	16

CHIRALPAK® HSA column; Mobile phase potassium phosphate buffer (pH 7.4; 67 mM):ACN (variable proportion); Flow rate 0.9 mL/min; Temperature 22 ± 2°C; Detection UV 254nm.

Table S3

The best chromatographic data obtained for enantiomeric mixtures of CDXs on CHIRALPAK® HSA at 37°C ± 2°C.

Enantiomeric mixture	k_1	k_2	α	Rs	ACN %
CDX **1**	4.11	10.03	2.44	3.14	16
CDX **6**	0.48	4.38	9.16	4.31	22
CDX **14**	6.28	8.43	1.34	1.00	14
CDX **15**	4.25	9.68	2.28	2.51	20
CDX **18**	1.02	7.28	7.14	4.97	22
CDX **19**	2.17	6.96	3.20	3.39	22
CDX **20**	2.32	5.44	2.34	2.20	22
CDX **23**	4.75	9.67	2.04	2.45	22
CDX **24**	5.23	11.16	2.13	2.66	18
CDX **25**	8.18	14.65	1.79	2.32	16
CDX **27**	0.48	4.38	9.16	4.31	23

CHIRALPAK® HSA column; Mobile phase phosphate buffer (pH 7.4; 67 mM):ACN (variable proportion); Flow rate 0.9 mL/min; Detection UV 254nm.

Table S4

Retention time (t_R), retention factor (*k*) and binding percentage (*%b*) values of CDXs on a CHIRALPAK® HSA column using different percentages of ACN in mobile phase.

Compound	25% [a]			22% [a]			20% [a]			17% [a]			15% [a]			12% [a]			10% [a]			7% [a]			2% [a]			0% [a]		R^2
	t_R	*k*	*b%*	t_R	*k*	*b%*	t_R	*k*	*b%*	t_R	*k*	*b%*	t_R	*k*	*b%*	t_R	*k*	*b%*	t_R	*k*	*b%*	t_R	*k*	*b%*	t_R	*k*	*b%*	*k*	*b%*	
Chlorpromazine	-	-	-	-	-	-	10.24	7.19	87.79	11.64	8.31	89.26	17.25	12.80	92.75	21.97	16.57	94.31	23.79	18.03	94.75	-	-	-	-	-	-	52.31	98.12	0.948
Indomethacin	-	-	-	-	-	-	9.13	6.30	86.30	13.55	9.84	90.78	15.66	11.53	92.02	20.44	11.39	91.93	-	-	-	-	-	-	-	-	-	31.20	96.89	0.961
Metronidazole	-	-	-	-	-	-	-	-	-	-	-	-	1.32	0.05	5.16	1.35	0.08	7.27	1.36	0.09	8.22	-	-	-	1.50	0.20	16.78	0.25	19.78	0.997
(*S*)-CDX **1**	-	-	-	-	-	-	3.74	1.99	66.54	8.46	5.76	85.22	13.83	10.06	90.96	29.57	22.66	95.77	35.55	27.44	96.48	-	-	-	-	-	-	483.95	99.79	0.975
(*R*)-CDX **1**	3.55	1.84	64.74	5.52	3.41	77.34	10.42	7.34	88.01	16.48	12.19	92.42	31.20	23.96	95.99	-	-	-	-	-	-	-	-	-	-	-	-	1035.14	99.90	0.988
(*S*)-CDX **2**	-	-	-	-	-	-	2.41	0.92	48.02	4.96	2.96	74.77	7.40	4.92	83.11	13.84	10.07	90.96	16.43	12.15	92.39	-	-	-	-	-	-	198.06	99.50	0.962
(*R*)-CDX **2**	-	-	-	-	-	-	2.41	0.93	48.07	4.92	2.94	74.60	7.39	4.91	83.08	13.69	9.95	90.87	16.16	11.93	92.26	-	-	-	-	-	-	191.51	99.48	0.961
(*S*)-CDX **3**	-	-	-	-	-	-	1.97	0.57	36.48	3.87	2.10	67.70	5.40	3.32	76.86	9.25	6.40	86.48	10.74	7.59	88.36	-	-	-	-	-	-	122.80	99.19	0.976
(*R*)-CDX **3**	-	-	-	-	-	-	2.03	0.62	38.42	4.02	2.22	68.90	5.76	3.61	78.29	10.47	7.37	88.06	12.34	8.87	89.87	-	-	-	-	-	-	156.03	99.36	0.953
(*S*)-CDX **4**	-	-	-	-	-	-	1.64	0.32	23.97	3.01	1.41	58.51	3.88	2.10	67.74	5.76	3.60	78.28	6.34	4.07	80.28	-	-	-	-	-	-	64.00	98.46	0.963
(*R*)-CDX **4**	-	-	-	-	-	-	-	-	-	2.95	1.36	57.56	3.77	2.01	66.82	5.48	3.38	77.17	5.96	3.77	79.02	8.83	6.07	85.85	-	-	-	17.13	94.48	0.982
(*S*)-CDX **5**	-	-	-	-	-	-	-	-	-	2.85	1.28	56.12	3.64	1.91	65.63	5.40	3.32	76.84	6.12	3.89	79.57	7.27	4.82	82.81	-	-	-	14.00	93.33	0.948
(*R*)-CDX **5**	-	-	-	-	-	-	1.59	0.27	21.33	3.11	1.49	59.86	4.05	2.24	69.14	6.50	4.20	80.78	7.39	4.91	83.07	-	-	-	-	-	-	108.47	99.09	0.987
(*S*)-CDX **6**	-	-	-	-	-	-	2.26	0.80	44.59	4.60	2.68	72.80	6.60	4.28	81.06	11.67	8.33	89.29	13.57	9.85	90.79	-	-	-	-	-	-	148.42	99.33	0.951
(*R*)-CDX **6**	4.98	2.98	74.88	9.06	6.25	86.21	17.25	12.80	92.76	28.86	22.08	95.67	54.24	42.39	97.70	-	-	-	-	-	-	-	-	-	-	-	-	2086.89	99.95	0.992
(*S*)-CDX **7**	-	-	-	-	-	-	-	-	-	3.81	2.05	67.19	5.41	3.33	76.89	9.35	6.48	86.63	10.86	7.69	88.49	17.89	13.31	93.01	-	-	-	50.41	98.05	0.982
(*R*)-CDX **7**	-	-	-	-	-	-	-	-	-	3.73	1.98	66.49	5.29	3.23	76.36	8.91	6.13	85.97	10.14	7.11	87.67	15.48	11.38	91.92	-	-	-	40.51	97.59	0.976
(*S*)-CDX **8**	-	-	-	-	-	-	-	-	-	3.35	1.68	62.69	4.61	2.69	72.88	7.89	5.31	84.16	9.07	6.25	86.21	14.70	10.76	91.50	-	-	-	40.63	97.60	0.983
(*R*)-CDX **8**	-	-	-	-	-	-	-	-	-	3.67	1.94	65.97	5.12	3.10	75.59	9.18	6.34	86.38	10.72	7.57	88.34	16.77	12.42	92.55	-	-	-	48.73	97.99	0.980
(*S*)-CDX **9**	-	-	-	-	-	-	-	-	-	2.53	1.02	50.53	3.05	1.44	58.99	4.08	2.26	69.35	4.31	2.45	71.00	4.74	2.79	73.63	-	-	-	6.42	86.52	0.973

Table S4 Continuation

Compound	25% [a]			22% [a]			20% [a]			17% [a]			15% [a]			12% [a]			10% [a]			7% [a]			2% [a]			0% [a]		R^2
	t_R	*k*	*b%*	t_R	*k*	*b%*	t_R	*k*	*b%*	t_R	*k*	*b%*	t_R	*k*	*b%*	t_R	*k*	*b%*	t_R	*k*	*b%*	t_R	*k*	*b%*	t_R	*k*	*b%*	*k*	*b%*	
(*R*)-CDX **9**	-	-	-	-	-	-	-	-	-	2.54	1.03	50.79	3.13	1.51	60.10	4.17	2.33	69.99	4.45	2.56	71.94	4.89	2.91	74.45	-	-	-	6.84	87.25	0.941
(*S*)-CDX **10**	-	-	-	-	-	-	-	-	-	2.38	0.90	47.41	2.79	1.23	55.20	3.58	1.87	65.11	3.82	2.06	67.28	3.90	2.12	67.91	-	-	-	4.54	81.94	0.951
(*R*)-CDX **10**	-	-	-	-	-	-	-	-	-	2.56	1.05	51.19	2.86	1.29	56.31	3.37	1.70	62.90	3.85	2.08	67.55	3.80	2.04	67.10	-	-	-	3.77	79.02	0.956
(*S*)-CDX **11**	-	-	-	-	-	-	-	-	-	2.62	1.09	52.20	3.11	1.48	59.76	4.23	2.38	70.41	4.67	2.73	73.22	4.94	2.95	74.70	-	-	-	7.01	87.52	0.942
(*R*)-CDX **11**	-	-	-	-	-	-	-	-	-	2.63	1.11	52.54	3.09	1.47	59.48	4.16	2.33	69.98	4.54	2.63	72.47	4.78	2.82	73.83	-	-	-	6.41	86.51	0.957
(*S*)-CDX **12**	-	-	-	-	-	-	-	-	-	2.39	0.91	47.63	2.73	1.18	54.20	3.53	1.82	64.60	3.80	2.04	67.11	3.76	2.00	66.72	-	-	-	4.24	80.91	0.951
(*R*)-CDX **12**	-	-	-	-	-	-	-	-	-	2.41	0.93	48.07	2.74	1.20	54.45	3.55	1.84	64.78	3.81	2.05	67.22	3.77	2.01	66.82	-	-	-	4.21	80.82	0.941
(*S*)-CDX **13**	-	-	-	4.88	2.90	74.37	7.84	5.27	84.05	12.57	9.06	90.06	20.97	15.77	94.04	50.14	39.11	97.51	-	-	-	-	-	-	-	-	-	735.70	99.86	0.991
(*R*)-CDX **13**	-	-	-	5.02	3.02	75.11	8.02	5.42	84.42	13.08	9.46	90.44	22.28	16.82	94.39	56.10	43.88	97.77	-	-	-	-	-	-	-	-	-	889.41	99.89	0.990
(*S*)-CDX **14**	-	-	-	3.73	1.99	66.52	5.71	3.57	78.10	8.78	6.02	85.76	14.32	10.45	91.27	34.54	26.63	96.38	-	-	-	-	-	-	-	-	-	485.74	99.79	0.989
(*R*)-CDX **14**	-	-	-	3.50	1.80	64.31	5.04	3.03	75.19	7.41	4.93	83.14	11.57	8.25	89.19	25.79	19.63	95.15	-	-	-	-	-	-	-	-	-	284.71	99.65	0.989
(*S*)-CDX **15**	5.87	3.69	78.69	12.17	8.74	89.73	29.36	22.49	95.74	65.25	51.20	98.08	-	-	-	-	-	-	-	-	-	-	-	-	-	-	-	16481.62	99.99	0.990
(*R*)-CDX **15**	4.35	2.48	71.26	7.60	5.08	83.55	13.07	9.45	90.43	23.01	17.41	94.57	39.69	30.75	96.85	-	-	-	-	-	-	-	-	-	-	-	-	1289.44	99.92	0.997
(*S*)-CDX **16**	-	-	-	-	-	-	3.23	1.58	61.30	8.30	5.64	84.94	13.08	9.46	90.44	29.72	22.78	95.79	37.65	29.12	96.68	-	-	-	-	-	-	662.98	99.85	0.972
(*R*)-CDX **16**	-	-	-	-	-	-	3.01	1.41	58.43	7.15	4.72	82.51	11.08	7.86	88.72	24.30	18.44	94.86	31.09	23.87	95.98	-	-	-	-	-	-	493.51	99.80	0.975
(*S*)-CDX **17**	-	-	-	-	-	-	3.18	1.55	60.73	8.19	5.55	84.74	12.92	9.34	90.33	29.35	22.48	95.74	37.12	28.69	96.63	-	-	-	-	-	-	660.54	99.85	0.971
(*R*)-CDX **17**	-	-	-	-	-	-	3.42	1.74	63.47	9.73	6.78	87.15	15.95	11.76	92.16	38.71	29.96	96.77	52.91	41.32	97.64	-	-	-	-	-	-	1185.77	99.92	0.976
(*S*)-CDX **18**	5.67	3.54	77.95	11.40	8.12	89.04	28.98	22.18	95.69	67.80	53.24	98.16	-	-	-	-	-	-	-	-	-	-	-	-	-	-	-	20502.18	99.99	0.988
(*R*)-CDX **18**	-	-	-	-	-	-	3.28	1.62	61.90	7.82	5.26	84.02	11.87	8.50	89.47	24.88	18.90	94.98	30.97	23.77	95.96	-	-	-	-	-	-	422.57	99.76	0.971
(*S*)-CDX **19**	5.55	3.44	77.46	11.06	7.85	88.70	28.59	21.87	95.63	59.11	46.28	97.89	-	-	-	-	-	-	-	-	-	-	-	-	-	-	-	14934.82	99.99	0.983
(*R*)-CDX **19**	-	-	-	-	-	-	5.38	3.31	76.78	14.60	10.68	91.44	24.40	18.52	94.88	56.11	43.89	97.77	-	-	-	-	-	-	-	-	-	2192.30	99.95	0.992
(*S*)-CDX **20**	-	-	-	-	-	-	2.90	1.32	56.88	6.11	3.89	79.56	16.10	11.88	92.24	42.56	33.05	97.06	-	-	-	-	-	-	-	-	-	4867.43	99.98	0.993

Table S4 Continuation

Compound	25% [a]			22% [a]			20% [a]			17% [a]			15% [a]			12% [a]			10% [a]			7% [a]			2% [a]			0% [a]		R^2
	t_R	*k*	*b%*	t_R	*k*	*b%*	t_R	*k*	*b%*	t_R	*k*	*b%*	t_R	*k*	*b%*	t_R	*k*	*b%*	t_R	*k*	*b%*	t_R	*k*	*b%*	t_R	*k*	*b%*	*k*	*b%*	
(*R*)-CDX **20**	-	-	-	-	-	-	5.72	3.57	78.13	12.86	9.29	90.28	26.31	20.05	95.25	61.62	48.29	97.97	-	-	-	-	-	-	-	-	-	2587.02	99.96	0.998
(*S*)-CDX **21**	-	-	-	-	-	-	3.68	1.95	66.07	9.67	6.73	87.07	15.16	11.12	91.75	30.50	23.40	95.90	59.24	46.40	97.89	-	-	-	-	-	-	989.01	99.90	0.988
(*R*)-CDX **21**	-	-	-	-	-	-	3.45	1.76	63.81	8.41	5.72	85.13	13.12	9.49	90.47	26.14	19.91	95.22	53.71	41.97	97.67	-	-	-	-	-	-	857.24	99.88	0.991
(*S*)-CDX **22**	-	-	-	6.27	4.01	80.05	10.38	7.31	87.96	17.01	12.61	92.65	28.53	21.82	95.62	35.41	27.33	96.47	-	-	-	-	-	-	-	-	-	335.81	99.70	0.964
(*R*)-CDX **22**	-	-	-	5.94	3.75	78.96	9.97	6.97	87.46	16.21	11.96	92.29	26.67	20.34	95.31	-	-	-	-	-	-	-	-	-	-	-	-	651.33	99.85	0.990
(*S*)-CDX **23**	7.40	4.92	83.11	15.92	11.74	92.15	25.12	19.10	95.02	42.69	33.15	97.07	-	-	-	-	-	-	-	-	-	-	-	-	-	-	-	2080.18	99.95	0.987
(*R*)-CDX **23**	5.51	3.41	77.30	10.11	7.09	87.64	17.90	13.32	93.02	31.82	24.46	96.07	66.83	52.46	98.13	-	-	-	-	-	-	-	-	-	-	-	-	2618.79	99.96	0.993
(*S*)-CDX **24**	4.05	2.24	69.11	7.23	4.78	82.71	14.53	10.62	91.40	27.92	21.33	95.52	61.34	48.07	97.96	-	-	-	-	-	-	-	-	-	-	-	-	4192.76	99.98	0.993
(*R*)-CDX **24**	-	-	-	5.23	3.18	76.08	8.39	5.71	85.10	13.73	9.98	90.90	26.11	19.89	95.21	-	-	-	-	-	-	-	-	-	-	-	-	792.14	99.87	0.987
(*S*)-CDX **25**	3.85	2.08	67.50	6.73	4.38	81.42	13.23	9.58	90.55	24.94	18.95	94.99	52.23	40.78	97.61	-	-	-	-	-	-	-	-	-	-	-	-	3188.60	99.97	0.993
(*R*)-CDX **25**	-	-	-	5.47	3.37	77.14	9.03	6.22	86.15	15.25	11.20	91.80	29.56	22.65	95.77	-	-	-	-	-	-	-	-	-	-	-	-	1052.45	99.91	0.988
(*S*,*S*)-CDX **26**	4.89	2.91	74.45	8.93	6.14	86.00	15.88	11.71	92.13	28.27	21.62	95.58	62.49	48.99	98.00	-	-	-	-	-	-	-	-	-	-	-	-	2690.30	99.96	0.991
(*R*,*R*)-CDX **26**	4.95	2.96	74.75	9.12	6.30	86.30	17.31	12.85	92.78	33.63	25.90	96.28	-	-	-	-	-	-	-	-	-	-	-	-	-	-	-	2927.52	99.97	0.995
(*S*,*R*)-CDX **27**	7.02	4.61	82.18	15.61	11.48	91.99	24.99	18.99	95.00	52.67	41.14	97.63	-	-	-	-	-	-	-	-	-	-	-	-	-	-	-	4335.11	99.98	0.998
(*R*,*S*)-CDX **27**	4.12	2.30	69.66	7.02	4.62	82.19	13.79	10.03	90.93	19.85	14.88	93.70	27.81	21.25	95.51	-	-	-	-	-	-	-	-	-	-	-	-	681.87	99.85	0.971
(*S*,*S*)-CDX **28**	-	-	-	4.27	2.41	70.70	6.71	4.37	81.38	10.27	7.22	87.83	19.47	14.58	93.58	-	-	-	-	-	-	-	-	-	-	-	-	517.61	99.81	0.981
(*R*,*R*)-CDX **28**	-	-	-	3.90	2.12	67.92	5.60	3.48	77.69	8.11	5.49	84.59	14.08	10.27	91.12	26.54	20.23	95.29	42.55	33.04	97.06	-	-	-	-	-	-	309.31	99.68	0.994
(*S*,*R*)-CDX **29**	-	-	-	3.50	1.80	64.26	-	-	-	7.12	4.69	82.43	11.65	8.32	89.27	20.90	15.72	94.02	31.80	24.44	96.07	-	-	-	-	-	-	217.72	99.54	0.997
(*R*,*S*)-CDX **29**	-	-	-	3.58	1.86	65.07	5.91	3.73	78.86	8.09	5.47	84.54	13.34	9.67	90.63	24.49	18.59	94.90	36.09	27.87	96.54	-	-	-	-	-	-	252.64	99.61	0.991
(*S*,*R*)-CDX **30**	-	-	-	4.49	2.59	72.13	7.21	4.77	82.66	12.74	9.19	90.19	21.20	15.96	94.10	43.34	33.67	97.12	-	-	-	-	-	-	-	-	-	702.59	99.86	0.998
(*R*,*S*)-CDX **30**	-	-	-	-	-	-	5.91	3.73	78.86	9.21	6.37	86.43	14.52	10.61	91.39	26.17	19.94	95.22	37.89	29.31	96.70	-	-	-	-	-	-	242.55	99.59	0.998
(*S*,*S*)-CDX **31**	-	-	-	5.01	3.00	75.02	7.79	5.23	83.95	13.25	9.60	90.56	21.88	16.50	94.29	41.99	32.59	97.02	-	-	-	-	-	-	-	-	-	556.16	99.82	0.998
(*R*,*R*)-CDX **31**	-	-	-	4.87	2.90	74.33	7.50	5.00	83.34	12.79	9.23	90.23	21.25	16.00	94.12	42.16	32.73	97.04	-	-	-	-	-	-	-	-	-	577.96	99.83	0.998

[a] Acetonitrile %

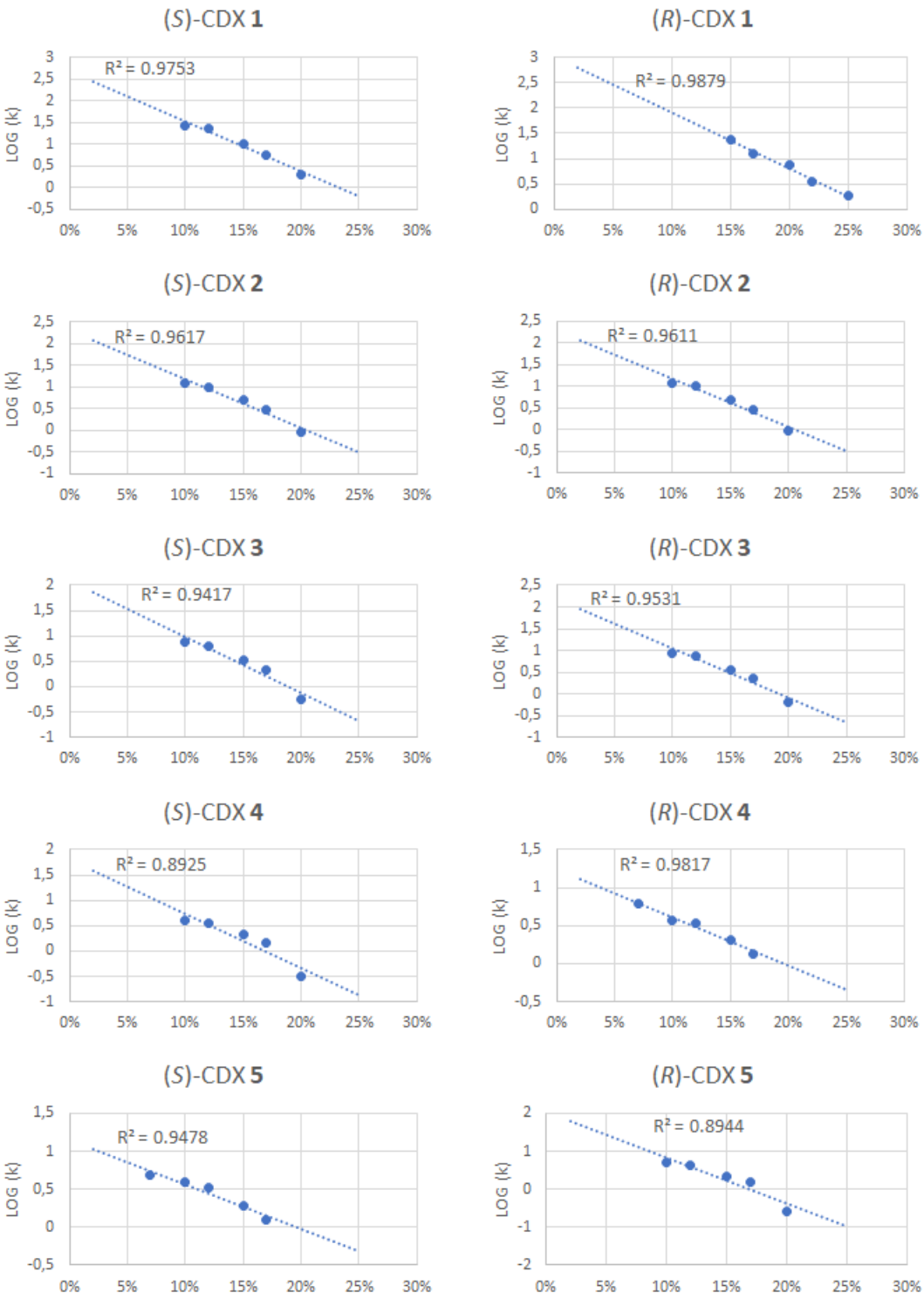


Fig. S1. Calibration curves of both enantiomers of CDX **1** – CDX **5**.

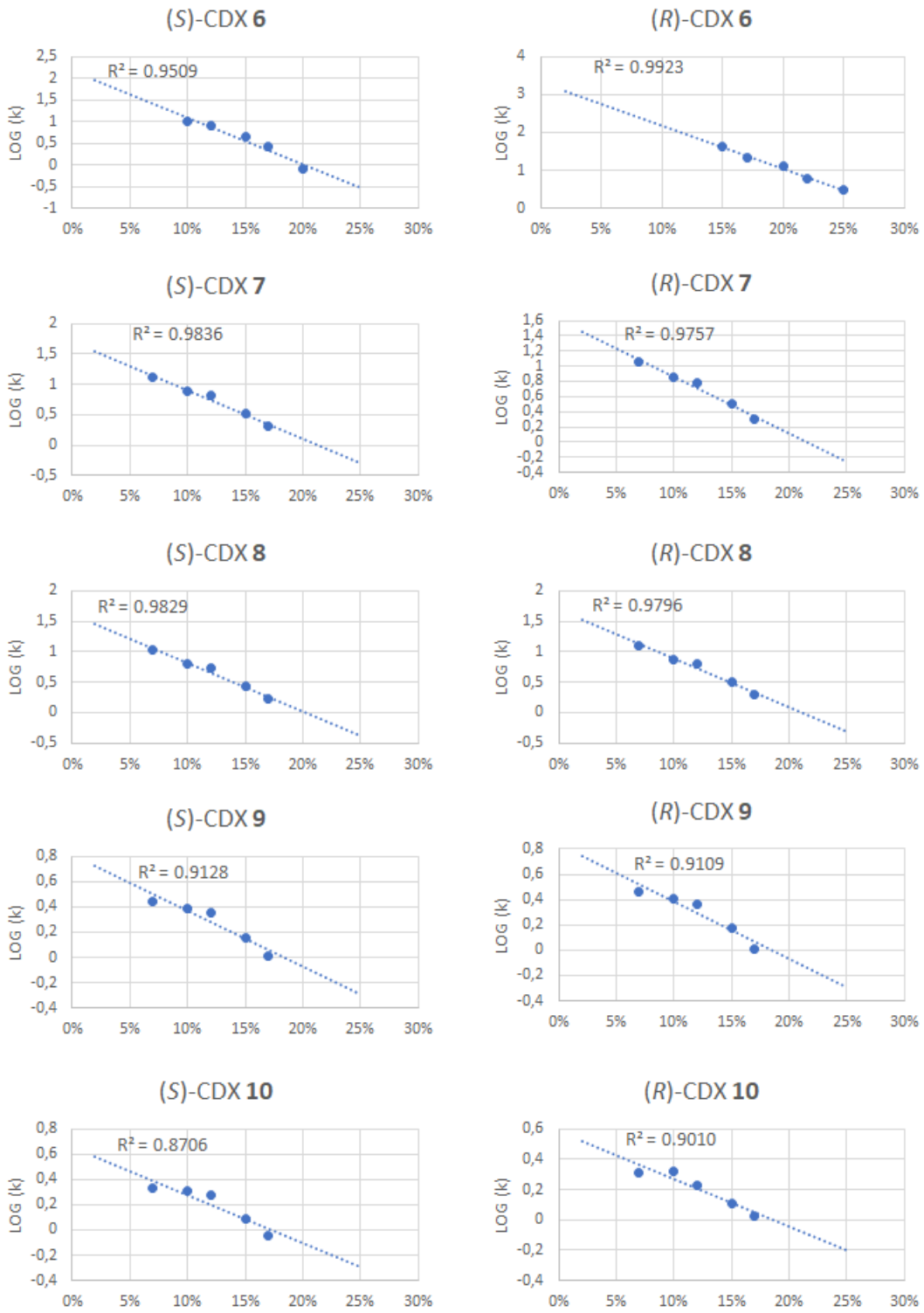


Fig. S2. Calibration curves of both enantiomers of CDX **6** – CDX **10**.

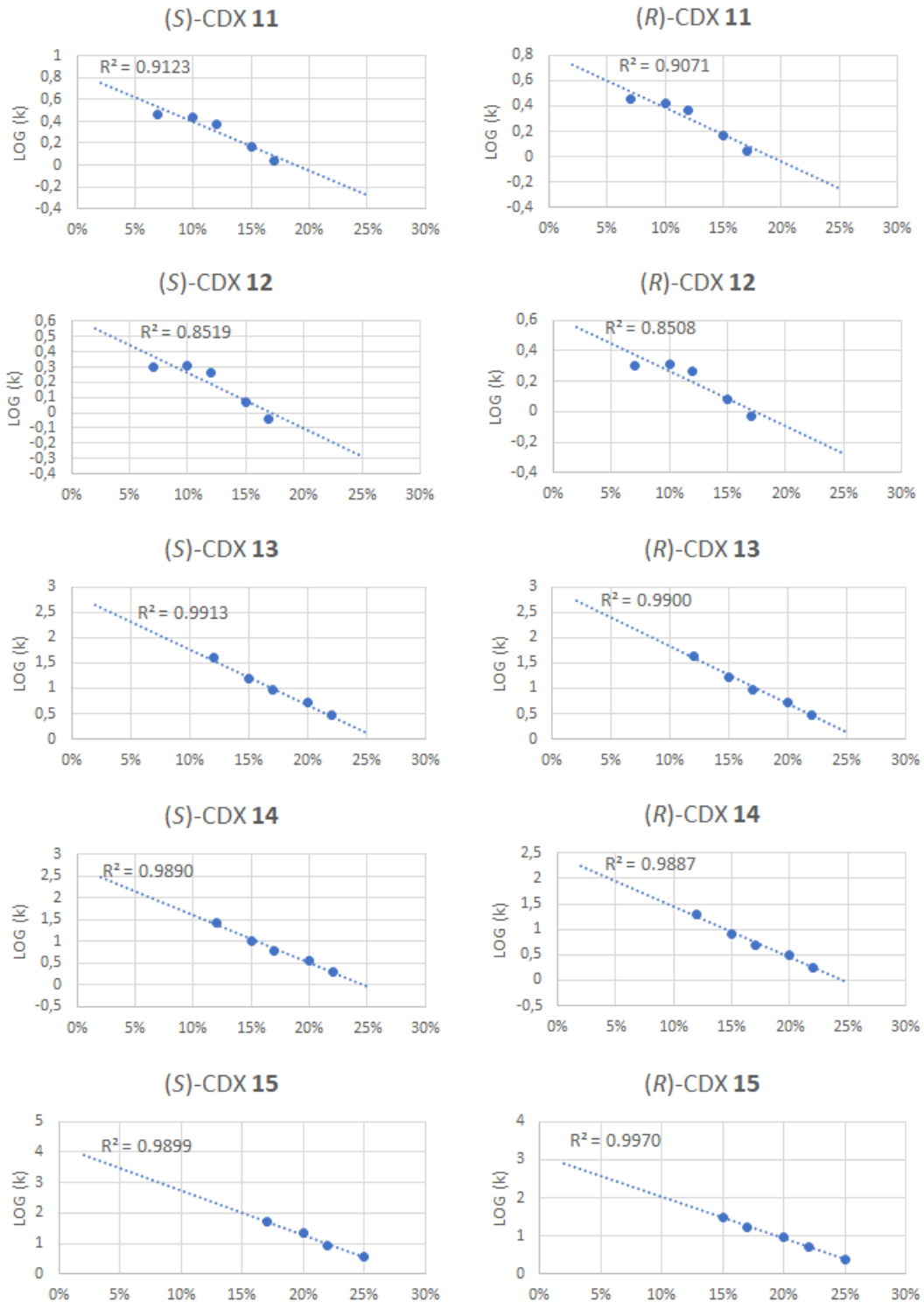


Fig. S3. Calibration curves of both enantiomers of CDX **11** – CDX **15**.

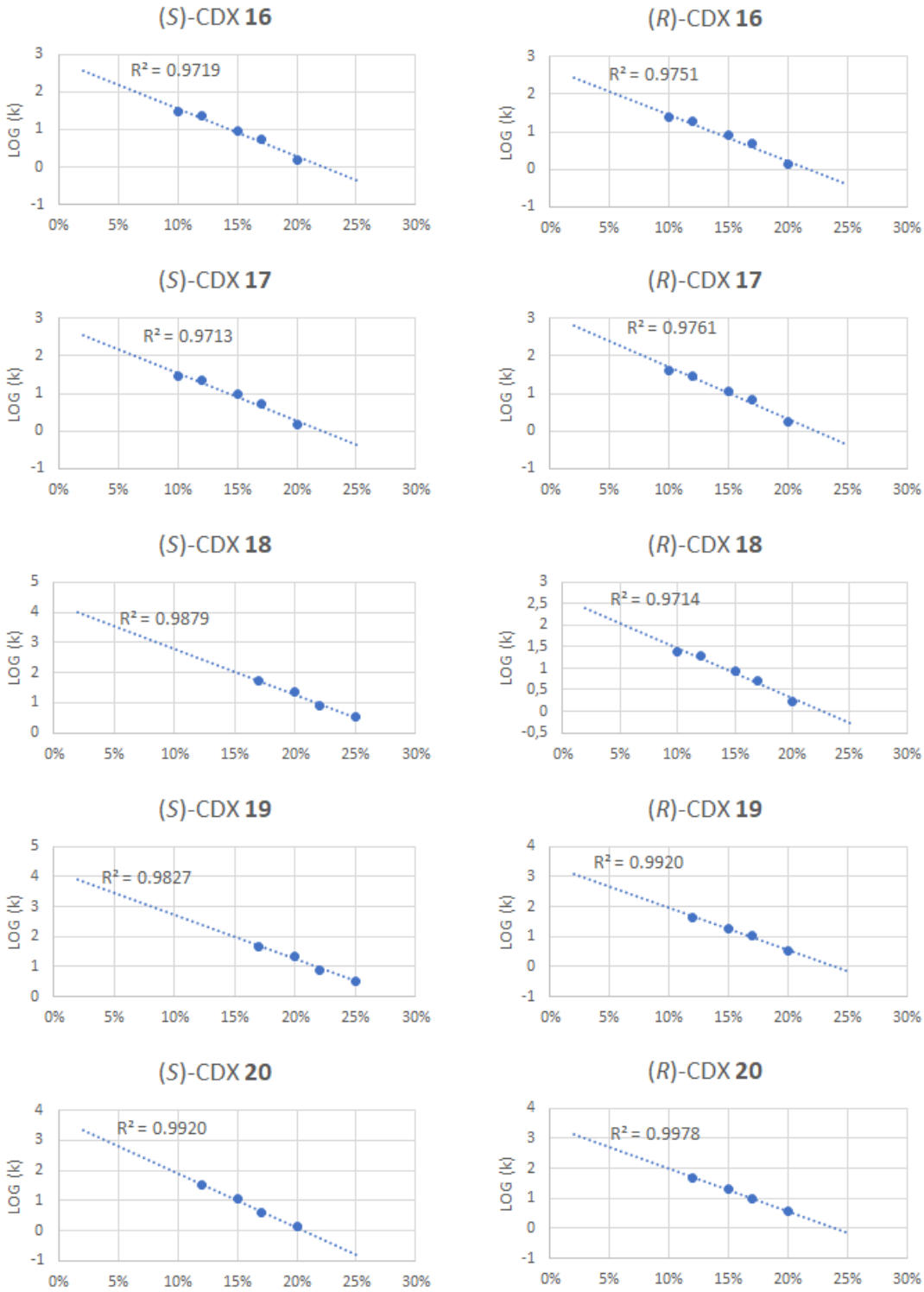


Fig. S4. Calibration curves of both enantiomers of CDX **16** – CDX **20**.

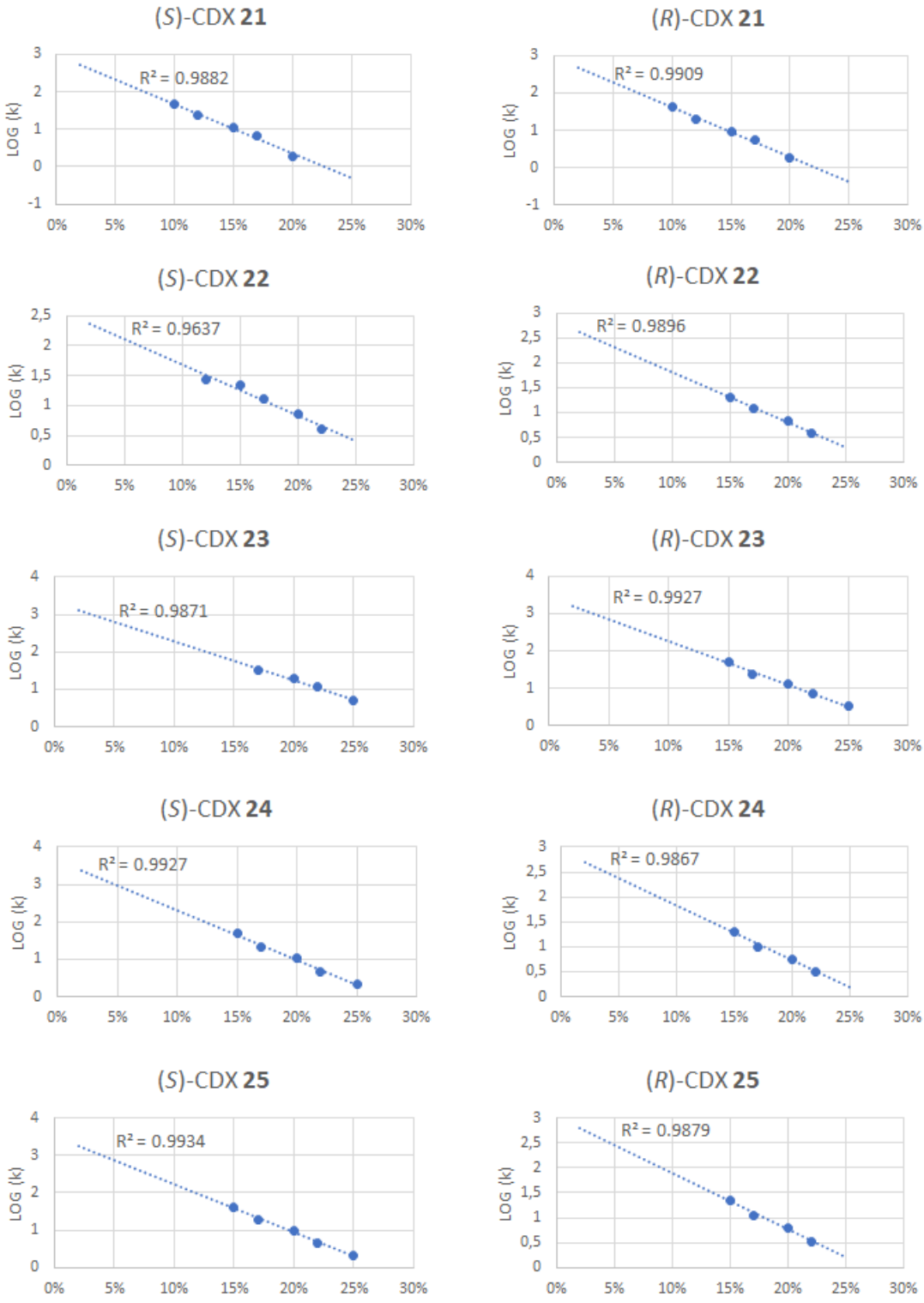


Fig. S5. Calibration curves of both enantiomers of CDX **21** – CDX **25**.

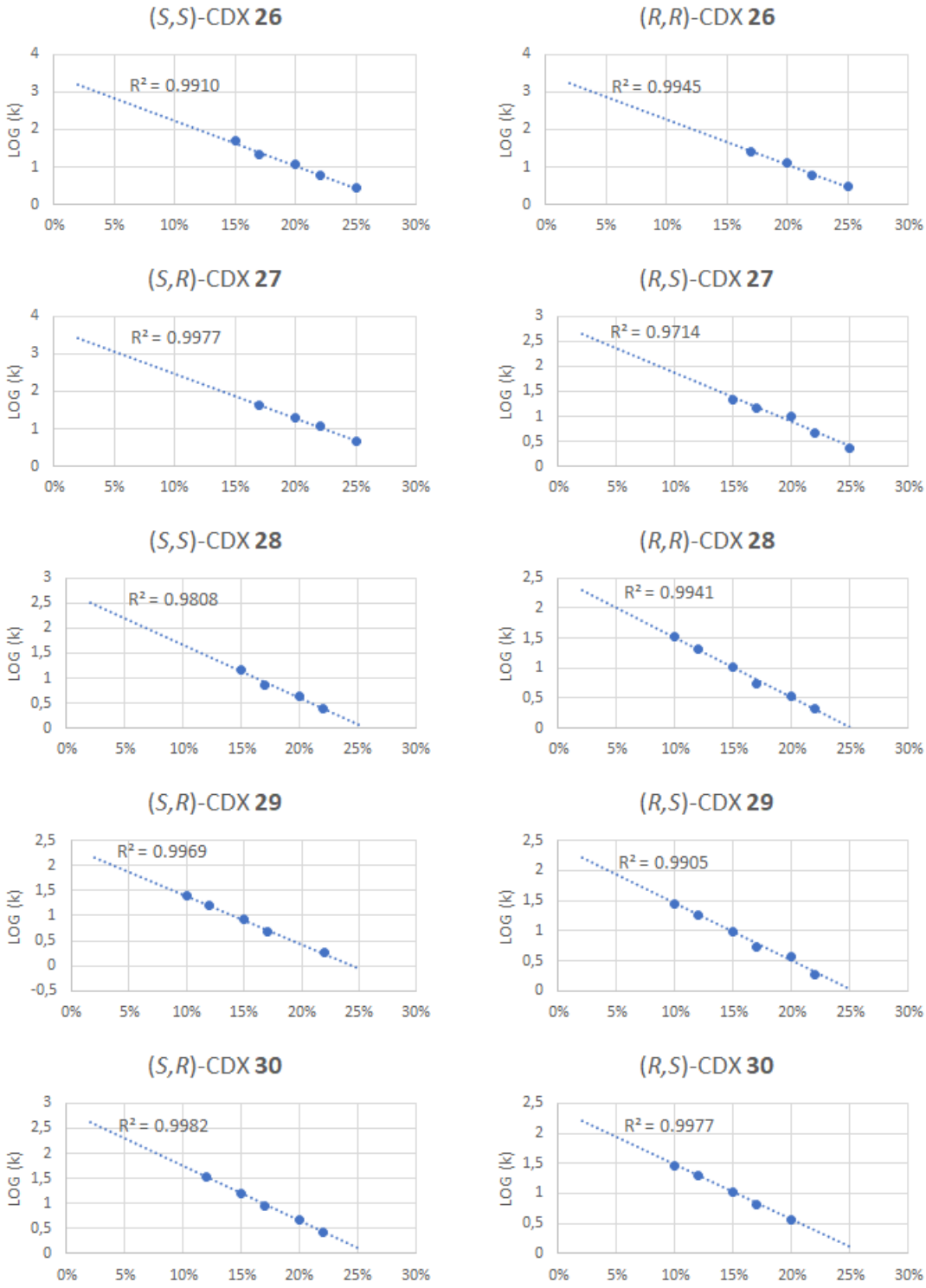


Fig. S6. Calibration curves of both enantiomers of CDX **26** – CDX **30**.

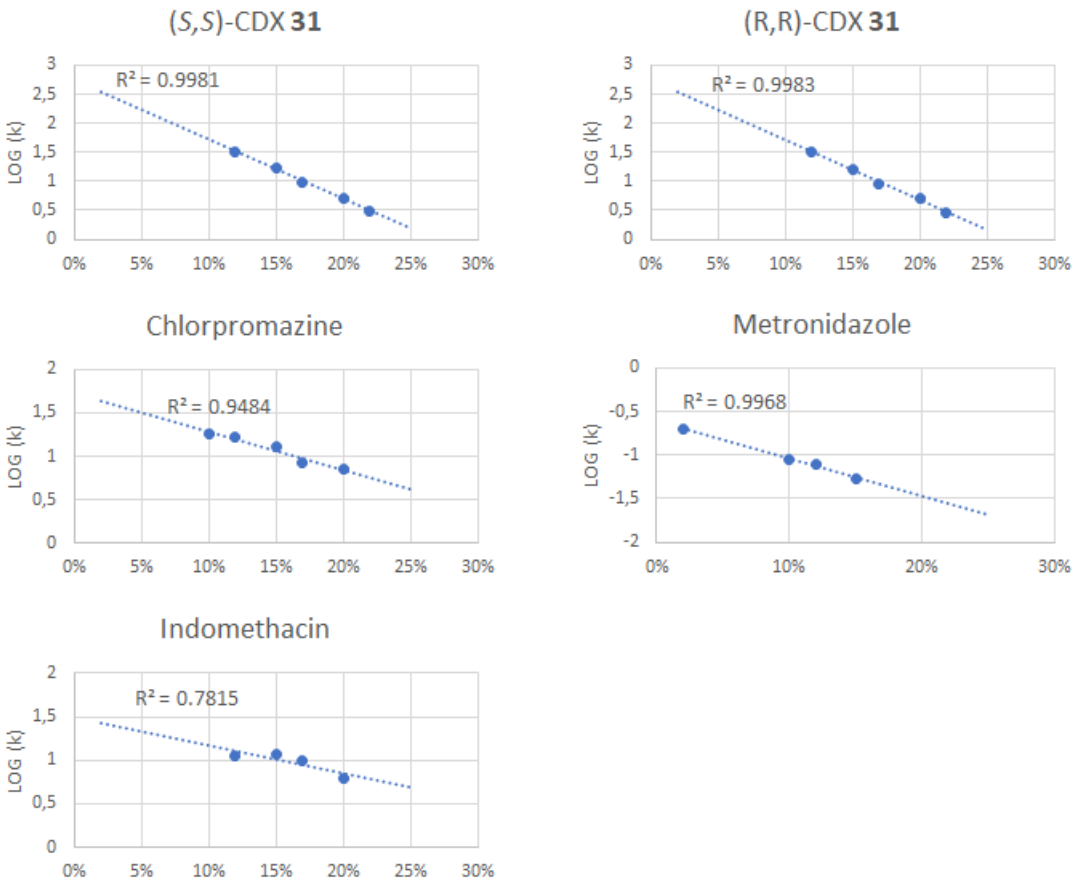


Fig. S7. Calibration curves of both enantiomers of CDX **31**, chlorpromazine, metronidazole and indomethacin.

CHAPTER IX

CONCLUSIONS

The results here presented fulfilled the initial aims of this thesis. Accordingly, the results concerning Aim 1 (chapters IV and V) point to the following conclusions:

Twelve new CSPs were successfully developed using a well-established synthetic methodology that, after the synthesis of suitable carboxylated derivatives as chemical substrates, only involved simple three steps: amidation, silylation and bonding to silica gel. The synthetized chiral selectors were covalently bonded to fully porous silica, which guarantee long-lasting columns, and showed high stability, versatility in the selection of the mobile phase composition and reproducibility. The enantioselective performance of the new CSPs was evaluated using several commercial and “in house” chiral analytes. Specificity for enantioseparation of some CDXs under normal-phase elution conditions was observed in the evaluation of the new CSPs. Although the chromatographic results obtained were not promising as expected, it was found that the number and position of the chiral moieties in the xanthone scaffold of the chiral selectors can interfere with the chiral recognition mechanism. The CSP comprising a chiral moiety with two aromatic rings and two stereogenic centers with (*R*)-configuration revealed poor enantioresolution capabilities for the tested compounds. For the CSPs comprising equal number of chiral units in the same positions, the nature of the substituent next to the stereogenic center was shown not to be pivotal because either the CSPs having an aromatic ring or an alkyl chain showed similar results. The central aromatic core of the selector, either xanthone or benzophenone scaffold, aligned with the xanthone tricyclic ring of the analytes to maximize π-stacking interactions, as well as hydrogen bonding interactions between the donor and acceptor polar groups of analytes and selectors, demonstrated to be essential for enantioselective recognition. The docking studies were proved to be a meaningful tool for the structural requirements necessary for the effective elucidation of the intermolecular CSP-analyte interactions.

Moreover, the results concerning Aim 2 point to the following conclusions:

Enantioseparation and/or assessment of the chiral recognition mechanisms of several CDXs, prepared “in-house”, were performed using different types of CSPs, namely Pirkle-type, polysaccharide-based, macrocyclic antibiotics-based and protein-based

CSPs. For some enantiomeric mixtures of CDXs on some tested CSPs, 100% EtOH was an efficient mobile phase for enantioseparation being its use an advantage considering the low toxicity of this solvent.

The Pirkle-type CSP (*S*,*S*)-Whelk-O1® and the polysaccharide-based CSP Lux® Celullose-2 (chapter VI) were successfully used for enantioseparation and determination of enantiomeric purity of the new synthetized chiral selectors, under polar organic elution mode. High enantioselectivity and resolution were observed in (*S,S*)-Whelk-O1® CSP for the enantiomeric mixtures of analytes comprising an aromatic ring linked to the stereogenic center(s), with α values ranging from 1.35 to 4.15, and Rs values ranging from 2.22 to 13.87. Among all the tested enantiomeric mixtures, those comprising three chiral moieties positioned in the xanthone scaffold gave the best chromatographic results. Enantiomers comprising an alkyl chain linked to the stereogenic centers were efficiently enantioseparated on a Lux® Celullose-2 CSP, with α values ranging from 2.16 to 1.86, and Rs values ranging from 3.38 to 2.93. Additionally, assessment of chiral recognition mechanisms on (*S*,*S*)-Whelk-O1 CSP was performed by molecular docking approach, which were in accordance with the chromatographic parameters. The nature and number of chiral moieties in the central aromatic scaffold of either xanthone or benzophenone derivatives were proved to be crucial for enantiorecognition. The simultaneous π-stacking interactions established by the aromatic ring at the stereogenic center and by the xanthone scaffold (with aromatic moieties of the selector) in addition to hydrogen interactions showed to be essential for enantioselective recognition.

The systematic study of enantioseparation for thirty-one enantiomeric mixtures of CDXs, prepared “in-house”, using four macrocyclic antibiotic CSPs (Chirobiotic® T, Chirobiotic® R, Chirobiotic® V and Chirobiotic® TAG) (chapter VII) confirmed their applicability for this class of compounds. The applicability increased considering the complementary profile in enantioselectivity of the different macrocyclic antibiotic selectors. The effects of the mobile phase composition, the percentage of organic modifier, the pH of the mobile phase, the nature and concentration of different mobile phase additives on the chromatographic parameters were investigated. The structural characteristics of the analytes and chiral selectors as well as the mobile phase composition proved to be fundamental factors for enantioselectivity. Chirobiotic® T and

Chirobiotic® V, under normal-phase and reversed-phase modes respectively, demonstrated to be the most effectives for the tested enantiomeric mixtures. Considering the importance of understanding the chiral recognition mechanisms associated with the chromatographic enantioresolution, and the scarce data available in this field for macrocyclic antibiotic-based CSPs, computational studies by molecular docking were carried out. Concerning Chirobiotic® T, R, V, and TAG columns, there was a 52%, 50%, 47%, and 80% agreement between docking scores and experimental results concerning the elution order of the enantiomers of the chiral analytes.

The chiral recognition mechanisms for the same library of thirty-one enantiomeric mixtures of CDXs, prepared “in-house”, was also investigated by molecular docking method for the protein-based CSP CHIRALPAK® HSA (chapter VIII). A good agreement (71%) between docking studies and experimental results was achieved, indicating that CDXs fit within the hydrophobic pocket of subdomain IIIA of HSA. The visual inspection of the most stable docked conformations for enantiomers complexes with the HSA-CSP revealed that the docking poses of the enantiomers were diverse, leading to different binding interactions.

Therefore, the current work represents a breakthrough, which contributes to a better knowledge in the area of chiral LC in general and in the area of CDXs in particular. The results obtained are important contributions to enlarge the applications of enantiomeric separation, to allow a closer look towards the mechanism of chiral molecular recognition as well as to have a better insight into the structural requirements of the analytes to be enantioseparated. The development of new CSPs for LC is a continuous and challenging issue. This work is an important contribution to improve the design of new selectors and further preparation of more efficient CSPs based on xanthone and benzophenone derivatives possessing wider applicability.

APPENDIXES

Table 1. Structures of chiral stationary phases based on xanthone and benzophenone derivatives.

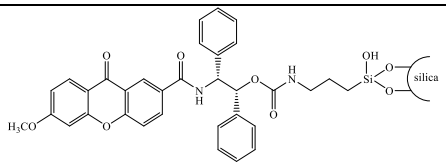
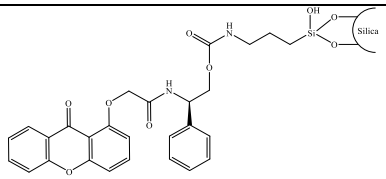
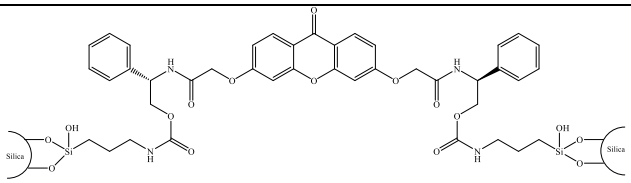
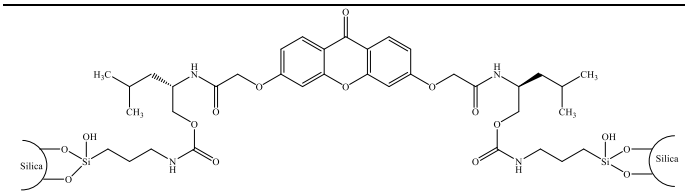
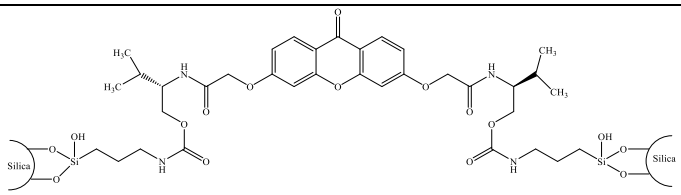
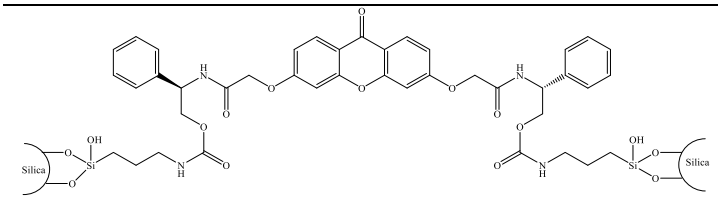
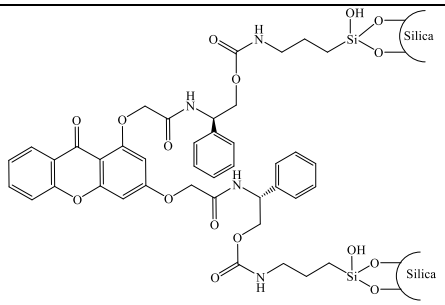
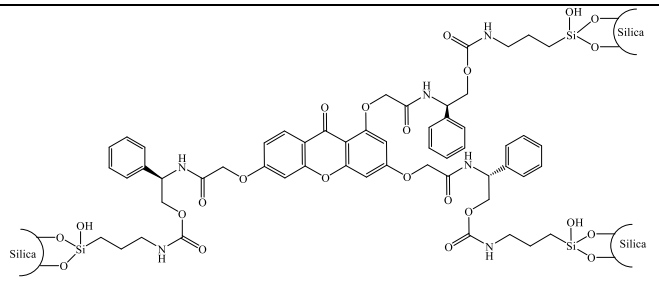
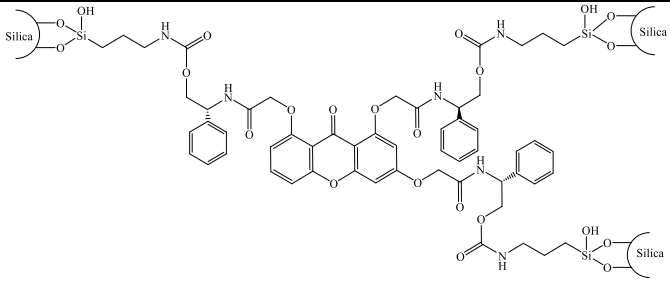
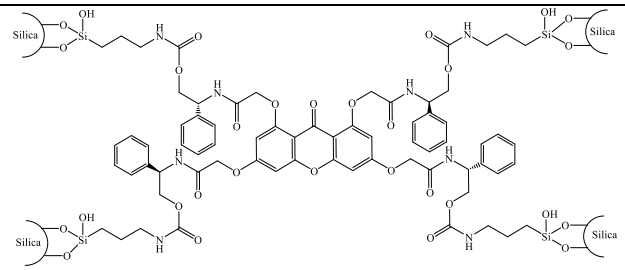
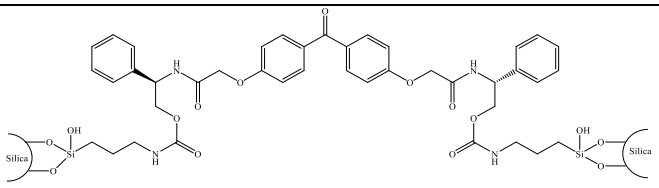
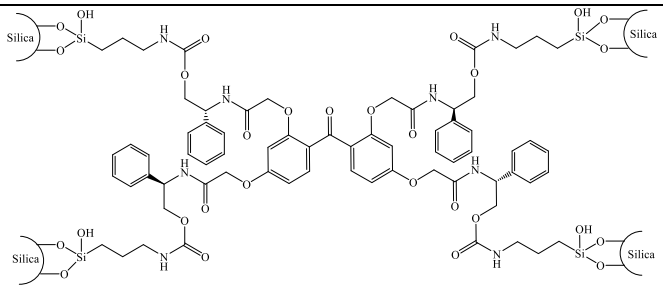
Structures	Thesis	Chapter	
		III	IV
	**CSP1**	**XCSP 5**	-
	**CSP2**	-	**CSP 1**
	**CSP3**	-	**CSP 2**
	**CSP4**	-	**CSP 3**
	**CSP5**	-	**CSP 4**
	**CSP6**	-	**CSP 5**
	**CSP7**	-	**CSP 6**

Table 1. Continuation

Structures	Thesis	Chapter	
		III	IV
	**CSP8**	-	**CSP 8**
	**CSP9**	-	**CSP 9**
	**CSP10**	-	**CSP 10**
	**CSP11**	-	**CSP 11**
	**CSP12**	-	**CSP 12**